473–664

ISSN 0003–2654

ROYAL SOCIETY OF CHEMISTRY

The Analyst

A monthly international journal dealing with all branches of the theory and practice of analytical chemistry, including instrumentation and sensors, and physical, biochemical, clinical, pharmaceutical, biological, environmental, automatic and computer-based methods

In This Issue...

SAC 89

Papers presented at the 8th SAC International Conference on Analytical Chemistry Cambridge UK 30 July - 5 August 1989

Vol. 115 No. 5 May 1990

The Analyst

The Analytical Journal of The Royal Society of Chemistry

Editorial Office: The Royal Society of Chemistry, Thomas Graham House, Science Park, Milton Road, Cambridge CB4 4WF. Telephone 0223 420066. Telex No. 818293 ROYAL. Fax 0223 423623.

Advertisements: Advertisement Department, The Royal Society of Chemistry, Burlington House, Piccadilly, London, W1V 0BN. Telephone 071-437 8656. Telex No. 268001. Fax 071-437 8883.

The Analyst (ISSN 0003–2654) is published monthly by The Royal Society of Chemistry, Thomas Graham House, Science Park, Milton Road, Cambridge CB4 4WF, UK. All orders accompanied with payment should be sent directly to The Royal Society of Chemistry, The Distribution Centre, Blackhorse Road, Letchworth, Herts. SG6 1HN, England. 1990 Annual subscription rate UK £220.00, EEC £233.00, Rest of World £253.00, USA $493.00. Purchased with *Analytical Abstracts* UK £476.00, EEC £520.00, Rest of World £547.00, USA $995.00. Purchased with *Analytical Abstracts* plus *Analytical Proceedings* UK £561.00, EEC £611.00, Rest of World £645.00, USA $1187.00. Purchased with *Analytical Proceedings* UK £279.00, EEC £296.50, Rest of World £321.00, USA $626.00. Air freight and mailing in the USA by Publications Expediting Inc., 200 Meacham Avenue, Elmont, NY 11003.
USA Postmaster: Send address changes to: *The Analyst,* Publications Expediting Inc., 200 Meacham Avenue, Elmont, NY 11003. Second class postage paid at Jamaica, NY 11431. All other despatches outside the UK by Bulk Airmail within Europe, Accelerated Surface Post outside Europe. PRINTED IN THE UK.

Information for Authors

Full details of how to submit material for publication in *The Analyst* are given in the Instructions to Authors in the January issue. Separate copies are available on request.

The Analyst publishes papers on all aspects of the theory and practice of analytical chemistry, fundamental and applied, inorganic and organic, including chemical, physical, biochemical, clinical, pharmaceutical, biological, environmental, automatic and computer-based methods. Papers on new approaches to existing methods, new techniques and instrumentation, detectors and sensors, and new areas of application with due attention to overcoming limitations and to underlying principles are all equally welcome. There is no page charge.

The following types of papers will be considered:

Full papers, describing original work.

Short papers: the criteria regarding originality are the same as for full papers, but short papers generally report less extensive investigations or are of limited breadth of subject matter.

Communications, which must be on an urgent matter and be of obvious scientific importance. Rapidity of publication is enhanced if diagrams are omitted, but tables and formulae can be included. Communications receive priority and are usually published within 5–8 weeks of receipt. They are intended for brief descriptions of work that has progressed to a stage at which it is likely to be valuable to workers faced with similar problems. A fuller paper may be offered subsequently, if justified by later work.

Reviews, which must be a critical evaluation of the existing state of knowledge on a particular facet of analytical chemistry.

Every paper (except Communications) will be submitted to at least two referees, by whose advice the Editorial Board of *The Analyst* will be guided as to its acceptance or rejection. Papers that are accepted must not be published elsewhere except by permission. Submission of a manuscript will be regarded as an undertaking that the same material is not being considered for publication by another journal.

Regional Advisory Editors. For the benefit of potential contributors outside the United Kingdom, a Panel of Regional Advisory Editors exists. Requests for help or advice on any matter related to the preparation of papers and their submission for publication in *The Analyst* can be sent to the nearest member of the Panel. Currently serving Regional Advisory Editors are listed in each issue of *The Analyst.*

Manuscripts (three copies typed in double spacing) should be addressed to:
The Editor, *The Analyst,*
Royal Society of Chemistry,
Thomas Graham House,
Science Park,
Milton Road,
CAMBRIDGE CB4 4WF, UK

Particular attention should be paid to the use of standard methods of literature citation, including the journal abbreviations defined in Chemical Abstracts Service Source Index. Wherever possible, the nomenclature employed should follow IUPAC recommendations, and units and symbols should be those associated with SI.

All queries relating to the presentation and submission of papers, and any correspondence regarding accepted papers and proofs, should be directed to the Editor, *The Analyst* (address as above). Members of the Analytical Editorial Board (who may be contacted directly or via the Editorial Office) would welcome comments, suggestions and advice on general policy matters concerning *The Analyst.*

Fifty reprints of each published contribution are supplied free of charge, and further copies can be purchased.

Titration from Metrohm sets standards, not limits

1000+ Applications
100 Electrodes
6 Potentiometric Titrators
4 Karl Fischer Titrators
4 Sample Changers

The choice is yours!

Ion analysis -
quite simply with Metrohm

Metrohm
Measurement in Chemistry
Worldwide with Metrohm

METROHM Ltd.
CH-9101 Herisau Switzerland
Phone 071 53 11 33
Telefax 071 52 11 14
Telex 88 27 12 metr ch

FIRST FOLD HERE

THE ANALYST READER ENQUIRY SERVICE
For further information about any of the products featured in the advertisements in this issue, write the appropriate number on the postcard, detach and post.

FOLD HERE

THE ANALYST READER ENQUIRY SERVICE

MAY'90

For further information about any of the products featured in the advertisements in this issue, please write the appropriate number in one of the boxes below.
Postage paid if posted in the British Isles but overseas readers must affix a stamp.

PLEASE USE BLOCK CAPITALS LEAVING A SPACE BETWEEN WORDS *Valid 12 months*

1 NAME

2 COMPANY

PLEASE GIVE YOUR BUSINESS ADDRESS IF POSSIBLE. IF NOT, PLEASE TICK HERE ☐

3 STREET

4 TOWN

5 COUNTY
POST CODE

6 COUNTRY

7 DEPARTMENT
DIVISION

8 YOUR JOB TITLE
POSITION

9 TELEPHONE NO

OFFICE USE ONLY REC'D PROC'D

FOLD HERE

Postage will be paid by Licensee

Do not affix Postage Stamps if posted in Gt. Britain, Channel Islands, N. Ireland or the Isle of Man

BUSINESS REPLY SERVICE
Licence No. WD 106

Reader Enquiry Service
The Analyst
The Royal Society of Chemistry
Burlington House, Piccadilly
LONDON
W1E 6WF
England

Foreword

8TH SAC INTERNATIONAL CONFERENCE ON ANALYTICAL CHEMISTRY

Cambridge, UK, 30 July–5 August, 1989

In keeping with the examples set by the two previous SAC Conferences, some of the papers presented at SAC 89 (8th in the series of triennial conferences) have been collected together to produce this Special Issue of *The Analyst*. The SAC Conferences were started in 1965 by the Society for Analytical Chemistry (hence SAC), and have been continued by the Analytical Division of the Royal Society of Chemistry, after the Society amalgamated with other professional chemical bodies to form The Royal Society of Chemistry. Unlike many conferences and scientific meetings which were held during the 1980s, SAC 89 presented a broad view of analytical research and development, allowing many varied topic areas to be discussed. Almost 300 summaries were submitted for presentation at the Conference, many of which were from outside the UK, confirming the status of the Conference as a truly international event. This issue of *The Analyst*, therefore, will act as a useful reference volume to illustrate those areas of analytical chemistry which were of research interest at the end of the decade.

The SAC 89 Conference was officially sponsored by the International Union of Pure and Applied Chemistry and the Federation of European Chemical Societies, and financial sponsorship was given by a small number of Chemical/Instrument companies in the UK. The Editorial Board is grateful for the support given by all of these organisations, that helped to make the Conference a success and this issue of *The Analyst* possible.

Four Plenary Lectures, 138 invited and contributed papers, 108 posters, five workshops and five update courses, comprised the scientific and technical programme of the Conference. The full programme together with abstracts of Conference papers, was published in the June 1989 issue of *Analytical Proceedings* (1989, **26**, 177–246) (Handbook Issue). The actual programme varied slightly from that published, owing to events beyond the control of the Executive Committee who organised the Conference.

The papers in this issue include three of the Plenary Lectures. Of the 69 papers submitted for publication, 37 appear in this Special Issue. Some of the papers submitted were rejected by the referees, and others, which were submitted late, will appear in future issues of this journal. Additional copies of this issue are available for personal purchase from the Royal Society of Chemistry, Distribution Centre, Blackhorse Road, Letchworth, Herts SG6 1HN (price £22/$49).

I wish to thank the Editorial Board for agreeing to devote this issue of *The Analyst* to SAC 89 and for allowing me the opportunity of introducing it. At the same time I should like to thank formally, the Executive Committee who gave freely of their time to organise the Conference, the permanent officers who administered the event so professionally and the many contributors who made it all worthwhile.

Brian W. Woodget
Chairman, SAC 89 Executive Committee

Flow Injection Analysis and Chromatography: Twins or Siblings?*

Plenary Lecture

Jaromir Růžička and Gary D. Christian
Department of Chemistry, University of Washington, Seattle, WA 98195, USA

The purpose of this survey of liquid chromatography and flow injection analysis, which reveals their common background and shared features, the various novel approaches possible and the lack of a unified theory, is to highlight the compatibility of these techniques and to promote the interaction and exchange of ideas between areas of the newly emerging discipline of "injection techniques," in the field of flow analysis.

Keywords: *Liquid chromatography; flow injection; injection technique*

Any measurement in a chemical laboratory involving liquid materials consists of solution handling, analyte detection, data collection and computation of results. Until about 25 years ago, research efforts in analytical chemistry were focused mainly on the last three areas whereas solution handling remained conceptually what it was in the late nineteenth century.[1] The problems of the incompatibility of modern analytical instrumentation with the unwieldiness of manual solution handling ("beaker" chemistry) are now being faced. However, significant changes are needed in many research laboratories, and in virtually all teaching laboratories, to replace calibrated glassware, beakers, extraction funnels and distillation apparatus by the more efficient flow injection operations.

Anyone who has used both a cuvette and a flow-through cell for measurements recognises the compatibility of flow microtechnology with detectors and computers. However, the concept of microflow operations can be extended well beyond this modest application: microlitre volumes of sample and reagent solutions can be metered exactly by means of injection and/or pumping. Volumes, and concentrations of flowing reactants, can be controlled precisely in space and time, thus allowing highly reproducible formation and detection of reaction products. Flow operations of this type are very versatile because the geometry and material of flow conduits can be optimised by moving, mixing, stopping, re-starting, reversing, oscillating, splitting and re-sampling the flowing streams (or portions of them) with the aim of controlling concentrations of reactants and their mutual contact times. In addition, injected samples may be transported by flow to contact reactive, separative, catalytic or sensing surfaces in a highly reproducible manner.

Although many advantages of flow operations have been exploited and optimised in chromatography and throughout much of this century, the remainder of the analytical community adopted the flow approach mainly in the form of flow-through detectors, leaving the bulk of solution handling operations to be performed in a batch mode. The reason for this development (or lack of it) has been conceptual rather than technological: the belief that the homogeneous mixing of reactants (and perhaps even the attainment of a chemical equilibrium) is the only reliable way of obtaining reproducible results. Even Skeggs'[2] ingenious idea of a continuous flow air-segmented system conformed with this belief, as his invention was aimed at achieving a homogeneous mixture of reactants within each individual segment of the liquid separated by air bubbles, thus maintaining the concept of a "beaker travelling on a conveyor belt." Consequently, the commercial and technical success of the AutoAnalyzer further perpetuated the notion that homogeneous mixing and the steady-state signal are the only reliable means of performing chemical assays reproducibly, even when evidence to the contrary was available in other fields of instrumental analysis (chromatography and electrophoresis).

It was the advent of flow injection analysis (FIA)[3] which changed that view by demonstrating that concentration gradients can be well controlled in space and time, thus allowing highly reproducible interaction of analytes with reagents, and that transient signals yield reproducible data regardless of whether the chemical reactions are taking place in homogeneous or heterogeneous systems.[4,5] To date, more than 2000 papers have been published describing the application of FIA to a wide variety of solution handling operations and instruments. It is, therefore, time to attempt another step into the future by examining the barriers between chromatography and FIA through comparison of the characteristic features of these techniques. The importance of such a comparison is beginning to be recognised as a symposium on this very topic was held recently at the 1989 Winter Conference on Flow Injection Analysis[6] and at an international meeting in Spain.[7]

Flow Injection Analysis

In order to discuss and compare the microflow analysis techniques of flow injection (FI) and chromatography, the principles, operations and definitions of FIA are briefly reviewed here. This will also serve as an introduction for the chromatographer who may not have used the technique. Flow injection analysis is based on the injection of a liquid sample into a moving continuous carrier stream of a suitable reagent.[4] The injected sample forms a zone which, during its transport towards a detector, disperses and reacts with the components of the carrier stream. The shape and magnitude of the resulting peak reflect the concentration of the injected analyte and provide kinetic information on the chemical reactions taking place in the flowing stream.

The saving of time, of reagent and sample consumption, of waste production and the simplicity of the experimental set-up have led to the conversion of hundreds of traditional spectrophotometric procedures into the FIA mode.[4,5,8] In addition to spectrophotometry, a wide variety of electroanalytical, solvent extraction, dialysis and gas diffusion, and the entire range of spectroscopic techniques, have been enhanced by the FI technique (Table 1).

The simplest and most widely adopted continuous flow injection mode can be illustrated by a diagram [Fig. 1(*a*)] showing the flow system and the resulting readout. A sample (S) injected into a continuously moving carrier stream of reagent disperses into a zone as it moves through a conduit on

* Presented at SAC 89, the 8th SAC International Conference on Analytical Chemistry, Cambridge, UK, 30 July–5 August, 1989.

Table 1. Detectors and techniques used in FIA

Amperometry/voltammetry	Reaction rate measurements
Ion-selective electrodes	Dialysis
Conductivity	Gas diffusion
Atomic spectrometry (AAS, ICP-AES)	Solvent extraction
Molecular spectrometry (UV, Visible, FT-IR)	Precipitation/dissolution
Fluorescence	Ion exchange
Chemiluminiscence	Electrolytic dissolution
Mass spectrometry	Electrodeposition
	Adsorption/desorption

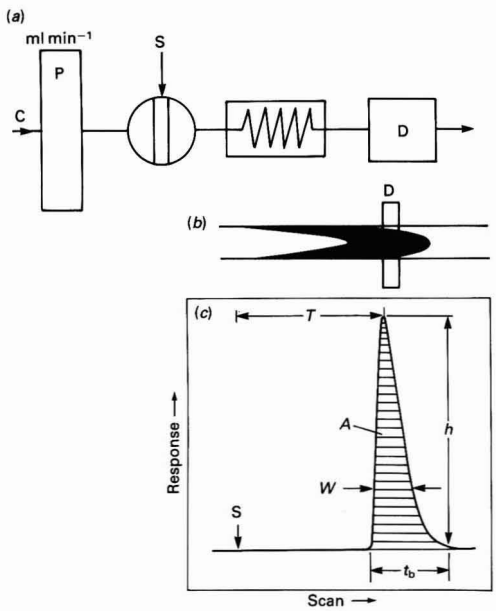

Fig. 1. (*a*) Schematic diagram of the simplest single-line FIA manifold: C, carrier stream; P, pump; S, injection valve reactor; and D, detector. (*b*) Schematic diagram of the dispersed sample zone as it passes through the observation field of the detector, D. (*c*) A typical peak recorded under continuous flow: S, point of injection; T, peak maximum appearance time; h, peak height; A, peak area; t_b, peak width from base line to base line; and W, peak width at a fixed arbitrary level as chosen for quantification. Note that whereas the analyte concentration response for a linearly responding detector is a linear function for h or A, it is logarithmic for W

the way to the detector. Chemical reactions take place in a microreactor (shown as a coil) from where the dispersed and reacted zone proceeds through a detector (D) to waste. The resulting "flowgram" (one hesitates to use the term fiagram as FIA is an acronym, not a word) exhibits a single peak for each injection and the height (h), width (W) or area (A) reflects the analyte concentration. The measurements are highly reproducible, although the sample zone is not mixed homogeneously with the reagent stream, but is dispersed into it and chemical reactions take place. This parabolic concentration gradient, when scanned by a detector, appears as a transient signal. In contrast to chromatography, the concentration gradient is more stratified and the peak is usually more skewed. Most frequently peak height, and for titrations peak width, is used for quantification of the analyte.

When multiple-wavelength detectors are used, such as atomic emission spectrometric, UV - visible spectrophotometric or Fourier transform infrared (FT-IR) spectroscopic

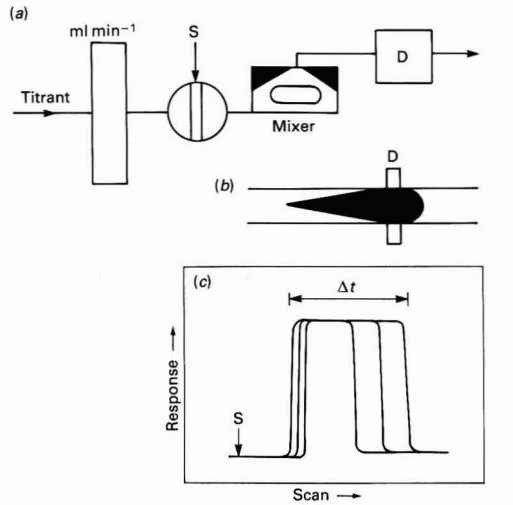

Fig. 2. Flow injection analysis titrations are performed in (*a*) a manifold which consists of S, a mixer injection valve; D, a detector and a pump which propels the carrier stream of titrant. (*b*) The mixer creates a homogenised exponential profile, shown schematically as it passes through the detector. (*c*) The resulting peak is composed of back-to-front titration curves, the distance Δt being a logarithmic function of the analyte concentration. Three injections of increasing analyte concentrations are shown, recorded from an identical starting point, S, to demonstrate this response

detectors, the flowgram exhibits an additional axis (wavelength), yielding multivariate information. Indeed, both spectroscopic and voltammetric detection have been used in FIA (Table 1). Multivariate information is often also obtained in the practise of modern chromatography and electrophoresis (multi-dimensional chromatographic modes and "hyphenated" techniques).

The next group of FIA techniques are titrations. Here, in a single-line manifold, the reaction coil is replaced by a gradient device (shown as a mixer, Fig. 2). The concentration of reagent in the carrier stream (serving as a titrant) is selected to be lower than that which corresponds stoichieometrically to the concentration of the injected analyte. Hence, if a sample of an acid (S) is injected into a carrier stream of base, the dispersing zone gradually becomes neutralised by the base penetrating through the interfaces at the leading and trailing edges. Therefore, each of these two boundaries is a continuum of acid to base ratios ranging from pure base to pure acid, where an element of fluid can be located within which the acid has been neutralised by the base. The distance between two such equivalent points, one at the leading edge of the zone and the other at its trailing edge, increases with increasing concentration of the injected acid and, therefore, the peak width, as displayed by means of a suitable indicator in the carrier, is proportional to the concentration of the injected acid. In Fig. 2, three injections are shown [recorded from the same starting point (S)] to indicate this increase in the value of Δt, which is the basis of the calibration graph. This titration in flow conceptually departs from the concept of classical titrations which, being based on homogeneous mixing, call for complete neutralisation of the entire volume of analyte pipetted into the titration vessel.[4] In contrast, FI titrations rely on the formation of an axial concentration gradient "stretched in time" by means of the mixer so that the titration process is digitalised as the successive elements of fluid pass through the detector. Note that in contrast to chromatography, the dispersed zone is visualised as a continuum of sample to

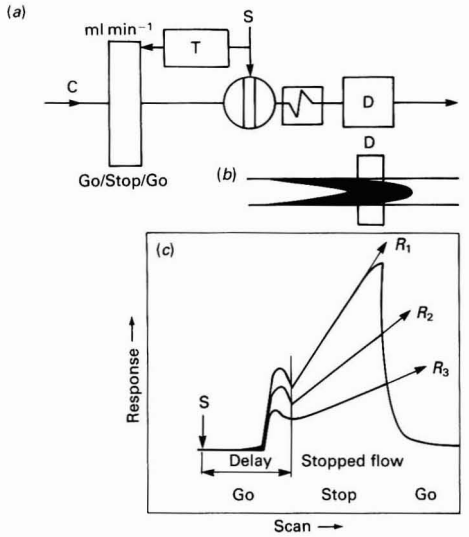

Fig. 3. (*a*) Reaction rate measurements by the stopped-flow method are performed in a manifold furnished with a timer, T, which is activated when the valve, S, is turned to the injection position. After a pre-selected delay time, the pump is stopped and then re-started after the stopped-flow period has elapsed. This allows a selected portion of the dispersed sample zone [shown schematically in (*b*)] to be arrested in the observation field of the detector. (*c*) The resulting peak is composed of the following three sections: continuous flow showing the peak maximum as recorded during the delay period; the reaction rate curve recorded during stopped-flow; and the washout tail. Three injections with increasing analyte concentrations are shown, recorded from identical starting points and showing increasing reaction rates R_1, R_2 and R_3

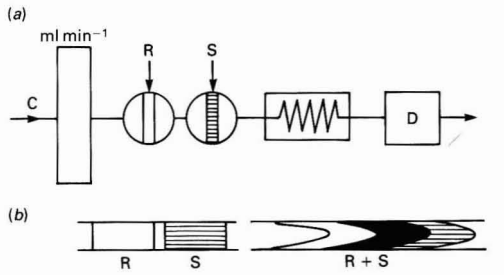

Fig. 4. (*a*) Single-line double-injection merging zones flow diagram. C, Carrier stream; R, reagent; S, sample solution, and D, detector. The double-looped valve is shown schematically as two separate valves which, however, turn synchronously and simultaneously. (*b*) Schematic diagram of the individual zones prior to their simultaneous injection and mutual merging as they travel through the mixing coil on the way to the detector

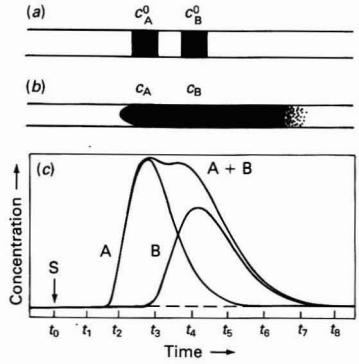

Fig. 5. Schematic diagram of (*a*) and (*b*) the merging zones and (*c*) the resulting concentration gradients observed at various times following sample injection, S. For details see text[4]

reagent ratios from which a pair of elements of fluid is selected for the readout.

Stopped-flow FIA allows us to exploit the physical and chemical kinetic processes taking place within the dispersing sample zone on the way from the injector to the detector.[4] One can gain an insight into these very complex processes by stopping the flow and observing the rate of the chemical reactions as they occur in the observation field of the detector (Fig. 3), where a selected section of a dispersed zone has been arrested. As physical dispersion virtually ceases when the carrier stream is stopped, the change of absorbance with time reflects the kinetics of the chemical reactions between the mutually dispersed components of the injected sample and carrier stream. In Fig. 3, three injections are shown recorded from the same starting point (S) to indicate the decrease in the slope of the reaction rate curves R_1, R_2 and R_3 for standards of decreasing analyte concentration and identical delay times. Note that because it is the change of signal with time rather than its absolute value which is the basis of calibration, the readout would not be affected by absorbing species in the injected sample. This feature, together with the flexibility of selecting the sample to reagent ratio (by selecting the delay time), has been found to be very valuable for biotechnological applications of FI, as it allows a wide range of enzymatic assays to be performed automatically on small volumes of samples. Note that in stopped-flow FIA only a single element is selected from the continuum (matrix) of the dispersed zone, which becomes the source of the readout. As the sample to reagent ratio changes continuously along the dispersed sample zone, there is an infinite range from which to select for measurement.

Yet another mode of FIA is the merging zones technique,[4,9] executed in a single-line manifold (Fig. 4). Water or another suitable solvent serves as a carrier stream into which both sample (S) and reagent (R) are injected simultaneously as two separate zones, using a double-looped valve. On the way towards the detector these zones gradually merge (R + S). This mutual merging yields a complex concentration pattern in which regions of pure and partly reacted components may be identified as they pass through the detector.

A schematic representation of the mutual dispersion of two zones, A and B (Fig. 5), reveals that the composite zone contains different concentration ratios of the original components, c_A and c_B, respectively, in addition to portions with pure component A or pure component B only. As each time slice, t_0, t_1, t_2, can be assigned to a certain concentration of A, B or their mixture, FI provides us with a highly reproducible matrix of concentration and times. Therefore, the merging zones technique allows simultaneous standardisation and assay by injecting the standard solution as A and the analyte solution as B when the carrier is the reagent. It also allows the determination of several analytes in the injected sample, even when using a single-wavelength detector, by permitting the sample components (A) to compete for a variable concentration of reagent (B).[9] With a multi-wavelength detector such as FT-IR, the landscape of the three-dimensional flowgram will become a multivariate space on which multi-component analysis can be performed. Further, different reagents injected sequentially as B will produce a different three-dimensional flowgram with the same sample zone (A) and hence each injection of a given sample with a different reagent will produce an additional fingerprint or landscape. Hence, hyphenation, available today only at a high cost by combining instruments in series, can be obtained inexpensively by the

judicious choice of a functional group reagent. With the assistance of chemometrics, random reagent access merging zone techniques may extend the capability of FIA for multi-component assays. This is not to say that the more powerful hyphenated chromatographic techniques will diminish in importance. These are often used for the characterisation of totally unknown materials, via structural elucidation. As the world moves increasingly to the measurement of larger molecules, even more sophisticated (and more expensive) combined techniques will be required.

The theory of FIA will take a long time to become fully developed. It is now well recognised that it has to deal with two processes occurring simultaneously: the physical process of dispersion and the chemical process of formation of the measurable species. However, the simplified theories developed so far deal mainly with the physical process, and even those are deficient, as they are either too complex or oversimplified. They naturally borrow very heavily from the wealth of chromatographic theory, although the classical descriptions based on the use of statistical moments have limited value for FI, where an individual element of fluid rather than the entire mass of the zone material is of interest. Therefore, focusing on the mean residence time is much less productive than considering residence times of individual elements of fluid, and the dispersion coefficient[4] of a selected element of the dispersing zone is a more useful description than the total amount of reactants involved. Therefore, existing models of microflow dynamics which have been applied successfully to chromatography will need major modification to become applicable to aspects of FIA. Additional consideration will have to deal not only with the continuously moving monotonous type of flow, but also with stopped-, pulsed- and even reversed-flow applications.[5,8,10,11]

As FIA is aimed at obtaining information from individual elements of the dispersed zone, it would be ideal if each element could be well mixed in the radial direction, rather than being stratified; however, as adjacent elements form a continuous concentration gradient in the axial direction, such an image of the dispersed zone is an obvious contradiction. Therefore, a "dualistic" view of the concentration gradient has to be adopted: a digitised one and a continuous one.

The digital image is useful because it allows us to optimise FIA manifolds and to conceive novel FI techniques. For this purpose, the dispersion coefficient, $D = c^0/c$, has been proposed,[4] to express the degree of dilution of the original sample solution in relation to that element of fluid within the dispersed zone from which the analytical readout is being taken, should it be the peak maximum (*cf.* Fig. 1) or an equivalence point (*cf.* Fig. 2) or some other section of the zone which may provide useful information (*cf.* Figs. 3–5). In this way, the value of D serves as a guide, allowing us to make comparisons with the assay conditions developed previously in a beaker (such as mixing ratios), while recognising the differences caused by the inhomogeneity of the reaction mixture, which continuously changes its composition on the way from the injector to the detector.

The continuous image of the dispersed zone has been described by statistical moments which lead to the concept of a mixing stage which in turn allows a measure of the intensity of the radial mass transfer rate in relation to the axial dispersion as it takes place in an FI channel.[4,12] Chromatographers will recognise here a degree of analogy with the concept of the height equivalent to a theoretical plate (HETP) with all its limitations. In both techniques it is desirable to have the material redistributed radially across the column as frequently as possible: in chromatography, to ensure contact between the stationary and mobile phases and to minimise band spreading, in FI to promote chemical reactions through improved radial mixing. Hence the plate height and mixing cell length are analogous parameters evaluated from statistical moments of the zone spreading. However, they both fail to deal adequately with a description of the chemical processes, as they assume total mixing and equilibrium throughout the plate (or mixing stage) volume.

The dynamics of chromatography and those of FIA therefore share numerous features which come to mind when reading the elegant classic text of Giddings.[13] Although seemingly less complex, the development of the theory of FIA will remain a formidable challenge for some time.

Flow Injection Analysis and Liquid Chromatography: Twins or Siblings?

To chromatographers, the schematic diagram of the FI analyser shown in Fig. 1 represents a high-performance liquid chromatographic (HPLC) system without a column. This undeniable resemblance of the flow schemes of these two methods leads to the conclusion that they are related. Indeed, one may say that FIA and chromatography are sub-sets of injection techniques belonging to the class of flow analysis. In fact, the flow scheme in Fig. 1 depicts either technique if the reactor were to be a column. As the above discussion dealt with FIA alone, it is now useful to seek a closer comparison with chromatography because, through such an analysis, we shall be able to elucidate their relationship and to discover novel injection techniques based on their common features.

Firstly, there is a difference in purpose: chromatographic techniques are aimed at the determination of many analytes in a single injected sample by resolving them through separation into a corresponding number of components which are then detected sequentially. The same mechanism also serves to eliminate matrix effects. The resulting readout is a chromatogram. Flow injection analysis is aimed at the determination of a single (or several) analyte(s) through chemical conversion, with detection within a single dispersed zone. Selective chemical conversions are also used to minimise matrix effects. The resulting readout is a flowgram.

Secondly, there is a difference in the means and the outcome: the transport of the sample from the injector to a detector in a flow-through system fulfills different functions,

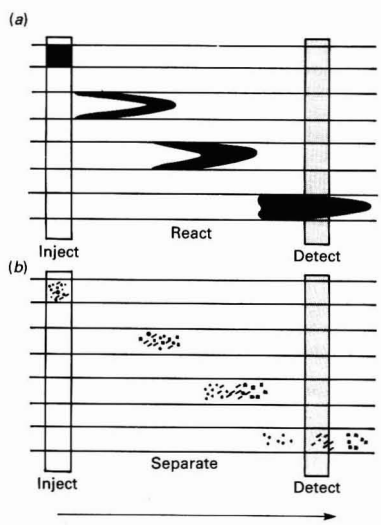

Fig. 6. Schematic representation of (*a*) the dynamics of FIA and (*b*) the chromatographic processes. Both techniques exploit the injection of analytes into a carrier stream which transports the material towards the detector. In FIA different analytes move down the system with the same mean velocity as they react with the carrier stream. In chromatography, different analytes move at different mean velocities, thus arriving at the detector at different times

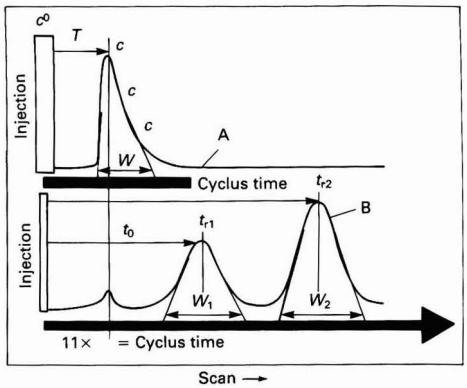

Fig. 7. Schematic representation of A, a flowgram and B, a chromatogram, revealing differences in peak shapes, duration of cyclus times and readout modes. For details see text. $D = c^0/c$; $T = t_0$

which rely on the exact repeatability of kinetic, physical and chemical processes taking place in the flowing stream. Hence, the resulting chromatogram is a consequence of differences in migration velocities between the analytes [Fig. 6(*b*)], due to differences in separation factors (ratio of distribution coefficients) and amplified through numerous repetitions (theoretical plates).

A flowgram is a result of dispersion of the sample zone into a carrier stream of reagent, and of the ensuing chemical reactions taking place in the flowing stream [Fig. 6(*a*)], where all analytes move through the system in the same fashion and at the same rate (because their distribution coefficients are virtually zero), while they are redistributed randomly in axial and radial directions by the hydrodynamics of flow and by molecular diffusion. Consequently, in a flowgram, the peak maximum appears at what a chromatographer will term the breakthrough time, t_0 (dead-time or dead-volume), whereas the first peak in a chromatogram always appears later at t_{r1}, the second peak even later at t_{r2}, etc. This observation leads to a comparison of the operational speed of these two methods (Fig. 7).

The cyclus time is the residence time of the sample zone between the injector and detector and is the period during which the flow channel is occupied; hence, its duration defines the injection frequency. In FIA this period is equal to $t_0 + W$, where W is the peak width at the base (Fig. 7), because no analyte is retained on the conduit walls or on the reactor packing. For this reason it is important that the FI analyser is hydrodynamically well designed, as $N = 16(W/t_0)^2$, where N is the number of mixing stages. At a continuous monotonous flow, N is a function of the radial mass transfer rate and hence of the reactor geometry, the velocity of flow and of the molecular diffusion coefficient.[4,12,13] The more intense the radial transfer rate, the shorter will be the length of the mixing stage and the larger the value of N. Hence for $N > 10$, when the peak shape becomes Gaussian, the cyclus time will be reduced to $t_0 + 0.5W$.

In chromatography the residence time of the injected material is much longer as, in addition to flow transport, various analytes which have been injected in a single zone migrate at different rates down the column, because the system is designed to impart a different interaction of these analytes with the stationary phase. Although physico-chemical interactions at the interface between the mobile and stationary phases are selected so that the capacity factor does not exceed 5, which results in a residence time of the last peak of at least $t_r = 6t_0$, the minimum cyclus time must be prolonged to at least 11 breakthrough times (t_0) as unknown matrix components may have capacity factors greater than 10. The rationale for this rule of thumb is that if a capacity factor is greater than 10 under given conditions, the species will not affect subsequent runs for some period of time. Hence, considering equal flow designs FIA offers at least a ten times higher sampling frequency than chromatography, whereas chromatography allows multi-component assay on a single sample injection. In chromatography, hundreds of components may be determined simultaneously, although only a few may be of actual interest. To process the data for 100 components may take an unacceptably long time.

As we shall see later, these capabilities make the two techniques competitive and complementary.

The limit of detection of any injection technique is a function of: (1) the sensitivity of the detector used for the detection of a given species; (2) the dispersion of the sample zone during transport through the flow channel and the flow cell; and (3) the injected sample volume.

In chromatography, the mass of injected analyte is restricted by column overloading, and the injected volume, V_i, is restricted by peak broadening and is (for 1% broadening): $V_i = 0.2t_rV/(N)^{\frac{1}{2}}$, where V is the flow-rate. This means that for a typical column with $N = 10\,000$, a flow-rate of 2 ml min^{-1} and a retention time of 1 min, the maximum injected sample volume is, in theory, 4 μl.[14] In practice, however, 10–20 μl are typically injected, resulting in a 20-fold dilution when the analyte reaches the detector. In FIA, such a narrow restriction on injected volume does not exist, as the FIA system cannot be overloaded unless $D = 1.0$ is reached, and peak broadening is not an important factor, because it can be compensated for by temporarily increasing the flow-rate (see flow programming in FIA below). As peak height in FIA increases linearly with injected sample volume up to the value of $S_{\frac{1}{2}}$ (the injected volume necessary to reach 50% of the steady-stage signal)[4] (and dilution may even approach zero), and as in chromatography a typical sample volume corresponds to only about one twentieth of $S_{\frac{1}{2}}$ without overloading the column then, all other factors being equal, FIA offers at least a 20 times higher sensitivity and a correspondingly lower limit of detection than chromatography. Of course, through the use of extremely sensitive detectors, chromatography is capable of measuring very small amounts of analytes. However, in the future also, FIA will be able to take advantage of similar detection systems for maximum detectability. In the meantime, the detector sensitivity requirement is lessened by the ability to inject larger sample volumes.

A further increase in the sensitivity of FIA can be obtained through chemical derivatisation, performed in the stopped-flow mode. The high sensitivity of FIA combined with its speed makes this technique ideal for less selective pre-chromatographic screening of samples, prior to implementation of the more selective but more time consuming chromatographic measurement.

The calibration of all injection systems relies on a periodic injection of a known (standard) analyte, as "what happens to one sample happens in exactly the same way to any other sample." Hence the readout for the known analyte can be compared with that of the unknown to be determined for the purpose of quantification and identification provided, of course, that the extensive parameters (injected volume, flow-rate, geometry of flow channel, detector configuration and response, temperature and pressure), and the resulting intrinsic parameters (concentration gradients of reactants, residence times and surface - liquid interactions), can be strictly reproduced from one sampling cycle to the next, time after time. Obviously such conditions are more difficult to maintain the longer the sampling cyclus is, and the more complex are the physico-chemical interactions taking place in the flow channel. The success of chromatography is a result of the tremendous effort spent on the research and technology of column packing, high-pressure pulseless pumping devices,

and of the durability of conduit components, which include connectors, flow cells and particularly injection valves. In contrast to chromatography, the processes in the FI analyser are less complex, the flow resistance of flow-through channels is low, resulting in a pressure requirement of 1 bar or less, and the shortness of the sampling cycli makes frequent recalibration practical.

The detectors and associated computers used in injection techniques have certain common features, such as low flow-cell volume, speed of response and data acquisition/reduction capability. However, in chromatography, traditionally, non-selective detectors have been preferred, as many different species must be sensed by the same detector sequentially, after they have been resolved on a column. In contrast, the only source of selectivity in FIA is selective detection enhanced by suitable chemical conversion, and this is often the choice in liquid chromatography. In addition to measurements in solutions, FIA is being used increasingly for the detection of chemical reactions taking place on solid surfaces (optosensing[15]), for the assay of heterogeneous samples with detection of precipitates formed during or after their separation (by turbidimetry or nephelometry[4,8,16]), and of cells, organelles, colloids and micellar solutions. In addition, novel types of detector are being introduced, such as flow cytometric[17] or flow spectrofluorimetric detectors, for heterogeneous samples.[18] There is no doubt that the future of selective detection in FIA is in hybrid detectors, where spectroscopic and electrochemical sensors will be serially connected and their signals processed, deconvoluted and correlated in real time by multivariate techniques. It is important to realise that high repeatability of sample interaction in time and space, provided by FI operation, is the necessary condition for the successful operation of any such serial detection system.

The programming of physical parameters within a single measuring cycle is an important tool of injection analysis. These parameters can either be kept constant or varied in a highly reproducible fashion.

In chromatography, many modes of programming have been exploited with great ingenuity, such as temperature, pressure and, above all, changes in the mobile phase composition. Although these parameters are usually kept at set values in FIA, flow-rate programming is the most important tool of this technique, as stopped-flow,[4] split and merging flows,[4] periodically slowed,[10] oscillating[11] and even the periodically pulse flow[19] allow control of the reaction times and of the sample zone dispersion far beyond that which is possible with a monotonous continuously moving stream, as used in chromatography. In this context, it is of historical interest to note that it was the lack of understanding of flow programming that led to the gloomy prediction of the limited scope of FIA.[20,21]

Chemical interactions are the very essence of all injection methods and they constitute the core of analytical chemistry, whether they are performed in homogeneous media or at the liquid - solid interface. Reviewing the range of mobile and stationary phases used in chromatography leaves one in awe of the ingenuity and efforts spent by generations of chemists, who developed and perfected this powerful methodology, in which microflow operation plays such an important role. Much of what has been learned about analyte interactions in the two-phase systems as used in chromatography is only now becoming transferred to FIA. In addition to heterogeneous interactions, FIA exploits, perhaps to a greater extent than chromatography, the wealth of solution chemistries which produce species detectable by molecular spectroscopies, by chemiluminescence or by electrochemical detectors. Enzymatic assays or any other catalysed reactions, which depend on reaction rate measurement, are advantageously performed using FIA stopped-flow techniques. In view of recent advances in detector cell volumes, knitted post-column reactors, etc., stopped-flow detection in chromatography should be more useful in the future. Multi-component analysis using diode arrays combined with the mutually penetrating zone technique is still in its infancy; however, it will mature to fill the gap between FIA and chromatography by allowing the

Table 2. Injection chemistry systems

Enhancement of instrumental methods by the FIA technique—

Technique	Enhancement*
Atomic spectrometry	ST, DL, M, CH, MC
Cytometry	ST, CH (staining)
Microfluorimetry	ST, CH, RR
Voltammetry	ST, CH, KA, RR
Electrophoresis	CH, KA
Mass spectrometry	ST, KA, M

Hybridised injection chemistry based instruments—

Sequence of functions	Technique	Application†
Derivatisation/detection	FIA	SASI
Dilution/derivatisation/detection	FIA	PC
Pre-concentration/derivatisation/detection	FIA	TA
Pre-concentration/derivatisation/elution/detection	FIA	TA
Separation/detection	Chromatography	SAMA
Separation/derivatisation/detection	Chromatography	SSAMA
Dilution/separation/detection	FIA/chromatography	PC
Pre-concentration/derivatisation/detection	FIA/chromatography	TA
Derivatisation/detection → separation/detection	FIA → chromatography	SS
Pre-concentration/elution → separation/detection	FIA → chromatography	TA
Derivatisation/detection or separation/detection	FIA or chromatography	DIONEX

* ST, sample throughput; DL, improved detection limit (and sensitivity); M, matrix removal; CH, chemical conversion; MC, microchemistry; RR, reaction rate measurement; and KA, kinetic advantage.

† SASI, serial assay of a single analyte: PC, process control; TA, trace analysis; SAMA, serial assay of many analytes; SSAMA, sensitised assay of many analytes; SS, screening of samples to distinguish low/high analyte content prior to chromatography; and DIONEX, environmental analyser capable of chromatographic or FI analysis.

determination of several species from a single injection without their physical separation. Considering that extensive dilution (up to 10^6 times[22]), pre-concentration,[4,23] and separation by solvent extraction,[4,8,24] dialysis[4,8] or gas diffusion[4,8,25] have also been performed by FIA, one may safely conclude that, given the relatively short period of its existence, FIA can offer much more than what has been seen so far.

Injection Techniques: Their Scope and Synergisms

The purpose of using the term injection techniques here is not to introduce a new terminology, or to stake new territory, but to free us from certain entrenched associations which prevent us from discovering novel approaches, by identifying areas of compatibility and synergism of analytical techniques based on injection into a flowing stream. We have undoubtedly failed to consider all the important parameters, operations and instrumental features relative to both chromatography and FIA. However, it is hoped that this discussion has highlighted enough common denominators for us to try to envisage what can be gained by combining features of injection-based techniques and to give others an impetus to follow. It is important to emphasise that these techniques are well on the way to operating on the microlitre scale, thus enabling desktop or portable instruments to be designed. Such instrumentation will fulfill the vision of the old school of microchemistry, which proposed the use of miniscule volumes of sample and reagent solutions for an assay. This represents the requirements of environmentalists, who strive for improved safety in the workplace, and the wish of the analytical chemist, who intends to perform an analysis in a laboratory or at any other place, should that be in a chemical plant, at a bedside, under the sea or on a mountain top.

Apart from obvious advantages of miniaturisation, well appreciated by chromatographers, microflow injection is a link between chemistry, detector and computer, allowing integration and hybridisation of their functions. Four areas of future development will emerge: (1) enhancement of traditional instrumental analysis; (2) design of injection-based instruments with hybrid functions; (3) design of injection-based chemical sensors; and (4) mutual enhancement of FIA and chromatography.

The combination of the concepts of FIA and liquid chromatography is within the scope of this paper and is, therefore, discussed below. Several of these ideas are outlined in Table 2.

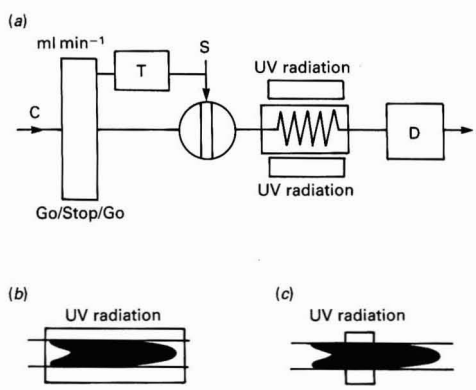

Fig. 8. (*a*) Schematic diagram of the manifold for reagentless FIA stopped-flow photolysis. The combination of photolysis by UV radiation and the stopped-flow method (*cf.* Fig. 3) allows more efficient degradation of the analytes by irradiating the zone when arrested in the irradiated coil. Note that either an entire zone [shown schematically in (*b*)] or section [shown schematically in (*c*)] can be illuminated prior to the subsequent detection

What Can Flow Injection Analysis Borrow From Chromatography?

Post-column derivatisation is so closely related to FIA that virtually all chemistries developed for this purpose can be directly transferred. A comparison of the most recent literature on post-column derivatisation[26–30] and FIA[4,5,8] reveals that these areas have addressed different types of compound, post-column derivatisation being focused more on the detection of broader groups of organic compounds, with the aim of increasing the sensitivity of their detection, or to convert them into species detectable by fluorescence, UV - visible spectrophotometry, voltammetry or conductivity. The transfer of these chemistries into the FIA domain will allow the determination of a wide variety of biologically active compounds, pharmaceuticals, substrates and products of fermentation, pesticides, drugs, vitamins and toxins (see, for example, Table 1 in reference 28, and references 26 and 27). It is true, however, that many of these reactions are non-selective, often aimed at the derivatisation of a functional group and therefore of little use when employed without separation. However, several alternatives make their use in FI worth considering: (1) determination of an analyte which is a major sample component, as in the production control of a known product; (2) serial screening of samples, prior to more time-consuming chromatography; (3) as the chemistry of choice to be coupled to a spectrometric technique of powerful resolution such as FT-IR; and (4) use in the stopped-flow FIA mode where selectivity may be obtained through reaction rate measurement.

Photolytic FIA is a straightforward parallel to the use of UV irradiation in post-column derivatisation[27,28] where this technique is applied to increase the reaction rate, to replace chemical reagents in a conversion scheme by radiant energy or to produce derivatives with favourable detection properties. As PTFE tubing is transparent to UV light in addition to being heat resistant, it can simply be wound as a coil around a light source. Although many organic compounds yield fluorescent fragments, others can be coupled through UV irradiation with suitable reagents. Aromatic pesticides,[31] phenothiazines,[32] sulphonamides,[33] stilbene derivatives[34] and vitamin homologues[35] have been determined by photolytic derivatisation with fluorescence detection. Even compounds with little or no UV absorbance can be converted to fluorophores and detected, with the aid of a suitable sensitiser. Alcohols, aldehydes and ethers have been determined by fluorescence using anthraquinone-2,6-disulphonate,[36] as were several pesticides using an *o*-phthalaldehyde - 2-mercaptoethanol reagent.[37] In addition to spectrometry, voltammetry has been used to detect species produced by photolysis. Here, UV irradiation has been used to produce compounds that can be oxidised at a platinum electrode, thus allowing voltammetric measurements in the potential region where dissolved oxygen does not interfere, or to produce a halide detectable at a silver electrode.[38] A combination of heat and photolysis in separate reactors has also been used for the determination of metabolites.[28]

In post-column derivatisation, photolytic reactors have been operated under continuous flow due to chromatographic coupling and, therefore, long coils have to be used and the lamp must be on continuously. In FI the flow can be stopped and the entire sample zone arrested in an irradiated coil [Fig. 8(*b*)]. Alternatively, carrying this approach one step further, the irradiation process can be "digitised" by focusing the radiation into a narrow field, much shorter than the dispersed zone [Fig. 8(*c*)], and by scanning the entire zone afterwards with the purpose of obtaining a blank and a photolysed section, by analogy with the merging zones concept shown in Figs. 4 and 5. As the lamp-on/lamp-off technique allows differentiation between degradable and non-degradable compounds, as has been well demonstrated in post-column derivatisation of antihypertensive drugs or of chlorinated

pesticides using amperometric detection, it is tempting to speculate that differential kinetic photolytic FI could be developed for the same purpose. There indeed seems to be ample room for innovative thought in this unexploited area. Many reaction/detection schemes are possible, of which reagentless stopped-flow FIA using FT-IR detection of photolytically generated fragments appears to be the most interesting proposal, as in combination with chemometrics it may perhaps replace or at least supplement the assay of organic compounds now performed by the more time-consuming chromatography - post-column derivatisation.

High pressure/high temperature FIA was proposed a few years ago and shown to be suitable for the hydrolysis of polyphosphates prior to their spectrophotometric determination.[39] Also, supercritical fluid FIA using CO_2 as solvent and thermal lens[40] or FT-IR detection[41] is feasible. Therefore, high temperature/high pressure FIA is a logical concept, justified whenever reaction rates or the solubility of respective compounds prevent the use of more moderate reaction conditions, whereas FI in the gas phase still awaits its recognition.

What Can Chromatography Borrow From Flow Injection Analysis?

Stopped-flow on-column manipulations can be useful in liquid chromatography and capillary electrophoresis due to the relatively small diffusion coefficients. This is an area of still unexplored possibilities for the study of physico-chemical processes, measurement of diffusion coefficients and investigation of the behaviour of stationary phases.

Stopped-flow post-column derivatisation is a straightforward technique, which first comes to mind if we visualise a system such as that shown in Fig. 3 where the coil has been replaced by a chromatographic column and augmented with an additional line for the addition of a post-column reagent. An advantage of such a technique would be its capability of measuring the reaction rate during post-column derivatisation and hence enhancing the sensitivity of detection due to the absence of band broadening during the reaction/stopped-flow time. Stopped flow might also bring about more effective use of post-column enzymic reactors. However, most importantly, it would allow reaction rate measurements (*cf.* Fig. 3) on eluate fractions to be performed, a feature of great value for preparative chromatography and for isolating enzymes or biologically important substrates, where continuous FIA has recently been used successfully.[42] However, inevitably, stopped-flow operation would "digitise" a chromatogram, thus either prolonging the chromatographic cyclus beyond practical limits or, if the eluate by-passes the detector during stopped-flow periods (using a valve nested flow cell), "blind spots" will be generated on corresponding sections of the chromatogram. We should mention that impressive state-of-the-art post- and on-column derivatisation techniques in chromatography are being developed, for example, the capillary zone electrophoresis systems described by Rose and Jorgenson[43] and Pentoney *et al.*[44]

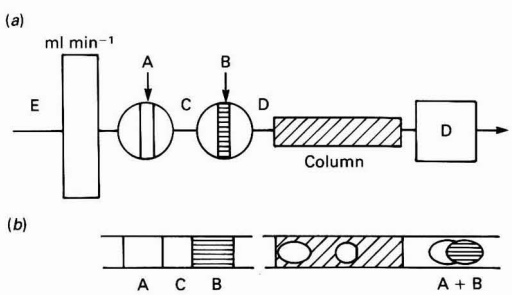

Fig. 9. Schematic diagram of (*a*) the manifold for merging zones chromatography and (*b*) the merging zones. This method, by analogy with merging zones flow injection (Figs. 4 and 5), results in deliberately created doublet peaks which can serve a variety of purposes (see text). The twin-looped valve, shown as two separate valves, functions as described in Fig. 4.

Merging zones chromatography by analogy with merging zone FIA (Figs. 4 and 5) would be performed in a system in which a double-injection valve would be used instead of a single-loop valve as in conventional chromatography (Fig. 9). This unusual injection mode may be used for three different purposes: internal standardisation, pre-column derivatisation and simplified gradient elution.

Internal standardisation by merging zones will allow standard and analyte chromatograms to be run simultaneously. By simultaneous injection of unknown analytes through one loop (A) and a mixture of known standards through another loop (B), two precisely spaced zones will be introduced sequentially on to the column. Given suitable zone spacing (C) and choice of standards based on their capacity factors, doublet peaks will be observed for identical analytes in standards and unknowns. The advantage of observing a double peak, rather than an enhanced single peak as obtained by conventional internal standard techniques, is that it will allow verification of the retention time of the standard analyte and will give an obvious positive identification of unknown peaks. The first feature may be useful for chemometric resolution of chromatographically unresolved peaks, as the mathematical models rely heavily on perfect reproducibility of retention times and peak shapes (tailing). Chemometricians have, in this respect, been much frustrated by subtle changes in column characteristics as they occur from one chromatographic run to the next, with consequent irreproducibilities of retention times and peak shapes (so called "rubber banding"). Simultaneous internal standardisation by merging zones may alleviate the problem. Obvious positive indentification may find use whenever a chromatogram is to be used as a legal document, as the presence of a double peak would eliminate any doubt as to the identity (position) of the species in question or to the proper execution of the chromatographic run.

Pre-column derivatisation on-line is often hindered by the non-compatibility of the derivatising reagent with the column material. This problem could be partly alleviated by injecting only a zone of reagent, rather than pumping it continuously through the injector and the column. The sequence, proximity (C) and volumes of sample (B) and reagent (A) zones would have to be calculated to allow proper material penetration and contact times to achieve the required derivatisation.

Gradient elution by merging zones would require a small-volume loop for sampling (A) and a long delay conduit (C), together with a second large-volume loop (B) for the eluent to be used. The eluent should reach the column only after the sample components have been adsorbed. Although simple in design and operation, gradient elution by merging zones would be less flexible than conventional gradient systems, which allow profiles of the eluent to be formed in nearly any desirable fashion.

The measurement of physico-chemical parameters in different circumstances than chromatography can provide highly precise data. Novotny and co-workers,[45,46] for example, have measured diffusion coefficients by near-critical chromatography which is really "chromatography" in an empty tube.

Packed Reactors in Chromatography and in Flow Injection Analysis

Pre-concentration, matrix removal and chemical conversion by means of solid reagents are performed by flow microanalysis with the aid of reactors packed with suitable solid

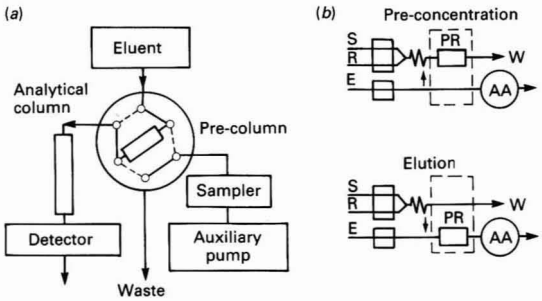

Fig. 10. (*a*) Pre-column trace enrichment[44] and (*b*) FIA pre-concentration.[46] In both schemes the pre-column and packed reactor (PR) are nested in the valve in the "straight flush" mode. In reference 46, detection was by atomic absorption (AA) spectrometry (for details see text). E = Eluent

materials. The common characteristics of these devices are their small size (typically 20 × 2 mm i.d.) and the coarseness of the packing material (50–200 μm particles) so that the flow resistance is low, allowing the use of the air pressure (vacuum) of a syringe, or of a peristaltic pump, to propel the flow.

Another important operational feature, shared by the pre-concentration performed on a packed reactor, can be described as the "all or nothing" principle: the combination of analyte/reagent/carrier stream composition is selected in such a way that the distribution ratio of selected species is either $\gg 100$ or $\ll 0.01$, resulting in either complete retention on, or complete release of analyte from, the solid surface. Affinity chromatography, representing an extreme of chromatographic selectivity, is a perfect example of the "all or nothing" principle.

Surface modified silica is most widely used as the solid support, although surface modified polymers are gaining ground owing to their better stability at higher pH values. Other useful materials are controlled pore glass for the covalent bonding of enzymes and reagents, and traditional ion exchangers for the pre-concentration of ionisable analytes.

Many of these materials are used as solid packing in pre-columns or guard columns for chromatography. An excellent review of their applications and properties is summarised in selected chapters[30,47,48] of recently published monographs.[26,27]

The pre-concentration of desired analytes and removal of unwanted matrix material are accomplished by passing a large volume of sample through a packed reactor and by subsequent elution of the analytes into a small volume of a suitable eluent. In this way, up to a 100-fold pre-concentration can easily be achieved.

Although trace enrichment has been used as a pre-column technique in chromatography for well over a decade,[26,27] the first paper on FIA pre-concentration only appeared in the early 1980s at about the same time as the work on short column affinity chromatography was published.[49] Whereas chromatography has mainly been concerned with increasing the sensitivity for the determination of organic compounds, FIA pre-concentration has mainly been aimed at matrix removal and pre-concentration of the desired metals followed by their determination by atomic absorption or inductively coupled plasma (ICP) atomic emission spectrometry.[4] Leaving aside semantics and priority issues, let us first compare these techniques as they are practised today.

Although graphically dissimilar, the flow diagrams in Fig. 10 represent two systems with an identical function: an on-line pre-concentration with a "straight flush" elution of the analytes. In both schemes the packed reactor (PR or pre-column) is nested in a valve, which has two positions: pre-concentrate and elute. In both schemes the enrichment increases with increasing volume of sample solution pumped through the microcolumn and is also dependent on the volume of the eluent into which the analyte is released. Obviously, the reproducibility of this pre-concentration critically depends on the reproducibility of timing, flow-rates, concentrations of reactants and contact times of liquid - solid surfaces. Both chromatographic and FIA modes of operation are eminently suited for this purpose; however, how do these two techniques actually differ? The answer to this question is already known. The flow scheme shown in Fig. 10(*b*) is essentially the same as that in Fig. 10(*a*) without a chromatographic column. Therefore, as we discussed previously, all other parameters being equal, pre-concentration and measurement by FIA will be at least 11 times faster and at least 20 times more sensitive than trace enrichment in chromatography. Also, the absence of the chromatographic column allows the FIA system to be operated at a low pressure and at a higher flow-rate with a simpler peristaltic pump. Further, there is less restriction on the composition of the eluent, which does not have to be compatible with the column material and separation performance. Also, the selection of reactor packing material is not limited by the requirements of a chromatographic column.

If, however, the chromatographic column, which is the source of resolution, is absent from the flow scheme, how can FIA satisfy the requirement of selectivity of determination? The answer is combined selectivity of reaction and detection. For this purpose, in addition to a non-selective sorption mechanism such as hydrophobic interaction, an additional selective (and preferably hydrophilic) reagent is used to promote the selective adsorption of an analyte on the reactor packing.

An example of such an approach is the determination of trace amounts of lead using octadecyl-bonded silica (ODS) as the solid support, an aqueous solution (pH 8) of sodium diethyldithiocarbamate (NaDDC) as the reagent and methanol as the eluent, together with atomic absorption spectrometric (AAS) detection.[50] When an acidified sample solution of lead(II) is pumped in a flow scheme such as that shown in Fig. 10(*b*), and merged with the reagent solution, water-insoluble $Pb(DDC)_2$ precipitates instantly in the mixing coil and is then adsorbed on the hydrophobic surface of the ODS in the packed reactor which is nested in the valve. As long as the packed reactor (PR) is in the pre-concentrate (upper) position this process continues, provided that the retention capacity of the solid phase is not exceeded. When the valve is turned to the elute position, the relatively non-polar methanol frontally and instantly elutes the lead chelate completely in a very narrow zone, which is carried into the nebuliser of an atomic absorption spectrometer. Other chelating agents such as dithizone and 8-hydroxyquinoline have been used for the pre-concentration of metals by FI and these model systems confirm that solvent extraction of metal chelates can be automated and performed on a micro-scale by sorbent extraction. Hence, highly selective solvent extraction procedures, originally performed manually in a separating funnel and more recently in FI systems,[4,8,24] can now be performed more efficiently without the need to use toxic organic solvents and often troublesome phase separators, these sorbent extractions taking advantage of a wide variety of sophisticated solvent extraction chemistries.[51–53] Additional experiments[50] with the azo dyes 1-(2-pyridylazo)-2-naphthol (PAN) and 4-(2-pyridylazo)resorcinol (PAR), which are used for the spectrophotometric determination of metals, have indicated that the range of reagents suitable for FI pre-concentration may be fairly large, possibly encompassing the majority of colorimetric indicators and reagents known today.[53,54]

The determination of phosphate using spectrophotometric detection has been investigated as a model system for the pre-concentration of anions.[55] Formation of phosphomolybdate and its subsequent reduction to molybdenum blue by

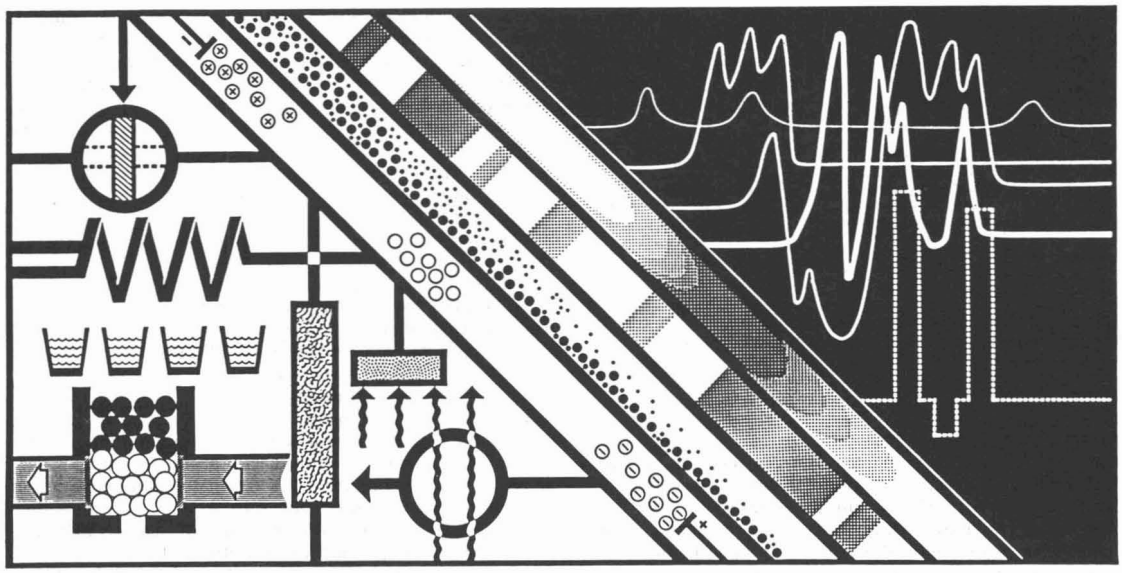

Fig. 11. Injection analysis, its components, concepts, inputs and readouts

ascorbic acid was performed in a flow system, Fig. 10(*b*). The sample was an aqueous solution of sodium orthophosphate, the reagent was an acidified solution of ammonium heptamolybdate and the eluent was a 2% solution of ascorbic acid in aqueous methanol. During the pre-concentration cycle the phosphomolybdate was adsorbed on the ODS, while the reduction and subsequent spectrophotometric detection of the eluted molybdenum blue was accomplished after the column had been switched into the eluent stream. Up to an 80-fold increase in sensitivity was obtained using a 2-min pre-concentration cycle, compared with the "classical" FIA procedure.

It follows from the foregoing that, in contrast to the operation of pre-column cartridges, where the surface of the adsorbent has a non-selective functionality permanently bonded to the solid surface, in FIA selective surface chemistry may be renewed for each pre-concentration cyclus. This can be achieved in several ways, either by pumping the selective reagent, as exemplified above, or by injecting the reagent into a merging zone arrangement similar to that shown in the flow scheme in Fig. 4.

Therefore, the wealth of materials developed for chromatography for the retention of a wide range of compounds, either non-polar (the sorbent being C_{18}), moderately polar (C_8), non-polar (phenyl) or ionisable (cation or anion exchangers), can also be exploited in FI together with other non-selective matrices such as sepharose gels. The non-selective retention properties of these stationary phases make them useful as a non-selective group of sorbents; however, the selectivity of pre-concentration can be achieved by the strategic choice of a suitable reagent. Whereas chelating reagents are suitable for the pre-concentration of metal ions, and ion associate or precipitate formation is suitable for the pre-concentration of anions, biospecific ligands covalently bound to a chromatographic bed material are useful for the pre-concentration of nucleic acids, plasma proteins and cells, as described in papers dealing with affinity chromatography.

Solid reagents and catalysts have been widely used in heterogeneous FI analysers. We recognise, however, that the purpose of packed reactors for these applications is not to separate analytes, but to provide reactive surfaces or a catalyst to interact with analytes in the flowing stream. Here again we observe an analogy with the use of solid-phase reactors and immobilised enzymes in post-column derivatisation[26,27] and FIA.[4,5,8]

Once again we arrive at the conclusion that chromatography and FIA are not identical, but related, not competitive but complementary. In chromatography the main source of selectivity is the resolution obtained by the chromatographic process; in FI it is the selectivity of the solution chemistry (or solution - surface chemistry) augmented by the selectivity of the detection. Although FIA is faster, chromatography is multi-component. However, the most important difference between these two related methods is in the way the solution - surface interactions are selected and controlled: in chromatography the functionality of the stationary phase must be permanent not only within a single chromatographic run but also during many subsequent runs. In FIA the functional groups may be renewed for each separate run and may even change during a single operational cycle, thus allowing a wider choice of reagents which may be less stable over a period of time and do not need to be covalently bound to the stationary phase.

Conclusion

It follows from the foregoing that the differences between liquid chromatography and FIA should not be viewed simply as differences in their histories, or in definitions, terminology, methodology or hardware. Although legitimate, these detract our attention from their fundamental underlying physicochemical similarities and their principal differences. The physical similarity, the injection of a sample zone into a carrier stream of fluid, with subsequent continuous detection, makes FIA, liquid chromatography, capillary electrophoresis and field-flow fractionation sub-divisions of injection techniques (Fig. 11). Liquid chromatographic techniques exploit situations in which the distribution coefficients (capacity factors) lie in the range 1–5, whereas FIA deals with non-retained or completely retained species. Hence, when the distribution coefficient is <0.01, chemical derivatisation in a liquid phase or quantitative elution of analytes from a solid support is performed, whereas when the distribution coefficient is >100, FIA is used for the pre-concentration of diluted analytes, or

exploits solution - surface chemistries with reagents that have been immobilised on surfaces strategically placed in a flow-through channel or a flow-through detector. Capillary electrophoresis exploits an electric field to separate charged species, whereas field-flow fractionation separates by means of transverse fields of power; however, they all depend on the injection of a sample into a flowing stream.

Having discussed the relationship between FIA and chromatographic techniques, let us investigate the scope of the injection-based techniques. To some it may appear heresy to define these techniques as sub-divisions of a general method. However, it is unarguable that the injection of A into a stream of B is the key operation, as it provides a highly reproducible original input for subsequent physical and/or chemical modulation. In FIA, this well defined initial impulse of analyte A injected into the reagent stream of B allows the subsequent gathering of data from a concentration gradient formed by physical dispersion and the ensuing chemical reactions, which take place during a pre-programmed passage of the analytes through a microflow conduit. In chromatography, the injection of analyte A into a carrier stream of eluent B is followed by a series of chemical and physical interactions on the column material, which change the shape of the original impulse and resolve it into a series of responses by selectively modulating the migration of the individual sample components through the column, *i.e.*, chromatography and FIA are impulse-response techniques, which upgrade measurements on all solution chemistries to the standards of modern instrumentation, where beams are chopped, lasers are pulsed and electrical signals are modulated in a wide range of frequencies and amplitudes.[4] When the consequences of this concept are recognised, as has already happened in the area of process control and discussed in a recent paper by Gisin and Thommen,[56] novel approaches to injection techniques will be identified and will become an integral part of chemical sensors and analytical instruments of the future.

Note added in proof. The International Symposium on Detection in Liquid Chromatography and Flow Injection Analysis (HPLC/FIA), held after submission of this paper, provided excellent examples of some of the concepts discussed here. A paper entitled "Integrated Photochemical Reaction/Electrochemical Detection in Flow Injection Analysis Systems: Kinetic Determination of Oxalate"[57] illustrates well the concept shown in Fig. 8. A paper entitled "Two-fold Use of an FIA Manifold as a Screening System and Post-column Reactor - Detector in HPLC"[58] is an excellent example of combining the techniques of FIA and HPLC for more efficient analyses, due to the more rapid screening capabilities of FIA. It is apparent from this symposium that the practitioners of chromatography and FIA are recognising the synergism and complementary aspects of the two techniques.

The authors thank Alison MacDonald for a critical review of this work, Ed Johnson, Milos Novotny and Kip Powell for critical comments, David Whitman for assistance in the preparation of the figures and the Pernovo Scientific Foundation for partial financial support.

References

1. Szabadvary, F., "History of Analytical Chemistry," Pergamon Press, Oxford, 1966.
2. Skeggs, L. T., *Anal. Chem.*, 1966, **38**, 107.
3. Růžička, J., and Hansen, E. H., *Anal. Chim. Acta*, 1975, **78**, 145.
4. Růžička, J., and Hansen, E. H., "Flow Injection Analysis," Second Edition, Wiley, New York, 1988.
5. Růžička, J., and Hansen, E. H., *Anal. Chim. Acta*, 1988, **214**, 1.
6. "Winter Conference on Flow Injection Analysis," Orlando, FL, January 5–7, 1989.
7. "International Symposium on Detection in Liquid Chromatography and Flow Injection Analysis (HPLC/FIA)," Cordoba, Spain, September 20–22, 1989.
8. Valcarcel, M., and Luque de Castro, M. D., "Flow Injection Analysis. Principles and Applications," Ellis Horwood, Chichester, 1987.
9. Whitman, D. A., *PhD Thesis*, University of Washington, 1989.
10. Růžička, J., and Flossdorf, J., *Anal. Chim. Acta*, 1989, **218**, 291.
11. Canete, F., Rios, A., Luque de Castro, M. D., and Valcarcel, M., *Anal. Chem.*, 1988, **60**, 2354.
12. Hungerford, J. M., and Christian, G. D., *Anal. Chim. Acta*, 1987, **200**, 1.
13. Giddings, J. C., "Dynamics of Chromatography," Marcel Dekker, New York, 1965.
14. Meyer, V. R., "Practical High-performance Liquid Chromatography," Wiley, New York, 1988.
15. Růžička, J., and Hansen, E. H., *Anal. Chim. Acta*, 1985, **173**, 3.
16. Valcarcel, M., and Gallego, M., *Trends Anal. Chem.*, 1989, **8**, 34.
17. Rabinovich, P., and Růžička, J., unpublished work.
18. Sernetz, M., and Willems, H., *Trends Anal. Chem.*, 1988, **7**, 370.
19. Clark, G. D., *PhD Thesis*, University of Washington, 1989.
20. Margoshes, M., *Anal. Chem.*, 1977, **49**, 17.
21. Snyder, L. R., *Anal. Chim. Acta*, 1980, **114**, 3.
22. Garn, M. B., Gisin, M., Gross, P., Schmidt, W., and Thommen, C., *Anal. Chim. Acta*, 1988, **207**, 225.
23. Bergamin, H. Fº., Reis, B. F., Jacintho, A. O., and Zagatto, E. A. G., *Anal. Chim. Acta*, 1980, **117**, 81.
24. Karlberg, B., and Thelander, S., *Anal. Chim. Acta*, 1978, **98**, 1.
25. Baadenhuisen, H., and Seuren-Jacobs, H. E. H., *Clin. Chem.*, 1979, **25**, 443.
26. Frei, R. W., and Zech, K., *Editors*, "Selective Sample Handling and Detection in High-performance Liquid Chromatography," Elsevier, Amsterdam, 1988.
27. Krull, I. S., "Reaction Detection in Liquid Chromatography," Marcel Dekker, New York, 1986.
28. Bachman, W. J., and Stewart, J. T., *LC-GC*, 1989, (7), 38.
29. Imai, K., and Toyoka, T., *in* Frei, R. W., and Zech, K., *Editors*, "Selective Sample Handling and Detection in High-performance Liquid Chromatography," Elsevier, Amsterdam, 1988, Chapter 4.
30. Nondek, L., and Frei, R. W., *in* Frei, R. W., and Zech, K., *Editors*, "Selective Sample Handling and Detection in High-performance Liquid Chromatography," Elsevier, Amsterdam, 1988, Chapter 7.
31. Miles, C. J., and Moye, H. A., *Chromatographia*, 1987, **24**, 628.
32. Brinkman, U. A. Th., Welling, P. L. M., de Vries, G., Scholten, A. H. T. M., and Frei, R. W., *J. Chromatogr.*, 1981, **217**, 463.
33. Stewart, J. T., and Bachman, W. J., *Trends Anal. Chem.*, 1988, **7**, 106.
34. Verbeke, R., and Vanhee, P., *J. Chromatogr.*, 1983, **265**, 239.
35. Lefevere, M. F., Frei, R. W., Scholten, A. H. M. T., and Brinkman, U. A. Th., *Chromatographia*, 1982, **15**, 459.
36. Gandelman, M. S., and Birks, J. W., *Anal. Chem.*, 1982, **54**, 2131.
37. Miles, C. J., and Moye, H. A., *Anal. Chem.*, 1988, **60**, 220.
38. Selavka, C. M., and Krull, I. M., *Anal. Chem.*, 1988, **60**, 250.
39. Hirai, Y., Yoza, N., and Ohashi, S., *Anal. Chim. Acta*, 1980, **115**, 269.
40. Leach, R. A., and Harris, J. M., *Anal. Chem.*, 1987, **59**, 2699 and 2704.
41. Olesik, S. V., French, S. B., and Novotny, M., *Anal. Chem.*, 1986, **58**, 2258.
42. Kunnecke, W., Kalisz, H. M., and Schmid, R., *Anal. Lett.*, in the press.
43. Rose, D. J., and Jorgenson, J. W., *J. Chromatogr.*, 1988, **447**, 117.
44. Pentoney, S. L., Jr., Huang, X., Burgi, D. S., and Zare, R. N., *Anal. Chem.*, 1988, **60**, 2625.
45. Roth, M., Steger, J. L., and Novotny, M. V., *J. Phys. Chem.*, 1987, **91**, 1645.
46. Olesik, S. V., Steger, J. L., Kiba, N., Roth, M., and Novotny, M., *J. Chromatogr.*, 1987, **392**, 165.

47. Nielen, M. W. F., Frei, R. W., and Brinkman, A. U. Th., *in* Frei, R. W., and Zech, K., *Editors*, "Selective Sample Handling and Detection in High-performance Liquid Chromatography," Elsevier, Amsterdam, 1988, Chapter 1.
48. Huber, R., and Zech, K., *in* Frei, R. W., and Zech, K., *Editors*, "Selective Sample Handling and Detection in High-performance Liquid Chromatography," Elsevier, Amsterdam, 1988, Chapter 2.
49. Walters, R. R., *Anal. Chem.*, 1983, **55**, 1395.
50. Růžička, J., and Arndal, A., *Anal. Chim. Acta*, 1989, **216**, 243.
51. Morrison, G. H., and Freiser, H., "Solvent Extraction in Analytical Chemistry," Wiley, New York, 1957.
52. Stary, J., "The Solvent Extraction of Metal Chelates," Pergamon Press, Oxford, 1964.
53. Cheng, K. L., Ueno, K., and Imamura, T., "Handbook of Organic Analytical Reagents," CRC Press, Boca Raton, FL, 1982.
54. Bishop, E., "Indicators," Pergamon Press, Oxford, 1972.
55. Lacey, N., paper presented at the "Winter Conference on Flow Injection Analysis," Orlando, FL, January 5–7, 1989.
56. Gisin, M., and Thommen, C., *Trends Anal. Chem.*, 1989, **8**, 62.
57. Leon, L. E., Rios, A., Luque de Castro, M. D., and Valcarcel, M., "International Symposium on Detection in Liquid Chromatography and Flow Injection Analysis (HPLC/FIA)," Cordoba, Spain, September 20–22, 1989, Poster PI 35.
58. Valcarcel, M., Luque de Castro, M. D., Lizaro, F., and Membiela, A., "International Symposium on Detection in Liquid Chromatography and Flow Injection Analysis (HPLC/FIA)," Cordoba, Spain, September 20–22, 1989, Poster PII 23.

Paper 9/02372K
Received June 6th, 1989

Evolutions in Chemometrics*

Plenary Lecture

Gerrit Kateman
Department of Analytical Chemistry, Faculty of Sciences, Catholic University of Nijmegen, Nijmegen, The Netherlands

Chemometrics started as part of analytical chemistry with the emphasis on statistics and pattern recognition. Although data processing still occupies a large part of chemometrics, new trends are emerging. The desire to lay a firm scientific base in analytical chemistry was a challenge to chemometrics. Information theory, state estimation and new ways of calibration are some examples of techniques that have emerged in the last 10 years. The desire to formalise and record analytical knowledge spurred the development of expert systems. Although these systems are available commercially many problems arise, for example, how to represent and introduce the vast amount of analytical knowledge. Development of learning systems will be required.

Keywords: *Chemometrics; expert system; learning system; genetic algorithm; neural network*

The birth date of chemometrics is not exactly known, only its name-giving day. In 1971, Wold[1] coined the word chemometrics and this summer the 18th anniversary of the name was celebrated in Umeå, Sweden. However, long before that date, techniques were available that today are considered to be chemometrical. In 1908, Gosset,[2] an amateur of statistics and a professional chemist, published a paper on the error of the mean, under his pen name, Student; the parameter known since as Student's t was introduced. It allows the quantitative comparison of the results of two items, such as methods of analysis or samples. Another statistical parameter in use was the standard deviation (SD). This, combined with Fisher's F-test, indicates the possibility that the scatter in the results of a particular experiment is better or worse than the scatter found in a very reproducible standard series of analytical results. Although these quality parameters were known, they were not in common use among analytical chemists. One major contribution of the practical use of statistics in analytical chemistry was the introduction of the control chart, familiarised by Shewhart in 1931.[3] Such a chart allows the continuous supervision of accuracy and precision in an analytical laboratory. It allows corrective measures to be taken when a control line is crossed. After 1940 a host of publications appeared on the application of statistical techniques in analytical chemistry. Most of these were directed to the application of statistics in the validation of analytical results. In analytical chemistry the application of statistical techniques was restricted to the comparison of analytical procedures, without establishing quality parameters for analytical methods other than accuracy (SD and variance).

In 1963, van der Grinten[4–7] published some simplified equations that were derived from Wiener's rules on control theory. This allowed quantitative evaluation of the value of measurements with respect to the object that was measured. Some of the results of the application of this theory on analytical data were published by Leemans[8] in 1971. From this work it became clear that, in addition to accuracy and reproducibility, the speed of analysis and the frequency of sampling, and their merit in the application of the results, could be quantified and optimised.

These developments were not alone in generating new views on analytical chemistry. In the early seventies a discussion of the necessity of analytical chemistry arose, mainly in the American analytical literature that culminated in the rhetorical question, "Analytical Chemistry, a fading discipline."[9] The discussion was pursued in Europe and resulted in a series of definitions of the analytical discipline.

One body of opinion[10] sees analytical chemistry as a "black box," a system with known input and output and rules interconnecting these. From this point of view, operations research, the science of the study of this type of system, could be applied to analytical chemistry. Massart and Kaufman[11] presented the first survey of research using this new approach.

Another phenomenon, parallel to the use of control theoretical concepts, and operations research, was the introduction in analytical chemistry of integrated systems of statistics and correlation analysis, known as pattern recognition.[12] This technique allows, for instance, the selection of those analytical results that are indispensable and sufficient for describing a certain phenomenon. Further, it is possible to classify analytical results in classes known beforehand or in classes that are given by the system itself and to select an analytical method that, given the properties of the problem under investigation, will give an optimum solution to the problem.

This was the situation when, in 1974, the International Chemometrics Society was founded. This body was intended to provide a meeting place for people engaged in chemometrics. The following definition of chemometrics was formulated by the Society[13] and forwarded to IUPAC: "Chemometrics is the chemical discipline that uses mathematical and statistical methods (a) to design or select optimal measurement procedures and experiments and (b) to provide maximum chemical information by analysing chemical data. In the field of analytical chemistry, chemometrics is the chemical discipline that uses mathematical and statistical methods to obtain in an optimal way relevant information about material systems."

It will become clear in this paper that the definition needs rephrasing, as developments in analytical chemistry demand more than simply mathematics or statistics.

Analytical chemists try to obtain information from material systems or objects by chemical, physical or physicochemical techniques. These techniques are often very sophisticated, very precise and sensitive and, as a rule, expensive. The input of analytical chemistry consists of samples, representative parts of the objects under investigation. The samples are prepared so as to convert them to a suitable form for measurements, and the data obtained are processed by sophisticated techniques. This output is intended for object or sample description, or for process monitoring or control, at the behest of the principal, owner, controller or manager of

* Presented at SAC 89, the 8th SAC International Conference on Analytical Chemistry, Cambridge, UK, 30 July–5 August, 1989.

the object or process. In this field, chemometrics covers the domain of the principal and his purposes, the object and its peculiarities and analytical chemistry with its chemical pre-processing and physical measurements. As the purpose of analytical chemistry is the collection of information, a principal concern is how to obtain more information, at less cost, with more confidence, and within the boundaries of what is physically possible. As information is the difference between knowledge (entropy) before and after measurements, an important influencing factor is the availability of prior knowledge, which can be exploited in several ways. Even more important is the notion that only relevant information is worth its price: "information is the difference that makes a difference."

In the same way as the field of medicine, chemical analysis is largely an art. Therefore, there are no scientific foundations to carry the entire analytical process from problem to solution. Most of the techniques are scientifically or technically sound and well founded, but it is not possible to predict theoretically the method that will give the ultimate answer to a specific problem. This absence of theoretical rules can be compensated by experience and hence chemical analysis depends on highly trained and experienced workers. They know the peculiarities of the sample and the instrument, they seek in the literature the most promising methods, and a choice is made to the best of their knowledge. If the method shows unexpected deviations during testing, they change conditions, reagents and instruments and obtain in most instances a result that can be trusted within known boundaries. The process of measuring and varying analytical performance parameters can be compared with the control of a technological process. In principle, the same procedures can be applied and many of the statistical and control theoretical procedures described elsewhere could be of use, following the tradition of analytical chemistry that every technique that is helpful should be used. However, an analytical laboratory is far more difficult to control than a chemical process, for various reasons. (1) Only a few performance parameters, *e.g.*, accuracy, precision and sensitivity, are known and fully understood. The measurement of these parameters is often time consuming and expensive and the number of measurements is often very low, hence "normal" statistics does not apply. (2) Most analytical chemical laboratories are relatively labour intensive, and human effort affects the quality of the work considerably. Quality defects caused by human error are very difficult to control and cannot be coped with completely by theory. (3) The results of analytical chemical measurements affect more than simply the institute or factory that the laboratory serves. For example, products are bought and sold all over the world, and water and air pollution is transported across boundaries of countries and continents. Therefore, the results of analytical laboratories should meet not only regional but also national and international standards.

These factors, in combination with the ease and low cost of changing an analytical procedure, are responsible for the astonishingly small number of exactly corresponding analytical procedures. Both comparison and control of incomparable procedures are difficult on a large scale.

In this abundance of problems, chemometrics attempts to develop tools that can be used to optimise the analytical task. The world in which we live can be divided into three parts for our purposes, *i.e.*, the real world, the instrumental world and the chemometrical world (Fig. 1). This picture should be extended to the organisation of the whole.

The real world poses problems that must be solved by analytical chemists. Therefore we do not need only instruments, but, in addition, a lot of thinking and organising. Chemometricians aim to solve the problems that are non-material. Hence chemometrics can be seen as a collection of tools capable of performing these tasks. Such tasks can be

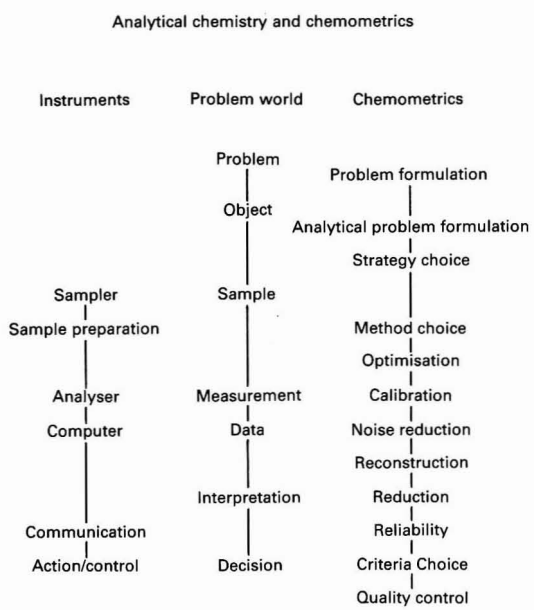

Fig. 1. Chemometrics and analytical chemistry

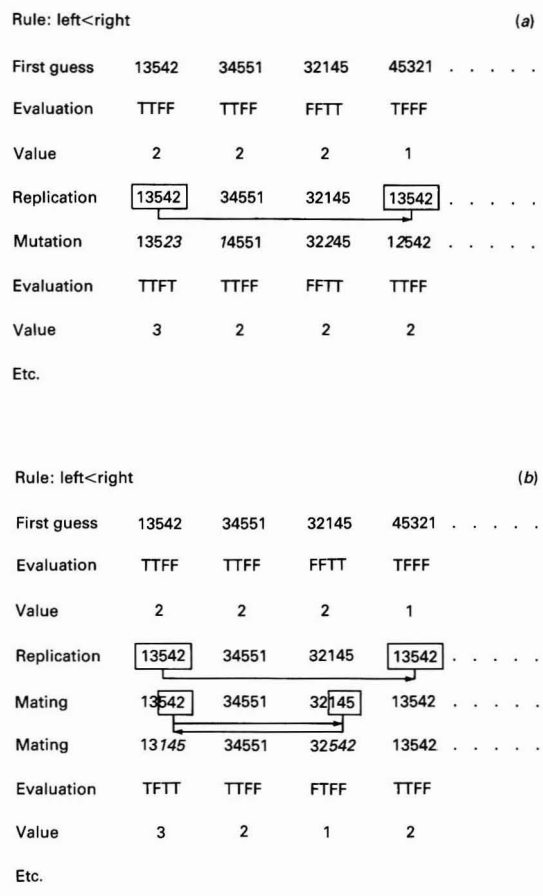

Fig. 2 (*a*) Model of a genetic algorithm with mutation; and (*b*) model of a genetic algorithm with mating or cross-over

divided into two groups. (a) Exploration: studying the area and doing tests, hoping to find something one needs; traversing a region for the purpose of discovery (of the environment in which the experiment is performed). (b) Exploitation: utilising for profit, getting the most out of data and information obtained from measurements.

In chemometrics, much research has been performed on the exploitation of data obtained by measurements. The tool used most is statistics, which allows the possibility of deciding whether the data are reliable, removing a substantial part of the noise and obtaining the most likely values from the data. Historically this has always been done by hardware, *e.g.*, resistance - capacitance filters, to diminish noise. Building better instruments has always been a challenge and the provision of calibration standards has been left to large and much valued institutes. One of the first applications of chemometrics was the use of round-robin tests; these were constructed by using a set of statistical methods as follows: experiment design; analysis of variance; and tests for normality. Later chemometrics focused on the exploitation of multi-dimensional data. However, one of the hidden goals of chemometrics is to lay a firm theoretical base for analytical chemistry, a goal that has not yet been accomplished. An example is the theoretical treatment of the difference between data and information and their interdependence.[14]

Both analytical chemistry and chemometrics show an evolutionary progress, not only in contrast to revolutionary progress but also in the biological sense. Many evolutionary

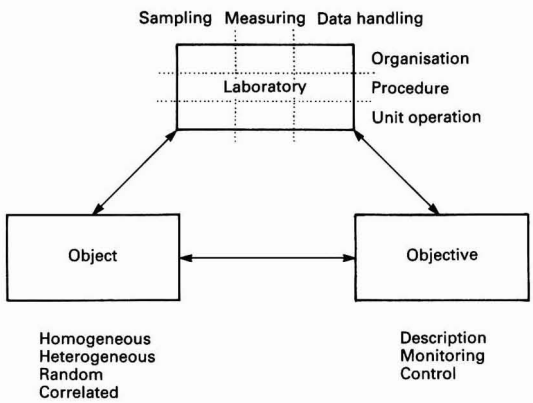

Fig. 3. Model of analytical chemistry

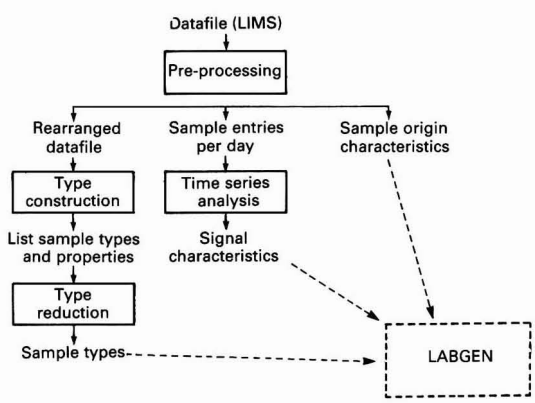

Fig. 4. Tasks of the laboratory simulation program LABGEN

models exist in the field of biology, of varying degrees of refinement, and dependent on molecular models and their use. Here one of the simpler models is used; one which is capable both of explaining development in chemometrics and posing a model for optimisation in chemometrics.[15] This model assumes a finite pool of individuals, each characterised by a string of genes, the pool being subject to random changes of two types. Mutation is the random replacement of one gene by another one. Mating or crossing over is characterised by the exchange of part of a gene string with the corresponding part of another individual. The pool is then evaluated: the individuals that show properties that differ least from a wanted property or individuals that yield most to pressure from the environment are duplicated at the expense of the most unfavourable.

This model is explained in Fig. 2. Each cycle of mutation/crossing over, evaluation and duplication is called a generation. Refinements are possible in the size of the pool, the possibility of expanding or shrinking the pool, the fraction of mutation/crossing over and the evaluation criterion. Applying this model to chemometrics we are faced with the first assumption, which has regard to the original pool. As discussed above, the basic techniques ("individuals" in our model) are statistics and data processing, characterised by names such as Fourier, Student, Shewhart, Wiener and Kalman. Mutation and mating of these techniques provided pattern recognition and data analysis with, for instance, principal component analysis, multi-component analysis and target transformation factor analysis. Automatic analysis and pattern recognition make use of, for example, experimental designs and Simplex optimisation. Noise reduction and calibration profit from estimations of state and parameter.[16–20] In these examples the mating mechanism seems to be the most prominent factor, mutation working only in minor parts. This is contrary to the situation in analytical chemistry, where small mutations often provide a slow but unmistakable progress.

The aforementioned techniques apply at two of the three levels of analytical chemistry, *i.e.*, unit operation and procedure (Fig. 3). At the organisational level, however, the theory is not yet mature. The combination of queueing theory and sampling theory provides us with the information yield of a laboratory organisation, but only for one server (technician or instrument).[21] For more complex organisations, simulation should be used, the techniques drawing on mathematics and statistics. However, although the handling of these simulation techniques becomes too difficult to be of practical use, new blood is introduced into the pool; artificial intelligence (AI) and the combination of these techniques made possible the use of simulation as an aid to management decisions.[22]

Artificial intelligence emerged from the need to handle symbolic knowledge, contrary to numeric knowledge, not only algorithmically but also heuristically. Further objectives for the development of the handling of knowledge are the possibilities of acquiring and digesting new knowledge continuously; this, would in fact be comparable to learning. From the potential to learn, follows the desire to generalise, *i.e.*, to be able to answer questions that are not available as answers in the knowledge base by "inventing" an answer from the incomplete knowledge available.

The merging of AI with simulation algorithms and statistics has helped in the construction of a system for laboratory management decision support, LABGEN[23,24] (Fig. 4). This involves an expert system asking its user many questions about the user's laboratory and its organisation. These questions cover items such as the technicians available, their skills, the instruments available and their mean time between failures. Moreover, many data are required about sample streams, distributions of arrival times and processing times, minimum and maximum batch sizes, due times, etc. These data can be obtained from a laboratory information management system

(LIMS). The system now builds its own simulation program and starts simulation runs. These simulations act as laboratory experiments on laboratory organisation. The effects of manpower, instrument quality, sample streams, priorities, etc., can be simulated and used to make decisions. In fact, this system merges many known techniques, and is the result of evolution over many years by mutation and mating. Of course, expert systems have other uses. Formalisation, recording and the incorporation of different techniques can be used as has been demonstrated, for example, in the ESPRIT* project on the evaluation of expert system shells for high-performance liquid chromatography (HPLC).[25] In this system the first step is a "first guess." Using all chemical and physical knowledge that is available, a proposal is made for an HPLC system that is able to perform the required task. (In the ESPRIT project this task is the purity check of a group of pharmaceutical compounds.) The next stages are to optimise the separation and the system, the latter by using, for example the well known relations between flow, plate number and time. Having acquired this knowledge, the performance of the proposed system is tested, a ruggedness test is applied and the performance data are produced. If the system falls short of the intended goal, the system optimisation is repeated, using the suggestions of the quality control module. Another feature is the logging of results in order to cope with the requirements of good laboratory practice.

During the development of these systems a number of problems emerged relating to the development of expert systems for analytical chemistry. Most of these would also be related to developments for other purposes, but some are specific as regards analytical chemistry. The representation of analytically important parameters can be difficult; whereas numeric values are fairly straightforward, symbolic values can cause problems. The description of an HPLC column, for instance, can take many forms, but to use an objective, repeatable description can be difficult. The incorporation of numeric calculations, such as those used in the system optimisation, can also be difficult. Most expert systems do not have the facilities to incorporate, *e.g.*, a spreadsheet in the system, or, for calculations, require a change from the expert system language, say LISP, to another language, *e.g.*, PASCAL or FORTRAN. A major problem, not exclusive to analytical chemistry, is the acquisition of knowledge. To obtain the knowledge of the expert in a structured, logical way is not easy. The expert can be reluctant to help perhaps because he knows that his knowledge is not logical or is not available in a structured format, or he does not want to share his knowledge with a computer. One scientific advantage, which is not very exciting for the knowledge engineer, is the situation in which the expert discovers the logics in his knowledge and, therefore, no longer needs an expert system as his problems can now be solved in an adequate manner. The last, but by no means the least, problem is the need to update the knowledge in the computer. Ideally, this new knowledge should be tested to see whether generalisations are possible to allow the solution of more problems. In fact, the objective is that the system should be able to learn, acquire and digest new knowledge.

Some of these problems could be overcome by the automation of knowledge acquisition. Several such projects

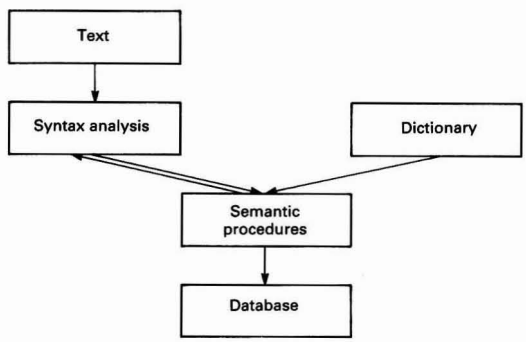

Fig. 5. Analysis of analytical chemical texts for automatic database construction

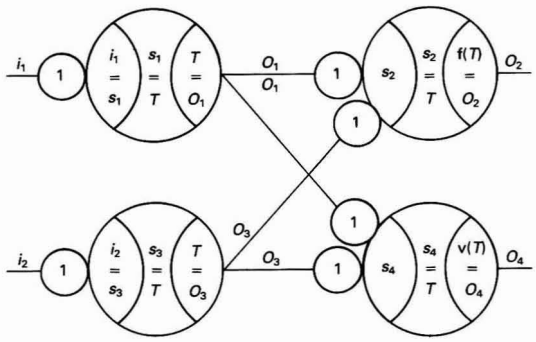

Fig. 6. Neural network. Input signals, i_k; input strength s_k (weight factor 1); state T [$T = f(s_k, T)$]; and output signal O_k [$O_k = f(T)$]

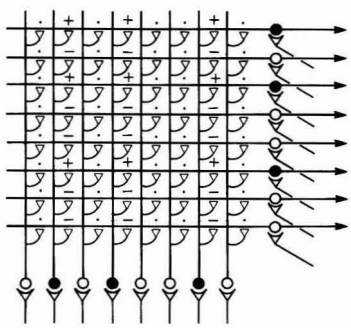

Fig. 7. Neural network: matrix connection of input and output signals. Bottom: incoming signals, ○, weight 0; ●, weight 1. Weight 0 leaves neurons neutral (·). Weight 1 makes neurons active, + if output should be positive (●), − if output should be negative (○). The product of the rows determines whether the output (right-hand side) will be positive or negative

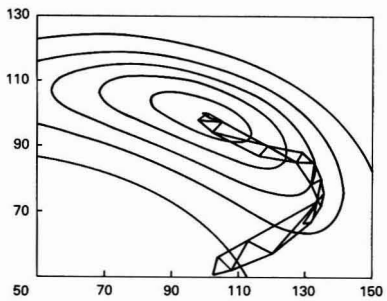

Fig. 8. Finding an optimum value by simplex optimisation

* A European Community sponsored co-operation between Philips Scientific, Cambridge, UK, Philips Forschungslabor, Hamburg, FRG, Philips Research, Eindhoven, The Netherlands, Organon International, Oss, The Netherlands, the Free University of Brussels, Belgium, and the Catholic University of Nijmegen, The Netherlands.

are underway and some have been completed, for example, the expert system builder.[26]

The front-end analyser (FEA)[27] from the described system for laboratory optimisation can be considered as a specimen of an automatic knowledge collection device, though its application is restricted to the expert system described here.

Another approach, with its source in linguistics, is that taken by Postma.[28] An analytical chemistry text, obtained from the literature or textbooks can be analysed semantically and syntactically. Hence it is possible to extract relevant information from the text and store it in a database, preferably in database frames, combinations of data, attributes and values (Fig. 5).

An entirely different approach emerged when Parallel Distributed Systems, also known as Neural Networks, became available. The original ideas came from Hebb[29] who, in 1949, proposed a model for the working of the human brain. The model was expanded by Rosenblatt[30] and, after two decades of little activity, has gained new attention. The result has been that it is now used in many scientific disciplines. Although the

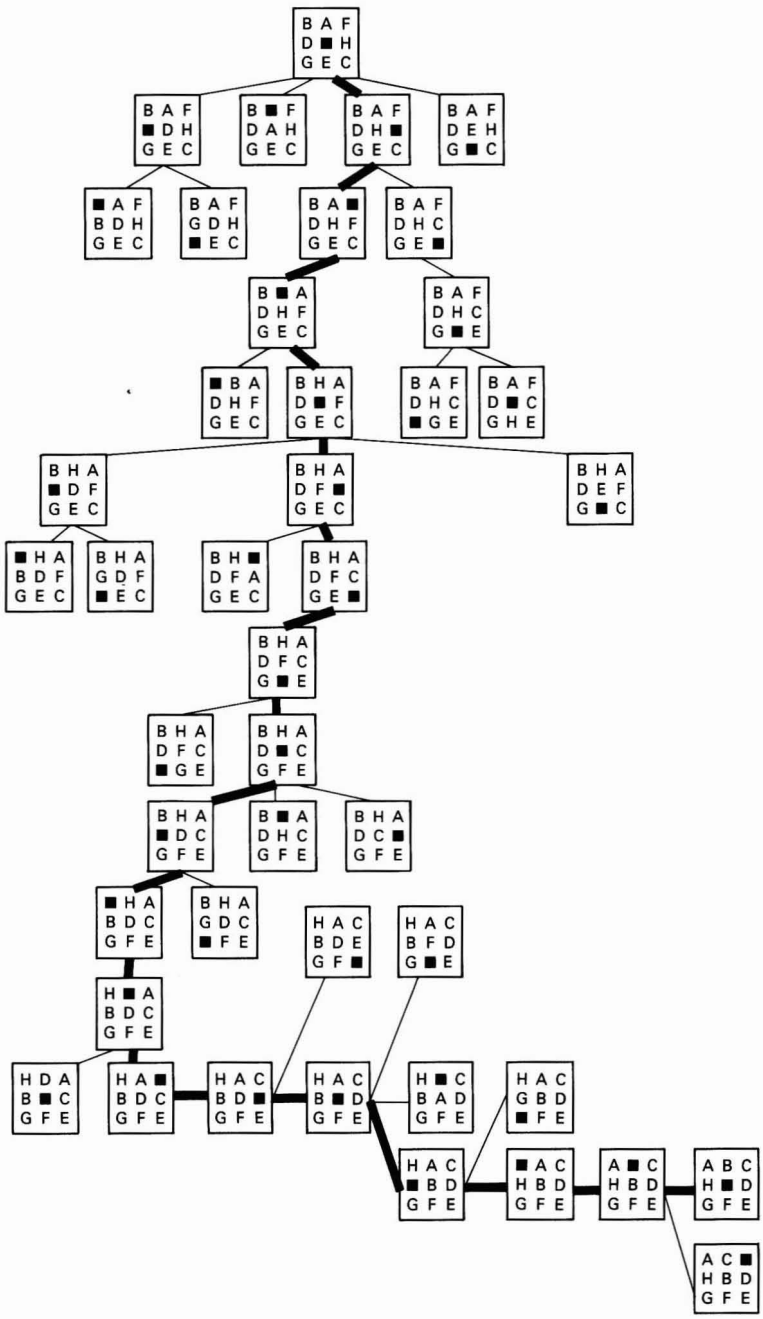

Fig. 9. Finding an optimum configuration by a genetic algorithm

model attracts much attention from psychologists, pedagogues and brain-scientists, only its applications to the field of analytical chemistry are discussed here. The basic idea is that an input signal applied to a "neural node" transforms the state of that node. The input signal can be given a weight and more input signals can be applied to the node. The node can give an output signal, which can also be altered by a weight function, the output signal being the input signal for another node or nodes (Fig. 6). Hence a network can be built that in its simplest form can be represented by the matrix shown in Fig. 7. When the input nodes are provided with a (coded) signal and the output nodes are simultaneously given the required output, simple algorithms set the value of the intermediate nodes in the matrix. After applying a number of input and output patterns, the intermediate nodes obtain a more or less stable equilibrium value. When these values are fixed, the application of an input signal that has been "learned" produces the appropriate output signal.

The advantages of this approach are obvious: no model of the relation between input and output signal is required. The system is purely heuristic. When the system has been trained, a near immediate answer can be obtained. Moreover, the system has the ability to generalise, *i.e.*, an input signal that has not been used in the training process can produce an output signal that might be a fairly good approximation of the right answer. The drawbacks are also obvious. Large matrices are required for the training of complicated input and output signals; as there is no theoretical relation between input and output, generalisation might be dangerous.

However, the nature of the system allows the processing of all operations in parallel, in arrays of fairly simple processors. Hence parallel computers, which are currently under development, can do the job quite easily. To date, applications in analytical chemistry are scarce. Frankel *et al.*[31] have described a system for the automatic classification of algae. Algal cells are presented consecutively to one or more laser beams, operating on different wavelengths. The absorbance and fluorescence are measured and used as input signals for a neural network. The class of the alga is used as the output. After training with 15000 examples, the system was able to distinguish new samples with >99% certainty.

Bos *et al.*[32] described a system that allows the use of the output of a set of ion-selective electrodes in a mixture of components as the input of a neural network. The net is trained to produce the real concentration in the solution, a test that can be of great value as ion-selective electrodes are far from selective. Parczewski and Kateman[33] developed systems for the choice of the appropriate analytical method for samples of different compositions and are at present developing a system for the elucidation of infrared spectra.

The results of evolution in chemometrics are to be seen in the development of so-called evolutionary or genetic algorithms. Clearly, the system shown in Fig. 2 could be used as an optimisation system.

Optimisation systems are well known in analytical chemistry, *e.g.*, the simplex system introduced by Deming and Morgan.[34] In such a system, the optimum in a multi-dimensional response-space will be reached by hill climbing. However, in a multi-mode system the obtained optimum depends on the starting point of the optimisation run. Although preliminary experiments, *e.g.*, analysing a lattice, can give clues to the starting point of the hill-climbing algorithms, the danger still exists that the real optimum has not been reached. Automatic operation is applicable only in well known response surfaces (Fig. 8).

A genetic algorithm, however, does not follow the continuous slopes of the hills, but "jumps" to the places dictated by the mutations or crossing over. By the nature of the system, in the region where the individual measurements are expected, the results gradually become better. This allows the system to find the real optimum (Fig. 9).

Holland *et al.*[35] changed the algorithm in such a way that it became possible to optimise both the data and the rules. Hence it is possible to have a self-optimising system that uses not only numerical data but also symbolic information, both in data and rules.

As the development of the optimum does not depend on continuous slopes but can jump into unknown regions, "discoveries" are possible when the system under investigation has not previously been mapped sufficiently. However, with our scientific methods of investigation, based mainly on continuous developments, discoveries can be expected.[36]

The following application to analytical chemistry has been developed by Lucasius and Kateman.[37] The elucidation of two-dimensional nuclear magnetic resonance (NMR) spectra of deoxyribonucleic acid (DNA) hairpins is a tedious task and although expert systems can aid in performing that task, they tried another approach. In a restricted area of the DNA string, hairpins can be simulated by making strings described by bonding distances, bonding angles and torsion angles. The simulated hairpin is used for the calculation of its two-dimensional NMR spectrum. The root mean square (RMS) difference between the calculated spectrum and the real measured system is used as the optimisation criterion in a genetic algorithm. The simulated hairpins are subjected to evaluation by mutation and crossing over of torsion angles; hence a slow but distinct diminshing of the RMS distance can be obtained. In this instance, as more solutions that produce the same RMS distance (the so-called degeneration) are possible slight modifications in the algorithm are required to allow the increased number of solutions to emerge. Although this system can automatically find optimum probable configurations, a simple graphical representation of the proposed structures allows the spectroscopist to delete proposed structures that are impossible due, for example, to steric hindrance, or are known to be highly improbable from experience. However, coupling to a neural network could teach the system to avoid improbable structures.

The field of chemometrics is still developing, albeit slowly and steadily rather than in large strides, by exploiting new areas that are introduced in a manner that can be called evolutionary, resembling mutation and crossing over. Optimisation, as in the evolutionary systems used in the computer, is likely, and even "discoveries" of unexpected new areas of use in analytical chemistry, are possible.

References

1. Kowalski, B., Brown, S., and Vandeginste, B., *J. Chemometr.*, 1987, **1**, 1.
2. Gosset, W. S., *Biometrika*, 1908, **6**, 1.
3. Shewhart, W. A., "Economic Control of the Quality of Manufactured Product," Van Nostrand, New York, 1931.
4. van der Grinten, P. M. E. M., *Control Eng.*, October 1963, 87.
5. van der Grinten, P. M. E. M., *Control Eng.*, December 1963, 51.
6. van der Grinten, P. M. E. M., *ISA J.*, December 1965, 48.
7. van der Grinten, P. M. E. M., *ISA J.*, January 1966, 58.
8. Leemans, F. A., *Anal. Chem.*, 1971, **43**, 36A.
9. Findeis, A. F., Wilson, M. K., and Meinke, W. W., *Anal. Chem.*, 1970, **42**, 26A.
10. Gottschalk, G., and Marr, I. L., *Talanta*, 1973, **20**, 811.
11. Massart, D. L., and Kaufman, L., *Anal. Chem.*, 1975, **47**, 1344A.
12. Jurs, P. C., Kowalski, B. R., Isenhour, T. L., and Reilley, C. N., *Anal. Chem.*, 1969, **41**, 690.
13. Kowalski, B. R., *Chem. Ind. (London)*, 1978, **22**, 882.
14. Eckschlager, K., and Stepanek, V., "Analytical Measurement and Information," Research Studies Press, Letchworth, England, 1985.
15. Holland, J. H., "Adaptation in Natural and Artificial Systems," University of Michigan Press, Ann Arbor, MI, 1975.
16. Thijssen, P. C., Wolfram, S. M., Smit, H. C., and Kateman, G., *Anal. Chim. Acta*, 1984, **156**, 87.

17. Thijssen, P. C., Smit, H. C., and Kateman, G., *Anal. Chim. Acta*, 1984, **162**, 253.
18. Thijssen, P. C., Smit, H. C., and Kateman, G., *Anal. Chim. Acta*, 1985, **173**, 265.
19. Thijssen, P. C., Prop, L. T. M., Kateman, G., and Smit, H. C., *Anal. Chim. Acta*, 1985, **174**, 27.
20. Brown, S. D., *Anal. Chim. Acta*, 1986, **181**, 1.
21. Janse, T. A. H. M., and Kateman, G., *Anal. Chim. Acta*, 1983, **150**, 219.
22. Klaessens, J., Saris, T., Vandeginste, B. G. M., and Kateman, G., *J. Chemometr.*, 1988, **2**, 49.
23. Klaessen, J., van Beijsterveldt, L., Saris, T., Vandeginste, B., and Kateman, G., *Anal. Chim. Acta*, 1989, **222**, 1.
24. Klaessens, J., Sanders, J., Vandeginste, B., and Kateman, G., *Anal. Chim. Acta*, 1989, **222**, 19.
25. Goulder, D., Blaffert, T., Blokland, A., Buydens, L., Chabra, A., Cleland, A., Dunand, N., Hindriks, H., Kateman, G., van Leeuwen, H., Massart, D., Mulholland, M., Musch, G., Naish, P., Peeters, A., Postma, G., Schoenmakers, P., de Smet, M., Vandeginste, B., and Vink, J., *Chromatographia*, 1988, **26**, 237.
26. Technical note ESB-96, Plessey, Christchurch, 1989.
27. Klaessens, J., van Schalkwijk, J., Cox, P., Bezemer, R., Vandeginste, B., and Kateman, G., *J. Chemometr.*, 1988, **3**, 81.
28. Postma, G., unpublished results.
29. Hebb, D. O., "The Organization of Behavior," Wiley, New York, 1949.
30. Rosenblatt, F., "Mechanisation of Thought Processes: Proceedings of a Symposium held at the National Physical Laboratory, November 1958," Volume 1, HM Stationery Office, London, pp. 421–456.
31. Frankel, D. S., Olson, R. J., Frankel, S. L., and Chisholm, S. W., *Cytometry*, November 1988, p. 1.
32. Bos, M., Bos, A., and van der Linden, W. E., *Anal. Chim. Acta*, in the press.
33. Parczewski, A., and Kateman, G., "Proceedings of the 5th International School on Expert Systems Technology," Rzeszow, 1989.
34. Deming, S. N., and Morgan, S. L., *Anal. Chem.*, 1973, **45**, 278A.
35. Holland, J. H., Holyoak, K. J., Nisbett, R. E., and Thagard, P. R., "Induction: Processes of Inference, Learning, and Discovery," MIT Press, Boston, MA, 1986.
36. Goldberg, D. E., "Genetic Algorithms in Search, Optimization and Machine Learning," Addison Wesley, London, 1989.
37. Lucasius, C. B., and Kateman, G., *in* Schaffer, J. D., *Editor*, "Proceedings of the Third International Conference of Genetic Algorithms," Morgan Kaufmann, San Mateo, CA, 1989, p. 170.

Paper 9/03356D
Received August 7th, 1989

Solution Chemiluminescence—Some Recent Analytical Developments*

Plenary Lecture

Alan Townshend
School of Chemistry, University of Hull, Hull HU6 7RX, UK

Some recent developments in analytical solution chemiluminescence (CL) are described. These include various approaches for monitoring CL, especially flow injection, applications based on luminol and peroxyoxalate CL, direct determinations based on the CL of the analyte, and the uses of CL for liquid chromatographic detection.

Keywords: *Chemiluminescence; flow injection; liquid chromatographic detection; luminol; peroxyoxalate*

Chemiluminescence (CL) is the emission of radiation, usually in the visible or near infrared region, as a result of a chemical reaction. One of the reaction products is formed in an electronic excited state, and emits the radiation on falling to the ground state. A general description of the reactions is

$$A + B \rightarrow C^* + D$$
$$C^* \rightarrow C + h\nu$$

where * indicates an electronic excited state.

The best known example of such a reaction is the oxidation of luminol (**I**) to produce excited 3-aminophthalate (**II**):

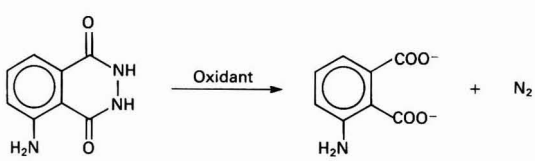

(I) (II)

The spectrum of the CL of this system is identical with the fluorescence spectrum of 3-aminophthalate.[1] Much of the current analytical interest in CL arises from this means of exciting molecules without the need for sample irradiation and the consequent problems of light scattering, unselective excitation and source instability.

In some instances, the excited product (C*) is an ineffective emitter, but by transfer of the excitation energy to an efficient fluorophore (F) added to the system, a considerable increase in luminescence may be achieved:

$$C^* + F \rightarrow C + F^*$$
$$F^* \rightarrow F + h\nu_1$$

The emission is now identical with the fluorescence of F, so that this process, known as sensitisation, enables the luminescence of F to be stimulated without the need for irradiation. The peroxyoxalate CL systems described below are good examples of this type of process.

Chemiluminescence can be produced in the gas phase,[2] including flames,[2,3] and on solid surfaces (*e.g.*, candoluminescence[4] and electroluminescence[5]). These phenomena have all been used analytically, often with great sensitivity, but will not be discussed here. This review will be concerned with CL in solution, and even here some considerable restrictions will be applied. For example, bioluminescence (BL) is the CL produced by a wide variety of organisms (fireflies, bacteria, etc.).[2] The reactions provide extremely sensitive analytical procedures, but are not discussed here. The uses of CL or BL reactions in immunoassays are being shown to provide extreme sensitivity, but again are not included. Finally, electrogenerated CL (*i.e.*, electrochemical reactions producing solution CL), although the subject of renewed interest,[6] remains of rather restricted application, and is omitted.

Chemiluminescent reactions can occur very rapidly (<1 s) or can be long lasting (>1 d). Although the duration is influenced by the reaction conditions, such a wide range presents a challenge to the development of instrumentation for CL monitoring. The light intensity produced is dependent on the CL quantum yield. For BL systems this is often high (*e.g.*, 0.88 for firefly luciferin[2]), resulting in detection limits down to 1×10^{-21} mol in the most favourable instance.[7] For non-biological systems, however, the most efficient system (peroxyoxalate) has a quantum yield of up to 0.50,[2] but other common systems, such as luminol or lucigenin, have quantum yields of only 0.01,[2] and many of the less well known systems that will be dealt with later in this review have quantum yields many orders of magnitude less. The highly selective nature of CL reactions, and the frequent, almost complete absence of background emission, however, means that it is possible to monitor even such very inefficient reactions without difficulty, thus allowing them to be used for analytical purposes.

Analytical interest in CL has increased considerably over the last decade. This is especially clear from the abundance of books and review articles that have appeared during this time,[2,8–20] and which the present author does not wish to duplicate. The present paper, therefore, is intended as a rather personal selection of recent developments and trends in analytical applications of solution CL, and of the instrumentation that has been developed for this purpose. The applications are divided into those procedures that involve established CL reactions, such as those of luminol or peroxyoxalates, and those that involve direct CL reactions.

Instrumentation

Until recently, the major application of CL has been the determination of adenosine 5′-triphosphate (ATP) in the clinical field, based on BL reactions. Such systems are highly sensitive, and the reactions can take several minutes. This has enabled very simple instrumentation to be used,[21] so that commercial luminometers have almost entirely been based on a direct injection batch procedure. The sample, in a cuvette, is placed in a light-tight box, the CL or BL reagent added (usually as drops from a syringe) and the light intensity monitored (usually over a pre-determined time interval) by an

* Presented at SAC 89, the 8th SAC International Conference on Analytical Chemistry, Cambridge, UK, 30 July–5 August, 1989.

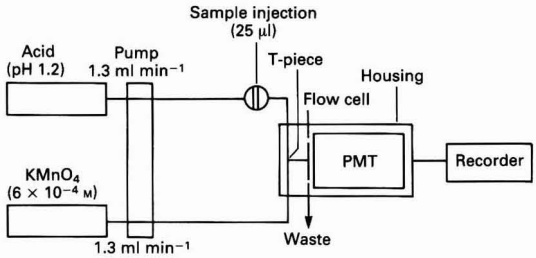

Fig. 1. Schematic diagram of a typical flow injection assembly for chemiluminescence monitoring (used for the detection of morphine)[88]

adjacent photomultiplier tube (PMT). Because there is only one emitting species, wavelength discrimination is not necessary. Recent developments in such commercial luminometers have been in the mechanisation or automation of the reagent addition systems, the addition of multi-cuvette holders and computerised data handling, but the basic concept is unchanged. Syringe-driven reagent-addition luminometers have been described, however, which perform very satisfactorily.[21,22]

The majority of the CL reactions discussed in this review are fast (*i.e.*, are complete in a few seconds) or can be made to be so. For the less efficient reactions, especially, a fast reaction is necessary in order to produce a reasonable burst of photons. Thus, the batch luminometer, which has a rudimentary reagent addition system and probably no mixing device, will not allow reproducible monitoring of fast CL reactions. The batch procedure also requires a separate cuvette for each sample, and the light-tight apparatus must be opened to insert each cuvette, or set of cuvettes, thus necessitating special precautions to protect the PMT. The recent modification of immunoassay-type microtitre plates to monitor CL or BL, whilst of considerable interest, does not solve these problems.[23]

Three other major approaches have been used to monitor CL reactions. Perhaps the most successful of these is based on flow injection (FI).[24] A typical instrumental set up is shown in Fig. 1. The sample is injected into one flowing stream of appropriate pH remote from the detector; the CL reagent flows in the other stream. The two streams meet head on at the T-piece, inside a light-tight casing, then flow through a flat coil placed immediately in front of a PMT. The coil serves to retain the solution in view of the PMT whilst it is emitting most intensely (*e.g.*, for 5–15 s). The external flow tubing can be of black, opaque plastic, thus preventing light piping, and the internal assembly can readily be made completely light tight, as it never has to be opened, except for repair. The whole assembly is very compact and inexpensive. It provides very rapid, reproducible mixing, thus giving reproducible emission intensities, and allows rapid sample throughput. The concept was introduced by Rule and Seitz[25] and has since been used by numerous workers, including ourselves,[26,27] with great effect.

The design of both the mixing device and of the means of retaining the emitting solution in view of the detector are important. Mixing is most effective at a T-piece, but a Y-junction can be used, and some workers have used conventional dispersion of an injected sample into the surrounding flowing reagent to achieve mixing. This last approach is reproducible, but not very rapid. A description of some of the retaining cells proposed has been given by Seitz.[10] Recently, the use of a flowing "film" of solution has been described for this purpose.[28] Petersson *et al.*[29] have designed an FI microconduit assembly for CL monitoring. Another major advantage of this flow approach is that the systems developed are readily useful for liquid chromatographic (LC) detection, and flow luminometers readily function as LC detectors, as will be described below.

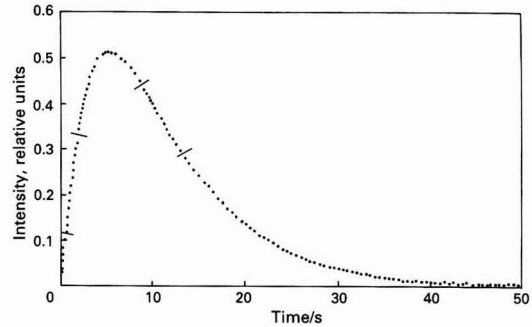

Fig. 2. Intensity - time profile obtained from the CL stopped-flow determination of 5.3×10^{-7} M H_2O_2 (3.2×10^{-4} M luminol and 4.0 μg ml^{-1} of cobalt). Reproduced, with permission, from reference 33

Table 1. Detection limits (DL) for H_2O_2 by chemiluminescence

Reagents	DL/mol l^{-1}	System	Reference
Luminol/Co^{2+}	5×10^{-12}	FI	36
TCPO*	1×10^{-9}		37, 38
Luminol/haemin	5×10^{-9}	Continuous flow	39
Luminol/Cu^{2+}	3×10^{-8}	Batch	35
Imm.† luminol/haemin	1×10^{-6}	FI	40
Imm. TCPO	1×10^{-8}	FI	41
Solid TCPO	6×10^{-9}	FI	42

* TCPO = bis(2,4,6-trichlorophenyl) oxalate.
† Imm. = immobilised.

About a decade ago, attempts were made to use centrifugal analysers for CL monitoring[30–32] because of their proven advantages of rapid and convenient multi-sample processing. Although CL could be measured in this way, the optical design and the intermittent light collection meant a considerable loss of potential sensitivity which would have greatly restricted the applications of the technique had it been pursued.

The stopped-flow approach has many attractive features when applied to CL monitoring. This was used most recently by Perez-Bendito and co-workers.[33] Again, very rapid mixing is achieved, the emitting solution may be retained in the measuring cell for whatever time is desired and, unlike the FI approach, the intensity - time variation can be monitored, thus allowing kinetic measurements to be made. A typical intensity - time plot for luminol oxidation, obtained in this way, is shown in Fig. 2. Up to 60 samples per hour were monitored by this technique.

Uses of Established CL Reactions

Luminol

Luminol (I), when oxidised by most strong oxidants in alkaline solution, gives rise to a characteristic blue luminescence. The reaction is catalysed by a number of metal ions of which iron(II), copper and cobalt are particularly effective.[8] The most obvious use of the reaction has been to determine oxidants. Mayneord *et al.*,[34] for example, applied the reaction to H_2O_2 determination in irradiated water; a modification of this procedure, 10 years later in 1965,[35] gave a detection limit of 3×10^{-8} M H_2O_2, limited by the blank response. It is interesting that since that time the detection limit for H_2O_2, using luminol or other CL reagents, in a variety of experimental arrangements hardly changed until Abbott[36] achieved a considerable improvement, using equipment similar to that shown in Fig. 1. Some detection limits reported for H_2O_2 are

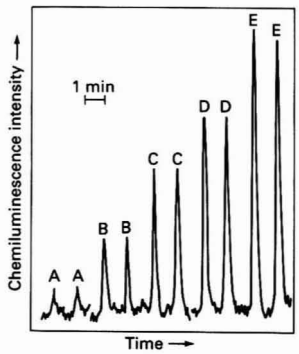

Fig. 3. CL - time responses for various concentrations of cobalt obtained after elution from a cation separation column with 3.0 mM $BaCl_2$ at pH 3.0. A, 1; B, 10; C, 20; D, 30; and E, 40 pg ml^{-1} of Co. Reproduced, with permission, from reference 48

summarised in Table 1. The procedure of Hool and Nieman[40] is unusual in that the reagents are released slowly into the solution by diffusion through a microporous membrane.[43] Phosphatidyl hydroperoxide (≥7 nmol) was detected by luminol - cytochrome C CL after LC separation.[44]

The luminol reaction has also been used to determine compounds which interact with the oxidant. For example, if hypochlorite is used as the oxidant, ammonia (0.1–5 mM) can be determined by an FI procedure by its reaction with the oxidant, thus decreasing the production of CL.[45] Alkyl phosphates or phosphonates react with H_2O_2 to give the corresponding peroxo compounds. These species oxidise luminol much more rapidly than H_2O_2 in alkaline solution, and can thus be determined very sensitively. By appropriate attention to the reaction conditions, a detection limit of 0.5 ng was obtained for the nerve gases DFP (diisopropyl fluorophosphate), sarin (*O*-isopropyl methylphosphonate) and soman (1,2,2-trimethylpropyl methyl fluorophosphate).[46]

Another ingenious application of the luminol reaction has been for the determination of thiols.[47] A thiol derivative of luminol (*N*-mercaptoacetylluminol) is bound to Sepharose 6B (a thiol polysaccharide) by an S–S bond. At pH 9.2, thiols exchange quantitatively with the luminol derivative on the Sepharose, and the released luminol is determined by its CL in a stopped-flow apparatus. The detection limit was 5×10^{-12} mol of thiol.

Determination of metal ions by their catalysis of the luminol or lucigenin reactions has been reported on numerous occasions.[8] Cobalt is particularly active but iron(II), copper, chromium and manganese are also good catalysts. The procedures for their determination are well known, and will not be elaborated here. A recent, interesting development has been the use of such reactions to detect metal ions separated by LC. Cobalt has received particular attention, with Sakai *et al.*[48] obtaining a detection limit of 0.1 pg of Co per 100 μl of sample, with ion-chromatographic separation and on-line luminol CL detection (Fig. 3). Jones *et al.*[49] obtained a detection limit of 0.1 pg of Co per 200 μl of sample after reversed-phase LC separation. Similar detection limits had earlier been obtained in an FI system.[26] The main problem with the chromatographic procedures is the need for better separations.

The effect of chelation of the catalytic metal ion has also been utilised. Polyamines such as ethylenediamine have been determined by reaction with salicylaldehyde to form a Schiff's base, which enhances the catalytic activity of manganese in the luminol - H_2O_2 reaction.[50] This type of reaction has also been used to distinguish between chelated and non- or weakly-complexed chromium(III). The strongly bound chromium has a much weaker catalytic effect.[51] Amino acids, separated by LC, have been detected by their effect on the copper catalysis of the luminol - H_2O_2 reaction.[52]

A major developing use of CL, mainly of luminol, or of firefly or bacterial BL, is to detect the products of enzyme-catalysed reactions.[2] Some luminol applications will be described here. The luminol is used to detect an oxidant, usually H_2O_2, produced in such a reaction. Glucose, for example, in blood or urine could be determined by oxidation in the presence of glucose oxidase to produce H_2O_2, which was detected by CL.[43, 53–56] Other substrates of oxidases can be determined similarly [*e.g.*, cholesterol,[57–59] uric acid[60] and reduced nicotinamide adenine dinucleotide (NADH)[61]] down to *ca.* 1×10^{-8} M.

Some compounds can be determined by a sequence of enzyme-catalysed reactions culminating in H_2O_2 production. A typical example is sucrose, which is converted in sequence to α-D-glucose (and fructose) and β-D-glucose before applying the glucose oxidase reaction. This sequence was used by Koerner and Nieman[62] in conjunction with their microperoxidase reactor to determine 5–1000 μM sucrose.

Finally, mention must be made of the greatly enhanced CL of luminol, produced when horseradish peroxidase is used as the catalyst, in the presence of substituted phenols (*e.g.*, *p*-iodophenol) or naphthols or 6-hydroxybenzothiazoles (including firefly luciferin).[63,64] So far, this has been used for enhancing sensitivity in CL immunoassay, but it should also be useful for other applications.

Peroxyoxalate Systems

Certain aryl (Ar) oxalate esters (**III**) react with H_2O_2, and, most efficiently of all non-biological systems, produce CL if a sensitiser is present.[65,66] The reaction is suggested to proceed via a cyclic intermediate, 1,2-dioxetanedione (**IV**), which then interacts with the sensitiser (F) to excite it and liberate carbon dioxide:

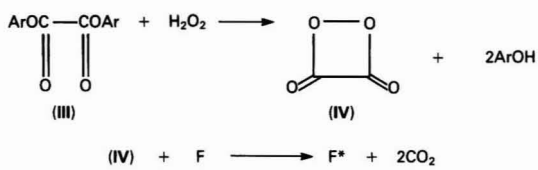

Almost all the analytical applications of this type of reaction, with the exception of H_2O_2 determination (see below), are concerned with the determination of molecules which act as sensitisers. In such applications, the intermediate (**IV**) replaces irradiating photons in exciting the fluorophore, F. It is not surprising, therefore, that the applications of oxalate ester CL are to molecules that have previously been determined by spectrofluorimetry, or have been converted into species that could so be determined. Compounds that are highly fluorescent, therefore, are very sensitively determined by this CL procedure. They include polycyclic aromatic hydrocarbons,[67] of which perylene is generally the most sensitive. The great advantage of chemical excitation is the greatly decreased background signal, thus enabling much improved detection limits to be achieved, often in the sub-fmol region.[68]

As with spectrofluorimetry, direct application of CL measurements to real samples is often impossible or undesirable, because of the effect of other sample components. Therefore, the use of oxalate ester CL for LC detection is widely applied to systems where fluorescence detection has already been shown to be useful. Thus, the technique has been applied with advantage to coal tar extracts[69] (Fig. 4) and urinary porphyrins, which exhibit native fluorescence, and also, for example, to dansylated amino acids,[70] steroids[71–73] and aliphatic amines,[74] and to fluorescamine labelled cate-

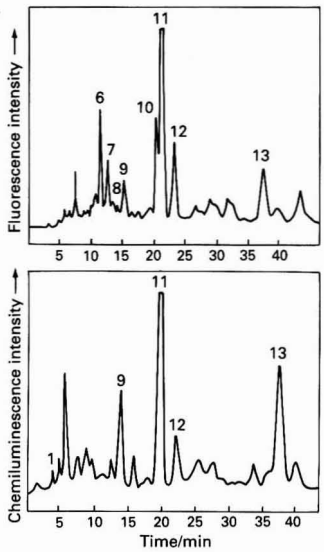

Fig. 4. Chromatograms of polycyclic aromatic hydrocarbons in a coal tar extract. Comparison of CL and fluorescence detection. Reproduced, with permission, from reference 69. 1, Indene; 6, fluoranthene; 7, pyrene; 8, 1,2-benzofluorene; 9, benz[*a*]anthracene; 10, benzo[*b*]fluoranthene; 11, perylene; 12, benzo[*a*]pyrene; and 13, 9,10-diphenylanthracene

cholamines.[75] The system has also been used for detection of dansylated amino acids separated by thin-layer chromatography.[76] Detection limits in the fmol region are often obtained for such favourable systems.

Peroxyoxalate systems have some advantages over luminol and similar CL reagents. Their efficiency and therefore sensitivity is greater, and they are not susceptible to metal ion catalysis or effects of oxygen. The detection limit for H_2O_2 is similar to values reported for the luminol system (Table 1), and the system has been applied to the determination of H_2O_2 produced by a photochemical reactor (detection limit, 1.5×10^{-8} M)[77] and to the determination of uric acid[78] or glucose[61] after enzymic generation of H_2O_2.

There are also some complications with peroxyoxalate systems that are not found in the non-sensitised CL and BL systems. The first is that the oxalate esters are generally not water soluble, and are more or less susceptible to hydrolysis. This places some restriction on their applicability to aqueous samples, although this is much less of a problem when used for LC detection. The second is that the luminescence intensity depends on the particular ester, and the "pH" used. Bis(2,4,6-trichlorophenyl) oxalate (TCPO) gives greatest intensity, *i.e.*, reacts fastest, at "pH" 7.5. In bis(2,4-dinitrophenyl) oxalate, the dinitrophenyl group is a better leaving group, so that reaction is faster, CL intensities are greater and measurable luminescence can be achieved at a "pH" as low as 3.5.[68] However, peroxyoxalate systems do exhibit CL in the absence of a sensitiser.[79] Although this is an extremely weak emission, it does provide a measurable background at high amplification, and thus restricts the signal to noise ratio. The intensity is also dependent on a number of experimental factors, such as solvent and reagent purity, solvent composition and, in flow systems, on pulsing originating in the pumps, a phenomenon which might arise from mixing variations. It is not surprising that this noise is greater with the more sensitive oxalate ester, and is usually the factor governing the limit of detection.

Much work is being carried out on improving the properties of oxalate esters used for CL generation. An alternative approach has been to accept the benefits of water insolubility, and to use solid TCPO[42] as the reagent, which dissolves very slowly in the flowing medium.

Table 2. Some direct chemiluminescent determinations

Analyte	Oxidant system	Detection limit/ mol l^{-1}	Reference
Sulphide . .	ClO^-	1×10^{-7}	81
	H_2O_2 - peroxidase	1.5×10^{-9}	82
Adrenaline . .	H_2O_2 - OH^-	6×10^{-7}	80
Humic acids . .	MnO_4^- - OH^-	0.7*	83
Paracetamol . .	Ce^{IV}	4×10^{-7}	84
Quinones . .	H_2O_2 - OH^-	1×10^{-5}	85
Hydrazine . .	ClO^-	*ca.* 10^{-8}	86,87
Morphine . .	MnO_4^- - H^+	1×10^{-10}	88
Naphthols . .	MnO_4^- - H^+	5×10^{-7}†	89
Tetracycline	Br_2 - OH^-	4×10^{-5}	90
	Dibromodimethyl-hydantoin	1×10^{-6}	91
Sulphenyl esters . .	Iodosobenzene	5×10^{-4}	92
Loprazolam . .	MnO_4^- - H^+	7×10^{-6}	93
Streptomycin . .	MnO_4^- - H^+	*ca.* 10^{-5}	36
Sulphite . .	MnO_4^- - H^+	1×10^{-6}†	94
	MnO_4^- - H^+	1.5×10^{-8}‡	95

* mg l^{-1}.
† With sensitiser.
‡ With 3-cyclohexylaminopropanesulphonic acid.

Direct Chemiluminescent Determinations

The determinations described above involved interaction of the analyte with well established CL reactions, often as a catalyst or sensitiser or after a sequence of other reactions. Further development of analytical procedures involving this very small number of CL reactions will require considerable chemical ingenuity, and must be very restrictive to the wider application of CL. The alternative approach, which is gathering momentum, is to seek CL reactions of the analytes themselves. The search is bringing to light a number of unsuspected CL systems, some of which are described below.

New CL reactions are generally discovered by testing the analyte with a wide range of oxidants (and reductants) under an equally wide range of conditions.[36,80] A typical set of oxidants might be H_2O_2, ClO^-, cerium(IV), IO_4^-, MnO_4^- (H^+ and OH^-) and Br_2, with the possibility of also adding catalysts and of carrying out the reactions at different pH values. There are some guidelines for predicting which analytes are likely to generate CL. For example, if oxidation of the molecule is known to give a fluorescent product (as was the case with morphine, tetracycline and streptomycin, as described below), or if the analyte itself has the type of structure that might lead to fluorescence, there is a possibility that oxidation of the analyte will give CL. Very often, however, the CL reactions discovered in screening tests cannot be predicted; frequently, also, a predicted CL reaction is found not to emit.

A selection of direct determinations based on CL is given in Table 2. The detection limits vary considerably, but many of the procedures use μl volumes of sample solution, so that even relatively insensitive procedures in concentration terms are able to detect down to nmol amounts.

The development of a procedure for morphine is typical.

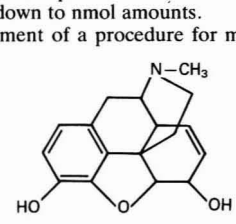

(V)

Morphine (**V**) can be determined spectrofluorimetrically after oxidation to a dimeric product, pseudomorphine.[96] It was possible, therefore, that the oxidation reaction would produce CL, as was found to be the case. Acidic permanganate gave the greatest intensity, with tetraphosphoric acid being the best acid.[36,88] A screen of related narcotic analgesics and of other drugs showed that, of the compounds tested, only morphine and some of its derivatives gave intense CL. These results showed that for intense CL to occur, there must be a free OH group at position 3. Therefore, heroin (3,6-diacetylmorphine) and morphine 3-glucuronide, an important metabolite of morphine, do not give intense CL. Interestingly, buprenorphine (**VI**), a drug attracting much attention as a morphine substitute, also gives intense CL, and can be determined on that basis.[97]

The very low detection limit for morphine indicated that CL detection might be suitable for forensic purposes, and thus an LC procedure was developed that could be applied to blood or urine samples. The original method,[98] after sample clean up, used an acidic eluent, which would mix post-column with the aqueous permanganate stream. The acidic eluent made it necessary to use a polymer column. The procedure had an on-column detection limit of 5 ng of morphine. Subsequent modification of the procedure, especially avoiding the use of the acidic eluent by incorporating the acid in the permanganate stream, has decreased the detection limit to 0.08 ng on-column.[99]

Another example of the unexpected occurrence of CL was found during a screen of benzodiazapines for CL in an acidic permanganate medium. Of seven compounds tested, only loprazolam (**VII**) was chemiluminescent.[93] There was no obvious structural reason for this.

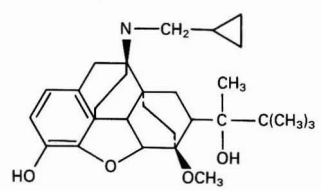

(**VI**)

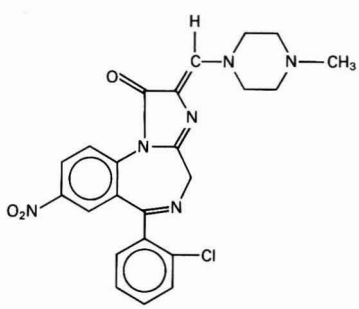

(**VII**)

Conclusions

Chemiluminescence can provide analytical procedures with extremely low detection limits. Better instrumentation will undoubtedly improve this situation further, because many systems are almost free of background luminescence. There will undoubtedly be a great expansion in the number of direct CL determinations that will be possible as more CL reactions are discovered. As with luminescence processes, CL can be affected (quenched or enhanced) by other compounds present in samples, so that useful applications will require such interactions to be understood and controlled. For this reason, the use of CL for LC detection is becoming recognised as a means of avoiding interferences and of achieving an extremely reproducible and very sensitive means of analysis.

I thank those who worked with me as students or visitors, or who subsequently have developed an interest in CL, for the major contribution they have made to this subject. They include J. L. and M. Burguera, A. R. Wheatley, R. W. Abbott, A. T. Faizullah, S. A. Al-Tamrah, A. A. Al-Warthan, A. C. Calokerinos, N. P. Evmiridis and, most recently, A. R. J. Andrews. I also thank the Analytical Chemistry Trust for the award of a studentship to A. R. Wheatley, and the SERC and the Home Office Forensic Service for CASE awards to R. W. Abbott and A. R. J. Andrews. Finally, I thank Dr. P. J. Worsfold, whose parallel, but independent, contributions in this area have done much to enhance our reputation in the area of chemi- and bioluminescence.

References

1. White, E. H., and Bursey, M. M., *J. Am. Chem. Soc.*, 1964, **86**, 940.
2. Campbell, A. K., "Chemiluminescence, Principles and Applications in Biology and Medicine," Ellis Horwood/VCH, Chichester, 1988.
3. Alkemade, C. Th. H., and Herrmann, R., "Fundamentals of Analytical Flame Spectroscopy," Adam Hilger, Bristol, 1979.
4. Belcher, R., Nasser, T. A. K., Shahiduallh, M., and Townshend, A., *Am. Lab.*, 1977, 61.
5. Haapakka, K., Kankare, J., and Kulmala, S., *Anal. Chim. Acta*, 1985, **171**, 259.
6. Haapakka, K., *Anal. Chim. Acta*, 1982, **141**, 263, and references cited therein.
7. Campbell, A. K., "Chemiluminescence, Principles and Applications in Biology and Medicine," Ellis Horwood/VCH, Chichester, 1988, p. 261.
8. Burguera, J. L., Burguera, M., and Townshend, A., *Acta Cient. Venez.*, 1981, **32**, 115.
9. Burguera, J. L., Burguera, M., and Townshend, A., *Rev. Roum. Chim.*, 1982, **27**, 879.
10. Seitz, W. R., *CRC Crit. Rev. Anal. Chem.*, 1981, **13**, 1.
11. De Luca, M. A., and McElroy, W. D., *Editors*, "Bioluminescence and Chemiluminescence," Academic Press, New York, 1981.
12. Kricka, L. J., and Carter, T. J. N., *Editors*, "Clinical and Biochemical Luminescence," Marcel Dekker, New York, 1982.
13. Kricka, L. J., and Thorpe, G. H. G., *Analyst*, 1983, **108**, 1274.
14. Burr, J. G., *Editor*, "Chemi- and Bioluminescence," Marcel Dekker, New York, 1985.
15. van Dyke, K., *Editor*, "Bioluminescence and Chemiluminescence, Instruments and Applications," CRC Press, Cleveland, 1985, Volumes I and II.
16. Fernandez-Gutierrez, A., and Munoz de la Pena, A., *in* Schulman, S. G., *Editor*, "Molecular Luminescence Spectroscopy, Methods and Applications, Part I," Wiley, New York, 1985, pp. 463–546.
17. Tsuji, A., and Maeda, M., *Bunseki*, 1987, 403.
18. Grayeski, M. L., *Anal. Chem.*, 1987, **59**, 1243A.
19. De Luca, M. A., and McElroy, W. D., *Methods Enzymol.*, 1987, **133**.
20. Zhang, F., and Chen, Y., *Fenxi Shiyanshi*, 1987, **6**, 51, and references cited therein.
21. Stanley, P. E., *in* Kricka, L. J., and Carter, T. J. N., *Editors*, "Clinical and Biochemical Luminescence," Marcel Dekker, New York, 1981, pp. 219–260.
22. Hayashi, Y., Ikeda, M., and Yuki, H., *Anal. Chim. Acta*, 1985, **167**, 81.
23. Bunce, R. A., Thorpe, G. H. G., Gibbons, J. E. C., Killeen, P. R., Ogden, G., Kricka, L. J., and Whitehead, T. P., *Analyst*, 1985, **110**, 657.
24. Burguera, J. L., and Burguera, M., *Acta Cient. Venez.*, 1983, **34**, 79.
25. Rule, G., and Seitz, W. R., *Clin. Chem.*, 1979, **25**, 1635.

26. Burguera, J. L., Townshend, A., and Greenfield, S., *Anal. Chim. Acta*, 1980, **114**, 209.
27. Townshend, A., *Anal. Proc.*, 1985, **22**, 370.
28. Swindlehurst, C. A., and Nieman, T. A., *Anal. Chim. Acta*, 1988, **205**, 195.
29. Petersson, B. A., Hansen, E. H., and Růžička, J., *Anal. Lett.*, 1986, **19**, 649.
30. Bowling, J. C., Dean, J. A., Goldstein, G., and Dale, J. M., *Anal. Chim. Acta*, 1975, **76**, 47.
31. Bostick, W. D., Bauer, M. L., McCracken, R., and Mrochek, J. E., *Anal. Chem.*, 1980, **52**, 300.
32. Wirth, M. J., Kostelo, A. C., Mohler, C. E., and Lentz, B. L., *Anal. Chem.*, 1981, **53**, 2045.
33. Gonzalez-Robledo, D., Silva, M., and Perez-Bendito, D., *Anal. Chim. Acta*, 1989, **217**, 239.
34. Mayneord, W. V., Anderson, W., Evans, H. D., and Rosen, D., *Radiat. Res.*, 1955, **3**, 379.
35. Armstrong, W. A., and Humphreys, W. G., *Can. J. Chem.*, 1965, **43**, 2576.
36. Abbott, R. W., *PhD Thesis*, University of Hull, 1986.
37. Rigin, V. I., *Russ. J. Anal. Chem.*, 1978, **33**, 1265.
38. Rigin, V. I., *Russ. J. Anal. Chem.*, 1979, **34**, 619.
39. Yoshizumi, K., Aoki, K., Nouchi, I., Okita, T., Kobayashi, T., Kamakura, S., and Tajima, M., *Atmos. Environ.*, 1984, **18**, 395.
40. Hool, K., and Nieman, T. A., *Anal. Chem.*, 1988, **60**, 834.
41. Gubitz, G., van Zoonen, P., Gooijer, C., Velthorst, N. H., and Frei, R. W., *Anal. Chem.*, 1985, **57**, 2071.
42. van Zoonen, P., Kamminga, D. A., Gooijer, C., Velthorst, N. H., and Frei, R. W., *Anal. Chim. Acta*, 1985, **167**, 249.
43. Pilosoff, D., and Nieman, T. A., *Anal. Chem.*, 1982, **54**, 1698.
44. Miyazawa, T., Yasuda, K., and Fujimoto, K., *Anal. Lett.*, 1987, **20**, 915.
45. Kraus, P. R., and Crouch, S. R., *Anal. Lett.*, 1987, **20**, 183.
46. Fritsche, U., *Anal. Chim. Acta*, 1980, **118**, 179.
47. Lippman, R. D., *Anal. Chim. Acta,* 1980, **116**, 181.
48. Sakai, H., Fujiwara, T., Yamamoto, M., and Kumamaru, T., *Anal. Chim. Acta*, 1989, **221**, 249.
49. Jones, P., Williams, T., and Ebdon, L., *Anal. Chim. Acta*, 1989, **217**, 157.
50. Matveeva, E. Ya., Kalinchenko, I. E., and Pilipenko, A. T., *Zh. Anal. Khim.*, 1981, **36**, 2215; *Anal. Abstr.*, 1982, **42**, 6C3.
51. Huizenga, D. L., and Patterson, H. H., *Anal. Chim. Acta*, 1988, **206**, 263.
52. Lowery, S. N., Carr, P. W., and Seitz, W. R., *Anal. Lett.*, 1977, **10**, 931.
53. Bostick, D. T., and Hercules, D. M., *Anal. Lett.*, 1974, **7**, 347.
54. Bostick, D. T., and Hercules, D. M., *Anal. Chem.*, 1975, **47**, 447.
55. Ridder, C., Hansen, E. H., and Růžička, J., *Anal. Lett.*, 1982, **15**, 1751.
56. Hara, T., Toriyama, M., and Imaki, M., *Bull. Chem. Soc. Jpn.*, 1982, **55**, 1854.
57. Pilosoff, D., Malvolti, N., and Nieman, T. A., *Anal. Chim. Acta*, 1985, **170**, 199.
58. Blum, L., Plaza, J. M., and Coulet, P. R., *Anal. Lett.*, 1987, **20**, 317.
59. Taniguchi, A., Hayashi, Y., and Yuki, H., *Anal. Chim. Acta*, 1986, **188**, 95.
60. Gorus, F., and Schram, E., *Arch. Int. Physiol. Biochim.*, 1977, **85**, 981.
61. Williams, D. C., Huff, G. F., and Seitz, W. R., *Anal. Chem.*, 1976, **48**, 1003.
62. Koerner, C. A., and Nieman, T. A., *Anal. Chem.*, 1986, **58**, 116.
63. Whitehead, T. P., Thorpe, G. H. G., Carter, T. J. N., Grocutt, C., and Kricka, L. J., *Nature (London)*, 1983, **305**, 158.
64. Thorpe, G. H. G., and Kricka, L. J., *Methods Enzymol.*, 1987, **133**, 331.
65. Rauhut, M. M., Bollyky, L. J., Roberts, B. G., Loy, M., Whitman, R. H., Semsel, A. M., and Clark, R. A., *J. Am. Chem. Soc.*, 1967, **89**, 6515.
66. Rauhut, M. M., *Acc. Chem. Res.*, 1969, **2**, 80.
67. Sherman, P. A., Holzbecher, J., and Ryan, D. E., *Anal. Chim. Acta*, 1978, **97**, 21.
68. Imai, K., and Weinberger, R., *Trends Anal. Chem.*, 1985, **4**, 170.
69. Sigvardson, K. W., and Birks, J. W., *Anal. Chem.*, 1983, **55**, 432.
70. Kobayashi, S., and Imai, K., *Anal. Chem.*, 1980, **52**, 424.
71. Koziol, T., Grayeski, M. L., and Weinberger, R., *J. Chromatogr.*, 1984, **317**, 355.
72. Nozaki, O., Ohba, Y., and Imai, K., *Anal. Chim. Acta*, 1988, **205**, 255.
73. Imai, K., Higashidate, S., Nishitani, A., Tsukamoto, Y., Ishibashi, M., Shoda, J., and Osuga, T., *Anal. Chim. Acta*, 1989, **227**, 21.
74. Melbin, G., and Smith, B. E. F., *J. Chromatogr.*, 1984, **312**, 203.
75. Kobayashi, S, Sekino, J., Honda, K., and Imai, K., *Anal. Biochem.*, 1981, **112**, 99.
76. Curtis, T. G., and Seitz, W. R., *J. Chromatogr.*, 1977, **134**, 343.
77. Gandelmann, M. S., Birks, J. W., Brinkman, U. A. Th., and Frei, R. W., *J. Chromatogr.*, 1983, **282**, 193.
78. Scott, G., Seitz, W. R., and Ambrose, J., *Anal. Chim. Acta*, 1980, **115**, 221.
79. Capomacchia, A. C., Jennings, R. N., Hemingway, S. M., D'Sousa, P., Prapaitrakul, W., and Gingle, A., *Anal. Chim. Acta*, 1987, **196**, 305.
80. Nakagama, T., Yamada, M., and Suzuki, S., *Anal. Chim. Acta*, 1989, **217**, 371.
81. Klockow, D., and Teckentrup, J., *Talanta*, 1976, **23**, 889.
82. Burguera, J. L., and Townshend, A., *Talanta*, 1980, **27**, 309.
83. Marino, D. F., and Ingle, J. D., Jr., *Anal. Chim. Acta*, 1981, **124**, 23.
84. Koukli, I. I., Calokerinos, A. C., and Hadjiioannou, T. P., *Analyst*, 1989, **114**, 711.
85. Burguera, J. L., and Burguera, M., *Talanta*, 1984, **31**, 1027.
86. Wheatley, A. R, *PhD Thesis*, University of Hull, 1983.
87. Faizullah, A. T., and Townshend, A., *Anal. Proc.*, 1985, **22**, 15.
88. Abbott, R. W., Townshend, A., and Gill, R., *Analyst*, 1986, **111**, 635.
89. Al-Tamrah, S. A., and Townshend, A., *Anal. Chim. Acta*, 1987, **202**, 247.
90. Al-Warthan, A. A., and Townshend, A., *Anal. Chim. Acta*, 1988, **205**, 261.
91. Owa, T., Masujima, T., Yoshida, H., and Imai, H., *Bunseki Kagaku*, 1984, **33**, 570.
92. Lancaster, J. S., and Worsfold, P. J., *Anal. Proc.*, 1989, **26**, 19.
93. Andrews, A. R. J., and Townshend, A., *Anal. Chim. Acta*, 1989, **227**, 65.
94. Yamada, M., Nakada, T., and Suzuki, S., *Anal. Chim. Acta*, 1983, **147**, 401.
95. Al-Tamrah, S. A., Townshend, A., and Wheatley, A. R., *Analyst*, 1987, **112**, 883.
96. Jane, I., and Taylor, J. F., *J. Chromatogr.*, 1975, **109**, 37.
97. Al-Warthan, A. A., and Townshend, A., *Anal. Chim. Acta*, 1986, **185**, 329.
98. Abbott, R. W., Townshend, A., and Gill, R., *Analyst*, 1987, **112**, 397.
99. Andrews, A. R. J., Townshend, A., and Gill, R., unpublished work.

Paper 9/04983E
Received November 22nd, 1989

Review of Current Techniques for the Verification of the Species Origin of Meat*

Ronald L. S. Patterson and Sheila J. Jones
AFRC Institute of Food Research (Bristol Laboratory), Langford, Bristol BS18 7DY, UK

An overview of developments that have occurred in meat species identification over the last decade is presented. It starts by noting the different requirements for speciation techniques over the period, describes the complex nature of meat in terms of chemical composition and shows how the chain of events from slaughter to retail gives rise to opportunities for deliberate adulteration or innocent contamination. The limitations of techniques such as electrophoresis and isoelectrofocusing are pointed out where the analysis of mixed meats is concerned; attention then focuses on the range of techniques based on antigen - antibody interactions: agar gel immunodiffusion, counter immuno-electrophoresis and enzyme-linked immunosorbent assay (ELISA) in three formats. The choice of analyte is discussed, firstly for the analyses of raw meat materials and secondly, for heat-processed meat products. In the first example, blood serum proteins are used almost exclusively despite the limitation that their presence does not necessarily denote the presence of the corresponding muscle tissue (meat). For cooked products, a new range of antisera are necessary, based on thermally stable components derived from the tissues. By using different formats of ELISA, it is demonstrated that different responses can be obtained for heat-processed meat *versus* processed offal, and that determination of a species meat content in a cooked mixed meat product is possible. Techniques for improving the specificity and performance of antisera are discussed briefly, with the future introduction of thermally stable, muscle-specific monoclonal antisera being seen as the way forward.

Keywords: *Meat; species identification; antisera; enzyme-linked immunosorbent assay*

About 10 years ago, interest arose in developing methods for the identification of the species origin of meat after removal from the carcass. The reason for undertaking research on meat speciation at that time was to evolve good analytical procedures for use by Trading Standards and Law Enforcement agencies in their attempts to combat increasing problems of adulteration in national meat supplies: instances of illegal species meats such as horse or kangaroo had been finding their way into the meat chain and were causing much concern. The underlying reasons for continuing research in this field today are similar, although with some shift in emphasis; less is now heard about gross amounts of horse or kangaroo meats in the bulk supplies, but rather more about a few per cent. of other "acceptable" meats being found in consignments that had been declared to be 100% of a pure single species. These problems come to light as a result of enforcement of the Trading Standards and Labelling regulations. This has required research to evolve improvements in sensitivity of detection, in addition to finding ways of reducing cross-reactions that could lead to erroneous conclusions where low levels of "contamination" are involved.

Meat

Meat can be presented in a variety of forms, each offering different opportunities for adulteration and/or contamination. For example, whole meat can be in the form of carcasses, sides, quarters, primal joints or domestic joints; in such circumstances, there are few problems as most species are still anatomically recognisable. Deboned meat, which is popular in wholesale because of its space- and (refrigeration) energy-saving advantages is usually boxed or vacuum-packed in plastic bags and stored and distributed in the frozen state; opportunities for adulteration of the supply are now possible, especially as much of the material is used for product manufacture directly from the frozen state without thawing. Alternatively, meat can be diced, chopped or minced and is usually handled in bulk; the composition of such material can be extremely variable and easily manipulated.

From the analytical chemist's point of view the composition of the meat is complex. The principal components are the proteins of the muscle, residual blood and collagenous materials, together with lipids and small amounts of free amino acids, enzymes, carbohydrates and minerals.

The presence of meat, *i.e.*, muscle protein, in a food can be established by analysing muscle hydrolysates for the amino acid, 3-methylhistidine.[1] This unusual amino acid arises *in vivo* by the specific methylation of one particular histidine residue in actin and also in one form of myosin in the myofibrillar protein. However, as this biological reaction is common to all species, it cannot be used for species identification purposes. Other components must therefore be used for species recognition, and generally they must be analysed without heating or hydrolysis, which would destroy their distinctive structures. Possibilities are, *e.g.*, the blood (serum) proteins, muscle proteins, components of the lipids and collagen.

Techniques

Electrophoresis

With raw, unheated meats, the proteins give most options, and the standard biochemical methods of electrophoresis and isoelectrofocusing, and variants of these procedures, have been used to good effect in speciation work, principally where single species of meat (or fish) have been concerned. The proteins are separated as characteristic band patterns in a supporting gel, and rendered visible, if necessary, by simple non-specific staining, or by enzymological or even immunological methods. The degree of separation can be manipulated by employing gels of different characteristics, *e.g.*, homogeneous gels, or concentration- or pH-gradient gels, or by use of denaturants such as urea or detergents that dissociate the tertiary protein structures. Successful applications to species recognition include isoelectrofocusing of aqueous extracts of raw meat, exploiting the coloured myoglobin bands,[2] or discriminating between appropriate species-

* Presented at SAC 89, the 8th SAC International Conference on Analytical Chemistry, Cambridge, UK, 30 July–5 August, 1989.

specific isoenzymes after specific visualisation.[3,4] Such methods are, however, much less effective in the resolution of mixtures of meats in which proteins from more than one species are present.[5]

For heat-processed meats, the extraction of protein normally requires the use of solubilisation agents. For example, cooked horse meat and beef can be distinguished electrophoretically after extraction into 8 M urea, "renaturation" by dialysis, separation in concentration-gradient gels and visualisation by non-specific dye-binding.[6] Alternatively, separation can be achieved after extraction into 6 M guanidine hydrochloride, dialysis into 1% Triton X-100, isoelectrofocusing in pH-gradient gels and visualisation by specific detection of renatured enzyme activity, *e.g.*, adenylate or creatine kinase.[7] These lengthy procedures are most appropriate as definitive, confirmatory tests after simpler, immunological screening, or for special discrimination between two immunologically related species.[8]

Immunological Procedures

These procedures are based on very specific antigen - antibody interactions, and can be used to detect and determine particular analytes without prior separation in complex mixtures such as biological fluids or food extracts. There are many analytical procedures in which immuno-reagents are used, but for the present purposes, the two most appropriate in species recognition are (1) the classical Ouchterlony double immunodiffusion technique,[9] and its variants; and (2) the more recent enzyme-linked immunosorbent assay (ELISA). Of the two, ELISA requires less antiserum and less time; it is also more sensitive and objective, but is more complicated and requires more expensive equipment and a higher degree of operator skill.

The proteins most commonly used are those of the blood because they are the easiest to extract and work with, but they are not muscle-specific and their presence in a sample does not necessarily denote the presence of the corresponding species of meat. For example, liver, which contains high levels of serum albumin, is classed as offal and not meat.[10] Nevertheless, the blood serum albumins are the basis of most commonly used speciation tests. Muscle proteins such as myosin, actin, titin, troponin, and myoglobin can be used as antigens for raising antisera,[11–13] but generally this approach has been restricted to the work of specialist laboratories. Even then, the resulting anti-species antisera are not always fully muscle- or species-specific.

Agar gel immunodiffusion (AGID)

This technique is carried out by placing a few millilitres of aqueous extract of soluble proteins from a meat sample in wells cut in a shallow layer (2–3 mm) of agarose gel. Antisera raised against the test species are placed in an adjacent well. The plate is then incubated to allow antibodies and antigens to diffuse together. If both are present, a visible opaque band will appear in the gel between the wells, and results are available within 24 h.[14,15] With an optimised procedure, using commercial precipitating antisera to species-specific blood proteins, it is possible to detect beef, horse, pig, poultry, sheep and kangaroo sera routinely, and thus infer the presence of the related meat(s). It is not, however, possible to distinguish sheep from goat, or horse from donkey, by this method. Subjective detection limits in raw beef are: sheep, 5%; pork, 10%; horse, 10%; chicken/turkey, 15%; kangaroo, 20%; beef itself could be detected at the 2% level in pork.

The same principle has been developed as a dry test,[16] now available commercially as the Domino 5 meat speciation test kit.[17] The kit contains sets of dry paper discs either with individual species antisera, or with reference antigens [several authentic species antigens (serum proteins) on one "multi-reference" disc], plus packs of blanks for coating with sample material. Pre-coated agar plates are also provided, and the appropriate paper discs are applied to the agar according to a template pattern provided. As before, antibodies and sample antigens diffuse towards each other in the gel and produce a precipitation line if the antigen and antisera are homologous. The kit is inexpensive and simple to operate and is therefore suitable for routine screening for major adulteration or misrepresentation. Sensitivity varies according to species: detection limits for pig, beef and horse meats lie between 5 and 10%, while that for mutton is nearer 20%.

Counter immuno-electrophoresis (CIE)

This is another technique for separating and identifying proteins, which has proved to be effective, especially in forensic work, and has been evaluated by the UK Veterinary Investigation Centre in Worcester for use in screening consignments of imported meat materials.[18] It is a combination of the principles of agar gel double immunodiffusion and electrophoresis, and results are generated more quickly than with simple AGID, which relies solely on spontaneous diffusion. In conventional gel electrophoresis, the gel is at neutral pH, and all the proteins move to the anode because of their negative charge. In CIE, however, the gel is alkaline. This causes electro-osmosis to occur and effectively changes the charge on weak, negatively charged proteins, including the gamma-globulins in serum, to positive; the gamma-globulins, therefore, now move to the cathode. By correct positioning of the wells in an alkaline gel, proteins from a meat extract and gamma-globulins from a specific antiserum can be made to move towards each other, and, if homologous, produce a precipitin band where they meet.

Both fresh meat and offal give similar results with this technique. The range of species detectable is limited to the range of specific antisera available, but considerably less antisera is required than with AGID. As with AGID, differentiation of closely related species is not possible. However, low levels of adulteration are detectable, *e.g.*, dilutions of one part in 300 of a meat species are readily detectable by use of CIE. This is a major asset when dealing with very low levels of adulteration or with material with little soluble protein, such as green offal, or with meat of a very high fat content. The time taken to obtain a result is about half that for AGID, and overall, the test is more cost-effective than the simple AGID test.

Enzyme-linked immunosorbent assay (ELISA)

In enzyme immunoassays, the antibody - antigen interaction is usually carried out in a monomolecular layer immobilised on the surface of a plastic microtitre plate. The extent of reaction is monitored by means of a subsequent colour-forming reaction, initiated by an enzyme chemically bonded either to one of these immuno-reagents or to a separate "antibody-detector" added as a second stage.[19,20] Measurement of the absorbance of the wells provides a measure of the reaction and allows comparison with standards and assay controls.

At least three forms of ELISA have been used in meat speciation work. The first to be applied was a straightforward form of ELISA (sometimes called indirect ELISA), in which all the soluble protein components of an extracted meat sample are absorbed directly on to the ELISA plate. The serum proteins in the sample are detected by introducing, firstly, the species-specific antibody, followed by a "first-antibody detector" with enzyme already linked to it. The "antibody-detector" can be either anti-immunoglobulin G (IgG) (*e.g.*, anti-rabbit IgG) or protein A. Enzyme substrate is added, and colour formation is proportional to the amount of antibody - enzyme complex formed and hence to the original concentration of serum albumin present on the plate.[19,21]

While this basic system is perfectly adequate for checking that beef is beef or pork is pork, it is not sensitive enough for the analysis of meat mixtures containing less than *ca.* 5% of another species component. This is because it depends on colour formation in direct proportion to the amount of each species antigen present. At low levels of adulteration, it is not safe to rely on a small increase of substrate colour, say 0.2 or 0.3 A, to indicate the presence of a species, even after compensating the assay results for, *e.g.*, background colour and second anti-antibody effect. In such instances, it is necessary to employ a double-antibody sandwich (DAS) version of ELISA, and several examples of this system for meat species identification have now been published.[22–26] These DAS-ELISA methods, which have the advantage of improved specificity and sensitivity for detection of components at low concentrations, require two species-specific antibodies; in our assay system, developed to detect very low levels of pig meat in beef, it was concluded that the greatest sensitivity resulted from using the better "mono"-specific (affinity-absorbed) anti-pig antibody for the "capture" stage on the plate.[25]

The microtitre wells are pre-coated with one of the "mono"-specific antibodies to capture the particular meat antigens from the extract when it is applied. Two or three repeat applications of the extract improve the sensitivity of the assay, allowing detection of 0.5% of a species adulterant. Second species "detector" antibodies are applied to form the top half of the sandwich. The "detector" antibody can be applied with either the enzyme attached directly or by use of anti-IgG or protein A with the enzyme attached. Addition of enzyme substrate then gives rise to colour formation in proportion to the amount of specific meat antigen originally present, with high specificity and sensitivity. This form of ELISA is the basis of two commercially available kits, the Australian "Checkmeat" system, which can be used to distinguish the closely related species sheep/goat, beef/buffalo and horse/donkey,[24,26] and Meat Speciation (Biokits, UK). A third kit by Sera Laboratories has been discontinued.

A competitive ELISA is a third variant of the system, which has been developed for meat species identification.[27] In this variant, each sample extract is incubated initially with a fixed, pre-determined amount of species-specific antibody reagent in phosphate-buffered saline/Tween (PBST) solution in a separate vessel. This prevents the interaction of that species-specific antibody with its authentic, purified antigen already pre-coated on the ELISA plate. If the sample extract does *not* contain the species antigen in question, then all the anti-species antibodies will remain free to interact with the plate-bound antigen. After addition of this solution to the wells of the plate, the assay is completed in the usual way by applying second, enzyme-labelled anti-antibodies, but in this instance, maximum or high colour development indicates a negative or low adulterant level response, and low colour, a full positive result. A well-developed, optimised competitive ELISA could be used to complete meat speciation tests in <1 h, especially if a plate shaker is used to speed up the interaction stages. Rapidity (10-min incubations) and sensitivity are the advantages of this method.

For the analysis of unknown meat homogenates or meat mixtures, the current range of ELISA tests, based on the detection of residual blood protein in the meat, should only be considered as *qualitative* even though the ELISA end-point values vary. In some circumstances, a semi-quantitative evaluation may provide useful information, *e.g.*, when sample treatments are clearly defined and portions of the original pure meats incorporated into a mixture can be retained for analysis. Normally, however, attempts to interpret assay data in terms of amounts of individual meat species have not been successful,[27] because the residual blood levels in different cuts or joints of meat are too variable to correlate accurately with the corresponding lean content.

Developments

Many, if not all, of the ELISA methods currently available for meat speciation make use of polyclonal antisera. Such antisera may need special immunosorbent purification, as previously indicated, to eliminate significant cross-reactions. Once effective ELISA methods are established for particular analyses, they require a continuous supply of antisera of consistent quality and characteristics to permit large-scale production of commercial test kits, and this can lead to problems of supply in the long term. The following techniques can be helpful in the production of polyclonal antisera in appropriate circumstances.

Immunosorbent (Affinity) Chromatography

Polyclonal antisera can be rendered species-specific by circulating them through a series of chromatographic columns containing the appropriate unwanted antigens in bound form. These remove the unwanted antibodies causing the cross-reactions. The desired species-specific antibodies are now trapped by and subsequently harvested from a final column containing the homologous antigen. This acts both as a purification and concentration step. The columns are re-usable after regeneration, although they are expensive to establish initially.

Absorption of Cross-reactions

During work-up, antisera can be rendered more specific by simply "absorbing" them in solution with the other, interfering antigens. This is an effective way of reducing minor cross-reactions, but removal of major cross-reactions by this procedure may render an antiserum too weak or ineffective for use in AGID tests because of the way the antibody - antigen aggregation proceeds in that situation; if only very specific antibodies are left that are capable of interacting with only one or perhaps two unique epitopes (active sites) on an antigen, they might fail to give a clear precipitin result because the secondary "precipitation" aggregates would not form. Clearly, this is where immunoassays have an advantage because only a single linking of antibody with antigen is needed before visualisation can take place by colour formation.

"Blocking" is a variant of the same procedure whereby an interfering species can be nullified during an ELISA of the type in which sample extract proteins are bound to the plate surface. Blocking is carried out by addition of heterologous antigens dissolved in PBST to the dilute anti-species antiserum in a separate vessel; cross-reactions then occur in the PBST solution rather than on the solid phase of the plate where they would otherwise remain and interfere.[28] After addition of the blocked antiserum to the wells of the plate, and the desired antigen - antibody reactions have taken place on the plate surface, the normal washing procedure removes the remaining heterologous antigens and the products of the blocking reaction. Thereafter, the remainder of the ELISA procedure is standard.

Closely Related Host Animal

One of the best ways of obtaining antibodies capable of differentiating two closely related species is to use one of the pair, or a very close relative of one of the species, as host animal in the production of the antiserum. Therefore, to differentiate sheep from goat, a goat would be immunised with sheep antigen, or to differentiate beef and buffalo, a cow would be immunised with buffalo antigen, and so on. This technique is not new, as Weitz[29] attempted differentiation of goat and sheep this way in 1952, using precipitin methodology. However, the differentiation of close relatives can now be fully exploited by the DAS-ELISA procedure, with very

Table 1. Response of the anti-pig reagent to heat-treated species offals and to a range of pork and beef mixtures

	Absorbance value at 405 nm (mean of three corrected values)			
	Pig	Beef	Sheep	Horse
(i) *Carcass component*—				
Typical muscle	1.57	0.01	0	0
Tongue	1.40	0.03	NT†	NT
Heart	0.48 (28.6%)*	0.02	0.01	0.06
Liver	0.37 (21.8%)	0.02	0.02	0
Lungs	0.22 (12.4%)	0.02	0.03	NT
Kidney	0.25 (14.2%)	0	0.02	NT
Brain	0.11 (5.4%)	0.01	NT	0.03
Spleen	0.25 (14.2%)	0.02	NT	NT
Gelatin	0.49 (29.0%)			
Fat (subcutaneous)	0.82 (50%)			
(mesenteric)	0.53 (31%)			
(ii) *Model pork/beef mixture*—	Linear regression constants: $y = mx + c$			
5% pork in beef	0.10 A	$m = 0.016$		
10% pork in beef	0.15 A	$c = 0.023$		
25% pork in beef	0.41 A	$r = 0.994$		
50% pork in beef	0.86 A			
75% pork in beef	1.37 A			
95% pork in beef	1.45 A			

(iii) Skimmed milk powder and soya protein gave absorbance values of <0.10

* Per cent. values refer to the equivalent percentage of pork in beef estimated from the linear response of six raw pork/beef mixtures (ii), and the responses of other species of pure muscle meats and offals extracted by equivalent heat treatment and analysed during the same assay for comparison.

† NT = Not tested.

effective results. Hence, when raising antisera, particular attention should be paid to the choice of host animal to be sure of obtaining the most appropriate immune response.

Monoclonal Antisera

The development of hybridoma technology has provided a means for the continuous production of antibodies, of characteristic activity and specificity, from single cell lines[30]; once selected by stringent screening procedures, the monoclonal antibodies are grown as "clones" by tissue culture techniques and are potentially immortal. In recent work, as part of our Anglo-Spanish research collaboration, three hybridoma cell lines were produced, which secrete monoclonal antibodies specific for the detection of (uncooked) chicken muscle proteins; two of the monoclonals can also be used to detect turkey protein, but the third cannot, thereby affording a means of distinguishing between chicken and turkey by indirect ELISA.[31] No cross-reaction occurs with similar soluble muscle protein extracts from pork, beef, lamb, horse or rabbit, or with other proteins such as casein, gelatin and soya. Further, results obtained from the analysis of chicken organs indicated that all three monoclonal antibodies are apparently muscle-specific when used in an "indirect" ELISA format, a similar finding to that reported later in this paper for heat-processed pig meat.

Heat Process/Retorted Meat Products

A major disadvantage of species recognition via blood proteins is that it is not applicable to the analysis of well-cooked or retorted meat products. While it can be shown that the response of beef to conventional antisera remains constant up to 60 °C, irrespective of whether the meat was raw (frozen) or had been cooked for 1 h in a water-bath at 50 or 60 °C, above this temperature there is a marked decrease in response, and eventually no evidence of beef can be detected after heating for 1 h at 80 °C or above. Heating to temperatures between 60 and 80 °C progressively destroys the antigenic sites on the blood proteins that are recognised by the antisera. Some products heated in commercial processes to nominally higher temperatures may still contain a core of less severely denatured protein, which can be recognised by these conventional methods. However, in order to detect proteins after thorough heating to >80 °C, either a heat-stable antigen must be selected or the heat-denatured protein "renatured" to restore its antigenicity. Heat-stable antigens that retain their immunological properties, even after autoclaving at 120 °C for 30 min, have been observed in autoclaved extracts of adrenals and adrenal/kidney tissue; one of these antigens is both species-specific and widely distributed in other organs including muscle, and has been made the basis (with the corresponding antibodies) of an immunodiffusion test.[32]

Detection of pig meat is of particular interest because of its rejection by Moslem peoples. Several independent ELISA methods have now been reported, which can identify pig meat in heated processed meats and meat products. The capture ELISA of Berger *et al.*[33] has the ability to detect very low levels of heated pig meat extract in beef, chicken or horse muscle extract. It is based on the detection of a highly soluble, heat-resistant component of fresh, unheated pork, which hitherto had been isolated in very pure form and used successfully as the immunogen. A simpler indirect assay, described by Kang'ethe and Gathuma,[34] detected similar, soluble "thermostable" antigen analytes derived from saline extracts of the meat. This approach was effective for the species identification of autoclaved, boiled or raw meats and, in the examples quoted, was capable of detecting *ca.* 3% of specified species in a mixture of meats. A third procedure, developed in our laboratory, was based on thermostable muscle components prepared by a special extraction and autoclaving procedure, and used as an antigen to produce the anti-species muscle antiserum.[35]

Research elsewhere has revealed other more unusual biochemical properties of pig muscle that can be used as indicators of its presence in raw and heated products. The rare muscle-specific peptide balanine (β-alanyl-3-methylhistidine), which, amongst the common meat species, is virtually unique to the pig, can be detected by high-performance liquid chromatography.[36] Also, a rare fatty acid, eicosa-11,14-dienoic acid (C 20 : 2), has been found in pork and lard by using gas chromatographic analysis of the methyl esters; in this

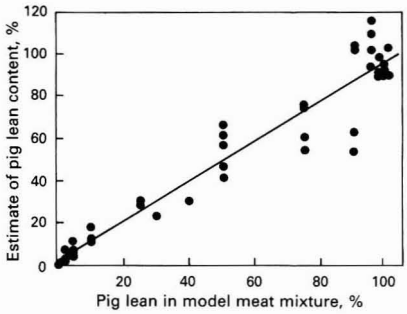

Fig. 1. Determination of pig lean meat in model meat mixtures. Correlation coefficient (r), 0.94; $y = 1.27 + 0.95x$

Table 2. Variation in response of different pig muscles to the anti-pig reagent, expressed as equivalent percentage of pig lean meat

Muscle	Equivalent of typical pork lean,* %
Longissimus dorsi	95.5‡
Semitendinosus (pale)†	140.8
Semitendinosus (dark)	146.1
Vastus	134.1
Gluteus medius	124.2
Triceps laterli	130.4
Diaphragm	86.9
Tongue	45.7

* "Typical" pork lean was prepared from a selected range of pig muscles.

† The *semitendinosus* muscle was divided into the pale and dark zones for separate extraction and analysis.

‡ Each value is the average calculation of two wells.

instance, a detection limit of 1% pork in beef and mutton was achieved.[37] Although these methods may be considered suitable for quality control in special circumstances, considerable investment in equipment and expertise is required.

In our system for the detection of heated pig meat in a variety of meat products, a protocol for sample preparation was developed and two ELISA procedures were evolved. An ELISA of the "indirect" type was used to screen the initial crude antiserum for specificity to pig protein, and to determine whether it responded exclusively to pig muscle proteins or also to, *e.g.*, components of porcine blood, offals, collagen and fat. Table 1 shows that various pig organs including heart muscle all gave significantly lower absorbance values than those of samples of the skeletal muscles. By using the same "indirect" procedure, increasing percentages (5–95%) of pork in beef mixture gave absorbance values that were linearly related to the percentage of pork lean ($r = 0.99$). Apparent equivalences of 20–30% pork lean were given by heart and liver; kidney, spleen and lungs gave 10–15%, and brain gave 5.4%. Gelatin (from pig skin) gave a high response equivalent to 29% pig lean, while some pig fat extracts gave responses equating up to 50% pork lean; this surprisingly high response may result from the active component residing in the connective tissue network, elements of which are common to both the musculature and the adipose tissue. Hence, although this form of the assay clearly detected less of the active antigen in the heat-treated organs and in fat than in the skeletal muscle and tongue, it did not provide an unequivocal means of distinguishing between the offals and lean meat mixtures containing <50% pork meat. However, there was no response either to skeletal muscle, tongue, heart or any of the offals of bovine, ovine or equine origin.

Comment

For the determination of lean meat content, a "competitive" step was introduced at the beginning of the assay to give optimum sensitivity to pork lean content between 5 and 100%, and to accommodate variations in the composition of sample extracts due to the presence of other non-meat components. In this form of the assay, in which high coloration is generated for low concentrations of the active antigen, the major pig offals, fatty tissues and gelatin gave only small reductions in absorbance from the maximum antibody binding value (*i.e.*, the high colour "blank" when no antigen is present); extracts of beef, sheep and chicken were also "negative." Fig. 1 shows results for pork lean content in a range of carefully formulated lean meat mixtures of low pork fat content; other meat species were beef, mutton and chicken. Overall, there was a significant linear relationship between the extracted content of pig lean and the original formulation ($r = 0.94$ on 52 points, $p < 0.001$). Hence, in contrast to the foregoing "indirect" procedure, this competitive form of the ELISA is virtually specific for the presence of the muscle antigens and so potentially offers a means for determining the lean meat content. This occurs because the assay in this form is not sufficiently sensitive to detect the relatively low concentration of the heat-stable antigen present in the tissues of the main offals, collagen or fat. However, as a result of the variation in response obtained for individual muscles of the carcass (Table 2), when compared against a "standard" mixture prepared from a selected range of pig muscles, the determination of lean meat content using this procedure still cannot be considered as absolute.

References

1. Jones, D., Shorley, D., and Hitchcock, C. H. S., *J. Sci. Food Agric.*, 1982, **33**, 677.
2. Sinclair, A. J., and Slattery, W. J., *Aust. Vet. J.*, 1982, **58**, 79.
3. King, N. L., and Kurth, L., *J. Food Sci.*, 1982, **47**, 1608.
4. Slattery, W. J., and Sinclair, A. J., *Aust. Vet. J.*, 1983, **60**, 47.
5. Jones, S. J., *in* Patterson, R. L. S., *Editor*, "Biochemical Identification of Meat Species," *Proceedings of the Commission of the European Communities Seminar*, Elsevier Applied Science, London, 1985, p. 193.
6. Babiker, S. A., Glover, P. A., and Lawrie, R. A., *Meat Sci.*, 1980, **5**, 473.
7. King, N. L., *Meat Sci.*, 1984, **11**, 59.
8. Kurth, L., and Shaw, F. D., *Food Technol. Aust.*, 1983, **35**, 328.
9. Ouchterlony, O., *Acta Pathol. Microbiol. Scand.*, 1949, **26**, 507.
10. Statutory Instruments 1987, No. 2236, "Food Hygiene—The Meat Inspection Regulations," HM Stationery Office, London, 1987, p. 1, para. 2.
11. Warnecke, M. O., and Saffle, R. L., *J. Food Sci.*, 1968, **33**, 131.
12. Hayden, A. R., *J. Food Sci.*, 1977, **42**, 1189.
13. Hayden, A. R., *J. Food Sci.*, 1979, **44**, 494.
14. Hayden, A. R., *J. Food Sci.*, 1978, **43**, 476.
15. Swart, K. S., and Wilks, C. R., *Aust. Vet. J.*, 1982, **59**, 21.
16. Jones, S. J., Patterson, R. L. S., and Kestin, S. C., "Proceedings of the Thirty-second European Meeting of Meat Research Workers," Ghent, 1986, Volume II, p. 485.
17. Anon, *Meat Manuf.*, 1987, **1**, 10.
18. Ansfield, M., and Allsup, T. N., *in* Patterson, R. L. S., *Editor*, "Biochemical Identification of Meat Species," *Proceedings of the Commission of the European Communities Seminar*, Elsevier Applied Science, London, 1984, pp. 160 and 176.
19. Kang'ethe, E. K., James, S. J., and Patterson, R. L. S., *Meat Sci.*, 1982, **7**, 229.
20. Hitchcock, C. H. S., and Crimes, A. A., *Anal. Proc.*, 1983, **20**, 413.
21. Whittaker, R. G., Spencer, T. L., and Copland, J. W., *J. Sci. Food Agric.*, 1983, **34**, 1143.
22. Neaves, P., Patel, P. D., and Woods, L. F. J., *BFMIRA Tech. Circ. No. 777*, British Food Manufacturing Industries Research Association, Leatherhead, Surrey, 1983.

23. Johnston, L. A. Y., Tracey-Patte, P. D., Pearson, R. D., Hurrel, J. G. R., and Aitkin, D. P., *in* Morris, B. A., and Clifford, M. N., *Editors*, "Immunoassays in Food Analyses," Elsevier Applied Science, London, 1985, p. 95.
24. Patterson, R. M., Whittaker, R. G., and Spencer, T. L., *J. Sci. Food Agric.*, 1984, **35**, 1018.
25. Jones, S. J., and Patterson, R. L. S., *Meat Sci.*, 1985, **15**, 1.
26. Patterson, R. M., and Spencer, T. L., *Meat Sci.*, 1985, **15**, 119.
27. Griffiths, N. M., and Billington, M. J., *J. Sci. Food. Agric.*, 1984, **35**, 909.
28. Jones, S. J., and Patterson, R. L. S., *J. Sci. Food. Agric.*, 1986, **37**, 767.
29. Weitz, B., *J. Hyg.*, 1952, **50**, 285.
30. Kohler, G., and Milstein, C., *Nature (London)*, 1975, **256**, 495.
31. Martin, R., Wardale, R. J., Jones, S. J., Hernandez, P. E., and Patterson, R. L. S., *Meat Sci.*, 1989, **25**, 199.
32. Hayden, A. R., *J. Food Sci.*, 1981, **46**, 1810.
33. Berger, R. G., Mageau, R. P., Schwab, B., and Johnston, R. W., *J. Assoc. Off. Anal. Chem.*, 1988, **71**, 406.
34. Kang'ethe, E. K., and Gathuma, J. M., *Meat Sci.*, 1987, **19**, 265.
35. Patterson, R. L. S., and Jones, S. J., "Proceedings of the Thirty-fifth International Congress on Meat Science and Technology," Copenhagen, 1989, Volume II, p. 529.
36. Carnegie, P. R., Illic, M. Z., Etheridge, M. O., and Collins, M. G., *J. Chromatogr.*, 1983, **261**, 153.
37. Saeed, T., Abu-Dagga, F., and Rahman, H. A., *J. Assoc. Off. Anal. Chem.*, 1986, **69**, 999.

Paper 9/03355F
Received August 7th, 1989
Accepted November 1st, 1989

Estimation of Analytical Values From Sub-detection Limit Measurements for Water Quality Parameters*

James E. Gaskin, T. Dafoe and P. Brooksbank
Water Quality Branch, Inland Waters Directorate, Environment Canada, Ottawa, Ontario K1A 0H3, Canada

A method is described for estimating analytical values for water quality parameters from sub-detection limit measurements. The method, which is referred to as the error approximation (EA) procedure, relies on quality control analytical procedures and on the assumption that the bulk of the analytical error associated with measurements at or near the detection limit exists within $k = -3$ to $+3$ standard deviations for normally (or approximately normally) distributed errors. The EA procedure also assumes that the analytical errors are equally distributed on each side of half the detection limit and that the sub-detection limit value lies between zero and the detection limit.

Keywords: *Detection limit; limit of quantification; quality control; error approximation procedure; censored data*

Non-detected (ND) values, which are often referred to as "censored data," occur regularly in the experimental analysis of water quality samples containing trace amounts of organic and inorganic chemical constituents. When only the largest values can be observed from an experimental analysis, the data are said to be "censored on the left." If only the smallest values can be observed, the data are said to be "censored on the right." Left-censored data are of major concern to water quality data analysts.

The censoring of water quality data results in a loss of information. Data that include ND values contain less information than data for which numbers are reported, even if some of those numbers are very imprecise.[1] The statistical literature contains a number of procedures for dealing with ND values. These procedures relate to parameter estimation, goodness of fit, regression and several other approaches. It is generally accepted that methods suitable for estimating ND values are sensitive to assumptions about the underlying distribution. Several distributions found in uncensored water quality data are used for purposes of simulation. Gilliom and Helsel[2] used the Monte Carlo simulation technique to mimic as closely as possible the types of data that actually occur for concentrations of trace constituents in water. They also developed ways for matching the estimated form of a distribution with a particular estimator (for mean, variance and median) by using the relative quartile range of the uncensored portion of the sample data. Porter[3] has provided goodness of fit tests, parameter estimation, tests for trend and two-sample comparisons using left-censored sample data from normally and lognormally distributed populations. Gilbert and Kinnison[4] have described in detail the use of estimators for samples from lognormally distributed populations. In addition, they have provided guidelines for determining when censored data can be considered to be distributed lognormally. Porter *et al.*[1] favour estimating the population mean and then using the confidence interval to indicate the information content of the water quality sample. These workers also support the reporting of negative results in order that valid inferences may be made from data sets. Different arbitrary values have been substituted for missing data in censored results. Nehls and Akland,[5] Gilbert and Kinnison,[4] McBean and Rover,[6] Helsel[7] and others have substituted values as varied as zero, half the detection limit and the detection limit. Winsorised procedures,[8] while addressing the estimation of means, standard deviations and confidence limits from data sets that contain ND values, have adopted the method of replacing ND values with the lowest non-censored value of the nearest neighbour. The trimmed means approach[9] is less exact and discards the missing ND values and a matching number of the highest values.

Experimental

Reagents

Analytical-reagent grade chemicals were used, and de-ionised, distilled water was used for preparing all aqueous solutions.

Apparatus

An inductively coupled argon plasma spectrometer (Model 3580) from Applied Research Laboratories, and a direct current argon plasma spectrometer (Spectrospan 6) from Spectrometric/Beckman, were used for the determination of Cu, Fe and Mn. A Technicon Autoanalyzer II was used for measuring nitrate concentrations.

The determination of polychlorinated biphenyls (PCBs) was carried out on a gas chromatograph [Hewlett-Packard (HP) 5890] coupled to a mass spectrometric detector (HP 5970).

Theory

Most analytical measurements are accompanied by errors that follow a normal distribution. When a sufficiently large number

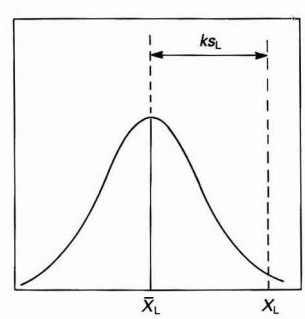

Fig. 1. Normal distribution curve for a measured X_L value

* Presented at SAC 89, the 8th SAC International Conference on Analytical Chemistry, Cambridge, UK, 30 July–5 August, 1989.

of observations is made, plotting the measured responses would produce a curve similar to that in Fig. 1.

For a limited number of measurements on a given water quality sample where the number of replicates is less than 20, the population mean, μ, is replaced by $\bar{X}_L$, and the population standard deviation, σ, by s_L in Fig. 1. The use of $k = 3$ allows a confidence level of 99.8% for measurements following a normal or approximately normal distribution. If X_L does not follow a normal distribution, then the probability that $X_L \geqslant \bar{X}_L + 3s_L$ would be $100(1 - 1/k^2)$ or 88.9% according to "Tschebyshev's inequality rule."[10]

Long and Winefordner[11] have suggested that values of $k < 3$ should not be used for limit of detection calculations.

The range of values for X_L can be demonstrated by

$$\bar{X}_L - ks_L \leqslant X_L \leqslant \bar{X}_L + ks_L \quad \ldots \quad (1)$$

where X_L is the lowest measurable value, $\bar{X}_L$ is the mean of the replicate X_L values and s_L is the standard deviation for the replicate values.

Another expression for referencing individual replicate values can be written as:

$$X_i = D(i - 1)/(n - 1) \quad \ldots \quad (2)$$

where X_i is an individual value for $i = 1, 2, 3, \ldots, n$, D is the detection limit value and n represents the number of replicate observations.

The expression:

$$X_L \geqslant \bar{X}_L + ks_L \quad \ldots \quad (3)$$

best represents the probability that the analyte would be detected if it were present in any measurable amount.

Results and Discussion

The data in Table 1 represent analytical results from three separate samples for three water quality parameters (dissolved Fe, dissolved Mn and PCBs). Quality control procedures were employed in each instance.

Calculations

Estimating the ND value for each water quality parameter in Table 1 simply involves finding the mean value ($\bar{X}_L$) and the sample standard deviation (s_L) from the experimental observations and then applying the value of $k = 3$ to equation (3).

For n data results: $X_1, X_2, X_3, \ldots, X_n$; $\bar{X}_L = 1/n(\Sigma X_i)$, and, $s_L = [\Sigma(X_i - \bar{X}_L)/(n - 1)]$.

The estimated values for the three parameters are:

(*a*) Dissolved Fe = [0.75 + 3(0.017)] μg l^{-1} = 0.80 μg l^{-1}

(*b*) Dissolved Mn = [0.83 + 3(0.016)] μg l^{-1} = 0.88 μg l^{-1}

(*c*) PCBs = [3.9 + 3(0.40)] ng l^{-1} = 4.1 ng l^{-1}

Table 1. Less than detection limit (DL) results for three water quality parameters

Dissolved Fe (ICP)*/μg l^{-1}	Dissolved Mn (ICP)*/μg l^{-1}	PCBs (GC - MS†)‡/ ng l^{-1}
0.73	0.81	3.5
0.75	0.83	4.2
0.75	0.85	3.7
0.76	0.83	3.8
0.75	0.81	4.3
0.75	0.82	
0.76	0.84	
0.75	0.85	
0.73	0.85	
0.74	0.82	

* DL = 1.00 μg l^{-1}.
† GC - MS = gas chromatography - mass spectrometry.
‡ DL = 5.0 ng l^{-1}.

Comparison Between Sub-detection Limit Data From Two Analytical Methods

Sometimes it may be possible to verify that the suggested EA procedure does indeed produce a reliable estimate of the analyte of interest. Verification may be effected by comparing the results obtained with a given method with those obtained using a more sensitive method. This approach can be illustrated by using the data in Table 2. The data for Cu were obtained by two methods, namely, directly coupled plasma (DCP) and inductively coupled plasma (ICP) atomic emission spectrometry.

Estimated values

$$X_{DCP} = [0.63 + 3(0.01)]\ \mu g\ l^{-1} = 0.66\ \mu g\ l^{-1}$$

$$X_{ICP} = [0.06 + 3(0.05)]\ \mu g\ l^{-1} = 0.21\ \mu g\ l^{-1}$$

Note that $DL_{ICP} < DCP_{estimate} < DL_{DCP}$ (DL = detection limit).

As $DCP_{estimate} > DL_{ICP}$, it is reasonable to suggest that if sub-samples corresponding to the measurements in Table 2 were subjected to both analytical methods, a measurement at or above the limit of quantification (LOQ) would be registered with the ICP method.

The relationship between LOQ and DL is given by the expression

$$LOQ = DL + 7s_b \quad \ldots \quad (4)$$

or

$$LOQ = R_b = 10s_b \quad \ldots \quad (5)$$

where R_b is the average signal (level) of the blank (sample) and s_b is the standard deviation of the replicate determinations. The LOQ may be defined as the lower limit for precise quantification as against qualitative detection.

Using equation (5) for the ICP data in Table 2, the LOQ is calculated as

$$LOQ = [0.06 + 10(0.05)]\ \mu g\ l^{-1} = 0.56\ \mu g\ l^{-1}$$

The LOQ for the ICP system is less than the lowest measurable value on the DCP system, and it is clearly demonstrated that an amount that is less than the detection limit on the less sensitive system (DCP) is predictably measurable on the more sensitive sytem (ICP).

Evaluation of the EA Procedure

A number of simple methods have been used occasionally to estimate means and variances from data containing ND results. Three such methods are: (*a*) Winsorisation; (*b*) trimmed means; and (*c*) substitution of arbitrary quantities. The Winsorisation method combines elimination and substitu-

Table 2. Less than detection limit (DL) results for Cu from two analytical methods

DCP*		ICP†	
Replicate No.	Measurement/ μg l^{-1}	Replicate No.	Measurement/ μg l^{-1}
1	0.62	1	0.10
2	0.64	2	0
3	0.64	3	0
4	0.63	4	0.10
5	0.63	5	0.10
6	0.62	6	0.10
7	0.61	7	0
8	0.62	8	0.10
9	0.62	9	0.10
10	0.62	10	0

* DL = 2.00 μg l^{-1}.
† DL = 0.20 μg l^{-1}.

tion procedures, and the trimmed means method is essentially an elimination process.

Table 3 shows results of measurements on 12 samples for the NO_3/NO_2 water quality parameter. Column 1 contains the experimental results for the 12 individual samples and columns 2 and 3 contain the replicated measurements for two samples (A and B) containing amounts of NO_3/NO_2 less than the detection limit (20 μg l^{-1}). Measurements in column 1 were conducted prior to those in columns 2 and 3.

When the two ND values are estimated by six estimation procedures: (*i*) Winsorisation (WINS); (*ii*) trimmed means (TRIMMS); (*iii*) error approximation (EA); (*iv*) substitution of the detection limit (SDL); (*v*) substitution of half the detection limit (SHDL); and (*vi*) substitution of zero (SZ), the results in Table 4 are obtained. Table 5 gives a summary of the means and variances calculated from the estimation procedures.

Table 3. Analytical results with ND values for NO_3/NO_2

Replicate determinations below the DL (20.0 μg l^{-1})		
Sample/μg l^{-1}	Sample A/μg l^{-1}	Sample B/μg l^{-1}
(A) ND	9.8	14.2
(B) ND	10.2	13.8
(C) 40.0	10.0	14.0
(D) 60.3	9.7	14.2
(E) 45.5	10.0	14.3
(F) 32.0	10.3	13.8
(G) 29.4	9.8	13.7
(H) 52.1	10.1	14.0
(I) 36.4	10.2	13.9
(J) 62.0	10.3	14.1
(K) 23.5		
(L) 48.6		

Table 4. Analytical results with estimated ND values for NO_3/NO_2 (μg l^{-1})

SDL	SHDL	WINS	EA	SZ	TRIMMS
20	10	23.5	10.7	0	—
20	10	23.5	14.6	0	—
23.5	23.5	23.5	23.5	23.5	23.5
29.4	29.4	29.4	29.4	29.4	29.4
32.0	32.0	32.0	32.0	32.0	32.0
36.4	36.4	36.4	36.4	36.4	36.4
40.0	40.0	40.0	40.0	40.0	40.0
45.5	45.5	45.5	45.5	45.5	45.5
48.6	48.6	48.6	48.6	48.6	48.6
52.1	52.1	52.1	52.1	52.1	52.1
60.3	60.3	52.1	60.3	60.3	—
62.0	62.0	52.1	62.0	62.0	—

Table 5. Summary and comparison of statistics obtained from Table 4

	Statistics	
Estimation procedure	Mean ($\bar{x}$)/μg l^{-1}	Variance (s^2)/μg l^{-1}
(*i*) WINS	38.2	137.4
(*ii*) TRIMMS	38.4	99.0
(*iii*) EA	37.9	278.2
(*iv*) SDL	39.2	218.1
(*v*) SHDL	37.5	302.9
(*vi*) SZ	35.8	418.0

The Winsorisation and trimmed means processes both lead to a shrinkage in the dispersion of values of a given data set and ultimately to a reduction in the size of the variance. Evidence of the latter is seen in Table 5 for the variance values associated with statistical methods (*i*) and (*ii*). On the other hand, substitution of zero or half the detection limit causes a greater spread among the data values and hence a subsequent increase in the size of the variance. The variance associated with the EA procedure lies between the smallest and largest variances. In general, if the detection limit is substituted for the ND value, $\bar{x}$ and s^2 will be biased high and low, respectively. With the substitution of zero, the reverse bias will occur with $\bar{x}$ and s^2. Substitution of half the detection limit will give a mean value, which is biased between the values obtained for the substitution of DL and zero; a biased s^2 value will also result.

Significance Testing

To test if there are any significant differences between the mean values in Table 5, an analysis of variance (ANOVA) of the data in Table 4 is required. The trimmed means process leads to an elimination of a chosen percentage of the lowest values and an equal percentage of the highest values in a data set. As a result of this elimination procedure, there is an absence of results in column 6 of Table 4, and this column must be omitted from the ANOVA process. The results of the analysis are shown in Table 6.

At a significance level of 0.05, there is insufficient evidence to reject the null hypothesis that the data samples come from populations with equal means. In essence, the ANOVA results appear to suggest that because the estimated means are not significantly different from each other, it is unimportant which estimation procedure is used. However, caution must be exercised in accepting such an inference, and the method which incorporates the least bias in its estimation procedure should be given preference when a particular procedure is being chosen for estimating ND values.

Conclusion

In the past, various statistical techniques have been used to estimate ND values for water quality parameters. Some of the techniques were simple, others fairly complicated. The simple techniques,[4,6,12] although useful, suffered from the arbitrary nature with which the selection of the substituted values was made. The more difficult techniques[4,13–16] depended heavily on the choice of the distribution function (normal, lognormal, etc.) that best fitted the experimental data.

The use of distribution functions to estimate maximum likelihood parameters from censored data have had the following shortcomings.

(1) Only relatively large data sets were adequate for the required data analysis.
(2) Estimation of censored data depended solely on non-censored data.
(3) Different data segments accumulated over the collection period (sometimes 3–10 years) were assumed to come from one data population. However, this assumption appears unjustified, as water quality samples collected at different intervals could have variable

Table 6. Results of the analysis of variance. DF = Degrees of freedom; SS = sum of squares; MS = mean square; F = the *F*-distribution ratio = [MS(factor)/MS(ratio)] in this context; and SIG. LEV. = significance level

0	1. DF	2. SS	3. MS	4. F	5. SIG. LEV.
1. Factor*	5	319.79	63.96	0.23	0.95
2. Error	55	15 542.35	282.59		
3. Total	60	15 862.14			

* The factor term refers to the different estimation procedures (SHDL, SDL, WINS, EA and SZ).

matrix effects, and differences in sample handling and operational procedures could bring about significant variation in the analytical measurements for the same parameter. Instead of being one data population, the data set could then be a composite of several data populations with unequal variances.

(4) If the comments in (1)–(3) are valid, then a significant amount of bias could be injected into the values of the estimated distributional parameters.

The EA method, for its part, provides an appropriate procedure for the estimation of values below the detection limit, if the analytical measurements are obtained under statistically controlled conditions. In any effort to obtain a measurement that is lower than the detection limit, a flagging mechanism must be in place during the laboratory analysis. The flag should indicate the presence of a zero value or a value that is less than the detection limit and the sample should then be re-analysed using effective quality control procedures. In this way, measurable sub-detection limit amounts if present, can be determined or estimated.

If the analytical measurements below the detection limit are less than the blank readings, then the missing values can be equated to zero.

References

1. Porter, P. S., Ward, R. C., and Bell, H. F., *Environ. Sci. Technol.*, 1988, **22**, 856.
2. Gilliom, R. J., and Helsel, D. R., "Estimation of Distributional Parameters for Censored Trace-level Water Quality Data," US Geological Survey open file report 84-729, US Geological Survey, Reston, VA, 1984.
3. Porter, P. S., *PhD Thesis*, Colorado State University, 1986.
4. Gilbert, R. O., and Kinnison, R. R., *Health Phys.*, 1981, **40**, 377.
5. Nehls, G. J., and Akland, G. G., *J. Air Pollut. Control Assoc.*, 1973, **23**, 180.
6. McBean, E. A., and Rover, F. A., *Groundwater Monit. Rev.*, 1984, 42.
7. Helsel, D. R., *in* El-Shaarawi, A. H., and Kwiatkowski, R. E., *Editors*, "Estimation of Distributional Parameters for Censored Water Quality Data," Statistical Aspects of Water Quality Monitoring, Proceedings of Workshop, CCIW, Ontario, Canada, 1985, pp. 137–157.
8. Atkinson, G. F., "Statistical Tests with Observations Below Detection Limits," Systems and Informatics Directorate, Environment Canada, Hull, Quebec, 1988.
9. Gaskin, J. E., "Approximate Estimation of Analytically Non-detected Values for Water Quality Parameters," Water Quality Branch, IWD, Environment Canada, Ottawa, Ontario, Canada, 1988.
10. Dowdy, S., and Wearden, S., "Statistics for Research," Wiley, New York, 1983, pp. 135 and 136.
11. Long, G. L., and Winefordner, J. D., *Anal. Chem.*, 1983, **55**, 712A.
12. Gilliom, R. J., and Helsel, D. R., "Estimation of Distributional Parameters for Censored Trace-level Water Quality Data," Water Resources Research, US Geological Survey, Reston, VA, 1986, Volume 22, No. 2, pp. 135–146.
13. McBean, E. A., *in* El-Shaarawi, A. H., and Kwiatkowski, R. E., *Editors*, "Alternatives for Identifying Statistically Significant Differences," Statistical Aspects of Water Quality Monitoring, Proceedings of Workshop, CCIW, Ontario, Canada, 1985, pp. 326–334.
14. Gupta, A. K., *Biometrika*, 1952, **39**, 260.
15. Cohen, A. C., *Technometrics*, 1959, 1.
16. Aitchison, J., and Brown, J. A. C., "The Lognormal Distribution," Cambridge University Press, Cambridge, MA, 1969.

Paper 9/04185K
Received October 2nd, 1989
Accepted December 12th, 1989

Simple and Unambiguous Method for Identifying Urinary Acylcarnitines Using Gas Chromatography - Mass Spectrometry*

Stephen Lowes and Malcolm E. Rose†
Department of Chemistry, The Open University, Walton Hall, Milton Keynes, MK7 6AA, UK

Several inherited metabolic disorders, particularly the organic acidurias and acidemias, are often characterised by excretion of acylcarnitines, especially octanoylcarnitine, in the urine. Clinical investigation of such serious disorders ideally requires a rapid, simple and selective method for determining acylcarnitines in urine. Initial results are given here of a method that may approach this ideal. The procedure involves chemical derivatisation, in which the zwitterionic acylcarnitines are cyclised to volatile lactones, and analysis by gas chromatography and gas chromatography - mass spectrometry. Preparation of urine samples by ion-exchange purification and an illustrative application of the proposed method to a clinical sample are also outlined.

Keywords: *Acylcarnitine; gas chromatography - mass spectrometry; chemical derivatisation; urine; clinical analysis*

In an energy producing pathway, fatty acids are broken down into acetyl units by a β-oxidation process occurring in human mitochondria.[1] To undergo β-oxidation, fatty acids are first activated by condensation with coenzyme A (CoA). However, the resulting medium and long chain fatty acyl-CoA compounds are unable to pass through the mitochondrial membrane. Carnitine (**I**) acts as a carrier for the acyl moieties by reacting with acyl-CoA compounds to give acylcarnitines (**II**). The mitochondrial membrane is permeable to the acylcarnitines so acyl moieties are transported into the mitochondria as zwitterions (**II**). Once inside the mitochondria, acylcarnitines undergo transesterification with CoA so that fatty acyl-CoA compounds and carnitine are regenerated. The resulting acyl-CoA species undergo β-oxidation involving a number of enzymes, notably medium chain acyl-CoA dehydrogenase (MCAD).

Whilst the transport of fatty acids to the site of β-oxidation is considered to be the principal role of carnitine, several other of its metabolic roles have been elucidated in the last decade.[2] For example, the carnitine released in the mitochondria is known to react with potentially toxic excesses of acyl groups again forming acylcarnitines, and thus allowing the acyl moieties to pass out of the cell to be excreted in the urine.

These processes involving acylcarnitines provide an excellent biochemical indication of many metabolic disorders, particularly the organic acidurias and acidemias. For instance, intermittent non-ketotic dicarboxylic acidurias are potentially amenable to diagnosis and biochemical characterisation by a good analytical method for urinary acylcarnitines. Most of these acidurias seem to be caused by a deficiency of MCAD and the disorder frequently presents itself as Reye's syndrome or sudden infant death syndrome. It is often characterised by excretion of acylcarnitines, especially octanoylcarnitine, in neonatal urine.[3] Also, some patients with unexplained intermittent ketosis excrete increased levels of acylcarnitines. The development of a reliable and selective analytical procedure for determining acylcarnitines in urine would further the understanding and aid the rapid diagnosis of such diseases.

Gas chromatography - mass spectrometry (GC - MS), because of its selectivity, sensitivity and routine nature,[4,5] is the favoured technique for neonatal screening of normal urinary organic acids. Unfortunately, methods based on GC

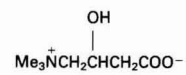

(**I**)

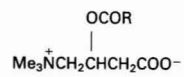

(**II**)

cannot be applied directly to acylcarnitines because the compounds (**II**) are non-volatile. The only reported method utilising GC involves hydrolysis of acylcarnitines, followed by an examination of the fatty acids liberated.[6] The procedure is lengthy and difficult to apply routinely and it is also possible that the fatty acid analytes originate from acyl-containing substances other than acylcarnitines.

Several other methods for analysing urine for acylcarnitines have been reported but none is yet ideal for routine clinical analysis. The methods have been reviewed recently.[7] They include two mass spectrometric approaches: fast atom bombardment followed by tandem mass spectrometry (FABMS - MS) and liquid chromatography - mass spectrometry (LC - MS). The latter is still proving itself at physiological levels but cannot be considered as routine for clinical work, and the former is complex, costly and generally unable to handle mixtures of isomeric acylcarnitines.[7] Therefore, GC - MS may be the technique that is most likely to provide a definitive and routine clinical method at a realistic cost. Any such method could be readily integrated into existing GC - MS screening procedures for urinary organic acids. In order to exploit the strengths of GC - MS in this area, we are developing an extremely simple derivatisation in which acylcarnitines are cyclised to give volatile lactones (Fig. 1). Importantly, the resulting acyl-containing lactones (**III**) retain a structural memory of their origin. That is, in (**III**) the fatty acid acyl unit is still bound to a diagnostic residue of carnitine, unlike the hydrolysis approach[6] in which the molecular integrity of the fatty acid acyl group with its carnitine parent is lost. In this paper, a preparation by use of ion-exchange purification, the chemical derivatisation, the examination of the lactones (**III**) by GC and GC - MS, and an initial application to a clinical sample are described.

* Presented at SAC 89, the 8th SAC International Conference on Analytical Chemistry, Cambridge, UK, 30 July–5 August, 1989.

† To whom correspondence should be addressed.

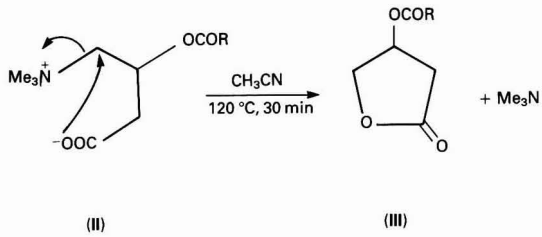

Fig. 1. Derivatisation of acylcarnitines (**II**) to volatile acyl-containing lactones (**III**, R = CH_3, C_7H_{15}, $C_3H_6C_6H_5$ or $C_{15}H_{31}$)

Experimental

Materials and Reagents

DL-Carnitine hydrochloride, thionyl chloride (gold label), acetyl chloride, palmitic acid, 4-phenylbutanoic acid and *N,N*-di-isopropylethylamine were obtained from Aldrich and used without further treatment. Trichloroacetic acid (gold label) was also obtained from Aldrich but was recrystallised from ethanol-free chloroform before use. Acetyl-, octanoyl- and palmitoyl-DL-carnitine hydrochloride were obtained from Sigma, malic acid, ethyl acetate (Distol grade) and acetonitrile (Distol grade) from Fisons, other solvents and octanoic acid from BDH, ReactiVials (1-ml volume) from Pierce and analytical-grade ion-exchange resins from Bio-Rad.

Gas Chromatography

A Carlo Erba Model 5300 Mega series gas chromatograph was used. A BP5 fused-silica column from SGE, 25 m × 0.33 mm i.d. and with a film thickness of 0.5 μm was used. Helium carrier gas flowed through the column with an average linear velocity of 35 cm s^{-1}. The hydrogen and air inlet pressures (for the flame-ionisation detector) were 70 and 120 kPa, respectively. The detector was maintained at 280 °C. The oven temperature was programmed from 87 to 250 °C at a rate of 10 °C min^{-1}. The temperature ramp rate started immediately after injection and on reaching 250 °C was maintained at this temperature for 15 min. Cold on-column injections were performed by using a 5-μl gas-chromatographic syringe (Hamilton) with a 7.5-cm needle. Retention times were measured from the time of injection.

Gas Chromatography - Mass Spectrometry

Two instruments were used for GC - MS. (*i*) A VG 20-250 quadrupole system coupled to a Hewlett-Packard Model 5890 gas chromatograph equipped with a fused-silica BP5 capillary column of dimensions 12.5 m × 0.25 mm i.d. and a film thickness of 0.5 μm. Split - splitless injection at 230 °C was used with column conditions as reported above for GC. The direct-line interface was maintained at 180 °C and source temperatures of 175–200 °C were used. (*ii*) An INCOS 50 bench-top quadrupole instrument coupled to a Varian Model 3400 gas chromatograph equipped with a 25-m fused-silica SE54 column and a splitless injector. Again the GC conditions were as reported above. With both instruments electron ionisation (EI) was employed, with an electron energy of 70 eV and an ion current of 100 μA.

Synthesis of Acylcarnitines

The synthesis of pure acylcarnitines from DL-carnitine hydrochloride and fatty acids having 2–18 carbon atoms has been described by Ziegler *et al.*[8] The reported methods were employed to prepare all acylcarnitines used in this study, except 4-phenylbutanoyl-DL-carnitine hydrochloride which was prepared by a modification of Method C.[8]

4-Phenylbutanoic acid (3 g, 9 mmol) was stirred at 55 °C before the addition of freshly distilled thionyl chloride (0.4 g, 3.4 mmol). The mixture was heated and stirred at 60 °C for 1 h, followed by 1 h at 70 °C and 1 h at 80 °C. A solution of DL-carnitine hydrochloride (0.8 g, 4 mmol) in trichloroacetic acid (3 g) at 60 °C was added to the reaction mixture. Stirring was continued at 80 °C for 2.5 h, then the mixture was poured into dry diethyl ether (50 ml). The precipitate was filtered off, washed with diethyl ether and dissolved in hot propan-2-ol (15 ml). This solution was filtered to remove any unreacted carnitine and the filtrate was added to dry diethyl ether (100 ml). The product was allowed to precipitate overnight; the precipitate was then filtered off, washed with diethyl ether and dried. A yield of 0.66 g (57%) was obtained, m.p. 156 °C. FABMS, *m/z* (relative abundance): 308 (100%, $[M - Cl]^+$), 147 (13%, $PhCH_2CH_2CH_2CO^+$), 144 (20%, $Me_3\overset{+}{N}CH{=}CHCH_2COOH$), 100 (32% $Me_3\overset{+}{N}CH{=}CHCH_3$), 91 (21%, $PhCH_2^+$), 85 (50%, $^+CH_2CH{=}CHCOOH$), 58 (42%, $Me_2\overset{+}{N}{=}CH_2$). Infrared (IR): wavenumber, 1735 (ester C=O stretch), 1710 cm^{-1} (acid C=O stretch). ^1H NMR ([$^2H_6$]-dimethyl sulphoxide, 90 MHz): δ 1.8 (m, 2 H, $CH_2CH_2CH_2$), 2.2–2.8 (m, 6 H, $CH_2CH_2CH_2$, CH_2COOH), 3.1 [s, 9 H, $(CH_3)_3$], 3.7 (d, 2 H, NCH_2), 7.2 p.p.m. (m, 5 H, Ph).

Satisfactory analytical data (NMR, FABMS) were obtained for the known acylcarnitines prepared according to the literature.[8] Acetylcarnitine hydrochloride, 76% yield, m.p. 208 °C (lit.,[8] 210 °C); octanoylcarnitine hydrochloride, 59% yield, m.p. 158 °C (lit.,[8] 160 °C); palmitoylcarnitine hydrochloride, 81% yield, m.p. 154 °C (commercial sample, 157 °C; lit.,[8] 161 °C). All three products showed two carbonyl stretching bands in the IR at 1710 (acid) and 1730–1740 cm^{-1} (ester).

Synthesis of Standard Lactones (III)

The preparation of the standard acyl-containing lactone compounds (**III**) was based on the synthesis of β-hydroxy-γ-butyrolactone followed by reaction with the corresponding acid chloride. The synthesis of β-hydroxy-γ-butyrolactone from malic acid was carried out as reported by Henrot *et al.*,[9] except that the reaction time for the reduction of the half-ester[9] was increased from 2 to 20 h in order to produce a significant yield (23% overall from malic acid).

In order to prepare the octanoyl-containing lactone (**III**, R = C_7H_{15}) β-hydroxy-γ-butyrolactone (0.5 g, 4.9 mmol) was dissolved in tetrahydrofuran [THF (10 ml)] and added dropwise to a solution of octanoyl chloride (1.36 ml in 10 ml of THF) at 0 °C. After warming to reflux, the reaction was allowed to proceed for 24 h. The solvent was removed and the product purified by chromatography on silica gel (EtO_2CMe - hexane, 1 + 1). Traces of octanoic acid were removed by washing a solution of the product in diethyl ether with three equal volumes of a saturated solution of $NaHCO_3$. The diethyl ether was removed to leave a clear oil (0.78 g, 70% yield).

Similarly acetyl-, palmitoyl- and 4-phenylbutanoyl-containing lactones were prepared by using acetyl chloride, palmitoyl chloride and 4-phenylbutanoyl chloride, respectively. Satisfactory analytical data were obtained for all four lactones prepared by use of ^{13}C and ^1H NMR, IR and EI mass spectra.

Compound (**III**, R = CH_3), 53% yield. EIMS: identical to that shown in Fig. 3(*a*). IR: wavenumber, 3000–2860 (CH stretch), 1790 (lactone C=O stretch), 1740 cm^{-1} (ester C=O stretch). ^1H NMR ($CDCl_3$, 90 MHz): δ 2.1 (s, 3 H, CH_3), 2.5–3.0 (m, 2 H, CH_2CO), 4.4 (m, 2 H, CH_2OCO) and 5.5 p.p.m. (m, 1 H, CHOCO).

Compound [**III**, R = $(CH_2)_6CH_3$], 70% yield. EIMS: identical to that shown in Fig. 3(*b*). IR: wavenumber, 2980–2860 (CH stretch), 1790 (lactone C=O stretch), 1740 cm^{-1} (ester C=O stretch). ^1H NMR ($CDCl_3$, 90 MHz): δ

0.8–1.7 [m, 13 H, $(CH_2)_5CH_3$], 2.3 (t, 2 H, side-chain CH_2CO), 2.5–3.0 (m, 2 H, ring CH_2CO), 4.4 (m, 2 H, CH_2OCO), 5.5 p.p.m. (m, 1 H, CHOCO). ^{13}C NMR ($CDCl_3$): δ 174 (lactone C=O), 173 (ester C=O), 74 (*C*HOCO), 69 (*C*H_2OCO), 35 (*C*H_2CO), 34 (*C*H_2CO), 32 (CH_2), 29 (CH_2), 28 (CH_2), 25 (CH_2), 23 (CH_2), 14 p.p.m. (CH_3).

Compound [**III**, R = $(CH_2)_{14}CH_3$], 70% yield. EIMS: identical to that shown in Fig. 3(*c*). IR: wavenumber, 2960–2860 (CH stretch), 1790 (lactone C=O stretch), 1740 cm^{-1} (ester C=O stretch). ^1H NMR ($CDCl_3$, 90 MHz): δ 0.8–1.7 [m, 29 H, $(CH_2)_{13}CH_3$], 2.3 (m, 2 H, side-chain CH_2CO), 2.7 (m, 2 H, ring CH_2CO), 4.4 (m, 2 H, CH_2OCO), 5.4 p.p.m. (m, 1 H, CHOCO). ^{13}C NMR ($CDCl_3$): δ 174 (lactone C=O), 173 (ester C=O), 74 (*C*HOCO), 69 (*C*H_2OCO), 35 (*C*H_2CO), 34 (*C*H_2CO), 32–23 (13 × CH_2), 11 p.p.m. (CH_3).

Compound [**III**, R = $(CH_2)_3Ph$], 44% yield. EIMS: identical to that shown in Fig. 3(*d*). IR: wavenumber, 3060–3020 (aromatic CH stretch), 3000–2850 (aliphatic CH stretch), 1795 (lactone C=O stretch), 1740 cm^{-1} (ester C=O stretch). ^1H NMR ($CDCl_3$, 90 MHz): δ 1.8–3.0 [m, 8 H, $(CH_2)_3$ and ring CH_2CO], 4.3 (m, 2H, CH_2OCO), 5.4 (m, 1 H, CHOCO), 7.2 p.p.m. (m, 5 H, Ph). ^{13}C NMR ($CDCl_3$): δ 174 (lactone C=O), 173 (ester C=O), 141 (Ph), 128 (Ph), 126 (Ph), 74 (*C*HOCO), 70 (*C*H_2OCO), 35 (*C*H_2CO), 34 (*C*H_2CO), 33 (Ph*C*H_2), 26 p.p.m. ($CH_2CH_2CH_2$).

Analytical Procedure

Derivatisation of aqueous mixtures of acylcarnitines

Standard solutions containing about 20 μg of each acylcarnitine were concentrated to less than 1 ml by lyophilisation, and transferred into a 1-ml ReactiVial for complete drying. The residue was treated with acetonitrile (0.5 ml) and *N,N*-diisopropylethylamine (0.5 μl). On sealing the ReactiVial, with a Teflon septum, the vessel was heated to 120 °C for 30 min to effect cyclisation (Fig. 1). The solvent was then removed under a stream of argon and the residue dissolved in ethyl acetate (0.2 ml). Any remaining solid material was filtered off and the filtrate analysed for the resulting lactones by GC and GC - MS (typical injection volumes, 1–2 μl).

Urine samples (spiked and clinical)

The double ion-exchange procedure used here was based on the work of Norwood and co-workers.[10,11] Bio-Rad AGI-X8, 100–200 mesh, formate form, anion-exchange resin (2 cm^3) was used to pack a column of 1 cm diameter. The resin was converted to the chloride form by eluting with 1 M HCl (10 ml). The column was then equilibrated with distilled water and the urine sample (0.5 ml) applied to the head of the column. Acylcarnitines, other cationic and neutral species were eluted with distilled water (2 ml). The eluent was acidified with 40 μl of 36% HCl.

Bio-Rad AG50W-X8, 100–200 mesh, hydrogen form, cation-exchange resin (2 cm^3) was used to pack a 1-cm diameter column. The acylcarnitine-containing eluent from above was applied to the column. Neutral and loosely bound cationic species were washed off with 0.01 M HCl (5 ml) and distilled water (5 ml). Acylcarnitines were eluted with 2 M NH_4OH in 20% aqueous ethanol, the first 1 ml being discarded and the following 6 ml collected and freeze-dried.

The resulting residue was dissolved in distilled water (0.5 ml), transferred into a 1-ml ReactiVial and freeze-dried in this vessel. The residue was then subjected to derivatisation in acetonitrile and base, as with the standard mixtures of acylcarnitines.

Results and Discussion

The derivatisation envisaged to convert the zwitterionic acylcarnitines (**II**) into lactones of sufficient volatility for GC involves intramolecular nucleophilic attack of the carboxylate anion on the carbon bearing the trimethylammonium group, resulting in the ejection of trimethylamine (Fig. 1). This scheme is attractive, firstly, because the product (**III**) retains a diagnostic residue of carnitine and secondly, because the process is simple, in principle requiring no reagents. Initial trials of the viability of this cyclisation were conducted on standard aqueous samples of acylcarnitines. Removal of water from the samples was addressed first because acylcarnitines are known to be labile towards hydrolysis and because gas chromatographic analysis was to be applied. Freeze-drying was found to be the most expedient method for removing water. This technique was used to prepare aqueous mixtures of all commercial acylcarnitine hydrochloride salts and synthetic 4-phenylbutanoyl-DL-carnitine hydrochloride [$(CH_3)_3\overset{+}{N}CH_2CH(OCOR)CH_2COOH.Cl^-$, R = CH_3, C_7H_{15}, $C_{15}H_{31}$, or C_3H_6Ph] for the derivatisation.

Several aprotic, non-nucleophilic solvents were tested for dissolving and cyclising the acylcarnitines and acetonitrile was found to be by far the most efficacious, under the conditions reported under Experimental. Additionally, acetonitrile is readily available and easily removed by evaporation following the 30-min derivatisation. A small amount of non-nucleophilic base (*N,N*-diisopropylethylamine) was also added to help maintain a carboxylate anion, as opposed to the less nucleophilic carboxyl group, in the acylcarnitine molecule. This procedure was more important for the derivatisation of commercial and synthesised acylcarnitines than for clinical samples because the former existed as their hydrochloride salts.

Fig. 2 shows the gas chromatogram resulting from the analysis of an aqueous mixture of the four acylcarnitines. The four major peaks, in order of elution, correspond to the expected acetyl-, octanoyl-, phenylbutanoyl- and palmitoyl-DL-carnitine derivatives; their retention times and mass spectra are identical with those of the corresponding, independently synthesised, acyl-containing lactones (**III**): the acetate, octanoate, 4-phenylbutanoate and palmitate esters of β-hydroxy-γ-butyrolactone. The three aliphatic lactones (**III**,

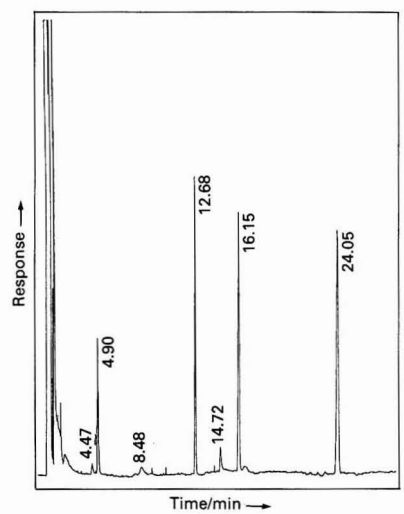

Fig. 2.: Gas chromatogram from a standard mixture of acylcarnitines containing acetylcarnitine (52 nmol), octanoylcarnitine (39 nmol), 4-phenylbutanoylcarnitine (36 nmol) and palmitoylcarnitine (29 nmol). After derivatisation to the acyl-containing lactones, the retention times are 4.90, 12.68, 16.15 and 24.05 min, respectively. Injection volume, 1 μl from a final solution of 200 μl

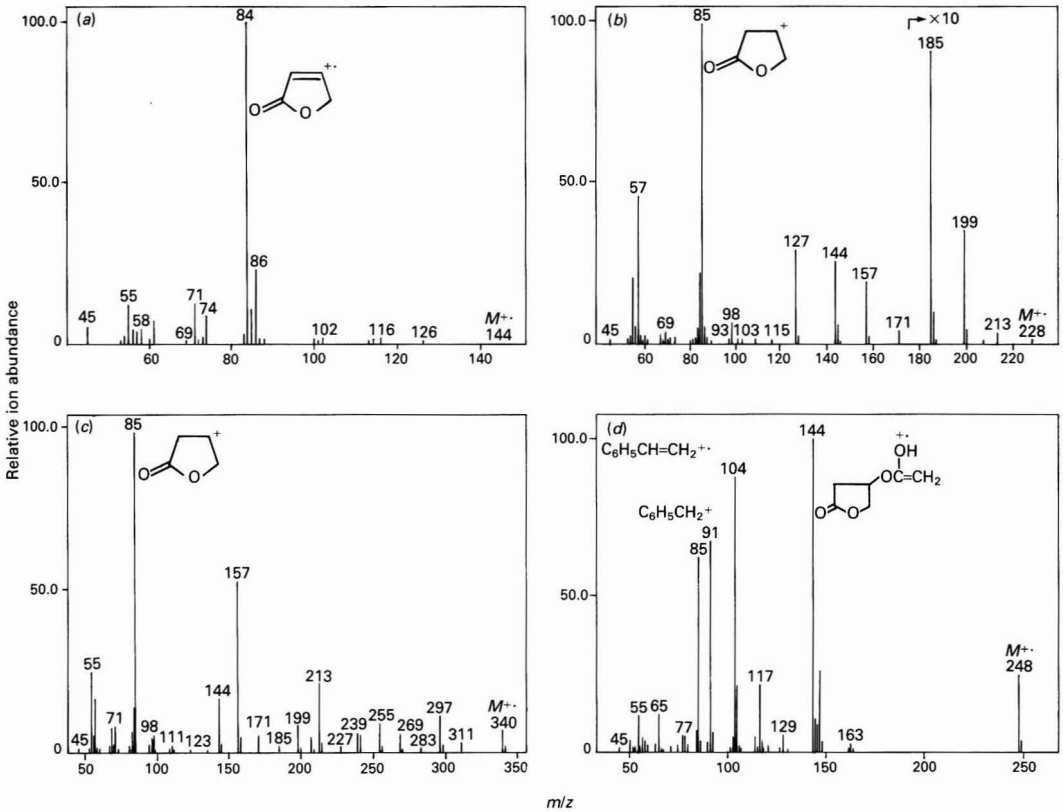

Fig. 3. Electron ionisation mass spectra of the derivatised acylcarnitines as in Fig. 2. (*a*) Acetate ester (**III**, R = CH_3); (*b*) octanoate ester (**III**, R = C_7H_{15}); (*c*) palmitate ester (**III**, R = $C_{15}H_{31}$); and (*d*) 4-phenylbutanoate ester of β-hydroxy-γ-butyrolactone (**III**, R = $C_3H_6C_6H_5$). In (*b*) the relative ion abundance scale has been increased by a factor of 10 above *m/z* 175

R = CH_3, C_7H_{15} or $C_{15}H_{31}$) gave small molecular ion peaks in their EI mass spectra (Fig. 3). The two long-chain lactones also produced a series of ions corresponding to cleavages along their aliphatic chains, as shown in structure (**IV**) and Fig. 3(*b*) and (*c*). Both of these lactones and the product of the internal standard (**III**, R = $CH_2CH_2CH_2Ph$) exhibited characteristic peaks at *m/z* 85 (the lactone ring residue) and *m/z* 144 (product of a McLafferty rearrangement). The aromaticity of the latter lactone stabilised its molecular ion, which produced a larger peak.

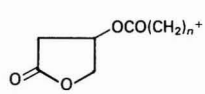

(**IV**)

n = 2, *m/z* 157	*n* = 8, *m/z* 241
n = 3, *m/z* 171	*n* = 9, *m/z* 255
n = 4, *m/z* 185	*n* = 10, *m/z* 269
n = 5, *m/z* 199	*n* = 11, *m/z* 283
n = 6, *m/z* 213	*n* = 12, *m/z* 297
n = 7, *m/z* 227	*n* = 13, *m/z* 311

Yields of the derivatisation reaction were determined by GC using standard solutions of the authentic, synthesised lactones (**III**). In each instance, a yield in excess of 70% was observed. The method proved successful with nmol amounts

(**III**)

Scheme 1.

of octanoylcarnitine providing a linear relationship between concentration and peak area. For example, in the range 1–90 nmol, the correlation coefficient was 0.996 (nine points), the detection limit for standard solutions being in the sub-nmol range. Hence, the sensitivity of the method appeared suitable for the determination of physiological levels of acylcarnitines in clinical samples. The detection limit was not determined accurately because, for urine samples, it was thought likely to be affected markedly (and adversely) by the selectivity of the preparation, *i.e.*, by the chemical background not present in standard solutions.

Precautions were required to control the conversion from acylcarnitine to acyl-containing lactone. Overheating or long reaction times resulted in the pyrolysis of the required lactone to the corresponding free organic acid and unsaturated lactone (Scheme 1). This effect is observed only as minor peaks when the acylcarnitines are heated at 120 °C for just 30 min (Fig. 2): octanoic acid, 4.47 min; phenylbutanoic acid, 8.48 min; palmitic acid, 14.72 min. Similarly, GC injection techniques

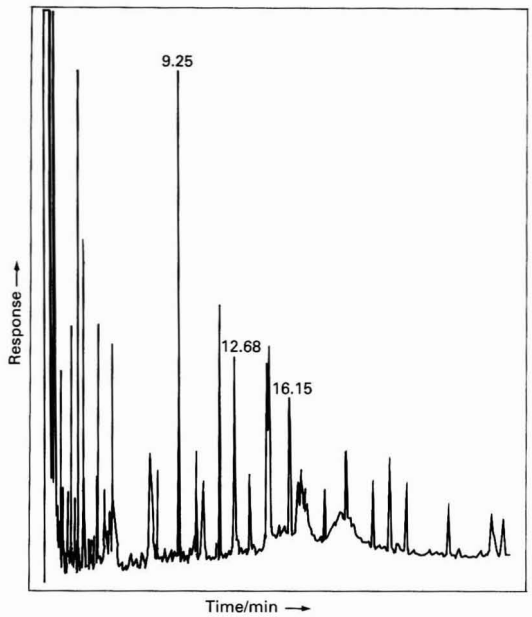

Fig. 4. Gas chromatogram from a clinical urine sample of an MCAD-deficient patient, after extraction and derivatisation as in Fig. 1

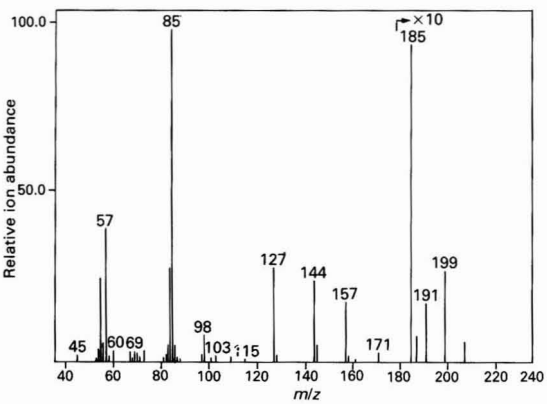

Fig. 5. Electron ionisation mass spectrum of the urinary component eluting at 12.68 min in the chromatogram of the clinical sample (Fig. 4). Comparison with Fig. 3(*b*) confirms that it is the lactone (**III**, R = C_7H_{15}) from octanoylcarnitine. The relative ion abundance scale has been increased by a factor of 10 above *m/z* 175

which require vaporisation of the sample accelerate the thermal decomposition. For this reason cold on-column injection was utilised for all GC analyses. When split - splitless injection was utilised for GC - MS analysis, the injector port temperature was not allowed to exceed 230 °C. However, this resulted in significant band broadening of the lactone from palmitoylcarnitine due to poor transfer out of the injection zone.

The complex matrix of urine demanded an extraction procedure for the analysis of clinical samples. After unsuccessful attempts with reported solvent extraction techniques, ion-exchange resins were found most suitable for sample preparation.[10,11] Removal of the anionic species on an AGI-X8 anion-exchanger followed by selective elution from an AG50W-X8 cation-exchange column provided a suitably

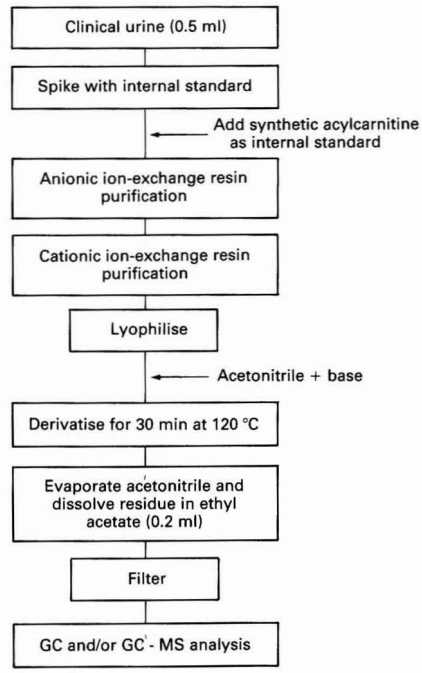

Fig. 6. Analytical procedure for monitoring acylcarnitines in urine

purified acylcarnitine fraction. Standard aqueous acylcarnitine mixtures were also subjected to this isolation procedure and then derivatised. The GC results, when compared with those from identical samples which were only freeze-dried prior to derivatisation, suggested an approximate 30% recovery from the combined ion-exchange procedure.

The suitability of the overall analytical procedure for urine analysis can be illustrated with a clinical, but well characterised, sample. Fig. 4 shows the gas chromatogram obtained by subjecting 0.5 ml of urine, from an infant suffering MCAD deficiency, to the ion-exchange preparation and derivatisation depicted in Fig. 1. The sample was spiked, after derivatisation, with the 4-phenylbutanoate ester of β-hydroxy-γ-butyrolactone to determine the potential of 4-phenylbutanoyl-DL-carnitine as an internal standard. The sizeable peak eluting at 12.68 min had an identical retention time to that of the lactone derivative from octanoylcarnitine. When examined by GC - MS the same peak exhibited the mass spectrum shown in Fig. 5. A comparison with the mass spectrum of the octanoyl containing lactone [Fig. 3(*b*)] clearly confirms the identification of octanoylcarnitine in the sample. The experiment was conducted qualitatively but the appearance of a good peak for the aromatic lactone (16.15 min) supports the use of 4-phenylbutanoyl-DL-carnitine as an internal standard for future quantitative analysis.

The identification of lactones from acylcarnitines in the clinical sample using the GC - MS data was effected as follows: (*i*) manually by examining mass spectra in the appropriate retention time windows, which was successful for octanoylcarnitine and the internal standard; (*ii*) by rapid location using mass chromatograms at *m/z* 85 and 144, which also located mass spectra consistent with the lactone from 3-phenylpropanoylcarnitine (a metabolite of 3-phenylpropanoic acid) and with the lactone from hexanoylcarnitine; and (*iii*) without human involvement by reverse library searching, *i.e.*, automatic searching of the data for specific spectra. Approach (*iii*) readily identified the lactone from octanoylcarnitine in the clinical sample that gave the chromatogram in Fig. 4 and could

be used to detect and automatically identify any derivatised acylcarnitine for which a mass spectrum is known and stored.

Conclusions

It has been shown that acylcarnitines can be derivatised simply and in high yield to give volatile lactones according to Fig. 1. The procedure provides products that are unambiguously derived from acylcarnitines, amenable to gas chromatography and GC - MS and can be detected at physiological levels. Therefore our initial results suggest that this method has potential for neonatal screening of acylcarnitines at a realistic cost. It makes obsolete the comment of Gaskell and Finlay,[12] that "conversion of the intact acylcarnitines to derivatives amenable to GC - MS was not possible." The unambiguous identification, by GC - MS, of octanoylcarnitine in the urine of a patient with MCAD deficiency is particularly encouraging.

Our current research involves firstly, improving the efficiency of extraction of acylcarnitines from urine, secondly, developing the technique into a quantitative assay for urinary acylcarnitines (a flow diagram for which is shown in Fig. 6), thirdly, extending the method to a wider variety of acylcarnitines [different R groups in (**II**)], fourthly, applying the method to other clinical samples and, if successful, fifthly, using the procedure for diagnosis and characterisation of inherited metabolic diseases.

This work was supported by the Analytical Chemistry Trust of the Royal Society of Chemistry with a SAC Studentship (to S. L.). We gratefully acknowledge the Foundation for the Study of Infant Deaths for a research grant for the purchase of a gas chromatograph (Project 110). Thanks are also expressed to Dr. A. T. Hewson (Sheffield City Polytechnic) for useful discussions, to Dr. R. J. Pollitt (Neonatal Screening Laboratory, Sheffield Children's Hospital) for both useful discussions and the provision of clinical samples, and to Finnigan MAT for the use of GC - MS instrumentation.

References

1. Bahl, J. J., and Bressler, R., *Ann. Rev. Pharmacol. Toxicol.*, 1987, **27**, 257.
2. Feller, A. G., and Rudman, D., *J. Nutr.*, 1988, **118**, 541.
3. Duran, M., Mitchell, G., De Klerk, J. B. C., De Jager, J. P., Hofkamp, M., Briunvis, L., Ketting, D., Saudubray, J. M., and Wadman, S. K., *J. Pediatr.*, 1985, **107**, 397.
4. Divry, P., Vianey-Liaud, C., and Cottee, J., *Biomed. Environ. Mass Spectrom.*, 1987, **14**, 663.
5. Bennett, M. J., Worthy, E., and Pollitt, R. J., *Anal. Proc.*, 1987, **24**, 322.
6. Bieber, L. L., and Kerner, J., *Methods Enzymol.*, 1986, **123**, 264.
7. Lowes, S., and Rose, M. E., *Trends Anal. Chem.*, 1989, **8**, 184.
8. Ziegler, H. J., Bruckner, P., and Binon, F., *J. Org. Chem.*, 1967, **32**, 3989.
9. Henrot, S., Larchevêque, M., and Petit, Y., *Synth. Commun.*, 1966, **16**, 183.
10. Norwood, D. L., Kodo, N., and Millington, D. S., *Rapid Commun. Mass Spectrom.*, 1988, **2**, 269.
11. Millington, D. S., Norwood, D. L., Kodo, N., Roe, C. R., and Inove, F., *Anal. Biochem.*, 1989, **180**, 331.
12. Gaskell, S. J., and Finlay, E. M. H., *Trends Anal. Chem.*, 1988, **7**, 202.

Paper 9/03747K
Received September 4th, 1989
Accepted November 1st, 1989

Study of Fatty Acid Profiles in Cancer Cells Grown in Culture Using Gas Chromatography - Mass Spectrometry*

Sima Pazouki and J. D. Baty
Department of Biochemical Medicine, Ninewells Hospital and Medical School, Dundee DD1 9SY, UK
Heather M. Wallace and Catherine S. Coleman
Clinical Pharmacology Unit, Departments of Medicine and Therapeutics and Pharmacology, University of Aberdeen, Polworth Building, Foresterhill, Aberdeen AB9 2ZD, UK

The determination of long-chain fatty acids in the phospholipid, triglyceride and free fatty acid fractions of HT29/219 colon cancer cells grown in a medium containing either foetal calf serum or horse serum, was carried out using gas chromatography - mass spectrometry. Several bonded-phase capillary columns were tested for the separation of the fatty acid methyl esters, and a 30-m poly(ethylene glycol) column was found to give optimum separation. The mass spectrometer was set to the multiple ion detection mode to increase the sensitivity of the recording of the characteristic ions, consisting of the molecular ion and the base peak. The phospholipid and triglyceride compositions of the cells were different when the cells were grown in media containing different sera. Differences were also found in the turnover of the acids in the different lipid fractions, the phospholipids being the most important, when the cells were grown in different media. The cellular metabolism and turnover of certain fatty acids differed from others in the same cell. These differences emphasise the importance of a precise knowledge of the lipid composition of the culture medium in *in vitro* studies of cancer cells.

Keywords: *Fatty acid; phospholipid; gas chromatography - mass spectrometry; cultured tumour cell*

There is considerable interest in the metabolism of fatty acids in cell cultures, especially with regard to tumour cells. The possible conversion of fatty acids to peroxides and the role of these compounds in carcinogenesis is still not resolved,[1] but peroxides of phospholipids have, for example, been identified in adipose tissue from patients with breast cancer.[2]

We have used gas chromatography - mass spectrometry (GC - MS) to study the metabolism of fatty acids in cancer cells and in this paper present some initial results relating to the optimisation of the method and data relating to the uptake of fatty acids from the culture medium into the growing cell. The main areas of interest are as follows. (1) The uptake and turnover of medium fatty acids into the phospholipid, triglyceride and free fatty acid fractions of the cells, over a specified time in culture. (2) Changes in the fatty acid profile of the different lipid classes when the medium is supplemented with different sera having different fatty acid contents. (3) Differences in the profiles of different cell lines grown in the same media. (4) Fatty acid changes in growing *versus* quiescent cells.

Experimental

Two human colon carcinoma lines, HT29/219 and HT115, and a human breast cancer cell line, ZR-75-1, were studied. The cells were grown in Dulbecco's modification of Eagle's medium supplemented with 10% v/v foetal calf serum (DFC_{10}) or horse serum (DH_{10}). They were seeded at a density of 1.9×10^4 cells cm^{-2} and maintained at 37 °C in a humidified atmosphere of 5% CO_2 - 95% air.

To analyse cellular lipids, cells were harvested into phosphate buffered saline at specific time intervals up to 120 h, an aliquot was taken for protein analysis and the total lipids extracted from the remainder using chloroform - methanol (2 + 1) containing 2,6-di-*tert*-butyl-4-methylphenol (butylated hydroxytoluene) as an antioxidant. The total lipid extract was then applied to silica gel G thin-layer chromatography (TLC) plates for separation of the different lipid classes. The solvent system used was hexane - diethyl ether - acetic acid (70 + 30 + 1). The separated phospholipid, triglyceride and free fatty acid bands were then scraped off the plates and the lipids eluted using chloroform - methanol (2 + 1). The phospholipids and triglycerides were transmethylated by a base-catalysed transesterification procedure[3] using sodium methoxide in methanol, and the free fatty acids were methylated using diazomethane.

As described by Christie,[4] the optimum columns for the separation of fatty acid methyl esters are bonded-phase capillary columns coated with polar phases. This choice is, however, not satisfactory when a mass spectrometer is used for detecting the eluting fatty acid methyl esters, because of high levels of bleed from these columns at elevated temperatures. Four bonded-phase capillary columns were tested: a 15-m non-polar methylsilicone column (DB-1), a 30-m 50% cyanopropyl column (DB-23), a 30-m 50% cyanopropylphenyl column (DB-225) and a 30-m poly(ethylene glycol) column (DB-WAX). A Hewlett-Packard benchtop GC - MS system was used.

Results

The non-polar DB-1 column gave poor resolution of the unsaturated acids, for example for the C18 : 1 (this nomenclature implies a carbon chain containing 18 carbon atoms and with one double bond), C18 : 2 and C18 : 3 acids as shown in the total ion current (TIC) trace (Fig. 1). To achieve a better resolution between the fatty acid methyl esters a polar, rather than a non-polar column was used. The DB-225 column gave good separation of most of the acids, including *cis*- and *trans*-isomers, but because the complete separation of all the fatty acid methyl esters of interest required the use of a temperature programme up to 220 °C, there was substantial bleed from this column which when used with MS detection, resulted in spectra that were difficult to interpret. The DB-23 column also gave good separation of all the fatty acid methyl esters, but again the amount of bleed was too high and this interfered with the interpretation of the mass spectra.

* Presented at SAC 89, the 8th SAC International Conference on Analytical Chemistry, Cambridge, UK, 30 July–5 August, 1989.

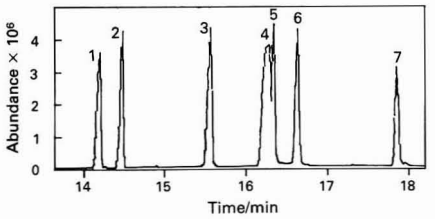

Fig. 1. Separation of fatty acid methyl esters on the DB-1 column. Temperature programme: 70 °C, 1 min; 70–265 °C, 10 °C min^{-1}; and 265 °C, 5 min. Column: DB-1, 15 m × 0.25 mm; film thickness, 0.25 μm. Peak identification: 1, C16 : 1; 2, C16 : 0; 3, C17 : 0; 4, C18 : 2 + C18 : 3; 5, C18 : 1; 6, C18 : 0; and 7, C20 : 4

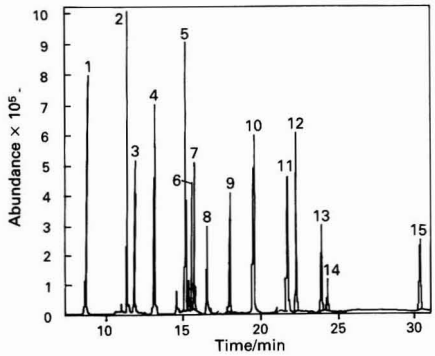

Fig. 2. Separation of a standard mixture of 15 fatty acid methyl esters on the DB-WAX column. Temperature programme: 70 °C, 2 min; 70–170 °C, 40 °C min^{-1}; 170 °C, 1 min; 170–220 °C, 3 °C min^{-1}; 220 °C, 10 min. Column: DB-WAX, 30 m × 0.25 mm; film thickness, 0.25 μm. Peak identification: 1, C14 : 0; 2, C16 : 0; 3, C16 : 1; 4, C17 : 0; 5, C18 : 0; 6, C18 : 1 9-*cis*; 7, C18 : 1 11-*cis*; 8, C18 : 2; 9, C18 : 3; 10, C20 : 0; 11, C20 : 3; 12, C12 : 4; 13, C20 : 5; 14, C22 : 0; and 15, C22 : 6

The other polar column, the DB-WAX, gave much lower levels of bleed, with a resolution equal to that of the cyanopropyl columns. Complete separation of all the acids was obtained on this column in less than 35 min, using a temperature programme (Fig. 2).

For improved sensitivity, the mass spectrometer was set to the multiple ion detection mode, and the molecular ion and the base peak for each fatty acid methyl ester was examined. Samples were injected on to the column using a Hewlett-Packard autosampler and the integrated data, consisting of retention times and peak areas, were transferred to a PC for analysis. This over-all automation meant that large numbers of samples could be analysed in a short period of time.

To improve the recognition of the molecular ion and the positions of double bonds within fatty acids, derivatives such as pyrrolidides and picolinyl esters have been recommended.[5,6] However, more than 90% of the lipids studied were either phospholipids or triglycerides which require a transesterification method for derivatisation and there are as yet no published methods for transesterification using picolinyl alcohol. Therefore, the methyl esters were used.

It is well documented that most cells in culture can synthesise lipids from glucose and amino acids available in the medium, but when the lipids are present in the extracellular medium, it has been shown that the *de novo* biosynthesis of fatty acids and cholesterol is inhibited and the cells take up lipids present in the medium.[7]

It was of interest to determine whether sera containing demonstably different lipid compositions had different effects

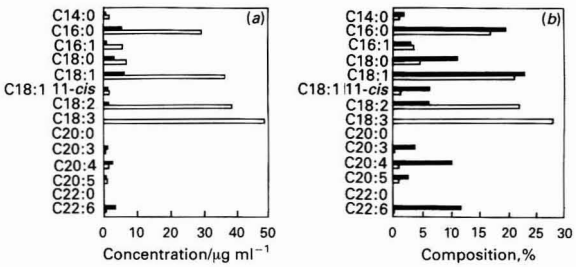

Fig. 3. Free fatty acids in foetal calf serum and horse serum. (*a*) Concentration (μg ml^{-1}); and (*b*) percentage distribution (%). Unshaded bars, horse serum; and shaded bars, foetal calf serum

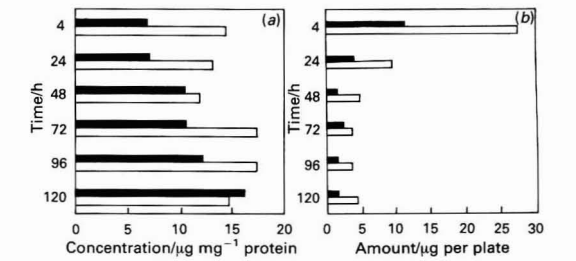

Fig. 4. Concentration of C16 : 0 during growth in (*a*) the phospholipid fraction of the cells; and (*b*) the free fatty acid fraction of the culture media. Unshaded bars, horse serum; and shaded bars, foetal calf serum

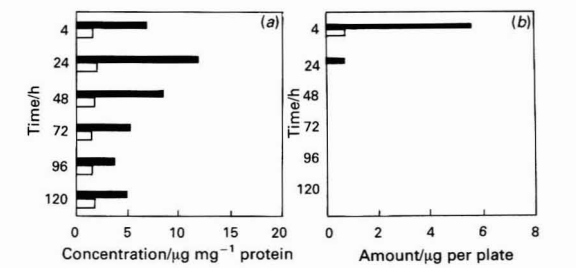

Fig. 5. Concentration of C20 : 4 during growth in (*a*) the phospholipid fraction of the cells; and (*b*) the free fatty acid fraction of the culture media. Unshaded bars, horse serum; and shaded bars, foetal calf serum

on the fatty acid composition of cells, and if so, if these effects were directly related to the fatty acid composition of the medium. It was therefore necessary to obtain detailed information about the fatty acid levels in the serum supplements used. As the free fatty acid fraction is believed to be the main class of lipid that supplies fatty acids to the cells in culture, the level of each fatty acid in this fraction for foetal calf serum and horse serum was measured.

The free fatty acid concentration and the composition of the foetal calf serum and horse serum are shown in Fig. 3. These results are very similar to those obtained by other workers.[7] As shown in Fig. 3(*b*), the composition of the fatty acids is very different in the two sera. The actual levels of the fatty acids in the two sera show an even greater difference [Fig. 3(*a*)]. Horse serum was found to contain approximately six times as much free fatty acid as the foetal calf serum, with very high levels of

the C18:2 and C18:3 acids, which are only present in trace levels in foetal calf serum, and lower levels of the C20:4 and C22:6 acids.

With these differences in mind, the levels and compositions of the different fatty acids in the phospholipid, triglyceride and free fatty acid classes of HT29/219 cells grown in either DFC_{10} or DH_{10} over a period of 120 h were studied.

Fig. 4 compares the level of C16:0 found in the phospholipid fraction of the cells with that in the medium. It can be seen that the level of C16:0 in the medium falls considerably in the first 48 h, in both DFC_{10} and DH_{10}, showing that C16:0 has been taken up by the cells. This has been confirmed by labelled fatty acid uptake experiments. The cellular phospholipid fraction, however, shows different patterns in DFC_{10}-grown cells compared with DH_{10}-grown cells. In DFC_{10}-grown cells the level of C16:0 in the phospholipid rises gradually up to 120 h (from *ca.* 7 μg mg^{-1} of protein to *ca.* 17 μg mg^{-1}). In DH_{10}-grown cells the C16:0 level in the phospholipid falls initially (4–48 h), then rises, and then falls again over 96–120 h. These results therefore show differences in the turnover of C16:0 in the phospholipids when cells are grown in different sera.

The pattern of cellular phospholipid changes is completely different for C20:4 (Fig. 5). The data for medium free fatty acids show that this acid is also taken up by the cells. This has been confirmed by labelling experiments. The uptake seems to be rapid, as after 24 h no more C20:4 was found in either medium. Levels of C20:4 in cellular phospholipids in the DFC_{10}-grown cells peak to a maximum at 24 h and then fall gradually. Cells grown in DH_{10} show more constant levels over 120 h.

On comparing the cellular phospholipid C16:0 and C20:4 results [Figs. 4(*a*) and 5(*a*)], distinct differences in the profiles of the two acids can be seen. This leads us to believe that they are metabolised differently in the cells; C20:4 seems to be used up for other cellular processes, perhaps prostaglandin production.

In conclusion, it has been shown that for the analysis of fatty acid methyl esters by GC - MS, a low bleed column is essential. Columns with the lowest bleed are those with non-polar methylsilicone phases. These phases, however, do not give sufficient resolution. Therefore a compromise has to be made, and the best polar column we have found for the analysis of fatty acid methyl esters is a Carbowax-type [poly(ethylene glycol)] phase column.

The use of the mass selective detector, in the single ion monitoring mode, as the detection system means that the compounds of interest can be detected with greater certainty than can be achieved from chromatographic retention time data alone. The retention time data, on the other hand, can often be of crucial importance as an aid to the identification of closely related isomers. The combination of the two therefore provides a powerful tool for the qualitative, and more importantly, quantitative analysis of lipids. In order to improve the accuracy of the quantitative analyses, multiple calibration lines were constructed using area and height data for the molecular ion and the base peak for each fatty acid methyl ester. This was carried out by means of a data handling program.

Using the methodology outlined in this paper the fatty acid profiles of different tumour cell lines growing in identical media and also the profiles of tumour cells treated with anti-proliferative drugs are being studied at present.

References

1. Cornwell, D. G., and Morisaki, N., *in* Pryor, W. A., *Editor*, "Free Radicals in Biology," Volume VI, Academic Press, New York, 1984, p. 95.
2. Hietanen, E., Punnonen, K., Punnonen, R., and Auvinen, O., *Carcinogenesis*, 1986, **7**, 1965.
3. Christie, W. W., *J. Lipid Res.*, 1982, **23**, 1072.
4. Christie, W. W., *in* Christie, W. W., *Editor*, "Gas Chromatography of Lipids," The Oily Press, Ayr, 1989, pp. 85–125.
5. Andersson, B. A., *Prog. Chem. Fats Other Lipids*, 1978, **16**, 279.
6. Harvey, D. J., *Biomed. Mass Spectrom.*, 1982, **9**, 33.
7. Spector, A. A., Mathur, S. N., Kaduce, T. L., and Hyman, B. T., *Prog. Lipid Res.*, 1981, **19**, 155.

Paper 9/03792F
Received September 5th, 1989
Accepted September 29th, 1989

Identification of Triacylglycerols by High-performance Liquid Chromatography - Gas - Liquid Chromatography and Liquid Chromatography - Mass Spectrometry*

N. W. Rawle
Dalgety PLC, Group Research Laboratory, Station Road, Cambridge CB1 2JN, UK
R. G. Willis and J. D. Baty
Department of Biochemical Medicine, Ninewells Hospital and Medical School, Dundee DD1 9SY, UK

Triacylglycerols from rat adipose tissue were chromatographed by high-performance liquid chromatography (HPLC), with a gradient of propan-2-ol in acetonitrile as the mobile phase. Fractions of the material eluting from the column were collected and analysed by automated gas - liquid chromatography of the fatty acid methyl esters obtained after transmethylation. Triacylglycerols were identified by using a combination of their fatty acid content and elution time from the HPLC column. Fractions corresponding to whole peaks or groups of peaks were also collected and re-chromatographed on a liquid chromatography - mass spectrometry system equipped with a belt interface. For most triacylglycerols, good agreement was obtained between the two methods, although mass spectrometric identification of the early eluting peaks was complicated by poor resolution of the triacylglycerols on the HPLC system.

Keywords: *Triacylglycerol; high-performance liquid chromatography; gas - liquid chromatography; mass spectrometry*

The study of triacylglycerols poses several problems for the analyst. In natural triacylglycerol mixtures, the number of possible molecular species is large, so that a single-step analysis is not usually sufficient for complete analysis. A triacylglycerol mixture may be analysed by hydrolysis followed by analysis of the component fatty acids by gas - liquid chromatography (GLC).[1,2] This provides no information about the distribution of the fatty acids between the triacylglycerols.

Some workers have used GLC to separate intact triacylglycerols,[3,4] but high temperatures are required to volatilise them. This can cause an excessive amount of stationary phase bleed from the column, particularly when relatively polar phases are used. Less polar phases are more thermally stable, but are less selective towards unsaturated triacylglycerols. When GLC is used in conjunction with mass spectrometry, this may cause problems in the identification of triacylglycerols which co-elute.[5]

The most popular method for the separation of triacylglycerols has been reversed-phase high-performance liquid chromatography (HPLC) with non-aqueous solvents used for the mobile phase.[6–11] The major problem in the analysis of triacylglycerols by HPLC is that of detection.[12] Triacylglycerol molecules do not possess a strong chromophore and cannot be derivatised without disruption of the original structure and consequent loss of information. Ultraviolet (UV) detection[13] at short wavelengths (190–230 nm) and infrared detection[14] have been used to monitor triacylglycerols. In both instances, detection is based on absorbance by carbonyl and isolated double bonds. Both detection systems limit the choice of solvents that can be used in the mobile phase and exhibit different responses towards saturated and unsaturated triacylglycerols. Base-line drift may occur during the operation of gradients. The refractive index detector suffers from poor sensitivity towards triacylglycerols and cannot be used in conjunction with gradient elution. Systems which involve the removal of solvent, such as flame ionisation[15] and mass detection,[16,17] can be applied to triacylglycerol analysis without the occurrence of base-line drift during gradient elution. Further information about the structure of the triacylglycerols may be obtained by transmethylating triacylglycerols that have been separated by HPLC and analysing the resulting fatty acid methyl esters by GLC.[11]

Gas chromatography - mass spectrometry (GC - MS)[5,18] and liquid chromatography - mass spectrometry (LC - MS)[19,20] have been used in the analysis of triacylglycerol mixtures. In the mass spectrometer, under electron impact conditions, triacylglycerols produce characteristic ions,[21] corresponding to $[M - RCOO]^+$, $[M - RCOOH]^+$, $[RCO + 74]^+$, $[RCO + 128]^+$ and $[RCO]^+$, where R represents the acyl chains of the component fatty acids of the triacylglycerol.

We are interested in studying the distribution of the fatty acids amongst the triacylglycerols in adipose tissue. Triacylglycerols which have been separated by HPLC are analysed further by two separate procedures. In one instance the triacylglycerols are analysed, as their component fatty acid methyl esters, by GLC. In the other they are analysed by LC - MS. In this paper the results obtained by using the two methods are compared.

Experimental

Reagents

Triacylglycerol and fatty acid methyl ester reference standards were purchased from Sigma (Poole, Dorset, UK). All solvents were of analytical-reagent or HPLC grade and supplied by BDH (Poole, Dorset, UK) or Rathburn Chemicals (Walkerburn, Peeblesshire, UK).

HPLC

High-performance liquid chromatography was performed with an Altex 100A dual-piston pump and Altex 110A pump, controlled by an Altex 420 programmer (Altex Scientific, Berkeley, CA, USA). A Rheodyne 7126 injection valve (Rheodyne I, Cotati, CA, USA) with a 20-μl loop and a column (25 cm × 4.6 mm i.d.) of 3 μm Spherisorb ODS 2 were used. The mobile phase was propan-2-ol - acetonitrile (32 + 68) for 50 min, then to propan-2-ol - acetonitrile (60 + 40) in 30 min, at a flow-rate of 0.8 ml min^{-1}. Ultraviolet detection

* Presented at SAC 89, the 8th SAC International Conference on Analytical Chemistry, Cambridge, UK, 30 July–5 August, 1989.

was with a Kratos Spectroflow 757 detector (Kratos Analytical Instruments, Ramsey, NJ, USA) at a wavelength of 213 nm. Fractions eluting from the column were collected with a Gilson 203 fraction collector (Gilson Medical Electronics, Villiers-le-Bel, France), which was controlled by a Hewlett-Packard 3388A integrator.

GLC

A Hewlett-Packard 7672A autosampler was used to inject fatty acid methyl ester solutions into a Hewlett-Packard 5710A gas chromatograph, equipped with a flame-ionisation detector. A glass column (2 m × 2 mm i.d.), packed with 10% SP-2330 on 100–120 Chromosorb W AW (Supelchem, Sawbridgeworth, Hertfordshire, UK) was used. The carrier gas was nitrogen at a flow-rate of 25 ml min^{-1} with an oven temperature of 155 °C. Autosampler control and data handling were performed by a Hewlett-Packard 3388A integrator.

LC - MS

Liquid chromatography – mass spectrometry was carried out with a PU 4003 HPLC system (Philips Analytical, Cambridge, UK) containing a column (25 cm × 2.0 mm i.d.) of 5 μm Spherisorb ODS 2, with acetone - acetonitrile (63.7 + 36.3) at a flow-rate of 300 μl min^{-1} as the mobile phase. Injection was via a septum injector and the HPLC system was linked to a VG 7070F double focus mass spectrometer (VG Organic, Altrincham, Cheshire, UK) via a belt interface. Resolution was 1000 (10% valley). A source temperature of 260 °C, an electron energy of 20 eV and an accelerating voltage of 4 kV were used. Ions were scanned from 640 to 195 u at 1 s $decade^{-1}$.

Procedure

A sample (*ca.* 50 mg) of adipose tissue was removed from an epididymal fat pad of a male Sprague - Dawley rat. The sample was homogenised in 15 ml of chloroform - methanol (2 + 1) and passed through a 0.45-μm nylon filter (Gelman Sciences, Northampton, UK). The extract was dried under a stream of nitrogen and re-dissolved in chloroform (2 ml). A portion (400 μl) of the extract was applied to a silica gel 60 thin-layer chromatography plate (BDH) which was developed with hexane - diethyl ether - acetic acid (85 + 25 + 1). The triacylglycerols were recovered from the plate with chloroform - methanol (2 + 1) and reconstituted in acetone. Approximately 0.5 mg of triacylglycerol, dissolved in 20 μl of acetone, was injected into the HPLC system. Fractions eluting from the detector were collected for further analysis by GLC or LC - MS.

GLC

Fractions of the material eluting from the HPLC column were collected at 0.2-min intervals. This interval was increased in stages to a final value of 1.0 min, to take band broadening into account. After addition of triheptadecanoin (16 μg) as internal standard for the GLC, each fraction was re-dissolved in diethyl ether (1 ml) and transesterified with sodium methoxide according to the method of Christie.[22] The resulting fatty acid methyl esters were dissolved in dodecane (150 μl), 1 μl of which was analysed by automated packed-column GLC.

LC - MS

Fractions corresponding to whole peaks or groups of peaks were collected from the HPLC column and dried under a stream of nitrogen. Each fraction was re-dissolved in 200–300 μl of acetone and a portion (10 μl) of this solution injected into the LC - MS system.

Results and Discussion

The HPLC trace of the triacylglycerols obtained with UV detection at 213 nm is shown in Fig. 1. The base-line drift occurring after 60 min, caused by the operation of the gradient elution, demonstrates the difficulty of quantification of triacylglycerols when short wavelength UV detection is used.

With HPLC - GLC, triacylglycerols were identified by a combination of their elution time from the HPLC column, compared with those of standard compounds, and their fatty acid content. For the identification of triacylglycerols by LC - MS, a reference library of 165 triacylglycerol mass spectra was compiled from published data[21] for the fragment ions corresponding to $[M - RCOO]^+$, $[M - RCOOH]^+$, $[RCO + 74]^+$, $[RCO + 128]^+$ and $[RCO]^+$. Triacylglycerols were therefore identified by a combination of their elution time from the HPLC and a comparison of their mass spectra with the library data.

The identities assigned by the two methods to the major triacylglycerols contained in the fractions are listed in Table 1. For fractions 2–8, good agreement between the two methods was achieved. For fraction 1, the LC - MS method wrongly identified the triacylglycerols contained in this fraction. This occurred because the second peak of fraction 1 contained a mixture of four triacylglycerols, namely LLL, PeLL, PePeL and PePePe. The resulting mixed spectrum caused the peak to

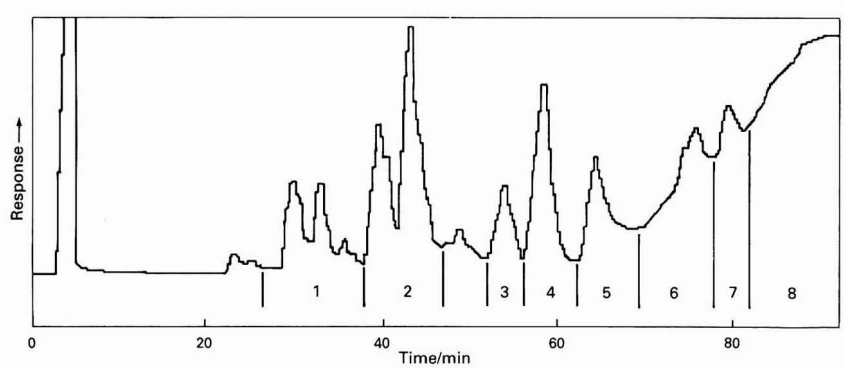

Fig. 1. Chromatogram of rat adipose tissue triacylglycerols obtained by HPLC with UV detection at 213 nm. For conditions see text. Fractions 1–8 were collected for further analysis by LC - MS

Table 1. Identities given to the major triacylglycerols present in fractions 1–8 by further analysis of the component fatty acid methyl esters by GLC or intact triacylglycerols by LC - MS

Fraction	GLC of fatty acid methyl esters*	LC - MS of intact triacylglycerols
1	MMM	MMM
	PePePe	PPePe
	PePeL	OLLn
	PeLL	
	LLL	
2	OLL	PeOL
	PLL	PPeL
	PeOL	
	PPeL	
3	OOL	OOL
4	PLO	PLO
5	PPL	PPL
6	OOO	OOO
	POO	POO
7	PPO	PPO
8	PPP	PPP
	POS	POS

* M = Myristic acid, P = palmitic acid, Pe = palmitoleic acid, S = stearic acid, O = oleic acid, L = linoleic acid, Ln = linolenic acid and POS is a triacylglycerol composed of palmitic, oleic and stearic acids. No distinction is made here between the three fatty acid positions of the triacylglycerols.

be wrongly identified as OLLn or PPePe. It is known that these triacylglycerols do not elute at this point, as the HPLC - GLC analysis of this fraction shows palmitic and oleic acids to be absent from these triacylglycerols.

This work shows the advantages of HPLC - GLC and LC - MS for the analysis of triacylglycerols over those methods which use more traditional modes of detection. Both methods allow identification of triacylglycerols, such as tripalmitin, which have only a very small response when UV detection is used. Because the mobile phase is removed prior to detection, base-line drift is not a problem when gradient elution is used. These methods provide structural information about the triacylglycerols, although no distinction is made between those molecules which are positional isomers.

When LC - MS is used, caution must be exercised in the interpretation of mass spectra, as incorrect identities can be assigned to triacylglycerols which elute together.

References

1. Jacobsen, B. K., Trygg, K., Hjermann, I., Thomassen, M. S., Real, C., and Norum, K. R., *Am. J. Clin. Nutr.*, 1983, **38**, 906.
2. Plakke, T., Berkel, J., Beynen, A. C., Hermus, R. J. J., and Katan, M. B., *Hum. Nutr. Appl. Nutr.*, 1983, **37A**, 365.
3. Mares, P., Skorepa, J., Sindelkova, E., and Tvrzicka, E., *J. Chromatogr., Biomed. Appl.*, 1983, **273**, 172.
4. Hamilton, R. J., *J. Chromatogr. Sci.*, 1975, **13**, 474.
5. Oshima, T., Yoon, H.-S., and Koizumi, C., *Lipids*, 1989, **24**, 535.
6. Aitzetmüller, K., *Prog. Lipid Res.*, 1982, **21**, 171.
7. Plattner, R. D., *Methods Enzymol.*, 1981, **72**, 21.
8. El-Hamdy, A. H., and Perkins, E. G., *J. Am. Oil Chem. Soc.*, 1981, **58**, 49.
9. El-Hamdy, A. H., and Perkins, E. G., *J. Am. Oil Chem. Soc.*, 1981, **58**, 867.
10. Dong, M. W., and DiCesare, J. L., *J. Am. Oil Chem. Soc.*, 1983, **60**, 788.
11. Baty, J. D., and Rawle, N. W., *J. Chromatogr.*, 1987, **395**, 395.
12. Robinson, J. L., and Macrae, R., *J. Chromatogr.*, 1984, **303**, 386.
13. Singleton, J. A., and Pattee, H. W., *J. Am. Oil Chem. Soc.*, 1984, **61**, 761.
14. Hamilton, R. J., Mitchell, S. F., and Sewell, P. A., *J. Chromatogr.*, 1987, **395**, 33.
15. Phillips, F. C., Erdahl, W. L., Nadenicek, J. D., Schmit, J. A., and Privett, O. S., *Lipids*, 1984, **19**, 142.
16. Stolyhwo, A., Colin, H., and Guiochon, G., *Anal. Chem.*, 1985, **57**, 1342.
17. Robinson, J. L., Tsimidou, M., and Macrae, R., *J. Chromatogr.*, 1985, **324**, 35.
18. Murata, T., and Takahashi, S., *Anal. Chem.*, 1973, **45**, 1816.
19. Myher, J. J., Kuksis, A., Marai, L., and Manganaro, F., *J. Chromatogr.*, 1981, **283**, 289.
20. Marai, L., Myher, J. J., and Kuksis, A., *Can. J. Biochem. Cell Biol.*, 1983, **61**, 840.
21. Barber, M., Merren, T. O., and Kelly, W., *Tetrahedron Lett.*, 1964, **18**, 1063.
22. Christie, W. W., *J. Lipid Res.*, 1982, **23**, 1072.

Paper 9/04758A
Received November 6th, 1989
Accepted December 19th, 1989

Validity of Empirical Formulae Obtained by Gas Chromatography - Microwave-induced Plasma Atomic Emission Spectrometry*

Antonio Luiz Pires Valente† and Peter C. Uden‡
Department of Chemistry, Lederle Graduate Research Towers, University of Massachusetts, Amherst, MA 01003-0035, USA

A survey of empirical formulae obtained by means of microwave-induced plasma atomic emission spectrometric detection coupled to a gas chromatograph shows that, in general, the largest errors in molecular formula coefficients occur for hydrogen. An evaluation of the most commonly used method for formula calculation is presented. An alternative method, in which the chromatographic properties of the samples are more intensively considered, is outlined. For the studied data set this method, compared to the conventional approach, improved the reliability of the calculated molecular formulae.

Keywords: *Element specific gas chromatographic detection; spectrometric detection; microwave-induced plasma; empirical formula measurement*

In the time since the first reports on formula determination using gas chromatography - microwave-induced plasma atomic emission spectrometry (GC - MIP),[1,2] several workers have stressed the usefulness of the approach. In general, the formulae obtained for compounds in standard mixtures have been considered by these workers to be accurate, and based on these results empirical formulae have been calculated for various "unknowns," showing good agreement with the expected compounds. However, conflicting results have also been reported in several instances, and arguments have been raised that the GC - MIP method may not always be adequate for formula determination, because the elemental response data obtained may be dependent on the molecular structure of the analyte.[3] Such a dependence would invalidate the usual approach for inter-elemental ratio calculations, as described by equation (1)[2,4,5]:

$$\frac{E}{C} = \frac{R_{E_u}}{R_{C_u}} \times \frac{R_{C_r}}{R_{E_r}} \times \frac{N_{E_r}}{N_{C_r}} \quad \ldots \quad (1)$$

where E/C is the calculated element : carbon ratio in the unknown, R_{E_u} and R_{C_u} are the measured element and carbon responses for the unknown and R_{C_r}, R_{E_r}, N_{C_r} and N_{E_r} are, as indexed, the carbon and element responses, and the number of atoms of each in a chosen reference compound. Equation (1) can be reduced to:

$$\frac{E}{C} = \frac{R_{E_u}/F_E}{R_{C_u}/F_C} \quad \ldots \quad (2)$$

where F_E and F_C are the response per atom of element and carbon, respectively. As F_E and F_C are calculated for the reference compound, equation (1) implies that the plasma always behaves in exactly the same way for a given element, independent of its source molecule. If this is not the case then the arguments raised against equation (1) are valid. However, these arguments are themselves restricted, as they consider the applicability of this approach to be threatened by only this one source of systematic error.

Setting aside non-systematic observational or instrumental error, there are two possible components of inaccuracy in the empirical formulae obtained in this fashion; the dependence of the detector response on analyte structure, noted above, and the amount of analyte measured. These two sources of error can only be studied when they cause detectable systematic deviations from the linear behaviour inherent in equation (1), and an experiment designed to study these two sources of systematic error can be experimentally demanding: several compounds must be used to try to assess the structural dependence, and a range of concentrations of each compound is necessary to study the possible concentration dependence. Moreover, if these systematic deviations are masked by the precision of the technique employed they become very difficult, perhaps impossible, to detect, and there will be no solid basis to conclude that the data do not behave as described by equation (1). It would be shown that it does apply, within the precision of the available method.

Regarding experimental factors which may affect the determination of empirical formulae by GC - MIP, there are three types of problem to be accounted for or overcome. (*i*) The best compromise of MIP power, plasma position in relation to the spectrometer entrance slit, and support gas flow-rate, must be established to optimise the signal for each of the elements to be detected. (*ii*) The determination of whether there are any theoretical or empirical bases which can help in characterising any dependence of response to molecular structure. (*iii*) The consideration of other experimental limitations that relate to both empirical formula determination and the achievement of quantitative GC analysis. These include reliability of standards, quality of sample preparation, reliability of the data acquisition systems and data treatment methods, and quality of instrumentation.

To summarise, even if class (*i*) problems can be overcome, any attempt at improving the data so that class (*ii*) questions may be assessed would have to keep in mind the limitations in precision inherent to class (*iii*) problems. For data collection with strip-chart recorders, using syringe injection, the precision to be expected for GC analysis lies between 3 and 5%.[6,7] It is within this limitation that the utility of equation (1) for the experimental data reported in this paper will be considered. The analytical method has been designed to allow the study of possible concentration or mass dependencies that may be due to the plasma fragmentation process, to the gas-chromatographic process, or to both.

Experimental

The multi-elemental GC - MIP system consisted of a Hewlett-Packard (Avondale, PA, USA) Model 5830 gas chromato-

* Presented at SAC 89, the 8th SAC International Conference on Analytical Chemistry, Cambridge, UK, 30 July–5 August, 1989.

† Present address: Instituto de Quimica, Universidade Estadual de Campinas, Campinas, São Paulo 13081, Brazil.

‡ To whom correspondence should be addressed.

graph interfaced to a Beenaker TEM_{010} atmospheric pressure cavity and an Applied Chromatographic Systems (Luton, Bedfordshire, UK) Model MPD 850 multi-channel polychromator. The design of the system has been described in detail elsewhere.[8] Carbon, chlorine and hydrogen were monitored at 247.9, 481.0 and 656.3 nm, respectively. The secondary slits of the spectrometer were aligned for optimum response (peaking) at the hydrogen line.

A representative analyte sub-set, consisting of six of the 13 chlorinated compounds studied by Slatkavitz and co-workers,[9,10] was used as the test sample. Each compound was weighed into toluene, a known mass of cyclohexane added as internal standard, and the volume made up to the mark with toluene. Two solutions of different concentrations were prepared, having the following concentrations of analytes and internal standard: 1,1-dichloroethane (29.94, 12.88 mg ml^{-1}), chloroform (59.61, 25.65 mg ml^{-1}), 1,1,1-trichloroethane (24.46, 10.53 mg ml^{-1}), 1,1,2,2-tetrachloroethane (36.97, 17.34 mg ml^{-1}), *m*-chlorotoluene (31.36, 13.49 mg ml^{-1}), *m*-dichlorobenzene (45.24, 19.46 mg ml^{-1}) and cyclohexane (10.12, 9.34 mg ml^{-1}). Based on preliminary tests on these compounds, these concentrations were defined such that the hydrogen peaks would be of measurable magnitude, and the peaks in each monitored line would be of comparable size, using the total signal amplifications (photomultiplier high-voltage setting plus output attenuation) in which the noise was low enough to preclude interference with the peak measurements. These mixtures were analysed under the following conditions: injected volume, 0.3 μl; column flow, 1 ml min^{-1}; split ratio, 1/250; injector temperature, 200 °C; column temperature, 70 °C for 1 min, then heated to 180 °C at 30 °C min^{-1} and held for 2 min; transfer line to the cavity, 200 °C; helium flow to sustain the plasma, 100 ml min^{-1}; forward power to the cavity, 56 W; and reflected power at the minimum readable level (<1 W). The spectrometer conditions for each line were: high voltage to photomultipliers and output attenuations, respectively, for C, 1200 V, ×32; Cl, 1400 V, ×64 for higher and ×32 for lower concentration solutions; and H, 1100 V, ×32. Signals were monitored with Omniscribe dual-channel recorders (Houston Instruments, Austin, TX, USA), set to 10 mV input voltage and a 10 cm min^{-1} chart speed. Although an internal standard method was used, three injections of each sample, intercalated with toluene injections, were made because it was observed that the 1,1,2,2-tetrachloroethane peak size sometimes increased over successive injections, probably because of adsorption in the syringe needle. The ratio of peak height of element to peak height of carbon in cyclohexane was compared, to assess the reproducibility of the chromatograms; as these ratios agreed to within 2%, their averages were used to represent the sample parameters.

Results and Discussion

In an extensive study Slatkavitz and co-workers[9,10] used experimentally determined empirical formulae to calculate the coefficients for the molecular formulae for a set of 13 chlorinated hydrocarbons. The Cl molecular coefficients of these formulae showed errors that ranged from 0 to 10%. As the highest (10%) error occurred for the Cl molecular coefficients in *m*-chlorotoluene (C_7) and *m*-chloronaphthalene (C_{10}), the results were considered acceptable, as the experimental conditions left no doubt as to the number of C atoms in the two compounds; higher relative molecular mass compounds than those identified would not have had the gas-chromatographic properties observed.[10] In the present work, this use of the chromatographic data as an aid in ascertaining the correct molecular formula was extended. However, the possibility that the error was a result of a response to structure dependence of the detector could not be ignored. For the H molecular coefficients, the analysis must be more detailed as the errors ranged from 0 to 40%.[10] These high errors could also have been due to the response to structure dependence.

By using the data from this study,[10] a correlation was made of the inter-elemental peak height dependence with the ratio of the number of the respective atoms in the 13 compounds by plotting the atomic ratio *versus* the peak-height ratio. For the Cl : C ratio the plot was found to be linear, except for CCl_4, C_2HCl_3 and $C_2H_4Cl_2$. This plot has the equation $y = 1.293x - 0.014$ (correlation coefficient, $r^2 = 0.999$). From this equation the molecular formulae for 13 compounds were interpolated and the Cl molecular coefficients listed in Table 1 were obtained. All the molecular coefficients were within a 0–6% error so it can be concluded that the total deviation for Cl molecular coefficients is not more than 6%, and that the three

Table 1. Theoretical formulae and calculated molecular coefficients

	Slatkavitz*		Present study			
					Error†	
Compound	Cl‡	H§	Cl	H	Cl	H
CH_2Cl_2	2.00	2.02				
$C_2H_4Cl_2$	1.97	3.90	1.99	4.10	0.3	2.5
$CHCl_3$	2.98	1.00	3.03	1.00	1.2	0
$C_2H_3Cl_3$	2.99	2.97	3.10	2.93	4.8	2.1
CCl_4	4.16					
C_2HCl_3	2.90	1.00				
$C_4H_8Cl_2$	2.01	7.87				
$C_2H_2Cl_4$	4.00	1.94	3.77	1.96	5.8	2.2
$C_4H_4Cl_2$	2.04	3.92				
$CH_3C_6H_4Cl$	0.97	6.50	1.01	7.93	5.8	13.3
$C_6H_4Cl_2$	2.00	4.06	2.08	4.08	4.1	2.0
$C_6H_3Cl_3$	3.03	3.06				
$C_{10}H_7Cl$	0.95	6.50				

* See references 8 and 10.
† With relation to known formulae.
‡ With $y = 1.293x - 0.014$ (see text for details).
§ With $y = 0.019 + 0.671x + 0.131x^2$ (see text for details).

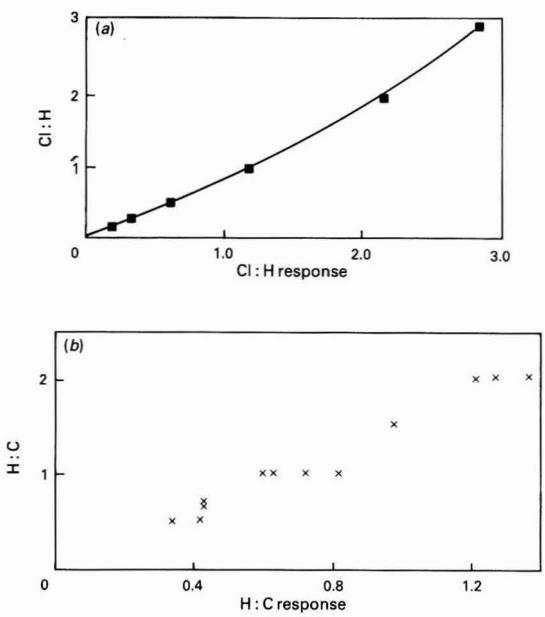

Fig. 1. Relationship of the number of atoms in the molecular formulae to the ratio of elemental response. (*a*) Cl : H; and (*b*) H : C (data from references 9 and 10)

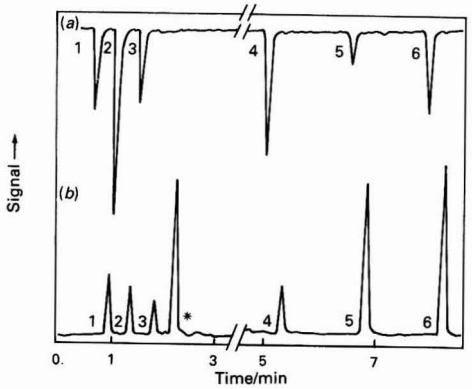

Fig. 2. Chromatograms of the lower concentration solution at (*a*) the chlorine 481.0-nm line; and (*b*) the carbon 247.9-nm line. 1, 1,1-Dichloroethane; 2, chloroform; 3, 1,1,1-trichloroethane; 4, 1,1,2,2-tetrachloroethane; 5, *m*-chlorotoluene; and 6, *m*-dichlorobenzene. The peak marked with an asterisk is the cyclohexane internal standard. The solvent (toluene) elutes after cyclohexane and before peak 4. Column, 5 m × 0.25 mm i.d. SE 30 FSO T

Table 2. Data analysis for the element relative to carbon (ERC) response behaviour towards the number of atoms in the molecular formulae*

Solution No.‡	Polynomial parameter† *A*	*B*	*K*	Correlation coefficient
Carbon line—				
1	0.0653	NC§	0.1391	0.9884
2	0.0829	NC	−0.1632	0.9984
Hydrogen line—				
1	0.1499	NC	−0.2190	0.9883
1	0.1245	0.0005	−0.0574	0.9783
2	0.1624	0.0006	−0.3783	0.9979
2	0.1902	NC	−0.6558	0.9957
Chlorine line—				
1	0.0500	NC	0.0978	0.9444
1	0.0783	−0.0002	−0.3877	0.9948
2	0.0635	NC	−0.2006	0.9987

* Corresponding to plots such as Fig. 4.

† From least-squares regression with first- and second-order polynomials of the type $y = Ax + Bx^2 + K$.

‡ Solutions 1 and 2 are, respectively, those with higher and lower concentrations.

§ NC = no *B* term, first-order polynomial.

compounds that were excluded in the derivation of the linear equation can be expected to behave in the same way as the other ten compounds.

Similar plots were made for H : C and Cl : H (Fig. 1). The Cl : H plot was clearly non-linear and was described by the polynomial $y = 0.019 + 0.671x + 0.131x^2$, with $r^2 = 0.998$, while the H : C plot revealed no functional relationship. When interpolation of the H molecular coefficients was made using the above polynomial, the reliability of the calculated H molecular coefficients improved and, when used together with the Cl molecular coefficients, it led to correct molecular formulae.

It is not clear from these results whether H or Cl was responsible for the non-linearity, because the observed Cl : C linearity could be the result of a non-linear response by Cl and C that was compensated when the ratios of the elemental response to the respective number of atoms were made. Thus, an experiment was designed to resolve this question. Six of the 13 compounds previously tested were chosen, to try to detect

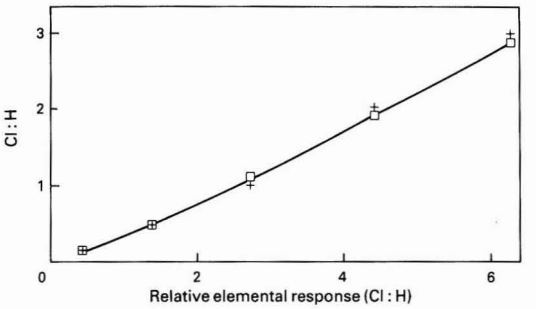

Fig. 3. Values for the ratio of Cl : H coefficients as a function of the Cl : H relative elemental response. +, Raw data; and □, polynomial (second order)

Table 3. Data analysis for the relationship between the relative elemental response and the inter-elemental content of a compound*

Elemental ratio	Polynomial parameter† *A*	*B*	*K*	Correlation coefficient
Cl : C	0.7905	NC‡	−0.0235	0.9965
H : C	2.1604	NC	−0.1120	0.9285
Cl : H	0.4994	NC	−0.1979	0.9926
Cl : H	0.3415	0.0233	−0.0322	0.9981

* Corresponding to the ratio of the number of atoms in the molecular formula *versus* the relative elemental response plots, as in Fig. 3.

† See Table 2.

‡ NC = no *B* term, first-order polynomial.

the source of the non-linearity. In order to avoid problems of poor injection repeatability, an approach derived from the internal standard method (ISM) was used. Use of the ISM approach also minimised changes in plasma characteristics which are due to both a black carbon deposit and a white deposit that grew in the quartz discharge tube as a consequence of molecular fragmentation in the plasma.

In consideration of their boiling-points, cyclohexene, cyclohexane and nonane were tested as internal standards; cyclohexane was chosen because it eluted before the solvent (toluene) and was well separated from the next eluting compound (Fig. 2). The measured peak heights for each compound at chlorine, hydrogen and carbon lines, after correction to the same ×16 attenuation value, were divided by the molar concentration of the compound to generate a parameter that was called the response per concentration unit (RCU). The same parameter was calculated by dividing the peak height for the internal standard (cyclohexane) at the carbon line by its molar concentration. Then, the values of the RCU for each element were divided by the carbon RCU of the internal standard. Each RCU was dependent on the injected volume, but not the ratio, as slight variations due to syringe repeatability tended to compensate when using the ISM approach. The ratio of the RCUs generates another "relative" parameter, the element relative to carbon (ERC), of the internal standard, response. The ERC is, to a first approximation, directly proportional to the number of atoms of the respective element, and thus the study of the behaviour of these relative responses against the number of atoms of the respective elements in the six compounds should provide information about possible structural dependencies of the detector response.

The number of atoms of the three elements studied (C, H, Cl) in the six compounds was plotted against the respective ERC and the data points for the two solutions were fitted by first- and second-order polynomials. For the most dilute solution, the linear equations of Table 2 give the best fits for

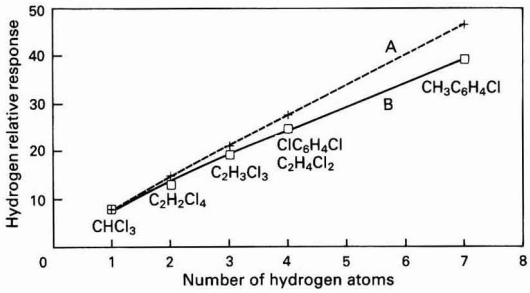

Fig. 4. Hydrogen relative response as a function of the number of H atoms in the molecular formulae. A, Solution of higher concentration; and B, solution of lower concentration

the carbon and chlorine data, but a second-order equation gives the best fit for the hydrogen data (the correlation coefficient of 0.9979 is slightly better than the corresponding 0.9957 of the linear plot); the non-linear equation also has an intercept (−0.3783) that better approaches the zero intercept expected for a functional relationship based on the ratio of peak size. The same data analysis applied to the higher concentration solution revealed very poor correlations (first- and second-order polynomials) for carbon and hydrogen with a possible tendency of the chlorine data to be better fitted by a second-order polynomial (Table 2).

To present data comparable to that of Slatkavitz,[10] we plotted each of the three possible atomic ratios (Cl : C, H : C, Cl : H) in the six compounds against the ratio of the respective ERC. This ratio is termed the relative elemental response and is strictly related to the element molar concentration because it is a relationship between "elemental responses per parent compound molar concentration unit." This reduced parameter allows the comparison of the detector response for elements in different compounds as if the compounds had the same molar concentration. For a given pair of elements in different compounds, and in the absence of either structural or concentration dependence of the detector response (and any other systematic error), this relative elemental response must have a linear relationship to the atomic ratios of the pair of elements in the different compounds.

As can be seen in Fig. 3 and in Table 3, the atomic ratio *versus* relative elemental response plot for the Cl : H pair is better described by a non-linear relationship, the Cl : C plot is linear and the H : C, in a similar fashion to the plot of Fig. 1(*b*), shows no functional behaviour. These results should be expected because, as discussed above for the ERC *versus* number of atoms plots, the H response does not show a linear correlation with the number of H atoms (Fig. 4).

The Cl : C linear equation and the Cl : H second-order equation from Table 3 were used to interpolate the corresponding minimum atomic ratios for the six compounds. This resulted in two different sets of minimum molecular coefficients for chlorine, and unit molecular coefficients for both C and H. A factor was calculated for each compound by dividing the Cl molecular coefficient obtained from the Cl : C relationship by the Cl molecular coefficient from the Cl : H ratio. These factors were taken as the H molecular coefficients. The Cl molecular coefficients were taken as those obtained from the more reliable linear Cl : C relationship. This both eliminated a dual (and cumbersome) set of Cl minimum molecular coefficients and generated the H molecular coefficients by a cross-correlation type of data analysis. These Cl, H and (C = 1) minimum molecular coefficients were used to reproduce the known molecular formulae which are listed in Table 1; these are shown, together with the errors for the number of atoms of each element in relation to the real value. As can be seen, except for the compound of highest hydrogen content, *m*-chlorotoluene, all hydrogen molecular coefficients have less than 5% errors and give the correct molecular formulae. Chlorine molecular coefficients all have less than 6% errors. The Cl molecular coefficients for the lower concentration solution were also calculated using equation (1) with $C_2H_4Cl_2$ as the reference compound and all were within the 5% error expected for the experimental procedure. It may thus be concluded that, although equation (1) does not apply to the calculation of hydrogen molecular coefficients, because the H behaviour is not linear, it may still be used as a good representation of the Cl : C ratio of elemental response per atom.

For the Cl : H ratio, the results indicated that the hydrogen response tended to be enhanced at higher hydrogen concentrations. This non-linear behaviour was not attributed to structural effects. Our results also indicate that, in contrast to hydrogen, the number of atoms *versus* response (ERC) plots were linear for both carbon and chlorine. Thus, the non-linearity observed for hydrogen was the result of an effect that only applied to that element.

The suggestion of a dependence of the hydrogen peak sizes on hydrogen concentration, rather than a structural effect, is based on the following considerations. Firstly, as can be seen in Fig. 4, *m*-chlorotoluene is the compound that probably causes the deviation from linearity; it was also the compound that showed the higher error (13.3%) for the hydrogen molecular coefficient when equation (1) was used for the calculations. Secondly, Fig. 4 also shows that the curves for the higher and lower concentration solutions tend to coincide as the number of hydrogen atoms per molecule diminishes. Thirdly, the data points for the H_1–H_4 compounds in Fig. 4 show a behaviour that could be taken as linear. However, except for the H_1 compound, $CHCl_3$, the two plots are non-coincident and separate further as the number of hydrogen atoms in the compounds becomes larger. Finally, data for the higher concentration solution in Table 2 indicate that the chlorine and carbon, and also the hydrogen, behaviour is not well represented by linear equations.

Conclusions

The results presented here indicate that errors in elemental molecular coefficients that arise when the linear equation (1) is used may be related to concentration dependencies of the size of chromatographic peaks of hydrogen. This indicates the need to study the dependence of peak size on the number of atoms of each element, for different concentration mixtures of a series of compounds: the series of compounds and the concentration range need to be sufficient to include the unknown. For this type of approach, the use of an internal standard method is appropriate, to avoid replicate injections of each standard sample which would lead to long-term changes in the plasma behaviour. The possible existence of different elemental responses can be used as a tool for data cross-correlation that can lead to reliable figures for atomic coefficients.

A GC - MIP system has two highly valuable characteristics in terms of chemical analysis: the compounds that reach the detector have a high degree of purity, achieved by high-resolution gas-chromatographic separation; and the elements of these compounds can be detected with a high degree of selectivity. This makes GC - MIP an important tool for formula determination studies, as analytes can be observed with very little, or no, matrix effect. Thus, it is imperative that this structural formula determination technique should not be considered invalid because linear, through the origin plots are not always observed; rather, there should be serious attempts to understand these deviations better so that the technique might be more fully exploited.

One of the authors, A. L. P. V., thanks the "Fundacao de Amaparo a Pesquisa do Estado de São Paulo (FAPESP)," São

Paulo, Brazil, for the sponsorship of postdoctoral study at the University of Massachusetts. This work was supported in part by the Dow Chemical Company, by Merck, Sharp and Dohme Research Laboratories and by the Baxter Healthcare Corporation.

References

1. Dagnall, R. M., West, T. S., and Whitehead, P., *Anal. Chem.*, 1972, **44**, 2074.
2. McLean, W. R., Stanton, D. L., and Penketh, G. E., *Analyst*, 1973, **98**, 432.
3. Dingjan, H. A., and de Jong, H. J., *Spectrochim. Acta, Part B*, 1981, **36**, 325.
4. Estes, S. A., Uden, P. C., and Barnes, R. M., *Anal. Chem.*, 1981, **53**, 53.
5. Windsor, D. L., and Denton, M. B., *Anal. Chem.*, 1979, **51**, 1116.
6. McNair, H. M., and Bonelli, E. J., "Basic Gas Chromatography," Fifth Edition, Varian Aerograph, Walnut Creek, CA, 1969, p. 160.
7. Grob, R. L., "Modern Practice of Gas Chromatography," Second Edition, Wiley, New York, 1985, p. 414.
8. Uden, P. C., Slatkavitz, K. J., Barnes, R. M., and Deming, R. L., *Anal. Chim. Acta*, 1986, **180**, 401.
9. Slatkavitz, K. J., Uden, P. C., Hoey, L. D., and Barnes, R. M., *J. Chromatogr.*, 1984, **302**, 277.
10. Slatkavitz, K. J., *PhD Dissertation*, University of Massachusetts, 1985.

Paper 9/03965A
Received September 18th, 1989
Accepted January 16th, 1990

On-line Pre-concentration of Refractory Elements for Atomiser, Source, Inductively Coupled Plasmas in Atomic Fluorescence Spectrometry (ASIA)*

Stanley Greenfield, Tariq M. Durrani, Satilmis Kaya and Julian F. Tyson†
Department of Chemistry, University of Technology, Loughborough, Leicestershire LE11 3TU, UK

A simple flow manifold coupled to an atomiser, source, inductively coupled plasmas in atomic fluorescence spectrometry (ASIA) system for the pre-concentration of refractory elements is described. A miniature column of Amberlite IRA-93 anion-exchange resin was used to pre-concentrate refractory elements such as tungsten, molybdenum, zirconium and vanadium as their oxyanions from synthetic aqueous solutions before detection. A study of the parameters that affect the performance of the method is described. The pre-concentrated species were eluted with a stream of ethanolic ammonia directly into the nebuliser of the atomiser plasma. The limits of detection based on a sample volume of 35 ml (sampling time 5 min at 7 ml min^{-1}) were 65 and 15 ng ml^{-1} for tungsten and molybdenum, respectively. Relative standard deviations of 4.28 and 5.24% were obtained for 0.5 and 0.1 μg ml^{-1} concentrations of tungsten and molybdenum, respectively. Further improvements in detection limits were obtained after modification to the instrument; although the main objective of this work was to develop a pre-concentration method applicable to the simultaneous determination of a number of refractory elements, this was not achieved. However, the proposed method could be used for pre-concentration of tungsten and molybdenum.

Keywords: *Pre-concentration; atomiser source inductively coupled plasma; atomic fluorescence spectrometry; refractory element; tungsten and molybdenum*

Atomic fluorescence spectrometry (AFS) has been of considerable interest to analytical atomic spectroscopists for a number of years.[1,2] The main advantage of this technique over other techniques, particularly inductively coupled plasma atomic emission spectrometry (ICP-AES), is the simplicity of the spectra obtained. This alleviates the problem of spectral interferences to which ICP-AES is prone. Unfortunately, analytical applications of the technique have suffered from the lack of commercial instrumentation. However, a commercial instrument has been introduced by Baird which uses pulsed hollow-cathode lamps as the source of excitation and an ICP as the atomiser.[3] The instrument used in the work described here[4] utilises a high-power plasma (source plasma) to excite atomic fluorescence from the atoms formed in a low-power plasma (atomiser plasma).

In general, detection limits for most elements determined using this technique are comparable to, or better than, those in ICP-AES, except for refractory elements. Refractory elements such as tungsten exhibit low sensitivity in the AFS technique, possibly owing to the formation of refractory oxides. The use of carbon-containing species has been recommended[5,6] for the reduction of oxides formed in the atomiser plasma. Carbon can be introduced by passing propane, at low flow-rates, into the injector tube of the atomiser plasma, to produce a long-tailed plasma resembling a flame. Alternatively, organic solvents can be introduced into the atomiser plasma. This leads to an increase in sensitivity but, unfortunately, neither approach provides sufficient sensitivity to permit detection limits comparable to those achievable by ICP-AES.

Pre-concentration of refractory elements prior to their nebulisation is an alternative for improving the sensitivity by this technique. A variety of pre-concentration techniques are available to enhance the sensitivity, including chelating ion-exchange resins,[7] solvent liquid - liquid extraction,[8] co-precipitation[9–11] and electro-deposition methods.[12] Recently, Furuta *et al.*[13] reported a pre-concentration flow injection system utilising a microcolumn of activated alumina to pre-concentrate molybdenum from sea water prior to determination by ICP-AES.

The aim of this study was to develop a rapid and simple on-line pre-concentration procedure that would allow a number of refractory elements to be determined simultaneously and rapidly.

Experimental

Apparatus

The ASIA system consists of two ICPs. The source plasma contained in a Greenfield torch and powered by a Radyne RD150 high-frequency generator (15 kW output at 7 MHz). The atomiser plasma is contained in a long-sleeved Baird torch, powered by a Radyne SC15 high-frequency generator (2.5 kW output at 36 MHz). A detailed description of the instrument and its operation has been given elsewhere.[5] During the course of this work, modifications to the instrument were made which are listed in Table 1. The Optica monochromator has been replaced with a Bentham Instruments computer-controlled monochromator with an improved light-gathering power. A single lens is used between the atomiser plasma and the monochromator entrance slits rather

Table 1. Modifications made to the ASIA system

Component	Description
Monochromator	Bentham M300 (computer controlled)
Photomultiplier tube	EMI 9558QB
Stepping motor drive	Bentham SMD 3B/IEEE
Power amplifier for SMD	Bentham SMD2
Microcomputer	Opus PC II
Peripherals	Hewlett-Packard HP 7470 A and MP-165 printer
Current amplifier	Bentham 265HF (programmable)
Lock-in amplifier	Bentham 223
Display unit	Bentham 217

* Presented at SAC 89, the 8th SAC International Conference on Analytical Chemistry, Cambridge, UK, 30 July–5 August, 1989.

† Present address: Department of Chemistry, Lederle Graduate Research Tower A, University of Massachusetts, Amherst, MA 01003, USA.

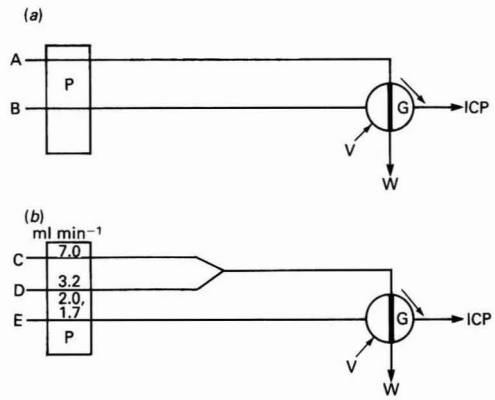

Fig. 1. Pre-concentration manifolds. (*a*) Single-line manifold: A, sample mixed with buffer at variable flow-rate; B, eluent at variable flow-rate; W, waste; P, pump; V, valve; G, column. (*b*) Dual-line manifold: C, sample; D, buffer; E, eluent

than the original two lenses, which allows greater collection of the fluorescence radiation from the atomiser plasma.

The pre-concentration manifold (Fig. 1) consisted of a Gilson Miniplus 2 (eight-channel) peristaltic pump and an Omnifit six-port injection valve incorporating a laboratory-made glass column (50 m × 2.3 mm i.d.) containing anion-exchange resin (Amberlite IRA-93, 16–50 mesh). All the connecting tubing consisted of 0.8 mm i.d. PTFE. Solutions were pumped with Tygon tubing of the appropriate size to obtain the desired flow-rates.

The column was prepared by placing a porous PVC membrane at one end of the column and aspirating a water slurry of the resin into the column until it was filled. Another PVC membrane was placed at the other end of the column and sealed to the plastic connectors using an epoxy resin. The column was placed in the injection loop of the valve so that the sample was loaded in one direction and eluted in the other, which prevented the resin from packing into one end of the column.

Reagents

All reagents were of analytical-reagent grade. Stock standard solutions of tungsten, molybdenum and vanadium were prepared from sodium tungstate (BDH), molybdenum oxide (BDH) and vanadium oxide (Aldrich), respectively. A stock solution of zirconium (995 μg ml^{-1}) from Aldrich was used. A series of working standard solutions for each of the four elements were prepared by dilution of the stock standard solutions with de-ionised water.

For the source plasma, a high-concentration solution of tungsten (40%, m/v) was prepared from dodecatungstosilicic acid (Fisons) dissolved in cold de-ionised water. A 20% (m/v) molybdenum solution was prepared by dissolving molybdenum oxide in the minimum amount of 35% ammonia solution. A stock solution of vanadium (1 mg ml^{-1}) was prepared by dissolving the oxide in 10 ml of concentrated hydrochloric acid. Molybdenum oxide and vanadium oxide were dried at 110 °C for 2 h before weighing.

Ethanolic 2.0 M ammonia solutions of tungsten were prepared by adding a measured volume of 35% ammonia solution to accurately measured volumes of tungsten stock solution in a calibrated flask, followed by the addition of a calculated volume of de-ionised water and dilution to volume with 99% ethanol with constant stirring. The ethanolic 2.0 M ammonia solutions were prepared freshly because solutions containing 80% or more of ethanol tend to form a precipitate after some time.

The buffer solutions were prepared from ammonium acetate (BDH) and potassium chloride (BDH). The pH of the ammonium acetate buffer solutions was adjusted to the appropriate value by adding acetic acid or ammonia solution, whereas the pH of the potassium chloride buffer solutions was adjusted by adding hydrochloric acid or ammonia solution.

Method Development

A systematic study was carried out to determine the optimum operating conditions of the instrument for the elements studied using an alternative variable search method,[14] while monitoring the total fluorescence signal. In emission experiments the figure of merit used was the signal to background ratio. The variables included plasma gas flow-rate, observation height and solution flow-rate. The emission lines selected for tungsten, molybdenum, zirconium and vanadium were 400.9, 379.8, 339.198 and 310.2 nm, respectively.

The performance of the pre-concentration manifold was studied by investigating the effect of buffer pH, sample and eluent flow-rates and eluent and buffer strengths. Measurements were made on-line for most of the parameters studied in the emission mode using the manifold in Fig. 1(*a*). The influence of pH on the retention of the metal species on the column was studied using 0.1 M potassium chloride (pH 1–3) and 0.5 M ammonium acetate (pH 3.5–8.0) buffers. The column efficiency was determined by passing metal solutions through the column at a flow-rate of 1 ml min^{-1}. The column effluents were analysed using the conventional continuous aspiration method. The results obtained were used to calculate the retention efficiency of the column for each of the four elements. The effect of sample flow-rate was studied by passing metal solutions through the column at different flow-rates and analysing the column effluent to determine the percentage retention of the elements. A number of eluents were studied, including nitric acid, hydrochloric acid, sodium carbonate and ammonia at concentrations between 1 and 4 M. Ammonia solutions were optimised for ethanol percentages for measurements made in the fluorescence mode.

Method Performance

The performance of the method was studied by constructing calibration graphs for molybdenum and tungsten. Standard solution at a flow-rate of 7 ml min^{-1} was merged with a buffer flowing at 3.2 ml min^{-1} at the optimum pH. This solution was then passed through the column for 5 min. After the analyte had been deposited on the resin column, elution was effected by switching the valve to allow a stream of 2.0 M ammonia solution in 75% ethanol at the optimised flow-rate to pass through the column. The valve was then switched to the "load" position and the column was washed with blank solution for 30 s to allow the column to reach the optimum pH. The procedure was repeated for the next solution.

Results and Discussion

Method Development

Fig. 2 shows that for tungsten, quantitative retention was obtained at pH 5 and below, whereas for molybdenum the response was fairly sensitive to pH, as indicated by the sharp maximum at pH 2.0. For zirconium and vanadium the behaviour of the resin was different, showing quantitative retention at and above pH 4.0 for both elements. This dissimilarity in the behaviour of the resin for the four elements studied can be attributed to the dissimilarity of the metal species formed in the solutions. These results show that pH 2.0 was suitable for the pre-concentration of tungsten and molybdenum. However, pH 4.5 was used for the pre-concentration of tungsten because of the gradual deterioration of the resin at pH 2.0.

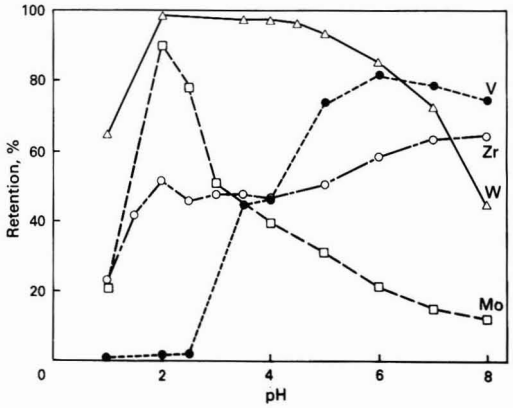

Fig. 2. Effect of varying pH on metal retention using the manifold in Fig. 1(*a*)

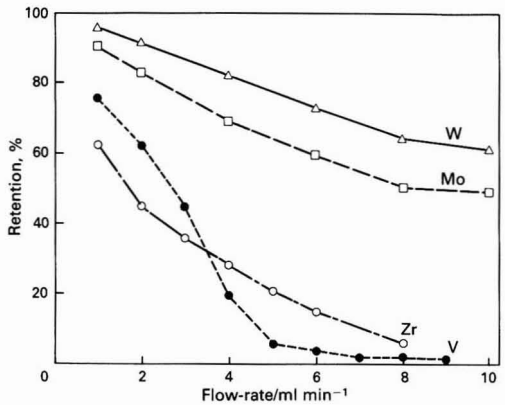

Fig. 3. Effect of varying sample flow-rate on metal retention using the manifold in Fig. 1(*a*)

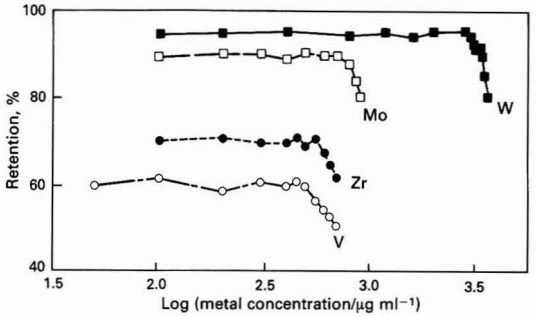

Fig. 4. Retention behaviour of the resin column

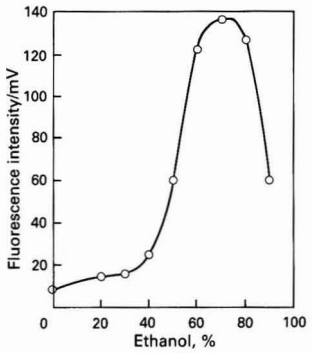

Fig. 5. Effect of percentage of ethanol on tungsten (750 μg ml^{-1}) atomic fluorescence signal, while aspirating a 40% tungsten solution into the source plasma

The effect of sample flow-rate on the retention of the metal species is shown in Fig. 3. The retention decreases as the flow-rate increases above 1 ml min^{-1}. This behaviour could be due to the kinetic effect relating the retention efficiency with the time the sample is in contact with the resin. Several factors are of value when making projections concerning the dynamic behaviour of resins, including the rate constant and the rate of interaction between the resin and the ions, which is a time-dependent factor. On the basis of the results obtained, these elements could be divided into two groups: (i) tungsten and molybdenum and (ii) zirconium and vanadium. The retention of zirconium and vanadium falls fairly rapidly as the flow-rate of the sample is increased above 1 ml min^{-1}. A possible reason for this behaviour of the resin could be the formation of unstable hydroxo complexes or polymerisation. The elements of the fourth and fifth groups such as zirconium and vanadium tend to hydrolyse, polymerise or precipitate even in fairly acidic solutions; hydrofluoric acid solutions have been recommended[15] for the formation of fluoro complexes, which are more stable than the hydroxo complexes. However, hydrofluoric acid could not be used with this particular manifold system because the column was made of glass.

The results of the retention efficiency experiments are shown in Fig. 4. The retention of tungsten, molybdenum, zirconium and vanadium falls after loading 3000, 700, 550 and 500 μg ml^{-1} of these elements, respectively. The retention efficiency calculations were made as recommended by Jacintho *et al.*[16]

Four types of eluents for eluting the retained metal species were investigated. It was found that nitric acid and hydrochloric acid at concentrations up to 4.0 M were less effective than ammonia solutions in eluting retained metal species from the resin column. The use of sodium carbonate solution resulted in a high blank value, which excluded its further use. A 2.0 M ammonia solution was found to be most suitable in eluting all the retained metal species for measurements made in the emission mode. However, for atomic fluorescence measurements a 75% ethanolic 2.0 M ammonia solution was found to be suitable.

As described earlier, special means are employed to maintain refractory elements as free atoms in the plasma tail plume for atomic fluorescence measurements. In this study, ethanol was used to provide the necessary reducing environment. The effect of ethanol on the atomic fluorescence signal of tungsten (Fig. 5) shows that the fluorescence signal increases as the percentage of ethanol increases until the 75% level is reached, after which a rapid decrease in signal occurs, probably owing to quenching of the fluorescence signal by the carbon species. Subsequently a 75% ethanolic 2.0 M ammonia solution was used to elute the sorbed metal ions. When using ethanol in the 2.0 M ammonia eluent there was no apparent effect on the eluting properties. An advantage of using ethanolic over aqueous ammonia solution was that there was less swelling of the resin column, which avoided any pressure build-up in the flow manifold, ensuring long-term operation of the column without leakage.

Table 2. Comparison of detection limits obtained by ASIA in the AFS mode (ng ml^{-1})

Element	Wavelength/nm	Previous system		Modified system	
		Conventional nebulisation	Pre-concentration	Conventional nebulisation	Pre-concentration
W	295.6	900	65	428	—
Mo	313.3	146	15	63	8

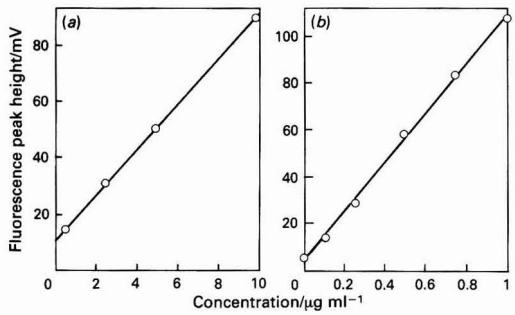

Fig. 6. Calibration graphs for (*a*) tungsten and (*b*) molybdenum, while aspirating 40 and 20% solutions of tungsten and molybdenum, respectively, into the source plasma

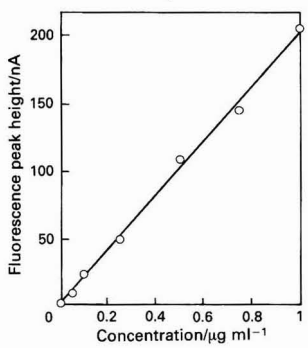

Fig. 7. Calibration graph for molybdenum while aspirating 20% molybdenum solution into the source plasma

Method Performance

It was observed in the study of the effect of various parameters on the method performance that only tungsten and molybdenum could be rapidly pre-concentrated. Zirconium and vanadium showed <5% retention on the column at a sample flow-rate of 8 ml min^{-1} and it was therefore considered unnecessary to continue with these elements. Calibration graphs for tungsten and molybdenum are presented in Fig. 6, and show good linearity. The relative standard deviations for tungsten at 10 and 0.5 μg ml^{-1} concentrations were 1.17 and 4.28%, respectively, and those for molybdenum at 1 and 0.1 μg ml^{-1} were 2.45 and 5.24%, respectively. The limits of detection based on three standard deviations of five replicate measurements of 0.5 μg ml^{-1} of tungsten and 0.1 μg ml^{-1} of molybdenum were 65 and 15 ng ml^{-1}, respectively. After modifications to the instrument, a calibration graph for molybdenum was constructed using the manifold in Fig. 1(*b*), the results of which are shown in Fig. 7. A detection limit of 8 ng ml^{-1} was obtained for a set of five replicate measurements on 50 ng ml^{-1} molybdenum solution using the procedure described earlier. The precision at this concentration was 4.76%. A comparison of the results obtained using the pre-concentration method and conventional nebulisation is shown in Table 2. Under the recommended conditions, the sampling frequency is 10 samples per hour.

Conclusions

This study has demonstrated that a pre-concentration manifold incorporating a microcolumn of an anion-exchange resin and subsequent elution of sorbed metal species using an organic solvent medium offers a method for the determination of refractory elements by AFS at the ng ml^{-1} level. It may be possible to increase the sensitivity by increasing the sample volume. However, the sampling frequency will be lowered accordingly.

Unfortunately, different conditions for pre-concentration were found to be necessary for different elements and the method would have only limited application to the ASIA work. As a consequence, further work with the proposed method was not pursued. However, the method would be of value if tungsten and/or molybdenum were to be determined by AFS. The manifold could be applied to other refractory elements that form oxyanions, *e.g.*, boron and chromium, for which the normal sensitivity in AFS is relatively low.

Financial support for T. M. D. from the Ministry of Science and Technology, Government of Pakistan, is gratefully acknowledged.

References

1. Epstein, M. S., Bayer, S., Bradshaw, J., Voigtman, E., and Winefordner, J. D., *Spectrochim. Acta, Part B*, 1980, **35**, 233.
2. Smith, B. W., Glick, M. R., Spears, K. N., and Winefordner, J. D., *Appl. Spectrosc.*, 1989, **43**, 376.
3. Demers, D. R., and Allemand, C. D., *Anal. Chem.*, 1981, **53**, 1915.
4. Greenfield, S., *Anal. Proc.*, 1984, **21**, 61.
5. Greenfield, S., and Thomsen, M., *Spectrochim. Acta, Part B*, 1986, **41**, 677.
6. Greenfield, S., and Thomsen, M., *Spectrochim. Acta, Part B*, 1985, **40**, 1369.
7. Phillips, R. J., and Fritz, J. S., *Anal. Chim. Acta*, 1980, **121**, 225.
8. Kim, C. H., Alexander, P. W., and Smythe, L. E., *Talanta*, 1975, **22**, 739.
9. Smith, C. L., Motooka, J. M., and Willsen, R., *Anal. Lett.*, 1984, **17** (A15), 1715.
10. Harda, H., and Kurata, N., *Bunseki Kagaku*, 1985, **34**, 175.
11. Akagi, T., Nojiri, Y., Matsui, M., and Haraguchi, H., *Appl. Spectrosc.*, 1985, **39**, 662.
12. Henriet, D., De Gelis, D., and Berneron, R., *Mem. Etud. Sci. Rev. Metall.*, 1983, **80** (2), 73.
13. Furuta, N., Brushwyler, K. R., and Hieftje, G. M., *Spectrochim. Acta, Part B*, 1989, **44**, 349.
14. Greenfield, S., Salman, M. S., Thomsen, M., and Tyson, J. F., *J. Anal. At. Spectrom.*, 1989, **4**, 55.
15. Nelson, F., Rush, R. M., and Kraus, K. A., *J. Am. Chem. Soc.*, 1960, **82**, 339.
16. Jacintho, A. O., Zagatto, E. A. G., Bergamin, Fº. H., Krug, F. J., Reis, B. F., Bruns, R. E., and Kowalski, B. R., *Anal. Chim. Acta*, 1981, **130**, 243.

Paper 9/03927I
Received September 14th, 1989
Accepted November 16th, 1989

Determination of Trace Elements in Trimethylgallium by Electrothermal Atomisation Atomic Absorption Spectrometry and Inductively Coupled Plasma Atomic Emission Spectrometry*

Kikuo Takeda, Masao Minobe, Takeshi Hoshika, Tsunenobu Jinno and Tadaaki Yako
Ehime Research Laboratory, Sumitomo Chemical Co., 5-1 Soubiraki-cho, Niihama, Ehime 792, Japan

Three different methods are described for the determination of trace elements in trimethylgallium (TMG), involving the use of electrothermal atomisation atomic absorption spectrometry (ETAAS) and inductively coupled plasma atomic emission spectrometry (ICP-AES). The TMG, diluted with xylene, was decomposed by its gradual addition to cooled hydrochloric acid in an atmosphere of argon. The gallium-free xylene phase obtained by the decomposition was used for the determination of organic silicon by ICP-AES. Inorganic silicon in the hydrochloric acid phase was determined by ETAAS, with the use of a lanthanum-coated graphite tube, after the concentration of inorganic silicon by diisopropyl ether extraction and lanthanum hydroxide coprecipitation techniques. Thirteen other elements were also determined by ETAAS after the separation of gallium by diisopropyl ether extraction. Detection limits for organic silicon, inorganic silicon and the other elements were 0.02, 0.05 and 0.01 p.p.m., respectively.

Keywords: *Trimethylgallium; coprecipitation with lanthanum hydroxide; electrothermal atomisation atomic absorption spectrometry; inductively coupled plasma atomic emission spectrometry; determination of trace impurities*

Organometallics such as trimethylgallium (TMG) are being increasingly employed in the large-scale production of compound semiconductors, by organometallic chemical-vapour deposition, for the fabrication of complex optoelectronic device structures. It is well known that the electrical properties of compound semiconductors are strongly dependent on the purity of the starting materials. For the successful production of these semiconductors, the organometallics must also be of the highest purity. It is, therefore, desirable to develop sensitive methods for the determination of trace impurities in, and for the purification of, organometallics. However, it is generally difficult to determine the impurities, because these are pyrophoric and react instantaneously with air and moisture. Bertenyi and Barnes[1] and Jones *et al.*[2] reported methods for the determination of impurities in TMG by inductively coupled plasma atomic emission spectrometry (ICP-AES). The detection limits of these methods are, however, almost p.p.m. to sub-p.p.m. levels. The purpose of this work was to develop a suitable decomposition procedure and highly sensitive methods for the determination of impurities in TMG by electrothermal atomisation atomic absorption spectrometry (ETAAS) and ICP-AES in spite of the difficulty of sample treatment.

Experimental

Apparatus

All AAS measurements were carried out with the use of a Hitachi Z-8000 Zeeman-effect atomic absorption spectrometer equipped with a Hitachi hollow-cathode lamp and a Hitachi tube-type graphite furnace. A Seiko Denshi Kogyo 1100H inductively coupled plasma atomic emission spectrometer was used for the determination of organic silicon. The decomposition apparatus employed is shown schematically in Fig. 1. The sealed PTFE decomposition bottle (200 ml) was connected to two bubblers (20 ml) each containing 10 ml of xylene in order to collect volatile organic silicon completely.

Reagents

All the chemicals used were of analytical-reagent grade, unless specified otherwise, and de-ionised, distilled water was used throughout.

Stock standard solutions for AAS (Wako Pure Chemicals; 1 mg ml^{-1}) were used for each element, except chromium and organic silicon. A stock standard chromium solution (1 mg ml^{-1}) was prepared by dissolving chromium metal in 6 M hydrochloric acid. A standard organic silicon solution was prepared by dissolving trimethylchlorosilane in xylene just prior to use.

Lanthanum solution (10 mg ml^{-1}) was prepared by dissolving 3.12 g of lanthanum nitrate (Wako Pure Chemicals) in 100 ml of water.

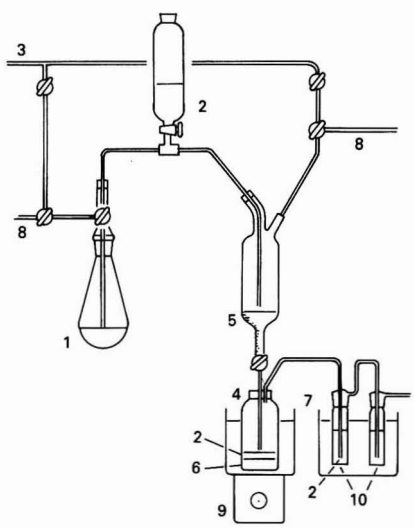

Fig. 1. Schematic diagram of the apparatus used to decompose TMG. 1, TMG; 2, xylene; 3, argon inlet; 4, decomposition bottle; 5, TMG diluted with xylene; 6, hydrochloric acid; 7, dry ice and hexane bath; 8, argon outlet; 9, magnetic stirrer; and 10, bubbler

* Presented at SAC 89, the 8th SAC International Conference on Analytical Chemistry, Cambridge, UK, 30 July–5 August, 1989.

Ammonia solution was of analytical super-high-purity grade (Tamapure-AA-100) from Tama Chemicals.

Hydrochloric acid was prepared with an all-PTFE sub-boiling distillation apparatus (Fujihara Seisakusyo).

Decomposition of TMG

The device shown in Fig. 1 was used to decompose TMG for the determination of trace impurities. A solution (40 ml) of 12 M hydrochloric acid and 20 ml of xylene were placed in the decomposition bottle (4). A 10-ml volume of xylene was also placed in each of the two bubblers (10). The decomposition bottle and the bubblers were cooled to −40 °C with dry ice and hexane. After the 200-ml specially designed measuring vessel (5), the decomposition bottle (4) and all the connecting tubes had been flushed with argon, 8.6 ml of TMG were transferred from the storage vessel (1) into the measuring vessel (5) through the PTFE tubes, with a slight positive pressure of argon, by using the graduation mark of the measuring vessel. After this, 100 ml of xylene (2) were placed in the measuring vessel, and the contents of the vessel were mixed by shaking. The TMG, diluted with xylene, was poured gently into the decomposition bottle at a rate of 10–20 drops min^{-1}, and the contents of the bottle were mixed continuously with a magnetic stirrer (9). The gaseous phase produced by decomposition of TMG was introduced into the two bubblers (10) in order to collect volatile organic silicon. After the reaction of TMG with hydrochloric acid was complete, the dry ice and hexane bath were removed from the decomposition bottle, and its contents were stirred at room temperature for 2 h. The contents of the bottle were then transferred into a PTFE separating funnel (200 ml) and separated into two phases.

Determination of Organic Silicon

The organic phase obtained by the decomposition process, and xylene in the bubblers, were introduced into the nebuliser of the ICP-AES system. The operating conditions were: radio-frequency power, 2.0 kW; nebuliser gas pressure, 1.5 kg cm^{-2}; coolant flow-rate, 18 l min^{-1}; auxiliary flow-rate, 2.0 l min^{-1}; and wavelength, 251.6 nm. A calibration graph of emission intensity *versus* silicon concentration was plotted, with the use of diluted standard organic silicon solutions containing 0.025–1.0 μg of silicon in 25 ml of xylene.

Determination of Inorganic Silicon

The hydrochloric acid phase (10 ml) obtained by the decomposition process and 10 ml of diisopropyl ether were placed in a PTFE vessel (30 ml) fitted with a cap. After shaking the vessel for a few minutes, the contents were left to stand, and the upper organic phase was removed by suction through a capillary tube. This extraction process was repeated twice. A 1-ml aliquot of lanthanum solution (10 mg ml^{-1}) was added to the remaining hydrochloric acid phase, and the pH of the mixture was adjusted to 9.5 by the addition of ammonia solution. This solution was allowed to stand for a few minutes and then centrifuged. The supernatant liquid was removed by decantation. The precipitate was dissolved in 0.5 ml of 6 M hydrochloric acid, and the solution was diluted to 1 ml with water. A 20-μl aliquot of the diluted solution was introduced into a lanthanum-coated graphite tube, and the absorption of silicon was measured by ETAAS. The operating conditions were: drying, 30 s at 80–120 °C; ashing, 30 s at 1000 °C; atomising, 7 s at 2800 °C; cleaning, 3 s at 2800 °C; and wavelength, 251.6 nm. A calibration graph of absorption *versus* silicon concentration was plotted, with the use of diluted standard inorganic silicon solutions containing 0.01–0.8 μg of silicon, prepared by the same procedure as described above, but without the sample.

Determination of 13 Other Elements

Hydrochloric acid (10 ml), obtained by the decomposition process, was placed in a PTFE vessel (30 ml) fitted with a cap, and 10 ml of diisopropyl ether were added. The vessel was shaken for a few minutes and left to stand, and the upper organic phase was removed by suction through a capillary tube. This extraction process was repeated three times. The resulting solution was evaporated to dryness, and the residue was dissolved in 1 ml of 6 M hydrochloric acid. The 13 elements (Al, Ca, Cd, Co, Cr, Cu, Mg, Mn, Ni, Pb, Ti, V and Zn) were determined by ETAAS under the optimum operating conditions shown in Table 1. A calibration graph of absorption *versus* concentration was plotted for each element, with the use of mixed standard solutions containing 0.01–0.20 μg of each element.

Results and Discussion

In spite of many efforts, the nature of the impurities in TMG has not been verified at present, because their concentration level is very low. In general, almost all organic metal compounds are immediately decomposed in the presence of mineral acids, and the metal ions produced are dissolved in mineral acids. Inorganic impurities are also readily transferred into mineral acids. On the other hand, organic silicon compounds are stable in mineral acids and cannot be dissolved in them. Therefore, when TMG, diluted with xylene, is decomposed by hydrochloric acid, organic silicon will remain in the xylene phase, while inorganic silicon and the other elements will be present in the hydrochloric acid phase.

Determination of Organic Silicon

In the decomposition procedure described above, when the xylene phase was not present in the hydrochloric acid phase in the decomposition bottle, the recovery of organic silicon was *ca.* 60%, because of the volatility of organic silicon compounds. On the other hand, the presence of the xylene phase increased the recovery of organic silicon, as shown in Table 2. Moreover, we also found that almost all the organic silicon could be collected by xylene in the first bubbler in both instances. We decided, therefore, to use xylene in the decomposition bottle and in the first bubbler for the determination of organic silicon by ICP-AES.

Table 1. Operating conditions for the atomic absorption spectrometer

Element	Al	Ca	Cd	Co	Cr	Cu	Mg	Mn	Ni	Pb	Ti	V	Zn
Wavelength/nm	309.3	422.7	228.8	240.7	359.3	324.8	285.2	279.6	232.0	283.3	364.3	318.4	213.8
Tube*	P	G	G	P	P	P	G	G	P	G	P	P	G
Heating conditions:†													
Ashing temperature/°C	700	600	300	600	700	600	500	500	700	400	900	900	300
Atomising temperature/°C	3000	2700	1500	2700	2900	2700	2000	2500	2700	2000	3000	3000	2000
Cleaning temperature/°C	3000	2800	1800	2800	3000	2800	2400	2800	2800	2400	3000	3000	2400

* Type of tube: G, graphite tube; P, pyrolytic graphite coated graphite tube.

† Other heating conditions: drying, 80–120 °C for 30 s; ashing, 30 s; atomising, 7 s; cleaning, 3 s.

It is known that normal nebulisation in ICP-AES alters the sensitivities for silicon when different organic silicon compounds are introduced into the nebuliser.[1] We also observed this phenomenon and found that the sensitivities correlated with the boiling-points of these organic compounds. Two different compounds, *i.e.*, trimethylchlorosilane (b.p. 57 °C) and methoxytrimethylsilane (b.p. 57 °C), showed the same sensitivities. It appears that, because high-purity TMG can normally be purified by distillation, the volatility of organic silicon in TMG is similar to that of pure TMG. Therefore, we decided to utilise trimethylchlorosilane as a standard substance, as its boiling-point is almost equal to that of TMG (57 °C).

The detection limit for the determination of organic silicon in TMG by ICP-AES was 0.02 p.p.m. as the metal base.

Determination of Inorganic Silicon

The hydrochloric acid phase obtained by the decomposition process contains a large amount of gallium converted into a water-soluble form. For the sensitive determination of silicon and the elimination of interference by matrix gallium, a procedure was carried out to remove gallium by extraction with diisopropyl ether,[3–8] and to collect silicon by coprecipitation with a metal hydroxide.

Extraction of gallium

In order to determine the amount of gallium remaining in the hydrochloric acid phase after the extraction with diisopropyl ether, the relationship between extraction time and the amount of gallium remaining was examined, with hydrochloric acid obtained by the decomposition of TMG as described above. The results showed that the amount of gallium remaining in the hydrochloric acid phase was less than 100 μg after three extractions. We decided, therefore, to extract with diisopropyl ether three times, because less than 100 μg of gallium did not interfere with the atomic absorption of silicon when this element was determined by ETAAS.

Selection of coprecipitant

There are only a few reports on the quantitative coprecipitation of trace amounts of silicon with metal hydroxides.[9,10] Hydroxides of lanthanum, indium and zirconium were examined as coprecipitants for the determination of silicon by ETAAS. Indium did not precipitate in a relatively concentrated solution of hydrochloric acid containing ammonia solution under the conditions described above. The use of zirconium was disadvantageous because of its poor solubility in acids. On the other hand, it was found that lanthanum hydroxide readily dissolved in hydrochloric acid and could collect trace amounts of silicon quantitatively. It was also found that the presence of lanthanum increased the sensitivity of the atomic absorption of silicon when this element was determined by ETAAS. Moreover, the use of lanthanum-coated graphite tubes also increased the sensitivity for silicon.[11] We decided, therefore, to use lanthanum hydroxide as coprecipitant for silicon. In the presence of 10 mg of lanthanum, used as coprecipitant in the resulting solution, and the use of a lanthanum-coated graphite tube, the slope of the calibration graph obtained by ETAAS was three times that of a calibration graph prepared without lanthanum, as shown in Fig. 2. The graphite tube was coated with 100 μl of lanthanum solution (10 mg ml^{-1}) five times. Further, the presence of lanthanum also improved the precision of the atomic-absorption measurements for silicon. The relative standard deviation of the atomic absorption obtained from ten replicate measurements for 0.2 μg ml^{-1} of silicon was 3.2% compared with 5.6% obtained in the absence of lanthanum.

Effect of pH on coprecipitation

The optimum pH range was studied with a hydrochloric acid solution (*ca.* 10 ml) containing 0.1 μg of silicon. Almost 100% recoveries were obtained over the pH range 9.2–10.8, as shown in Fig. 3. The pH was, therefore, adjusted to *ca.* 9.5 for the coprecipitation.

Effect of amount of coprecipitant

The amount of lanthanum necessary for the coprecipitation was examined, with a solution (10–20 ml) containing 0.1 μg of silicon. It was found that >3 mg of lanthanum should be added to the sample solution for quantitative collection.

Detection limit

The detection limit of this method, consisting of the extraction and coprecipitation procedures, was examined. The detection

Table 2. Recovery of organic silicon in the decomposition of TMG

Conditions of decomposition bottle	Silicon in xylene phase, %		
	In decomposition bottle	In the first bubbler	In the second bubbler
Hydrochloric acid only	61.4	36.3	2.3
Hydrochloric acid and xylene	84.1	13.6	2.3

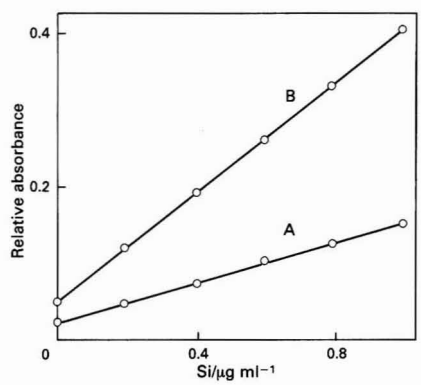

Fig. 2. Calibration graphs for silicon. A, Graphite tube in the absence of lanthanum in solution; and B, lanthanum-coated graphite tube in the presence of lanthanum in solution

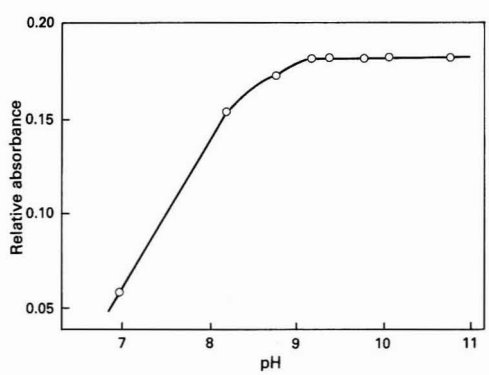

Fig. 3. Effect of pH on the recovery of silicon by coprecipitation with lanthanum hydroxide. Si taken, 0.1 μg; La added, 10 mg

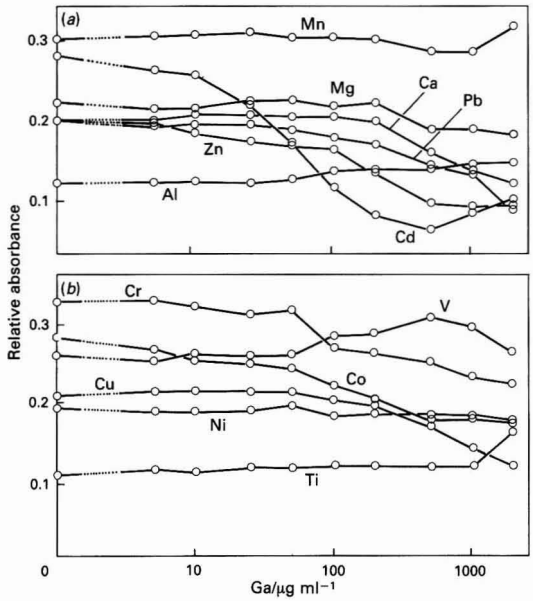

Fig. 4. Influence of gallium on the atomic absorption of 13 elements

limit (defined as three times the standard deviation of the reagent blank) of this method was 0.04 p.p.m. of inorganic silicon as the metal base.

Determination of 13 Other Elements

It is known that gallium is extracted with diisopropyl ether quantitatively and that many other elements are not extracted in high concentrations (>6 M) of hydrochloric acid.[4–8] This extraction method was applied to the determination of 13 other elements (Al, Ca, Cd, Co, Cr, Cu, Mg, Mn, Ni, Pb, Ti, V and Zn).

Interference of matrix gallium

As all the gallium cannot be removed completely by extraction, the interference was studied with 6 M hydrochloric acid solutions containing 0–2000 μg ml^{-1} of gallium. The concentrations of Cd, Mg, Mn and Zn were 0.005 μg ml^{-1}, those of Ti and V were 0.5 μg ml^{-1}, and the others were 0.05 μg ml^{-1}. It was found that the atomic absorption of Co, Cr, Cu and Zn gradually decreased in the presence of gallium. The results obtained are shown in Fig. 4. It was necessary to carry out the extraction four times in order to remove gallium at concentrations up to 10 μg ml^{-1}, which did not interfere with the determination of all 13 elements by ETAAS.

Detection limits

All the detection limits were less than 0.01 p.p.m. of each element as the metal base.

Recoveries

The efficacy of these methods was evaluated by investigating the recoveries by the recommended procedures. Trimethylgallium was spiked with trimethylchlorosilane and hydrochloric acid used in the decomposition was spiked with the 13 other elements. The recoveries of all the elements were between 86 and 104%. The results are shown in Table 3. It appears that the proposed methods are applicable to the analysis of TMG.

Table 3. Recoveries obtained by the proposed methods

Element	Taken/μg	Found/μg	Recovery, %
Organic Si	0.20	0.20	101
Inorganic Si	0.20	0.19	95
Al	0.050	0.052	104
Ca	0.050	0.050	100
Cd	0.050	0.046	92
Co	0.050	0.045	90
Cr	0.050	0.044	88
Cu	0.050	0.051	102
Mg	0.050	0.052	104
Mn	0.050	0.047	94
Ni	0.050	0.049	98
Pb	0.050	0.051	102
Ti	0.050	0.048	96
V	0.050	0.049	98
Zn	0.050	0.043	86

Table 4. Typical analytical data for impurities in TMG

Element	μg g^{-1}	Element	μg g^{-1}
Organic Si	0.03	Mg	<0.01
Inorganic Si	<0.05	Mn	<0.01
Al	0.22	Ni	<0.01
Ca	0.03	Pb	<0.01
Cd	<0.01	Ti	<0.01
Co	<0.01	V	<0.01
Cr	<0.01	Zn	0.02
Cu	<0.01		

Analysis of High-purity TMG

The proposed methods were used for the determination of impurities in high-purity TMG. The results are shown in Table 4. It was found that these methods could be used for the evaluation of high-purity TMG.

Conclusion

Methods have been developed for the decomposition of TMG and for the highly sensitive determination of impurities in TMG. In order to increase the sensitivity, organic silicon, inorganic silicon and 13 other elements were determined under matrix-free conditions by the techniques of decomposition with hydrochloric acid, extraction with diisopropyl ether, and coprecipitation with lanthanum hydroxide.

References

1. Bertenyi, I., and Barnes, M., *Anal. Chem.*, 1986, **58**, 1734.
2. Jones, A. C., Jacobs, P. R., and Cafferty, R., *J. Cryst. Growth*, 1986, **77**, 47.
3. Nachtrieb, N. H., and Fryxell, R. E., *J. Am. Chem. Soc.*, 1949, **71**, 4035.
4. Ramamurty, C. K., Kaiser, G., and Tolg, G., *Mikrochim. Acta*, 1980, **1**, 79.
5. Oldfield, J. H., and Bridge, E. P., *Analyst*, 1961, **86**, 267.
6. Owens, E. B., *Appl. Spectrosc.*, 1959, **13**, 105.
7. Saltman, W. M., and Nachtrieb, N. H., *Anal. Chem.*, 1951, **23**, 1503.
8. Nakamura, Y., Kobayashi, Y., and Abe, K., *Bunseki Kagaku*, 1986, **35**, 685.
9. Harada, Y., and Kurata, N., *Bunseki Kagaku*, 1986, **35**, 641.
10. Young, P. N. W., *Analyst*, 1974, **99**, 588.
11. Lo, D. B., and Christian, G. D., *Can. J. Spectrosc.*, 1977, **22**, 45.

Paper 9/03728D
Received September 1st, 1989
Accepted December 20th, 1989

Determination of Cadmium by Electrothermal Atomisation Atomic Absorption Spectrometry After Electrodeposition on a L'vov Platform*

Juan C. Vidal, Francisco Monreal and Juan R. Castillo†
Analytical Chemistry Department, Faculty of Sciences, University of Zaragoza, 50009-Zaragoza, Spain

The use of the L'vov platform as an electrode for electrodeposition and the subsequent determination of Cd by electrothermal atomisation atomic absorption spectrometry are described. A preliminary electroanalytical study of the L'vov platform as a cathodic macro-electrode for the pre-concentration of Cd (amalgamated on a mercury film) has been carried out. After the film had been formed, the platform was transferred into a graphite tube to atomise the element. The reliability of the method was tested for the determination of Cd; the method was found to be highly sensitive due to the electroanalytical step.

Keywords: *L'vov platform; anodic stripping voltammetry; electrothermal atomisation atomic absorption spectrometry; cadmium determination*

The electrodeposition of trace metals prior to their determination by atomic absorption spectrometry (AAS) is of great interest in ultratrace analysis, mainly due to the low detection limits (down to 10 ng ml^{-1}) that can be achieved and the minimisation of matrix interferences.[1] These extremely low detection limits are important in many analytical applications, such as high technology materials, environmental pollution or ultrapure reagents for chemical analysis.

In this technique, electrolytic pre-concentration is carried out by plating the metals on a graphite rod,[2] on metal wires of high melting-point metals such as W or Ir,[3,4] on a mercury film electrode,[5] on a hanging mercury drop electrode[6] or on a tubular pyrolytic graphite coated graphite furnace used as a cathode.[2,7–9] These devices, used as electrodes, are then transferred into an absorption spectrometer to atomise and determine the electrodeposited metals. In some of these arrangements, flow systems have been designed to minimise errors[7,8] (*e.g.*, contamination and/or adsorption).

By carefully controlling the potential and pH it is also possible to pre-concentrate only the fraction of metal that is electrochemically labile or active, which permits the selective deposition of metals such as Co, Ni, Pb, Zn, Mn, Cr, Tl, Sb or Bi.[10] Metals bound in non-labile complexed forms or adsorbed on colloidal species might not be deposited (unless released by, for example, acid digestion or UV irradiation). Labile/inert discrimination of Pb, Co and Ni[8] and redox state discrimination of Cr^{VI}/Cr^{III}[7] has been achieved with electrodeposition prior to electrothermal atomisation in a graphite furnace.

In this work, a pyrolised graphite L'vov platform was used as the cathode for the electrolytic deposition of Cd in the presence of added Hg^{II} ions (to form an amalgamated film on the graphite substrate). The platform was then introduced into the graphite tube for conventional electrothermal atomisation. Effective, reproducible electrodeposition of (amalgamated) Cd was achieved, as shown by the results of experiments using the platform as a cathode in a pre-concentration step followed by stripping as in anodic stripping voltammetry (ASV, linear scan).

Experimental

Apparatus

A Perkin-Elmer Model 3030 atomic absorption spectrometer with a deuterium lamp as background corrector and fitted with a Perkin-Elmer HGA-400 graphite furnace with pyrolytic graphite coated graphite tubes and L'vov platforms was used for the determinations. A Perkin-Elmer Cd hollow-cathode lamp (maximum intensity 8 mA, working intensity 6 mA) was also used.

Controlled potential electrodeposition and ASV measurements were made with an Inelecsa potentiostat interfaced to an Acer 500+ computer (IBM compatible) and a Star LC-10 printer for recording the voltammograms. A mercury pool and Pt were used as the reference and counter electrodes, respectively. Pyrolytic graphite coated graphite L'vov platforms were used as cathodic working electrodes. The L'vov platforms were placed on a split in a cylindrical PTFE insulator holder (length 75 mm, diameter 10 mm) and the internal electrical contact was made with a Pt wire. Great care was taken to ensure that the PTFE holder was water-tight. This construction permits electrodeposition of amalgamated Cd only in front of the platform (the only surface exposed to the electrolytic solution) and not on the side or back.

Reagents

All chemicals were of analytical-reagent grade (Merck) unless stated otherwise. High-purity water was obtained from a Millipore Milli-Q water system.

Standard Cd solution, 1000 mg l^{-1}. Prepared by dissolving 1 g of Cd metal in the minimum volume of 1% v/v HCl and diluting to 1000 ml with water. Working solutions were prepared daily by dilution with high-purity water.

Mercury(II) solution, 1000 mg l^{-1}. Prepared by dissolving 0.4273 g of $Hg(NO_3)_2.2H_2O$ in 250 ml of water.

Supporting electrolyte solutions of KCl, $NaH_2PO_4.2H_2O$ and KNO_3 (Suprapur, Merck), 0.125 M. Prepared by dissolving the appropriate amount of each salt in 250 ml of water. These solutions were purified by passing them through a column of Chelex-100 (potassium and sodium form, respectively) as described by van Loon.[11]

Standard metal solutions, 1000 mg l^{-1}. Solutions of foreign metal ions were used for the interference studies.

Procedure

Prepare the sample solutions by taking a known volume of the Cd solution and diluting to 25 ml with water, supporting electrolyte and Hg^{II} solutions to obtain final concentrations of 10^{-3} M KNO_3, 20 μg ml^{-1} of Hg^{II} and 1–3 ng ml^{-1} of Cd.

Place 25 ml of the sample solution in the electrolytic cell and remove the dissolved oxygen by bubbling oxygen-free nitro-

* Presented at SAC 89, the 8th SAC International Conference on Analytical Chemistry, Cambridge, UK, 30 July–5 August, 1989.

† To whom correspondence should be addressed.

Table 1. Optimised instrumental parameters for the determination of Cd by ETAAS

Step	Temperature/°C	Ramp/s	Hold/s
Drying	140	5	25
Charring	250	5	20
Atomisation	1600	0	2
Cleaning	2500	2	3

Wavelength: 228.8 nm
Slit width: 0.7 nm
Argon flow-rate: 50 ml min^{-1}
Lamp intensity: 6 mA
Deuterium lamp corrector: On

gen through the solution for 10 min. Introduce the working electrode (L'vov platform, previously conditioned as described below, in the PTFE holder) into the solution and apply an electrolysis potential (E_e) of −1050 mV for 4–10 min (electrolysis time, t_e) with a stirring rate of 800 rev min^{-1}. After electrodeposition, lift the L'vov platform, taking care not to touch its front with the fingers, and dry it carefully by dabbing with smooth paper. Transfer the platform into a graphite tube, place in the atomic absorption spectrometer and measure the absorbance using the instrumental parameters shown in Table 1.

Results and Discussion

Preliminary Electroanalytical Study With the L'vov Platform as an Electrode

Preliminary voltammetric studies were carried out by using the L'vov platform as a cathodic macro-electrode. Anodic stripping voltammograms were recorded (with a linear scan of potential, scan rate 6.66 mV s^{-1}) after an initial electrolytic pre-concentration step (E_e = −1050 mV, t_e = 4–10 min, stirring rate of solution = 800 rev min^{-1}) and a second nesting step [solution not stirred, rest time (t_r) = 30 s]. Narrow, well defined peaks were obtained in the third step which involved anodic stripping of mercury and Cd(Hg) from the platform. In this instance, the peak width at half-height approaches its lowest value (37 mV) for the slow scan rate of 6.66 mV s^{-1}, as predicted by the Randles - Sevcik theory.[12] Also, the rapid decrease of the current to zero after its maximum indicates the rapid removal of mercury and Cd from the platform.

The pyrolytic graphite coated graphite of the L'vov platform proved to be a good substrate for forming an adherent film of a strongly attached amalgam, similar to a conventional mercury film electrode (MFE) employed in ASV but larger (surface area 0.6 cm^2). The plating efficiency was improved by stirring (convection) the solution at a rate of 800 rev min^{-1} (with a stirring rod). This rate was controlled because the precision of the deposition of the metal is greatly influenced by the rate of diffusive - convective mass transport.

The platform was conveniently sealed using a PTFE tube, hence preventing the solution from penetrating between the electrode and the inside of the holder, which would produce a high background current in the recorded voltammograms and in the measurement of the electrolysis current (first step) or the blank solutions.

Mercury film thicknesses [l (cm)] ranging from 17 to 40 μm were obtained by measuring the current in the electrolysis step[13]: $l = 2.43 \times 10^{11} i_e t_e / r^2$, where i_e is the mean electrolysis current (μA), t_e is the electrolysis time (s) and r^2 is the electrode area (cm^2). Smaller film thicknesses (0.25–2.70 μm) were obtained without stirring the solution during the electrolysis, because of a low plating efficiency, which in turn produced a broadening of the voltammogram peaks because of incomplete stripping of the Cd deposited in the film layer. The potential of the maximum of the stripping peak for Hg^{II} only (E_p) also changes if the solution is not stirred. Hence, E_p = +80 mV (with stirring, 800 rev min^{-1}, t_r = 30 s) and E_p = +30 mV (without stirring).

Table 2. Temperature programme for pre-conditioning the L'vov platforms

Step	Temperature/°C	Ramp/s	Hold/s
1	2650	20	1
2	20	1	20
3	2650	10	1
4	20	1	20
5	2650	10	1
6	20	1	20
7	2650	10	2

To prevent saturation of the mercury film with metals deposited in a real sample (in addition to Cd), it is convenient to know the mass of Hg deposited on the electrode surface. Hence the initial concentration of Hg^{II} in the sample solution influences the film thickness and the amalgam concentration. The amount of mercury deposited was calculated using Faraday's law:

$$\text{Hg deposited } (\mu g) = i_e(\mu A) t_e(s) 200.59 \times 10^6/2 \times 96\,493$$

Two solutions (25 ml) containing 1×10^{-3} M KNO_3 and 1.0 and 6.20 μg ml^{-1} of Hg^{II}, respectively, were prepared to study this effect. With E_e = −800 mV and t_e = 2 min, Hg^{II} was plated on a platform and then rapidly stripped into a separate solution (25 ml of 10^{-3} M KNO_3), as in the "medium-exchange" technique.[12] This process was repeated four times observing the value of i_e in each instance (to calculate the amount of Hg deposited) and measuring the value of the maximum peak current [i_p (μA)] of the stripping voltammograms. The amounts of Hg^{II} deposited were calculated to be 2.43, 2.28, 2.40 and 2.46 μg (i_p of the stripping peaks ranged from 3.5 to 2.5 μA). In this instance, a decrease of about 10% in total mercury (and in the i_p of the stripping peaks) is observed in each step. This reduction in the amount of Hg in each electrolysis step indicates an extremely low concentration of this element.

With a 6.5 μg ml^{-1} solution of Hg^{II}, the amounts of Hg^{II} deposited in five steps were 4.68, 3.55, 2.84, 2.68 and 2.59 μg (i_p ranged from 26.00 to 6.10 μA). In this instance Hg^{II} plated in each electrolysis was about 3%, as can be seen from the calculated amount of Hg^{II} and from the decreasing value of i_p of the stripping voltammograms.

In this study, a second anodic scan using the same L'vov platform (after the first voltammogram for Hg^{II} had been obtained and without performing a new electrolysis) showed a small peak which indicated that Hg^{II} is not completely stripped from the platform in a single anodic scan; hence the platform must be cleaned by, for example, polishing with fine alumina powder. This cleaning is essential for reducing the background intensity caused by the slow deterioration and increase in porosity of the graphite substrate (see below). The performance of the platform was satisfactory for a minimum of *ca.* 35 electrodeposition/heating cycles. Nevertheless, this background intensity was independent of t_e and increased with increasing values of E_e (*ca.* 5 μA for E_e = −0.6 V and t_e = 2–12 min, and *ca.* 8.75 μA for E_e = −1000 mV and t_e = 2–12 min). Values of t_r ranging from 30 to 120 s had no effect on the background current or on the value of i_p for the Cd(Hg) anodic peaks. Also, conditioning of the platform with the temperature programme shown in Table 2 gave a marked decrease in the background current and elimination of the contamination of Hg (and Cd) from the previous cycle. The presence of trace amounts of O_2 also increased the background current of the voltammogram and decreased the stripping peaks of Cd(Hg).

Fig. 1 shows values of i_p for increasing concentrations of Hg^{II}. The Hg plated varies linearly with the concentration of Hg^{II} in the solution in the range 0.5–6 μg ml^{-1} (linear

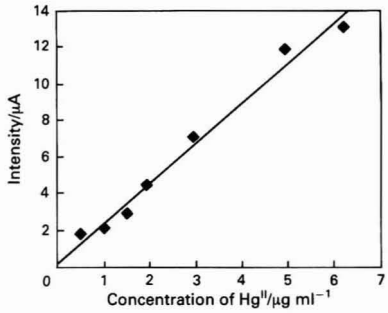

Fig. 1. Calibration graph for the anodic stripping of Hg^{II} deposited on a L'vov platform. $E_e = -1050$ mV; $t_e = 4$ min; $t_r = 30$ s; and [KCl] = 1×10^{-3} M

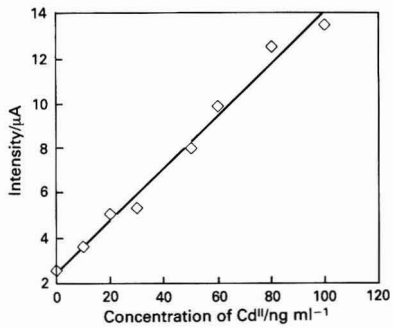

Fig. 2. Calibration graph for the anodic stripping of Cd(Hg) deposited on a L'vov platform. $E_e = -1050$ mV; $t_e = 8$ min; $t_r = 30$ s; $[Hg^{II}] = 1250$ ng ml^{-1}; and [KCl] = 1×10^{-3} M

equation: $i_p(\mu A) = 2.182\{[Hg^{II}]\ (\mu g\ ml^{-1})\} + 0.250$ [regression coefficient (R) = 0.9955]).

Electrochemical stripping voltammograms for 50 ng ml^{-1} of Cd^{II} (linear scan, scan rate 6.66 mV s^{-1}) gave the following results [mean of eight determinations (n = 8)]: $i_p = 8.40 \pm 0.78$ μA [coefficient of variation (CV) = 9.35%]; $E_p = -890 \pm 10$ mV (CV 1.16%). (Optimised parameters: $E_e = -1050$ mV; $t_e = 8$ min; $t_r = 30$ s; N_2 purge time = 10 min; and stirring rate = 800 rev min^{-1}.) The concentrations were as follows: $[Cd^{II}]$ = 50 ng ml^{-1} (sample volume 25 ml); $[Hg^{II}]$ = 1.24 μg ml^{-1}; and [KCl] = 10^{-3} M. A value of E_p greater than −1050 mV and up to −1500 mV gave a slight increase in sensitivity for the Cd peak but the increase in the background current (i_r) was unacceptable (from *ca.* 5 to 10 μA). In contrast, varying t_e from 4 to 12 min did not increase i_r (keeping E_e constant).

Fig. 2 shows values of i_p for increasing concentrations of Cd^{II} in the solution. The linearity between i_p and the Cd^{II} concentration [$i_p(\mu A) = 0.116\ \{[Cd^{II}]\ (ng\ ml^{-1})\} + 2.47$; R = 0.9920] is clear. The sensitivity, calculated from the calibration graph, is 0.116 ng^{-1} ml. To ensure proper plating of Cd, it was necessary (as observed experimentally) to have an [Hg]:[Cd] ratio of 20 or more. In practice, a concentration ratio >20 was chosen to prevent saturation of the Hg film.

Another aspect of interest was the purification of the supporting electrolyte solutions (prepared with Suprapur salts, Merck), which was achieved by passing them through a column of Chelex-100 (300 × 10 mm i.d.).[11] This produced a slight decrease in i_r by contamination from Cd or other metals from this solution. A concentration of the supporting electrolyte of 1×10^{-3} M proved to be sufficient, as indicated by the electrical conductivity and the Cd stripping peaks.

Table 3. Linear equations for calibration graphs in the determination of Cd by ETAAS. Equations (1) and (2): direct injection, calibration using peak height and peak area, respectively. Equations (3)–(6): after the pre-concentration step [t_e = 4 min for equations (3) and (4) and 10 min for equations (5) and (6)]; calibrations in peak height and peak area, respectively

Equation	R	Linear range, p.p.b.
(1) $A = 0.103\ \{[Cd^{II}]\ (ng\ ml^{-1})\} + 0.032$	0.9990	0.5–6
(2) $A = 0.087\ \{[Cd^{II}]\ (ng\ ml^{-1})\} + 0.005$	0.9995	0.5–8
(3) $A = 0.189\ \{[Cd^{II}]\ (ng\ ml^{-1})\} + 0.041$	0.9926	0.5–4
(4) $A = 0.178\ \{[Cd^{II}]\ (ng\ ml^{-1})\} + 0.010$	0.9978	0.5–5
(5) $A = 0.945\ \{[Cd^{II}]\ (ng\ ml^{-1})\} + 0.070$	0.9926	0.1–0.8
(6) $A = 0.890\ \{[Cd^{II}]\ (ng\ ml^{-1})\} + 0.041$	0.9978	0.1–0.9

Table 4. Analytical characteristics for the determination of Cd by ETAAS. Comparison of results with direct injection (20 μl) and with previous electrodeposition in a mercury film (t_e = 4 and 10 min). Values are given for calibration using peak heights and peak areas, respectively

Analytical characteristic	Direct injection	Electrolytic deposition	
		t_e = 4 min	t_e = 10 min
Sensitivity/ng^{-1} ml	0.133	0.189	0.945
	0.098	0.178	0.890
Detection limit/ng ml^{-1}	0.115	0.101	0.020
	0.089	0.078	0.011
Linearity of calibration graph/ng ml^{-1} of Cd	0.5–6	0.5–4	0.10–0.80
	0.5–8	0.5–5	0.10–0.90
CV, %	7.04	13.64	13.44
	8.80	13.50	13.22

Determination of Cd by Electrothermal Atomisation Atomic Absorption Spectrometry (ETAAS) With the L'vov Platform

The L'vov platform was first described by L'vov in 1977.[14] Its main advantage in electrothermal atomisation is based on delaying sample vaporisation until the tube atmosphere is at a higher, steadier temperature because the temperature of the platform (heated primarily by radiation) lags behind that of the graphite tube. This leads to a reduction in vapour-phase interferences and reduces the effect on the analyte signal of matrix-dependent variations in the appearance temperature.[15] The L'vov platform is widely used in ETAAS, particularly with biological samples, to reduce matrix interferences.

Before using the platform as an electrode, the analytical performance of the determination of Cd by simple injection on to this platform was measured for comparison. The optimised programme for the determination of Cd was the same as that shown in Table 1. The injection of 20 μl of a 2 ng ml^{-1} Cd solution gave the following absorbances (n = 10): A (peak height) = 0.230 ± 0.016 (CV = 7.04%); A (peak area) = 0.175 ± 0.015 (CV = 8.80%).

Table 3 shows the corresponding equations of the calibration graphs. The sensitivity and detection limits are compared in Table 4. The sensitivity was calculated from the mean of the slope of the calibration graph, as defined by IUPAC.[16] The detection limit was measured with blank solutions and calculated according to IUPAC recommendations[16]: detection limit (concentration) = $K\sigma/S$, where K = 3 (with a confidence level of 99.6%), σ is the standard deviation of the absorbance of the blank solutions (n = 10) and S is the sensitivity calculated from the calibration graph.

The tolerance limits of Hg^{II}, KCl and KNO_3 in the determination of 2 ng ml^{-1} of Cd (20 μl, direct injection) were in a [salt]:[Cd] ratio of 400, 2000 and 2200, respectively, showing a slight increase in the absorbance (interference) at higher ratios. These values are important because of the use of these salts in the electrodeposition of Cd.

In comparing the analytical characteristics shown in Table 4, because of the higher sensitivity achieved with the pre-concentration step (in this concentration range and with t_e = 4 min) it was necessary to measure the absorbance in the atomisation step without the stop-flow of argon (50 ml min^{-1}), whereas with direct injection stop-flow was used to increase the sensitivity. Obviously, increased sensitivity is obtained in the stop-flow mode (and with greater values of t_e), but the results were compared for solutions of similar concentrations.

The electrolytic deposition of Cd can lead to contamination of this element by the salts used in preparing the supporting electrolyte and by the added Hg^{II} ions. Blank solutions with a 10^{-3} M concentration of the various salts used as supporting electrolytes were prepared and their absorbances were compared in order to study their influence. The best results (lowest blank absorbances) were obtained with KNO_3 compared with the use of KCl and $NaH_2PO_4.2H_2O$: the approximate absorbances were (peak height) 0.029 ± 0.005 and (peak area) 0.009 ± 0.003, after passing the solutions through a column of Chelex-100. This purification with an ion-exchange resin also gave a decrease in the blank absorbances. The contamination due to the addition of $Hg(NO_3)_2$ was found to be less important because of its lower concentration (20 μg ml^{-1} of Hg^{II} in a 25-ml sample volume).

The absorbances for 2 ng ml^{-1} of Cd at different pH values showed no variation in the pH range 6–8. The pH was adjusted by adding dilute HCl or NaOH solution to the sample solution. Attempts to increase the hydrogen overvoltage in alkaline solution and the drop of background current levels produced an increase in the absorbances of the blank solutions, probably due to the contamination from the NaOH. Sample solutions with very low pH values gave a very slight decrease in the Cd absorbances with respect to the determination of Cd in solutions at a nearly neutral pH.

The determination of Cd (n = 8) (initial concentration of Cd^{II}, 2 ng ml^{-1}; sample volume, 25 ml) by electrolysis - ETAAS gave the following results: A (peak height) = 0.398 ± 0.054 (CV = 13.64%); A (peak area) = 0.370 ± 0.050 (CV = 13.50%). The linear equation of the calibration graph is shown in Table 3. Of course, an increase in sensitivity can be achieved with greater values of t_e. For instance, the detection limit obtained with t_e = 10 min (50 pg ml^{-1}; n = 10) is much greater than that with t_e = 4 min (0.49 ng ml^{-1}; n = 10).

The determination of 0.400 ng ml^{-1} of Cd^{II} gave the following results: A (peak height) = 0.439 ± 0.059 (CV = 13.44%); A (peak area) = 0.386 ± 0.052 (CV = 13.22%). The calibration graph, with t_e = 10 min, can be described by the linear equations shown in Table 3 and has the overall analytical characteristics shown in Table 4.

It is important to note that the better reproducibility in the determination of Cd with increasing values of t_e is due mainly to the better precision of the blank absorbances and not to an increase in these values (the absorbances of the blank solutions did not increase when t_e was increased from 4 to 12 min).

Owing to the contamination and the high absorbances of the blank solutions obtained after prolonged storage (2–3 d) or repetitive use, the L'vov platforms were pre-conditioned immediately before use. For the cleaning pre-treatment, the L'vov platforms were heated using the temperature shown in Table 2 and subsequently polished with fine alumina powder.

It is not advisable to apply a positive (anodic) potential to the L'vov platform in order to remove the amalgam film when cleaning, particularly in the presence of halides,[17] owing to the formation of a film of HgCl (calomel) that seriously degrades the performance of the graphite electrode surface and which is difficult to remove.

Effect of Foreign Ions

The selectivity of the method was assayed by adding different amounts of potentially interfering species. The tolerance limits given in Table 5 were calculated with respect to a Cd solution with a difference in absorbance of less than the CV, *i.e.*, 13.57%.

Table 5. Tolerance limits for the determination of Cd by electrolytic pre-concentration (t_e = 4 min) and ETAAS [Cd^{II}] = 2 ng ml^{-1}, [Hg^{II}] = 20 μg ml^{-1} and [KCl] = 1×10^{-3} M. Values of absorbances were taken as the means of three measurements

Tolerance ratio, interferent ion : Cd	Tolerance limit/ ng ml^{-1}	Ion assayed
1000 : 1	2000	Ca, Sr, Ba
500 : 1	1000	As, Mn, Cr
250 : 1	500	Ni, Zn, Pb, Cu, Fe^{III}

Table 6. Results for the determination of Cd in analytical-reagent grade KCl (Probus) (n = 6)

Sample	Calibration	Cd concentration in KCl/μg g^{-1}
KCl (without purification) . .	Peak height	18.5 ± 2.2
	Peak area	13.6 ± 2.2
KCl (with purification) . .	Peak height	10.8 ± 2.1
	Peak area	6.7 ± 2.1

Concentrations higher than the tolerance limits for certain ions (*e.g.*, Pb, Cu and Cr) produce a slight decrease in absorbances with respect to Cd only indicating rapid saturation of the Hg film. In this instance, an increase in the Hg^{II} concentration in the original solution can increase the tolerance limit; however, this is not advisable because of film sagging and the possibility of the loss of amalgamated material during transfer into the graphite tube of the furnace and the spectrometer, which can occur if the mercury film thickness is greater than 100 μm.[5]

Application to the Analysis of an Analytical Reagent

The proposed method was applied to the determination of Cd in an analytical-reagent grade product (potassium chloride, Probus, Barcelona, Spain, reference 144310). The specifications of this reagent are as follows: minimum purity, 99%; insoluble residue, 0.005%; maximum concentration of impurities: Ca + Mg, 0.05; SO_4^{2-}, 0.001; Ba, 0.001; iodide, 0.002; bromide, 0.01; perchlorate, 0.003; nitrate, 0.001; iron, 0.0003; sodium, 0.02; and metals (as Pb), 0.0005%.

The electrodeposition conditions were E_e = −1050 mV and t_e = 6 min. The standard additions method was used (two additions to give 0, 1 and 2 ng ml^{-1} of Cd added to the sample) and each analysis was repeated six times. The Cd content in the KCl was determined before and after passing 500 ml of a 2×10^{-4} M solution through a column of Chelex-100 (potassium form, prepared as described in reference 12). The Cd concentration in the KCl solution was determined (ng ml^{-1}) and the results are presented in Table 6 with respect to the mass of KCl taken (*i.e.*, μg of Cd per g of KCl). A small difference in the Cd content is found between peak height and peak area absorbance measurements, but this is acceptable at these concentrations.

Conclusion

A method is described in which a L'vov platform is used as a pyrolytic graphite substrate electrode for the pre-concentration of Cd amalgamated in a mercury film and its subsequent transfer into a graphite furnace tube. A preliminary electroanalytical study has shown that the L'vov platform can be used conveniently as a mercury film macro-electrode on which films 17 to *ca.* 50 μm thick can be deposited and subsequently transferred into the atomisation device of an atomic absorp-

tion spectrometer. The method permits the concentration of trace amounts of reducible metals in a single electrolytic step, leaving the matrix and other electrochemically inactive interfering elements in the sample solution. Hence the procedure allows the determination of ultratrace metals with enhanced sensitivity and selectivity.

This work was financed by project PB 86/0183 of the DIGICYT (Spanish Education and Science Department).

References

1. Sioda, R., Batley, G. E., Lund, W., Wang, J., and Leach, S. C., *Talanta*, 1986, **33**, 421.
2. Thomassen, Y., Larsen, B. V., Langmyhr, F. J., and Lund, W., *Anal. Chim. Acta*, 1976, **83**, 103.
3. Newton, M. P., and Davis, D. G., *Anal. Chem.*, 1975, **47**, 2003.
4. Dawson, J. B., Ellis, D. J., Hartley, T. F., Evans, M. E. A., and Metcalf, K. W., *Analyst*, 1974, **99**, 602.
5. Matusiewicz, H., Fish, J., and Malinski, T., *Anal. Chem.*, 1987, **59**, 2264.
6. Fairless, C., and Bard, A. J., *Anal. Chem.*, 1973, **45**, 2289.
7. Batley, G. E., and Matousek, J. P., *Anal. Chem.*, 1980, **52**, 1570.
8. Batley, G. E., and Matousek, J. P., *Anal. Chem.*, 1977, **49**, 2031.
9. Desimoni, E., Palmisano, F., Sabbatini, L., and Torsi, G., *Ann. Chim. (Rome)*, 1979, **69**, 381.
10. Florence, T. M., *Analyst*, 1986, **111**, 489.
11. van Loon, J. C., "Selected Methods of Trace Metal Analysis: Biological and Environmental Samples," *Volume 80 in Chemical Analysis*, Wiley-Interscience, New York, 1985, p. 312.
12. Wang, J., "Stripping Analysis," VCH, Deerfield Beach, 1985, pp. 26 and 48.
13. Batley, G. E., and Florence, T. M., *J. Electroanal. Chem.*, 1974, **55**, 23.
14. L'vov, B. V., *Spectrochim. Acta, Part B*, 1977, **33**, 153.
15. Hinderberger, E. J., Kaiser, M. L., and Koirtyohann, S. R., *At. Spectrosc.*, 1981, **2**, 1.
16. Irving, H. M., Freiser, H., and West, T. S., "Compendium of Analytical Nomenclature," IUPAC Analytical Chemistry Division, Pergamon Press, Oxford, 1977.
17. Florence, T. M., *Anal. Chim. Acta*, 1980, **119**, 217.

Paper 9/03351C
Received August 7th, 1989
Accepted September 27th, 1989

Determination of Vanadium in Water by Electrothermal Atomisation Atomic Absorption Spectrometry After Extraction With 8-Hydroxyquinoline in Isobutyl Methyl Ketone*

Pilar Bermejo-Barrera, Elisa Beceiro-Gonzalez, Adela Bermejo-Barrera and Francisco Bermejo-Martinez

Analytical Chemistry, Nutrition and Bromatology Department, Faculty of Chemistry, 15706 Santiago de Compostela, Spain

A sensitive method for the determination of vanadium in water by electrothermal atomisation atomic absorption spectrometry (ETAAS) is described. The vanadium is chelated with 8-hydroxyquinoline in isobutyl methyl ketone and determined by ETAAS after pre-heating the pyrolytic graphite coated graphite tube of a graphite furnace atomiser before injection. The effects of the pH and amount of reagent required for the extraction were studied. The precision, accuracy and interferences of the method were also investigated. The proposed method allows concentrations of vanadium of 0.16 μg l^{-1} to be detected.

Keywords: *Vanadium; water; 8-hydroxyquinoline; electrothermal atomisation; atomic absorption spectrometry*

Vanadium is widely distributed in the Earth's crust, its compounds can be highly toxic to man and animals and cause environmental diseases when released into the atmosphere on combustion of fossil fuels, which are known to have high vanadium contents.[1] In spite of its toxicity at high levels, vanadium is an essential trace element, possessing specific physiological functions.[2,3] The determination of vanadium receives increasing attention in pollution studies in addition to nutritional studies.

Because of the low levels of vanadium in water (of the order of μg l^{-1}), it is only in recent years that methods for its exact determination have been developed. Catalytic methods,[4] neutron activation analysis,[5] inductively coupled plasma atomic emission spectrometry[6] and electrothermal atomisation atomic absorption spectrometry (ETAAS)[7] have been used for the determination of vanadium; however, to determine vanadium in water samples, the low concentrations involved make it necessary to perform pre-concentration.

Pre-concentration of vanadium for ion exchange,[6,8,9] coprecipitation of vanadium with iron(II) hydroxide[5,10–12] and with diethyldithiocarbamate[13] and the complexation and extraction of vanadium with 5,7-dichloroquinolin-8-ol in diisobutyl ketone[14] and with 4-(2-pyridylazo)resorcinol - tetraphenylarsonium chloride in chloroform - acetone[15] have previously been used.

Electrothermal atomisation atomic absorption spectrometry has been used to determine vanadium in different media, but presents some problems owing to the formation of vanadium carbide during the ashing and atomisation steps, which decreases the sensitivity. These problems are minimised by pre-heating the graphite tube before sample injection.[16]

This paper describes the determination of vanadium in water by ETAAS after its extraction with 8-hydroxyquinoline in isobutyl methyl ketone (IBMK) and pre-heating the graphite tube before sample injection.

Experimental

Apparatus

A Perkin-Elmer Model 2280 atomic absorption spectrometer with a hollow-cathode lamp operating at 15 mA and with a slit width of 0.7 nm was used. Measurements were made at 318.8 nm. A deuterium arc background corrector was used. A Perkin-Elmer Model HGA-400 graphite furnace atomiser with pyrolytic graphite coated graphite tubes (Part No. 135-653) was operated under the conditions given in Table 1. Samples were injected manually using a Gilson micropipette. The volume injected was 50 μl. Signals were recorded on a Perkin-Elmer Model 56 recorder with a range of 5 mV. The height of the absorbance peak was measured.

Reagents

Vanadium(V) stock standard solution, 1000 μg ml^{-1}. Prepared by dissolving 1.1483 g of ammonium vanadate in 500 ml of ultrapure water.

All test solutions were prepared with ultrapure water and used immediately.

8-Hydroxyquinoline solution, 2%. Prepared by dissolving 2 g of 8-hydroxyquinoline in IBMK and making up to 100 ml.

Isobutyl methyl ketone (IBMK). Merck.

Hydrochloric acid, 0.1 *and* 0.01 M.

Sodium hydroxide solution, 0.1 *and* 0.01 M.

Ultrapure water (specific resistivity 18 MΩ). Obtained from a Milli-Q system (Millipore).

Unless stated otherwise, all reagents were of analytical-reagent grade and the presence of vanadium was not detected in the working range.

All glassware was kept in 10% nitric acid for at least 48 h and subsequently washed three times with ultrapure water before use.

Procedure

Transfer 10 ml of sample at pH 3 into a test-tube, add 1 ml of 2% 8-hydroxyquinoline solution and shake vigorously for 1 min. Allow the two phases to separate and then pipette off 50 μl of the organic phase for spectroscopic analysis.

Table 1. Furnace conditions

Step	Temperature/ °C	Ramp time/s	Hold time/s	Ar flow-rate/ ml min^{-1}
Dry	200	10	30	300
Char	1500	5	30	300
Atomise . .	2800	0	5	Stop
Clean . .	2800	0	5	300
Pre-heating	200	1	10	300

* Presented at SAC 89, the 8th SAC International Conference on Analytical Chemistry, Cambridge, 30 July–5 August, 1989.

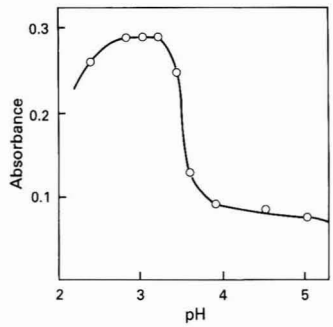

Fig. 1. Effect of the pH on extraction of the vanadium(V) - 8-hydroxyquinoline complex. Vanadium concentration, 10 μg l^{-1}

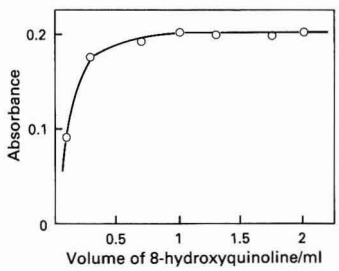

Fig. 2. Effect of the amount of 8-hydroxyquinoline on extraction of the vanadium(V) - 8-hydroxyquinoline complex. Vanadium concentration, 10 μg l^{-1}

Results and Discussion

Extraction pH

The effect of changes in the pH at which vanadium(V) was complexed and extracted was studied using 10 μg l^{-1} of vanadium solution in 10-ml flasks and carrying out the extraction procedure at different acidities. The results (Fig. 1) show that the optimum pH range is 2.80–3.20.

Amount of 8-Hydroxyquinoline

Different amounts of 8-hydroxyquinoline were added to a series of 10 μg l^{-1} vanadium solutions and the mixtures were made up to 2 ml with IBMK and subjected to the extraction procedure. It was found that 1 ml of a 2% 8-hydroxyquinoline solution in IBMK was sufficient for complete extraction and that an excess of 8-hydroxyquinoline did not have any adverse effect (Fig. 2). The same procedure (with 1 ml of 8-hydroxyquinoline solution) was then applied to 10, 20, 100 and 500 μg l^{-1} vanadium solutions (the pipetted organic phases of the 20, 100 and 500 μg l^{-1} solutions were diluted 2, 10 and 50 times with IBMK, respectively, before injection into the atomisation chamber). The signals obtained were all identical with those of the 10 μg l^{-1} solution, showing that 1 ml of the ligand solution is sufficient for vanadium concentrations up to at least 500 μg l^{-1}. This means that when the concentration of vanadium in the sample is high (greater than the upper limit of the calibration range), it is not necessary to repeat the determination with a smaller amount of sample, but it is sufficient just to dilute the organic phase that is pipetted off from the extraction mixture.

Interference

Experiments were performed to discover the degree to which the proposed method is susceptible to interference from elements known to interfere with the formation of the vanadium(V) - 8-hydroxyquinoline complex or with the determination of vanadium by ETAAS, including those forming refractory compounds at high temperatures. The elements studied were Al, Ba, Ca, Fe, Mg and Mo.

Table 2. Recovery of vanadium from a water sample (ten replicate analyses)

Vanadium concentration/μg l^{-1}				
		After addition		
Before addition	Added	$\bar{X}$	SD*	Average recovery, %
1.19	3	4.13	0.25	99.9
1.19	7	8.24	0.24	104.3

*SD = standard deviation

An interference was defined as being significant if a change of more than 10% in the measurements was observed. The determination of vanadium was possible in the presence of a 900-fold excess of Mg and Ba, a 700-fold excess of Ca, a 300-fold excess of Al and a 200-fold excess of Mo and Fe. The levels of these elements in water are less than those necessary to produce interference.[17] On the other hand amounts of the anions usually present in water (S^{2-}, CO_3^{2-}, F^-, SO_4^{2-}, Cl^-) do not produce any interference.

Calibration and Sensitivity

To obtain a calibration graph, standard vanadium solutions containing 1–10 μg l^{-1} of vanadium were brought to pH 3.0, made up to 10 ml with ultrapure water and subjected to the extraction procedure. The standard additions method was used, 0, 1, 3, 5 and 7 μg l^{-1} of vanadium being added to a water sample. Equations (1) and (2) were obtained for the calibration and standard additions graphs, respectively

$$\text{Absorbance} = 0.0096 + 0.0334x,\ r = 0.996 \quad \ldots \quad (1)$$

$$\text{Absorbance} = 0.0210 + 0.0382x,\ r = 0.998 \quad \ldots \quad (2)$$

where x is the concentration of vanadium in μg l^{-1}. The absorbance of the analytical blank was 0.012 ± 0.001.

The limit of detection (LOD), the lowest concentration level that can be determined to be statistically different from a blank,[18] is defined as the mean blank reading plus three times the within-batch standard deviation, corresponding to a 99% confidence level. The limit of quantification (LOQ) is defined as the level above which quantitative results can be obtained with a specified degree of confidence. At the 99% confidence level the value recommended is ten times the within-batch standard deviation. The values obtained were 0.16 μg l^{-1} for the LOD and 0.38 μg l^{-1} for the LOQ; both limits are based on ten replicate determinations of the blank.

The characteristic mass is defined as the mass of analyte in picograms required to give a signal of 0.0044 A s for integrated absorbance. The characteristic mass obtained was 6.82 ± 0.77 pg.

Precision and Accuracy

The precision [relative standard deviation (RSD) or coefficient of variation (CV)] of the method (instrumental and matrix factors) obtained for five replicate analyses of a single sample during the same run was 1.17% (for 3.2 μg l^{-1} of vanadium).

The within-batch precision of the method, obtained for ten replicates of three samples with 3, 5 and 7 μg l^{-1} of vanadium added, was 5.72, 3.41 and 2.71%, respectively.

To study the accuracy of the method, an International Atomic Energy Agency Standard Reference Material, IAEA SRM W-4 Water, with a vanadium content of 5.8 μg l^{-1} and with a confidence interval (significance level 0.05) of 4.9–10

μg l^{-1} was used. Using the proposed method the content of vanadium determined in this SRM was 5.50 ± 0.45 μg l^{-1}.

The accuracy of the method was also investigated by measuring the recovery of standard additions of vanadium to water samples. When ten replicates of 3 and 7 μg l^{-1} of vanadium were added to a water sample, the recoveries were 99.9 and 104.3%, respectively (Table 2).

Determination of Vanadium in Mineral Waters

The proposed method was applied to the determination of vanadium in eight different mineral water samples. The additions method with 0, 1, 3 and 5 μg l^{-1} of vanadium added to a water sample was used. Two sub-samples of each of the extracted samples were subjected to ETAAS. The values obtained were in the range 0.68–6.63 μg l^{-1} of vanadium.

Conclusion

The main difficulty in determining vanadium in water is its low concentration. The work described in this paper has shown that adequate sensitivity and selectivity can be attained using ETAAS by pre-heating the pyrolytic graphite coated graphite tube before injection and by concentrating the samples through complexation and extraction with 8-hydroxyquinoline in IBMK.

Vanadium carbide could be formed in the graphite tube during the atomisation process,[19] resulting in a decrease in sensitivity. By pre-heating the tube before injection, the reaction proposed by Styris and Kaye[16] (atomisation of vanadium from the oxide) $V_2O_3(s) + 3C(s) \rightarrow 2V(s) + 3CO(g)$ probably occurs, thus allowing the improved results described above. On the other hand, injection at 200 °C may allow more rapid drying of the sample with the result that the sample occupies a smaller surface area in the graphite tube and this could lead to more efficient atomisation. The proposed method allows concentrations of vanadium of 0.16 μg l^{-1} to be detected.

References

1. Lee, D. H. K., "Metallic Contaminants and Human Health," Academic Press, New York, 1972, p. 153.
2. Nielsen, F. H., *in* Prasad, A. S., *Editor*, "Current Topics in Nutrition and Disease, Volume 6, Clinical, Biochemical and Nutritional Aspects of Trace Elements," Alan R. Liss, New York, 1982, p. 379.
3. Macara, I. G., *Trends Biochem. Sci.*, 1980, **5**, 92.
4. Fishman, M. J., and Skougstad, M. W., *Anal. Chem.*, 1964, **36**, 1643.
5. Murthy, R. S. S., and Ryan, D. E., *Anal. Chem.*, 1983, **55**, 682.
6. Hirata, S., Umezaki, Y., and Ikeda, M., *Anal. Chem.*, 1986, **58**, 2602.
7. Fujiwara, K., Morikawa, T., and Fuwa, K., *Bunseki Kagaku*, 1986, **35**, 361.
8. Korkisch, J., and Krivanec, H., *Anal. Chim. Acta*, 1976, **83**, 111.
9. Shriadah, M. M. A., and Ohzeki, K., *Analyst*, 1985, **110**, 677.
10. Shrivastava, A. K., *Int. J. Environ. Anal. Chem.*, 1986, **27**, 1.
11. Burba, P., and Willmer, P. G., *Fresenius Z. Anal. Chem.*, 1986, **324**, 298.
12. Weisel, C. P., Duce, R. A., and Fasching, J. L., *Anal. Chem.*, 1984, **56**, 1050.
13. Hirayama, K., and Leyden, D. E., *Anal. Chim. Acta*, 1986, **188**, 1.
14. Miyazaki, A., Kimura, A., Bansho, K., and Umezaki, Y., *Anal. Chim. Acta*, 1982, **144**, 213.
15. Monien, H., and Stangel, R., *Fresenius Z. Anal. Chem.*, 1982, **311**, 209.
16. Styris, D. L., and Kaye, J. H., *Anal. Chem.*, 1982, **54**, 864.
17. Catalan, J., "Química del Agua," Blume, Madrid, 1982.
18. Keith, L. H., Crummett, W., Deegan, J., Jr., Libby, R. A., Taylor, J. K., and Wentler, G., *Anal. Chem.*, 1983, **55**, 2210.
19. Matousek, J. P., and Powell, H. K., *Spectrochim. Acta, Part B*, 1988, **43**, 167.

Paper 9/03334C
Received August 4th, 1989
Accepted September 29th, 1989

Comparative Study of Chemical Modifiers for the Determination of Molybdenum in Milk by Electrothermal Atomisation Atomic Absorption Spectrometry*

Pilar Bermejo-Barrera, Consuelo Pita Calvo, Francisco Bermejo-Martinez
Analytical Chemistry, Nutrition and Bromatology Department, Faculty of Chemistry, 15706 Santiago de Compostela, Spain

A comparative study of various chemical modifiers for the determination of molybdenum in milk by electrothermal atomisation atomic absorption spectrometry was carried out. Methods with nitric acid or barium difluoride as the chemical modifier and in the absence of a chemical modifier were studied by introducing the milk samples directly into the graphite furnace with octyl alcohol. The graphite furnace programme, amount of modifier and the calibration and additions graphs were studied in all instances. The characteristic masses were 17.82, 18.64 and 12.08 pg of molybdenum in the absence of a chemical modifier and with nitric acid or barium difluoride as the chemical modifier, respectively. The precision, accuracy and interferences of the method were also investigated.

Keywords: *Electrothermal atomisation; atomic absorption spectrometry; molybdenum; milk*

Molybdenum has been shown to be an essential trace element in man.[1] Its nutritional importance during the first months of life necessitates the determination of molybdenum in milk.

Although there are a number of techniques available for the determination of molybdenum in biological materials, recent interest has been focused on the use of electrothermal atomisation atomic absorption spectrometry (ETAAS). There are, however, problems associated with the use of this technique. The formation of stable, non-volatile carbides of molybdenum on the graphite surface is a serious impediment.[2,3] Carbon deposits in the furnace tube from undigested milk samples enhance the effect of molybdenum carbide formation. Atomisation from a pyrolytic graphite coated graphite surface and "maximum power" has therefore been recommended.[4] Slow, tailed atomisation peaks are typical and a high temperature clean out stage is usually necessary in the temperature cycle of the furnace, the tube life being shortened under these conditions.

Moreover, the direct determination of molybdenum in milk presents some problems with regard to sample introduction and matrix interferences. The determination of molybdenum has been reported without a chemical modifier[5] and with dilute nitric acid as a chemical modifier.[6]

On the other hand, barium difluoride has been proposed as a chemical modifier for the determination of molybdenum in serum samples,[7] because the presence of fluoride salts in the tube produces preferential formation of very volatile molybdenum fluorides, hence reducing carry-over between injections.

The aim of the present study was to develop a suitable method to determine molybdenum in milk by ETAAS. A comparative study has been carried out on the determination of molybdenum in milk without a chemical modifier and with nitric acid or barium difluoride as a chemical modifier.

Experimental

Apparatus

A Perkin-Elmer Model 2280 atomic absorption spectrometer with a hollow-cathode lamp operating at 15 mA and with a slit width of 0.7 nm was used. Measurements were made at 313.3 nm. A deuterium arc background corrector was used. A Perkin-Elmer Model HGA-400 graphite furnace atomiser, with pyrolytic graphite coated graphite tubes (Part No. 135-653), was operated under the conditions given in Table 1. Samples were injected manually using a Gilson micropipette. The volume injected was 20 μl. Signals were recorded on a Perkin-Elmer Model 56 recorder with a range of 5 mV. The height of the absorbance peak was measured.

Table 1. Furnace conditions

Step	Temperature/ °C	Ramp time/s	Hold time/s	Ar flow-rate/ ml min^{-1}
Dry	150	20	40	300
Carbonise ..	600	20	20	300
Char	1700	10	20	300
Atomise ..	2700*	0	5	Stop
Clean	2700	1	3	300

* Without a chemical modifier the atomisation temperature was 2800 °C.

Reagents

Molybdenum(VI) stock standard solution, 1000 μg ml^{-1}. Prepared by dissolving 0.1840 g of $(NH_4)_2MoO_4.3H_2O$ in 100 ml of ultrapure water.

All test solutions were prepared with ultrapure water and used immediately.

Nitric acid, 65%. Merck.

Barium difluoride, Suprapur. Merck.

Octyl alcohol.

Ultrapure water (*specific resistivity* 18 MΩ). Obtained from a Milli-Q system (Millipore).

National Institute of Standards and Technology Standard Reference Material, NIST SRM 1549 *Non-Fat Milk Powder*.

All material was kept in 10% nitric acid for at least 48 h and subsequently washed three times with ultrapure water before use.

Procedure

To overcome problems in the sample introduction and with carbon residues, whole milk samples with the appropriate amount of chemical modifier were introduced with octyl alcohol into the furnace using a two-step piston micropipette. Both the milk, with the modifier, and the octyl alcohol were

* Presented at SAC 89, the 8th SAC International Conference on Analytical Chemistry, Cambridge, 30 July–5 August, 1989.

taken up into the tip of the pipette in sequence and then loaded into the graphite furnace together.

Results and Discussion

Optimisation of the Graphite Furnace Programme

Experiments were carried out to determine the best temperatures and times for the various steps of drying, ashing and atomisation. To avoid problems related to the spluttering and foaming of milk samples, the samples were injected together with octyl alcohol. Optimum drying conditions were set to provide a smooth, even evaporation of the solvent with no spluttering. The importance of carbonisation at 600 °C was established. It is known that at high temperatures in alcoholic solutions molybdenum forms carbonyl compounds such as $Mo(CO)_6$, which enhance the molybdenum emission signal[8] and can lead to irreproducible results in atomic absorption spectrometry. These problems can be easily suppressed by the proper choice of carbonisation temperature. To optimise the charring and atomisation temperatures, charring and atomisation curves were constructed for milk samples containing 10 μg l^{-1} of added molybdenum and the optimum concentration of chemical modifier; the results are shown in Fig. 1. In all instances the optimum charring temperature was 1700 °C. The dip in the charring curve with barium difluoride must be related to chemical reactions of molybdenum with the graphite material[4] or to the presence of volatile molybdenum fluorides. The optimum atomisation temperature was 2700 °C with nitric acid or barium difluoride as the chemical modifier, but in the absence of a chemical modifier the optimum temperature was 2800 °C. The internal gas-stop mode and "maximum power" were used at the atomisation stage.

The use of the gas-stop mode in the atomisation step can produce tube memory effects. To overcome this, the tube was fired at 2700 °C for 3 s with the internal gas at the maximum flow-rate of 300 ml min^{-1}.

Among different atomisation techniques, tube wall atomisation has been found to be superior to platform atomisation. Integrated absorbance and peak height modes produce similar results. The life of a tube is 100 burns. The furnace conditions are shown in Table 1.

Amount of Chemical Modifier

In order to determine the optimum amounts of the chemical modifiers, different amounts of nitric acid or barium difluoride were added to a series of samples containing 500 μl of milk and 10 μg l^{-1} of molybdenum. The mixtures were made up to a fixed volume with ultrapure water and subjected to the furnace programme.

The optimum amounts were 0.3% v/v nitric acid and 0.005% m/v barium difluoride.

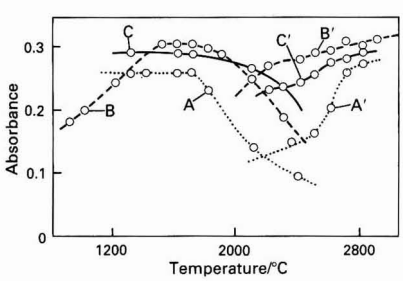

Fig. 1. A, B and C, Charring curves and A′, B′ and C′, atomisation curves of molybdenum. A and A′, Without a chemical modifier; B and B′, with barium difluoride as a chemical modifier; and C and C′, with nitric acid as a chemical modifier

Calibration

To obtain calibration graphs, standard solutions containing 5–30 μg l^{-1} of molybdenum with the optimum amount of a chemical modifier were subjected to the furnace programme. The standard additions method was used, 0, 5, 10 and 20 μg l^{-1} of molybdenum and the optimum amount of a chemical modifier being added to a milk sample. The slopes of the calibration and additions graphs, the average blank and the relative standard deviations are shown in Table 2. Chemical interference from octyl alcohol was not observed and, therefore, it was not necessary to add this chemical to the standard solution used for calibration.

Sensitivity

In this work calculation of the detection limit follows the recommendations of the ACS Committee of Environmental Improvement,[9] in which two limits are given. The limit of detection (LOD), the lowest concentration level that can be determined to be statistically different from a blank, is defined as three times the within-batch standard deviation of a single blank determination, corresponding to a 99% confidence level. The limit of quantification (LOQ) is defined as the level above which quantitative results can be obtained with a specified degree of confidence. At the 99% confidence level the value recommended is ten times the within-batch standard deviation. Table 3 summarises both these limits in terms of concentration. All the limits listed are based on ten replicate determinations of the blank with the modifier. An improvement in the detection limit is possible by using larger sample volumes.

The characteristic mass (m_0) is defined as the mass of analyte in picograms required to give a signal of 0.0044 A s for integrated absorbance. The values obtained are shown in Table 3.

Precision and Accuracy

The precision [relative standard deviation (RSD) or coefficient of variation (CV)] of the method (instrumental and matrix factors) obtained for ten replicate analyses of one milk sample during the same run was 1.76% (for 18.71 μg l^{-1} of molybdenum) without a chemical modifier, 1.72% (for 12.68 μg l^{-1} of molybdenum) with nitric acid as a chemical modifier and 2.55% (for 13.08 μg l^{-1} of molybdenum) with barium difluoride as a chemical modifier.

Table 2. Calibration and standard additions data

	Chemical modifier		
	None	0.3% v/v HNO_3	0.005% m/v BaF_2
Calibration slope/l μg^{-1}	0.0052	0.0062	0.0091
r (calibration)	0.9996	0.9967	0.9998
Additions slope/l μg^{-1}	0.0050	0.0080	0.0099
r (additions)	0.9944	0.9990	0.9993
Average blank ± SD*	0.006 ± 0.001	0.002 ± 0.001	0.011 ± 0.001

* SD = standard deviation

Table 3. Detection and quantification limits and characteristic mass data

	Chemical modifier		
	None	0.3% v/v HNO_3	0.005% m/v BaF_2
LOD/μg l^{-1} . .	0.62	1.53	0.89
LOQ/μg l^{-1} . .	1.56	3.95	1.96
m_0/pg	17.82	18.64	12.08

Table 4. Recovery studies: NIST SRM 1549 at 15% m/v (ten replicate analyses)

Molybdenum added/μg l^{-1}	Recovery, %		
	Without a chemical modifier	HNO_3 as chemical modifier	BaF_2 as chemical modifier
0	97.54	97.13	92.24
5	95.90	105.17	97.67
10	100.00	108.05	93.02
20	95.08	109.20	106.20

The within-batch precision of the method, obtained for ten replicates of four samples with 0, 5, 10 and 20 μg l^{-1} of added molybdenum, varied over the range 0.93–2.43% without a chemical modifier, 1.64–3.66% for nitric acid as a chemical modifier and 1.12–4.89% for barium difluoride as a chemical modifier.

To study the accuracy of the method, a National Institute of Standards and Technology Standard Reference Material, NIST SRM 1549 Non-Fat Milk Powder, with a molybdenum content (non-certified) of 0.34 μg g^{-1} was used. Molybdenum contents obtained were 0.36 ± 0.02, 0.34 ± 0.03 and 0.35 ± 0.02 μg g^{-1} without a chemical modifier and with nitric acid or barium difluoride as the chemical modifier, respectively. The accuracy of the method was also investigated by determining the recovery of standard additions of molybdenum to milk samples. To carry out this study the SRM 1549 was prepared at 15% m/v. The results are given in Table 4.

Interference

Experiments were performed to discover the degree to which the proposed method is susceptible to interference from elements known to interfere with the determination of molybdenum by AAS, including those forming refractory compounds at high temperatures. The elements studied were Al, Cu, Fe, W and V. The molybdenum concentration used was 10 μg l^{-1}.

An interference was defined as being significant if a change of more than 5% in the measurements was observed. Molybdenum can be determined without a chemical modifier in the presence of a 2000-fold excess of Cu, Fe and W, a 1000-fold excess of Al and a 100-fold excess of V. With nitric acid as the chemical modifier molybdenum can be determined in the presence of a 2000-fold excess of Cu, Al and W, a 1500-fold excess of Fe and a 100-fold excess of V. With barium difluoride as the chemical modifier molybdenum can be determined in the presence of a 2000-fold excess of Cu, Al, Fe and W and a 100-fold excess of V.

The levels of these elements in milk are less than those necessary to produce interference.[10] In addition, amounts of the anions usually present in milk (PO_4^{3-}, Cl^-, HCO_3^-, SO_4^{2-}), do not produce any interference.

Conclusions

The direct injection of a milk sample into the graphite furnace presents some difficulties with regard to spluttering and foaming of the sample. These problems were avoided by injecting octyl alcohol together with the milk, but its low surface tension can produce some losses during the injection. Problems caused by the milk matrix during the carbonise, char and atomise steps owing to the formation of molecular compounds that produce non-atomic absorption can be avoided by using an appropriate temperature and a deuterium arc background corrector.

When nitric acid was used as the chemical modifier there was a significant difference between the slopes of the calibration and additions graphs and the detection and quantification limits were worse than without a chemical modifier and when barium difluoride was used as a chemical modifier.

The results obtained without a chemical modifier and with barium difluoride as the chemical modifier were similar with respect to the slopes of the calibration and additions graphs, precision, accuracy and sensitivity, but the interference from Al was less with barium difluoride.

Lowering the molybdenum atomisation temperature by using barium difluoride, as a result of the preferential formation of very volatile molybdenum fluorides, together with the reduced carry-over between injections and the increase in the tube life due to the absence of the acidic medium, were the most important advantages of this chemical modifier for the direct determination of molybdenum in milk samples.

References

1. Morrison, C. H., *CRC Crit. Rev. Anal. Chem.*, 1979, **8**, 287.
2. Sneddon, J., Ottaway, J. M., and Rowston, W. B., *Analyst*, 1978, **103**, 776.
3. Muller-Vogt, G., Wendl, W., and Pfundstein, P., *Fresenius Z. Anal. Chem.*, 1983, **314**, 638.
4. Shaole, W., Chakrabarti, C. L., Marcantonio, F., and Headrick, K. L., *Spectrochim. Acta, Part B*, 1986, **41**, 651.
5. Mingorance, M. D., and Lachica, M., *Anal. Lett.*, 1985, **18**, 1519.
6. Casey, C. E., and Neville, M. C., *Am. J. Clin. Nutr.*, 1987, **45**, 921.
7. Ericson, S. P., McHalsky, M. L., and Jaselkis, B., *At. Spectrosc.*, 1987, **8**, 101.
8. Sanz Medel, A., Sanchez Uria, E., and Arribas, S., *Analyst*, 1985, **110**, 563.
9. Keith, L. H., Crummett, W., Deegan, J., Jr., Libby, R. A., Taylor, J. K., and Wentler, G., *Anal. Chem.*, 1983, **55**, 2210.
10. Iyengar, G. V., *in* "Elemental Composition of Human and Animal Milk," International Atomic Energy Agency, Vienna, 1982.

Paper 9/03194D
Received July 27th, 1989
Accepted September 30th, 1989

Evaluation of Biological Sample Mineralisation Methods for the Determination of Fluorine by Graphite Furnace Molecular Absorption Spectrometry*

M. Gómez, I. Rodríguez, C. Cámara and M. A. Palacios
Departamento de Química Analítica, Facultad de Ciencias Químicas, Universidad Complutense, 28040 Madrid, Spain

Various mineralisation methods were evaluated as means of treating different liquid and solid biological samples for the determination of fluorine by the formation of aluminium monofluoride in an electrothermal graphite furnace and molecular absorption spectrometry (AlF - MAS). Simple sample dilution and the use of 0.01 M Al^{3+} + 0.01 M Sr^{2+} solution as a matrix modifier are sufficient to determine the fluorine content in most liquid samples, although some require the addition of 0.3 M ammonium nitrate to the matrix modifier solution in order to diminish background absorbance. In solid samples, treatment methods routinely used with fluoride ion-selective electrodes such as microdiffusion, furnace ashing - microdiffusion and oxygen flask combustion, were tested for compatibility with AlF - MAS. The results were compared with those obtained with a fluoride ion-selective electrode. The proposed mineralisation methods were checked for applicability to different plants, foodstuffs and other biological materials. Some of the methods gave an over-all precision of better than 10%, which is often acceptable, and all methods gave recoveries above 80%. Differences between labile + ionic fluoride and total fluorine can be established by sample treatment.

Keywords: *Aluminium fluoride molecular absorption spectrometry; fluoride ion-selective electrode; fluorine determination; liquid and solid biological samples; oxygen flask combustion*

Fluorine is an essential element whose toxic effects at high concentrations make it necessary to develop efficient methods for the determination of total fluorine and diffusible (ionic + acid-labile) fluoride in biological materials. The fluoride ion-selective electrode (ISE) is an effective and easy-to-use potentiometric technique for the determination of fluoride in aqueous solutions[1] and has largely replaced the various spectrophotometric methods formerly used. However, there are two unresolved problems in the analysis of solids: the preparation of an appropriate analyte solution without losses or contamination, and the liberation of fluoride from its complexes, by either masking or separation.

Methods and procedures for the loss-free liberation of diffusible and total fluorine from a variety of matrices have been reviewed recently by the Analytical Chemistry Division Commission of IUPAC[2] and oxygen flask combustion and alkali fusion with subsequent microdiffusion for total fluorine, as opposed to microdiffusion and acid extraction for diffusible fluoride, have been proposed when a fluoride ISE is applied.[3]

Molecular absorption of aluminium fluoride (AlF) measured at 227.45 nm in a carbon furnace or dinitrogen oxide - acetylene flame is a direct and sensitive method for the determination of trace amounts of fluoride[4] and the development of methods to liberate fluoride from the liquid or solid matrix before determination in a graphite furnace is a promising line of investigation. Dittrich *et al.*[5] extracted fluoride from aqueous solution with triphenyltin hydroxide in isobutyl methyl ketone and stripped it with barium hydroxide. Interferences from anions and cations were reduced and the sensitivity and accuracy were improved. Takatsu *et al.*[6] directly determined ultratrace levels of fluorine in bovine milk, concluding that AlF - molecular absorption spectrometry (MAS) is a convenient technique but not yet simple to apply because of the difficulty in controlling interferences from inorganic and organic matrices. Fuwa and co-workers[7,8] determined fluorine in urine and blood serum by AlF - MAS and with an ISE. Urine and serum samples were prepared by dilution without pre-treatment. Ashing of serum was performed at 600 °C with sodium hydroxide and sodium carbonate followed by steam distillation with sulphuric acid as a standard method for purposes of comparison. The slightly higher AlF - MAS values obtained for digested serum compared with non-digested serum suggested the possibility of contamination during the complicated dry ashing - distillation method or the existence of another form of fluorine (*e.g.*, volatile organic fluorine) that was lost in the non-digestion procedure before the AlF absorbance signal was read. Venkateswarlu *et al.*[9] determined total fluorine by AlF - MAS in serum from chemical plant workers handling fluorochemicals. Their process used sodium biphenyl for the conversion of organic fluorine into inorganic fluoride before applying a reverse extraction technique. Satisfactory agreement was achieved between total fluoride results, and evidence was found for the partial loss of covalent fluorine when direct AlF - MAS was used.

For solid biological samples, Tsunoda *et al.*[10] used ashing with sodium carbonate in a porcelain crucible at 550 °C. The method was applied successfully to a standard reference material, *viz.*, National Institute of Standards and Technology (NIST), Standard Reference Material (SRM) 1571 Orchard Leaves.

In this work, some sample treatment methods routinely used for the determination of total fluorine and diffusible fluoride by ISE techniques were adapted for use with AlF - MAS.

Experimental

Apparatus

A Perkin-Elmer 1100B atomic absorption spectrometer equipped with a deuterium lamp for simultaneous background correction was used for AlF - MAS measurements. A furnace programme (HGA 400) and pyrolytic graphite furnaces with a L'vov platform were used. A platinum hollow-cathode lamp provided a light source for molecular absorption at 227.45 nm. The spectral bandpass was 0.07 nm throughout. Argon (flow-rate 200 ml min^{-1}) was used to purge air from the cuvette. A pH - mV meter (Crison Digit 501), a fluoride ISE (Orion Model 94-09) and a reference electrode (Ag - AgCl,

* Presented at SAC 89, the 8th SAC International Conference on Analytical Chemistry, Cambridge, UK, 30 July–5 August, 1989.

Table 1. Procedures for AlF molecular absorption at 227.45 nm with a graphite furnace

Procedure	Temperature/ °C	Ramp/s	Hold/s	Ar flow-rate/ ml min^{-1}
Application of Al^{3+} solution, 20 µl*	—	—	—	200
Drying	110	20	30	200
Stop and cooling of furnace	—	—	—	—
Application of F^- solution, 10 µl	—	—	—	—
Drying	110	20	30	200
Ashing I	700	10	30	200
Ashing II	700	0	2	0 (stop flow)
Vaporisation	2400	0	4	0 (stop flow)

* Aluminium nitrate solution and strontium nitrate concentrations 0.01 M or aluminium nitrate solution and strontium nitrate solution 0.01 M and ammonium nitrate solution 0.3 M.

Orion 90-01) were used in the potentiometric method. Platinum (50 ml), nickel (50 ml) and vitrified porcelain (100 ml) crucibles were used for ashing. Polystyrene Petri dishes (55 × 10 mm) without ribs were used in the diffusion method. Spherical Schöniger flasks (1000 ml) with platinum and nickel wire as sample supporters were used for oxygen flask combustion and the filter-paper used was hardened and ash-free (Whatman 541). A flask shaker (Griffin), magnetic stirrer, muffle furnace, adjustable pipettes (Finn) with polypropylene tips and polypropylene tubes and containers were used. Solutions (fluoride standard, buffers, etc.) were stored in polyethylene bottles.

Chemicals

All reagents were of analytical-reagent grade. Distilled water, further purified in a Millipore Milli-Q system, was used throughout. Fluoride stock standard solution, 1000 µg ml^{-1}, was prepared by dissolving Suprapur sodium fluoride in distilled water. The buffer solution used for the adjustment of total ionic strength in the fluoride ISE method was TISAB III containing cyclohexane-1,2-diaminetetraacetic acid (Orion 940911). A solution containing 10^{-2} M Al^{3+} + 10^{-2} M Sr^{2+} as nitrate was used. For microdiffusion the solutions used were 8 M perchloric acid, 2 M silver perchlorate and 0.5 M sodium hydroxide in methanol.

AlF - MAS Conditions for Fluoride Determination

The graphite furnace programme for the determination of fluoride is summarised in Table 1. Peak-height measurements were made.

Liquid Sample Treatment

Liquid samples were diluted in the range 1 + 1 to 1 + 50 with distilled water. For the determination of fluoride with a fluoride ISE, samples were not diluted because of the lower sensitivity and wide linear range of this technique. Carbonated drinks and beer were partially de-gassed by shaking for 30 min before dilution. Vinegar was partially neutralised to pH 6 with 1 M sodium hydroxide solution before dilution and the precipitate was removed by centrifugation at 1000 *g*. Tea infusion was prepared by suspending 7 g of pulverised tea leaves in 500 ml of hot water, shaking for 15 min, filtering the suspension and diluting to 500 ml. Urine samples needed to be fresh (<1 d old) because a precipitate tended to form progressively during storage, with the risk of irreversible adsorption of fluoride.

Solid Sample Treatment

Solid sample treatments applied were (a) microdiffusion, (b) MgO ashing - microdiffusion and (c) oxygen flask combustion.

Microdiffusion (for AlF - MAS and fluoride ISE)

Acid-diffusible (ionic + acid-labile) fluoride was isolated from unashed samples by acidic diffusion. The undersides of Petri dish lids were impregnated with 0.5 ml of 0.5 M sodium hydroxide in methanol. A uniform layer was obtained on the whole surface. Lids were dried in an oven at 60 °C and stored in a desiccator over solid potassium hydroxide. Unashed sample (100–300 mg for AlF - MAS and 300–500 mg for the fluoride ISE) was placed directly in a polystyrene Petri dish to which 4 ml of 8 M perchloric acid and 200 µl of 2 M silver perchlorate had been added. The Petri dish was immediately covered with a prepared lid and the sample was digested in an oven at 60 °C for 18–24 h. The dishes were removed from the oven and the lids placed in a desiccator with potassium hydroxide as desiccant. Blanks were prepared in parallel.

Measurement with AlF - MAS. The alkaline layer on the lid was dissolved in 2 ml of water by magnetic stirring, neutralised to pH 7 with nitric acid and diluted to a final volume of 5–25 ml. Subsequently, the experimental conditions given in Table 1 were applied.

Measurement with fluoride ISE. The alkaline layer on the lid was dissolved in 2.5 ml of TISAB III buffer (pH 5.0) and diluted to 25 ml. The solution was transferred into a small plastic beaker and the diffused fluoride was determined with a fluoride ISE. Calibration graphs for fluoride in the ranges 10^{-2}–10^{-5} and 10^{-5}–10^{-7} M were prepared under the same conditions as for the samples. The sample concentration in the latter range was extrapolated using a second-order calibration graph and fitting with the aid of a suitable programme. Because of the lack of precision in this range, the concentration obtained is only orientative.

Oxygen flask combustion (for AlF - MAS and fluoride ISE)

From 100 to 200 mg of sample were ignited by the usual oxygen flask combustion method. When measurement was by AlF - MAS, 15 ml of Al^{3+} + Sr^{2+} solution as absorbing agent and standard additions were used. When measurement was with a fluoride ISE, 5–10 ml of 0.4 M citrate buffer (pH 6.0–6.2) were added as absorbing agent. TISAB III (5 ml) was added before diluting the solution to 25 ml. Calibration was with standard solutions containing the same concentrations of TISAB (5 ml) and citrate buffer solution. Two calibration graphs, for the ranges 10^{-2}–10^{-5} and 10^{-5}–10^{-7} M, were prepared. In both AlF - MAS and fluoride ISE measurements, complete absorption was ensured by continuous shaking in a flask shaker for 30 min.

Furnace ashing (for AlF - MAS)

Fluorine-free MgO. In order to obtain fluorine-free MgO, the following treatment was applied. Ammonium carbonate (110 g) from Merck and 55 ml of ammonia solution (Merck) were dissolved in distilled water and diluted to 500 ml. Dry magnesium chloride (400 g) from Merck was dissolved in 500

ml of warm distilled water and 20 ml of the ammonium carbonate solution were stirred into this solution. The mixture was heated and, when it began to boil, heating was discontinued and the precipitate was allowed to settle for a few minutes. The mixture was filtered through a Büchner funnel using suction and the precipitate was discarded. The precipitation and filtration procedure was repeated three times using 20 ml of ammonium carbonate solution each time. Finally, the clear filtrate from the last precipitation was treated with the remainder of the ammonium carbonate reagent. The pooled filtrates were stirred well and heated to boiling. When boiling began, heating was discontinued and the precipitate was allowed to settle, filtered off and washed several times with hot distilled water until the washings were free from chloride. The residue was dried at 100 °C and small amounts (1–2 g) were ignited at 1000 °C in a platinum crucible to form the oxide.

Furnace ashing - microdiffusion. Samples (100–500 mg) were weighed into a nickel, platinum or vitrified porcelain crucible together with 100 mg of MgO (fluorine free) as fixative agent and suspended in 5 ml of water by stirring carefully to form a slurry. The crucible was placed on an electric hot-plate and the contents were evaporated to dryness slowly to avoid frothing. Complete dryness was obtained in 1 h. Next, the crucible was transferred into a muffle furnace, heated slowly from 100 to 550 °C and kept at 550 °C for 4–6 h depending on sample type. Hot water was used to transfer the contents of the crucible quantitatively into a Petri dish, after which the procedure described under Microdiffusion (for AlF - MAS and fluoride ISE) was followed.

Results and Discussion

Liquid Samples by AlF - MAS

Fluorine in liquid samples such as wine, vinegar, beer, carbonated drinks, tea infusion and urine was determined by the AlF - MAS and fluoride ISE techniques with no treatment other than dilution. It is generally recognised in the literature that the ISE analysis of such samples involves no critical steps such as sample pre-treatment or decomposition, and that potentiometry can be applied directly as there are no uncontrolled interferences resulting from the composition of the matrix. When AlF - MAS was applied, ammonium nitrate was added as matrix modifier to some samples in order to decrease the background absorbance.[11] The results are given in Table 2.

Table 2. Determination of fluoride in selected liquid samples

Sample	Fluoride/μg ml^{-1} AlF - MAS method	Fluoride ISE method
Red wine, Rioja*	0.150 ± 0.013	0.150 ± 0.011
Red wine, Valdepeñas*	0.142 ± 0.011	0.140 ± 0.009
White wine, Capel*	0.300 ± 0.021	0.300 ± 0.015
White wine, Soldepeñas*	0.085 ± 0.006	0.074 ± 0.008
Rosé wine, R. de Duero*	0.094 ± 0.006	0.094 ± 0.010
Rosé wine, C. de Gredos*	0.127 ± 0.011	0.127 ± 0.008
Vinegar*	0.389 ± 0.025	0.400 ± 0.020
Beer, Aguila*	0.338 ± 0.038	0.337 ± 0.040
Carbonated beverage, La Casera	0.098 ± 0.004	0.094 ± 0.006
Tea infusion, Hornimans	3.64 ± 0.15	3.300 ± 0.20
Urine 1*	0.715 ± 0.029	0.698 ± 0.030
Urine 2*	0.441 ± 0.020	0.445 ± 0.018
Urine 3*†	0.716 ± 0.033	0.540 ± 0.04

* With NH_4NO_3 as matrix modifier.

† Urine from patient with anaemia treated with iron(III) compound.

The good agreement between the results obtained by the two methods suggests that both are valid for the determination of fluoride in these types of liquid samples and that most of the fluorine is in the form of free fluoride ion. The accuracy was established by determining the recovery of added ionic fluoride (as NaF) by the proposed procedures. In all instances it was higher than 98%. The precision measured as the relative standard deviation varied between 4 and 12%.

Fluorine in orange juice and commercial bovine milk could not be determined by AlF - MAS despite the fact that the ashing temperature was varied between 700 and 900 °C and the ashing time between 30 and 240 s. Low recoveries of fluoride, pronounced matrix effects and high carbonaceous residues on the L'vov platform occurred.

Solid Samples by AlF - MAS

Microdiffusion

To determine ionic or labile fluoride in unashed samples, the diffusion of hydrogen fluoride from acid solution and subsequent measurement with a fluoride ISE appeared to be the most suitable method for routine analysis because of its simplicity. The strongest interferences in fluoride diffusion are from aluminium, iron and silicon. Aluminium and iron form very strong fluoride complexes and silicon interferes because in acidic media it forms a viscous gel containing micellar spaces in which HF is trapped, slowing the rate of diffusion of fluoride. On the other hand, high acidity may decompose some organofluorine compounds and monofluorophosphate and labile F^- may be determined together with ionic F^-.

The diffusion conditions for the fluoride ISE are well established.[3,12,13] Silver perchlorate is added to the sample slurry to avoid diffusion of HCl. The recoveries depend on the diffusion temperature (50–60 °C), diffusion time (18–48 h), volume : concentration ratio of the diffusible acid (usually 2–4 ml of 3–8 M perchloric) and the amount of methanol - sodium hydroxide solution in the lid of the Petri dish. As AlF - MAS is a fairly sensitive technique requiring only small volumes, we examined the analytical parameters for diffusion and subsequent AlF - MAS measurement. The optimum conditions for microdiffusion are summarised under Microdiffusion (for AlF - MAS and fluoride ISE) and those for measurement under Measurement with AlF - MAS. The calibration slopes for blanks, samples or sodium fluoride are almost identical and hence standard additions to samples are no longer needed. This makes the method less time consuming because the only calibration graph required for analysis is that obtained by standard additions to the blanks.

The microdiffusion method was tested with sodium fluoride standard solution containing 12.5 μg of F^- as sodium fluoride, added to each sample before microdiffusion - fluoride ISE, and 0.2 μg of F^- added before microdiffusion - AlF - MAS. Table 3 gives the results obtained for different samples. The recoveries varied from 80 to 109% for six replicates of each of the four samples analysed by the two methods. There is good agreement between the results obtained by the fluoride ISE and AlF - MAS techniques, with the exception of the diet sample. This anomaly could be attributed to the fluoride concentration being excessively low for determination with a fluoride ISE.

Oxygen flask combustion

Oxygen flask combustion is a well established method for the determination of fluorine in organic compounds and is usually employed as a reference method when other procedures are applied. It involves less risk of losses by volatilisation but only a limited amount (0.1–0.2 g) of dry sample can be ignited, which prevents the determination of very low concentrations of F^-. When the oxygen flask combustion - fluoride ISE method was used, a coefficient of variation of 20% for samples containing less than 2–3 p.p.m. of fluoride was obtained.

Table 3. Comparison of AlF - MAS and fluoride ISE methods: unashed microdiffusion method

Sample	*n*	AlF - MAS Fluoride/μg g^{-1}	AlF - MAS Recovery, %	Fluoride ISE Fluoride/μg g^{-1}	Fluoride ISE Recovery, %
Spruce needles*	6	2.89 ± 0.08	80	2.67 ± 0.09	80
Hay powder	5	1.25 ± 0.01	100	1.42 ± 0.05	92
Spanish diet	6	1.04 ± 0.09	109	0.65 ± 0.06	—
Tea leaves	6	260 ± 5	85	256 ± 3	89

* The same microdiffusion product was analysed by the two methods.

Table 4. Comparison of AlF - MAS and fluoride ISE methods: oxygen flask combustion

Sample	*n*	AlF - MAS Fluoride/μg g^{-1}	AlF - MAS Recovery, %	Fluoride ISE: fluoride/μg g^{-1}
Spruce needles*	4	5.77 ± 0.40	100	—
Spruce needles†	4	5.90 ± 0.35	100	3.73 ± 0.04
Hay powder	4	1.49 ± 0.10	92	4.37 ± 0.06
Tea leaves	3	265 ± 12	98	258 ± 10
Single-cell protein‡	3	15.98 ± 1.62	—	11.28 ± 0.70
A-11 milk powder§	2	0.26 ± 0.07	—	—

* Ni wire in oxygen flask combustion.
† Pt wire in oxygen flask combustion.
‡ Recommended value 16.6 μg g^{-1}.
§ Recommended value [International Atomic Energy Agency (IAEA)] 0.27 μg g^{-1}.

Table 5. Comparison of microdiffusion, MgO ashing - microdiffusion and oxygen flask combustion methods

Sample	Fluoride/μg g^{-1} Microdiffusion	DL*	Ashing - microdiffusion	DL*	Oxygen flask	DL*
Single-cell protein†	12.17 ± 1.4	1.4	14.65 ± 4.64	9.86	15.98 ± 1.62	2.45
Spruce needles	2.89 ± 0.03	0.59	4.37 ± 0.1	2.27	5.8 ± 0.24	0.18
A-11 milk powder‡	—	—	<DL	—	0.26 ± 0.07	0.05
Hay powder	1.25 ± 0.01	0.1	<DL	—	1.49 ± 0.14	0.05

* Detection limit.
† Recommended value 16.6 μg g^{-1}.
‡ Recommended value [International Atomic Energy Agency (IAEA)] 0.27 μg g^{-1}.

When the fluoride concentration in the samples is high enough, such as in tea leaves, measurement with an ISE is recommended.

We combined oxygen flask combustion with MAS. The absorbent solution was 10^{-2} M Al^{3+} + 10^{-2} M Sr^{2+}, this matrix being necessary to form AlF radicals in the furnace. The optimum volume of absorbent solution seems to be 15 ml but a smaller volume can be used.

No contamination from the platinum wire was noted and the use of a nickel instead of a platinum wire gave the same results except for a slower ashing step. In order to detect platinum interference with the 227.45-nm AlF - MAS signal we measured the absorbance of a platinum solution at this wavelength. A 10 p.p.m. concentration of platinum produces a signal 20% above the background. It is clear that if any dissolved platinum exists, its concentration is below the interference level. Standard additions are necessary in this method because it does not include a prior fluoride separation step as in the diffusion method.

Table 4 compares the AlF - MAS and fluoride ISE methods for selected samples and gives percentage recoveries. The coefficient of variation with the AlF - MAS method is usually below 10% whereas with the ISE method it varies from 5 to 20%.

Furnace ashing - microdiffusion

Of the various methods described in the literature, ashing followed by microdiffusion for the separation and concentration of fluorine prior to measurement with an ISE seemed to be the most promising approach for samples with low fluoride contents. Alkaline earth elements have been used both as matrix modifiers in AlF radical formation[14] and as fixative agents to stabilise fluoride during sample mineralisation.[3] This study attempted to adapt the ashing and the ashing plus microdiffusion methods for use with AlF - MAS. The application of 0.1 M strontium in the form of $Sr(NO_3)_2$ or $Sr(OH)_2$ suspension as a fixative agent in sample mineralisation was evaluated. Insoluble precipitates were obtained in the final solution after treatment of the residue with 6.4% nitric acid and neutralisation with 1:5 ammonia. Fluoride ion was partially absorbed into the precipitate and hence the reproducibility and recovery were not good enough for fluoride MAS determination. When Ca as a 10^{-2} M suspension of CaO was used as a fixative agent in sample mineralisation under the experimental conditions, serious interferences due to inhibition of H_4AlF formation were observed. Under the conditions specified in the ashing procedure, only Mg as MgO provided satisfactory mineralisation without interferences in AlF - MAS. However, the sensitivity and reproducibility were always lower than those obtained with a strontium matrix modifier. The working conditions giving the best sensitivity and precision were achieved by combining MgO mineralisation with subsequent microdiffusion as indicated under Furnace ashing - microdiffusion. After much effort spent trying to free this reagent from fluoride, we found that even under optimum conditions the signal of the blanks was very high and hence the detection limit was also very high. The method was applied to the determination of total fluoride in single-cell protein and spruce needles. The results were comparable to those given by the oxygen flask method. The fluoride content in milk powder and hay powder was below the detection limit (Table 5).

Conclusions

Simple sample dilution and the use of 0.01 M Al^{3+} + 0.01 M Sr^{2+} solution as a matrix modifier are sufficient to determine the fluorine content in most liquid samples, although some require the addition of 0.3 M ammonium nitrate to the matrix modifier solution in order to diminish background absorbance.

Microdiffusion used alone allows the determination of ionic and labile fluoride (that is why this method gives lower results than those in which total fluorine is determined). Standard additions need only be applied to the blank.

Oxygen flask combustion appears to be the most rapid of the three methods proposed and has the added advantages that Al^{3+} + Sr^{2+} (used as the matrix modifier in graphite furnace) can be used as a fluoride absorbing reagent and that the risk of contamination is relatively low.

The detection limit of the ashing - microdiffusion method is very high. This is attributed to the large amounts of fluoride present as impurities in the MgO reagent. Such contamination of the MgO makes this method applicable only to samples containing large amounts of fluoride.

Some of our results have not been compared with certified values as the latter are difficult to obtain for biological samples. The only informative values available for A-11 milk powder and single-cell protein are in good agreement with those given by the oxygen flask determinations.

We propose sample mineralisation by oxygen flask combustion combined with graphite furnace MAS as the most satisfactory method for the determination of total fluoride in biological samples, and the application of microdiffusion alone for the determination of ionic and labile fluoride.

The determination of fluoride by AlF - MAS is much more sensitive than that by the fluoride ISE method, and we therefore recommend the former for samples of low fluoride content.

The authors thank CYCIT (Project 85/0035), the International Atomic Energy Agency for financial support and Max Gormann for revision of the manuscript.

References

1. Frank, M. S., and Ross, J. W., *Anal. Chem.*, 1968, **40**, 1169.
2. Campbell, A. D., *Pure Appl. Chem.*, 1987, **59**, 695.
3. Gustafsson, L., and Njenga, L. W., *Anal. Chim. Acta*, 1988, **212**, 133.
4. Dittrich, K., *CRC Crit. Rev. Anal. Chem.*, 1986, **16**, 225.
5. Dittrich, K., Shkinev, U. M., and Spivakov, B. V., *Talanta*, 1985, **32**, 1019.
6. Takatsu, A., Chiba, K., Ozaki, M., Fuwa, K., and Haraguchi, H., *Spectrochim. Acta, Part B*, 1984, **39**, 365.
7. Chiba, K., Tsunoda, K., Haraguchi, H., and Fuwa, K., *Anal. Chem.*, 1980, **52**, 1582.
8. Tsunoda, K., Chiba, K., Haraguchi, K., and Fuwa, K., *Anal. Chem.*, 1979, **51**, 2059.
9. Venkateswarlu, P., Winter, L. D., Prokop, R. A., and Hagen, D. F., *Anal. Chem.*, 1983, **55**, 2232.
10. Tsunoda, K., Fujiwara, K., and Fuwa, K., *Anal. Chem.*, 1977, **49**, 13.
11. Gomez Gomez, M., Palacios Corvillo, M. A., and Cámara Rica, C., *Analyst*, 1988, **113**, 1109.
12. Dabeka, R. W., Mckenzie, A. D., and Conacher, H. B. S., *J. Assoc. Off. Anal. Chem.*, 1979, **62**, 1065.
13. Culik, B., *Anal. Chim. Acta*, 1986, **189**, 329.
14. Itai, K., Tsunoda, H., and Ikeda, M., *Anal. Chim. Acta*, 1985, **171**, 293.

Paper 9/03280K
Received August 2nd, 1989
Accepted November 1st, 1989

Decomposition of Cinnabar and Organomercurials in Geological Materials With Nitric Acid - Sulphuric Acid for the Determination of Total Mercury by Cold Vapour Atomic Absorption Spectrometry*

Arnold Kuldvere
Geological Survey of Norway, P.O. Box 3006 Lade, N-7002 Trondheim, Norway

Data are presented to show that cinnabar (HgS) dissolves very slowly in HNO_3 - H_2SO_4 at room temperature and at temperatures below that of a boiling water-bath. On a boiling water-bath, however, cinnabar was found to be decomposed rapidly by this acid mixture. The experiments illustrated the influence of the temperature on the speed of the reaction. On the basis of these experiments a digestion procedure was developed that uses HNO_3 - H_2SO_4 (2 + 3) for the extraction of total mercury from geological samples (rocks, soils and sediments) containing cinnabar and organomercurials.

Keywords: *Total mercury determination; cold vapour atomic absorption spectrometry; decomposition of cinnabar and organomercurials; geological sample*

Cold vapour atomic absorption spectrometry is a widely used method for the analysis of environmental samples because of its cost effectiveness and low detection limits. The cold vapour atomic absorption spectrometric determination of mercury in air and gases was first reported in 1930.[1] The reduction - aeration method for mercury in solution samples, however, was not introduced until more than 30 years later by Poluektov and Vitkun[2] and Poluektov *et al.*[3] Hatch and Ott[4] modified the method by allowing the mercury vapour to recirculate continuously in a closed system until a peak absorbance was observed. Their digestion procedure, however, in which rock and mineral samples are first digested in H_2SO_4 and H_2O_2 by applying heat, and then oxidised further with $KMnO_4$, does not decompose organic mercurials completely.[5]

Since this earlier work a wide range of digestion procedures for various mercury-containing materials have been proposed and many reviews on this subject presented.[6–11] All procedures must fulfil the same general requirements. A good digestion procedure must be able to extract the analyte element quantitatively. If a sample contains organic material, mercury compounds resistant to some acids (such as cinnabar) or organomercurials that are difficult to decompose (such as phenylmercury and its derivatives), then the procedure must be modified accordingly.

Cinnabar (HgS) is often present in geological materials such as rocks, soils and sediments,[12,13] and organomercurials occur in soils and sediments implicated in mercury transformations and pollution.[14–16] Partially digested final solutions can give rise to matrix effects[17–20]; hence the complete decomposition of cinnabar and organomercurials is necessary for the determination of total mercury. Cinnabar is reported to be insoluble in HNO_3.[21] It is also resistant to attack by HNO_3 or H_2SO_4.[13] It has also been reported that metallic mercury was not recovered quantitatively using an H_2SO_4 digestion procedure[22] and that metallic mercury is insoluble in cold H_2SO_4.[21]

For the reasons mentioned above, some workers[14,23,24] have claimed that cinnabar is also resistant to attack by HNO_3 - H_2SO_4. However, in the present work it is shown that the decomposition of HgS by HNO_3 - H_2SO_4 depends on the temperature and considerable amounts of HgS can be dissolved on a boiling water-bath in a short period of time.

* Presented at SAC 89, the 8th SAC International Conference on Analytical Chemistry, Cambridge, UK, 30 July–5 August, 1989.

Experimental

Apparatus

A Perkin-Elmer Model 403 atomic absorption spectrometer, equipped with an MHS-1 mercury hydride system and a Model 056 recorder, was used. The light source for mercury was an electrodeless discharge lamp (EDL), with an external power supply, operating at 5 W. The operating parameters for the instrument and accessories are given in Table 1.

Argon was used as the purge gas and 150-ml Erlenmeyer flasks (Pyrex) with standard 29/32 tapered joints were used as the reaction vessels in which the reduction of mercury(II) with $SnCl_2$ was carried out.

In order to ensure that the equipment used did not contribute to contamination of the samples and standards with mercury, all glassware was cleaned by adding concentrated HNO_3 to it and keeping it in a boiling water-bath for at least 1 h. After rinsing with water, the flasks were filled with, or soaked in, dilute HNO_3 containing $K_2Cr_2O_7$ (0.01% m/v $K_2Cr_2O_7$ in 5% v/v HNO_3) for at least 24 h before use.

Reagents and Solutions

All chemicals were of analytical-reagent grade, and glass-distilled water was used throughout.

Table 1. Instrument parameters

Atomic absorption spectrometer—	
Light source	EDL
Wavelength	253.6 nm
Slit (spectral slit width)	3 (0.2 nm)
Recorder full-scale	0.25 A
Recorder response (time constant)	2 (1 s)
Recorder—	
Chart speed	10 mm min^{-1}
Range	2 mV
MHS-1 system—	
Programme	Hg II
Reduction solution (10% m/v $SnCl_2.2H_2O$ in 5% v/v HCl)	2.5 ml
Sample dilution (150-ml Erlenmeyer flask, 4% v/v HCl)	20 ml
Temperature of silica cell	250 °C

Acid digestion mixture. A mixture of two volumes of concentrated HNO_3 (Merck) and three volumes of concentrated H_2SO_4 was used.

Tin(II) chloride solution. A 10% m/v solution of $SnCl_2.2H_2O$ in 5% v/v HCl (Merck) was used. Argon was bubbled through the solution to free it from contamination by mercury.

Potassium permanganate solution. A 5% m/v solution of mercury-free $KMnO_4$ (Merck) in water was used.

Mercury(II) stock solution, 1 g l^{-1}. Prepared by diluting the contents of an ampoule containing Titrisol-grade mercury (Merck) to 1 l with a solution containing 5% v/v HNO_3 and 0.01% m/v $K_2Cr_2O_7$.

Mercury(II) sulphide (cinnabar). Purchased from Merck [Quecksilber(II) sulfid, Article No. 4477].

Mercury(II) working standard. 0.1 mg l^{-1}. Prepared by serial dilution of the stock solution, maintaining the concentration of HNO_3 and $K_2Cr_2O_7$ at 5% v/v and 0.01% m/v, respectively.

Sample dilution solution. An 80-ml volume of concentrated HCl (Merck) was diluted to 2 l with water.

Digestion Procedure

All results are reported on a dry mass basis. The water content of the wet samples was determined by taking different amounts of the samples and drying them to constant mass at 105 °C in an air oven.

Representative wet geological samples (1–4 g; depending on the water and mercury content) were placed in 250-ml calibrated flasks (Pyrex, France). A 10-ml volume of the acid digestion mixture was added and the flasks were allowed to stand overnight at room temperature and then on a water-bath (95–100 °C) for *ca.* 24 h. The flasks were heated on a hot-plate at 155–165 °C until the evolution of brown fumes of oxides of nitrogen ceased (*ca.* 30 min). To the samples, which at this stage were still a dark colour, HNO_3 was added dropwise until the colour of the mixture changed from dark to light, indicating that the organic matter had been destroyed.

The flasks were removed from the hot-plate and allowed to cool to room temperature. A few drops of 5% m/v $KMnO_4$ solution were added until the pink colour persisted (2–5 drops). To the completely decomposed samples 20 ml of water were added and the salts dissolved by shaking the flasks. The sample solutions were filtered through folded No. 595.5 filters (Schleicher and Schnell) into 50-ml polyethylene flasks fitted with screw-caps. The residue in the calibrated flasks was washed several times with water, the washings filtered through the same filter into the same flask and the solutions made up to the mark with water.

It is important that the pink colour of the solution persists until the mercury content is determined, otherwise some loss of mercury may occur as a result of reduction, particularly from solutions with a low mercury concentration. The pink colour normally persists for at least 1 d. Blanks and standards were prepared throughout the entire procedure; however, the differences in the results were negligible, regardless of whether or not the standards were used throughout the procedure.

Measuring Procedure

An appropriate volume of the final sample solution (usually 0.1–5 ml) was transferred into an Erlenmeyer flask (the reaction vessel). A 20-ml aliquot of 4% v/v HCl was then added, the system closed and the programme started (Table 1). Peak-height readings were taken and compared with those given by a standard working solution. Background correction was applied but was found to be unnecessary. For samples with low mercury contents, the entire 50 ml of the final sample solution were taken for measurement; in this instance, the calibration graph was also constructed from measurements made on a 50-ml sample volume.

Results and Discussion

Dissolution of HgS

Mercury(II) sulphide occurs in two forms: the black sulphide, metacinnabarite and the red sulphide, cinnabar. The black form is converted by heat into the red form. Both forms are the most insoluble of the metallic sulphides.

Cinnabar is not dissolved either by HNO_3 or H_2SO_4.[13] It is dissolved by HCl (at room temperature) with the evolution of H_2S (Table 2), although it has been claimed that (as regards mineral acids) HgS is only soluble in aqua regia.[14,22,25] Aqua regia is a mixture of HNO_3 and HCl; the former oxidises the sulphide to free sulphur, the latter provides chloride ions to form the stable $[HgCl_4]^{2-}$ complex.

When $K_2S_2O_8$ was added to H_2SO_4, HgS was attacked very effectively by this mixture; however, when $K_2S_2O_8$ was added to HNO_3, no reaction was observed (Table 2). In HNO_3 - H_2SO_4, $K_2S_2O_8$ also had no effect (Table 2). It has been stated in the literature that HNO_3 - H_2SO_4 does not attack cinnabar.[14,23,24] Fig. 1 shows that cinnabar is attacked slowly by this acid mixture at room temperature. After 2 weeks, 15 mg of cinnabar had been dissolved completely in 10 ml of HNO_3 - H_2SO_4 at room temperature. The solubility is temperature-dependent as can be seen from Fig. 1; the same amount of cinnabar was dissolved by heating on a boiling water-bath for a period of 30 min.

Dissolution of Organomercurials

This subject has been widely reported in the literature.[5–14] The present work shows that the proposed procedure decomposes

Table 2. Effect of $K_2S_2O_8$ on the decomposition of cinnabar in HNO_3, H_2SO_4 and HNO_3 - H_2SO_4 (2 + 3). The experiments were carried out on a water-bath using 35 mg of HgS and 10 ml of extraction medium in each extraction. For details see text

Decomposition medium	Average time required for complete decomposition/min	
	Without $K_2S_2O_8$	With the addition of 2 g of $K_2S_2O_8$
HNO_3	Not decomposed*	Not decomposed*
H_2SO_4	Not decomposed*	15
HNO_3 - H_2SO_4 (2 + 3)	60	70
HCl	10	—

* In another experiment 5 mg of cinnabar and 25 ml of acid were heated on a boiling water-bath for 2 weeks. None of the HgS was dissolved.

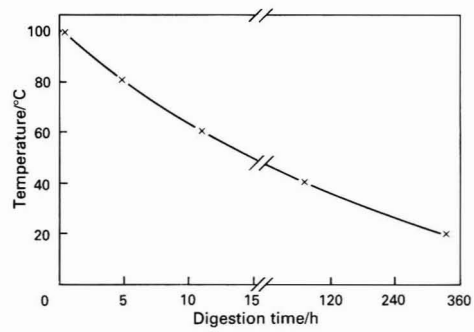

Fig. 1. Effect of temperature on the solubility of 15 mg of cinnabar in 10 ml of HNO_3 - H_2SO_4 (2 + 3). For details see text

methylmercury chloride by treatment on a water-bath. For complete decomposition of phenylmercury acetate, the hot-plate treatment was found to be necessary (Table 3).

Digestion

The described procedure is able to destroy organic matter and decompose HgS without the use of $K_2S_2O_8$ or other oxidising agents. The few drops of $KMnO_4$ solution, added at the end of the digestion period, serve to control the decomposition of organic matter and to preserve Hg^{II} in the final solution. As shown in Table 2, there is no advantage in adding $K_2S_2O_8$ to a mixture of HNO_3 and H_2SO_4. When $KMnO_4$ is used for the oxidation of large amounts of organic matter at lower temperatures, the addition of $K_2S_2O_8$ is mandatory, otherwise the organomercurials will not be destroyed.[22]

The procedure is an open-digestion method. Nevertheless, mercury is not lost as shown by the recovery studies (Tables 3 and 4) and by the analysis of a number of certified reference materials[26] (Table 5). The lengthy pre-oxidation step, initially at room temperature and then on a water-bath, destroys most of the organic matter at this stage of the procedure. The high neck of the calibrated flask acts as an air-condenser; the top part of the neck is at room temperature. The method has been used at the Geological Survey of Norway for a long period of time for the determination of mercury in rocks, soils and sediments and for the analysis of environmental organic materials with a few modifications. In the latter work,[27] mercury was determined in seaweed. The complete (or nearly complete) destruction of organic matter makes the use of antifoaming agents unnecessary and eliminates matrix effects, such as those described by Stuart[17] and Munaf *et al.*[20]

Table 3. Recovery of organic mercury and HgS at two different stages during the digestion step, using the recommended procedure

	Recovery,%	
Mercury compound*	Digestion stopped after treatment on water-bath	Samples taken through the entire procedure
Methylmercury chloride	100.1	98.2
	100.8	103.6
	Mean: 100.5	Mean: 100.9
	Relative error: +0.5	Relative error: +0.9
Phenylmercury acetate	65.4	104.1
	75.0	97.8
	60.2	101.0
	Mean: 66.9	Mean: 101.0
	Relative error: −33.1	Relative error: +1.0
HgS (cinnabar)	99.1	99.6
	100.4	101.0
	102.0	100.5
	Mean: 100.5	Mean: 100.4
	Relative error: +0.5	Relative error: +0.4

* Added to 1 g of sediment.

Table 4. Recovery of mercury added to a rock and soil sample. The mercury was added from a standard solution

	Concentration of mercury/ng g^{-1}			
	Certified value	Added	Found	Recovery of mercury added,%
Rock sample 415	87	50	129	94
		25	120	107
Soil sample 226/87	65	50	121	105
		25	82	91
		10	85	113

Reliability

The accuracy and precision of the method are shown by the recovery studies (Tables 3 and 4) and by the determination of mercury in a number of certified reference materials (Table 5). The precision can also be seen from the results presented in Table 6. The relative standard deviation (RSD) for samples with mercury concentrations at the p.p.b. level is 12–19% and for those with mercury concentrations at the p.p.m. level 8%. For soils, rocks and sediments, the detection limit in routine work is 5 ng g^{-1}.

Conclusions

Cinnabar is not resistant to attack by HNO_3 - H_2SO_4. It is soluble in H_2SO_4 in the presence of sufficient $K_2S_2O_8$, but not in HNO_3. In HCl, cinnabar dissolves with the evolution of H_2S and the formation of the stable $[HgCl_4]^{2-}$ complex.

The proposed procedure, using HNO_3 - H_2SO_4 (without the addition of other oxidising agents), is satisfactory for the decomposition of cinnabar and organomercurials and can be used for the determination of total mercury in geological materials.

Table 5. Determination of mercury in certified reference materials using the described extraction procedure. Recommended values (95% confidence level): 036 SO-1, 21 p.p.b.; 045 ASK-3, 8 p.p.m.; and CPB-1, 5.5 ± 0.5 μg g^{-1} of mercury

Mercury found, p.p.m.*		
036 SO-1†	045 ASK-3‡	CPB-1§
24	7.28	5.75
19	7.24	4.70
22	8.48	4.85
Mean: 22	8.00	5.55
Relative error: +5%	8.90	4.95
	8.88	Mean: 5.23
	7.86	RSD: 8.6%
	7.54	
	7.43	
	8.42	
	Mean: 8.00	
	RSD: 8.0%	

* Values for 036 SO-1 in p.p.b.
† Soil sample (see reference 26).
‡ Sulphide ore (see reference 26).
§ Lead Concentrate. Canadian Certified Reference Materials Project, Canada Centre for Mineral and Energy Technology, Ottawa, Canada.

Table 6. Determination of mercury in a rock and soil sample using the described method

Mercury found, p.p.b.	
Rock sample 415*	Soil sample 226/87*
81	72
65	50
78	75
91	49
108	75
90	50
87	80
85	69
91	70
91	60
Mean: 87	Mean: 65
RSD: 12%	RSD: 19%

* Using the method of Chiu and Hilborn[24] (aqua regia digestion in an open system), the values obtained were 90 and 60 p.p.b. of mercury for the rock and soil samples, respectively (means of three analyses).

The author thanks Frank Berge for analytical help.

References

1. Müller, K., *Z. Phys.*, 1930, **65**, 739.
2. Poluektov, N. S., and Vitkun, R. A., *Zh. Anal. Khim.*, 1963, **18**, 33.
3. Poluektov, N. S., Vitkun, R. A., and Zelyukova, T. V., *J. Anal. Chem. USSR*, 1964, **19**, 873.
4. Hatch, W. R., and Ott, W. L., *Anal. Chem.*, 1968, **40**, 2085.
5. Melton, J. R., Hoover, W. L., and Howard, P. A., *Soil. Sci. Soc. Am., Proc.*, 1971, **35**, 850.
6. Jenne, E. A., *At. Absorpt. Newsl.*, 1974, **13**, 106.
7. Ure, A. M., *Anal. Chim. Acta*, 1975, **76**, 1.
8. Manning, D. C., *At. Absorpt. Newsl.*, 1970, **9**, 97.
9. Helsby, C. A., *Mikrochim. Acta*, 1976, **1**, 307.
10. Gorsuch, T. T., "The Destruction of Organic Matter," Pergamon Press, Oxford, 1970.
11. Bock, R., "Handbook of Decomposition Methods in Analytical Chemistry," Blackie, London, 1979.
12. Frieberg, L., and Vostal, J., "Mercury in the Environment," CRC Press, Cleveland, OH, 1972.
13. Jonasson, I. R., Lynch, J. J., and Trip, L. J., *Geol. Surv. Can.*, Report No. 73–21, Energy, Mines and Resources, Ottawa, 1973.
14. Jacobs, L. W., and Keeny, D. R., *Environ. Sci. Technol.*, 1974, **8**, 267.
15. Jensen, S., and Jernelove, A., *Nature (London)*, 1969, **223**, 753.
16. Cranston, R. E., and Buckly, D. E., *Environ. Sci. Technol.*, 1972, **6**, 274.
17. Stuart, D. C., *Anal. Chim. Acta*, 1978, **96**, 83.
18. Stuart, D. C., *Anal. Chim. Acta*, 1978, **101**, 429.
19. Stuart, D. C., *Anal. Chim. Acta*, 1979, **106**, 411.
20. Munaf, E., Goto, M., and Ishii, D., *Fresenius Z. Anal. Chem.*, 1989, **334**, 115.
21. "Handbook of Chemistry and Physics," Sixty-ninth Edition, CRC Press, Boca Raton, FL, 1988–1989.
22. Iskander, I. K., Syers, J. K., Jacobs, L. W., Keeney, D. R., and Gilmour, J. T., *Analyst*, 1972, **97**, 388.
23. Agemian, H., and Chau, A. S. Y., *Analyst*, 1976, **101**, 91.
24. Chiu, C. H., and Hilborn, J. C., *Analyst*, 1979, **104**, 1159.
25. Pauling, L., "College Chemistry," W. H. Freeman, San Francisco, CA, 1952, p. 570.
26. *Geostand. Newsl.*, 1989, **13**, July (Special Issue).
27. Kuldvere, A., and Andreassen, B. T., *At. Absorpt. Newsl.*, 1979, **18**, 106.

Paper 9/03704G
Received August 31st, 1989
Accepted January 3rd, 1990

Evaluation of Oxidant Media for the Determination of Lead in Food Slurries by Hydride Generation Atomic Absorption Spectrometry*

Yolanda Madrid, Milagros Bonilla and Carmen Cámara
Departamento de Química Analítica, Facultad de Ciencias Químicas, Universidad Complutense, 28040 Madrid, Spain

Several oxidant media were evaluated for the generation of lead hydride from slurry samples and their application to the determination of lead in vegetables and fish by hydride generation atomic absorption spectrometry. Three oxidant - acid media were compared: hydrogen peroxide - nitric acid, ammonium persulphate - nitric acid and potassium dichromate - lactic acid. The powdered samples were suspended in Triton X-100 and shaken with 10.0 g of blown zirconia spheres until a slurry was formed. The potassium dichromate - lactic acid medium was the most satisfactory for the determination of lead in fish and vegetables, providing the lowest detection limits as a result of its high sensitivity and low blank values. The ammonium persulphate - nitric acid medium gave good accuracy, precision and selectivity for vegetables (1–2 p.p.m. of lead); however, with fish (0.1–1 p.p.m. of lead) it was only a semi-quantitative medium for the determination of lead owing to its lack of sensitivity and selectivity. The hydrogen peroxide - nitric acid medium was unsatisfactory for the generation of lead hydride from slurry samples because of decomposition of hydrogen peroxide by the organic matter in the sample.

Keywords: *Lead hydride generation; lead determination; food sample; atomic absorption spectrometry; slurry procedure*

In recent years interest has grown in the direct analysis of suspensions or slurries of solids by atomic absorption spectrometric methods, which show advantages of speed, ease of analysis and reduction of blank levels. Many of these studies have employed flame atomic absorption spectrometry, but the atomisation efficiency is dependent on sample transport efficiency, particle size, atomisation temperature and sample matrix.

Although electrothermal atomisation atomic absorption spectrometry can tolerate large particle sizes and has been used successfully for the determination of lead in soil, environmental samples,[1–4] foodstuffs and biological samples, sampling difficulties and high matrix salt levels can become an important source of errors. Hydride generation appears to offer a viable alternative for overcoming many of these problems.

Haswell *et al.*[5] determined arsenic in environmental samples by cold acid solubilisation - hydride generation atomic absorption spectrometry. Samples were weighed directly into the glass hydride generation vessel and 10 ml of 4 M hydrochloric acid added. Arsine was generated by adding 1% m/v sodium tetrahydroborate(III). The influence of particle size, homogeneity and matrix on the reproducibility and amount of analyte released was examined. The technique gave similar results to those obtained by the aqua regia digestion procedure.[5]

Madrid *et al.*[6] reported a simple and rapid method for the determination of lead in foodstuffs and biological samples that combines a slurry procedure with lead hydride generation atomic absorption spectrometry. Powdered samples were suspended in Triton X-100 and shaken with 10.0 g of blown zirconia spheres until a slurry was formed. Determination of lead in slurries was carried out by hydride generation atomic absorption spectrometry in an ammonium persulphate - nitric acid medium. The effect of various concentrations of thixotropic thickening agent on the efficiency of lead hydride generation and slurry stability and the influence of an antifoaming agent were studied.

In this work we studied several oxidant media for lead hydride generation from slurried food and vegetable samples and compared their accuracy, precision and selectivity in the determination of lead by hydride generation atomic absorption spectrometry.

* Presented at SAC 89, the 8th SAC International Conference on Analytical Chemistry, Cambridge, UK, 30 July–5 August, 1989.

Experimental

Apparatus

Lead determinations were performed with a Perkin-Elmer Model 2380 atomic absorption spectrometer equipped with an electrodeless discharge lamp operated at 10 W from an external power supply. A spectral band width of 0.7 nm was selected to isolate the 217.0-nm lead line. The signals were recorded on a Perkin-Elmer Model 56 recorder set at the 10-mV range. A laboratory-built hydride generation system was used that had three valves to control the three flows: purge, mixing and sodium tetrahydroborate(III) addition.[7] Background correction was not used.

Reagents

All reagents were of analytical-reagent grade or higher purity and de-ionised water from a Milli-Q system was used. A 1000 mg l^{-1} lead(II) stock standard solution was prepared by dissolving 0.3991 g of $Pb(NO_3)_2$ (Merck) in 250 ml of 0.2% v/v nitric acid. Working solutions were prepared each day by diluting appropriate aliquots of the stock solution. Sodium tetrahydroborate(III) solutions (10, 8 and 4% m/v) were prepared by dissolving sodium tetrahydroborate(III) powder (Carlo Erba) in de-ionised Milli-Q water and stabilising in 0.1% sodium hydroxide solution.[8] Solutions were prepared daily and filtered before use.[9] Working oxidant solutions were prepared by appropriate dilution of 10, 9 and 5% m/v stock solutions of ammonium persulphate (lead-free after extraction with dithizone solution in chloroform), hydrogen peroxide and potassium dichromate, respectively.

Procedure for Slurry Preparation

Freeze-dried powdered samples (0.25–1.0 g) were weighed accurately and placed in small polyethylene bottles with 10.0 g of blown zirconia spheres (Glen Creston, Stanmore, Middlesex, UK), after which 5.0 ml of 1% m/m Triton X-100 solution were added. The bottles were shaken for about 10 min in a

flask shaker until a slurry was formed. Slurries were separated from the zirconia spheres using a Büchner funnel and transferred into a calibrated flask. A few drops of anti-foaming agent were added before the slurry was diluted.

Sample Analysis

Lead hydride generation was carried out in ammonium persulphate - nitric acid, hydrogen peroxide - nitric acid and potassium dichromate - lactic acid media. The optimum conditions for lead hydride generation in each medium are summarised in Table 1.

Table 1. Optimum conditions for lead hydride generation

Parameter	Hydrogen peroxide - nitric acid[7]	Ammonium persulphate - nitric acid[10]	Potassium dichromate - lactic acid[11]
Acid concentration, % v/v	0.5	2.0	2.0
Oxidant concentration, % m/v	1.8 (v/v)	3.0	0.3
Sodium tetrahydroborate(III) concentration, % m/v	10	8.0	4.0
Ni^{II} concentration (as catalyst), p.p.m.	2.5	—	—
Sample volume/ml	5.0	5.0	5.0
Mixing flow-rate/ml min^{-1}	60	20	20
Purge flow-rate/ml min^{-1}	675	800	800

Procedure in ammonium persulphate - nitric acid medium

To analyse slurry samples, 0.5–5 ml of the prepared sample were placed in a reaction flask of the hydride generation system, 1.0 ml of 10% v/v nitric acid and 1.5 ml of 10% m/v ammonium persulphate were added and the volume was made up to 5 ml with de-ionised Milli-Q water. Lead hydride was generated by adding 2.0 ml of 8% m/v sodium tetrahydroborate(III) solution.

Procedure in hydrogen peroxide - nitric acid medium

A volume of sample solution (2.0–5.0 ml), 25 μg of nickel, 1.0 ml of 2.5% v/v nitric acid and 1.0 ml of 9% v/v hydrogen peroxide were placed in a reaction flask, diluted to 5.0 ml with de-ionised Milli-Q water and then 5.0 ml of 10% m/v sodium tetrahydroborate(III) were added to generate lead hydride.

Procedure in potassium dichromate - lactic acid medium

To determine lead, 0.5–2.0 ml of slurry sample, 1.0 ml of 10% v/v lactic acid and 0.3 ml of 5% m/v potassium dichromate were placed in a reaction flask and diluted to 5.0 ml with de-ionised Milli-Q water. Lead hydride was generated by adding 2.0 ml of 4% m/v sodium tetrahydroborate(III) solution.

In all instances, analyte peaks were recorded as peak height. To determine the amount of lead, six distinct portions were taken from each sample, weighed, slurried, and then each portion was analysed in triplicate. The same procedure was followed for the blank. To avoid possible errors due to

Table 2. Lead concentration in foods determined using the ammonium persulphate - nitric acid medium

Sample	Concentration of powdered sample in slurry, % m/v	Lead content (slurry procedure)/ μg g^{-1}*	Certified value or value obtained by other procedure/ μg g^{-1}	LOD/ μg g^{-1}	LOQ/ μg g^{-1}	Slope ratio
IAEA V10 Hay (powdered)†	2.0	1.60 ± 0.07	1.61§	0.30	0.90	1.11
BCR CRM 281 Ryegrass‡	2.0	2.32 ± 0.10	2.38 ± 0.11§	0.20	0.60	1.7
Lettuce	2.0	2.87 ± 0.16	2.90 ± 0.16¶	0.40	1.20	1.16
Mussel	2.0	1.96 ± 0.06	1.98 ± 0.08¶	0.30	0.9	1.5
Sardine	2.0	<LOD	—	0.20	0.6	1.48
Atlantic bluefin tuna	2.0	<LOD	—	0.6	1.8	7
Anchovy	4.0	<LOD	—	0.3	0.9	2.5
Atlantic pomfret	2.0	<LOD	—	0.7	2.1	6.5
Prawn	2.0	No hydride generation				
IAEA H9 Diet†	10.0	0.10 ± 0.07	0.098§	0.07	0.21	1.6

* Mean value expressed as $\bar{X} \pm \sigma$.
† IAEA = International Atomic Energy Agency.
‡ BCR CRM = Bureau Communities of Reference, Certified Reference Material.
§ Certified value.
¶ Value obtained by other procedure (sample solutions prepared by mineralisation in a PTFE pressure bomb with nitric acid and V_2O_5).

Table 3. Lead concentration in foods determined using the potassium dichromate - lactic acid medium

Sample	Concentration of powdered sample in slurry, % m/v	Lead content (slurry procedure)/μg g^{-1}*	Certified value or value obtained by other procedure/ μg g^{-1}	LOD/ μg g^{-1}	LOQ/ μg g^{-1}	Slope ratio
IAEA V10 Hay (powdered)†	2.0	1.64 ± 0.07	1.61§	0.10	0.30	3.00
BCR CRM 281 Ryegrass‡	2.0	2.36 ± 0.15	2.38 ± 0.11§	0.14	0.32	2.6
Lettuce	2.0	2.90 ± 0.03	—	0.16	0.48	1.8
Mussel	2.0	1.26 ± 0.10	—	0.10	0.30	0.9
Sardine	2.0	0.14 ± 0.01	0.13 ± 0.02¶	0.04	0.12	1.31
Atlantic bluefin tuna	2.0	0.43 ± 0.04	0.42 ± 0.03¶	0.09	0.27	1.2
Anchovy	4.0	0.24 ± 0.01	0.23 ± 0.04¶	0.05	0.15	2.3
Atlantic pomfret	2.0	0.40 ± 0.09	—	0.09	0.27	1.5
Prawn	2.0	No hydride generation				
IAEA H9 Diet†	10.0	No hydride generation				

*, †, ‡, §, ¶ See Table 2.

inhomogeneity and settling out, shaking of the flask is recommended before each sample is removed. Analyses were performed by the standard additions method.

Results and Discussion

The results of the comparative study of vegetable and fish samples are given in Tables 2 and 3. Detection and quantification limits (LOD and LOQ, respectively) were calculated using the IUPAC method.[12] Standard additions graphs were prepared for blanks and for samples, and from these the blank to sample slope ratios were derived to compare the selectivities of the methods.

Comparison of Oxidant - Acid Media

Hydrogen peroxide - nitric acid

This medium was unsuitable for the generation of lead hydride from slurry samples because of decomposition of hydrogen peroxide by the organic matrix. Further, the low sensitivity provided by this medium made it necessary to increase the concentration of powdered sample in the slurry, with the result that it became almost impossible to determine lead because of sampling difficulties and the increased matrix effect.

Ammonium persulphate - nitric acid

This medium gave good results with vegetables for selectivity and quantification, with good agreement between the certified values and those obtained by the slurry procedure. With fish, however, except for mussel, the method lacked the necessary sensitivity and selectivity to determine lead. It was concluded that this medium yields only semi-quantitative results for the analysis of fish slurry.

Potassium dichromate - lactic acid

The results in Tables 2 and 3 show that this medium is satisfactory for the determination of lead in fish and vegetable slurries. The efficiency of lead hydride generation from fish samples with this medium was better than that with the ammonium persulphate - nitric acid medium above. This is illustrated by the slope ratio values of nearly 1 for Atlantic pomfret and Atlantic bluefin tuna with this medium, whereas with the ammonium persulphate - nitric acid medium these values were much higher, indicating an inferior ability to generate lead hydride from the two fish samples. The potassium dichromate - lactic acid medium gave lower detection limits owing to its high sensitivity and the low lead levels in the blanks. When mussel was analysed, however, this medium gave lower results than the ammonium persulphate - nitric acid medium and wet digestion procedures. This could be attributed to the inability of potassium dichromate to remove the lead completely from this sample, unlike ammonium persulphate, which is a sufficiently strong oxidant to eliminate lead totally.

Conclusions

The results reported here show that of the three oxidant media tested, potassium dichromate gives the best results for the determination of lead in slurry samples. Ammonium persulphate - nitric acid gives only semi-quantitative results with fish slurry samples. The hydrogen peroxide - nitric acid medium is inadequate for the generation of lead hydride from slurry samples.

This hydride generation atomic absorption spectrometric procedure is concluded to be a rapid and simple method for the determination of lead in a wide variety of samples. The slurry preparation requires less manipulation than mineralisation, reducing the risk of sample contamination.

The authors thank Professor Les Ebdon for his assistance, CICYT for financial support under contract number 85/0035 and the International Atomic Energy Agency for providing the samples.

References

1. Hinds, M. W., Katyal, M., and Jackson, K. W., *J. Anal. At. Spectrom.*, 1988, **3**, 83.
2. Stephen, S. C., Littlejohn, D., and Ottaway, J. M., *Analyst*, 1985, **110**, 1147.
3. Stephen, S. C., Littlejohn, D., and Ottaway, J. M., *Fresenius Z. Anal. Chem.*, 1987, **328**, 346.
4. Ebdon, L., and Lechotycki, A., *Microchem. J.*, 1986, **34**, 340.
5. Haswell, S. J., Mendham, J., Butler, M. J., and Smith, D. C., *J. Anal. At. Spectrom.*, 1988, **3**, 731.
6. Madrid, Y., Bonilla, M., and Cámara, C., *J. Anal. At. Spectrom.*, 1989, **4**, 167.
7. Bonilla, M., Rodríguez, L., and Cámara, C., *J. Anal. At. Spectrom.*, 1987, **2**, 157.
8. Hajos, A., "Complex Hydrides, Studies in Organic Chemistry 1," Elsevier, Amsterdam, 1979, p. 43.
9. Knechtel, J. R., and Fraser, J. L., *Analyst*, 1978, **103**, 104.
10. Madrid, Y., Bonilla, M., and Cámara, C., *J. Anal. At. Spectrom.*, 1988, **3**, 1097.
11. Meseguer Talavera, J., *Masters Thesis*, Universidad Complutense, Madrid, 1989.
12. Long, L. G., and Winefordner, J. D., *Anal. Chem.*, 1983, **55**, 713A.

Paper 9/03289D
Received August 2nd, 1989
Accepted November 1st, 1989

Bismuth(III) Hydride Generation, its Separation and the Determination of Bismuth(III) by Atomic Absorption Spectrometry Using Flow Injection*

Wing-Fat Chan and Ping-Kay Hon†
Department of Chemistry, The Chinese University of Hong Kong, Shatin, NT Hong Kong

A PTFE membrane backed by a stainless-steel screen was used to separate bismuth(III) hydride in a flow injection process. The atomic absorption signal gave a linear range of 0–50 p.p.b. of bismuth(III) in a sample size of 200 μl. Good precision (1.6% relative) and a low detection limit [0.17 ng of bismuth(III)] were observed. A sampling rate of up to 300 samples h^{-1} was obtained. Parameters and interfering ions which might affect the final atomic absorption signal of bismuth(III) were studied.

Keywords: *Bismuth(III) determination; atomic absorption spectrometry; hydride generation; poly(tetrafluoroethylene) separator; flow injection*

The determination of mercury by cold vapour atomic absorption spectrometry is well known for its high sensitivity and selectivity. Other metals that readily form hydrides can also be determined by a similar procedure. An additional step is required to decompose the metal hydride thermally in the absorption cell in order to realise the atomic absorption. Conventional atomic absorption spectrometry is a batch process, which limits the sampling rate. Therefore, in order to increase the sample throughput, the flow injection technique has been incorporated into the atomic absorption spectrometric method. If a U-tube type separator is used for the gas separation, a steady state should be maintained.[1–5] It has been demonstrated that some membranes are successful for the separation of organic liquids and gases from an aqueous phase.[6] In this paper a PTFE membrane with a stainless-steel screen backing has been used to separate bismuth(III) hydride from a liquid phase. Bismuth(III) was then determined by atomic absorption spectrometry using flow injection.

Experimental

Apparatus

A Perkin-Elmer Model 360 atomic absorption spectrometer was used. A quartz T-tube (17 × 0.7 cm i.d.) with a side-arm (*ca.* 6 × 0.4 cm i.d.) was used as the absorption cell. It was heated electrically to 900 °C. The light source was a Varian Techtron bismuth hollow-cathode lamp. A Cole-Parmer strip-chart recorder and a laboratory-built two-channel peristaltic pump and sample injection valve were used. Thin-walled silicone rubber tubing of 0.8 mm i.d. was used as the pumping tube. The gas - liquid separator was made from two blocks of acrylic plastic. One plastic block, with a groove of 1.0 × 3 × 50 mm, was used for the liquid sample. The other block, with a groove of 3 × 3 × 50 mm was used for the carrier gas. The membrane was PTFE tape, 0.075 mm thick and 12 mm wide. A stainless-steel screen, 200 mesh, 10 × 60 mm, was used for the backing. Adhesive tape was used to fix the edges of the screen to the plastic block. The PTFE membrane was then placed on the top of the screen. The plastic blocks were held together with rubber bands. Fig. 1 is a schematic diagram of the flow injection system. The gas - liquid separator assembly is shown in Fig. 2.

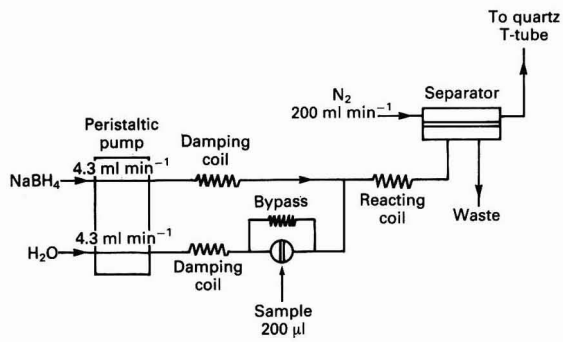

Fig. 1. Schematic diagram of the flow injection system

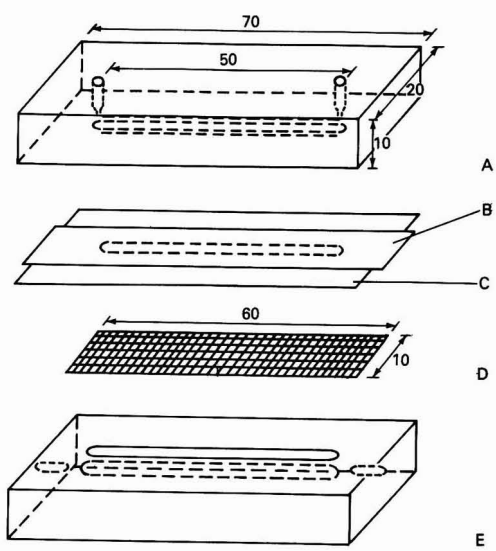

Fig. 2. Schematic diagram of the gas - liquid separator assembly. A and E, Plastic blocks; B, PTFE tape; C, adhesive tape; and D, stainless-steel screen. All dimensions are in mm

* Presented at SAC 89, the 8th SAC International Conference on Analytical Chemistry, Cambridge, UK, 30 July–5 August, 1989.
† To whom correspondence should be addressed.

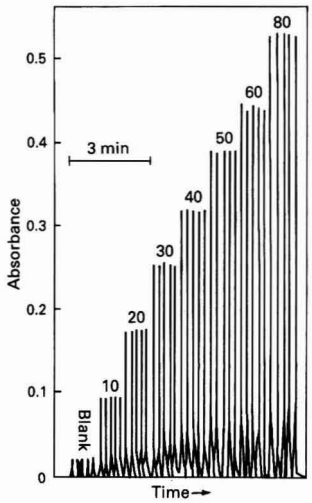

Fig. 3. Typical results for the determination of bismuth(III). The values above the peaks are the amounts of bismuth(III) in p.p.b.

Reagents

All reagents were of analytical-reagent grade. A stock solution of 1000 p.p.m. of bismuth(III) was prepared by dissolving 1.000 g of bismuth metal in the minimum volume of 1 + 1 nitric acid and diluting to 1 l with 2% nitric acid. Standard solutions of 10, 20, 30, 40 and 50 p.p.b. of bismuth(III) were prepared from the stock solution. An appropriate amount of hydrochloric acid was added to give a final acid content of 0.40 M. Sodium tetrahydroborate ($NaBH_4$) solution was prepared fresh by dissolving 2.5 g of $NaBH_4$ (powder, Sigma) in 25 ml of 1 M sodium hydroxide and then diluting to 500 ml with distilled water.

Procedure

The absorption wavelength was set at 233.1 nm. The lamp current was 10 mA, the slit width was 0.7 nm (band pass) and the energy gain was set at 50. The absorption T-tube was heated to 900 °C. The nitrogen carrier gas flow-rate was 280 ml min^{-1}. Distilled water and $NaBH_4$ solution were pumped at the same flow-rate of 4.3 ml min^{-1}. The sample loop, with a volume of 200 µl, was first filled and then the valve was rotated to allow the sample to be carried by the water stream to the reacting coil where it was mixed with the $NaBH_4$ solution. On entering the gas - liquid separator, the bismuth(III) hydride gas diffused through the membrane and was carried by the nitrogen into the absorption cell. Five injections were run for each sample.

Results and Discussion

Linearity, Precision, Accuracy and Detection Limit

Fig. 3 shows a typical series of results. Good linearity was observed in the range 0–50 p.p.b. of bismuth(III), with a correlation coefficient of 0.9994. The sensitivity, determined from the slope in the linear region for 1% absorption, was 0.12 ng of bismuth(III). The precision from 15 × 30 p.p.b. replicate injections was found to be 0.5 p.p.b. (or 1.6% relative). The detection limit, defined as $2\sigma/m$ where m is the slope of the linear portion of the calibration graph and σ is the standard deviation of replicate measurements near the blank level, was found to be 0.85 p.p.b. of bismuth(III) (or 0.17 ng). The accuracy was checked by determining bismuth(III) in a National Institute of Standards and Technology Standard Reference Material, NIST SRM 361 Special Low Alloy Steel AISI 4340 and two real samples, a leaded gun metal and a British Chemical Standard Certified Reference Material, BCS-CRM 347 Electronic Flowsolder. The results were in good agreement with the certified or listed values, Table 1. A sampling rate of up to 300 samples h^{-1} could be obtained.

Table 1. Determination of bismuth(III) in real samples

Sample	Bismuth(III) content, % Certified or listed	Found
NIST SRM 361 AISI 4340 ..	4×10^{-4}	4.1×10^{-4}
Leaded gun metal*	5×10^{-3}	4.9×10^{-3}
BCS-CRM 347	8×10^{-2}	8.4×10^{-2}

* The leaded gun metal has a high copper content, 84.08%; other metals present: Sn, 7.3; Sb, 0.22; and As, 0.14%.

Table 2. Effect of foreign ions on the absorption signal of bismuth(III). Amount of bismuth(III), 30 p.p.b.

Ion	Amount, p.p.m.	Error, %	Ion	Amount, p.p.m.	Error, %
Cu^{II} ..	0.10	−5.6	Sb^{III} ..	12	−4.2
Ni^{II} ..	0.25	−4.6	Sn^{II} ..	100	−5.0
Fe^{III} ..	130	−5.0	Ca^{II} ..	3000	+1.0
Co^{II} ..	3.5	−5.6	Mg^{II} ..	1200	−4.9
Cr^{III} ..	2000	−1.3			
Se^{II} ..	0.6	−4.5			
Te^{II} ..	0.4	−5.0	CrO_4^{2-} ..	2000	−4.1
As^{III} ..	12	−4.3	SO_4^{2-} ..	5000	−1.4
Ge^{IV} ..	95	+6.7	$C_2O_4^{2-}$ ..	200	+6.2

Experimental Conditions

The following parameters were investigated and optimised.

Groove dimensions

For the liquid side of the separator a gradual increase in signal for a groove width from 2 to 4 mm was observed, then the signal decreased for a groove width of 5 mm. A groove width of 3 mm was therefore chosen in order to minimise the possibility of distortion of the membrane at a high solution flow-rate. The highest signal was observed for a groove length of 50 mm. For a groove length greater than 50 mm the signal was reduced significantly. The depth of the groove, from 0.5 to 1.0 mm, had no effect on the signal. The groove dimensions for the gas stream were not critical.

Membrane backing material

Filter-paper was tested as the backing material. It lasted for several runs. Both a stainless-steel screen and nylon cloth were satisfactory supporting materials; however, the former was much more rigid. Nylon mesh as a membrane backing material has been described by Pacey *et al.*[7]

Sample volume

The signal reached a maximum and levelled off at a sample volume of 300 µl. A sample volume of 200 µl was chosen because a higher sampling rate would be obtained.

Nitrogen flow-rate

High nitrogen flow-rates decreased the signal as the bismuth(III) hydride was diluted and the residence time in the absorption cell also decreased. The optimum nitrogen flow-rate was 280 ml min^{-1}.

Solution flow-rate

The signal increased steadily for flow-rates in the range 1–5 ml min^{-1}. At low flow-rates, sample diffusion was significant

and peak broadening resulted. At high flow-rates, the pressure increased significantly and caused leakage. The optimum value was therefore 4.30 ml min^{-1}.

Acid concentration

Thompson and Thomerson[8] reported that by using $NaBH_4$ as the reductant, the signal was independent of the hydrochloric acid concentration in the range 1–4 M. Åstrom[1] and Yamamoto *et al.*[4] reported that the signal reached a maximum at an acid concentration of *ca.* 0.5 M. A further increase in acid concentration had no effect on the signal. In this work the signal levelled off at a hydrochloric acid concentration in the sample of 0.2 M.

Sodium tetrahydroborate concentration

The signal increased sharply for concentrations of $NaBH_4$ in the range 0.1–0.5%. A further increase in concentration gave only a slight increase in the signal. This result was consistent with the observations made by Åstrom[1] and Yamamoto *et al.*[4]

Length of reaction coil

The length of the reaction coil had no significant effect on the signal. This is because the reduction of a metal ion by $NaBH_4$ to form a metal hydride is a fast process.

Interference Studies

Åstrom[1] reported that a number of elements: Ni, Cu, Co, As, Sb and Sn at 100 p.p.m. each interfered in the determination of bismuth(III) by generating its hydride. The most serious interfering elements were Ni and Cu, suppressing the signal by 100%, Co with 80% suppression and As with 30% suppression. Our results confirmed the findings of Åstrom.[1] The effect of other ions is shown in Table 2. As copper has a large effect on the signal, then for the analysis of a real sample known to contain a high percentage of copper, the signal would be reduced significantly and the standard additions technique should be used. This was the case in the analysis of the leaded gun metal.

Conclusion

By using the readily available PTFE tape and stainless-steel screen (both were obtained in a local hardware store), a gas - liquid separator can easily be constructed. The separator has a high efficiency and a long lifetime. With a small sample volume (200 μl) a high sampling rate of 300 samples h^{-1} can be achieved, compared with 700 μl and 180 samples h^{-1} in the work of Åstrom.[1] Under the optimum experimental conditions, good precision (1.6%) and accuracy have been shown for the analysis of real samples. The detection limit, 0.17 ng, is about four times better than that reported by Åstrom,[1] 0.7 ng. Interferences are seldom encountered. If the samples are known to contain large amounts of interfering elements, good accuracy can still be achieved using the standard additions method. The separator not only works for metal hydrides, it also separates other gases efficiently, *e.g.*, NH_3, SO_2, H_2S, CO_2, etc., generated from aqueous solutions. They can then be detected and determined by other specific and sensitive methods.

The authors thank Mr. S. F. Luk for his work on some of the interference studies and Dr. O. W. Lau for her encouragement on the preparation of the manuscript.

References

1. Åstrom, O., *Anal. Chem.*, 1982, **54**, 190.
2. Sturman, B. T., *Appl. Spectrosc.*, 1985, **39**, 48.
3. Ikeda, M., *Anal. Chim. Acta*, 1985, **167**, 289.
4. Yamamoto, M., Yasuda, M., and Yamamoto, Y., *Anal. Chem.*, 1985, **57**, 1382.
5. Crock, J. G., *Anal. Lett.*, 1986, **19**, 1367.
6. Nord, L., and Karlberg, B., *Anal. Chim. Acta*, 1980, **118**, 285.
7. Pacey, G. E., Straka, M. R., and Gord, J. R., *Anal. Chem.*, 1986, **58**, 502.
8. Thompson, K. C., and Thomerson, D. R., *Analyst*, 1974, **99**, 595.

Paper 9/03273H
Received August 2nd, 1989
Accepted October 10th, 1989

Use of Masking Agents in the Determination of Lead in Tap Water by Flame Atomic Absorption Spectrometry With Flow Injection Pre-concentration*

Stephen R. Bysouth† and Julian F. Tyson†
Department of Chemistry, University of Technology, Loughborough, Leicestershire LE11 3TU, UK
Peter B. Stockwell
PS Analytical Ltd., Unit B4, Chaucer Business Park, Watery Lane, Kemsing, Sevenoaks, Kent TN15 6QY, UK

The selectivity of immobilised 8-hydroxyquinoline for lead is shown to be improved by the use of masking agents during pre-concentration, prior to determination by flame atomic absorption spectrometry. Interference by iron, copper, aluminium and zinc is suppressed by including triethanolamine, thiourea, fluoride, acetylacetone or cyanide in the buffer as masking agents. Species such as iron or copper can completely prevent the pre-concentration of lead. This is shown to be overcome by using a buffer consisting of 0.2 M boric acid, 2% triethanolamine, 2% thiourea and 2% acetylacetone, even when the interfering species is in a 200-fold excess over lead. Recoveries from tap water samples, to which various amounts of lead had been added, ranged from 94 to 108%. Results of analyses of tap water samples using this method were in good agreement with those obtained by electrothermal atomic absorption spectrometry.

Keywords: *Lead pre-concentration; flow injection; interference masking; flame atomic absorption spectrometry; tap water analysis*

The determination of lead in drinking water is becoming increasingly important. The current maximum permissible level in drinking water before entering the distribution network is 50 p.p.b.[1] Normal flame atomic absorption spectrometry (FAAS), with detection limits greater than 10 p.p.b., does not provide sufficient sensitivity for the determination of lead at this level. Currently electrothermal atomic absorption spectrometry (ETAAS) is the preferred method of analysis[2] but it is not simple to use. The interfacing of flow injection manifolds to FAAS instruments is convenient and simple,[3] and enhances the capability of the flame technique. Numerous examples of flow injection pre-concentration techniques have been described,[4–8] some of which have detection limits equal to those obtained by ETAAS. Although these methods enable very low levels of determinand to be measured, very little work has been undertaken on the effects of possible interferents. In a previous paper[9] it was shown that the pre-concentration of lead from dilute solutions, using a simple manifold incorporating a small column of immobilised chelating agent, was possible and a detection limit of 1.3 p.p.b. was achieved. The procedure was shown to suffer from interference from other transition metal ions such as iron(III) and copper(II) which can be adsorbed on the column. Other potential interferents, such as calcium, were found not to have a large effect at moderate concentrations. If these pre-concentration methods are to be reliable in the presence of trace amounts of interferents, or capable of being used in the presence of larger amounts of interferents, methods for overcoming the effects of species that compete for the active sites on the stationary phase must be studied. Masking of interferent species in solution has been used extensively for many chemical reactions, especially in complexometric titrations.[10]

In this paper, the effects of interferent species are demonstrated. The development and use of a buffer solution, containing suitable masking agents for the suppression of some interferences, and its use in determining lead in tap water, as a model system, are described.

Experimental

Apparatus

A manifold (Fig. 1) containing Tefzel tubing (Omnifit, Cambridge, UK) with an i.d. of 0.5 mm based on a prototype pre-concentration unit (PS Analytical, Sevenoaks, Kent, UK), which consisted of a double injection valve and three pumps with associated timing circuitry, was constructed. This device allowed pre-concentration for a variable time followed by washing for a variable time before simultaneous injection of acid eluent and column contents. The manifold was connected to a flame atomic absorption spectrometer (Philips, Model SP9, Philips Analytical, Cambridge, UK) optimised for the determination of lead at 283.3 nm in an air - acetylene flame. Peaks were recorded using a PM 8251 chart recorder (Philips). A pre-concentration time of 134 s and a wash time of 32 s were used for all analyses. The column consisted of a

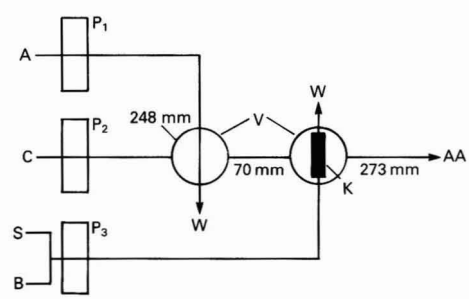

Fig. 1. Pre-concentration manifold. P_1, P_2 and P_3, Peristaltic pumps; V, double injection valve; W and AA, connections to the waste and spectrometer, respectively; and K, column connected to the valve by two 50 mm lengths of tubing. A, acid eluent (pumped at 3 ml min^{-1}); C, water carrier (pumped at 5.5 ml min^{-1}); B, buffer (pumped at 0.8 ml min^{-1}); and S, sample (pumped at 5.5 ml min^{-1})

* Presented at SAC 89, the 8th SAC International Conference on Analytical Chemistry, Cambridge, UK, 30 July–5 August, 1989.

† Present address: Department of Chemistry, Lederle Graduate Research Tower A, University of Massachusetts, Amherst, MA 01003, USA.

microbore glass column 50 × 3 mm i.d. (Omnifit) fitted with porous poly(vinyl chloride) frits and packed with 8-hydroxyquinoline immobilised on 35–70 mesh silica gel as described previously.[9] A pH meter (Philips PW 9420) fitted with a glass electrode (Philips Type CE1) was used for pH determination.

Reagents

All standards and acids were of SpectrosoL grade (BDH, Poole, Dorset, UK) or AAS grade (Fisons, Loughborough, Leicestershire, UK) and other reagents were either AnalaR (BDH) or AR (Fisons) grade. Water used for dilution was obtained from an RG reverse osmosis - de-ionisation unit (LiquiPure).

Procedures

Four solutions each containing 50 p.p.b. of lead were prepared. To three of them were added 10 p.p.m. of either copper, iron or aluminium. Nitric acid was added to give a final concentration of 0.01 M and a solution of 0.01 M nitric acid was used as the blank. Each of these solutions was pre-concentrated three times. Six buffers, which consisted of 0.05 M borax and 0.05 M borax plus one of the following masking agents (1% m/v): sodium fluoride, sodium cyanide, triethanolamine, acetylacetone and thiourea, were investigated. Each buffer was adjusted to pH 8 by the addition of boric acid slurry. Elution was effected with 1.0 M hydrochloric acid.

After the suitability of each masking agent had been investigated, a buffer consisting of 0.2 M boric acid, 2% triethanolamine, 2% thiourea and 2% acetylacetone was used for the pre-concentration of samples containing 50 p.p.b. of lead and various concentrations of interferent ions, and in the determination of lead in four spiked tap water samples with calibration against acidified lead standards.

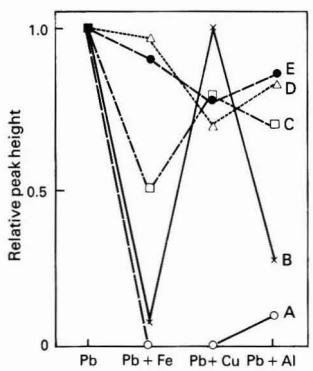

Fig. 2. Relative peak heights compared with a 50 p.p.b. lead standard. Pre-concentration with: A, borax - boric acid buffer; B, borax - boric acid buffer with added cyanide; C, borax - boric acid buffer with added thiourea; D, borax - boric acid buffer with added triethanolamine; and E, borax - boric acid buffer with added fluoride

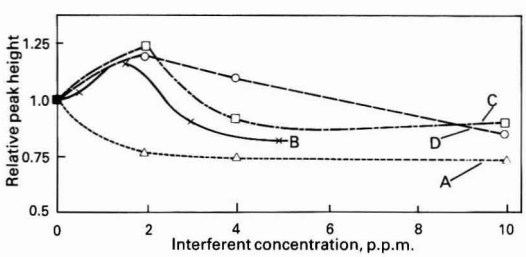

Fig. 3. Effect of increasing interferent concentration on the relative peak heights for pre-concentration of a 50 p.p.b. lead solution using the buffer with masking agents. Added interferents: A, zinc; B, copper; C, aluminium; and D, iron

Six tap water samples and four aqueous standards were obtained from the National Rivers Authority Environmental Laboratory (NRAL), Nottingham, UK, in which the lead content had been determined by ETAAS. These samples had been preserved by inclusion of 0.1 M nitric acid. Six standards including a blank, preserved using 0.1 M nitric acid, were also supplied to the NRAL by us, and analysed by ETAAS. In order to perform pre-concentration, the molarity of the acid in these samples and standards was reduced from 0.1 to 0.01 M by the addition of 5 ml of 0.8 M sodium hydroxide solution to 45 ml of sample. All solutions supplied by the NRAL were then analysed using the six standards and an additional standard of 100 p.p.b. treated in the same way. Each pre-concentration was performed in triplicate, whereas four determinations over two batches were performed for each sample analysed by ETAAS. The pH of each solution was measured before and after addition of sodium hydroxide.

All the solutions analysed, including the blanks, were pre-concentrated in a random order and no carry-over was observed.

Results and Discussion

The pre-concentration and wash times of 134 and 32 s, respectively, were chosen because these times gave suitable detection limits and were as close as could be achieved to those used previously.[9] It is recognised that the choice of pre-concentration time is an important parameter in the optimisation of a procedure for dealing with unknown samples. An algorithm for this choice is currently under development[11] and is based on the concept of extending the conventional calibration range rather than producing a set of discontinuous calibration functions. In order to achieve a calibration the pre-concentration time is chosen such that the upper limit of quantification of the new concentration range corresponds to the lower limit of quantification of the initial range. In turn, this means that the time selected produces a pre-concentration factor equal to the ratio of the upper to lower limits of quantification.

The effect of adding masking agents to the buffer on the interference of different interferent ions is shown in Fig. 2. Clearly, triethanolamine, fluoride and thiourea reduce the interference of all the species investigated, but cyanide is more specific, only having a significant effect on interference by copper ion. Sodium fluoride caused a white precipitate to form in the reagent, sodium cyanide was considered undesirable because of its toxicity and borax ($Na_2B_4.10H_2O$) was found to be unnecessary for adjusting the pH to 8. These three compounds were not included in the mixed reagent.

The effect of increasing interferent ion concentration is shown in Fig. 3. There is an apparent increase in the signals when the concentration of each interferent ion is 2 p.p.m. This may be caused by imperfect matching of the acidity of the

Table 1. Recoveries for spiked tap water determined using five lead standards to give a 17 point linear calibration graph, correlation coefficient 0.9992. Each sample was analysed by pre-concentration FAAS three times

Nominal concentration, p.p.b.	Mean concentration found, p.p.b.	Confidence interval (95%)	Recovery, %
26.0	28.0	0	107.7
42.0	40.4	5.7	96.2
89.0	84.5	6.2	94.9
65.0	64.2	3.0	98.8

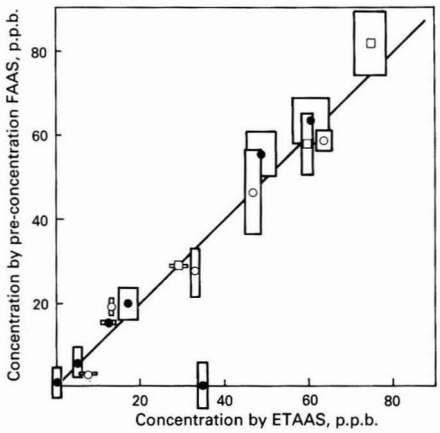

Fig. 4. Regression line of the results of ETAAS and pre-concentration FAAS of tap water samples and aqueous standards. ○, Solutions used as standards for pre-concentration and analysed by ETAAS and pre-concentration FAAS; □, solutions used as standards for ETAAS and analysed by ETAAS and pre-concentration FAAS; and ●, tap water samples. Rectangles about the points represent 95% confidence intervals for each method

samples. In all instances, the extent of the interference is less than that obtained when using a buffer without masking agents (Fig. 2).

The recoveries for the spiked tap water samples are given in Table 1. Even when non-matrix matched standards were used only one result showed bias at the 95% confidence level.

The 100 p.p.b. standard gave a peak absorbance of 0.351, indicating that there is some scope for increasing the pre-concentration time. The results for the analysis of tap water samples by pre-concentration FAAS and by ETAAS are presented as a regression line, Fig. 4. Clearly one sample has not been pre-concentrated and it was found that even after addition of sodium hydroxide, the pH was 1.45. The pH of all the other solutions after addition of sodium hydroxide was approximately 2.0. Apparently, if the pH is 1.45 there is insufficient buffer capacity in the reagent - sample mixture entering the column to bring the pH to the desired level. The imprecision of the results obtained by pre-concentration FAAS is reflected in the calibration obtained with a detection limit of 6.8 p.p.b. This imprecision is due to the type of pump used for pumping the reagent - buffer mixture. Previously,[9] a detection limit of 1.3 p.p.b. was obtained by using a micro-processor controlled, stepper-motor driven pump. The type of pumps used in the prototype device possess considerable momentum during pumping and consistent roller pressure is difficult to maintain, causing imprecision in timing and flow-rate, respectively. However, the precision for three results is better than that obtained for ETAAS. Concentration values of 0.025 p.p.b. for the blank generated by our laboratory, with a 95% confidence interval of 0%, and −0.052 p.p.b. for the blank generated by the NRAL, with a 95% confidence interval of 0.894%, were obtained. When the regression line was calculated by least squares, and excluding the outlier in order that ETAAS and pre-concentration FAAS can be compared, a slope of 1.02, an intercept of −0.20 and a correlation coefficient of 0.9902 were obtained, with 95% confidence intervals of 0.10 and 5.72 for slope and intercept, respectively; the slope is not significantly different from 1.0 and the intercept is not significantly different from 0.

Conclusion

An increase in selectivity of immobilised 8-hydroxyquinoline, for the pre-concentration of lead, by the addition of masking agents to the buffer has been demonstrated. With this system interferent ions with concentrations up to 200-fold in excess of that of lead could be tolerated but the resulting signals were reduced by 25% compared with those obtained in the absence of interferent species. Sample throughput is not high, but all sample pre-treatment can be carried out on-line if the samples are at the correct pH. Adjustment of pH can also be incorporated into the system.

The analysis of tap water samples by pre-concentration FAAS was accurate but the precision was not as good as that obtained for ETAAS. The precision and sensitivity can be improved by careful control of sample flow-rate using pumps with precise pumping characteristics and by increasing the sampling time.

It has been shown that column techniques of pre-concentration can suffer from interference by competing species, and that this can be reduced using appropriate masking agents. Although a flame spectrometer was used for detection in this instance, use of the correct interface can allow the application of flow injection techniques to other detectors such as electrothermal spectrometers themselves. This gives rise to the possibility of determining lead at the parts per trillion level.

The authors thank the SERC for financial support for S.R.B., and P. B. Smith of the National Rivers Authority Environmental Laboratory, Nottingham, for provision of samples and analyses by ETAAS.

References

1. "EC Directive Relating to the Quality of Water Intended for Human Consumption," 80/778/EEC, *Off. J. Eur. Commun.*, July 1980; OJL 229, 30th August, 1980.
2. Smith, P. B., personal communication.
3. Tyson, J. F., Adeeyinwo, C. E., Appleton, J. M. H., Bysouth, S. R., Idris, A. B., and Sarkissian, L. L., *Analyst*, 1985, **110**, 487.
4. Malamas, F., Bengtsson, M., and Johansson, G., *Anal. Chim. Acta*, 1984, **160**, 1.
5. Marshall, M. A., and Mottola, H. A., *Anal. Chem.*, 1985, **57**, 729.
6. Risinger, L., *Anal. Chim. Acta*, 1986, **179**, 509.
7. Olsen, S., *Dan. Kemi.*, 1983, **3**, 68.
8. Olsen, S., Pessenda, L. C. R., Růžička, J., and Hansen, E. H., *Analyst*, 1983, **108**, 905.
9. Bysouth, S. R., Tyson, J. F., and Stockwell, P. B., *Anal. Chim. Acta*, 1988, **214**, 329.
10. Perrin, D. D., "Masking and Demasking of Chemical Reactions," Wiley-Interscience, London, 1970.
11. Bysouth, S. R., and Tyson, J. F., unpublished work.

Paper 9/03928G
Received September 14th, 1989
Accepted January 2nd, 1990

Spectrofluorimetric Optosensing of Aluminium in a Flow Injection System: Determination of Aluminium in Dialysis Fluids and Concentrates*

Maria Rosario Pereiro García, Marta Elena Díaz García and Alfredo Sanz-Medel†
Department of Physical and Analytical Chemistry, Faculty of Chemistry, University of Oviedo, 33006 Oviedo, Spain

An on-line pre-concentration - optical fibre spectrofluorimetric detection procedure is described for the determination of trace amounts of Al in the μg l^{-1} range. The active solid phase for Al, packed into the flow cell, was the 8-hydroxyquinoline derivative Kelex 100 immobilised on Amberlite XAD-7. Different parameters were investigated with the aim of selecting the reagent solid phase, and several flow cell designs were studied. Optimisation of the operating conditions and figures of merit of the analytical system are given. The method was applied successfully to the determination of Al in dialysis fluids and concentrates.

Keywords: *Aluminium determination; optical sensor; flow injection; spectrofluorimetric optosensing; dialysis fluid and concentrate*

Optosensing at active surfaces[1] represents a novel approach to the detection of chemical and biological species based on the interaction of radiation with the surface of a solid phase able to react selectively with the analyte. On-line monitoring and *in situ* continuous measurements of the analyte, flowing in a stream, can be achieved by careful selection of the active solid phase. This active phase usually consists of a suitable reagent of the analyte immobilised on an appropriate solid support (*e.g.*, silica gel or ion exchanger). The changes in the optical properties of this active surface, due to the selective reaction, provide the basis for the monitoring of the analyte concentration in the flowing stream. The flow-through cell where the analyte retention/reaction takes place can be simply a modified sample cell in a classical spectrophotometer.[2,3] However, the use of non-transmitting solid supports makes the measurement of transmitted light (absorbance) difficult; hence, in order to measure the intensity of reflected light (reflectance) it is preferable to monitor the change in colour occurring at the immobilised reagent solid phase.[4] Bearing this in mind, fluorescence measurements should be particularly appropriate for monitoring at active surfaces because emission of light is measured and, moreover, the intrinsic sensitivity of luminescence (fluorescence, phosphorescence or chemiluminescence) is far superior to that attainable by absorbance or reflectance measurements.

In any event, the advantages offered by such chemical transducers based on active solid phases are realised better with the aid of optical fibres. Chemical transduction with optical fibres has attracted considerable interest during the last few years because, among other favourable properties, optical fibres allow miniaturisation of the sensing device (*e.g.*, for *in vivo* applications) and remote sensing as is the case in the most popular fibre optic sensors, the probe-type sensors or "optrodes."[5–7] As in the flow-through cells referred to above, the response of an optrode is also based on optosensing at an active surface (the microzone where the reaction selective to the desired analyte takes place). The use of flow-through cells, however, offers some important possibilities: the numerous flow injection (FI) techniques now available can be employed and it is easy to renew the reagents which should not be, or intentionally are not, immobilised on the active surface. As a result, irreversible chemistry can be applied to these devices for on-line chemical transduction (without resorting to "disposable" probes). Moreover, rather than a continuous signal, there is a base line (hence problems resulting from base-line drift can be avoided) and this allows for easy calibration. Finally, sample pre-treatment can be integrated into the system.[8–12]

Our recent research has included the development of new methodologies to determine low levels of Al in samples of clinical interest: a variety of deleterious physiological effects have been observed related to the presence of Al in patients with chronic renal failure.[13] Encephalopathy, anaemia, osteomalacic osteodistrophy and cardiotoxicity are disorders related to Al intoxication. The necessity for Al control in dialysis patients and research into Al toxicity explain the current demand for analytical techniques to monitor this metal at trace and ultratrace levels in blood serum and in potential sources for the patient (*e.g.*, dialysis concentrates and water).

Most determinations of Al in dialysis concentrates have been carried out on diluted dialysis fluids which are prepared before use from the concentrates (a *ca.* 35-fold dilution with water) usually by graphite furnace atomic absorption spectrometry (GFAAS). The extremely high salt content of these solutions appears to be responsible for the unreliable results obtained to date.[14]

8-Hydroxyquinoline-5-sulphonic acid has been immobilised previously on an anion-exchange resin and used as a fluorescent sensor of several ions including Al.[15] Reversibility data and analytical applications were not described, however.

Isshiki *et al.*[16] studied the interactions between 12 metals and Kelex 100 (an 8-hydroxyquinoline derivative) immobilised on solid supports. In the present paper a spectrofluorimetric optosensor for Al^{III}, based on an active surface of Kelex 100 adsorbed on Amberlite XAD-7, for the on-line monitoring of Al in dialysis fluids and concentrates is described.

Experimental

Reagents

Analytical reagent-grade chemicals were employed for the preparation of all the solutions. Freshly prepared ultrapure water (Milli-Q 3RO/Milli-Q2 system, Millipore) was used in all experiments. The preparation and handling of solutions and containers, to minimise any possible risk of Al contamination, was carried out as described elsewhere.[17]

A 1000 μg ml^{-1} Al stock solution was prepared by dissolution of the pure metal in hydrochloric acid (1 + 1).

* Presented at SAC 89, the 8th SAC International Conference on Analytical Chemistry, Cambridge, UK, 30 July–5 August, 1989.

† To whom correspondence should be addressed.

Two types of resin were used: the cross-linked polymer of methyl methacrylate, Amberlite XAD-7 (20–50 mesh), from Sigma, and the cross-linked copolymer of styrene and divinylbenzene, Amberlite XAD-4, from BDH. For comparative purposes both resins were ground to 50–100 mesh. The Amberlite impurities were removed by washing with ethanol in order to displace air from the pores of the resin and to remove residual monomers and solvents, and with water.

The selected reagent, Kelex 100, the main component of which is 7-(4-ethyl-1-methyloctyl)-8-hydroxyquinoline, was provided by Schering (Industrial Chemicals). This spectrofluorimetric reagent was purified by vacuum distillation as described previously (p <0.5 mmHg, T = 160 °C).[18]

Impregnated resins (active phases) were prepared by placing 1 g of each dry support in a 250-ml round-bottomed flask and adding 300, 215 and 100 mg, respectively, of Kelex 100 diluted in each instance with 35 ml of heptane. The heptane was removed at room temperature on a rotary evaporator and the temperature was then raised to 100 °C. Fresh heptane (10 ml) was added and the evaporation was repeated.[19] The loaded resins were then washed with 2 M HCl until no absorbance at 360 nm (due to free reagent) was detected in the wastes. In order to evaluate the exact amount of reagent adsorbed per gram of each support, each waste was diluted to 500 ml with 2 M HCl and the absorbance at 360 nm was measured. The amounts of Kelex 100 adsorbed (calculated from the difference between Kelex 100 added and reagent found in the wastes) were: 291, 210 and 97 mg per gram of Amberlite XAD-7, and 212 mg per gram of Amberlite XAD-4.

It is worth mentioning that, in spite of the fact that the reagent mechanism is a simple adsorption process, no washing out was observed when the active phase was treated repeatedly with acid (*e.g.*, 2 M HCl) or base (2 M NaOH) (bending of the long hydrophobic tail of the reagent and hydrophobic forces thus developed with the non-ionic resin beads may be responsible for the strong adsorption observed).

Instrumentation

A Shimadzu Model RF-5000 spectrofluorimeter coupled to a data station (Shimadzu, Model DR-15) was employed for fluorescence measurements.

The flow cell was fabricated from a Perspex block (see Fig. 1): to introduce the optical fibre a 2.2 mm i.d. bore was situated perpendicular to the axis of a cylindrical compartment (6 × 1 mm i.d.) as shown in Fig. 1. The active phase was loaded as a suspension into the flow cell with the aid of a peristaltic pump. Small pieces of nylon netting were placed at the ends of the compartment to prevent movement of the resin particles by the carrier stream.

Optical communication between the spectrofluorimeter and the flow cell was achieved with a laboratory-built 30 cm long silico - silicone fibre bundle (from Quartz & Silice), consisting of 22 individual strands (PCS 200, core diameter of each strand, 0.2 mm) randomly bifurcated at the remote end. One of the two arms was focused to the xenon arc lamp and the other to the detector within the sample compartment. The common end was coupled, with the aid of an appropriate connector, to one end of the optical fibre (PCS 1000, Quartz & Silice, core diameter 1 mm) which, finally, was introduced into the flow cell (as shown in Fig. 1).

This type of connection between the common end of the bundle and the 1 mm core diameter optical fibre offers two advantages: firstly, it allows both arms of the bifurcated fibre to be focused correctly and fixed in the sample compartment of the spectrofluorimeter; hence, the changing of flow cells, or probes, is very easily carried out (simply by moving the PCS 1000 optical fibre). Secondly, with this design, the fluorescence sensitivity is improved because the whole surface under the optical fibre is illuminated and, at the same time, all the fluorescence gathered.

The FI set-up consisted of a peristaltic pump with four channels (Gilson Miniplus 2), two rotating valves (Omnifit), connecting tubing made of PTFE, connections (all made from low-pressure tubing 0.8 mm i.d.) and fittings. The dimensions of the column used to eliminate interferences were 250 × 3 mm i.d. Details of its construction have been given elsewhere.[20] The manifold for the elimination of interferences is shown in Fig. 2.

The procedure was as follows: the sample, usually 1 ml, is injected through the valve A into a channel of 0.1 M ammonium acetate buffer (pH = 2.5) and then mixes in a T-piece with the same carrier to achieve the appropriate pH for retaining interferences from Fe^{III}, Cu^{II} and Cr^{III} in column B (see Fig. 2) packed with Kelex 100 adsorbed on Amberlite XAD-7 (20–50 mesh). Under such conditions Al^{III} is not retained but is propelled forward until it reaches a second T-piece where the sample pH is raised to 5. In this medium, Al^{III} at a total flow-rate of 0.75 ml min^{-1} (0.25 ml min^{-1} in each channel) will be retained in the flow cell D yielding a highly fluorescent complex ($\lambda_{ex.}$ = 420 nm and $\lambda_{em.}$ = 512 nm), which is monitored via the optical fibre. After the Al fluorescence measurement has been taken, 2 ml of 2 M HCl are injected through the valve C (to strip the Al retained on the solid phase, before proceeding with the next sample injection).

Iron(III), copper(II) and chromium(III) are impurities present in the samples only at very low levels. Therefore, the cleaning of column B (by injecting 2 ml of 2 M HCl through the valve A) was carried out after every 6–8 sample injections.

The pH measurements were made with a WTW pH meter and a Radiometer GK-2401-C combination glass - saturated calomel electrode.

Results and Discussion

Selection of Reagent Phase

The choice of the solid support was the first parameter evaluated (Table 1). Amberlite XAD-4 and XAD-7 (both

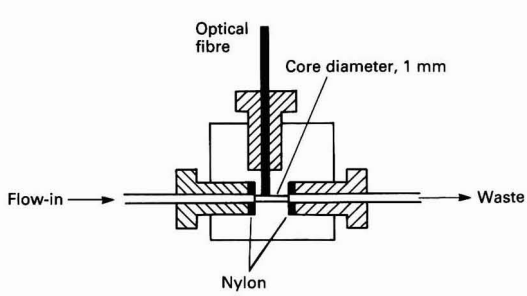

Fig. 1. Schematic diagram of the flow cell employed

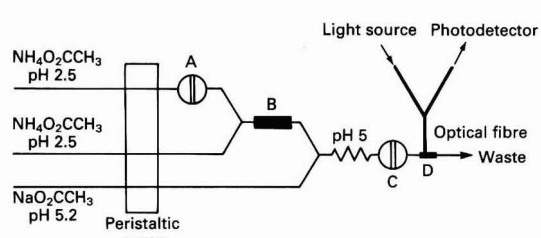

Fig. 2. Schematic flow diagram of the system employed. A, sample valve; B, mini-column used to eliminate interferences; C, elution valve; and D, flow cell

Table 1. Selection of reagent phase (1 μg of Al was injected in all instances)

		Fluorescence intensity, arbitrary units
Support	Amberlite XAD-7	11.5
	Amberlite XAD-4	3.1
Grain size (mesh)	20–50	11.5
	50–100	22.0
Reagent concentration (mg of reagent per gram of support)	291	21.0
	210	22.0
	97	11.4

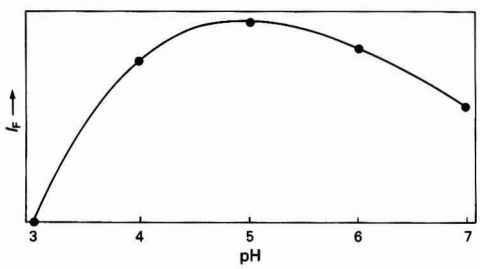

Fig. 3. Effect of pH on the spectrofluorimetric signal of Al

Table 2. Choice of Al leaching agent (1 μg of Al was injected in all instances). Leaching time, 3 min

	Assayed releasing solution					
	HCl		NaOH		KF	
	1 M	2 M	1 M	2 M	1 M	2 M
Al eluted,%	66	100	100	100	31	46

20–50 mesh and with 0.210 g of reagent per gram of solid support) were examined; the better fluorescence signals for Al (1 μg) were obtained with Amberlite XAD-7. Hence, using Amberlite XAD-7, different grain sizes were tested and improvements in the analytical signal were observed with 50–100 mesh resin. Unfortunately, 100–200 mesh cannot be used owing to the high pressure developed along the flow system. Finally, using the selected support, studies of optimum reagent concentration (291, 210 and 97 mg of reagent per gram of solid support) were carried out and the optimum results (1 μg of Al injected) were obtained with 0.210 g of reagent per gram of solid support.

Flow Cell Studies and Flow-rate Optimisation

The dimensions and geometrical position of the optical fibre in the flow cell were studied.

Different flow cells were explored (all were fabricated from Perspex blocks and had a 2.2 mm i.d. bore) for introducing the optical fibre perpendicular to the axis of a cylindrical compartment (6 mm long with an i.d. of 3, 2 and 1 mm, respectively). For comparative purposes, in some flow cells, the bore for the optical fibre was located in the middle of the reagent compartment, in others the bore was at the near side of the upper stream.

Results demonstrated that the flow cell with a 1 mm i.d. and with the bore for the optical fibre situated at the side of the upper stream offers the best fluorescence signals (1 μg of Al injected) and the shortest time for regenerating the solid phase.

Table 3. Effect of foreign cations on the recovery of 1.0 μg of Al using a simple system (single-channel configuration)

Cation	Interferent : Al ratio, m/m	Relative fluorescence intensity
—	—	100
Na^{I}	10^5	100.0
Ca^{II}	1000	100.0
Mg^{II}	500	100.0
K^{I}	500	100.0
Zn^{II}	10	99.5
	100	102.5
Mn^{II}	10	99.0
	100	91.7
Cr^{VI}	10	99.0
	20	100.0
	100	81.0
Cr^{III}	1	99.5
	2	82.5
	10	49.0
Fe^{III}	0.1	86.0
	0.5	66.0
	1	0
Cu^{II}	0.1	100.0
	0.5	88.0
	1.0	0

Table 4. Effect of foreign anions on the recovery of 1.0 μg of Al using a simple system

Anion	Interferent : Al ratio, m/m	Relative fluorescence intensity
—	—	100
EDTA	10	42
	100	0
F^-	10	32
	100	0
PO_4^{3-}	10	100
	100	91
Cl^-	60 000	100
Acetate	30 000	100

The retention of Al was virtually unchanged at carrier flow-rates from 0.5 to 0.75 ml min^{-1}, but decreased significantly above this rate; the flow-rate used for the analysis was kept constant at 0.75 ml min^{-1}.

Aluminium Uptake as a Function of pH and Selection of Leaching Agent

The pH of the carrier influences the Al uptake and therefore the final fluorescence signal. The results of the effect of carrier pH (pH range 3–7) are shown in Fig. 3. As can be seen, the highest analytical signal was obtained between pH 4.5 and 5.5. A pH of 5.0 was selected for subsequent studies.

The elution of Al from the flow cell was studied by using NaOH, HCl and KF solutions at various concentrations, as stripping agents. Table 2 shows the recovery of Al after passing each eluent for 3 min; 2 M HCl was preferred to NaOH solutions because, firstly, the reagent phase regenerated very slowly from the basic form, and, secondly, using NaOH, the elution of any Fe and Cu retained does not occur.

Influence of Salt Content and Effect of Various Ions

The effect of adding increasing amounts of NaCl (a fundamental component in dialysis concentrates) on the Al signal (1 ml

Table 5. Results of the determination of Al in dialysis fluids and concentrates

Sample	Al concentration/μg l^{-1} Proposed method	GFAAS
Dialysis fluids—		
1	30.4 ± 0.6	32.6 ± 3.0
2	40.5 ± 0.7	44.3 ± 0.2
3	56.6 ± 0.6	58.9 ± 0.9
4	77.7 ± 0.6	73.5 ± 2.3

Sample	Al found by proposed method/ μg l^{-1}	Al^{III} added/ μg l^{-1}
Dialysis concentrates—		
1	36.8 ± 1.1	40.0
2	53.6 ± 1.2	60.0
3	116.2 ± 2.2	120.0
4	131.2 ± 2.3	135.0

of 1 μg ml^{-1} of Al) was investigated and the results showed that up to 40 000 μg ml^{-1} of Na (maximum level tested) did not affect the Al signal.

Other metals (K, Mg and Ca) at the high concentration levels present in dialysis concentrates did not interfere with the determination of Al (see Table 3). The effect of other cations such as Cu^{II}, Zn^{II}, Fe^{III}, Cr^{III}, Cr^{VI} and Mn^{II} was also tested. As shown in Table 3 in an FI system having only a channel of sodium acetate buffer (pH 5.0), the presence of Fe^{III}, Cu^{II} and Cr^{III} strongly decreased the emission signal.

It has been reported[16] that Fe^{III} and Cu^{II} are retained completely at pH 2.5 using Kelex 100 immobilised on a solid support. Considering that Al^{III} is not retained at this pH, we designed and tested the three-channel configuration shown in Fig. 2 to eliminate interferences. Using this system, Cu^{II} and Cr^{III} up to a 100-fold excess and Fe^{III} up to a 30-fold excess over Al did not interfere with the Al signal.

Chloride and acetate did not interfere at all, but anions that form complexes with Al, namely, fluoride, ethylenediaminetetraacetic acid (EDTA) and phosphate, inhibited the retention of the metal and hence affected the final spectrofluorimetric detection of Al (see Table 4).

Analytical Performance

Analytical performance characteristics of the proposed method were evaluated under selected conditions: calibration graphs prepared from the results of triplicate 1-ml injections of Al standard solutions were linear from 0.035 to 1 μg ml^{-1} of Al. The detection limit, calculated as three times the standard deviation of the blank signal, was 0.007 μg ml^{-1} of Al and the relative standard deviation (n = 10) at the 0.1 μg ml^{-1} level was 0.8%.

Obviously the fluorescence signal observed depends on the total Al^{III} from the sample retained on the active surface (rather than on its concentration in the injected solution) because of the pre-concentration process taking place on the solid phase. Hence, it is possible to increase the sensitivity and useful range of the method simply by changing the injected sample volume (*i.e.*, the same analytical signal was obtained on injecting 1 ml of 0.15 μg ml^{-1} of Al as when 10 ml of 0.015 μg ml^{-1} were injected).

Analysis of Dialysis Fluids and Concentrates

The proposed method was applied to the determination of Al in dialysis concentrates and fluids. The samples did not require any previous treatment and were analysed using the FI system described above (see Fig. 2).

The results obtained for the dialysis fluids were compared with those obtained by GFAAS[21] for the same samples. Table 5 shows that the two methods provided equivalent results for the analysis of dialysis fluids.

For the determination of Al in dialysis concentrates the more commonly used technique of GFAAS is unreliable.[14] Therefore the analysis was performed on synthetic "reference" samples (prepared from a dialysis concentrate that did not originally give Al signals by GFAAS and was then spiked with Al). As Table 5 shows, the results obtained agree well with the expected results for this type of analysis.

Conclusions

It has been shown that remote monitoring of ultratrace amounts of Al is feasible by using on-line pre-concentration - optical fibre spectrofluorimetric detection. The proposed method offers excellent analytical characteristics including sensitivity and adequate selectivity, versatility and convenience of use. In fact, this technique shows great promise for application to FI or even to the continuous monitoring of low levels of Al in dialysis concentrates and other sources of exposure to this metal by renal failure patients in hospital dialysis units.

The future of the technique (on-line optosensing at active surfaces using optical fibres) appears very bright both from a methodological and fundamental standpoint: it is possible that other related optical properties (phosphorescence, light polarisation, optical activity, chemiluminescence, etc.) could be exploited for sensing and their eventual application to real sample analysis could become a reality. From a basic point of view, the experimental design described offers great potential, as yet unexploited, for fundamental studies on the binding, reaction kinetics and suitability of different metal complexes, packings and designs for an appropriate optrode for a desired chemical or biological species.

Financial support from the "Fundación para la Investigación Científica Aplicada y la Tecnología" (FICYT) for this research and helpful suggestions from Dr. R. Narayanaswamy (UMIST, UK) are gratefully acknowledged.

References

1. Růžička, J., and Hansen, E. H., *Anal. Chim. Acta*, 1985, **173**, 3.
2. Yoshimura, K., *Anal. Chem.*, 1987, **59**, 2922.
3. Lazaro, F., Luque de Castro, M. D., and Valcarcel, M., *Anal. Chim. Acta*, 1988. **214**, 217.
4. Guthrie, A. J., Narayanaswamy, R., and Russell, D. A., *Analyst*, 1988, **113**, 457.
5. Seitz, W. R., *C.R.C. Crit. Rev. Anal. Chem.*, 1988, **19**, 135.
6. Narayanaswamy, R., and Sevilla, F., III, *J. Phys. E*, 1988, **21**, 10.
7. *Talanta*, 1988, **35**, No. 2 (special issue).
8. Narayanaswamy, R., and Sevilla, F., III, *Analyst*, 1986, **111**, 1085.
9. Yerian, T. D., Christian, G. D., and Růžička, J., *Analyst*, 1986, **111**, 865.
10. Woods, B. A., Růžička, J., and Christian, G. D., *Anal. Chem.*, 1987, **59**, 2767.
11. Narayanaswamy, R., and Sevilla, F., III, *Fresenius Z. Anal. Chem.*, 1988, **329**, 789.
12. Russell, D. A., and Narayanaswamy, R., *Analyst*, 1989, **114**, 381.
13. Galle, P., *Recherche*, 1986, **61**, 857.
14. Pereiro García, M. R., López García, A., Díaz García, M. E., and Sanz-Medel, A., *J. Anal. At. Spectrom.*, 1990, **5**, 15.
15. Zhujun, Z., and Seitz, W. R., *Anal. Chim. Acta*, 1985, **171**, 251.
16. Isshiki, K., Tsuki, F., Kuwamoto, T., and Nakayama, E., *Anal. Chem.*, 1987, **59**, 2491.

17. Cannata, J. B., Suarez, S. C., Cuesta, V., Rodriguez, R. M., Allende, M. T., Herrera, J., and Perez, J., *Proc. Eur. Dial. Transplant Assoc. Eur. Renal Assoc.*, 1984, **21**, 354.
18. Mourier, P., Cote, G., and Bauer, D., *Analusis*, 1982, **10**, 468.
19. Parrish, J. R. *Anal. Chem.*, 1977, **49**, 1189.
20. Pereiro García, M. R., Díaz García, M. E., and Sanz-Medel, A., *J. Anal. At. Spectrom.*, 1987, **2**, 699.
21. Sanz-Medel, A., Rodriguez Roza, R., González Alonso, R., Noval Vallina, A., and Cannata, J., *J. Anal. At. Spectrom.*, 1987, **2**, 177.

Paper 9/03279G
Received August 2nd, 1989
Accepted November 28th, 1989

Effect of Coated Open-tubular Inorganic-based Solid-state Ion-selective Electrodes on Dispersion in Flow Injection*

Jacobus F. van Staden
Department of Chemistry, University of Pretoria, Pretoria 0002, South Africa

The shape and quality of the analytical signal obtained from coated open-tubular inorganic-based solid-state ion-selective electrodes interfaced to a flow injection system are directly influenced by both the electrode and the flow injection system. The electrode characteristics and response, in a flow-through system, are controlled by the chemical properties of the specific electrode used and the partial dispersion arising from the flow dynamics of the system. The efficiency of electrode functioning depends on the nature of the electrode membrane surface, the way in which the electrode is coated, the conditioning of the electrode and contributions from diffusion - convection transport, all resulting in a concentration - time profile. The effects of these parameters on the dynamic linear response range, practical response time and peak shape are described. The Gaussian peak shape is distorted at the lower front and back part of the peak, which is attributed to the predominance of an electrode mechanism at low chloride concentrations. At the centre portion of the sample plug, however, where the chloride concentration is higher, the influence of dispersion flow dynamics becomes predominant.

Keywords: *Flow injection; tubular solid-state chloride-selective electrode; flow-through system; dispersion*

The evaluation of the performance of electrochemical flow-through sensors in unsegmented continuous flow systems dates back as far as 1970, when Pungor's group were the first to report on the use of graphite electrodes for the voltammetric detection of samples injected into continuously flowing streams.[1] It was not until the mid-1970s, however, with the development of flow injection (FI),[2] that analytical chemists became aware of the scope and potential of this technique. The introduction of FI marked an important breakthrough in automatic continuous flow systems and this concept has nowadays developed into a well established analytical technique.[3–5]

The incorporation of flow-through electrochemical detectors, especially tubular ion-selective electrodes (ISEs), as an extension of the manifold tubing in FI systems, has become increasingly attractive as a result of various advances.[6–9]

Various mathematical models have been used to describe the process of dispersion in FI systems.[3–5] All involve the concept of an ideal or theoretical manifold with or without a chemical reaction including several different ways of sample introduction (*e.g.*, syringe sluice or time injection, hydrodynamic injection, plug injection valve function or as a delta injection function). Nearly all mathematical models are based on the use of a single-line manifold with a number of assumptions, as indicated by Stone and Tyson.[10,11] In FI systems[10,11] the manifolds are often more complicated as reagent streams are added sequentially downstream to the carrier stream, accelerating the flow-rate; the injection valve, connectors and detector disrupt the laminar flow profile and the manifold tubings are coiled. The expression that takes strictly into account both convective and diffusional transport and therefore best describes the over-all physical dispersion phenomena[4] is the diffusion - convection equation resulting in a concentration - time profile. This equation is one of the few models that takes the contribution of the injection valve into consideration.[12–17] Stone and Tyson[10,11] used the single well stirred mixing tank model[18] to measure solute concentration within a finite volume rather than a plane. The volume of the measurement cell is usually much smaller than that of the manifold and injection valve system, and for that reason the dispersion of the sample plug in this part of the FI system has been neglected and the contribution of the measurement cell has been excluded from most of the mathematical physical models.[19] However, Betteridge *et al.*[20] have shown that tubular conductivity cells, and Stone and Tyson[10,11] that photometric cells, contribute significantly to the shape of the output signal of FI systems. It is therefore clear that the measurement cell should be included in the mathematical models for FI systems. Vanderslice *et al.*[12] provided an expression for base line to base line time from numerical integration of the diffusion - convection equation. This was extended by Gomez-Nieto *et al.*[21] to an experimental approach to calculate base-line peak width. We applied the latter expression for the prediction of peak width at different peak heights for FI manifolds with spectrophotometric or inductively coupled plasma detection.[22]

The shape and quality of the analytical signal obtained from a coated open-tubular inorganic-based solid-state ion-selective electrode incorporated into an FI system are directly influenced by both the electrode and FI manifold. The electrode characteristics and response in an FI flow-through system are basically controlled by two mutually dependent components: (i) a contribution from the type of electrode used, which depends on the chemical properties of the specific electrode used at the moment in time, *e.g.*, a silver - silver chloride or silver - silver sulphide electrode, *i.e.*, the electrode aspect; and (ii) a contribution from the partial dispersion originating from flow dynamics resulting in a concentration - time profile coming from both convection and diffusion transport, *i.e.*, the FI manifold aspect.

This paper reports the results obtained in a study of the effects of coated open-tubular inorganic-based solid-state ion-selective electrodes on the dispersion in FI from both the electrode and FI manifold aspects for silver - silver chloride ion-selective electrodes.

Experimental

Reagents and Solutions

All reagents were prepared from analytical-reagent grade chemicals unless specified otherwise. Doubly distilled, de-ionised water was used throughout. The water was tested beforehand for traces of chloride. All solutions were de-

* Presented at SAC 89, the 8th SAC International Conference on Analytical Chemistry, Cambridge, UK, 30 July–5 August, 1989.

gassed before measurements by use of a water vacuum pump. The main solutions were prepared as follows.

Ionic strength adjustment reagent (ISA)

Dissolve 202.22 g of potassium nitrate in 2 dm^3 of distilled water in a calibrated flask to obtain a 1 mol dm^{-3} solution of potassium nitrate.

Standard chloride solutions

Dissolve 32.9680 g of dried sodium chloride in 2 dm^3 of distilled water to give a stock solution with a chloride concentration of 10 000 mg dm^{-3}. Prepare working standard chloride solutions by dilution of appropriate aliquots of the stock solution to cover the range 50–2000 mg dm^{-3}.

Instrumentation

Coated tubular flow-through electrode construction

The basic design, preparation and conditioning of the coated tubular flow-through solid-state chloride-selective membrane electrode were similar to those described previously.[6]

FI system

The tubular flow-through chloride-selective electrode was incorporated in a manifold system with sampler unit, sampling valve and peristaltic pump similar to the system described previously.[6] The potentials were measured at room temperature with an Orion Model 901 microprocessor Ionalyzer. The detector output was directed via a Model TM-40 LabMaster analogue to digital (A/D) converter with 12-bit resolution and a maximum conversion rate of 40 kHz to an XT IBM-compatible microcomputer, 640-kbyte RAM, equipped with mathematics coprocessor 80827, EGA colour graphics card with 256-kbyte graphics memory and high-resolution monitor. The results were plotted on a Hewlett-Packard Model 7475A-compatible serial plotter. The constructed flow-through tubular indicator electrodes were used in conjunction with an Orion Model 90-02 double-junction reference electrode with 10% m/v potassium nitrate as the outer chamber filling solution.

Data acquisition and assimilation

The detector output, normally channelled to a recorder, was simply connected by a screened cable to the daughter board of the LabMaster card through the P1D (D refers to daughter board) pins connector. The major function of the LabMaster daughter board was to perform the actual conversion from analogue data, received from the detector output, to digital data which the computer could use. This A/D conversion was carried out using one of the eight true differential channels with 12-bit resolution. The daughter LabMaster card communicated with the computer through the mother LabMaster card. The conversion was started with an ASYST software (ASYST Software Technologies, Version 1.04; Macmillan Software, New York) command using the AMD 9513 programmable timer inserted in the LabMaster board. An XT IBM-compatible microcomputer, 640-kbyte RAM, equipped with an 80287 mathematical coprocessor, EGA colour graphics card with 256-kbyte graphics memory, high-resolution monitor and ASYST software, was used to acquire, process and display data obtained from the coated open-tubular solid-state chloride-selective electrode FI system. The background noise received with the raw data from the electrode was removed by applying the DS (data sets) Cat and Smooth unary operation of the file processor of the ASYST software. With the DS Cat and Smooth operation, consecutive data sets in long data files are catenated and then smoothed by convolution with a filter computed from a low-pass Blackman window frequency response. Selection of a cut-off frequency (cycles per point) is available in a prompt list to allow flexibility in the amount of smoothing. These raw and background-corrected data were plotted on the HP 7475A-compatible serial plotter.

Results and Discussion

The shape and quality of the analytical signal obtained from the coated open-tubular solid-state chloride-selective electrodes incorporated into the FI system are directly influenced by both the electrode and FI manifold. These two mutually dependent components basically control the electrode characteristics and response in the FI flow-through system.

Electrode Aspect

With respect to the electrode, the efficiency of electrode functioning depends on a number of factors,[23] including the: (i) nature of the electrode membrane surface; (ii) way in which the electrode is coated; (iii) conditioning of the electrode; (iv) dynamic linear response range; (v) practical response time; and (vi) electrode selectivity.

The memory effect or practical response time of an ion-selective electrode in an FI system is determined to a great extent by the dynamic properties on the electrode surface and the properties of the electrode membrane film. If an ISE is used as a sensor in FI, it responds dynamically (with the "wash-in" and "wash-out" of an analyte sample plug in the flow detection conduits) and not strictly according to the static type of equilibrium conditions found in manual methods. The practical response time of an ISE in FI systems is also a contributing factor in determining the sample throughput of such a system and the carry-over and reproducibility of results. Any contribution of the practical response time as an additional dispersion effect to the electrode output signal and therefore, ultimately the peak measurement, might result in peak broadening and hence, have an adverse influence on the sampling rate.

The linear response range, which arises from variations in response electrode potentials between different analyte or sample concentrations, is caused by a charge-transfer mechanism both on the electrode interface and in the membrane.

The electrochemical behaviour of such an electrode may be ascribed to one or more of the following aspects[24–29]: (i) adsorption of ions at, and dissolution of ions from, the membrane surface; (ii) redox reactions at the electrode - solution interface; (iii) rapidity and reversibility of ion-exchange processes; (iv) diffusion processes; and (v) influence of the activity of defects in the solid state.

It has been observed[23] that in coated tubular solid-state ion-selective electrodes, the chemical properties of the electroactive materials used in forming the membrane surface of the precipitate-based ion-selective electrode, and also the thin film responsible for transporting any potential changes to the metal wire conductor linking the electrode to the measuring instrument, are crucial to the final peak signal obtained. The defect crystal structure of the solid-state insoluble salt serves as an important mediator for the charge transfer through the thin membrane layer.

In FI systems, any change in response contributed from the electrode material due to electrochemical behaviour at a specific moment is reflected in the output signal as variation in peak height or peak width. In this way, any changes in the activities of primary cations and anions, and any interferences from secondary ions, are detected. The shape of the peak obtained is also a function of the concentration of the analyte plug moving over the active membrane conduit of the ion-selective electrode and the peak shapes obtained for relatively high and low analyte concentrations differ. The lower limits of response of the halide-selective electrodes with membranes made from silver salts are governed, theoretically, by the solubility of the membrane material, which provides

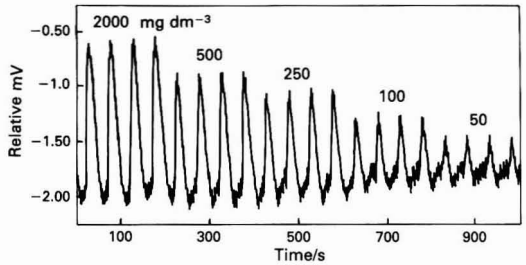

Fig. 1. Raw data for a typical representative run with different standard chloride solutions, as acquired by the ASYST system via a LabMaster board from the tubular electrode - FI system and as it appeared on the monitor screen. From left to right, 2000–50 mg dm^{-3} standard chloride solutions; each standard injected four times

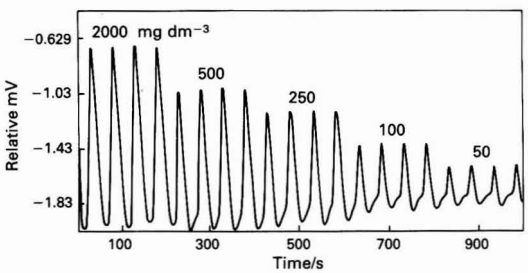

Fig. 2. Typical representative DC Cat and Smooth operated background-corrected graph of the raw data acquired in Fig. 1

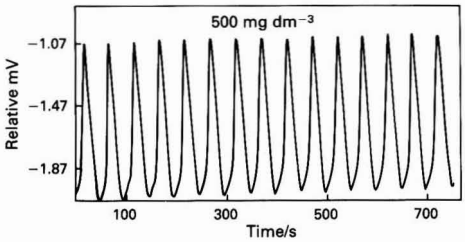

Fig. 3. Typical representative DC Cat and Smooth operated background-corrected graph of a run with 15 repetitive injections of 500 mg dm^{-3} standard chloride solutions with the FI system and coated tubular ISE

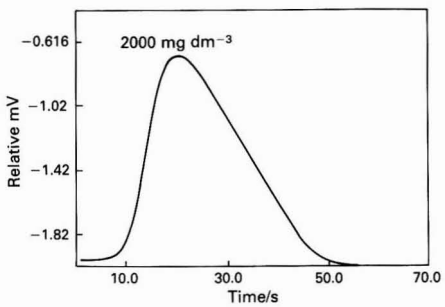

Fig. 4. Enlargement of the second peak from an injection of 2000 mg dm^{-3} standard chloride solution with a cut-off frequency of 55 s, revealing basic information on a single peak

small activities of the membrane components in solution, depending on the solubility constant of the silver halide.[30]

The theoretical relationship between analyte concentration and electrode response can be described by a form of the Nernst equation, which includes the relevant solubility products and activity coefficients.[31,32] In simplified form relevant to the contribution of silver - silver chloride electrodes to the analytical signal in an FI system, the initial electrode potential, E_i, corresponding to the carrier and reagent streams of ISA buffer alone (*i.e.*, the base line) is given by

$$E_i = E^\circ - \left(\frac{RT}{F}\right) \ln [Cl^-_i]$$

where the symbols have their conventional meanings. When the chloride ion, with no interferences, moves across the sensing membrane, the final electrode potential, E_f, is given by

$$E_f = E^\circ - \left(\frac{RT}{F}\right) \ln [Cl^-_f]$$

Therefore, the peak height is

$$\Delta E = E_i - E_f = \left(\frac{RT}{F}\right) \ln \frac{[Cl^-_f]}{[Cl^-_i]}$$

FI Manifold Aspect

Although the electrode surface can act in a dominant manner (especially at the lower limits of response due to the electrochemical behaviour of the electrode, which is also a function of the specific electrode material) the dispersion process in the electrode tube also contributes to the concentration - time profile shown as a peak. Since the concept of FI was introduced in the mid-1970s, various attempts and approaches have been used to derive general expressions or to quantify the process of dispersion in FI systems. These models also involve analyte detection of the already either partially or fully injection- and manifold-dispersed sample plug, measuring the mean concentration in the cross-section of the flow in the middle of the measurement cell or the average integral concentration in the whole volume of the measurement cell, as performed by Stone and Tyson.[10,11] The shape of the analytical peak obtained from a coated open-tubular inorganic-based solid-state ion-selective electrode interfaced to an FI system at different stages, forms a very important part in describing the output of the analytical signal obtained at a specific moment as a result of either the electrode's behaviour or the dispersion process, or both. The output analytical signal is therefore a very important part of the system. In the straight, short, tubular analytical detector where a constant laminar flow exists, with no possible disturbance, the diffusion - convection equation with concentration - time profile is applicable, but with correct measurement points.

Pungor and co-workers[33,34] used the diffusion - convection equation with the resulting concentration - time profile as a mathematical theoretical background to quantify a distorted dispersed plug received further downstream in the manifold as a dispersion model in analytical systems.

Two mechanisms from the convection - diffusion equation[4,33] contribute to sample zone deformation under laminar flow conditions. The primary convective transport deforms the whole slug by a velocity distribution. This deformation causes, however, a secondary molecular diffusional transport phenomenon acting against the deformation as a combination of axial and radial diffusion. At the front side of the tube-deformed slug there will be a considerable concentration gradient towards the tube wall, whereas at the rear side there will be a gradient towards the axis. If an ion-selective electrode is incorporated into the conduits of an FI manifold at a distance, x, from the injector valve, the ion-selective electrode will either measure some kind of average concentra-

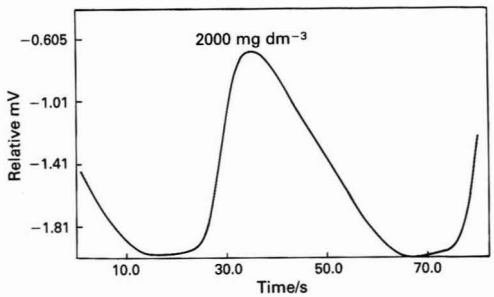

Fig. 5. Enlargement of the second peak from an injection of 2000 mg dm^{-3} standard chloride solution with a cut-off frequency of 80 s, revealing extended basic information on a single peak

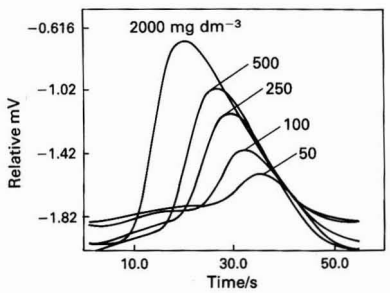

Fig. 6. Enlargements of the second peak from different injected standard chloride solutions (see Fig. 2) covering the range 50–2000 mg dm^{-3} with a cut-off frequency of 55 s and using the tailing part of each curve for simultaneous overlapping

tion in the section at x, or it will measure a local point concentration somewhere in the cross-section, for example, at the tube wall or in the centre of the tube at x. The construction of a coated tubular solid-state ion-selective electrode is in the form of a short, straight tube, which means that the electrode also measures an average concentration over the whole electrode tube or electrode volume. Horvai and Pungor[33] described two important kinds of cross-sectional average concentrations, the mean concentration, c_m, and bulk concentration, c_b, both of which can be measured by the ion-selective electrode; c_m is a function of the cross-section of the tube and the solute concentration only, whereas c_b also includes the local point values of the velocity and the flow-rate. In other words, c_m is the usual average of the local values over the cross-section, whereas c_b is the cross-sectional average concentration weighted by the local velocity. Horvai and Pungor[33] defined both types of concentration mathematically and also used the original Taylor models to predict the detector output signal with the aid of mathematical equations.

In the tubular ion-selective electrodes, measurement usually occurs at the tube walls (where the deformed sample slug local point distribution, at the radial distance from the tube centre, approaches the tube radius and the local point velocity value tends to drop to zero). It is therefore c_m that is mainly measured. The detector signal obtained in this way is a peak in the form of a concentration - time profile that is the result of the diffusion - convection processes.

The raw data for a representative run, as acquired by the ASYST system via a LabMaster board and as it appeared on the monitor screen, is presented in Fig. 1. It is clear from the plotted version that there is a large amount of background noise with the raw data. By applying the DS Cat and Smooth unary operation of the file processor of the ASYST (see under

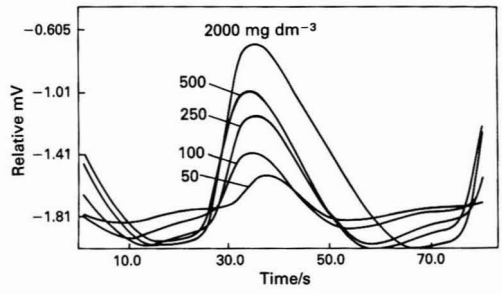

Fig. 7. Enlargements of the second peak from the different injected standard chloride solutions (see Fig. 2) covering the range 50–2000 mg dm^{-3} with a cut-off frequency of 80 s and using the peak maximum of each curve for simultaneous overlapping

Data acquisition and assimilation), the background noise was removed. The background-corrected graphs, as they appeared on the monitor screen, are presented here.

Fig. 2 is a typical representative DC Cat and Smooth operated background-corrected graph of a run for the determination of chloride with the FI system and coated tubular ISE. Standard chloride solutions in the range 50–2000 mg dm^{-3} were injected, each four times. Fig. 2 revealed some changes in peak shape between the output signals obtained from different standard solutions. This is particularly noticeable in the lower part of the different peaks. Fig. 3, however, indicated that the peak shapes for 15 repetitive injections of, for example, 500 mg dm^{-3} standard chloride solutions are reproducible.

In Figs. 4 and 5, the enlargement of the second peak from an injection of 2000 mg dm^{-3} is illustrated, first with a cut-off frequency at 55 s (Fig. 4) and second with a cut-off frequency at 80 s (Fig. 5). The cut-off frequency of 55 s (Fig. 4), however, only revealed the basic information on a single peak. In Fig. 5 this is extended to include information on part of the falling curve of the preceding peak in addition to information on part of the rising curve of the following (third injection) peak by extending the cut-off frequency to 80 s. Comparison of these two figures revealed that much more information is obtained with a cut-off frequency of 80 s.

Figs. 6 and 7 show an enlargement of the second peak from the different injected chloride standards covering the range 50–2000 mg dm^{-3}. In Fig. 6 a cut-off frequency of 55 s was used. The main aim with this cut-off frequency was to try to obtain an overlapping of individual peaks from different concentrations at a fixed point and to study the response behaviour of the electrode for different chloride concentrations from this common point. The tailing part of each curve was used for simultaneous overlapping. By using the cut-off frequency at 80 s (Fig. 7), the falling and rising curves of the preceding and following peaks were also included with the corresponding individual main peaks. Here the aim was to let the different individual main peaks overlap at the peak maximum.

The results show clearly that the coated tubular solid-state chloride ion-selective electrode contributes to the peak shape obtained and that this type of contribution cannot be ignored in any FI system. It is also clear from the results that the output form obtained for a certain part of the peak is controlled by the electrode mechanism, whereas the flow dynamics of the manifold system dominate another output region of the peak. The Gaussian peak shape is distorted at the lower front and rear part of the peak (Figs. 6 and 7). This is attributed to dominance of the electrode mechanism, which is in agreement with the adsorption - desorption mechanism that occurs at low concentrations.

The following conclusions can be drawn from the experimental curves. The adsorption - desorption mechanism

is not so dominant for relatively high standard chloride concentrations, as indicated by the curve for the 2000 mg dm^{-3} solution in both Figs. 6 and 7. The influence of the adsorption - desorption mechanism increases as the chloride concentration decreases, with the largest contribution at 50 mg dm^{-3}, as indicated in both Figs. 6 and 7. The rate of adsorption is slower than the rate of desorption at the electrode surface, as indicated in Fig. 6. This is particularly noticeable at 50 mg dm^{-3}, where the adsorption - desorption mechanism dominates. The adsorption process takes more than 30 s, whereas it appears that the desorption process needs only about 20 s. This phenomenon is not so noticeable at 2000 mg dm^{-3}, where the flow dynamics process predominates. The decrease in adsorption rate with decrease in chloride concentration tends to decrease the practical response time, as reflected in a shift in peak maximum to the right in Fig. 6. The increase in the dominance of the electrode mechanism with decrease in chloride concentration becomes more obvious in Fig. 7, where the peak maxima of the different individual main peaks overlap.

The results in Figs. 6 and 7 also illustrate clearly that for the top part of the peak, where the centre portion of the sample plug with a higher chloride concentration is moving through the electrode conduit, the influence of dispersion flow dynamics becomes predominant. Measurement of the mean concentration, c_m, on the tube walls of the electrode, as reflected in the results obtained, shows that the detector signal forms a distorted Gaussian peak with a larger tail than normal. The tailing effect becomes more evident with an increase in chloride concentration, with the greatest effect on the 2000 mg dm^{-3} peak, as illustrated in Fig. 6. The reason for this is that the dispersed sample zone from the FI manifold enters the tubular electrode where further dispersion occurs. The sharper increase in the rising part of the curve is attributed to the tendency of particles ahead of the sample zone to move to the tube walls owing to molecular diffusion. The tailing of the curves is attributed to the tendency at the rear of the sample zone to move to the tube centre.

The author thanks the Foundation for Research Development of the Council for Scientific and Industrial Research, Pretoria, and the University of Pretoria for financial support. He also thanks Miss A. Botha, L. van Vuuren and R. Coetzee for assistance in performing some of the experiments.

References

1. Nagy, G., Feher, Zs., and Pungor, E., *Anal. Chim. Acta*, 1970, **52**, 47.
2. Růžička, J., and Hansen, E. H., *Anal. Chim. Acta*, 1975, **78**, 145.
3. Růžička, J., and Hansen, E. H., "Flow Injection Analysis," Second Edition, Wiley, New York, 1988.
4. Valcárcel, M., and Luque de Castro, M. D., "Flow Injection Analysis. Principles and Applications," Ellis Horwood, Chichester, 1987.
5. Burguera, J. L., "Flow Injection Atomic Spectroscopy," Marcel Dekker, New York, 1989.
6. van Staden, J. F., *Anal. Chim. Acta*, 1986, **179**, 407.
7. Meyerhoff, M. E., and Kovach, P. M., *J. Chem. Educ.*, 1983, **60**, 766.
8. Meyerhoff, M. E., and Fraticelli, Y. M., *Anal. Lett.*, 1981, **14**, 415.
9. Pungor, E., Féher, Zs., Nagy, G., Tóth, K., Horvai, G., and Gratzl, M., *Anal. Chim. Acta*, 1979, **109**, 1.
10. Stone, D. C., and Tyson, J. F., *Anal. Proc.*, 1986, **23**, 23.
11. Stone, D. C., and Tyson, J. F., *Anal. Chim. Acta*, 1986, **179**, 427.
12. Vanderslice, J. T., Stewart, K. K., Rosenfeld, A. G., and Higgs, D. J., *Talanta*, 1981, **28**, 11.
13. Meschi, P. L., and Johanson, D. C., *Anal. Chim. Acta*, 1981, **124**, 303 and 315.
14. Vanderslice, J. T., Beecher, G. R., and Rosenfeld, A. G., *Anal. Chem.*, 1984, **56**, 268.
15. Painton, C. C., and Mottola, H. A., *Anal. Chim. Acta*, 1984, **158**, 67.
16. Betteridge, D., Marczewski, C. Z., and Wade, A. P., *Anal. Chim. Acta*, 1984, **165**, 227.
17. Vanderslice, J. T., Rosenfeld, A. G., and Beecher, G. R., *Anal. Chim. Acta*, 1986, **179**, 119.
18. Tyson, J. F., and Idris, A. B., *Analyst*, 1981, **106**, 1125.
19. Kolev, S. D., and Pungor, E., *Anal. Chem.*, 1988, **60**, 1700.
20. Betteridge, D., Cheng, W. C., Dagless, E. L., David, P., Goad, T. B., Deans, D. R., Newton, D. A., and Pierce, T. B., *Analyst*, 1983, **108**, 1.
21. Gomez-Nieto, M. A., Luque de Castro, M. D., Martin, A., and Valcárcel, M., *Talanta*, 1985, **32**, 319.
22. Kempster, P. L., van Vliet, H. R., and van Staden, J. F., *Talanta*, 1989, **36**, 969.
23. van Staden, J. F., *Anal. Proc.*, 1987, **24**, 331.
24. Morf, W. E., Kahr, G., and Simon, W., *Anal. Chem.*, 1974, **46**, 1538.
25. Vesely, J., paper presented at the Symposium on Ion-selective Electrodes, Hruba Skala, Czechoslovakia, 4–5 November, 1970.
26. Ross, J. W., *in* Durst, R. A., *Editor*, "Ion-selective Electrodes," NBS Special Publication, No. 314, National Bureau of Standards, Washington, DC, 1969, p. 77.
27. Vesely, J., Jensen, O. J., and Nicolaisen, B., *Anal. Chim. Acta*, 1972, **62**, 1.
28. Harsanyi, E. G., Tóth, K., and Pungor, E., *Anal. Chim. Acta*, 1984, **161**, 333.
29. van Staden, J. F., *Fresenius Z. Anal. Chem.*, 1988, **332**, 157.
30. van Staden, J. F., *Anal. Chim. Acta*, 1989, **219**, 55.
31. Buck, R. P., *in* Freiser, H., *Editor*, "Ion-selective Electrodes in Analytical Chemistry," Volume 1, Plenum Press, New York, 1978, pp. 89–96.
32. Hulanicki, A., and Lewenstam, A., *Anal. Chem.*, 1981, **53**, 1401.
33. Horvai, G., and Pungor, E., *CRC Crit. Rev. Anal. Chem.*, 1987, **17**, 231.
34. Kolev, S. D., and Pungor, E., *Talanta*, 1987, **34**, 1009.

Paper 9/04004H
Received September 21st, 1989
Accepted October 11th, 1989

Applications of the Single Well Stirred Tank Model for Dispersion in Flow Injection*

Julian F. Tyson†
Department of Chemistry, University of Technology, Loughborough, Leicestershire LE11 3TU, UK

The single well stirred tank model in which dispersion is modelled by the passage of a slug of fluid through the tank has been used to compare the sensitivity that can be obtained by the use of three types of flow injection manifold, which incorporate on-line chemical reaction. These manifolds are the single-line manifold, the double-line manifold and the single-line manifold used in the reverse mode (*i.e.*, the reagent is injected into the sample which constitutes the carrier stream). The model indicates that each manifold type will give the same sensitivity, but that operating conditions and throughput will be different for each. The model calculations for the determination of phosphate, based on parameter values from the literature, suggest that the commonly applied guideline of designing "medium dispersion" manifolds for on-line chemical derivatisations is sub-optimal in terms of maximising sensitivity and that the guideline should be that the dispersion coefficient has a value of <2. Practical problems related to refractive index and base-line absorbance effects mean that the double-line manifold is the most suitable for trace analysis and the design of such a manifold is illustrated for the determination of chloride with a detection limit of 11 p.p.b.

Keywords: *Flow injection; dispersion model; sensitivity comparison; design guideline; chloride determination*

In order to achieve the best detection limit for an analytical procedure it is necessary to maximise the sensitivity and minimise the factors that contribute to the over-all noise. For flow injection (FI) procedures that involve an on-line chemical reaction, the sample solution is mixed with the reagent solution. The extent of this mixing is a parameter to be optimised because although limited mixing may reduce the extent of sample dilution, it may not permit complete formation of the reaction product owing to an insufficient excess of reagent over determinand at the time when the analytical measurement is made. In most FI procedures this time corresponds to the maximum of the transient product concentration profile.

As part of a continuing study of the design of an FI manifold for the spectrophotometric determination of trace anions the factors affecting both the sensitivity and the noise in various manifold designs have been evaluated.[1,2] It has been shown that significant contributions to base-line noise arise from the pulsations due to the peristaltic pump and the mixing of streams with different physical properties at confluence points. It has also been found that detection limits can be severely affected by the use of reagents which absorb at the analytical wavelength and by the differences in refractive index between sample and reagent solutions. The noise contributions can be considerably reduced by the use of pulse dampers and of manifold components, downstream of confluence points, designed to promote mixing between merging streams. Such components include tightly coiled open tubular reactors (OTRs) and packed bed reactors (PBRs). It has been suggested that the single-line manifold (SLM) is limited with regard to the sensitivity, *i.e.*, the slope of the calibration graph, by the onset of double peaks[3] and that the reverse FI mode, in which the reagent is injected into the sample, has greater sensitivity than the normal mode.[4]

In this paper the relative sensitivities of three possible manifold configurations are examined. These configurations include the single-line manifold in normal mode (nSLM), the double-line manifold (DLM) and the SLM used in reverse mode (rSLM). The DLM is used in the normal mode. The basis for comparison is to consider all the dispersion effects to be modelled by the plug flow through a single well stirred tank. The performance of each of the three manifolds will be illustrated by reference to an example taken from the literature,[5] namely, the determination of orthophosphate by measurement of the absorbance due to the product of the reaction in acid solution in the presence of a reducing agent, between the determinand and molybdate. This reaction is typical of many spectrophotometric methods in common use in that it is normally carried out with a large concentration excess of reagent over determinand.

Theoretical

Manifold Design and Terminology

The extent to which the product of an on-line chemical reaction is formed depends on several factors. These include the stability constant and rate of the reaction under consideration, and the concentration excess of reagent over determinand at the peak maximum. This last factor is in turn controlled by the concentration of the reagent (c_0^r) and the concentration of the determinand (c_0^d). For any given analysis the concentration excess of reagent over sample will be least for the standard of maximum concentration ["top" standard (c_0^{dtop})].

If the ratio of concentrations at time $t = 0$ is given by $R_0^{r/d}$ and the ratio of the concentrations of reagent to determinand at the peak maximum is given by $R_p^{r/d}$, then the ratio of these two ratios, $R_p^{r/d}/R_0^{r/d}$, is equal to the ratio of dispersion coefficients, D/D^r, where D is the dispersion coefficient of the injection material given by c_0^d/c_p^d and D^r is the dispersion coefficient of the reagent defined in an exactly analogous way as for the injected determinand solution, namely as c_0^r/c_p^r. This ratio of dispersion coefficients will be referred to as the α-value.

The Single Well Stirred Tank Model

Single-line manifold (normal mode)

Equations for the well stirred model developed previously[6] give rise to the following relationships for D and D^r:

$$D = [1 - \exp(-V_i/V)]^{-1} \quad .. \quad .. \quad .. \quad (1)$$

$$D^r = [\exp(-V_i/V)]^{-1} \quad .. \quad .. \quad .. \quad (2)$$

* Presented at SAC 89, the 8th SAC International Conference on Analytical Chemistry, Cambridge, UK, 30 July–5 August, 1989.

† Present address: Department of Chemistry, Lederle Graduate Research Tower A, University of Massachusetts, Amherst, MA 01003, USA.

Thus the relationships between D and D^r are $D = D^r/(D^r - 1)$ and $D^r = D/(D - 1)$. These two equations can be combined into:

$$1/D + 1/D^r = 1 \quad .. \quad .. \quad .. \quad .. \quad (3)$$

The relationship between the hypothetical volume of the tank, V, and the volume injected V_i is given by the following equation,

$$V_i = V \ln D^r \quad .. \quad .. \quad .. \quad .. \quad (4)$$

From the definition of α given above it follows that

$$\alpha = D - 1 \text{ or } D = \alpha + 1 \quad .. \quad .. \quad .. \quad (5)$$

from which, when the top standard is injected

$$D = (R_p^{r/d}/c_0^r)c_0^{dtop} + 1 \quad .. \quad .. \quad .. \quad (6)$$

$$= \beta c_0^{dtop} + 1 \quad .. \quad .. \quad .. \quad .. \quad (7)$$

where $\beta = R_p^{r/d}/c_0^r$ .. .. (8)

and $\alpha = \beta c_0^{dtop}$ .. .. (9)

The sensitivity of the method, b, being the slope of the calibration graph is given by

$$b = kc_p^d/c_0^d = k/D \quad .. \quad .. \quad .. \quad .. \quad (10)$$

where k is the constant of proportionality between absorbance, A, and the concentration measured, c_p^d.

Single-line manifold (reverse mode)

By analogy with equations (1) and (2), the dispersion coefficients for the determinand species (in the carrier stream) and for the reagent (the injected solution) are given by

$$D = [\exp(-V_i/V)]^{-1} \quad .. \quad .. \quad .. \quad (11)$$

$$D^r = [1 - \exp(-V_i/V)]^{-1} \quad .. \quad .. \quad .. \quad (12)$$

The α-value (D/D^r) is thus given by

$$\alpha = D - 1 \quad .. \quad .. \quad .. \quad .. \quad (13)$$

As equation (13) is identical with equation (5) the same α-value is obtained regardless of which solution is the injectate and which is the carrier. This symmetry is reflected in the form of the relationship between the dispersion coefficient values given in equation (3).

Double-line manifold

Equations for the DLM have also been derived previously.[7,8] The relationship between the dispersion coefficient for the injected material, D, and the various model parameters (see Fig. 1) is given by

$$D = \{f^d[1 - \exp(-V_i/Vf^d)]\}^{-1} \quad .. \quad .. \quad (14)$$

where $f^d = u^d/Q$, $f^r = u^r/Q$ and $Q = u^r + u^d$ and u^d, u^r and Q are the determinand stream, reagent stream and total flow-rates, respectively. The reagent dispersion coefficient, D^r, is equal to f^r, the fraction of the total flow contributed by the reagent carrier stream. The α-value for this manifold is therefore given by

$$\alpha = D/D^r = D/(1 - f^d) \quad .. \quad .. \quad .. \quad (15)$$

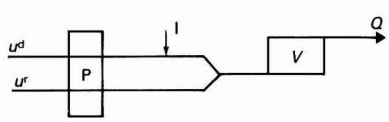

Fig. 1. Schematic diagram of the model for the DLM. u^d, Flow-rate of the determinand carrier stream; u^r, flow-rate of the reagent stream; P, pump; I, injection point; V, volume of the well stirred mixing tank; and Q, total flow-rate. The model assumes (a) plug flow between the injection point and the tank and (b) complete mixing at the confluence point

The sensitivity is given by equation (10).

Comparison of manifolds

To compare the sensitivities obtained with each of these manifold designs and to examine typical performance parameters, an example of an FI method for which a considerable amount of literature exists has been chosen, namely the determination of phosphate for which the following reaction is the first stage

$$PO_4^{3-} + 24H^+ + 12MoO_4^{2-} \rightleftharpoons PMo_{12}O_{40}^{3-} + 12H_2O \quad (16)$$

One source of information[5] concerning the FI format of this reaction gives the following data for an SLM: $V_i = 30$ µl, $c_0^{dtop} = 40$ p.p.m. (1.29×10^{-3} M), $c_0^r = 0.005$ M $(NH_4)_6Mo_7O_{24}$ (0.035 M Mo) and $D = 4$. In using these data for illustrative purposes, it is assumed that the values represent an optimised parameter set, *i.e.*, that the conditions produce the maximum sensitivity which can be obtained with this reagent if the top standard in the calibration sequence has a concentration of 40 p.p.m.

Single-line manifold (normal mode)

From equations (3)–(5), it can be calculated that for this manifold $D^r = 4/3$, $V = 104$ µl and $\alpha = 3$. From equations (6) and (7) it may be calculated that, for the top standard, $R_p^{r/d} = 81.4$ and $\beta = 2326$. The ratio of reagent to determinand at time $t = 0$ is 27.13.

The sensitivity of the procedure obtained from equation (10) is $0.25k$. If the assumed constraints apply the sensitivity is fixed. However, as the sensitivity is inversely proportional to the dispersion coefficient [equation (10)], the sensitivity may be increased if the α-value can be decreased [equation (5)]. Equations (8) and (9) show that for a given chemistry and reagent concentration, α will decrease if the top standard concentration is decreased. Examples of the changes that can be produced are given in Table 1, together with an indication of the injection volume necessary for a manifold of hypothetical mixing volume of 104 µl. The relationship between bk^{-1} ($1/D$) and the concentration of the top standard is given in Fig. 2.

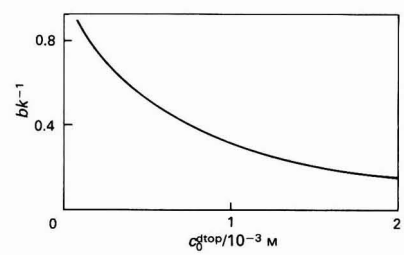

Fig. 2. Plot of bk^{-1} *versus* concentration of the top standard

Table 1. Increase in sensitivity obtained for SLM in normal mode by reducing the concentration of the top standard

$c_0^{dtop}/10^{-5}$ M	α	D	$bk^{-1}(1/D)$	V_i/µl
200*	4.65	5.65	0.177	20.3
100	3.33	4.33	0.301	37.0
25.0	0.581	1.581	0.632	104
3.12	0.0726	1.0726	0.932	280

* This value corresponds to approximately 64 p.p.m. of phosphorus.

Table 2. Manifold parameters for DLM as a function of top standard concentration

$c_0^{dtop}/10^{-5}$ M	α	D	$bk^{-1}(1/D = f^d)$	V_i/μl	V_i/μl*
200	4.65	5.65	0.177	81.4	20.3
100	3.33	4.33	0.301	106	37.0
25.0	0.581	1.581	0.632	291	104
3.12	0.0726	1.0726	0.932	429	280

* Injection volumes for the SLM with the same hypothetical mixing chamber volume.

Table 3. Comparison of injection volumes for three manifold designs

$c_0^{dtop}/10^{-5}$ M	α	D	bk^{-1}	V_i DLM/μl	V_i nSLM/μl	V_i rSLM/μl
200	4.65	5.65	0.177	84.8	20.3	180
100	3.33	4.33	0.301	111	37.0	152
25.0	0.581	1.581	0.632	303	104	47.6
3.12	0.0726	1.0726	0.932	447	280	7.29

Double-line manifold

By combining equations (10) and (14), the sensitivity (b) is given by

$$b = kf^d - kf^d\exp(-V_i/Vf^d) \quad \ldots \quad \ldots \quad \ldots \quad (17)$$

In order to maximise the value of b the first term on the right-hand side of equation (17) should be made as large as possible and the second term should be made as small as possible. This latter term can be reduced to zero for an infinitely large value of V_i: under these circumstances a dispersion coefficient of $1/f^d$ is obtained. Substituting this value into equation (15) gives an α-value for maximum sensitivity of $D - 1$. This value is the same as that obtained for the SLM.

It can be shown[8] that the injection volume required to give a peak height of 99% of that obtained under infinite volume conditions is given by $4.6V/D$. The implications for the manifold design parameters of fractional flow-rate for the determinand carrier stream (f^d) and volume injected (V_i) are shown in Table 2. For comparison, the corresponding injection volumes for the SLM are also given in Table 2. These values indicate that for the same total flow-rate, the throughput of the DLM would be less than that of the SLM.

Single-line manifold (reverse mode)

As can be seen from equation (13), the α-value for this manifold configuration is the same as that for the nSLM and the DLM and thus is capable of producing the same sensitivity as these two manifold designs. However, the operating parameters of this manifold differ markedly from those of the nSLM in that the increased sensitivity that can be obtained by decreasing the concentration of the top standard is achieved by decreasing the volume of reagent injected. A comparison of injection volumes is given in Table 3.

Discussion

The single well stirred tank model for dispersion shows that, contrary to previous reports,[3,4] all of these manifolds are capable of producing the same sensitivity when the constraints of the same α and β values are applied. However, the model indicates that the throughput will be considerably different for the nSLM and the DLM. Although the peak width will be narrow for the high sensitivity rSLM, the concept of sample throughput has less meaning in this instance, as the sample is the carrier stream and it is likely that this type of manifold would only be employed in situations where intermittent monitoring of a process stream was required, and also because the main consideration here is manifold design for maximum sensitivity. One possible reason for the consideration that the DLM provides for higher sensitivity than the SLM is that a study of the parameters of both manifolds, which investigated

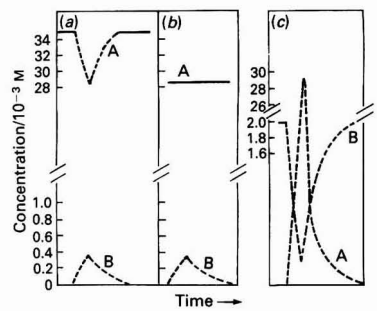

Fig. 3. Concentration gradients of A, reagent and B, determinand for (*a*) the SLM, (*b*) the DLM and (*c*) the rSLM

the effect of increasing the volume injected for a fixed concentration, would show the SLM to be limited by the appearance of double peaks, whereas the DLM would show a more gradual transition to a limiting sensitivity value (it is not possible for double peaks to be formed with this manifold) as there is no reagent concentration gradient in a DLM. There has been very little discussion of the role of $R_p^{r/dtop}$ values in manifold design in previous publications and it is likely that comparisons have been made between manifolds in which a variety of $R_p^{r/dtop}$ values would have been produced.

In comparing the nSLM with the rSLM it can be shown that if a given manifold is switched from one configuration to the other (*i.e.*, the roles of sample and reagent are reversed) an increase in sensitivity will be obtained if the dispersion coefficient (D) of the manifold is >2. Dispersion coefficient values greater than 2 are likely to be encountered as many manifolds designed for on-line reaction will have been designed as so-called "medium dispersion" manifolds,[9] for which D is normally taken to have a value of between 3 and 10. Thus, it is likely that a manifold designed according to this specification will show an increase in sensitivity when used in the reverse mode. When $D = 2$, no change in the sensitivity will be obtained on changing from normal to reverse mode.

The proposed model indicates that for fixed values of c_0^r and $R_p^{r/dtop}$ (*i.e.*, for a fixed β value) the sensitivity can only be increased by reducing the concentration for the top standard in the sequence. This, in effect, allows the same $R_p^{r/dtop}$ value to be obtained at a lower value of D. Further, the calculations suggest that the concept of a "medium dispersion" manifold, for which $3 < D < 10$, may not be a helpful guide for manifold design as the best performance may be obtained at D values below 2.

Although the model indicates that the three manifold configurations have the same sensitivity, the physically

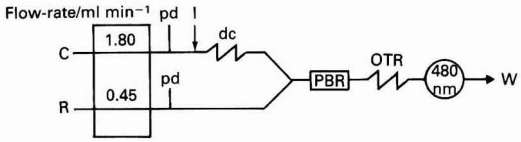

Fig. 4. Schematic diagram of the manifold for the determination of chloride. C, Sample carrier stream (water); R, reagent; pd, pulse damper; I, injection valve (1000 μl); dc, delay coil (2.1 m × 0.8 mm i.d.); PBR, packed bed reactor (6 cm × 2 mm i.d.); OTR, open tubular reactor (1 m × 0.8 mm i.d.); and W, waste

Table 4. Off-line formation of reaction product between 2 p.p.m. chloride and various reagent dilutions

Absorbance	Reagent dilution factor(D^r)	$D^r/(D^r-1)$ ($=D$)	c_0^d, p.p.m.	Sensitivity/ absorbance p.p.m.$^{-1}$
0.025	20.0	1.053	2.11	0.0119
0.031	16.7	1.064	2.13	0.0146
0.034	14.3	1.075	2.15	0.0158
0.039	12.5	1.087	2.17	0.0179
0.056	11.1	1.099	2.20	0.0255
0.069	10.0	1.111	2.22	0.0311
0.073	6.67	1.198	2.40	0.0305
0.093	5.00	1.250	2.50	0.0372
0.121	4.00	1.333	2.67	0.0454
0.130	3.33	1.429	2.86	0.0455
0.145	2.50	1.667	3.33	0.0435
0.153	2.00	2.000	4.00	0.0383
0.159	1.67	2.492	4.99	0.0319
0.156	1.43	3.326	6.65	0.0235
0.143	1.25	5.000	10.00	0.0143

Table 5. Calibration data for chloride

Concentration, p.p.b.	0	10	30	50	70	100	150
Absorbance/10^{-3} ..	0.3	1.0	1.8	3.2	4.4	5.8	8.2

dispersed concentration gradients for each are different, as shown in Fig. 3. The shapes of the profiles for the rSLM are typical illustrations of the situation which causes the appearance of double peaks. This suggests that it may not be necessary to have such a large reagent to sample excess at the peak maximum and that, in an optimisation strategy designed to achieve maximum sensitivity, the value of $R_p^{r/dtop}$ should be carefully studied.

It should be noted that the concentration of the reagent can be controlled. Equations (6)–(10) show that the sensitivity can be increased by increasing the concentration of the reagent.

Application of Model Calculations to the Determination of Chloride

Some of the above concepts were applied to the determination of chloride with a commercially available reagent. Previous work with this system[2] has indicated that the best detection limits cannot be achieved with the SLM because, at low determinand concentrations, there is considerable base-line distortion due to (*a*) refractive index effects (the reagent has a refractive index considerably different to that of dilute aqueous salt solutions) and (*b*) the absorption of the reagent at the analytical wavelength (which would give rise to negative peaks at low determinand concentrations even in the absence of refractive index effects). Both of these effects can be overcome by the use of a DLM. Contributions to base-line noise from pump pulsations and incomplete mixing downstream of the confluence point may be reduced by the use of pulse dampers and a combination of OTR and PBR, respectively.[2,10] A further source of base-line distortion has been observed with a DLM, namely, the momentary interruption of the sample carrier stream flow during the injection process. This distortion can be time-resolved from the analytical signal by the insertion of a delay coil in the sample line upstream of the confluence point.[10]

In order to determine the optimum $R_p^{r/dtop}$ value an off-line experiment was performed.

Experimental

The manifold used is shown in Fig. 4. All chemicals used were of analytical-reagent grade. The chloride reagent (BDH, Poole, Dorset, UK) consisted of mercury(II) thiocyanate 0.625 g l^{-1} (1.97×10^{-3} M), iron(III) nitrate 30.3 g l^{-1} (7.5×10^{-2} M), nitric acid 3.3 g l^{-1} (3.67×10^{-2} M) and methanol 15% v/v. Chloride standard solutions were prepared by serial dilution of a stock solution with a concentration of 1000 p.p.m. (BDH).

The absorbance of solutions containing 2 p.p.m. of chloride and various dilutions of the reagent was measured in 10-mm cells by a Philips PU 8600 UV - visible spectrometer. An aqueous solution of tartrazine (0.001% m/v, BDH) was used to establish the physical dispersion coefficient of the manifold. After determination of the optimum α and D values, the appropriate flow-rate ratios and injection volumes were calculated and a calibration for chloride over the range 0–150 p.p.b. was obtained. The detection limit was calculated from the absorbance residuals after an unweighted least-squares regression procedure had been applied to fit a straight line calibration function to the data.[11]

Results and Discussion

The results for the off-line measurement of the net absorbance for a chloride solution with a concentration of 2 p.p.m. are given in Table 4. This experiment is considered to model the performance of an SLM. The reagent dilution factors are thus analogous to D^r values so that D values can be calculated from equation (3). These values are given in Table 4. From these values an initial concentration of determinand can be calculated as, for each measurement, the "peak" concentration of chloride is 2 p.p.m. Hence a "sensitivity" value for the SLM analogue of this experiment could be calculated.

The results show that a D value of between 1.33 and 1.43 should be used. The model calculations discussed earlier showed that the DLM designed for maximum sensitivity would have the same α-value as the maximum sensitivity SLM and thus the requirement is for an α-value of between 0.33 and 0.43. For a DLM the α-value is controlled by the flow-rate ratio. As a single pump was used and pump tubing is only available in certain discrete sizes, it was not possible to adjust this ratio to exactly the required value. Hence, the value of 0.8 for f^d (rather than a value between 0.70 and 0.75) which arises from the flow-rates of 1.80 and 0.45 ml min^{-1} for u^d and u^r, respectively.

The injection of 564 μl of the tartrazine solution gave a physical dispersion coefficient, for $f^d = 0.8$, of 1.29. The volume of the equivalent well stirred tank, V, was calculated from equation (4) to be 200 μl, hence the volume of 1000 μl injected is sufficient to produce a physical dispersion coefficient of approximately 99.9% of the infinite volume value.

The calibration data are given in Table 5, from which the detection limit[11] is calculated to be 11 p.p.b. As the calibration range can be used for concentrations of up to 2 p.p.m., the dynamic range of the method is over two orders of magnitude. When a chart recording of the response to the standard of lowest concentration (10 p.p.b.) was examined, it appeared that a practical detection limit below the value calculated above could be achieved.

Conclusions

Application of the single well stirred tank model for dispersion shows that the SLM (both normal and reverse mode) and the

DLM all have the same inherent sensitivity for FI methods employing on-line chemical reaction. The model also indicates that the need to maintain a large excess of reagent over determinand at the peak maximum may not be necessary and that the use of the guideline of $3 < D < 10$ for manifolds used for on-line chemical derivatisation probably leads to a sub-optimal design in terms of sensitivity. The guideline should suggest $D < 2$.

The provision of chemicals and reagents by BDH is gratefully acknowledged.

References

1. Marsden, A. B., and Tyson, J. F., *Anal. Proc.*, 1985, **25**, 89.
2. Tyson, J. F., and Marsden, A. B., *Anal. Chim. Acta*, 1988, **214**, 447.
3. Růžička, J., and Hansen, E. H., "Flow Injection Analysis," Second Edition, Wiley, New York, 1988, p. 305.
4. Johnson, K. S., and Petty, R. L., *Anal. Chem.*, 1982, **54**, 1185.
5. Růžička, J., and Hansen, E. H., "Flow Injection Analysis," Second Edition, Wiley, New York, 1988, pp. 299–304.
6. Tyson, J. F., *Anal. Chim. Acta.*, 1986, **179**, 131.
7. Tyson, J. F., Bysouth, S. R., Stone, D. C., and Marsden, A. B., *Analusis*, 1988, **16**, 155.
8. Tyson, J. F., *Quim. Anal.*, 1989, **8**, 171.
9. Valcarcel, M., and Luque de Castro, M. D., "Flow Injection Analysis," Ellis Horwood, Chichester, 1987, p. 91.
10. Wang, X., Marsden, A. B., Fogg, A. G., and Tyson, J. F., *Anal. Proc.*, 1989, **26**, 51.
11. Miller, J. C., and Miller, J. N., "Statistics for Analytical Chemistry," Second Edition, Ellis Horwood, Chichester, 1988, pp. 101–136.

Paper 9/03942B
Received September 14th, 1989
Accepted December 7th, 1989

Shapes of Flow Injection Signals: Effect of Refractive Index on Spectrophotometric Signals Obtained for On-line Formation of Bromine From Bromate, Bromide and Hydrogen Ion in a Single-channel Manifold Using Large-volume Time-based Injections*

Arnold G. Fogg, Edward Cipko, Luciano Farabella and Julian F. Tyson†
Chemistry Department, Loughborough University of Technology, Loughborough, Leicestershire LE11 3TU, UK

The shapes of the spectrophotometric signals obtained with a single-channel manifold for large-volume (4 ml) time-based injections for the six possible combinations of the reagents bromate, bromide and nitric acid in the injectate and carrier stream, by which bromine can be formed on-line, have been determined. The injectate and carrier stream were 5.25×10^{-4} M in bromate, 0.030 M in bromide and 1 M in nitric acid when these reagents were present. The signals consisted of two separate peaks caused by formation of bromine at the front and rear boundaries of the injected bolus. When both injectate and carrier stream were 1 M in nitric acid (*i.e.*, for the reagent combination $H^+BrO_3^- - H^+Br^-$) the two peaks were of equal height, and the signal was virtually the same whichever solution was used as the injectate. In reagent combinations where only one solution contained nitric acid the peaks were different in size, the smaller peak being that produced by the boundary in which the acidic solution was flowing behind the other solution. This difference in size between the front and rear peaks was shown to be caused by refractive index effects. When the refractive indices of the two solutions were matched either by increasing the potassium bromide concentration or by making the non-acidic solution 7% in sodium nitrate, the peaks became equal in size. When the potassium bromide concentration was increased there was an appreciable increase in peak size (about 4-fold): the changes in the amount of bromine formed must be due to kinetic or equilibrium effects. This increase in size did not occur when sodium nitrate was used to balance the refractive indices.

Keywords: *Flow injection; spectrophotometric detection; on-line bromine formation; refractive index effect; large-volume and time-based injections*

Interest in flow injection signal shapes in this series of studies arose from the application of reverse flow injection (rFI) amperometric methods in single-channel manifolds. Reverse flow injection was used in two ways: either (*i*), reagent was injected into a sample stream[1]; or (*ii*), a monitorand was formed in the bolus by dispersion of a concentration limiting reagent contained in the carrier stream. This monitorand then reacted with a determinand which had been injected with an excess of a second reagent used to form the monitorand.[2–4] Examples of these two ways of using rFI are the determination of phosphate by injecting an acidified molybdate reagent into a phosphate sample stream,[1] and the iodimetric determination of sulphite in which iodine is formed on-line from iodate (and an excess of iodide) in the carrier stream, and an excess of acid, present with sulphite, in the injectate.[4] In these methods conventional injection volumes (*ca.* 100 µl) were used.

It eventually became clear that rFI signals were different in shape from the more conventional or normal flow injection (nFI) signals.[4,5] The schematic diagram (Fig. 1) illustrates simply the formation of nFI and rFI signals. In nFI the product is formed initially at the extremities of the bolus, but soon sufficient reagent has reached the centre of the bolus for all the sample to be converted to product: further dispersion simply dilutes this product. The conventionally shaped flow injection signal is obtained. The main difference between the nFI and rFI situations is that in rFI the sample is present essentially in infinite supply in the carrier stream. The equivalent concentration of sample throughout the reagent bolus increases from zero to a value approaching that in the carrier stream. Clearly, rFI signals would be expected to be broader than nFI signals and more prone to double-peak formation (especially when a determinand is injected into a monitorand formed in the rFI manner). The formation of double peaks was observed in the amperometric monitoring of iodine formed in the rFI manner, and this became more apparent when sulphite was injected with the acid (see Fig. 3 in reference 4).

Recently, the on-line formation of iodine was monitored spectrophotometrically in order to gain greater insight into the shapes of these signals.[6] Large-volume (2 ml) injections were used to isolate the dispersions at the front and rear boundaries of the injected bolus. Time-based injections, where both boundaries travel the same distance to the detector, were used to eliminate differences in dispersion caused by the rear boundary travelling further than the front boundary, which

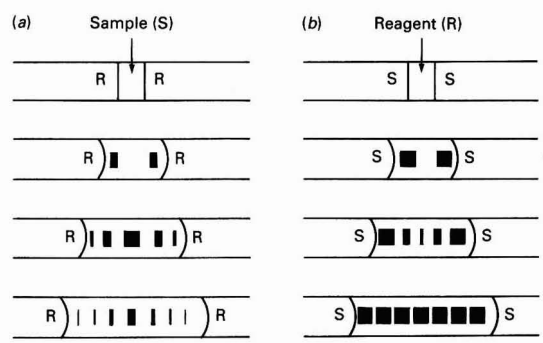

Fig. 1. Schematic diagram showing the formation of (*a*) nFI and (*b*) rFI signals, as dispersion increases with the distance travelled by the bolus in the transmission tubing. The size of each shaded area represents the extent of formation (*i.e.*, the concentration) of the reaction product which is monitored at the detector

* Presented at SAC 89, the 8th International Conference on Analytical Chemistry, Cambridge, UK, 30 July–5 August, 1989.

† Present address: Department of Chemistry, University of Massachusetts, Amherst, MA 01003, USA.

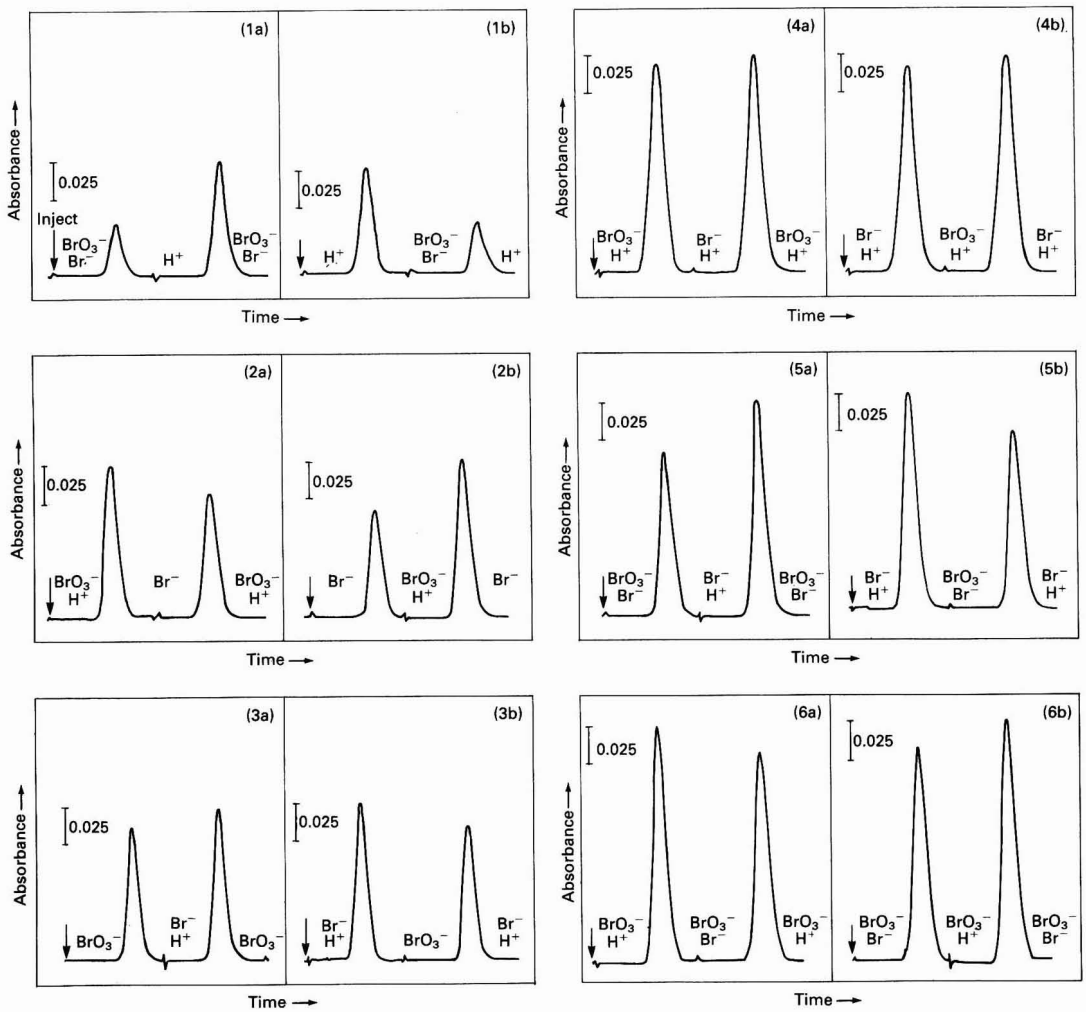

Fig. 2. Signals obtained with time-based injections for different combinations of reagents. The signals are numbered according to the information given in Table 1. The experimental conditions are described in the text. Flow-rate, 2 ml min^{-1}, [bromate], 5.25×10^{-4} M; [bromide], 0.030 M; and [nitric acid], 1 M. Non-acidic solutions were adjusted to pH 11.0 with sodium hydroxide solution. (The disturbance of the signal between the peaks is caused by the injection valve switching back to the carrier stream)

occurs in slug injection. Three reagents are used in the on-line formation of iodine, *viz.*, iodate, iodide and acid. These are present in two solutions. One solution must contain two of the reagents, but the other solution may contain one or two reagents, *i.e.*, one reagent can be present in both solutions. Thus, there are six possible reagent combinations, each of which is represented by two practical systems because each solution can serve as injectate or carrier stream. At large injection volumes each signal consisted of two peaks caused by iodine formation at the front and rear boundaries independently. The signals for four reagent combinations, including IO_3^--I^- - H^+, showed clearly that the size and shape of each particular peak (half of the signal) was determined simply by the composition of the solutions at the boundary and their positions relative to each other in the flow stream; for these four combinations of reagents the two peaks of each signal were clearly of different heights. Thus, for the reagent combination IO_3^--I^- - H^+ the larger peak was the one produced by the boundary in which the acidified solution was in the front. Unfortunately, for the two combinations of reagents which involved iodide and acid being present in the same solution interpretation of the signals was difficult because of the formation of iodine by oxidation by air.

In the present work the on-line formation of bromine by reaction of bromate, bromide and acid was monitored spectrophotometrically. It was felt that the results of this study could be interpreted more readily than those of the iodine system because bromine is not formed by air oxidation of bromide in acidified solutions.

Experimental

A single-channel manifold incorporating a six-port rotary valve was used to carry out time-based injections under computer control as described previously.[6] The transmission tubing was made of PTFE (3 m × 0.8 mm i.d.). Ismatec Reglo pumps were used and the detector was a Pye Unicam SP-6-250 visible spectrophotometer fitted with a 10-mm path length 8-μl quartz flow cell. Bromine was monitored at 393 nm. To study the refractive index effects measurements were also made at

550 nm where absorption by bromine was negligible. Refractive index measurements were made with an Abbe refractometer.

Results and Discussion

Nitric acid was used as the source of hydrogen ion: the use of hydrochloric acid was avoided because chloride is oxidised to chlorine by bromate, and was shown to distort the flow injection signals. The combinations of reagents by which bromine can be formed on-line in a single-channel manifold are listed in Table 1: these are numbered in a manner identical with the iodine system which was studied previously.[6] Typical signals obtained with these systems using time-based injections are shown in Fig. 2. The signals were obtained under the following experimental conditions: flow-rate, 2 ml min^{-1}; injection volume, 4 ml; bromate, bromide and nitric acid concentrations, 5.25×10^{-4}, 0.030 and 1 M, respectively; non-acidic solutions were adjusted to pH 11.0 with a sodium hydroxide solution. Note that the bromate concentration (5.25×10^{-4} M) used was two orders of magnitude higher than that of the iodate (6.67×10^{-6} M) used in the previous study,[6] because of the lower molar absorptivity of bromine.

The signals shown in Fig. 2 can be compared with those obtained previously for the iodine system.[6] In the present system the base lines obtained for all combinations of reagents remained at the same zero absorbance level for injectate and carrier stream because there was no problem with extraneous formation of bromine by air oxidation. Thus, with bromine the signals from all the combinations are available for more immediate interpretation than those for the iodine system. When the role of the two solutions is reversed the position of the peaks is reversed for all combinations. For all combinations here it can be seen that the height and shape of each peak (half signal) is determined by the composition of the two solutions at the boundary producing the signal and their relative positions in the flow stream. This was observed unambiguously for only four of the combinations in the iodine system, the situation in the other two combinations being obscured by air oxidation problems. The main feature that can be seen in the bromine system, but not in the iodine system, is that for systems 4a and 4b the two peaks of each signal are of approximately equal height; in this reagent combination acid is present in both solutions. At this stage it was considered that the faster rate of diffusion of hydrogen ion might explain the unequal peak heights observed with combinations other than 4, but this was eventually proved not to be the case.

At this stage in the experimental work the effect of including sulphite with the nitric acid in system 1a on the size and shape of the two peaks obtained in the 4-ml injection was studied. This system is the same as that reported recently for the spectrophotometric determination of sulphite using system 1a,[7] except that a 4-ml time-based injection is made here instead of a 15-μl slug injection. The effect of injecting nitric acid solutions containing an increasing amount of sulphite is shown in Fig. 3(*a*)–(*f*). The highest concentration of sulphite used is sufficient to reduce any bromine formed, but a large signal consisting of a negative peak and a positive peak remains. Clearly this effect is due to refractive index differences between the two solutions used as carrier stream and injectate. This we should have anticipated as Betteridge *et al.*[8] have demonstrated pronounced refractive index effects in single-channel manifolds using conventional FI injection volumes. The refractive index of an electrolyte solution increases with concentration, and the refractive index of a 1 M

Table 1. Combinations of reagents by which bromine can be formed on-line in a single-channel manifold. Bromate is present in solution A in all combinations. In systems designated a, solution A is the carrier stream. In systems designated b, solution B is the carrier stream, *e.g.*, for system 4a, the carrier stream contains BrO_3^-–H^+ and the injectate Br^-–H^+. A particular reagent is present in both solutions (A and B) in one combination

Combination number	Composition of solution A	Composition of solution B	Comments
1	BrO_3^-–Br^-	H^+	
2	BrO_3^-–H^+	Br^-	
3	BrO_3^-	Br^-–H^+	
4	BrO_3^-–H^+	Br^-–H^+	H^+ in both solutions
5	BrO_3^-–Br^-	Br^-–H^+	Br^- in both solutions
6	BrO_3^-–H^+	BrO_3^-–Br^-	BrO_3^- in both solutions

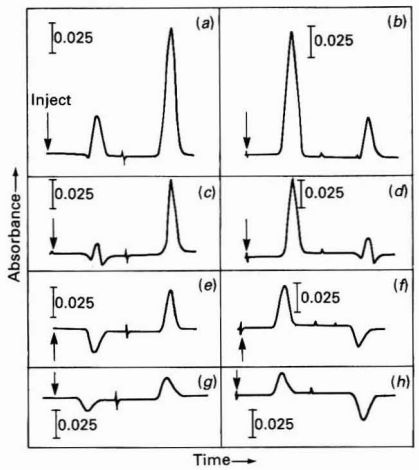

Fig. 3. (*a*)–(*f*) Signals obtained at 393 nm when increasing concentrations of sulphite were added to the nitric acid in reagent combination 1. [Sulphite]: (*a*) and (*b*), 2.87×10^{-5} M; (*c*) and (*d*), 2.87×10^{-4} M; and (*e*) and (*f*), 2.87×10^{-3} M. (*g*) Signal obtained when 1 M nitric acid solution was injected into water and (*h*) *vice versa*

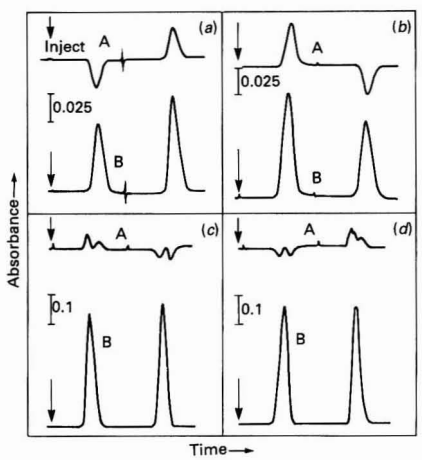

Fig. 4. Effect of balancing the refractive indices of injectate and carrier stream, by increasing the concentration of potassium bromide, on the signals obtained at A, 550 and B, 393 nm for reagent combination 1. [Potassium bromide]: (*a*) and (*b*) 0.030 M; and (*c*) and (*d*) 3.00 M. (*a*) and (*c*) Carrier, BrO_3^-–Br^-; injectate, H^+; and (*b*) and (*d*) carrier, H^+; injectate, BrO_3^-–Br^-

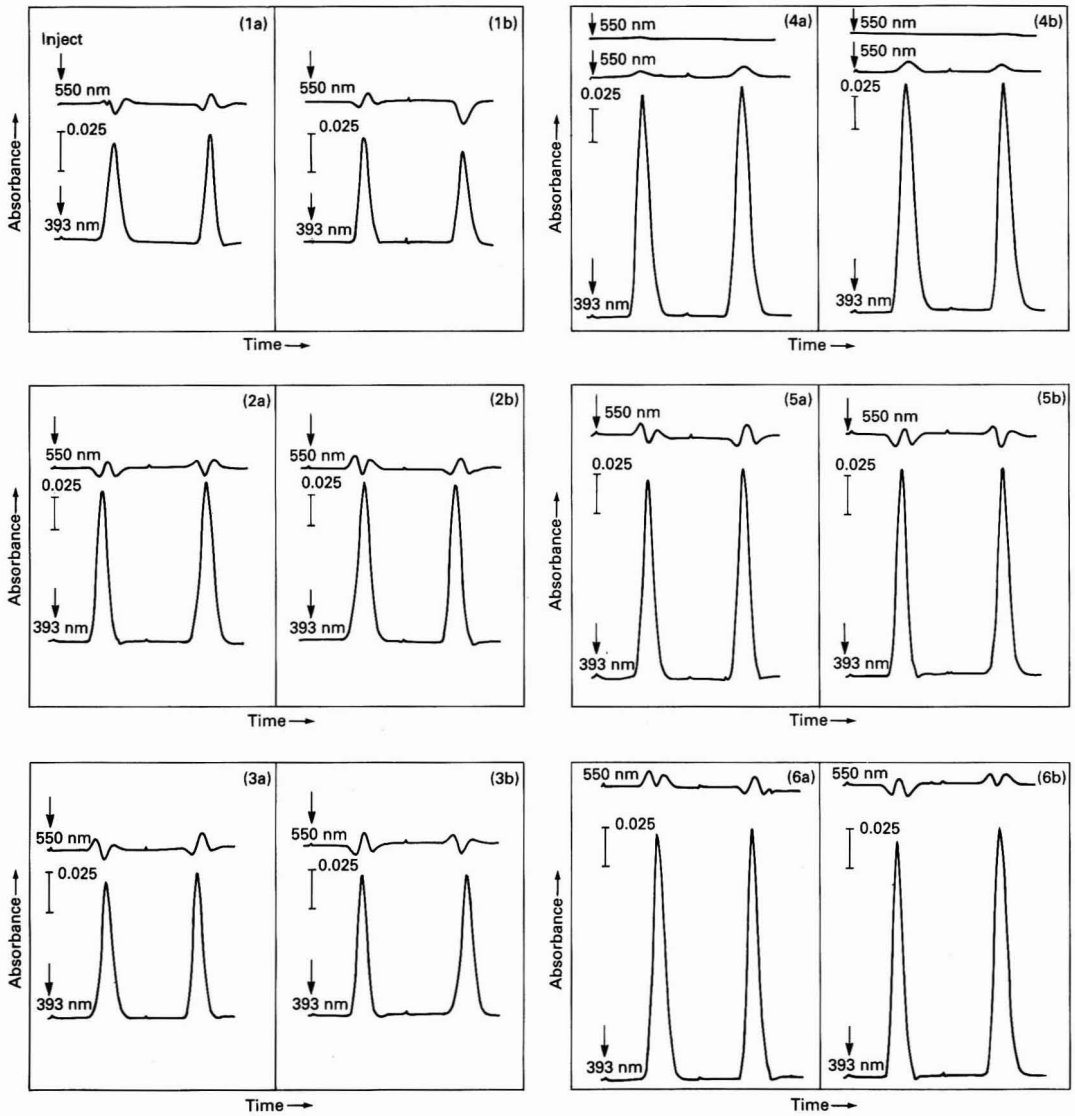

Fig. 5. Effect of balancing refractive indices in all combinations by making non-acidic solutions (and both solutions for system 4) 7% m/v in sodium nitrate. For combination 4 the signal at 550 nm is also recorded in the absence of bromate to illustrate the residual bromine signal. The signals are numbered according to the information given in Table 1

nitric acid solution is appreciably higher (1.3405) than those of 0.03 M potassium bromide (1.3330) or 5×10^{-4} M potassium bromate solution. As can be seen in Fig. 3(*g*) and (*h*), similar signals were obtained when 1 M nitric acid solution was injected into a water carrier stream and *vice versa*. A study of the effect of sulphite addition on the two-peak signals was postponed pending further studies of the refractive index effect and is not reported further here.

The effect of balancing the refractive indices of the two solutions was observed. The effect was first checked for reagent combination 1 by increasing the concentration of potassium bromide. When the potassium bromide concentration in the carrier stream had been increased 20-fold (refractive index of carrier stream 1.3405) the heights of the two peaks measured at 393 nm became equal (see Fig. 4). In order to study the refractive index signal without interference from the bromine signal measurements were also made at 550 nm, at which wavelength the bromine signal was negligible. The size of the signal at 550 nm for the carrier stream with the high potassium bromide concentration was much reduced, but was not eliminated. The addition of more bromide not only caused the peaks at 393 nm to become equal in height but the peaks obtained were considerably larger than before, indicating that more bromine is formed under these new solution conditions. This must be caused by kinetic or equilibrium effects in the formation of bromine.

The effect of making the non-acidic solutions (or both solutions in the case of combination 4) 7% m/v in sodium nitrate is shown in Fig. 5. This addition results in much closer matching of peak heights. Note that at 550 nm for combination

4 the signal is purely positive, which may indicate that there is a residual bromine signal at this wavelength; one would expect the refractive index signal in this combination to be eliminated completely. This was confirmed by monitoring the signal at 550 nm after omitting bromate from the solutions and explains the shapes of the signals for other combinations at 550 nm. Note also that on the addition of sodium nitrate there is no large increase in peak height as was the case when extra potassium bromide was added.

Clearly, when using flow injection with spectrophotometric detection in single-channel manifolds one should be aware of the effects of changes in refractive index on the signals obtained. However, even if a refractive index component is present in the observed signals, calibration graphs will still be valid provided that the standard and sample solutions are similar in composition. Alternatively, the effect of refractive index can be eliminated by matching the refractive indices of the injectate and carrier stream as illustrated above. The present work on large-volume injections is being extended to observe the effects of refractive index and refractive index matching on the signals obtained with small-volume injections. Further work is in progress on the shapes of flow injection signals obtained in single-channel manifolds using both visible spectrophotometric and amperometric detection.

References

1. Fogg, A. G., and Bsebsu, N. K., *Analyst*, 1984, **109**, 19.
2. Fogg, A. G., Bsebsu, N. K., and Abdalla, M. A., *Analyst*, 1982, **107**, 1462.
3. Fogg, A. G., Ali, M. A., and Abdalla, M. A., *Analyst*, 1983, **108**, 840.
4. Fogg, A. G., Guta, C. W., and Chamsi, A. Y., *Analyst*, 1987, **112**, 253.
5. Fogg, A. G., *Analyst*, 1986, **111**, 859.
6. Fogg, A. G., Wang, X., and Tyson, J. F., *Analyst*, 1989, **114**, 1119.
7. Fogg, A. G., Wang, X., and Tyson, J. F., *Analyst*, 1990, **115**, 305.
8. Betteridge, D., Dagless, E. L., Fields, B., and Graves, N. F., *Analyst*, 1978, **103**, 897.

Paper 9/03536B
Received August 18th, 1989
Accepted October 10th, 1989

Reductive Reverse Flow Injection Amperometric Determination of Nitrate at a Platinum Electrode After On-line Reduction to Nitrosyl Chloride in Concentrated Sulphuric Acid Medium Containing Chloride*

Arnold G. Fogg, S. Paul Scullion and Tony E. Edmonds
Department of Chemistry, Loughborough University of Technology, Loughborough, Leicestershire LE11 3TU, UK

A simple method has been developed for the determination of nitrate using flow injection with amperometric detection. The nitrate sample, which is made 2 M in hydrochloric acid, is the carrier stream, and into this is injected a small volume (25 μl) of concentrated sulphuric acid. The nitrosyl chloride and chlorine formed are detected as a combined reduction signal at a platinum electrode held at +0.70 V *versus* Ag - AgCl. As formation of nitrosyl chloride only occurs in the initial stages of dispersion of the sulphuric acid into the sample solution (*i.e.*, at high concentrations of sulphuric acid), incorporation of a 40-cm long single bead string reactor as the transmission tubing between the injection valve and the detector, which reduces this dispersion, increases the size of the signal and provides conditions in which gas (mainly hydrogen chloride) formed on-line, which otherwise results in a noisy base line, is re-dissolved before reaching the detector. Calibration graphs were rectilinear over the range from 9×10^{-5} M (the detection limit) to 5×10^{-3} M. Coefficients of variation were typically less than 4%. Other common constituents of hydroponic fluids did not interfere.

Keywords: *Nitrate determination; reverse flow injection; nitrosyl chloride; amperometric detection; platinum electrode*

Several flow injection methods for the determination of nitrate based on electrochemical detection have been reported. They include the use of a copper electrode, which could be regenerated *in situ*, to reduce nitrate directly,[1] a gas permeable membrane detector used to measure nitrogen oxide produced upstream by direct reduction of nitrate on a silver cathode[2] and the use of pneumatoamperometry in which nitrate is reduced to nitrogen oxide in 50% sulphuric acid solution by hydroquinone using an ammonium molybdate catalyst.[3] Recently, a method involving the oxidation of iodide to triiodide by nitrite has been reported[4]; in this method nitrate was reduced to nitrite using a cadmium column and triiodide was detected amperometrically at twin platinum wire electrodes. A disadvantage of these methods is that oxygen is an interferent and must be removed. In addition, the copperised cadmium column used to reduce nitrate is reported to be subject to interference from sulphite,[5] sulphate,[6] metal ions[6] and chloride.[7] Phosphate has also been shown to interfere[8] with the reduction process to an extent dependent on the amount of phosphate to which the reductor column has been exposed.

Recently[9] we reported a reverse flow injection procedure with amperometric detection at a glassy carbon electrode for the determination of nitrate in a plentiful sample solution, such as a hydroponic fluid, in which a solution of thiophene-2-carboxylic acid in concentrated sulphuric acid solution (25 μl) was injected into the sample solution stream. The concentrated sulphuric acid became diluted very rapidly after injection whereas nitration reactions generally only occur in solutions of acid concentration greater than about 70%. Nevertheless, under these conditions thiophene-2-carboxylic acid is nitrated extremely rapidly and to a sufficient extent to be appropriate for use as a reagent in this method. The need to inject concentrated sulphuric acid is not ideal, but the major disadvantage of this method was the contamination of the electrode, which became apparent after 15–20 injections.

In this paper an even simpler method is recommended which is free from electrode contamination. This method is not based on the formation of an organic nitro compound, but on the on-line reduction of nitrate to nitrosyl chloride in the presence of chloride in a concentrated sulphuric acid medium. Afghan *et al.*[10] reported that chloride catalysed the reduction of nitrate to nitrite in strongly acidic media. They developed a visible spectrophotometric method for use with AutoAnalyzer systems for the determination of chloride, based on the reaction of the reduced nitrogen species with chromotropic acid. Nakamura[11] and Velghe and Claeys[12] used this reduction reaction in order to measure nitrate. Both methods are based on reacting the reduced nitrogen species with a suitable organic reagent and using ultraviolet (UV) spectrophotometric detection. Velghe and Claeys[12] indicated that nitrosyl chloride was the nitrosating agent in the nitrosation of phenol. Armstrong[13] found that in the presence of chloride, solutions of nitrate exhibited a shift in UV absorbance maximum in strongly acidic solutions (>35% H_2SO_4). They assumed that the absorbing species was nitrosyl chloride.

Nitrosyl chloride is reduced at a platinum electrode at low positive potentials without interference from dissolved molecular oxygen. Previously we reported a flow injection amperometric method for determining nitrite, which required injecting sample solutions into an acidified bromide carrier stream and monitoring nitrosyl bromide at a glassy carbon electrode at a low positive potential.[14] This method was developed from the work of Coenegracht *et al.*[15] who developed a method for determining the excess of nitrite monoamperometrically at a platinum electrode during the titration of aromatic amines with nitrite. The classical method of determining sulphonamide drugs uses this reaction with biamperometric detection at two platinum electrodes. The presence of bromide in the titration solution speeds up the rate of diazotisation but also makes detection of the biamperometric end-point easier. In this work, which involves concentrated sulphuric acid solutions, it was impracticable to use bromide. Reduction of nitrosyl chloride at a glassy carbon

* Presented at SAC 89, the 8th SAC International Conference on Analytical Chemistry, Cambridge, UK, 30 July–5 August, 1989.

electrode leads to contamination of the electrode, so the nitrosyl chloride was monitored at a platinum electrode.

Experimental

The flow injection system consisted of a multi-channel peristaltic pump (Gilson Minipuls), a Rheodyne rotary injection valve (Model 5020) with an injection loop of approximately 25 μl, an amperometric flow cell connected to an electrochemical detector and a Linseis *y* - *t* recorder. When using a glassy carbon working electrode (3 mm diameter) a Metrohm VA611 detector was used in conjunction with a laboratory-built Kel-F flow cell[16] which incorporated an Ag - AgCl reference electrode and a stainless-steel auxiliary electrode. However, for the platinum working electrode (1.5 mm diameter) a Dionex pulsed amperometric detector was used in the fixed potential mode in conjunction with a Dionex flow cell which incorporated an Ag - AgCl reference electrode, separated from the flowing solution by an ion-exchange membrane and a stainless-steel counter electrode. Transmission tubing made from PTFE (Phase Separations) with an internal diameter of 0.58 mm was used. The flow injection system was a single-line manifold in which the valve was connected to the detector by means of a single bead string reactor (SBSR) or via a coiled tube. The SBSR contained glass beads (35–40 mesh), which had been acid washed, and was connected directly to the valve.

For the studies of the effect of temperature variation on the signals obtained a constant-temperature water-bath was used. The carrier stream reservoir bottle and as much of the transmission tubing as possible were placed in this water-bath.

A PAR 174A polarographic analyser was used to carry out linear sweep and cyclic voltammetry; an Hg - Hg_2SO_4 reference electrode and a platinum foil counter electrode were used. The voltammetric cell was of the H-cell design, with the counter electrode separated from the main body of the cell by a glass frit and the reference electrode connected to the cell by a Luggin capillary. An inlet to the cell to allow the introduction of gas was separated from the cell by a coarse glass frit. The reference electrode was prepared by covering the platinum wire contact with triply distilled mercury and depositing a paste prepared from mercury(II) sulphate and 9 M sulphuric acid over the mercury layer. The cell was then filled with 9 M sulphuric acid and left for 24 h to equilibrate.

The UV - visible spectra were recorded on a Shimadzu UV-160 spectrophotometer using 1 cm path length silica cells.

The solutions for linear sweep and cyclic voltammetry were prepared by adding small aliquots of solutions of the appropriate concentrations to 150 ml of 9 M sulphuric acid solution; the solutions were stirred for 30 s before taking the measurements. The platinum electrode was prepared by immersing it in a 6 M nitric acid solution before holding it at +0.1 V in a de-oxygenated solution of 0.1 M sulphuric acid until the current had stabilised.

For flow injection, the carrier stream was made 2 M in hydrochloric acid and the required concentration in nitrate. The flow-rate was set at 6 ml min^{-1} and the potential was set at +0.7 V. It was found necessary to hold the electrode at the measuring potential for about 20 min before use in order to obtain a stable signal. Concentrated sulphuric acid was used as the injected reagent. The platinum electrode was polished with the "fine" polishing powder supplied by the manufacturer (Dionex) for 2–3 min before use each day.

Results and Discussion

The results described in this section were obtained using the platinum working electrode. A typical linear sweep voltammogram for a 0.1 M HCl solution of a nitrate sample treated with sulphuric acid is shown in Fig. 1. Two reduction waves were observed with peak potentials of 0.55 and 0.27 V *versus* Hg - Hg_2SO_4, although the potential of the first wave was difficult to determine due to the large anodic process present at potentials greater than 0.6 V. The small peak observed at approximately −0.05 V was probably due to reduction of an oxide species on the electrode surface as it was not present following pre-treatment of the electrode and increased with time after pre-treatment. The anodic wave at potentials greater than 0.6 V was believed to be due to oxidation of chloride to chlorine as no wave was present at this potential when chloride was absent. The peaks at 0.55 and 0.27 V reached maximum heights after about 30-min reaction time. Cyclic voltammetry gave an anodic peak on the reverse scan (not shown) at 0.34 V, which represents a 70-mV separation with the peak obtained on the forward scan at 0.27 V. The first wave was too close to the anodic wave for its reversibility to be assessed by cyclic voltammetry. Linear sweep voltammograms of a solution of nitrite in 9 M sulphuric acid in the absence of chloride showed three cathodic waves with half-wave potentials of 0.39, 0.01 and −0.30 V (Fig. 2) and an anodic wave which started at approximately 0.60 V. Addition of 1.3 ml of concentrated HCl (final concentration 0.1 M) produced a marked change in the voltammograms with the peak potential of the first wave being at 0.28 V and the height being approximately the same as for the first peak obtained in the absence of chloride. The second peak was also shifted to −0.10 V and was less well defined. The third electrochemical process at 0.04 V was unchanged. No major change in peak

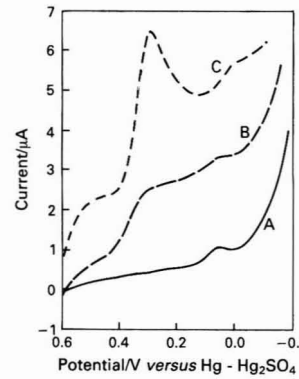

Fig. 1. Linear sweep voltammograms of nitrate in 9 M sulphuric acid solution at a platinum electrode. Scan speed, 10 mV s^{-1}; and nitrate concentration: A, 0; and B and C, 1×10^{-3} M. Chloride concentration: A, 0; and B and C, 0.1 M. B was recorded immediately on mixing and C, 10 min after mixing

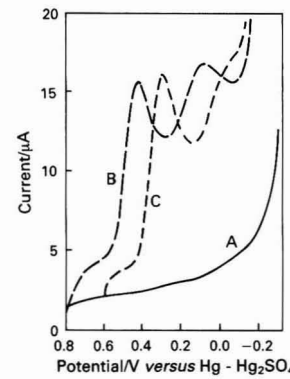

Fig. 2. Effect of the addition of chloride on linear sweep voltammograms of nitrite in 9 M sulphuric acid solution. Scan speed, 10 mV s^{-1}; and nitrite concentration: A, 0; and B and C, 1×10^{-3} M. Chloride concentration: A and B, 0; and C, 0.1 M

height was observed with increasing time after mixing, in contrast to the situation for the reaction with nitrate. The effect of increasing the chloride concentration was to shift the potential of the first peak to less positive values at 51 mV per decade change in chloride concentration. Cyclic voltammetry (5 mV s^{-1}) of nitrite with and without chloride gave cathodic - anodic peak separations of 70 mV. These results indicate that a nitrogen(III) species is being reduced at the electrode, and that nitrate is being reduced to this species by chloride in the concentrated sulphuric acid medium.

Schmid and Lobeck[17] studied the voltammetric characteristics of nitrite in 6 M sulphuric acid using a platinum electrode. They found three cathodic waves with $E_{\frac{1}{4}}$ values of 0.9, 0.55 and 0.2 V *versus* a normal hydrogen electrode; these they attributed to the following reduction processes:

$$NO^+ + e^- \rightarrow NO$$
$$NO + e^- \rightarrow NO^-$$
$$NO^- + 2e^- + 3H^+ \rightarrow NH_2OH$$

The first wave was shown to be diffusion controlled in highly acidic media (>9 M sulphuric acid), but kinetically controlled at lower acidities due to the slow formation of NO^+ preceding the electron transfer:

$$HNO_2 + H^+ \rightarrow NO^+ + H_2O$$

The size and potentials of the cathodic waves obtained here are in good agreement with the results of Schmid and Lobeck.[17] Coenegracht *et al.*[15] investigated the reaction of nitrite with chloride and bromide and attributed the reduction wave, at +0.6 V *versus* a saturated calomel reference electrode (SCE) obtained at platinum electrodes, to reduction of nitrosyl halide.

Further evidence to support the theory that nitrosyl chloride is the species being reduced was obtained by studying the effect of addition of chloride on the voltammetric response obtained when both nitrite and nitrate were present in solution. The results of this study are given in Table 1. Clearly, addition of nitrate increases 5-fold the size of the reduction peak of nitrite in the absence of chloride. In the presence of both nitrate and chloride, however, the peak size (now for reduction of nitrosyl chloride) is reduced again to approximately the same size as in the absence of nitrate.

Table 1. Inhibition by chloride of the catalytic reduction of nitrate by nitrite. Scan speed 5 mV s^{-1}, solutions stirred for 30 s before each scan

Solution composition*	E_p/V	i_p/μA
1.3×10^{-3} M NO_2^- . .	−0.390	4.5
1.3×10^{-3} M NO_3^- . .	−0.375	21.0
$+1.5 \times 10^{-2}$ M HCl	−0.310	6.5
$+3.0 \times 10^{-2}$ M HCl	−0.270	5.3

* Solutions in 9 M sulphuric acid, same solution used with sequential additions made as shown.

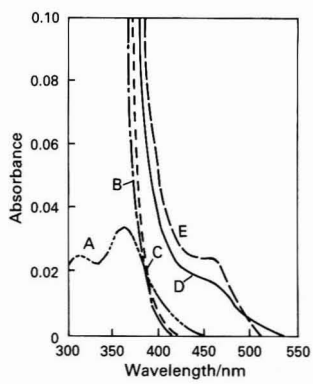

Fig. 3. Effect of the addition of chloride on the UV - visible spectra of nitrate and nitrite in 9 M sulphuric acid solution. [Nitrate] and [nitrite], 0.01 M; and [chloride], 1 M. A, Chloride only; B, nitrite only; C, nitrate only; D, nitrate and chloride; and E, nitrite and chloride

Nitrate has been shown previously[17] to have a catalytic effect on the reduction of nitrite. A mechanism has been suggested by Vetter[18] as follows:

$$HNO_2 + H^+ \rightarrow NO^+ + H_2O$$
$$NO^+ + NO_3^- \rightarrow 2NO_2$$
$$H^+ + NO_2 \rightarrow HNO_2^+$$
$$HNO_2^+ + e^- \rightarrow HNO_2$$
$$NO_3^- + 3H^+ + 2e^- \rightarrow HNO_2 + H_2O$$

Addition of chloride and the formation of nitrosyl chloride might be expected to remove NO^+ from solution thus preventing the catalytic action of nitrate.

Supporting evidence that the peak at +0.27 V is due to nitrosyl chloride was obtained from UV - visible spectrophotometry. An additional absorption peak is seen at approximately 450 nm on addition of chloride to nitrite or nitrate in 9 M sulphuric acid (Fig. 3). The absorption peak remained of constant height for nitrite solutions but increased with time when nitrate solutions were used, indicating continuing reaction. Nitrosyl chloride has been studied in the gas phase[19] and shown to have a weak absorption band in the visible region at 475 nm. Both Schmid and Maschka[20] and Bayliss and Watts[21] investigated the reaction of nitrite with chloride in aqueous acidic solutions, and attributed transition bands at approximately 450 nm to nitrosyl chloride.

The first voltammetric peak obtained with the nitrate reaction mixture is believed to be due to the reduction of chlorine. Armstrong[13] studied the UV spectrum of nitrate in solutions of sulphuric acid (>45%) with and without chloride present, and proposed that chloride reduces the nitrate to nitrosyl chloride, whilst the chloride is oxidised to chlorine. Using an extraction procedure with carbon tetrachloride an absorption peak was obtained at 320 nm which was attributed to chlorine. Chlorine can be reduced to chloride on platinum electrodes.[21]

If the reduction wave at +0.27 V is due to reduction of nitrosyl chloride, it would appear from the data obtained here that nitrosyl chloride is the predominant species present in solution. However, Schmid and Maschka[20] calculated the equilibrium constant for the reaction

$$HNO_2 + Cl^- + H^+ \rightarrow NOCl + H_2O$$

to be 1.1×10^{-3} at 25 °C from absorbance measurements at 430 nm. Bayliss and Watts[21] criticised this value, as 430 nm is not the maximum of the visible transition and the absorbance to concentration ratio did not reach a maximum even in the most concentrated acid.

In summary, it is believed that the chemical reduction of nitrate by chloride in concentrated sulphuric acid solutions is as proposed by Armstrong[13]:

$$HNO_3 + 2HCl \rightarrow HNO_2 + H_2O + Cl_2$$
$$HNO_2 + HCl \rightarrow NOCl + H_2O$$

or

$$HNO_3 + 3HCl \rightarrow NOCl + 2H_2O + Cl_2$$

The chlorine, nitrosyl chloride and nitrous acid are reduced at a platinum electrode as follows:

$$Cl_2 + 2e^- \rightarrow 2Cl^-$$
$$NOCl + e^- \rightarrow NO + Cl^-$$
$$HNO_2 + H^+ \rightarrow NO^+ + H_2O$$
$$NO^+ + e^- \rightarrow NO$$

Flow Injection

Initial studies were made using glassy carbon electrodes but prolonged use of these electrodes affected the electrode

surface and a re-polishing procedure had to be undertaken after 30–60 min of use. Wang and Hutchins[22] have described an electrode pre-treatment procedure for use on glassy carbon electrodes in chloride media, the results of which are attributed to chlorine attack on the carbon, which may explain the effect seen here. Unless otherwise stated all work described below was performed with a platinum electrode.

Effect of chloride/bromide concentration in the carrier stream

When chloride was added as hydrochloric acid the nitrate signal was slightly higher than when chloride was added as potassium chloride. More importantly, however, the use of hydrochloric acid gave a lower blank value when sulphuric acid was injected into the carrier stream (see Table 2). Clearly the use of an acidic carrier stream is advantageous and this was adopted here. The linear sweep voltammograms indicate that the reaction only proceeds if the sulphuric acid concentration is >45%, and the use of hydrochloric acid in the carrier stream allows a longer reaction time before the hydrogen ion concentration falls below this critical value. The signal obtained on injection into a blank carrier stream is due to background faradaic and capacitance currents.

Initially a 1 M hydrochloric acid concentration was used in the carrier stream but at nitrate concentrations greater than 1 mM the signal response became non-rectilinear. It was found that a 2 M hydrochloric acid concentration gave a linear response over the nitrate concentration range of interest (5×10^{-4}–5×10^{-3} M). At higher chloride concentrations peak heights became erratic due to the formation of bubbles of hydrogen chloride following the injection (see later).

Bromide, as potassium bromide, was used in the carrier stream with and without the presence of chloride. Although the signals were higher with bromide present, the reproducibility was poor with coefficients of variation of approximately 15%. The signals obtained when injecting into a blank carrier stream containing bromide were also higher. The equilibrium constant for nitrosyl bromide formation has been shown to be 40 times greater than that for nitrosyl chloride formation,[23–25] and has been shown to give larger reduction currents at equivalent concentrations.[14,15] No further work was carried out with bromide present.

Effect of sulphuric acid concentration of injectate

It can be seen from Table 3 that a small decrease in the concentration of the sulphuric acid injected into the carrier stream produced a large decrease in signal size. All further work was performed by injecting concentrated sulphuric acid (98%).

Effect of length and type of transmission tubing

The decrease in signal size with increasing length of transmission tubing above the minimum practical length (0.5 m) (Fig. 4), together with the data shown in Table 3 showing the effect of even a slight dilution of the concentrated sulphuric acid, indicates that the reaction takes place within the first few centimetres of tubing. The ratio of the signal to the peak height obtained when injecting into a blank carrier stream was found to be virtually independent of tubing length. The use of "knotted" tubing or an SBSR immediately after the injection valve was found to increase the peak height. The use of a 40-cm SBSR connected to the valve increased the peak height by *ca.* 25% of that obtained with a coiled piece of tubing of the same length whilst giving a slightly lower blank signal.

It has been shown that SBSRs increase mixing while limiting dispersion[25] when compared with "normal" coiled tubing. Results obtained here are consistent with this theory and a 40-cm SBSR was used in all further work. Use of longer SBSRs was impracticable as the increased back-pressure generated caused tubing connections to leak. A further advantage of the SBSR was the prevention of bubbles forming on the tubing. Large numbers of small bubbles were formed immediately following injection of the concentrated sulphuric acid and these were believed to consist of hydrogen chloride with possibly a small amount of chlorine formed during the

Table 2. Comparison of peak heights obtained when potassium chloride or hydrochloric acid was added to the sample carrier stream. Flow-rate = 2.5 ml min^{-1}, transmission tube length = 2 m, glassy carbon electrode, measurement potential = +0.3 V and injection volume = 25 µl

	Peak height/µA	
Reagent	Nitrate (1×10^{-3} M)	Blank
1 M HCl	2.6	−0.2
1 M KCl	2.3	0.5

Table 3. Effect of the concentration of the sulphuric acid injected on peak height. $[NO_3^-] = 10^{-3}$ M, [HCl] = 1 M, glassy carbon electrode, measurement potential = +0.3 V, transmission tube length = 2 m, flow-rate = 2.5 ml min^{-1} and injection volume = 25 µl

Sulphuric acid, %	Peak height/µA
98*	2.55
90	0.42
75	0.02
50	0.00

* Concentrated.

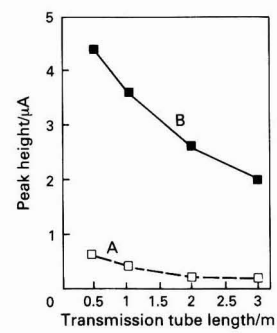

Fig. 4. Effect of transmission tube length (open tube) on the flow injection signal height obtained at a glassy carbon electrode. Flow-rate, 2.5 ml min^{-1}; potential, +0.3 V; injection volume, 25 µl; and carrier stream, 1 M hydrochloric acid. [Nitrate]: A, 0; and B, 1×10^{-3} M

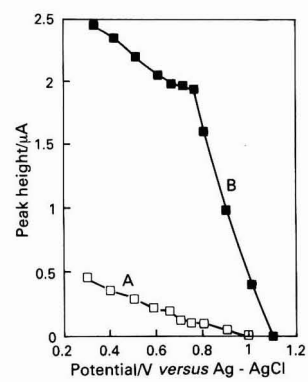

Fig. 5. Effect of measurement potential on the flow injection signal size obtained at a platinum electrode. Flow-rate, 6 ml min^{-1}; injection volume, 25 µl; transmission tube, 40-cm SBSR. [Nitrate]: A, 0; and B, 5×10^{-4} M

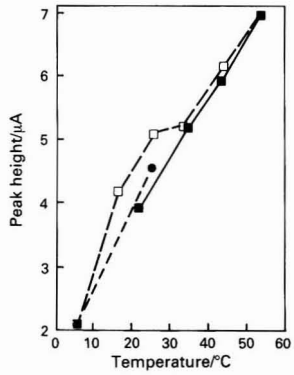

Fig. 6. Effect of temperature on the peak height. Flow-rate, 6 ml min^{-1}; injection volume, 25 μl; transmission tube, 40-cm SBSR. [Nitrate], 1×10^{-3} M. ■, Temperature increasing; □, temperature decreasing; ●, final temperature

Table 4. Calibration data. Flow-rate = 6 ml min^{-1}, measurement potential = +0.7 V, injection volume = 25 μl, temperature = 24.5 °C and 40-cm SBSR. Coefficient of variation at each nitrate level (6 determinations) = <4%

[Nitrate]/ 10^{-3} M	Peak height/ μA
5.0	19.8
4.0	16.1
3.0	12.1
2.0	7.94
1.0	3.84
0.8	3.01
0.6	2.29*
0.4	1.50*
0.2	0.84*
0.0	0.24*

* Negative peak of approximately −0.2 μA preceded the positive signal.

reduction. Using ordinary coiled tubing, not all of this gas re-dissolved and a build-up of bubbles occurred, which gave spurious peaks when they became detached from the tubing wall. This problem was not encountered when using the SBSR, as the bubbles were quickly re-dissolved as the acid was diluted during further dispersion. It should be noted that the back-pressure provided by the Dionex cell is also important in preventing bubble formation.

Effect of injection volume

When used in conjunction with a 40-cm SBSR and a 2 M hydrochloric acid carrier stream it was found that injection volumes >25 μl generated more hydrogen chloride than could be re-dissolved before reaching the detector. This resulted in poor reproducibility and a noisy base line. A volume of 25 μl was the smallest that could be injected conveniently by means of the valve and this volume was therefore used in all further work.

Effect of applied potential

The hydrodynamic potential - current curve given in Fig. 5 shows that maximum sensitivity was obtained at the least-positive potentials, although the blank signals also increased. A potential of +0.3 V was used for most of the work performed here. However, it was found that the use of an applied potential of +0.7 V gave an increase in the signal to blank ratio and also overcame interference from Cu^{2+} and Fe^{3+} (see later).

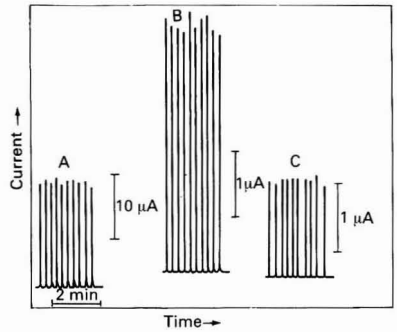

Fig. 7. Typical flow injection signals obtained for calibration purposes. [Nitrate]: A, 4×10^{-3}; B, 1×10^{-3}; and C, 4×10^{-4} M

Table 5. Effect of addition of plant mineral nutrients on signal size relative to signal size with no added nutrient. Flow-rate = 6 ml min^{-1}, measurement potential = +0.3 V, temperature = 25 °C, injection volume = 25 μl and transmission tube = 40-cm SBSR

Nutrient	Amount added/ mg l^{-1}	Relative signal size, % Nitrate (5×10^{-4} M)	Nitrate (5×10^{-3} M)
Cl^-	200	104	99
	500	105	98
	1000	97	99
	5000	105	96
PO_4^{3-}	10	101	97
	100	97	98
$H_2BO_3^-$	10	98	100
	100	95	99
MoO_4^{2-}	10	106	99
	100	104	100
Mg^{2+}	100	99	99
	500	98	97
Zn^{2+}	10	100	102
	100	97	102
Ni^{2+}	10	95	101
	100	99	100
Mn^{2+}	10	99	103
	100	100	102
Cu^{2+}	1	95	98
	10	63	89
	100	*	*
Ca^{2+}	100	102	97
	500	100	99
NH_4^+	10	101	99
	100	100	99
Fe^{2+}	1	98	97
	10	86	97
	100	66	78
Fe^{3+}	1	97	101
	10	57	98
	50	*	80
EDTA†	10	104	101
	50	105	98

* Background current swamps peak.
† EDTA = Ethylenediaminetetraacetic acid.

Effect of flow-rate

Little difference in peak height was seen over a flow-rate range of 2–6 ml min^{-1}, but reproducibility was marginally improved at the highest flow-rate studied. At flow-rates lower than 4 ml min^{-1}, peak heights were decreased slightly and coefficients of variation of >6% were obtained. A flow-rate of 6 ml min^{-1} was therefore used.

Table 6. Effect of addition of all mineral nutrients at highest levels indicated in Table 5 on peak height and reproducibility. Flow-rate = 6 ml min^{-1}, measurement potential = +0.3 V, temperature = 25 °C, injection volume = 25 µl and transmission tubing = 40-cm SBSR. Nitrate concentration = 5×10^{-4} M

Mineral nutrients	Peak height/ µA	Coefficient of variation, %
No	1.74	3.4
Yes	1.81	4.4

Effect of temperature

The reaction is sensitive to temperature (Fig. 6) and at 25 °C a 1 °C increase in temperature produced a 3% increase in peak height. A type of hysteresis was evident when the temperature was increased then lowered and increased again. Although the initial increase in signal size with increasing temperature was reproducible, the effect of decreasing the temperature from 60 °C was somewhat variable; this may have been caused by inadequacies in the thermostatic control. As the temperature of greenhouses in which hydroponics are used is known to vary considerably, it would appear to be necessary to control the temperature of the flow injection system.

Linearity and reproducibility of the reaction

A rectilinear response was obtained over a measured nitrate concentration range of 1×10^{-4}–5×10^{-3} M and the signal size and coefficients of variation obtained are given in Table 4. Typical flow injection traces are shown in Fig. 7. A limit of detection, measured as twice the size of the blank signal, of 9×10^{-5} M nitrate was obtained.

Effect of possible interferents

The composition of hydroponics various according to their application.[26] The most commonly used mineral nutrients were added to the nitrate solutions at concentrations in excess of those normally found, and the results are shown in Table 5. Chloride was added as the potassium salt, sulphate and molybdate as the sodium salts, phosphate as orthophosphoric acid and other metals as sulphates.

Interference caused by Cu^{2+} and Fe^{3+} was due to the metal ion being reduced at the electrode rather than interference with the reaction, as the background current increased with increasing concentration of both metals. Using an applied potential of +0.7 V no interference was evident for concentrations of Cu^{2+} and Fe^{3+} up to 100 mg l^{-1} but Fe^{2+} does reduce the peak height. The Fe^{2+} is oxidised at +0.7 V and is also known to react with nitrate in concentrated sulphuric acid to produce nitrosyl hydrogen sulphate.[27] Iron is normally added to hydroponics as the Fe^{3+} - EDTA complex and the concentration of Fe^{2+} is believed to be negligible. As a final check, the various species listed above (except for Fe^{2+}) were added at the highest concentrations indicated in Table 4 to a 5×10^{-4} M nitrate solution with little change in peak height or reproducibility (Table 6).

The authors thank the Agricultural and Food Research Council for financial support, and they were grateful to the late Mr. A. B. Marsden for advice in the preparation and use of single bead string reactors.

References

1. Albery, W. J., Haggett, B. G. D., Jones, C. P., Pritchard, M. J., and Svanberg, L. R., *J. Electroanal. Chem.*, 1985, **188**, 257.
2. Trojanek, A., and Opekar F., *J. Electroanal. Chem.*, 1986, **214**, 125.
3. Nygaard, D. D., *Anal. Chim. Acta*, 1981, **130**, 391.
4. Hulanicki, A., Matuszewski, W., and Trojanowicz, M., *Anal. Chim. Acta*, 1987, **194**, 119.
5. Wood, E. D., Armstrong, F. A. J., and Richards, F. A., *J. Mar. Biol. Assoc. U.K.*, 1967, **47**, 23.
6. "Nitrate and Nitrite in Water and Seawater," Industrial Method No. 158-71 W/A, Technicon Industrial Systems, Tarrytown, NY, 1977.
7. "Standard Methods for the Examination of Water and Freshwater," Fifteenth Edition, American Public Health Association, New York, 1981, p. 370.
8. Skicko, J. I., and Tawfik, A., *Analyst*, 1988, **113**, 297.
9. Fogg, A. G., Scullion, S. P., and Edmonds, T. E., *Analyst*, 1989, **114**, 579.
10. Afghan, B. K., Leung, R., Kulkarni, A., and Ryan, J. F., *Anal. Chem.*, 1975, **47**, 556.
11. Nakamura, M., *Analyst*, 1981, **106**, 483.
12. Velghe, N., and Claeys, A., *Analyst*, 1983, **108**, 1018.
13. Armstrong, F. A. J., *Anal. Chem.*, 1963, **35**, 1293.
14. Fogg, A. G., Bsebsu, N. K., and Abdalla, M. A., *Analyst*, 1982, **107**, 1040.
15. Coenegracht, P. M. J., Franke, J. P., and Metting, H. J., *Anal. Chim. Acta*, 1973, **65**, 375.
16. Taylor, M. G., *PhD Thesis*, Loughborough University of Technology, 1988.
17. Schmid, G., and Lobeck, M. A., *Ber. Bunsenges Phys. Chem.*, 1969, **73**, 189.
18. Vetter, K. J., *Z. Elektrochem.*, 1959, **63**, 1189.
19. Goodeve, C. F., and Katz, S., *Proc. R. Soc. London, Ser. A*, 1939, **172**, 432.
20. Schmid, H., and Maschka, A., *Z. Phys. Chem., Abt. B*, 1941, **49**, 171.
21. Bayliss, N., and Watts, D. W., *Aust. J. Chem.*, 1956, **9**, 319.
22. Wang, J., and Hutchins, L. D., *Anal. Chim Acta*, 1985, **167**, 325.
23. Schmid, H., and Hallaba, E., *Monatsh. Chem.*, 1956, **87**, 560.
24. Schmid, H., and Fouad, M. G., *Monatsh. Chem.*, 1957, **88**, 631.
25. Reijin, J. M., Van der Linden, W. E., and Poppe, H., *Anal. Chim. Acta*, 1981, **126**, 1.
26. Noggle, G. R., and Fritz, G. J., "Introductory Plant Physiology," Prentice Hall, Englewood Cliffs, 1976, p. 236.
27. Asplund, J., *J. Hazard Mater.*, 1984, **9**, 13.

Paper 9/03095F
Received July 24th, 1989
Accepted October 6th, 1989

Simultaneous Determination of Total and Free Calcium in Milk by Flow Injection*

Jacobus F. van Staden and Ancel van Rensburg
Department of Chemistry, University of Pretoria, Pretoria 0002, South Africa

A fast and reliable procedure for the determination of total and free calcium in milk is described. The method is based on the flow injection (FI) technique. Total calcium is determined by atomic absorption spectrometry (AAS) (422.7 nm) and free calcium by spectrophotometry (580 nm). Interference in the determination of free calcium is eliminated by using a dialyser, which also separates the total and free calcium. Interference from phosphates in milk in the determination of total calcium by AAS is overcome by using a dinitrogen oxide - acetylene flame with the necessary suppression with K^+. With 30-μl samples the FI system covers a standard working range of 100–1500 mg dm^{-3} of Ca^{2+}. The system is suitable for the simultaneous determination of total calcium (relative standard deviation <1.30% for 1300–1500 mg dm^{-3} of total calcium) and free calcium (relative standard deviation <0.85% for 120–170 mg dm^{-3} of free calcium) in milk at a sampling frequency of about 60 samples h^{-1}. The results obtained agree reasonably well with results from the AAS method.

Keywords: *Milk; flow injection spectrometry; dialysis membrane; total and free calcium determination*

The high biological value of calcium in milk is well known. Calcium forms an integral part of the daily diet of people as, for example, one of the components necessary in the formation of bone structure, especially for infants and children.

Two-thirds of the calcium present in milk is bound to proteins, while the remaining third is diffusible. The univalent ions Na^+, K^+ and Cl^- exist in milk largely as free ions, but the multivalent ions such as Ca^{2+} and Mg^{2+} form complexes.[1]

The two methods that appear to be used almost universally for the determination of calcium in milk are atomic absorption spectrometry (AAS) and spectrophotometry. The former is particularly useful in the determination of total calcium, while spectrophotometry with dialysis can be used to determine free calcium. It is possible to determine both total and free calcium simultaneously by incorporating a dialyser into the conduits of a flow injection (FI) system. In the determination of total calcium by AAS the dinitrogen oxide - acetylene flame is used to overcome interference from phosphates in milk. This, however, enhances the partial ionisation of calcium, which is suppressed by the addition of a more readily ionisable element such as potassium (as KNO_3).

The spectrophotometric method for the determination of free calcium is based on the reaction between a metal indicator and calcium using the correct conditions, *e.g.*, pH. Calmagite[2] and cresolphthalein complexone (CPC)[3,4] are two metal-complexing agents that can be used for the spectrophotometric determination of calcium. The use of CPC is preferred, owing to some disadvantages in the use of calmagite. Magnesium forms a more stable complex with calmagite than does calcium.[5] Phosphate, copper, iron and aluminium interfere[5,6] in the analytical procedure while the free indicator gives background absorbance at pH 10 in the spectrophotometric method. Cresolphthalein complexone forms $Ca(CPC)^{4-}$, $CaH(CPC)^{3-}$ and $Ca_2(CPC)^{2-}$ complexes with Ca^{2+} (or Mg^{2+}).[3] A weak absorbing complex $H_2(CPC)^{4-}$ is also formed.[3] The concentration of these species is a function of pH, metal ion concentration and ionic surroundings. The colour formed by the CPC complex is the result of the formation of a lactone ring in the phthalein molecule.[3] The colour formation is enhanced by bivalent metals and an increase in pH.

The reaction between CPC and calcium at pH 10–11 can be written as[7]:

$$H_2(CPC)^{4-} \underset{}{\overset{Ca^{2+}}{\rightleftharpoons}} Ca(CPC)^{4-}$$

$$\underset{\text{colourless}}{[H_3(CPC)^{3-}]} \overset{Ca^{2+}}{\rightleftharpoons} \underset{\text{pink}}{[CaH(CPC)^{3-}]}$$

Many variants of the manual method have been used. The batchwise mode involved in manual procedures is, however, time consuming for laboratories in which a high sample output is necessary. Most continuous-flow analytical procedures involve the use of a procedure similar to that used by Kessler and Wolfman[8] for the determination of calcium with CPC and diethylamine - sodium acetate as a base component. The absorbance of the calcium - CPC complex is measured at 580 nm and pH 12.0. Working at this pH and wavelength gave less interference from magnesium. Gitelman[9] improved this method by introducing quinolin-8-ol to eliminate interference from magnesium and by measuring the absorbance of the complex at 570 nm. Roach[10] applied this method with a sampling rate of 60 samples h^{-1} to the determination of calcium in animal feeds, measuring the absorbance of the complex at 580 nm and pH 10.7. Moorehead and Biggs[11] modified this method by replacing the toxic and volatile diethylamine (pK_a 11.0) with the more stable 2-amino-2-methylpropan-1-ol (AMP) (pK_a 9.6) as a base solution. The CPC reagent is almost colourless at pH 10, but highly coloured at pH 12; therefore, the blank was reduced and the sensitivity was increased. Moorehead and Biggs reported that as the interference from magnesium was eliminated by using quinolin-8-ol, it was not necessary to work at the higher pH. Basson and van Staden[12] found that AMP as base gave a sufficiently stable solution for the FI determination of calcium in animal feeds, which obviates the use of toxic potassium cyanide as stabiliser.

Proteins in milk interfere in the determination of calcium when using CPC as reagent and should therefore be eliminated. This can be carried out by wet digestion, and deproteinising with sodium tungstate and sulphuric acid, or by dialysis. One of the disadvantages of deproteinising and wet digestion is that it leads to a decrease in the sampling rate, whereas dialysis not only eliminates interference from

* Presented at SAC 89, the 8th SAC International Conference on Analytical Chemistry, Cambridge, UK, 30 July–5 August, 1989.

proteins but also facilitates the determination of free calcium. Joe *et al.*[13] reported a segmented, continuous-flow method for the determination of calcium in milk at a sampling rate of 20 samples h^{-1}, involving digestion of the samples before analysis. An automated segmented continuous-flow system equipped with a dialyser has also been reported for the determination of calcium in blood.[14] Flow-through dialysers are extremely useful components in analytical flow systems, particularly in manifolds for FI. As the efficiency of dialysis in a continuously moving stream is only *ca.* 0.5–4%, the dialyser serves not only as a separator of substances to be determined from interfering components, but also as an effective diluter of substances.

The determination of total and free calcium in milk, however, still remains a problem. It was obvious that the best way to solve this problem was the incorporation of a dialyser as part of the manifold in the FI system. Basson and van Staden[15] described an FI dialysis system for the determination of calcium in milk, measuring the absorbance of the dialysed calcium as a calcium - CPC complex at 580 nm. The method, however, suffers severe drawbacks due to the fact that it is only suitable for determining either total or free calcium. Protein digestion was used to produce total calcium. The pre-treatment of samples is time consuming, expensive and may also result in lack of precision. By combining an FI dialysis system with suitable detectors it was possible to distinguish between total and free calcium. Taking advantage of this possibility, an FI method was developed for the simultaneous determination of these two calcium components in milk, and this paper describes the work carried out in this regard.

Experimental

Reagents and Solutions

All reagents were prepared from analytical-reagent grade chemicals unless specified otherwise. Doubly distilled water was used throughout. The main solutions were prepared as follows.

Cresolphthalein complexone reagent. The solution was prepared by dissolving 0.10 g of CPC, obtained from BDH, in 40 cm^3 of 5.0 mol dm^{-3} hydrochloric acid in a 2-dm^3 flask. Then 2.0 g of quinolin-8-ol were added while swirling the flask gently. The solution was diluted quantitatively with distilled water.

Base solution. The solution was prepared by dissolving 70.0 g of AMP in 500 cm^3 of distilled water.

Standard calcium solution. A calcium stock solution was prepared by dissolving 24.98 g of analytical-reagent grade calcium carbonate carefully in approximately 0.5 mol dm^{-3} hydrochloric acid, added dropwise until all of the calcium carbonate had just dissolved. The solution was boiled for a few minutes in order to remove carbon dioxide. The calcium solution was then neutralised with approximately 0.1 mol dm^{-3} potassium hydroxide solution, adjusting the pH to *ca.* 6 whereafter it was diluted to 1 dm^3 with distilled water in order to obtain a stock solution containing 10 g dm^{-3} of calcium. Working solutions containing calcium in the range 100–1500 mg dm^{-3} were prepared by suitable dilution of the stock solution. The same standard working solutions were used for both total and free calcium in the proposed FI system. The recorder range on the dual pen recorder was attenuated in such a way that differentiation between the two detecting devices was possible on recorder tracings.

Potassium solution. For the removal of ionic interference 6.4650 g of potassium nitrate were dissolved in 1 dm^3 of water to give a solution containing 2500 μg cm^{-3} of K^+.

Apparatus

A Carle micro-volume two-position sampling valve with two identical sample loops, each having a volume of 30 μl, was used. The sampling unit was made by Cenco and was used with a Cenco peristaltic pump, operating at 10 rev min^{-1}. An optimum sample throughput of 60 samples h^{-1} was obtained. A Philips SP6-550 spectrophotometer was used at 580 nm and a Varian AA-175 atomic absorption spectrometer at 422.7 nm. The spectrometer lamp current was 10.5 mA and the slit width 1 nm. In the flow system, transmission tubing with an i.d. of 0.76 mm was used. A 160 × 30 × 25 mm dialysis unit was incorporated into the FI system, using a Technicon Type C dialysis membrane with a dialysis membrane path length of 300 mm. The i.d. of both the donor and recipient channels was 0.5 mm.

Results and Discussion

The flow diagram for the simultaneous determination of total and free calcium is shown in Fig. 1. The manifold consists of Tygon tubing (0.76 mm i.d.), cut into the required lengths and wound around glass tubes of length 10 cm and width 1 cm. The efficiency of on-line continuous dynamic dialysis depends on various factors, including the flow-rates of the pumping tube in the carrier and recipient streams and the pressure drop in the carrier stream. Dispersion in a long dialyser is also less with co-flow than with counter-flow, and co-flow was therefore preferred in the proposed system.

It was also clear from the results obtained that optimum precise mass transfer of free Ca^{2+} through the semi-permeable Technicon Type C membrane was possible when the same carrier and recipient flow-rates were used. This ensured that the dialysis process did not alter the geometry of the sample plug injected, but that the dialysate formed an identical diluted protein-free plug on the recipient side of the membrane. The use of acidified CPC reagent as recipient stream resulted in a slight increase in peak height. This indicated that acidified CPC as recipient stream disturbs the dialysis process in such a way that more calcium is dialysed than with water as recipient stream. For optimum performance and to obviate any possibility of a decrease in accuracy due to this phenomenon, CPC reagent was added further downstream after dialysis had been completed (Fig. 1). This was followed by an optimised amount of AMP solution as originally described by Gitelman[9] and Basson and van Staden.[15] Water was also used as carrier stream for optimum performance, and potassium nitrate was introduced further downstream (Fig. 1) in the total calcium channel before detection by AAS. The addition of

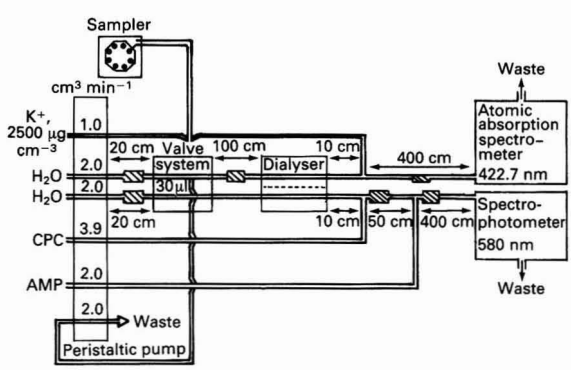

Fig. 1. Flow diagram for the simultaneous determination of total and free calcium in milk. Valve loop size, 30 μl; sampler, 60 s; wash, 0 s; valve actuation, at 58 s; sampling rate, 60 samples h^{-1}; tubing i.d., 0.76 mm

Table 1. Determination of total and free calcium by AAS and by the proposed method (Fig. 1)

	Free calcium			Total calcium		
No.	AAS, p.p.m.	FI, p.p.m.	RSD, *%	AAS, p.p.m.	FI, p.p.m.	RSD, *%
1	155	160	0.58	1310	1350	1.05
2	150	158	0.78	1300	1340	1.03
3	132	150	0.65	1308	1342	1.23
4	148	155	0.85	1300	1337	0.99
5	160	165	0.76	1450	1500	1.30

* Mean result of 15 analyses in each instance, with relative standard deviation for the proposed FI method.

potassium suppresses calcium ionisation, ensuring optimum accurate determination of total calcium. Incorporation of a dialyser into the conduits of the FI system also facilitates the possibility of the use of a single series of standard working calcium solutions in the range 100–1500 mg dm^{-3} for the simultaneous determination of total and free calcium. A single series of standard working calcium solutions (range 100–1500 mg dm^{-3}) was therefore injected into the proposed FI on-line dialysis system for calibration of both total and free calcium. The calcium standards for the determination of total calcium were channelled directly via the donor carrier stream to the AAS detector for measurement. The calcium standards for the determination of free calcium were at the same time dialysed, and the dialysate was channelled as a product, after reaction with CPC, to the spectrometer. In this way, it was unnecessary to remove the dialyser to allow calibration for total calcium.

Results revealed that the Technicon Type C membrane used showed a dialysis efficiency of 2.8% for a 300-mm dialysis membrane path length when 30-μl portions of a series of standard solutions were injected and water was used as carrier donor and recipient stream at flow-rates of 3.9 cm^3 min^{-1}, respectively. Calculations demonstrated that this amounted to a theoretical loss of 42 mg dm^{-3} on the total calcium value, due to diffusion through the membrane alone if a real sample calcium level of 1500 mg dm^{-3} was present. The percentage dialysis increased slightly to *ca.* 3.10% when milk protein (mainly casein) samples were injected, using the same experimental conditions as above. This gave a theoretical loss of 47 mg dm^{-3} on the total calcium value of 1500 mg dm^{-3}. Although the protein raised the dialysis rates in such a way that it seemed that the percentage dialysis increased to give a difference of about 0.3%, results indicated that it could be the maximum difference possible. In the proposed FI on-line dialysis system, the standards and samples were handled in exactly the same way, high flow-rates of 3.90 cm^3 min^{-1} in both the donor and recipient streams were used, and the plug flow sample mode gave an optimum membrane surface area/sample ratio; all factors enhanced the already insignificant differences in the amount of calcium lost to a more insignificant difference in results. It was also clear from the calculations carried out above that the minor differences obtained, due to the slightly different diffusion rates observed for sample and standards, did not influence the results significantly. The above-mentioned experimental conditions used also tended to equalise diffusion rates between samples and standards. This is confirmed by the results shown in Table 1.

No fouling problems were experienced with any of the dialysis membranes used, which is a possibility, owing to the nature of the samples. This was also attributed to the small amount of milk samples injected and to the procedure of pumping doubly distilled water for about 15 min through both channels during the shut-down period of the FI system.

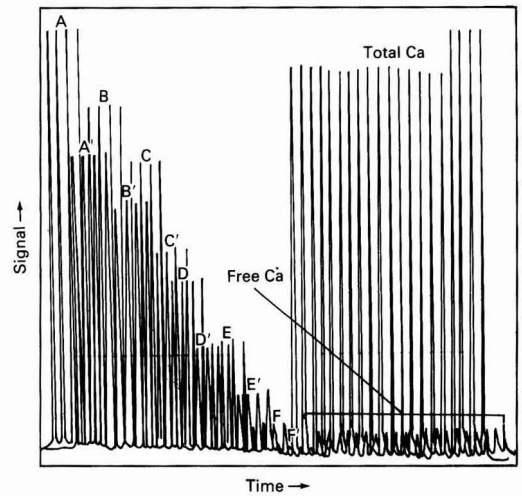

Fig. 2. Typical strip-chart recording for the simultaneous determination of total and free calcium in milk. Recorder paper speed, 30 cm h^{-1}; and recorder range, 10 mV (for total calcium) and 2 mV (for free calcium). Concentration of calcium in the standard calcium solution: for total calcium, A, 1500; B, 1000; C, 600; D, 400; E, 200; and F, 100 mg dm^{-3}; and for free calcium, A', 1500; B', 1000; C', 600; D', 400; E', 200; and F', 100 mg dm^{-3}. Five samples were injected, each four times

Fig. 2 illustrates recorder tracings of a representative run at a sampling rate of 60 samples h^{-1} for the determination of total and free calcium. Each standard and sample was injected four times. The performance of the proposed method is shown in Table 1. The results obtained for total calcium by the proposed FI system were also compared with values obtained for the same milk samples analysed manually by a standard AAS method. Milk samples were also dialysed on a non-segmented continuous-flow system and the dialysate was collected. The results obtained for free calcium by the proposed method were compared with the values obtained for the milk dialysate analysed manually by a standard AAS procedure and by a direct standard FI procedure. It is clear from Table 1 that comparable results were obtained with the proposed FI system and standard method. The relative standard deviations for milk samples having different concentrations of total and free calcium were better than 1.30 and 0.85%, respectively, for 15 analyses of each sample.

Conclusion

The proposed FI method, involving the use of a dialyser, is suitable for the determination of total and free calcium in milk. It can be carried out at a sampling rate of 60 samples h^{-1} with a significant improvement in accuracy and precision over the existing manual methods and can therefore be used for rapid, accurate and reliable routine analysis. Another advantage of the proposed method is the use of a single series of calcium standards for the determination of both total and free calcium.

The authors thank the Foundation for Research Development of the Council for Scientific and Industrial Research, Pretoria, and the University of Pretoria for financial support.

References

1. Webb, B. H., Johnson, A. H., and Alford, J. H., "Fundamentals of Dairy Chemistry," AVI, Westport, CT, 1974, p. 469.
2. Lindstrom, F., *Anal. Chem.*, 1960, **32**, 1123.

3. Anderegg, G., Flaschka, H., Sallman, R., and Schwarzenbach, G., *Helv. Chim. Acta*, 1954, **37**, 113.
4. Schwarzenbach, G., *Analyst*, 1955, **80**, 713.
5. Vogel, A. I., "A Textbook of Quantitative Inorganic Analysis," Longmans, London, 1961, Chapter 4.
6. McCullough, R. L., MacKay, J. K., and Padmanabhanm, G. R., *in* "Automation in Analytical Chemistry," Technicon Symposia, 1967, Volume 1, Mediad, New York, 1968, pp. 233–238.
7. Wanninen, E., *in* Bishop, E., *Editor*, "Indicators," Pergamon Press, Oxford, 1972, pp. 252 and 340.
8. Kessler, G., and Wolfman, M., *Clin. Chem.*, 1964, **10**, 686.
9. Gitelman, H. J., *Anal. Biochem.*, 1967, **18**, 521.
10. Roach, A. G., *in* "Automation in Analytical Chemistry," Technicon Symposia, 1965, Mediad, New York, 1966, pp. 137–141.
11. Moorehead, W. R., and Biggs, H. G., *Clin. Chem.*, 1974, **20**, 1458.
12. Basson, W. D., and van Staden, J. F., *Analyst*, 1978, **103**, 296.
13. Joe, M. M., Sakai, D., and Moffit, R. A., *in* "Automation in Analytical Chemistry," Technicon Symposia, 1966, Volume 1, Mediad, New York, 1967, pp. 595–597.
14. Ratliff, C. R., Casey, A. E., and Trasher, G. S., *in* "Automation in Analytical Chemistry," Technicon Symposia, 1966, Volume 1, Mediad, New York, 1967, pp. 321–325.
15. Basson, W. D., and van Staden, J. F., *Analyst*, 1979, **104**, 419.

Paper 9/02347J
Received June 5th, 1989
Accepted August 14th, 1989

Selective Determination of Triton-type Non-ionic Surfactants by On-line Clean-up and Flow Injection With Spectrophotometric Detection*

M. Eugenia León-González, M. Jesús Santos-Delgado† and Luis M. Polo-Díez
Departamento de Química Analítica, Facultad de Ciencias Químicas, Universidad Complutense de Madrid, 28040 Madrid, Spain

A flow injection method is proposed for the determination of Triton-type non-ionic surfactants, employing reagent injection and spectrophotometric detection. The method is based on the reaction between these surfactants and alizarin fluorine blue. Interferences from ionic and amphoteric surfactants were eliminated by selective retention on a column containing an ion-exchange resin inserted in the flow system, whereas interferences from non-ionic surfactants were eliminated by selective retention on a column containing Amberlite XAD-4 adsorption resin followed by elution of the Triton-type surfactants. Beer's law is obeyed at 432 nm in the ranges 0.2–12.0 mg l^{-1} and 2.0–120 μg l^{-1} of Triton-type surfactants, with relative standard deviations (n = 10) of 5.7 and 0.49%, respectively. The validity of the proposed method was tested by the analysis of several samples and by an analysis of variance (ANOVA) statistical comparison with two other methods.

Keywords: *Flow injection; spectrophotometry; non-ionic surfactant; alizarin fluorine blue*

Non-ionic surfactants have many applications in industry, where their control is vital because of their intrinsic activity and synergistic effect on pesticides.[1] In particular, Triton-type (*e.g.*, polyethylene glycol octyl phenyl ether) non-ionic surfactants are used widely in cosmetic and pharmaceutical formulations because of their emulsifying, detergent and wetting powers, and in the tanning and textile industries. Their determination in the presence of other ionic and non-ionic surfactants requires the use of chromatographic techniques, although liquid and gas chromatography only allow the determination of all the homologous groups of non-ionic surfactants without differentiating the group members.[2–6]

Environmental analysis and industrial control of this type of surfactant require the application of fast, reproducible and selective analytical methods; hence there is a need for automation.

In this paper, a method is proposed for the determination of Triton-type non-ionic surfactants in the presence of other surfactants. The method combines flow injection (FI) with spectrophotometric detection and is based on the reaction of the surfactants with alizarin fluorine blue (AFB) and the insertion of columns containing ion-exchange or adsorption resins in the flow system.

Experimental

Apparatus

A Tecator 5020 analyser was used. It consists of two pumps controlled by a microprocessor connected to the injection system, a Tecator L-100-1 injection valve capable of injecting variable volumes, a flow cell with an internal volume of 18 μl and a path length of 10 mm, an FIAstar 5020 spectrophotometer connected to an Alphacom printer and to the microprocessor and reaction and injection coils made of PTFE.

A Radiometer M-82 instrument equipped with a GK-2320 E combined glass - calomel electrode and a 50-kHz ultrasonic bath were also used.

Reagents

All chemicals were of analytical-reagent grade and purified water was obtained using a Milli-Q system.

The following stock solutions were used: 1.0×10^{-4} M aqueous AFB solution; 0.01 M acetic acid - sodium acetate buffer (pH 4.5); and 10 and 50 mg l^{-1} solutions of Triton X-100, X-405 and WR-1339 surfactants. Dilute solutions of 0.2–12.0 mg l^{-1} and 2.0–120 μg l^{-1} of these surfactants were prepared daily by appropriate dilution with water.

Amberlite IRA-904 and IR-120 ion-exchange resins and Amberlite XAD-4 adsorption resin were used.

Procedure

A diagram of the FI system is shown in Fig. 1. A 100-μl volume of a 1.0×10^{-4} M AFB solution was injected into a 0.01 M

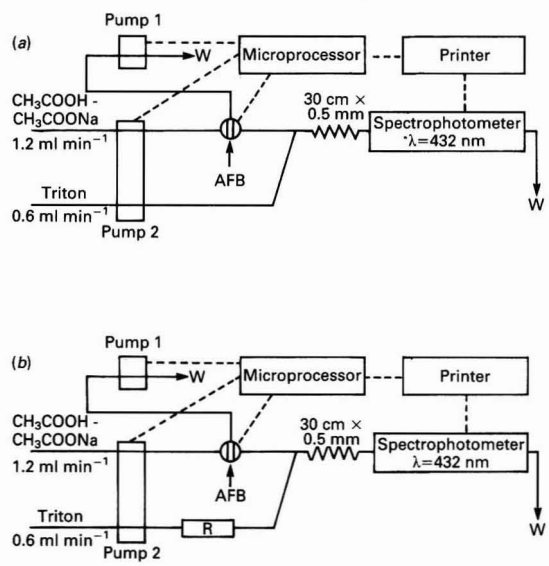

Fig. 1. Schematic diagram of the flow system: (*a*) without a column; and (*b*) with a column. R, Resin; and W, waste

* Presented at SAC 89, the 8th SAC International Conference on Analytical Chemistry, Cambridge, UK, 30 July–5 August, 1989.

† To whom correspondence should be addressed.

acetic acid - sodium acetate carrier solution. The carrier joins the sample either directly or after passing through a microcolumn. Ionic and amphoteric surfactants can be retained by inserting a column of cation-exchange (IRA-904) or anion-exchange (IR-120) resin in the channel of the water sample (0.2–12 mg l^{-1} of Triton-type surfactant); after *ca.* ten injections the resin was washed for 1 min by passing 0.1 M HCl in 10% methanol or 0.1 M NaOH in 10% methanol through the cation-exchange (IRA-904) or anion-exchange (IR-120) resin, respectively, by means of a programmable pump. Alternatively, the Triton-type surfactants can be retained by passing 100 ml of the aqueous sample (2–120 μg l^{-1} of surfactant) through a column of Amberlite XAD-4 adsorption resin; elution was carried out with 1 ml of ethanol which passes through the sample channel using a programmable pump.

Samples

Samples of detergent and wetting products for contact lenses and eye make-up removers were analysed directly after suitable dilution with water. Tanning-bath samples (from tanneries) were treated with 0.1 M NaOH solution, to eliminate chromium salts, and filtered before analysis.

Results and Discussion

Alizarin fluorine blue is a dye, the spectrum of which is a function of pH as its ionic forms are of various colours. Its absorption spectrum undergoes a hypsochromic shift and exhibits a large hyperchromic effect in the presence of small amounts of Triton-type non-ionic surfactants (Triton X-100, X-405 and WR-1339) at a pH between 4 and 5. For 2.0 mg l^{-1} of Triton-type surfactants, a hypsochromic shift of 40 nm and a hyperchromic effect of 0.5 A are observed, which is equivalent to a sensitisation factor of 4. These effects have been attributed by some workers[7] to non-polar interactions between the surfactant and AFB in other, similar systems.

The presence of surfactants may affect the stability of the π and π^* orbitals and the probability of electronic transitions. This has led us to evaluate the possibility of determining Triton X-100, X-405 and WR-1339 by spectrophotometric detection at 432 nm, a wavelength at which the absorbance difference between the dye and the AFB - non-ionic surfactant system is at a maximum (Fig. 2).

Choice of Manifold and FI Technique

A reagent - injection FI system was used because it gives more stable and reproducible base lines. Also, reagent consumption is lower, as it is possible either to recirculate the dye or to pump the injection-valve waste independently, by controlling the start and stop times with a microprocessor coupled to the system.

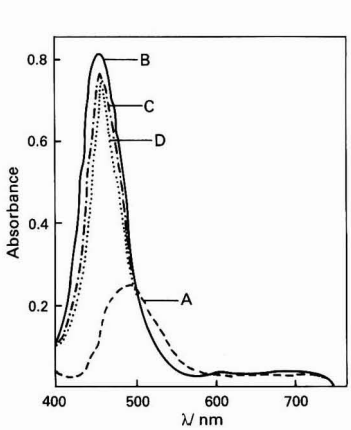

Fig. 2. Absorption spectra: A, AFB; B, AFB - Triton X-100; C, AFB - Triton X-405; and D, AFB - Triton WR-1339

Flow System Optimisation

The hydrodynamic and chemical variables studied and the optimum results obtained are shown in Table 1. The use of a 30 cm × 0.5 mm i.d. reactor is recommended. Several reactor geometries were tested, *viz.*, straight, coiled and knotted; the last offered the best sensitivity. Ionic strength does not appear to affect the analytical signal significantly for concentrations lower than 1 M NaCl. As regards the optimum pH, a value of 4.5 (buffered with acetic acid - sodium acetate) was chosen as this is an equilibrium pH between the yellow and red forms of the AFB dye. Further, small amounts of Triton-type surfactants appear to shift the equilibrium towards the yellow form, resulting in a maximum hypsochromic shift and a maximum hyperchromic effect at this pH.

Interferences

The selectivity study was carried out by observing the effect of cationic, anionic , non-ionic and amphoteric surfactants on the FI peak height in the Triton-type surfactant - AFB system. The Kirkbright criterion[8] with an interval of $\pm 2s$ was applied.

The maximum ratio of interfering surfactant allowed for 2.0 mg l^{-1} of Triton-type surfactant is shown in Table 2. The non-ionic surfactants all show a positive interference, possibly because they interact with AFB in the same way as do the Triton-type surfactants. Anionic surfactants cause the FI peak height to decrease, probably owing to polar and non-polar interactions between the non-ionic and cationic surfactants.

The influence of the amphoteric surfactant 4-picoline dodecyl sulphate was also tested. At an interferent to Triton-type surfactant ratio of 10 : 1, a slight negative interference was observed for the three non-ionic surfactants studied.

The interferences produced by ionic and amphoteric surfactants were minimised by selective retention on a column of ion-exchange resin inserted in the FI flow system [Fig. 1(*b*)]. Anion-exchange (Amberlite IR-120) and cation-exchange (Amberlite IRA-904) resins were used with samples containing a cationic or anionic surfactant to Triton-type surfactant ratio of 60 : 1 and an amphoteric surfactant to Triton-type surfactant ratio of 10 : 1; these ratios are higher than those usually found in these types of sample.

The influence of the length and i.d. of the ion-exchange column was studied; it was observed that the peak height decreased as either variable increased. The column dimensions chosen were length 2.5 cm and i.d. 1.5 mm, which provided good selectivity and acceptable reproducibility.

The retention of ionic or amphoteric surfactants is almost complete and is limited only by saturation of the ion-exchange

Table 1. Results of the optimisation studies

Variable	Range studied	Optimum
Volume of sample injected/μl	50–200	100
Flow-rate/ml min^{-1}:		
carrier	0.6–3.0	1.2
surfactant	0.3–1.5	0.6
Reactor length/cm	12–60	30
Reactor i.d./mm	0.35–0.70	0.50
Reactor shape	Knotted, coiled, straight	Knotted
[AFB]/M	0.01×10^{-4}–5.0×10^{-4}	1.0×10^{-4}
pH	4.1–6.1	4.5
Ionic strength (NaCl)/M	0.1–1.0	≥1

columns, which increases with the concentration of the interfering surfactant, and with the number of determinations. This saturation can be minimised by washing the cation- or anion-exchange columns as described under Procedure by passing 0.1 M HCl in 10% methanol or 0.1 M NaOH in 10% methanol through the cation-exchange (IRA-904) or anion-exchange (IR-120) resin, respectively, for 1 min. In the least favourable situation, up to ten injections per sample, depending on the ionic surfactant content, can be made without washing the column. The reproducibility is poorer when washing is not carried out between consecutive samples. Therefore, a maximum wash time of 1 min is recommended after each sample; this does not significantly affect the sampling rate which is *ca.* 60 injections h^{-1}.

The interferences produced by other non-ionic surfactants were minimised by selective retention on, and elution from, a column of Amberlite XAD-4 adsorption resin inserted in the FI flow system; elution was carried out with 1 ml of ethanol as described under Procedure. Up to 1 l of sample can be passed through the resin. The sampling rate depends on the Triton-type surfactant concentration of the sample and, consequently, on the sample volume necessary to obtain a signal above the detection limit. This allows the determination of Triton X-100, X-405 and WR-1339 concentrations at about the μg l^{-1} level. The selectivity in the presence of Amberlite XAD-4 adsorption resin is higher than that obtained in its absence, a fact that allows the determination of Triton-type surfactants in the presence of other non-ionic surfactants (Table 2).

Table 2. Tolerable upper limits of interferents in the determination of Triton-type surfactants

Interferent	Tolerable interferent to Triton-type surfactant ratio* Without column	With column
Non-ionic species—		
Brij 30	1.5	150
Tween 20	2.0	150
Tween 40	2.0	150
Tween 60	2.0	150
Tween 80	2.0	150
Pluronic L-61	2.0	150
Pluronic L-64	2.0	150
Pluronic F-68	2.0	30
Sucrose palmitate stearate 15	2.0	150
Sucrose palmitate stearate 7	2.0	150
Sucrose dipalmitate 11	2.0	150
Nonylphenyl ethoxylate	0.5	2
Anionic species—		
Sodium pentanesulphonate	5.0	70
Sodium heptanesulphonate	5.0	70
Sodium dodecyl sulphate	5.0	70
Sodium benzenesulphonate	5.0	70
Cationic species—		
Cetylpyridinium chloride	0.1	70
Tetrapropylammonium bromide	0.1	70
Tetrabutylammonium nitrate	0.1	70
Benzyldiisobutylphenoxyethoxy-dimethylammonium chloride (Hyamine 1622)	0.1	70
Cetyltrimethylammonium bromide	0.1	70
Alkylbenzyldimethylammonium chloride (Hyamine 3500)	0.1	70
Alkyl C_9–C_{15} benzyltrimethyl-ammonium chloride (Hyamine 2389)	0.1	70
Amphoteric species—		
4-Picoline dodecyl sulphate	10	30

* Kirkbright criterion[8] (±2*s*).

Analytical Characteristics

The analytical characteristics of the three surfactants studied are shown in Table 3. The linear range is slightly wider for Triton X-100. The sensitivity, expressed as the detection limit,[9] is higher for Triton X-100. The linear range and reproducibility are not affected by the addition of the ion-exchange microcolumns, whereas the detection limit varies slightly (Table 3). In contrast, the selectivity study (Table 2), carried out for a 2.0 mg l^{-1} Triton-type surfactant concentration, showed a marked increase in the maximum allowable interferent to Triton-type surfactant ratio.

The analytical characteristics show a marked change in the presence of Amberlite XAD-4 adsorption resin (Table 3). The linear range allows the determination of μg l^{-1} levels of the Triton-type surfactants; the detection limits are *ca.* 0.3 μg l^{-1} and the relative standard deviation is less than 0.5% for ten determinations of a Triton-type surfactant at the 20 μg l^{-1} concentration level. It is possible to determine Triton-type surfactants in the presence of a 150-fold excess of other non-ionic surfactants.

Determination of Surfactants in Real Samples

In order to test the validity of the proposed method, it was applied to the determination of Triton-type non-ionic surfactants in real samples, such as products for use with contact lenses and cosmetics, and in the process water from tanneries, all of which contain considerable amounts of other surfactants. In each determination, the standard additions method was used to quantify the matrix effect. Comparison of the calibration and standard additions slopes revealed no significant differences; hence it was concluded that there is no matrix effect under the established conditions.

The accuracy and precision of the proposed FI method were evaluated by comparison with a manual method[10] and another FI method[11] using the analysis of variance (ANOVA) technique.[12–14] The results of this comparison (Table 4) show that there are no significant differences between the three methods at the 95% probability level; this demonstrates that there are no systematic errors and the method is therefore validated.

Conclusions

An automated method is proposed for the determination of Triton-type non-ionic surfactants over a wide concentration range. The method was made reproducible and sensitive by minimising the interferences from ionic and amphoteric surfactants by passing the carrier stream through a column of ion-exchange resin; the interferences from non-ionic surfac-

Table 3. Analytical characteristics

Surfactant	Linear range/mg l^{-1}	s_r,* %	Detection limit/mg l^{-1}
Without column—			
Triton X-100	0.2–12.0	5.7	0.032
Triton X-405	0.4–10.0	5.6	0.036
Triton WR-1339	0.4–10.0	5.7	0.037
With ion-exchange column (Amberlite IRA-904 or IR-120)—			
Triton X-100	0.2–12.0	5.7	0.033
Triton X-405	0.4–10.0	5.6	0.037
Triton WR-1339	0.4–10.0	5.7	0.038
With adsorption column (Amberlite XAD-4)—			
Triton X-100	2.0–120†	0.49	0.30†
Triton X-405	3.0–110†	0.28	0.33†
Triton WR-1339	3.0–110†	0.30	0.34†

* s_r = Relative standard deviation; n = 10 at the 2.0 mg l^{-1} or 20 μg l^{-1} concentration level.

† Values in μg l^{-1}.

Table 4. Determination of Triton-type non-ionic surfactants by different methods

Sample	Proposed method		Picrate - FI method[11]		Picrate batch method[10]	
	Surfactant*/ mg l^{-1}	s_r, †%	Surfactant*/ mg l^{-1}	s_r, †%	Surfactant*/ mg l^{-1}	s_r, †%
Products for contact lenses—						
Bolor degreasing	60.2	0.47	59.8	0.25	59.9	0.32
Lentiflex degreasing	89.9	0.40	90.4	0.51	90.2	0.32
Lentiflex detergent	149.5	1.38	149.5	0.65	149.2	0.81
Dual-wet wetting	5.99	1.28	6.00	0.61	5.83	0.87
Lentiflex wetting	5.16	1.40	5.16	0.72	5.10	0.83
Eye make-up remover—						
Yves Rocher	663	0.54	662	0.15	661	0.37
Tatianne	453	0.79	453	0.36	450	0.54
Tanning water	294.5	0.65	294.5	0.35	294.0	0.40

* Means of six determinations.
† s_r = Relative standard deviation.

tants were minimised by passing the carrier stream through a column of Amberlite XAD-4 adsorption resin; the latter also allowed the pre-concentration of Triton-type non-ionic surfactants. The validity of the proposed method was confirmed for a number of samples by applying the ANOVA technique in order to compare it with two other methods.

The financial support of the Spanish CICYT (project PA86-0371) is gratefully acknowledged.

References

1. Attwood, D., and Florence, A. T., "Surfactant Systems. Their Chemistry, Pharmacy and Biology," Chapman and Hall, New York, 1980.
2. Chmil, V. D., Pilenkova, I. I., Fatyanova, A. D., and Zorova, A. I., *Metody Opred. Pestits.*, 1980, **4**, 60.
3. Bouska, J. B., and Phillips, S. F., *J. Chromatogr.*, 1980, **183**, 72.
4. Coupkova, M., Janes, K., Sanitrak, J., and Loupeak, J., *J. Chromatogr.*, 1978, **160**, 73.
5. Otsuki, A., and Shiraishi, H., *Anal. Chem.*, 1979, **51**, 2329.
6. Marcomini, A., Capri, S., and Giger, W., *J. Chromatogr.*, 1987, **403**, 243.
7. Mittal, K. L., "Solution Chemistry of Surfactants," Volume 1, Plenum Press, New York, 1979.
8. Kirkbright, G. F., *Talanta*, 1966, **13**, 7.
9. IUPAC, "Compendium of Analytical Nomenclature," Pergamon Press, Oxford, 1978.
10. Merino-Teillet, M. L., León-González, M. E., Santos-Delgado, M. J., and Polo-Díez, L. M., *Analyst*, 1987, **112**, 1323.
11. León-González, M. E., Santos-Delgado, M. J., and Polo-Díez, L. M., *Fresenius Z. Anal. Chem.*, in the press.
12. Polo-Díez, L. M., Pedraz-Peñalva, F., and González-Tablas, M., *An. Quím.*, 1984, **80B**, 261.
13. Hilman, J., and Glass, G. V., *J. Educ. Meas.*, 1967, **4**, 41.
14. Cochran, W. G., and Cox, G. M., "Diseños Experimentales," Trillas, Madrid, 1974.

Paper 9/03285A
Received August 2nd, 1989
Accepted October 4th, 1989

Continuous Flow Molecular Emission Cavity Analysis of Cephalosporins by Alkaline Degradation to Sulphide*

Nikos Grekas and Antony C. Calokerinos†
Laboratory of Analytical Chemistry, University of Athens, 106 80 Athens, Greece

A continuous flow method for the determination of some cephalosporins (cephradine, cephalexin, cephalosporin C, cefadroxil, cephapirin and cephalothin) in the general range 10.0–250.0 μg ml^{-1} is described. The sample is mixed with sodium hydroxide and remains for 20 min at 90 °C in the delay coil of an air-segmented system. The solution is then mixed with an excess of orthophosphoric acid, and the hydrogen sulphide evolved is continuously transferred into the cavity for generation of the S_2 molecular emission. The analysis is automated, requires no sample pre-treatment and samples can be analysed at a rate of 30 per hour with a relative error of 1–2%. The method was evaluated by carrying out recovery experiments and by the analysis of commercial formulations. Results agreed well with those obtained by the standard methods.

Keywords: *Cephalosporin determination; alkaline degradation; continuous flow molecular emission cavity analysis; routine assay*

Cephalosporins (CPs) are penicillinase-resistant antibiotics with significant activity against gram-positive and gram-negative bacteria. Several analytical methods have been devised for the determination of CPs. The most commonly used chemical method involves reaction with hydroxylamine. The reaction product forms a stable coloured complex with iron(III) in acidic solutions. The absorbance is then measured at 480 nm. This method is proposed for the determination of some CPs, such as cefadroxil, by the United States Pharmacopeia.[1] Nickel(II) catalyses the reaction and stabilises the coloured complex.[2] Other spectrophotometric methods have also been proposed for the analysis of CPs.[3–6] Complex samples such as biological fluids, have been analysed after high-performance liquid chromatographic separation.[7,8] Iodimetry is proposed by the British Pharmacopoeia for the assay of CPs in pharmaceutical preparations.[9]

Degradation products of CPs in alkaline medium have been identified by differential-pulse polarography.[10–12] The main products are sulphide, ammonia and diketopiperazine derivatives. Therefore, many analytical methods have been developed for the quantitative analysis of CPs via their alkaline degradation. Sulphide can be determined titrimetrically[13] or by the methylene blue method.[14,15] Ammonia can be determined by the indophenol reaction.[16] Diketopiperazine derivatives allow the sensitive spectrofluorimetric determination of CPs in biological fluids.[17–19]

Recently, a continuous flow molecular emission cavity analyser has been developed for the determination of organic sulphur compounds after their alkaline degradation to sulphide.[20] The air-segmented solution is then acidified, hydrogen sulphide is swept by nitrogen into the cavity and the S_2 emission intensity is measured. The application of this method to the determination of CPs is described. The procedure is relatively free from interferences and has been applied successfully to the determination of thiamine in formulations.[21] Minor modifications of the method allow the determination of some CPs, which is described in this paper. The results are in good agreement with those obtained by the standard methods.

Experimental

Apparatus

The laboratory-assembled molecular emission cavity analyser and the continuous-flow system were used as described previously.[20,21] The manifold is shown in Fig. 1.

Reagents

All solutions were prepared from analytical-reagent grade materials using de-ionised, distilled water. All CPs except cephalexin were purchased from Sigma. Cephalexin was obtained as a gift from the Greek National Pharmaceutical Industry.

Stock cephalosporin solution, 1000 μg ml^{-1}. Dissolve *ca.* 0.1 g of the CP, weighed accurately, in water and dilute to 100 ml. More dilute solutions were prepared by appropriate dilution.

Alkaline solution, 0.20 M *NaOH* - 0.02 M *ethylenediaminetetraacetic acid (EDTA)*. Dissolve 8.0 g of sodium hydroxide and 7.5 g of Na_2EDTA dihydrate (Titriplex III, Merck) in water and dilute to 1 l.

Orthophosphoric acid, 3.0 M

Sample Preparation

Assays in dosage forms

Tablets. Five tablets were weighed and finely powdered. An accurately weighed portion of not less than 200 mg was transferred into a 200-ml calibrated flask and diluted to volume with water. The powder was completely disintegrated by a mechanical shaker and the solution was filtered. From this sample solution, working solutions were prepared by appropriate dilution, so that the final CP concentration was in the working range.

Powder for injections. A portion was accurately weighed and diluted with water so that the final CP concentration was in the working range.

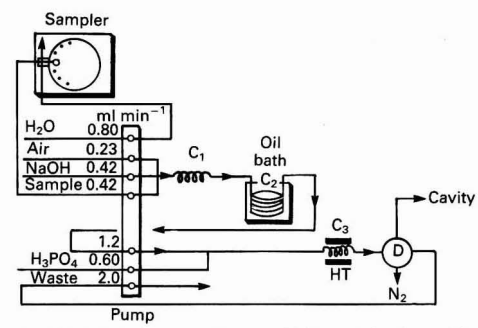

Fig. 1. Schematic diagram of the manifold used for the continuous flow molecular emission cavity analysis (CF-MECA) of CPs (not to scale). C_2, Delay coil; C_1 and C_3, mixing coils; and HT, heating tape

* Presented at SAC 89, the 8th SAC International Conference on Analytical Chemistry, Cambridge, UK, 30 July–5 August, 1989.

† To whom correspondence should be addressed.

Table 1. Experimental parameters for CF-MECA of CPs (other parameters as in Fig. 1)

Parameter	Description	Parameter	Description
Cavity position	Flame centre, 26 mm above burner head	Wavelength/nm	384
		Slit width/mm	2 (4 nm spectral band pass)
Flow-rates (l min^{-1})		Alkaline solution	0.20 M NaOH + 0.02 M EDTA
Hydrogen	0.85	Orthophosphoric acid	3.0 M
Nitrogen	1.60	Temperature/°C	
Nitrogen carrier	0.010	Delay coil	90
Cooling water	0.1	Mixing coil	45
Photomultiplier voltage/V	900	Sample time/s	60
		Wash time/s	60

Table 2. Chemical structures of the CPs examined

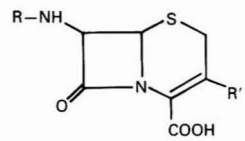

Cephalosporin (relative molecular mass)	Abbreviation	R	R′
Cephalosporin C (415.4)	CPC	$HOOCC(NH_2)H(CH_2)_3CO–$	$–CH_2OCOCH_3$
Cefadroxil (363.4)	CPF	p-$OHC_6H_4CH(NH_2)CO–$	$–CH_3$
Cephalexin (347.4)	CPL	$C_6H_5CH(NH_2)CO–$	$–CH_3$
Cephradine (349.4)	CPD	$C_6H_7CH(NH_2)CO–$*	$–CH_3$
Cephalothin (396.4)	CPT	$(SC_4H_3)CH_2CO–$†	$–CH_2OCOCH_3$
Cephapirin (445.4)‡	CPR	$(NC_5H_4)SCH_2CO–$§	$–CH_2OCOCH_3$

* C_6H_7 = cyclohexadienyl.
† SC_4H_3 = 2-thienyl.
‡ Relative molecular mass of the sodium salt.
§ NC_5H_4 = 4-pyridyl.

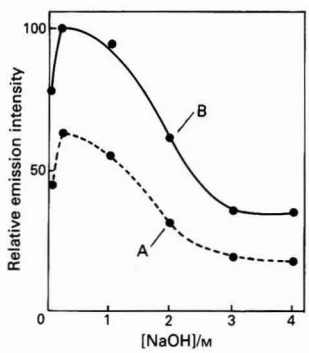

Fig. 2. Effect of sodium hydroxide concentration on the emission intensity from A, 100.0 and B, 150.0 μg ml^{-1} of cefadroxil

Capsules. The contents of five capsules were powdered and the procedure for the tablets was followed. The average mass of each capsule content was given by the manufacturer.

Powder for oral suspension. The procedure proposed by the manufacturer was followed.

Measurement procedure

Initiate the instrument set under the optimised conditions (Fig. 1 and Table 1), but keep the sampling needle always in the wash position. Ignite the flame and establish the base line. Condition the cavity by allowing *ca.* 0.2 ml of sulphide solution (500 μg ml^{-1}) to enter the system and generate intense S_2 emission. After re-establishment of the base line, activate the sampler and the analysis proceeds automatically. Construct the calibration graph of emission intensity (I/mV) *versus* concentration of CP (c/μg ml^{-1}), or preferably, the log$I$ - log$c$ graph and determine the CP content of the samples. Include a control standard solution for every 12 samples.

Results and Discussion

Optimisation of the Method

Flame composition and reagent flow-rates were the same as optimised previously for other organic sulphur compounds[20,21] (Fig. 1 and Table 1). Degradation of CPs was carried out in a 20-min delay coil at 90 °C. The extent of hydrolysis and therefore the amount of sulphide produced at this temperature was greatly affected by the sodium hydroxide concentration. Unexpectedly, the emission intensity was found to decrease with increasing alkali concentration (Fig. 2). Therefore, low concentrations of sodium hydroxide had to be introduced into the manifold in order to increase the degradation of CPs to sulphide. In comparison with other sulphur compounds, such as thiamine,[21] this effect was peculiar as the sulphur yield was expected to increase with alkali concentration. This observation was further confirmed by a simple experiment in which a standard solution of the CP was mixed with sodium hydroxide in a 50-ml beaker thermostated at 90 °C. After mixing, the sampling needle withdrew solution for 60 s and the emission intensity was recorded. Sampling was repeated after a wash interval of 60 s. Fig. 3 shows the results obtained from the hydrolysis of 100.0 μg ml^{-1} of cefadroxil. Similar profiles were recorded with the other CPs examined. Therefore, all the CPs tested required a lower alkali concentration than thiamine. All other experimental parameters were the same as used previously for the determination of thiamine.[21]

Analytical Parameters

Table 2 summarises the CPs studied. The yield of sulphide (Y,%) for each CP was calculated by

$$Y,\% = \frac{S^{2-}\text{ found (μg ml}^{-1})}{[\text{CP (μg ml}^{-1})/M_r\text{ (μg μmol}^{-1})]\,N\,(32.06\text{ μg μmol}^{-1}\text{ of S})} \times 100$$

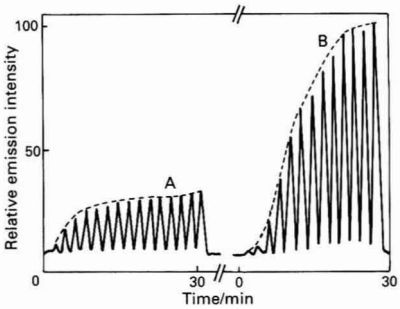

Fig. 3. Typical recording obtained from the hydrolysis of 100.0 μg ml^{-1} of cefadroxil with A, 2.0 and B, 0.10 M sodium hydroxide

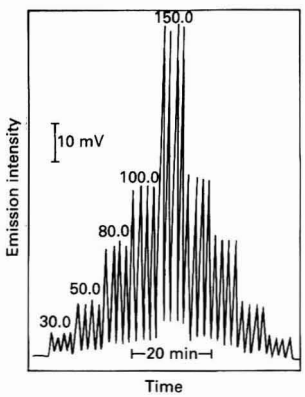

Fig. 4. Typical recorder outputs for a series of cephradine standards under the proposed conditions (numbers on the peaks are concentrations of CP in μg ml^{-1})

Table 3. Yield of sulphide produced from the CPs examined

CP*	CPD	CPL	CPF	CPC	CPT	CPR
Y,%	74.9	74.4	66.6	51.4	25.4	24.4

* 100.0 μg ml^{-1}.

where N = number of sulphur atoms per molecule of CP, and M_r = relative molecular mass of the CP. Molar yields were in the range 24.4–74.9% (Table 3).

Fig. 4 shows a typical recording for a series of cephradine standards carried out by the proposed procedure. All other CPs tested gave similar recordings. The linearity of the log$I$ - log$c$ calibration graph was very good (Fig. 5). The analytical parameters for each CP examined are summarised in Table 4. The coefficients of variation for 40.0 and 150.0 μg ml^{-1} of cefadroxil were 1.8 and 1.0% (n = 10), respectively, which were typical for all CPs. When aqueous solutions of CPs were analysed by the proposed procedure, the average error was in the range 1–2%.

Accuracy

As common pharmaceutical excipients do not interfere with the method,[21] it can be applied to the determination of CPs in formulations. The accuracy was examined by performing recovery experiments on solutions prepared from various CP

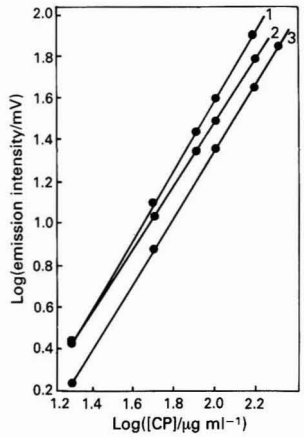

Fig. 5. Calibration graphs for 1, cephradine; 2, cefadroxil; and 3, cephalexin

Table 4. Analytical characteristics for the determination of CPs by the proposed method*

		Log$I$/log$c$ calibration graph			
CP	LOD†/ μg ml^{-1}	Linear range/ μg ml^{-1}	Slope	Intercept	r (n = 5)
CPD . .	5.00	10.0–150.0	1.68	−1.75	0.99995
CPF . .	5.00	10.0–150.0	1.55	−1.59	0.9998
CPL . .	7.00	15.0–200.0	1.64	−1.91	0.99992
CPC . .	10.0	20.0–250.0	1.67	−2.21	0.9999
CPT . .	10.0	20.0–250.0	1.71	−2.17	0.99994
CPR . .	10.0	25.0–250.0	1.67	−2.27	0.9998

* By using the same procedure, sulphide can be determined in the range 1.00–10.0 μg ml^{-1} (log$I$ = 0.107 + 1.86 log$c$, r = 0.9994, n = 10).

† LOD = limit of detection: signal to noise ratio = 3.

Table 5. Recovery experiments of CPs added to sample solutions of commercial formulations

Formulation	(CP)	Initially present/ μg ml^{-1}	Added/ μg ml^{-1}	Recovered/ μg ml^{-1}	Recovery, %
Velosef	(CPD)				
Capsules	250 mg	46.6	26.8	26.7	99.6
			53.5	54.0	100.9
	500 mg	38.9	26.8	27.4	102.2
			53.5	52.8	98.7
Moxacef	(CPF)				
Tablets	1 g	43.4	29.0	29.1	100.3
			58.0	57.2	98.6
Capsules	500 mg	39.4	30.0	30.2	100.7
			60.0	58.9	98.2
Cefatrex	(CPR)				
Powder for injection	1 g	98.7	42.4	41.0	96.7
			84.8	85.3	100.6
Medalexine	(CPL)				
Capsules	500 mg	72.9	29.0	28.8	99.3
			58.0	56.6	97.6
Powder for oral suspension	500 mg per 5 ml	80.3	29.3	28.6	97.6
			58.7	59.0	100.5
Keflex	(CPL)				
Tablets	500 mg	65.5	29.0	29.3	101.0
			58.0	59.5	102.6
				Mean:	99.7

Table 6. Determination of CPs by CF-MECA and standard methods

Formulation	CP/mg Claimed	Found CF-MECA*	Found Standard method	Relative difference (CF-MECA − standard),%
Capsules	(mg per capsule)			
Velosef	250	256.2 ± 2.0	247.8	+3.4
	500	517.9 ± 5.9	509.7	+1.6
Medalexine	500	508.5 ± 5.6	496.8	+2.4
Moxacef	500	499.8 ± 6.0	512.0	−2.4
Tablets	(mg per tablet)			
Keflex	500	512.0 ± 5.1	500.3	+2.3
Powder for oral suspension	(mg per 5 ml)			
Medalexine	500	504.9 ± 6.6	516.0	−2.2
			Mean:	2.4

* ± standard deviation (n = 3).

pharmaceutical preparations. A mean recovery of 99.7% was found (range 96.7–102.6%) (Table 5).

The proposed method was also evaluated by analysing commercial formulations of CPs, and comparing the results with those obtained by the standard methods. A satisfactory agreement between the results was obtained (Table 6) with a mean relative difference of 2.4% (range 1.6–3.4%). The relative standard deviation for continuous flow molecular emission cavity analysis (CF-MECA) of these formulations varied from 0.8 to 1.3%.

The general linear range (10.0–250.0 μg ml^{-1}) is appropriate for the determination of CPs in urine, where their concentration is relatively high. Nevertheless, recoveries of CPs from urine samples were <90%, even after extensive dilution (1 + 49). This was probably due to the presence of metal ions, which remove sulphide to form insoluble products.

Conclusions

The proposed automated method is accurate, precise and sensitive. It is not an indicator of stability, as sulphide is one of the degradation products of CPs. Penicillins do not produce sulphide after alkaline degradation. The observation has been made by other workers[14] and has been confirmed in this work. Therefore, the method allows the determination of CPs in the presence of penicillins. This potential application is useful for the determination of trace amounts of CPs in penicillins.

One of us (N. G.) thanks the University of Athens for financial support.

References

1. United States Pharmacopeial Convention, "US Pharmacopeia," Twenty-first Edition, Mack, Easton, PA, 1985, p. 1146.
2. Mays, D. L., Bangert, F. K., Cantrell, W. C., and Evans, W. G., *Anal. Chem.*, 1975, **47**, 2229.
3. Bodnar, J. E., Evans, W. G., and Mays, D. L., *J. Pharm. Sci.*, 1977, **66**, 1108.
4. Abdel-Khalek, M. M., and Mahrous, M. S., *Talanta*, 1983, **30**, 792.
5. Abdel-Khalek, M. M., and Mahrous, M. S., *Talanta*, 1984, **31**, 635.
6. Sengun, F. I., and Ulas, K., *Talanta*, 1986, **33**, 363.
7. Danzer, L. A., *Clin. Chem.*, 1983, **29**, 856.
8. Tokuma, Y., Shiozaki, Y., and Noguchi, H., *J. Chromatogr.*, 1984, **311**, 339.
9. "British Pharmacopoeia," HM Stationery Office, London, 1980, pp. 524 and 744.
10. Fogg, A. G., Fayad, N. M., Burgess, C., and McGlynn, A., *Anal. Chim. Acta*, 1979, **108**, 205.
11. Fogg, A. G., Fayad, N. M., and Burgess, C., *Anal. Chim. Acta*, 1979, **110**, 107.
12. Fogg, A. G., and Martin, M. J., *Analyst*, 1981, **106**, 1213.
13. Fogg, A. G., Abdalla, M. A., and Henriques, H. P., *Analyst*, 1982, **107**, 449.
14. Abdalla, M. A., Fogg, A. G., and Burgess, C., *Analyst*, 1982, **107**, 213.
15. Abdalla, M. A., Fogg, A. G., Baber, J. G., and Burgess, C., *Analyst*, 1983, **108**, 53.
16. Fogg, A. G., and Abdalla, M. A., *J. Pharm. Biomed. Anal.*, 1985, **3**, 315.
17. Barbhaiya, R. H., and Turner, P., *J. Pharm. Pharmacol.*, 1976, **28**, 791.
18. Heald, A. F., Ita, C. E., and Schreiber, E. C., *J. Pharm. Sci.*, 1976, **65**, 768.
19. Yu, A. B. C., Nightingale, C. H., and Flanagan, D. R., *J. Pharm. Sci.*, 1977, **66**, 213.
20. Grekas, N., and Calokerinos, A. C., *Anal. Chim. Acta*, 1988, **204**, 285.
21. Grekas, N., Calokerinos, A. C., and Hadjiioannou, T. P., *Analyst*, 1989, **114**, 1283.

Paper 9/03272J
Received August 2nd, 1989
Accepted September 12th, 1989

Purification of Human Glutamate Dehydrogenase (GDH) and an Adsorptive Voltammetric Investigation of the Interaction of GDH With Rabbit Anti-human GDH Antibody*

Patricia Carty and Richard O'Kennedy
School of Biological Sciences, Dublin City University, Dublin 9, Ireland

Encarna Lorenzo Abad,† José M. Fernández Alvarez, Juana Rodriguez Flores‡ and Malcolm R. Smyth§
School of Chemical Sciences, Dublin City University, Dublin 9, Ireland

Keith Tipton
Department of Biochemistry, Trinity College Dublin, Dublin 2, Ireland

A procedure for the isolation of glutamate dehydrogenase (GDH) from human liver, which involves the use of ion-exchange chromatography on diethylaminoethyl cellulose and affinity chromatography on guanosine triphosphate conjugated to Sepharose 4B, is described. The adsorptive voltammetric behaviour of human GDH, bovine GDH and rabbit anti-human GDH antibody was optimised with respect to accumulation potential, accumulation time and scan rate. The lower limits of detection were 0.2 and 1.2 mg l^{-1} for human and bovine GDH, respectively, and the lower limit of detection for rabbit anti-GDH antibody was 0.04 mg l^{-1}. The interaction of human GDH with rabbit anti-human GDH antibody was also examined using this method.

Keywords: *Glutamate dehydrogenase; adsorptive stripping voltammetry; anti-glutamate dehydrogenase antibody*

L-Glutamate dehydrogenase (GDH) (E.C. 1.4.1.3) is an enzyme which catalyses the reversible oxidative de-amination of L-glutamate to α-ketoglutarate and ammonia. The equilibrium for the reaction lies in favour of glutamate formation. There is a growing awareness that perturbations in amino acid neurotransmission may be involved in a number of neurological diseases. Altered levels of GDH have been found in patients suffering from olivopontocerebellar atrophy,[1] Reye's syndrome,[2] epilepsy[3] and diabetes.[4]

Measurement of GDH enzymatic activity has normally been made by spectrofluorimetric analysis[5] or by following the decrease in absorbance at 340 nm as nicotinamide adenine dinucleotide (NADH) is oxidised to NAD^+.[6] Adsorptive voltammetry, used to determine the enzyme levels, is simple to perform, rapid, and cheaper than the other available methods. Recently, we investigated the application of adsorptive stripping voltammetry (AdSV) to the trace determination of a variety of proteins and for the study of antibody - antigen interactions.[7–9] This paper describes the isolation and purification of human GDH and the application of AdSV to the study of human and bovine GDH and the monitoring of the interaction of human GDH with rabbit anti-human GDH antibody.

Experimental

Materials

All reagents were of analytical-reagent grade. Solutions for voltammetry were prepared in de-ionised water that was produced by passing distilled water through a Millipore (Harrow, Middlesex, UK) Milli-Q water purification system. A 0.1 M stock solution of phosphate buffer, pH 7.4, was prepared using Aristar grade potassium dihydrogen orthophosphate and dipotassium hydrogen orthophosphate. This was diluted 1 + 1 with Milli-Q purified water and used throughout the voltammetric investigations.

Bovine liver GDH was obtained from Sigma (Poole, Dorset, UK), Sepharose 4B from Pharmacia (Milton Keynes, Buckinghamshire, UK) and diethylaminoethyl (DEAE) cellulose (DE-52) from Whatman (Springfield Mill, Maidstone, Kent, UK). Tris(hydroxymethyl)aminomethane (Tris) was obtained from Riedel de Häen (Seelze, FRG) and all other chemicals from BDH (Poole, Dorset, UK).

Apparatus

Voltammograms were obtained by using a Princeton Applied Research (PAR; Princeton, NJ, USA) Model 264 polarographic analyser combined with a PAR Model 175 universal programmer, a PAR Model 303A static mercury drop electrode (SMDE), a PAR Model 305 magnetic stirrer and an Omnigraph Model 2000 x - y recorder. High-performance liquid chromatography (HPLC) analysis was carried out with a Waters Associates (Milford, MA, USA) Model 6000A dual piston pump in association with a Model 440 ultraviolet detector and a U6K injection system. A Protein Pak 300 SW gel filtration column was obtained from Waters Associates. Sodium dodecyl sulphate polyacrylamide gel electrophoresis (SDS PAGE) was carried out using a Pharmacia vertical electrophoresis unit. HPLC and SDS PAGE were used to test the purity of the GDH and antibody preparations.[10,11]

Procedures

Purification of GDH from human liver

L-Glutamate dehydrogenase was purified from human liver according to the method described by McCarthy *et al.*[12] During purification the enzyme was found to be unstable in buffers containing Tris. Therefore, Tris buffer was replaced by 20 mM sodium - potassium phosphate buffer, pH 7.4. The human liver was obtained within 12 h of death and was transported on ice to the laboratory. All purification steps were carried out at 4 °C.

* Presented at SAC 89, the 8th SAC International Conference on Analytical Chemistry, Cambridge, UK, 30 July–5 August, 1989.

† Permanent address: Departamento de Química, Universidad Autónoma, Madrid, Spain.

‡ Permanent address: Departamento de Química General, Universidad de Castilla-La Mancha, Ciudad Real, Spain.

§ To whom correspondence should be addressed.

Homogenisation

The liver (128 g) was homogenised in a Waring Blender for 90 s in a medium consisting of 500 ml of 4 mM sodium - potassium phosphate buffer, pH 7.4, containing 0.5 mM ethylenediaminetetraacetic acid (EDTA) and 0.1 mM phenylmethanesulphonyl fluoride.

Ammonium sulphate precipitation

Ammonium sulphate was added to the homogenate to give a 20% m/v saturated solution and homogenisation was continued for another 30 s at full speed. The mixture was stirred for 20 min and then centrifuged at 10 000 *g* for 30 min in a Sorval RC5B centrifuge. The pellet was discarded and solid ammonium sulphate was added slowly with continuous stirring to give a 50% m/v saturated solution. The mixture was stirred for 20 min and the precipitate formed was removed by centrifugation and re-suspended in 20 mM sodium - potassium phosphate buffer, pH 7.4 (buffer A), to give a total volume of 200–250 ml. This solution was dialysed overnight against three changes of buffer A.

Diethylaminoethyl cellulose ion-exchange chromatography

The dialysed sample was applied to a column (12 × 3.5 cm i.d.) of DEAE cellulose. The column was equilibrated with buffer A and washed until the absorbance of the eluent at 280 nm was less than 0.1 A. The elution of the enzyme was achieved with a linear gradient of 2 l of 20–150 mM sodium - potassium phosphate buffer, pH 7.4; 25-ml fractions were collected. The fractions of peak enzyme activity were pooled and concentrated using an Amicon ultrafiltration apparatus with an XM-50 membrane.

Affinity chromatography of GDH on guanosine triphosphate (GTP) Sepharose 4B

Twenty-three millilitres (50 units) of the concentrated enzyme solution were then applied to a 6 × 1.4 cm i.d. column of GTP-Sepharose 4B which was equilibrated in buffer A. The column was washed with buffer A until the absorbance of the eluent at 280 nm was below 0.01 A. The enzyme was eluted with a 400 ml linear gradient of 0–400 mM potassium chloride solution in buffer A. Fractions of 12 ml were collected and assayed for enzyme activity.[12] The fractions containing peak GDH activity were combined and concentrated by ultrafiltration to give a final protein concentration of 1.5 mg ml^{-1}. The enzyme solution was dialysed overnight against three changes of buffer A. Glycerol was added to the dialysed enzyme preparation to give a final concentration of 30% v/v and the solution was stored at −20 °C.

Production and purification of rabbit anti-human GDH antibody

The human liver GDH purified by affinity chromatography was used to raise polyclonal antibodies in New Zealand white rabbits, and the resulting antibodies were purified by affinity chromatography on GDH coupled to a Sepharose 4B chromatography column.[13]

Voltammetric Studies

For all voltammetric investigations, 5.0 ml of the supporting electrolyte (0.1 M potassium phosphate buffer, pH 7.0) solution were made up to 10.0 ml with Milli-Q water and purged with oxygen-free nitrogen for 8 min (and for 2 min in subsequent runs). The required accumulation potential (E_{acc}), +0.15 V, was then applied to the electrode for a selected accumulation time (t_{acc}), while the solution was stirred at 400 rev min^{-1}. After a 30-s rest period, a differential-pulse scan was initiated in the negative direction. The optimum conditions which were most commonly used were: scan rate (ν) 10 mV s^{-1} and pulse amplitude 50 mV. The scan was terminated at −1.0 V, and the adsorptive stripping cycle was repeated with a new drop. After the background electrolyte response had been recorded, aliquots of the respective protein solutions were introduced into the cell, and purged with oxygen-free nitrogen for 2 min. Care was taken not to allow frothing of the protein solutions at this point. The choice of a 2-min purging time for protein solutions was made following a study of the voltammetric responses with various purge times. All the results were obtained at 20 °C.

Interaction of Human GDH With Anti-human GDH Antibody

Human GDH was pre-incubated overnight with anti-GDH in the following proportions (GDH + rabbit anti-human GDH): 1 + 7, 2 + 3, 3 + 5, 1 + 1, 5 + 3, 3 + 1 and 7 + 1 at 4 °C. The solutions were centrifuged at 10 000 *g* for 5 min and 40 µl of the supernatant were added to 10 ml of the electrolyte solution for differential-pulse voltammetry.

Results and Discussion

Purification of GDH From Human Liver

A flow chart outlining the method of purification of GDH is shown in Fig. 1. Following chromatography on a GTP affinity column, a single peak of GDH was obtained (Fig. 2). The purity of this peak was determined using both SDS PAGE[10] and HPLC.[11] The results indicated that only one major protein, GDH, was present in the affinity-purified fraction (Fig. 3). Therefore, the method developed is ideal for the purification of human GDH. The same preparation was then used for AdSV. Bovine GDH, as obtained from Sigma, was not purified further. SDS PAGE indicated that the bovine enzyme contained contaminants at the 0.5% level with relative molecular masses of 51 000 and 27 000.

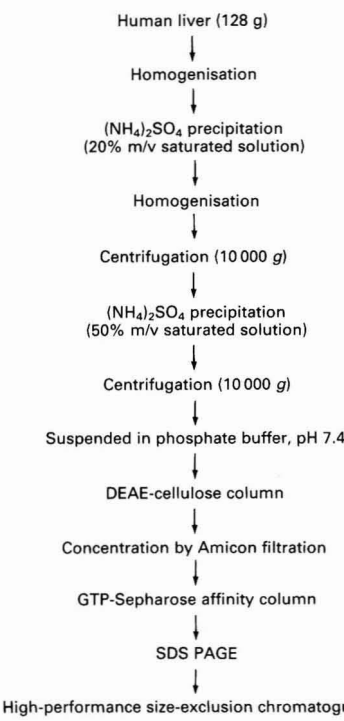

Fig. 1. Purification of human GDH

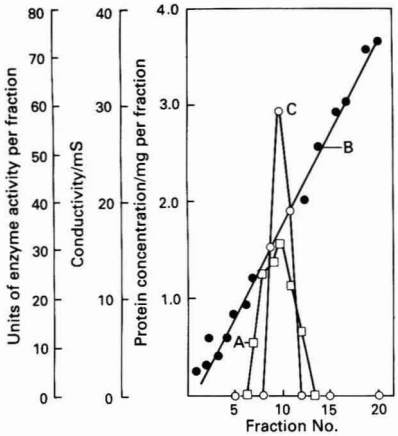

Fig. 2. Affinity chromatography of human GDH on a GTP affinity column. A, Protein concentration; B, conductivity; and C, enzyme activity

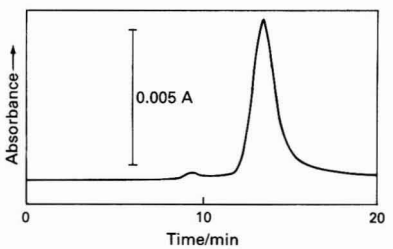

Fig. 3. HPLC profile of GDH (1 mg ml^{-1}) obtained using a Protein Pak 300 SW column. Eluent, 0.1 M phosphate buffer, pH 7.0; and flow-rate, 0.5 ml min^{-1}. The absorbance was measured at 280 nm

Cyclic Voltammetric Behaviour of Human and Bovine GDH

Both human and bovine GDH showed adsorption characteristics at the SMDE. Thus, at very low concentrations, no response was attained under solution-phase conditions, whereas respective symmetrical and well defined peaks were obtained when the potential was scanned in the negative direction following a previous accumulation step. A cyclic voltammogram obtained for a 1.2×10^{-6} M solution of bovine GDH using a t_{acc} of 120 s is shown in Fig. 4, A. From this voltammogram it can readily be seen that the enzyme undergoes an irreversible reduction process at the mercury electrode. In order to ascertain whether this process was a faradaic or a "pure" tensammetric one, successive voltammograms were recorded for the same drop (Fig. 4, B–D). The peak heights in the resulting curves equal those obtained when no accumulation is carried out (t_{acc} = 0 s). According to Kalvoda[14] this is indicative of an irreversible faradaic electrode process rather than a tensammetric one, which would yield progressively decreasing peak heights for repetitive scans.

Several accumulation - stripping experiments carried out by using increasing scan rates showed a linear dependence of the stripping peak intensity (i_p) on the first power of the scan rate (v) in the range 10–100 mV s^{-1} (r = 0.9999), as expected for an adsorption-controlled process.

It has been proved that GDH accumulates effectively at the SMDE under both electrolytic and open circuit conditions. In the first instance the range of potentials at which the accumulation is feasible is restricted from +0.2 to −0.2 V, whilst in the second instance it is extended to −0.4 V.

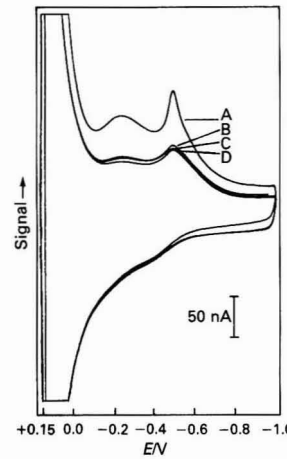

Fig. 4. Multi-cyclic voltammogram for a 1.2×10^{-6} M solution of bovine GDH. A, Obtained after a t_{acc} of 120 s; B–D, successive scans at the same drop

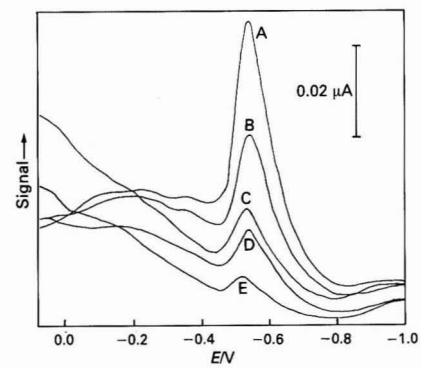

Fig. 5. Effect of t_{acc} on the adsorptive stripping voltammetric behaviour of human GDH (10 mg l^{-1}). Conditions as under Experimental. t_{acc}: A, 900; B, 600; C, 300; D, 180; and E, 60 s

Table 1. Influence of accumulation time, accumulation potential, scan rate and pulse amplitude on the peak potential and current of the stripping peak of human GDH (10 mg l^{-1})

t_{acc}/s	E_{acc}/V	v/mV s^{-1}	$-\Delta E$/mV	i_p/nA	$-E_p$/V
60	0.05	10	50	9	0.55
180	0.05	10	50	21	0.56
300	0.05	10	50	27	0.56
600	0.05	10	50	50	0.56
900	0.05	10	50	93	0.56
300	0.10	10	50	28	0.54
300	0.15	10	50	29	0.56
300	0.20	10	50	7	0.56
300	0.15	2	50	7	0.54
300	0.15	5	50	19	0.55
300	0.15	20	50	22	0.56
300	0.15	10	25	10	0.55
300	0.15	10	100	40	0.51

Moreover, the peak intensity remained essentially unaltered when the accumulation was carried out under open circuit conditions for any selected value of the starting potential. However, a sharp decrease of the stripping current was observed as E_{acc} was changed from positive to negative values.

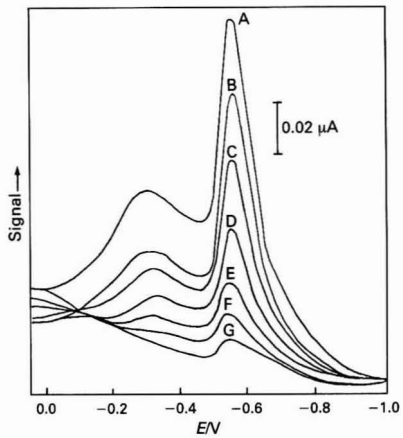

Fig. 6. Effect of t_{acc} on the adsorptive stripping voltammetric behaviour of bovine GDH (20 mg l^{-1}). Conditions as under Experimental. t_{acc}: A, 780; B, 720; C, 480; D, 300; E, 180, F, 120; and G, 60 s

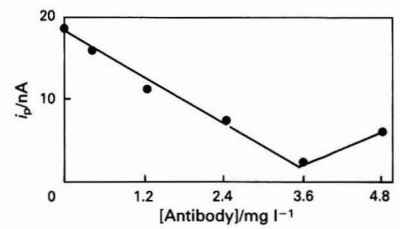

Fig. 7. Variation of the peak current of human GDH with increasing concentrations of anti-human GDH. $E_p = -0.55$ V

These experimental findings show that the enzyme adsorbs by itself at the SMDE, yielding a stripping peak that does not involve any mercury salt being formed with the sulphydryl moieties in the enzyme.[15] It has been reported[16] that no organomercury compounds are formed when the pre-concentration step is accomplished at open circuit. On the other hand, the enhanced response achieved at positive values of E_{acc}, when the pre-concentration was carried out under electrolysis, can be explained by taking into account that the isoelectric point (p*I*) of GDH is between 4.0 and 5.0[15] and the experiment is being carried out at pH 7.0. Under these conditions the molecule is negatively charged, and consequently shows an improved adsorption at the positively charged electrode, whereas a negatively charged electrode would provoke repulsions with the negatively charged enzyme.

Adsorptive Voltammetry of Human GDH

The effect of t_{acc} on the adsorptive stripping voltammetric behaviour of human GDH is shown in Fig. 5. By using an accumulation potential of +0.05 V (*versus* Ag - AgCl), a well defined peak was obtained at −0.55 V, which increased linearly with t_{acc} up to 15 min. The combined effects of E_{acc}, v and pulse amplitude on the adsorptive stripping voltammetric behaviour of human GDH are summarised in Table 1. The optimum E_{acc} and v for the determination of human GDH are +0.15 V and 10 mV s^{-1}, respectively. A pulse amplitude of 100 mV gave rise to a 4-fold enhancement in i_p compared with a pulse amplitude of 25 mV. However, this gain in sensitivity was accompanied by considerable peak broadening. Overall, a pulse amplitude of 50 mV was the best compromise between sensitivity and resolution requirements. Although higher currents were obtained for longer accumulation times, the increase in sensitivity achieved was at the expense of longer analysis times. For an accumulation time of 300 s, using the optimum conditions cited above, a linear calibration graph was obtained for human GDH between 0.7 and 2.4 mg l^{-1} with a slope of 0.66 nA mg^{-1} l (r = 0.999). The adsorptive accumulation results in extremely low detection and determination limits,[17] which were found to be 0.2 and 1.2 mg l^{-1}, respectively.

Adsorptive Voltammetry of Bovine Liver GDH

The effect of t_{acc} on the adsorptive voltammetric behaviour of bovine GDH is shown in Fig. 6. By using an E_{acc} of +0.05 V (*versus* Ag - AgCl), a well defined stripping peak is observed, with a peak potential of −0.55 V. In the time intervals studied the peak height increases linearly with time. A linear calibration graph was obtained for bovine GDH between 0.4 and 3.2 mg l^{-1} with a slope of 2.5 nA mg^{-1} l ($r = 0.991$) using a t_{acc} of 300 s. The limits of detection and determination[17] were 1.2 and 3.3 mg l^{-1}, respectively.

Adsorptive Voltammetry of Anti-human GDH Antibody

By use of an E_{acc} of +0.15 V and a v of 10 mV s^{-1}, a well defined stripping peak was obtained at −0.55 V, which increased linearly with t_{acc} up to 15 min. The optimum conditions in adsorptive voltammetry for anti-human GDH antibody are the same as those for human and bovine liver GDH. Using a t_{acc} of 300 s a linear calibration graph was obtained for anti-human GDH antibody between 19 and 57 μg l^{-1} with a slope of 0.1 nA μg^{-1} l (r = 0.99).

Study of the Interaction of Human GDH With Rabbit Anti-human GDH Antibody

The interaction of human GDH with anti-human GDH antibody was monitored by AdSV using the optimum conditions of E_{acc} and v described for anti-human GDH antibody. The t_{acc} used was 300 s. A decrease in i_p was seen for increasing concentrations of anti-human GDH antibody up to the point where the two proteins were of the same concentration in solution. When the concentration of anti-human GDH antibody exceeded that of GDH, the peak current was seen to increase (Fig. 7). The decrease in the i_p on addition of low concentrations of antibody to GDH may be as a result of the removal of GDH from solution due to the precipitation of the antibody - antigen complex.[18] This demonstrates the possibility of using this technique in a direct electrochemical immunoassay for GDH. Such a system might provide a very useful method of determining the concentrations of GDH in samples from patients with neurological diseases.

We gratefully acknowledge the financial support of the Health Research Board of Ireland and the Research and Postgraduate Studies Committee, Dublin City University, for this research. J. M. Fernández Alvarez thanks the Spanish Ministry for Education and Science for a post-doctoral scholarship.

References

1. Plaitakis, A., Nicklas, W. J., and Desnick, R. J., *Ann. Neurol.*, 1980, **7**, 297.
2. Holt, J. T., Arvan, D. A., Mayer, T., Smith, T. J., and Bell, E. J., *Biochim. Biophys. Acta*, 1983, **749**, 42.
3. Sherwin, A., Quesney, F., Gauthier, S., Olivier, A., Robitaille, Y., McQuaid, P., Harvey, C., and van Gelder, N., *Neurology*, 1984, **34**, 927.

4. McDaniel, H., Jenkins, R., and Parrish, W., *Clin. Res.*, 1988, **36**, A42.
5. Colon, A. D., Plaitakis, A., Perakis, A., Berl, S., and Clarke, D. D., *J. Neurochem.*, 1986, **46**, 1811.
6. Begermayer, H. U., *Editor*, "Methods in Enzymatic Analysis," Second Edition, Volume 2, Academic Press, New York, 1974, p. 650.
7. Rodriguez Flores, J., and Smyth, M. R., *J. Electroanal. Chem.*, 1987, **235**, 317.
8. Smyth, M. R., Buckley, E., Rodriguez Flores, J., and O'Kennedy, R., *Analyst*, 1988, **113**, 31.
9. Rodriguez Flores, J., O'Kennedy, R., and Smyth, M. R., *Biosensors*, 1988, **4**, 1.
10. Laemmli, U. K., *Nature (London)*, 1979, **227**, 680.
11. Carty, P., and O'Kennedy, R., *J. Chromatogr.*, 1988, **442**, 279.
12. McCarthy, A. D., Walker, J. M., and Tipton, K. F., *Biochem. J.*, 1980, **191**, 605.
13. Carty, P., Tipton, K. F., and O'Kennedy, R., *Biochem. Soc. Trans.*, 1990, **18**, 307.
14. Kalvoda, R., *J. Electroanal. Chem.*, 1984, **180**, 307.
15. Boyer, P. D., *Editor*, "The Enzymes," Third Edition, Volume XI, Academic Press, New York, 1975, p. 322.
16. Stankovich, M. T., and Bard, A. J., *J. Electroanal. Chem.*, 1977, **75**, 487.
17. Manson, J. H., *Anal. Chem.*, 1980, **52**, 2241.
18. Hudson, L., and Hay, F. C., *Editors*, "Practical Immunology," Second Edition, Blackwell Scientific Publications, London, 1980, p. 107.

Paper 9/04370E
Received October 10th, 1989
Accepted November 11th, 1989

Poly(vinyl chloride) Matrix Membrane Electrode for the Selective Determination of Heroin (Diamorphine) in Illicit Powders*

Saad S. M. Hassan and Marawan A. Hamada
Department of Chemistry, Faculty of Science, Ain Shams University, Cairo, Egypt

The potentiometric response characteristics of a poly(vinyl chloride) membrane electrode for heroin based on its ion-pair complex with tetraphenylborate were examined. The influence of pH, temperature and time on the performance of the electrode system was investigated. The electrode shows a near-Nernstian response over the heroin concentration range 10^{-2}–10^{-4} M with good precision. The mean relative standard deviation for the determination of heroin in 40 μg ml^{-1}–1 mg ml^{-1} aqueous heroin hydrochloride solutions is 1.2%. The electrode exhibits good selectivity for heroin in the presence of a number of adulterants and basic organic compounds commonly present in illicit heroin powders. The method was applied to the direct potentiometric determination of heroin in illicit powders (10–36% heroin) and the results agreed fairly well with those obtained by gas - liquid chromatography.

Keywords: *Heroin membrane electrode; poly(vinyl chloride) membrane; potentiometric heroin determination; heroin - tetraphenylborate complex; illicit heroin powder*

The use of heroin (diamorphine) as an illicit "street drug" is increasing rapidly, and much effort has been devoted towards developing and improving methods for its determination. In some legislative systems, the penalties for drug crimes are determined by the concentration of narcotic constituents in the actual drug preparation.[1] Such analyses may also establish possible common origins of drug seizures. Methods in current use for the determination of heroin include thin-layer chromatography,[2,3] gas - liquid chromatography (GLC),[4,5] high-performance liquid chromatography,[6,7] infrared spectrometry,[8] spectrophotometry,[9] spectrofluorimetry,[10] circular dichroism,[11] mass spectrometry,[12] polarography[13] and electrophoresis.[14]

Potentiometric methods with ion-selective membrane electrodes can provide valuable means of monitoring heroin because of their low cost, ease of use and maintenance and the simplicity and speed of the assay procedure. Although ion-selective electrodes for the determination of both opiate[15] and non-opiate[16–18] alkaloids have been reported, no electrodes responsive to heroin have so far been described. For this reason, we decided to investigate the response characteristics of a poly(vinyl chloride) - tetraphenylborate (TPB)-based heroin membrane electrode. This electrode system proved useful for the direct potentiometric determination of heroin at levels down to 40 μg ml^{-1} with good precision. The low detection limit (*ca.* 20 μg ml^{-1}) makes it suitable for the determination of heroin in illicit powders. The results obtained for six real samples of different origins compared favourably with those obtained by GLC.

Experimental

Apparatus

Potentiometric measurements were made at 25 ± 1 °C using an Orion Model SA 720 digital pH - millivoltmeter with the PVC heroin - TPB membrane electrode *versus* a double-junction Ag - AgCl reference electrode (Orion 90-02) containing 10% m/v potassium nitrate in the outer compartment. An Orion combination glass electrode (Model 91-01) was used for pH adjustment.

Gas - liquid chromatographic measurements were carried out using a Pye Unicam Model 104 instrument operated under the following conditions: column, glass, 6 ft × ¼ in i.d., packed with 3% OV-25 on Gas-Chrom Q (100–120 mesh); column temperature, 265 °C; injection temperature, 274 °C; carrier gas, nitrogen at a flow-rate of 60 ml min^{-1}; detector, flame ionisation; and detector temperature, 275 °C.

Reagents

All chemicals were of analytical-reagent grade and solutions were prepared with de-ionised water. Sodium tetraphenylborate(III) (NaTPB), poly(vinyl chloride) (PVC), dioctyl phthalate (DOP), dibutyl sebacate (DBS) and tetrahydrofuran (THF) were obtained from Aldrich. A standard World Health Organisation (WHO) heroin hydrochloride sample of purity not less than 97% and different illicit heroin powders of different origins were obtained through the Department of Narcotics, Criminal Laboratory, Ministry of Interior, Doha, Qatar.

Electrode Preparation

The heroin - TPB ion-pair complex was prepared by mixing 5 ml of 10^{-2} M aqueous heroin hydrochloride solution and 5 ml of 10^{-2} M NaTPB solution. The white precipitate was filtered off, washed with de-ionised water and dried at room temperature (m.p. 168 °C). Elemental analysis of the complex gave C 78.1, H 6.2, TPB ion-pair complex, $C_{21}H_{24}O_5N.C_{24}H_{20}B$ (C 78.37, H 6.39, N 2.03%). The infrared spectrum of the complex displayed almost all the absorption bands that appeared in the individual spectra of heroin hydrochloride and NaTPB.

The membrane of the electrode was prepared with the composition 2% heroin - TPB, 28% PVC and 70% plasticiser (DOP or DBS). The master membrane was fabricated by dissolving 150 mg of powdered PVC, 370 mg of plasticiser and 10 mg of the heroin - TPB ion-pair complex in 6 ml of THF. The solution was poured into a Petri dish (3 cm diameter) and the solvent was evaporated at room temperature. Discs were cut from the membrane for the electrode assembly. The electrode was constructed according to the method of Moody and Thomas[19] with a mixed internal solution of sodium chloride (5×10^{-3} M) and heroin hydrochloride (5×10^{-3} M).

The electrode was pre-conditioned after preparation by soaking for at least 24 h in 10^{-3} M aqueous heroin hydrochloride solution and stored in the same solution when not in use. The electrode was washed with de-ionised water and blotted with tissue-paper between measurements.

* Presented at SAC 89, the 8th SAC International Conference on Analytical Chemistry, Cambridge, UK, 30 July–5 August, 1989.

Electrode Calibration

A 10^{-2} M standard aqueous heroin hydrochloride solution was prepared by dissolving 0.20 g of pure heroin hydrochloride in 50 ml of 0.1 M citrate buffer (pH 5). By appropriate dilution with the citrate buffer, a series of standard solutions in the concentration range 10^{-3}–10^{-5} M were obtained. Aliquots of 25 ml of these solutions were transferred into 100-ml beakers and the PVC heroin - TPB membrane electrode in conjunction with an Orion double-junction Ag - AgCl reference electrode (Model 90-02) was immersed in the solutions. The measured potential was plotted against the logarithm of the heroin concentration.

Determination of Heroin

For direct potentiometric assay of heroin in illicit powders, typically a 50–100-mg portion of the powder was finely powdered and transferred with 0.1 M citrate buffer (pH 5) into a 25-ml calibrated flask. The solution was diluted to the mark with buffer, shaken for 5 min and transferred into a 100-ml beaker. The PVC heroin - TPB membrane electrode and Orion double-junction Ag - AgCl reference electrode were immersed in the solution. The electrode system was allowed to equilibrate with stirring and the e.m.f. was recorded and compared with the calibration graph. Alternatively, the standard additions method was used by recording the e.m.f. before and after the addition of 2.5 ml of standard aqueous 10^{-2} M heroin hydrochloride solution to the above solution. The change in the potential readings was recorded and used for calculation of the heroin content.

For the GLC determination of heroin, a portion of illicit heroin powder equivalent to *ca.* 25 mg of heroin hydrochloride was transferred into a 1-ml stoppered glass tube and 0.5 ml of chromatographic-grade methanol was added. After shaking for 5 min, a 2–5 μl aliquot of the solution was injected on to the GLC column. The peak heights for three replicate injections were recorded and their average value was compared with a standard calibration graph prepared for pure heroin hydrochloride under similar conditions.[20]

Results and Discussion

Electrode Characteristics

The critical response characteristics of a PVC heroin - TPB membrane electrode with DOP plasticiser are given in Table 1. Calibrations were made at a constant pH and ionic strength using 0.1 M citrate buffer (pH 5). The performance characteristics of an electrode incorporating DBS as membrane plasticiser are also included in Table 1 for comparison. Both electrodes display a linear response for aqueous heroin hydrochloride solutions over the concentration range 10^{-2}–10^{-4} M. The potential readings are stable and consistent to ±1.2 mV within the same day and are reproducible to within ±3 mV day-to-day for at least 4 weeks. The calibration slopes are 55.2 ± 0.8 and 52.1 ± 0.9 mV decade^{-1} for the DOP- and DBS-plasticised membranes, respectively. The detection limit, as defined by an e.m.f. difference of 18 mV between the calibration graph and the extrapolated linear section, is better than 5×10^{-5} M (*ca.* 20 μg ml^{-1}). This indicates the feasibility of using this electrode to determine heroin in illicit powders.

Table 1. Response characteristics of the PVC heroin - TPB membrane electrode with DOP and DBS plasticisers

Parameter	DOP	DBS
Slope/mV decade^{-1}	55.2 ± 0.8	52.1 ± 0.9
Intercept/mV	235.3 ± 0.8	216.2 ± 1.1
Correlation coefficient, r	0.998	0.997
Lower limit of linear range/M	6×10^{-5}	8×10^{-5}
Detection limit/M	4.5×10^{-5}	4.8×10^{-5}
Dynamic response time for 10^{-3} M heroin/s	10.5	20.5

Effect of pH, Time and Temperature

The pH dependence of the electrode potentials was measured as described previously.[21] Although the potential readings displayed by the PVC heroin - TPB membrane electrode are reasonably stable for 1 min in unbuffered solutions of pH 4–7, prolonged immersion of the electrode in these solutions shows a marked potential drift, probably owing to hydrolysis of heroin to 6-acetylmorphine and/or morphine. Measurements in a buffer solution of pH 5 provided stable potential readings within ±1 mV for up to 7 min.

The static response time of the PVC heroin - TPB membrane electrode is fast (*ca.* 40 s for 10^{-3} M heroin), but the dynamic response is even better. The electrode consistently responded in less than 20 s and frequently in less than 10 s to a halving or doubling of the heroin concentration, including injection of diluent or concentrate, mixing and recording of potential.

Most potentiometric measurements were made at 25 ± 1 °C, but a set of duplicate experiments was carried out at higher temperatures to investigate the effect of temperature on the electrode response. The potential responses of the electrode for 10^{-2}–10^{-4} M aqueous heroin hydrochloride solutions were followed as a function of temperature in the range 25–55 °C. Only a slight increase in the electrode potentials as the temperature increased (*ca.* 0.25 mV °C^{-1}) was observed without any significant deterioration in the electrode slope, selectivity or response time, indicating the high thermal stability of the membrane. The response times, influence of pH and temperature were almost identical for electrodes incorporating either DOP or DBS as membrane plasticiser.

Effect of Foreign Compounds

Illicit heroin powders may contain not only heroin but also low levels of morphine, acetylcodeine, codeine and some opium alkaloids.[1] The response of the PVC heroin - TPB membrane electrode to these interferents and the effects of some other alkaloids and basic compounds were checked. The selectivity coefficients ($k^{pot}_{her,B}$) were used to evaluate the degree of interference. The values given in Table 2 were obtained using

Table 2. Potentiometric selectivity coefficients ($k^{pot}_{her,B}$) for the PVC heroin - TPB membrane electrode with DOP and DBS plasticisers

	$k^{pot}_{her,B}$	
Interferent, B	DOP	DBS
Morphine	7.2×10^{-2}	1.8×10^{-1}
Codeine	9.5×10^{-2}	1.1×10^{-1}
Acetylcodeine	7.6×10^{-2}	6.0×10^{-2}
Nicotine	1.4×10^{-2}	1.2×10^{-1}
Brucine	1.1×10^{-2}	1.4×10^{-1}
Caffeine	3.0×10^{-2}	6.9×10^{-2}
Ephedrine	1.4×10^{-2}	2.9×10^{-2}
Sulphanilic acid	5.0×10^{-3}	1.2×10^{-2}
Anthranilic acid	4.6×10^{-3}	9.0×10^{-3}
Acetamide	1.4×10^{-2}	2.9×10^{-2}
Diethylamine	1.4×10^{-2}	1.9×10^{-2}
Propylamine	1.0×10^{-2}	1.5×10^{-2}
Urea	1.7×10^{-2}	2.0×10^{-2}
Alanine	6.0×10^{-3}	1.6×10^{-2}
Phenylalanine	5.7×10^{-3}	1.3×10^{-2}
NH_4^+	1.1×10^{-2}	2.4×10^{-2}
Na^+	5.5×10^{-3}	1.1×10^{-2}
K^+	7.9×10^{-3}	1.8×10^{-2}
Ca^{2+}	7.9×10^{-3}	2.1×10^{-2}
Ba^{2+}	1.0×10^{-2}	2.4×10^{-2}

Table 3. Direct potentiometric determination of heroin hydrochloride in aqueous solutions using the PVC heroin - TPB membrane electrode

Heroin hydrochloride/ μg ml^{-1}		Relative standard deviation
Added	Found*	(n = 5), %
40.0	39.5	1.4
80.0	79.5	1.4
160.0	158.4	1.3
200.0	198.6	1.2
320.0	316.5	1.1
400.0	394.0	1.3
600.0	592.8	1.2
720.0	713.5	1.1
800.0	788.8	1.2
1000.0	989.0	1.3

* Average of five measurements.

Table 4. Determination of heroin in illicit heroin powders using the PVC heroin - TPB membrane electrode and GLC methods

	Heroin found, %	
Sample No.	Electrode method	GLC method
1	10.4 ± 1.3	10.0 ± 1.4
2	14.5 ± 1.3	14.0 ± 1.4
3	19.6 ± 1.2	19.1 ± 1.3
4	30.2 ± 1.3	29.6 ± 1.4
5	32.6 ± 1.3	32.0 ± 1.5
6	36.0 ± 1.2	35.5 ± 1.4

the standard separate solutions methods.[16,22] The concentrations of heroin hydrochloride and the interferents were kept at a level of 10^{-3} M in solutions of the same pH and ionic strength (0.1 M citrate buffer of pH 5). The results showed that the PVC heroin - TPB membrane electrode with either DOP or DBS plasticiser is selective for heroin over many organic bases and alkaloids.

Illicit heroin powders commonly contain adulterants such as starch, powdered milk, lactose and local anaesthetics such as lidocaine and procaine.[23] None of these diluents at levels as high as 10–100 times that of heroin affected the response of the electrode. The nature of the membrane plasticiser can exert a considerable effect on the electrode selectivity. The membrane incorporating DOP is 1.2–12.7 times more selective for heroin in the presence of foreign compounds than that containing DBS plasticiser. The higher selectivity of the DOP-containing membrane is probably due to the higher viscosity of this plasticiser. Electrodes containing this membrane plasticiser also offer some additional advantages (see Table 1) that recommend its use for the screening of heroin.

Determination of Heroin

Results for measurements on pure aqueous heroin hydrochloride solutions at concentrations of 40 μg ml^{-1}–1 mg ml^{-1} using the PVC heroin - TPB membrane electrode (DOP plasticiser) and the standard additions (spiking) technique[16] are given in Table 3. The mean relative standard deviation is 1.2%. Potentiometric titration of 3–7 mg of heroin hydrochloride with standard 10^{-2} M aqueous NaTPB solution using the PVC heroin - TPB membrane electrode as an indicator electrode shows a potential break of *ca.* 90 mV at the stoicheiometric 1:1 molar reaction. The mean standard deviation is 0.7%.

The heroin contents of some illicit heroin powders of different origins were determined by the electrode method and the results are given in Table 4. The average relative standard deviation for five replicate assays for each sample was 1.2%. To assess the accuracy of the results, the same samples were analysed using GLC for comparison.[20] The two sets of results were in good agreement, although the GLC technique always gave results 0.4–0.6% lower than those obtained by the electrode method. In six different illicit samples, the heroin hydrochloride contents were found to be in the range 10–36%, depending on the origin.

In conclusion, the proposed membrane electrode system offers a simple, rapid and accurate screening technique for the determination of heroin in illicit powders.

References

1. Maehly, A., and Strömberg, L., "Chemical Criminalistics," Springer, Berlin, 1981, p. 19.
2. Marumo, Y., Inoue, T., Niwase, T., and Niwaguchi, T., *Kagaku Keisatsu Kenkyusho Hokoku*, 1978, **31**, 280.
3. Davey, E. A., Murray, J. B., and Rogers A. R., *J. Pharmacol.*, 1968, **20**, 51s.
4. Gloger, M., and Neumann, H., *Forensic Sci. Int.*, 1983, **22**, 63.
5. Mueller, E. M., Neumann, H., Fritschi, G., Halder, T., and Schneider, E., *Arch. Kriminol.*, 1984, **173**, 29.
6. Evren, N., Sener, B., and Noyanalpan, N., *Gazi. Univ. Eczacilik Fak. Derg.*, 1985, **2**, 67; *Anal. Abstr.*, 1986, **48**, 4E4.
7. Laurent, C. J. C. M., Billiet, H. A. H., and de Galen, L., *J. Chromatogr.*, 1984, **285**, 161.
8. Ravreby, M., *J. Forensic Sci.*, 1987, **32**, 20.
9. Lawrence, A., and Kovar, J., *Anal. Chem.*, 1984, **56**, 1731.
10. Wintersteiger, R., and Zeipper, U., *Arch. Pharm.*, 1982, **315**, 657; *Anal. Abstr.*, 1983, **44**, 2E11.
11. Bowen, J. M., Terry, A., Kennedy, R. K., and Purdie, N., *Anal. Chem.*, 1982, **54**, 66.
12. Joyce, J. R, Ardrey, R. E., and Lewis, I. A. S., *Biomed. Mass Spectrom.*, 1985, **12**, 588.
13. Popescu, S. D, and Baiulescu, G. E., *Rev. Chim. (Bucharest)*, 1977, **28**, 894.
14. Sinibaldi, M., and Rinalduzzi, B., *Anal. Lett.*, 1971, **4**, 125.
15. Goina, T., Habai, S., and Rosenberg, L., *Farmacia (Bucharest)*, 1978, **26**, 141.
16. Ma, T. S., and Hassan, S. S. M., "Organic Analysis Using Ion Selective Electrodes," Volumes I and II, Academic Press, London, 1982.
17. Hassan, S. S. M., and Tadros, F. S., *Anal. Chem.*, 1984, **56**, 542.
18. Hassan, S. S. M., and Saoudi, M. M., *Analyst*, 1986, **111**, 1367.
19. Moody, G. J., and Thomas, J. D. R., *in* Freiser, H., *Editor*, "Ion Selective Electrodes in Analytical Chemistry," Plenum Press, New York, 1978, Chapter 4.
20. Sobol, S. P., and Sperling, A. R., *in* Davies, G., *Editor*, "Forensic Science," American Chemical Society, Washington, DC, 1975, pp. 170–182.
21. Hassan, S. S. M., and Elnemma, E. M., *Analyst*, 1989, **114**, 1033.
22. IUPAC Analytical Chemistry Division, Commission on Analytical Nomenclature, *Pure Appl. Chem.*, 1978, **48**, 127.
23. Lawn, J. C., Hill, C. E., Feldkamp, R. H., Hoover, R. D., Rice, S. T., and Wong, B. J., "Drugs of Abuse," US Government Printing Office, Washington, DC, 1985, p. 16.

Paper 9/03787J
Received September 5th, 1989
Accepted November 14th, 1989

Biochelation Cartridge for the Solid-phase Extraction of Trace Metals*

Jeremy D. Glennon and Supalax Srijaranai
Department of Chemistry, University College Cork, Cork, Ireland

The characterisation and metal complexation capacities of biochelating silicas utilising hydroxamate complexation are described. Metal complexation on the silica displayed the characteristic optical properties of the free complexes in aqueous solution. Unsubstituted and *N*-methyl-substituted monohydroxamate silicas are compared with the biochelator, desferrioxamine immobilised on to silica; the latter displayed an over-all lower capacity as a function of pH. A trace metal cartridge utilising the biochelating silica showed good stability, pre-concentration and elution properties for a number of metals.

Keywords: *Hydroxamic acid; biochelating silica; trace metal pre-concentration; solid-phase extraction*

Three main approaches to the solid-phase extraction of trace metals can be identified. Ion-exchange materials have been extensively used[1] and other workers have immobilised metal complexes on to octadecylsilica for metal pre-concentration and elution by exploiting metal complex hydrophobicities. For example, Al^{III}, Cd^{II} and Fe^{III} complexes of 8-hydroxyquinoline in alkaline solution (pH 8–9) can be retained on a C_{18} cartridge and can be eluted in methanol for subsequent analysis by atomic absorption.[2] The use of chemically immobilised chelating groups for the solid-phase extraction and chromatographic analysis of metal ions presents new possibilities in trace metal analysis.

Hydroxamic acids, well known for their biochelation activity, have also attracted attention as analytical reagents owing to their good complexing behaviour with a broad range of metal ions.[3–5] A number of papers concerning the synthetic methods, properties and applications of solid phases containing hydroxamic acid groups have also been published. The most notable of these is the work of Ramadan and Porath[6] involving the coupling of hydroxamic acid groups to epoxy-activated Sepharose. Most of these reports, however, are concentrated on polymeric hydroxamic acids for which a variety of synthetic methods, properties and some interesting applications have been found. Vernon and Eccles[7,8] obtained several successful analytical separations using a hydroxamic acid resin. The synthetic route involved the production of cross-linked poly(acrylonitrile) followed by hydrolysis and conversion of the polymeric acrylamide to hydroxamic acids. Different hydroxamic acid polymeric backbones have been studied by several researchers.[9,10] The conventional cross-linked polycarboxylic acid cation exchangers such as Amberlite IRC 50[11] and other poly(methacrylic acid) resins[12] were also used. Phillips and Fritz[13,14] described an alternative use of Amberlite XAD-4 as a precursor, with a sequence of reactions including the production of carboxy XAD-4, the acid chloride and finally the hydroxamic acid.

Silica-bound chelating agents have also received attention because of the well documented advantages over cross-linked polymers.[15] The separation of metal ions on several new silica-bound azo-coupled chelating solid phases has been described.[16] More recently a silica-immobilised 2-{[2-(triethoxysilyl)ethyl]thio}aniline was prepared as a selective sorbent for the separation and pre-concentration of palladium.[17] Hydroxamic acid functional groups have been immobilised by the esterification of modified hydroxylated silochrome silica and reaction with hydroxylamine.[18,19] This paper reports the characterisation of chemically immobilised hydroxamic acids on silica and describes the solid-phase extraction properties of a trace metal cartridge utilising the solid phase.

Experimental

Materials

Unless stated otherwise, all chemicals were of analytical-reagent grade quality. A series of biochelating silica phases with unsubstituted and substituted hydroxamic acids (see Fig. 1) have been synthesised in the laboratory at University College Cork using silica (40 μm) obtained from Analytichem International (Harbor City, CA, USA). Hydroxylammonium chloride, potassium hydroxide, sodium hydroxide, indole and disodium ethylenediaminetetraacetate (EDTA) were obtained from BDH (Poole, Dorset, UK). *N*,*N*′-Carbonyldiimidazole, *N*-methylhydroxylammonium chloride and acetohydroxamic acid (AHA) were purchased from Sigma (Poole, Dorset, UK). Desferrioxamine mesylate (DFA) was obtained from Ciba Geigy (Horsham, Sussex, UK).

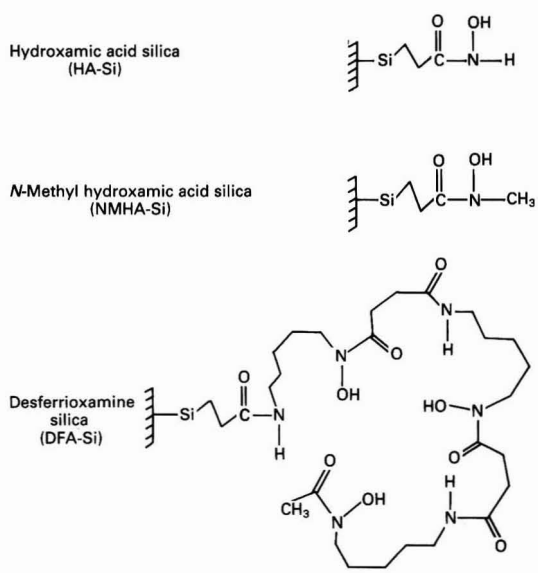

Fig. 1. Schematic diagram showing the biochelating silicas utilising hydroxamate complexation

* Presented at SAC 89, the 8th SAC International Conference on Analytical Chemistry, Cambridge, UK, 30 July–5 August, 1989.

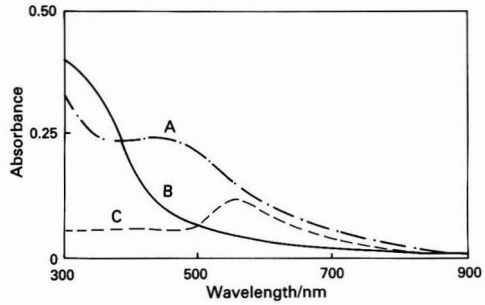

Fig. 2. Absorption spectra of metal complexes on HA-Si. A, Fe^{III}; B, V^{V}; and C, Au^{III}

Table 1. Maximum absorption wavelengths of Fe^{III} complexes for the chelating hydroxamic acid silica phases and free hydroxamic acids. Ratios in parentheses represent compositions of the complexes

Fe^{III} complex	Maximum wavelength/nm
Fe-AHA	510(1:1); 460(1:2); 420(1:3)
Fe-DFA	420
Fe-HA-Si	465
Fe-NMHA-Si	462
Fe-DFA-Si	449

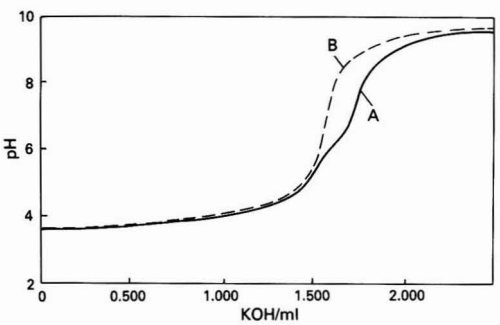

Fig. 3. Titration curves of: A, HA-Si and, B, CM-Si

Metal ion stock solutions (0.01 M) were prepared from the metal ion salts. Solutions of Fe^{III}, Al^{III}, Cd^{II}, Co^{II}, Cu^{II} and Ni^{II} were prepared from their nitrate salts, Au^{III} solution from the chloride and Zn^{II} from the sulphate. The solution of V^{V} was prepared from NH_4VO_3. Nitric acid and sodium hydroxide were used to obtain the desired pH of each metal solution. De-ionised water from an Elgastat spectrum water purification unit, with a resistivity of 15 MΩ cm or better, was used throughout the experiment.

Instrumentation

Titrations were performed with a Radiometer automatic titration apparatus consisting of a digital (PHM 84) pH meter, an autoburette (ABU 80), a titrator (TTT 80) and an automatic recorder (REC 80 Servograph). The 50-ml titration vessel was thermostatically controlled at 25 ± 0.05 °C using a HAAKE FE2 temperature-control unit. A Radiometer G 2040-C glass electrode and a K 4040 calomel reference electrode were employed.

The Radiometer (PHM 84) pH meter was also used to measure the pH of the metal solutions. Ultraviolet and visible absorption spectra were performed on a Shimadzu UV 260 spectrophotometer. Diffuse reflectance spectra were recorded on a Beckman DK-2A ratio-recording spectrophotometer. A Masterflex peristaltic pump equipped with two channel head pumps (Cole-Parmer Instruments, Chicago, IL, USA) was used for the cartridge experiment. Atomic absorption analyses were carried out using either a Pye Unicam SP 190 spectrophotometer or a graphite furnace atomic absorption spectrometer (Perkin-Elmer Model 2380).

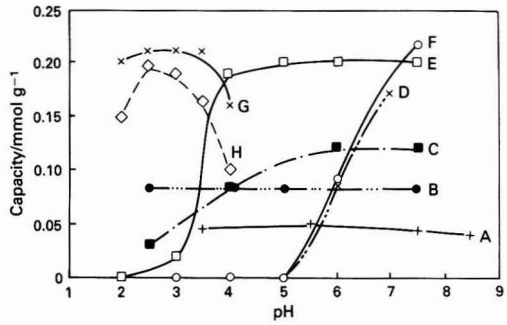

Fig. 4. Complexation capacities of metal ions on HA-Si as a function of pH: A, Au^{III}; B, Al^{III}; C, Ni^{II}; D, Co^{II}; E, Cu^{II}; F, Zn^{II}; G, Fe^{III}; and H, V^{V}

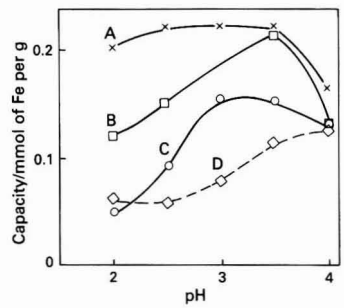

Fig. 5. Complexation capacity for Fe^{III} on silica phases as a function of pH: A, HA-Si; B, NMHA-Si; C, DFA-Si; and D, CM-Si

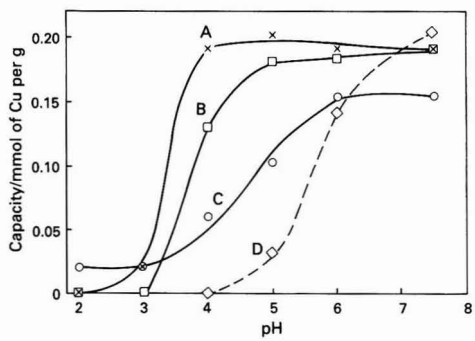

Fig. 6. Complexation capacity for Cu^{II} on silica phases as a function of pH: A, HA-Si; B, NMHA-Si; C, DFA-Si; and D, CM-Si

Procedures

Characterisation of the chelating silicas

The characterisation of the hydroxamic acid chelating silica was carried out by spectrophotometric and titrimetric methods. Carboxymethyl silica (CM-Si) was used throughout for comparison. The solid-state absorption spectra of the hydroxamic acid chelating silica and its metal complexes were

Table 2. Pre-concentration of metal ions from synthetic sea water on HA-Si

Metal ion	Volume of test solution/ml	Concentration factor	Metal added/ μg	Metal found μg	Metal found %	CV*
Fe^{III}	1000	200	10.00	9.80	98.00	0.06
Fe^{III}	100	20	10.00	10.10	100.10	0.03
Cu^{II}	100	10	2.50	2.50	100.00	0.10
Cu^{II}	100	10	5.00	5.20	104.00	0.05
Cu^{II}	100	10	10.00	9.70	97.00	0.03
Zn^{II}	100	10	5.00	3.95	79.00	0.06
Zn^{II}	100	10	10.00	7.73	77.30	0.02

* CV = Coefficient of variation (n = 5).

obtained as slurries in ethylene glycol and by diffuse reflectance. The sorbents were ground to fine powders before measurement. A slurry of each sample was placed in a 1-mm cell and the spectra recorded.

Titrations of the hydroxamic acid chelating silica were carried out and compared with those of CM-Si. Samples of the silicas (0.05-g amounts) were equilibrated in dilute acid by shaking overnight with 20 ml of carbonate-free 0.001 M HCl. The suspensions were then titrated with 0.02 M KOH.

The presence of chemically bound hydroxamic acid groups on the silica was examined further by spectrophotometry following hydrolysis of the hydroxamate groups. Samples of the chelating silica (0.1 g) were hydrolysed by refluxing with 4 ml of 2 M HCl at 90 °C for 4 h. After cooling, the hydrolysed product was then filtered and the filtrate was analysed for liberated hydroxylamine by spectrophotometric analysis of the liberated hydroxylamine complex and indole at 400 nm.[20]

Metal ion complexation capacities

The metal ion complexation capacities of the chelating silicas were studied as a function of pH by both batch and cartridge methods.

In the batch experiment, a 25-ml sample solution of metal ion was adjusted to the desired pH and shaken with 0.1 g of sorbent at room temperature for 15 min. The suspension was then filtered through a filter-paper and finally washed with water. The filtrate and all washing portions were analysed for metal ion using atomic absorption spectrometry (except for V^{V} for which a spectrophotometric technique was employed).

The cartridge method was carried out using a cartridge (plastic container, 1.3 × 0.9 cm i.d.) packed with *ca.* 0.6 g of sorbent. A 25-ml sample solution of the metal ion was adjusted to a suitable pH and was passed through the cartridge using a peristaltic pump at a flow-rate of 1 ml min^{-1}; the effluent and washings were then collected for analysis. The amount of complexed metal ion was also determined by stripping the metal ion from the cartridge by passing EDTA (0.08 M) through the cartridge and by collecting 5-ml fractions of the eluent. The concentration of the metal ion was then determined as before.

Pre-concentration of metal ions

The pre-concentration of Fe^{III}, Cu^{II} and Zn^{II} from aqueous samples was studied using the cartridge system. Samples of synthetic sea water[21] spiked with metal ions were passed through the cartridge. After the pre-concentration step, the metal ions were eluted from the cartridge using 0.08 M EDTA for Fe^{III} and acidified water (pH 2.0) for Cu^{II} and Zn^{II}. The effluent was collected in 5-ml fractions for the analysis.

Results and Discussion

The presence of hydroxamic acid groups on hydroxamic acid silica (HA-Si) was confirmed by a number of investigations. The absorption spectra of Fe^{III}, Au^{III} and V^{V} on HA-Si were investigated by two methods, namely, as slurries in ethylene glycol and by diffuse reflectance. The results obtained are shown in Fig. 2; these provide strong evidence of the presence of hydroxamate chelating groups on the silica phase. In particular, for Fe^{III}, the maximum absorption wavelengths obtained for these complexes are comparable to the characteristic absorption wavelengths of the free complexes in aqueous solution (Table 1). Further, in comparison with CM-Si, the titration curve (Fig. 3) for HA-Si shows an extra inflection in the pH range associated with proton liberation from hydroxamic acid groups. Representative pK_a values include those for AHA (9.74) and propionohydroxamic acid (9.56). The method was not used to quantify the amount of hydroxamate groups on the surface, as proton liberation is liable to be time dependent and incomplete in the heterogeneous system involved.

Information relating to the concentration of hydroxamic groups on the surface of HA-Si was obtained from two sources. The spectrophotometric analysis of liberated hydroxylamine following acid hydrolysis yielded a value of 0.29 mmol g^{-1}. The second approach uses the complexation capacity of the chelating silica for the metal ions at the optimum pH for complexation. The results obtained were 0.22 mmol g^{-1} for Fe^{III} at pH 2.5 and 0.20 mmol g^{-1} for Cu^{II} at pH 5.0.

Metal Complexation Capacity and Elution

Fig. 4 shows the complexation capacities, in terms of mmol of metal ion per gram of the HA-Si, as a function of pH for Fe^{III}, V^{V}, Cu^{II}, Ni^{II}, Co^{II}, Cd^{II}, Zn^{II}, Al^{III} and Au^{III}. The results provide very useful information for analytical applications as there are several metal ions which are strongly complexed with the chelating hydroxamic acid silica and the differences in the pH dependency of binding provide the opportunity of using the chelating silica for pre-concentration and separation of metal ions.

A comparison of the metal complexation capacities for Fe^{III} and Cu^{II} for the three phases is provided by Figs. 5 and 6, respectively. All the biochelating phases display metal binding at lower pH compared with CM-Si, a feature characteristic of hydroxamate complexation. However, what is not typical is the general order of abilities of the biochelating phases to bind metals in acidic solution, *i.e.*, HA-Si >*N*-methylhydroxamic acid silica (NMHA-Si) >DFA-Si, as trihydroxamates are noted for extensive metal complexation in acidic solution. The complexation capacities at optimum pH are in the order HA-Si ≈ NMHA-Si > DFA-Si, which can be understood in terms of the lower concentration of NMHA and DFA on the surface of the silica or of steric hindrance from the bulky groups of these phases compared with that of the unsubstituted HA-Si phase.[9]

The elution of metal ions from the biochelating hydroxamic acid silicas was examined using the cartridge. Several competing ligands such as EDTA, AHA and dithionite were investigated. The results showed that most of the complexed

metal ions, *i.e.*, Fe^{III}, Cu^{II}, Ni^{II}, Zn^{II}, Co^{II}, Cd^{II} and Al^{III}, are eluted quantitatively with a small volume (5 ml) of 0.08 M EDTA with the notable exceptions of Au^{III} and V^{V}. It is also clear from studies of the pH variation that elution can be achieved readily by pH control for certain metal ions, in particular, Cu^{II}, which is eluted quantitatively with acidified water (pH 2.0).

Application

The complexation capacities obtained for the biochelating hydroxamic acid silicas were sufficiently high to provide quantitative extraction or pre-concentration of the metal ions from a large volume of trace metal solution. The pre-concentration of trace amounts of Fe^{III}, Cu^{II} and Zn^{II} from spiked synthetic sea water was studied using HA-Si. The results, given in Table 2, show promise for the application of the biochelating silicas to the pre-concentration of Fe^{III} and Cu^{II}. Further studies on the uptake and elution of Zn^{II} are necessary to optimise recovery from sea water. In addition, the phases are stable to metal loading and washing cycles and exhibit minimum reduction in metal complexation capacity on repetitive usage.

References

1. Leyden, D. E., and Wegscheider, W., *Anal. Chem.*, 1981, **53**, 1059A.
2. Schwedt, G., and Sicker, U., *LoborPraxis*, 1983, **7**, 816.
3. Agrawal, Y. K., and Roshania, R. D., *Bull. Soc. Chim. Belg.*, 1980, **89**, 159.
4. Agrawal, Y. K., and Patel, S. A., *Rev. Anal. Chem.*, 1980, **4**, 237.
5. Senior, A. T., and Glennon , J. D., *Anal. Chim. Acta*, 1987, **196**, 333.
6. Ramadan, N., and Porath, J., *J. Chromatogr.*, 1985, **321**. 81.
7. Vernon, F., and Eccles, H., *Anal. Chim. Acta*, 1976, **82**, 369.
8. Vernon, F., and Eccles, H., *Anal. Chim. Acta*, 1976, **83**, 187.
9. Shah, A., and Devi, S., *Analyst*, 1985, **110**, 1501.
10. Shah, A., and Devi, S., *Analyst*, 1987, **112**, 325.
11. Petrie, G., Locke, D., and Meloan, C. E., *Anal. Chem.*, 1965, **37**, 919.
12. Cornaz, J. P., Hutschneker, K., and Deuel, H., *Helv. Chim. Acta*, 1957, **40**, 2015; *Chem. Abstr.*, 1958, **52**, 6892e.
13. Phillips, R. J., and Fritz, J. S., *Anal. Chim. Acta*, 1980, **121**, 225.
14. Phillips, R. J., and Fritz, J. S., *Anal. Chim. Acta*, 1982, **139**, 237.
15. Leyden, D. E., and Luttrell, G. H., *Anal. Chem.*, 1975, **47**, 1612.
16. Faltynski, K. H., and Jezorek, J. R., *Chromatographia*, 1986, **22**, 5.
17. Seshadri, T., and Haupt, H. J., *Anal. Chem.*, 1988, **60**, 47.
18. Vertinskaya, T. E., Kudryavtsev, G. V., Tikhomirova, T. I., and Fadeeva, V. I., *Zh. Anal. Khim.*, 1985, **40**, 1387.
19. Fadeeva, V. I., Tikhomirova, T. I., Yuferova, I. B., and Kudryavtsev, G. V., *Anal. Chim. Acta*, 1989, **219**, 201.
20. Seifter, S., Gallop, P. M., Micheals, S., and Meilman, E., *J. Biol. Chem.*, 1960, **235**, 2613.
21. Lyman, J., and Fleming, R. H., *J. Mar. Res.*, 1940, **3**, 136.

Paper 9/04034J
Received September 21st, 1989
Accepted November 20th, 1989

Linear Plots for Complexometric Potentiometric Titrations of Mixtures of Two Metal Ions*

Carlo Maccà
Department of Inorganic, Metallorganic and Analytical Chemistry of the University, Via Marzolo 1, I-35131 Padova, Italy

The application of Gran plots to potentiometric complexation titrations of mixtures of two metals with a selective electrode for one of the metal ions is surveyed. New developments are discussed; only 1:1 reactions are considered. Depending on the ratio between the conditional stability constants of the two metal chelates, the first and/or second equivalence point can be found by using different forms of approximately linear Gran functions. Criteria for identifying the linear range of Gran functions using logarithmic diagrams are illustrated. Rigorous equations for linearised titrations are introduced.

Keywords: *Potentiometric titration; complexometric titration; Gran plot; logarithmic diagram*

Gran plots[1,2] are used extensively for determining the equivalence point in potentiometric titrations. Their application to complexometric titrations of metals by chelating agents using ion-selective electrodes has been discussed.[3–6]

Gran plots were first derived for titrations of solutions containing a single analyte. The plot of the Gran function against the titrant volume is linear and extrapolation yields the equivalence volume when the titration reaction is quantitative. Titrations that do not satisfy this condition give curved plots. When a large part of the plot deviates appreciably from ideal linear behaviour, an incorrect end-point is obtained. Nevertheless, Gran plots can have sufficiently large linear ranges and give fairly accurate and precise end-points even when the steepness of the titration curve at the equivalence point is insufficient to yield a satisfactory end-point using traditional methods. A general approach for the determination of the titration range useful for linear extrapolation has been described, and application to complexometric titrations of single metals has been discussed.[7,8]

Potentiometric titrations of mixtures of metals with an electrode selective for one of the metal ions have been discussed and conditions for obtaining titration curves with sharp end-points, suitable for separate determination of the metals, have been given.[9–11] The steepness of the titration curve at the equivalence point of interest can be considerably decreased compared with titrations of solutions that contain only the given metal. Moreover, a poor selectivity and detection limit of the measuring electrode can also produce undesirable effects. Therefore, alternative end-point methods deserve attention. The performance of Gran plots for these titrations has not yet been examined in sufficient detail.

In this paper, the Gran function and new approximate and exact linear equations for titrations of mixtures of two metals (reacting in a 1:1 ratio with the titrant chelating agent) are discussed. The general approach for the determination of the linear range of Gran plots[7,8] is applied to these titrations.

General

Consider the titration of a solution containing two metals, M and N (initial volume V^0, concentrations C^0_M and C^0_N) with a chelating agent, Y (titrant concentration C), forming the complexes MY and NY with stability constants K_{MY} and K_{NY}. The variables measured in potentiometric titrations are the volume, V, and the electromotive force, E, of the cell formed by an electrode sensitive to the ion M and a reference electrode. In an adequately buffered test solution, E is ideally expressed by the equation:

$$E = E' + S \log[M] \quad .. \quad .. \quad .. \quad (1)$$

where E' is the conditional standard potential, S is the slope factor (which in practice can be slightly different from the theoretical Nernstian[12] factor) and [M] is the conditional concentration of ion M, *i.e.*, the total concentration of unreacted metal. However, N can interfere with the response of the indicating electrode to the primary ion M. For the present purpose, it is convenient to define $k_{M,N}$ as the "conditional" selectivity coefficient, related to the response of the electrode to the conditional concentrations of M and N. Finally, the detection limit,[12–14] D, for the electrode response to M should be taken into account, because it can be approached even when the amount of titrant is smaller than the total amount of metals. The following equation is generally used[12] as the complete equation for the response of the electrode:

$$E = E' + S \log([M] + k_{M,N}[N]^{m/n} + D) \quad .. \quad (2)$$

where m and n are the charges of the two ions. The selectivity coefficient can reasonably be assumed to be constant throughout the part of the titration of interest. D is variable to a certain extent, depending on the nature of the electrode, the titrated solution, the titrant[11,15] and, in general, the working conditions; the qualitative evaluation of its effect, obtained by using a constant value, can be useful, however.

The metal that forms the more stable complex reacts first with the titrant. When K_{MY} is much larger than K_{NY}, and both constants are large enough, two equivalence points are found by potentiometric titration with an electrode sensitive to M. The first corresponds to n^0_M, and the second to the sum $n^0_M + n^0_N$. When the first condition is not met, only the second equivalence point is usually taken into consideration.[9–11]

The applicability and limitations of Gran plots for titrations of mixtures can be conveniently discussed using logarithmic diagrams, which are most suitable for multi-component systems.[8]

Logarithmic Diagrams and Titration Curves

The logarithmic diagram for the titration of a mixture of metals is obtained simply by juxtaposition of the diagrams for the titrations of single metals.[4,5] The logarithm of the conditional concentration of any ith species, log[i], is plotted against pY, the conditional concentration of the chelating agent. The diagram is easily completed by a plot representing the contribution of the interfering ion N to the concentration of M sensed by the electrode, $(m/n)\log [N] + \log k_{M,N}$; the

* Presented at SAC 89, the 8th SAC International Conference on Analytical Chemistry, Cambridge, UK, 30 July–5 August, 1989.

horizontal line representing the detection limit, log D, can also be plotted when D can be assumed to be constant.

Logarithmic diagrams are best used in combination with the equation of the relative titration error.[16] The relative error, ε, or the titration ratio, f, can be advantageously taken as the experimentally controlled variable instead of V. For two-step titrations, the relative error and the titration ratio can be defined in terms either of the first equivalence point (I), equation (3), or of the second (II), equation (4), depending on the purpose of the titration.

$$\varepsilon_I = f_I - 1 = \frac{n^t - n^0_M}{n^0_M} = \frac{(V^0 + V)([Y] + [NY] - [M])}{C^0_M V^0} \quad .. \quad (3)$$

$$\varepsilon_{II} = f_{II} - 1 = \frac{n^t - (n^0_M + n^0_N)}{n^0_M + n^0_N} = \frac{(V^0 + V)([Y] - [M] - [N])}{(C^0_M + C^0_N)V^0} \quad (4)$$

The right-hand sides of equations (3) and (4) were obtained by substitution of the mass balances of the reactants:

$$n^0_M = C^0_M V^0 = (V^0 + V)([M] + [MY]) \quad .. \quad (5)$$

$$n^0_N = C^0_N V^0 = (V^0 + V)([N] + [NY]) \quad .. \quad (6)$$

$$n^0_Y = CV = (V^0 + V)([Y] + [MY] + [NY]) \quad .. \quad (7)$$

With logarithmic diagrams, which neglect dilution, the following approximate forms, obtained by setting $V^0 + V \approx V^0$, are used:

$$\varepsilon_I \approx \frac{[Y] + [NY] - [M]}{C^0_M} = \frac{[Y] + [MY] + [NY]}{C^0_M} - 1 = \frac{[Y] - [M] - [N]}{C^0_M} + \frac{C^0_N}{C^0_M} \quad (3')$$

$$\varepsilon_{II} \approx \frac{[Y] - [M] - [N]}{C^0_M + C^0_N} = \frac{[Y] + [MY] + [NY]}{C^0_M + C^0_N} - 1 = \frac{[Y] + [NY] - [M] - C^0_N}{C^0_M + C^0_N} \quad (4')$$

The three equivalent forms of equations (3′) and (4′) are suitable in different parts of the titration; the form containing the smaller conditional constants (which are obtained from the diagram with less absolute uncertainty) should be used every time. The logarithm of the modulus of the titration error can be easily plotted on the logarithmic diagram[8] using these equations.

A fairly indicative titration curve is calculated by obtaining from the diagram the log[i] values to be substituted into equations (3′) and (4′) at a suitable series of values of pY, and plotting log([M] + $k_{M,N}$[N]$^{m/n}$ + D) against ε or f.[17] A constant value of D can be assumed for qualitative purposes.[4,5]

Figs. 1(*a*) and 2(*a*) depict the logarithmic diagrams for titrations with $m = n$ and $K_{MY} >> K_{NY}$ and $K_{MY} << K_{NY}$, respectively. The theoretical (ideal) titration curve, log[M] *versus* f_I, is plotted as a solid line in Figs. 1(*b*) and 2(*b*); the broken curve represents the quantity measured in practice, *i.e.*, log([M] + $k_{M,N}$[N]$^{m/n}$ + D).

It should be noted that equations (3) and (4) are implicit forms of the exact equation for the titration curve. They can be developed after substitution of the functional expressions of the equilibrium concentrations in terms of [M]:

$$[MY] = \frac{C^0_M V^0 - (V^0 + V)[M]}{V^0 + V} \approx C^0_M - [M] \quad .. \quad (8)$$

$$[Y] = \frac{C^0_M V^0 - (V^0 + V)[M]}{K_{MY}(V^0 + V)[M]} \approx \frac{C^0_M - [M]}{K_{MY}[M]} \quad .. \quad (9)$$

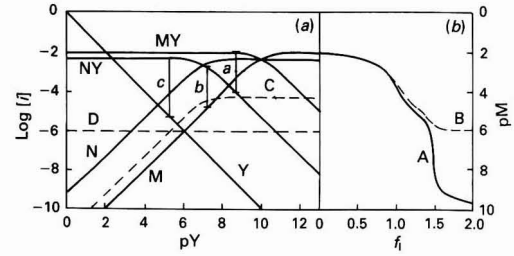

Fig. 1. (*a*) Logarithmic diagram for the titration by Y of: 1.00×10^{-2} M M (conditional formation constant $K_{MY} = 10^{10.00}$) and 0.50×10^{-2} M N ($K_{NY} = 10^{7.00}$). Lines C and D: contributions of the interference by N (isovalent ions, $k_{M,N} = 0.01$) and of the detection limit (10^{-6} M), respectively, to the response of an electrode for M. Vertical segments are distances log δ characterising the critical conditions for linearity of the Gran plots for the first equivalence point, equation (15) (segment a, δ = 0.01) and for the second (segment b, initial condition, for δ = 0.01; segment c, final condition, for δ = 0.001). (*b*) Titration curve of pM *versus* f_I: A, ideal; and B, with the contribution of the electrode interference by N and of the detection limit

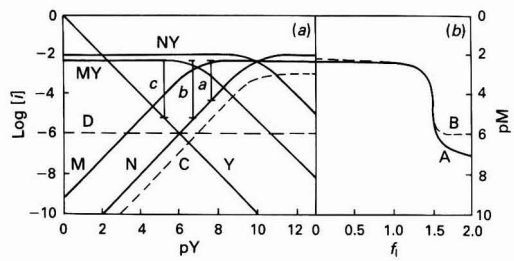

Fig. 2. (*a*) Logarithmic diagram for the titration by Y of: 0.50×10^{-2} M M (conditional formation constant $K_{MY} = 10^{7.00}$) and 1.00×10^{-2} M N ($K_{NY} = 10^{10.00}$). Lines C and D: as Fig. 1(*a*), but for $k_{M,N} = 0.1$. Vertical segments are distances log δ characterising the critical conditions for linearity of the Gran plots for the second equivalence point (segment a, initial condition, for δ = 0.01; segment b, the same for δ = 0.001; segment c, final condition, for δ = 0.01). (*b*) Titration curve of pM *versus* f_I: A, ideal; and B, with the contribution of the electrode interference by N and of the detection limit

$$[N] = \frac{C^0_N V^0}{(V^0 + V)(1 + K_{NY}[Y])} \approx \frac{C^0_N}{1 + K_{NY}[Y]} \quad .. \quad (10)$$

$$[NY] = \frac{C^0_N V^0}{(V^0 + V)(1 + 1/K_{NY}[Y])} \approx \frac{C^0_N}{1 + 1/K_{NY}[Y]} \quad (11)$$

Direct calculation of the titration curve is greatly simplified if dilution can be neglected.[9–11] Equation (3′) or (4′) is then used together with the approximate forms of equations (8)–(11); [M] is conveniently taken as the master variable in the calculations.

Discussion

$K_{MY} >> K_{NY}$

When MY, the complex formed by the metal sensed by the electrode, is much more stable than NY, the theoretical titration curve has two distinct steps[9,10] [Fig. 1(*b*)] at the equivalence points for the titration of M and M + N, respectively.

First equivalence point

In the first part of the titration, M is titrated. The ideal linear function, F_I, expresses the stoicheiometric excess of the titrated substance, *i.e.*, the difference between $n^0_M = C^0_M V^0$,

the total amount of analyte, in moles, and $n^t = CV$, the added amount of titrant[7,18]:

$$F_I = n^0_M - n^t \quad .. \quad .. \quad .. \quad .. \quad (12)$$

This quantity can be calculated from the experimental data. When F_I is plotted against n^t, or against a quantity proportional to n^t, such as V, the titrant volume, or f, the titration ratio, the equivalence volume can be obtained by linear extrapolation to $F_I = 0$, where $n^t = n^0_M$ (the equivalence point condition, by definition).

By using the appropriate mass balances [equations (5)–(7)], the following equation can be written:

$$F_I = (V^0 + V)\,([M] - [Y] - [NY]) \quad .. \quad .. \quad (13)$$

On the assumption that in this part of the titration the titrant reacts quantitatively with M, *i.e.*, that [Y] and [NY] are negligible, equation (13) can be approximated by the total equilibrium amount (the "conditional" amount) of unreacted metal, n_M:

$$F_I \approx F' = n_M = (V^0 + V)\,[M] \quad .. \quad .. \quad (14)$$

On the further assumption that the electrode potential can be expressed by the ideal equation (1), equation (14) becomes identical with the Gran function[1] for the titration of M alone:

$$F' = G = (V^0 + V)\,10^{-E'/S}\,10^{E/S} \propto (V^0 + V)\,10^{E/S} \quad (15)$$

In practice, the factor $10^{-E'/S}$ is neglected, and the right-hand term is plotted against V; however, this is immaterial for the following discussion.

If the two stability constants are not sufficiently far apart, on approaching the first equivalence point, N begins to react appreciably before the reaction of M is complete. When [NY] begins to be appreciable in equation (13), the Gran function [equations (14) and (15)] shows appreciable positive deviations from the ideal linear function[6]:

$$F' - F_I = n_M - (n^0_M - n^t) = (V^0 + V)\,([Y] + [NY]) \quad .. \quad (16)$$

{for completeness, [Y], which is generally negligible, is not omitted in equations (16)–(18) and (20)}. Deviations increase on approaching the equivalence point and cause the plot of G to be curved upward. Points affected by deviations likely to yield an appreciable error must be discarded when G is extrapolated against V to obtain the equivalence volume. A simple criterion for the choice of the titration range useful for linear extrapolation of the equivalence point has been obtained[7,8] on the basis of the following considerations.

Let the maximum relative titration error admitted be δ (typically 0.1 or 1%), corresponding to the absolute error δn^0_M. The straight line through the initial point (with abscissa $x = 0$, ordinate $y = n^0_M$) that intercepts the abscissa at the point affected by this error, $x = n^0_M\,(1 + \delta)$, is represented by the equation $y = n^0_M - n^t/(1 + \delta)$; this equation can be approximated to $y = n^0_M - n^t\,(1 - \delta) = F_I + \delta n^t$ for any reasonable value of δ ($\delta < 0.05$). Extrapolation through the initial point and the single experimental point (at n^t_c) coincident with the above straight line yields a titration error equal to δ. For the points at $n^t > n^t_c$, the deviation of the ordinate of the Gran plot from the ideal linear plot, equation (16), is larger than δn^t; if a titration error smaller than δ is required, it is advisable to exclude these points from the extrapolation. As a fairly large linear titration range (with n^t_c close to n^0_M) is desirable, and more than two points are generally employed for extrapolation, the maximum allowed deviation can be approximated by δn^0_M. Hence the equation

$$\frac{F' - F_I}{F_I^0} = \frac{n_M - (n^0_M - n^t)}{n^0_M} = \frac{(V^0 + V)\,([Y] + [NY])}{V^0 C^0_M} = \delta \quad (17)$$

can be taken as the limiting condition for linearity (F_I^0, the initial value of the stoicheiometric excess of M, is obviously equal to n^0_M). The approximate form

$$\frac{[Y] + [NY]}{C^0_M} = \delta \quad .. \quad .. \quad .. \quad .. \quad (18)$$

which holds for negligible dilution, is more conveniently used for calculating the critical value $[M]_c$, after substitution for [Y] and [NY] by equations (9) and (11).

The quantity defined by the left-hand side of equation (18) can be obtained directly from the logarithmic diagram as the antilogarithm of the vertical distance between the auxiliary curve representing log([Y] + [NY]) and the ordinate value $\log C^0_M$. The value of pY where this distance is equal to $\log\delta$ is easily identified. The corresponding values of [M] and of ε_I, equation (3) (and hence of f_I), can be also calculated from the diagram, as seen above.

In practice, however, according to equation (2), equation (15) is equivalent to

$$G = (V^0 + V)\,([M] + k_{M,N}[N]^{m/n} + D) \quad .. \quad (19)$$

In this part of the titration D is generally negligible, and the absolute deviation is

$$G - F_I = (V^0 + V)\,([Y] + [NY] + k_{M,N}[N]^{m/n}) \quad .. \quad (20)$$

A logarithmic diagram containing the plot of $(m/n)\log[N] + \log k_{M,N}$ can be used to calculate absolute and relative deviations for appreciable interference. In the part of the titration in which Y reacts quantitatively with M, [Y] and [NY] can be neglected; therefore, the deviation of G from F_I is due only to the term resulting from the interference, $(V^0 + V)k_{M,N}[N]^{m/n}$. For isovalent ions ($m = n$) the deviation, virtually equal to $k_{M,N}\,n^0_N$, is constant and the plot of G is linear. Hence, the first equivalence point obtained by linear extrapolation of G in this part of the titration is affected by a systematic error equal to $k_{M,N}n^0_N$. This error can be calculated and corrected for when the selectivity coefficient and the concentration of N are known. Correspondingly, titrations of a mixture of M and N of known composition can be used for obtaining the value of the selectivity coefficient[19] from the experimental error. When $m \neq n$, the contribution of the interference is variable even in the part of titration in which N does not react appreciably, and the plot is slightly curved; the curvature is negligible for negligible dilution ($V \ll V^0$).[19]

Second equivalence point

In the second part of the titration, the quantity giving the required linear plot against n^t, f or V is the difference between the total amount of metals and the amount of titrant added:

$$F_{II} = n^0_M + n^0_N - n^t = (C^0_M + C^0_N)V^0 - CV = (V^0 + V)\,([M] + [N] - [Y]) \quad (21)$$

For simplicity, the case in which the interference of N in the electrode response is negligible will be considered first.

Gran function. If K_{NY} is sufficiently smaller than K_{MY}, but still large, N begins to react with Y at the first equivalence point, and reacts quantitatively until to the second. Hence, both [M] and [Y] are negligible with respect to [N] in equation (21), which thus can be approximated by the equation:

$$F_{II} \approx F'' = (V^0 + V)\,[N] \quad .. \quad .. \quad .. \quad (22)$$

Moreover, the excess of titrant with respect to the first equivalence point is quantitatively converted to NY, so that it can be expressed by the approximate equation:

$$CV - C^0_M V^0 = (V^0 + V)\,([Y] + [NY] - [M]) \approx (V^0 + V)\,[NY] \quad (23)$$

(both [Y] and [M] are negligible with respect to [NY]).

Finally, for the mass balance of M, equation (5) can be approximated by the equation:

$$C^0_M V^0 \approx (V^0 + V)\,[MY] \quad .. \quad .. \quad .. \quad (24)$$

([M] is negligible with respect to [MY]). Substitution by the above equations into the expressions for the stability constants yields the approximate equations (25) and (26):

$$[Y] = \frac{[MY]}{K_{MY}\,[M]} \approx \frac{C^0_M V^0}{K_{MY}\,(V^0 + V)\,[M]} \quad .. \quad .. \quad (25)$$

$$[N] = \frac{[NY]}{K_{NY}\,[Y]} \approx \frac{C\,V - C^0_M V^0}{K_{NY}\,(V^0 + V)\,[Y]} \quad .. \quad .. \quad (26)$$

and equation (27) is obtained from equation (22):

$$F'' \approx G_{II} = \frac{K_{MY}\,(CV - C^0_M V^0)\,(V^0 + V)\,[M]}{K_{NY}\,C^0_M V^0} \quad .. \quad (27)$$

By substitution for [M] using equation (1), equation (27) yields the approximate function for linear extrapolation of the second equivalence point, analogous to but not identical with the usual Gran functions. By neglecting the constant factors, it can be used in the simpler form:

$$G_{II} = (CV - C^0_M V^0)\,(V^0 + V)\,10^{E/S} \quad .. \quad .. \quad (28)$$

For calculation of G_{II}, the amount of M, $C^0_M V^0$, is required. This quantity is either known (for instance, in "titrations with an auxiliary metal," where a known amount of M is added to a test solution containing N in order to permit the titration of N with the electrode for M) or can be obtained from the first equivalence point.

Deviations of the Gran plot from the ideal linear plot. Deviations of the Gran function, G_{II}, from F_{II} reflect the approximations made in the formulation of equation (27). It is convenient to examine separately the different contributions. As the purpose of this part of the titration is most often the determination of the amount of N, the relative deviations are best referred to this amount, *i.e.*, to the value of F_{II}, equation (22), at the first equivalence point, $F^0_{II} = C^0_N V^0$.

Neglecting [M] and [Y] with respect to [N] in equation (22) causes a deviation of F'' from F_{II}, represented by the equation:

$$\frac{F'' - F_{II}}{n^0_N} = \frac{(V^0 + V)\,([Y] - [M])}{C^0_N V^0} \approx \frac{[Y] - [M]}{C^0_N} \quad .. \quad (29)$$

This deviation is negative in the proximity of the first equivalence point (where [Y] << [M]) and positive in the proximity of the second (where [Y] >> [M]). The further approximations cause relative deviations of G_{II} from F'', which are proportional to the ratio between the quantity neglected and the exact quantity. Therefore, the deviation of G_{II} from F'' due to the approximation in equation (23) is proportional to ([Y] − [M])/([NY] + [Y] − [M]). This ratio is negative, approximately equal to −[M]/([NY] − [M]), or, simply, to −[M]/[NY] in the proximity of the first equivalence point; it is positive, equal to [Y]/([NY] − [Y]) ≈ [Y]/[NY] ≈ [Y]/C^0_N, in the proximity of the second. The deviation due to the approximation in equation (24) with respect to equation (5) is proportional to [M]/C^0_M. The theoretical values of these ratios are calculated at a given value of [M] by substitution for the conditional concentrations using equations (9) and (11). More conveniently, these ratios are obtained from the logarithmic diagram at given values of pY and, indirectly, of [M] and ε or *f*.

Taking all these contributions into account in the calculation of the total deviation would be complicated. However, the smaller contributions to the over-all relative deviation of G_{II} from F_{II} can be frequently neglected with respect to the larger. In this way, the two values of pY (and, indirectly, of [M] and ε) at which the relative deviation of the Gran plot for the second equivalence point from the ideal linear plot is equal to a given value δ and to − δ, respectively, can be easily found, as shown under Examples.

The titration points corresponding to the relative deviations −δ (in the proximity of the first equivalence point) and δ (in the proximity of the second) are sufficiently indicative of the limits of the titration range where linear extrapolation of G_{II} yields an error not higher than δ (particularly when several experimental points are regularly distributed within this range). In principle, this part of the titration, where the smallest deviations occur in the intermediate stage, could not be treated according to the same simple criteria as the first part of the titration, in which the initial points are affected by the smallest deviations; however, the experimental limitations of the potentiometric measurements do not warrant the complex rigorous treatment.

Further deviations of G_{II} from F_{II} are caused by the electrode interference of N. The effect can be very large even for small values of $k_{M,N}$, because the ratio between [N] and [M] can be very large in this part of the titration. The experimental Gran function (28), taking into account the interference of an isovalent ion, becomes equivalent to

$$G_{II} = \frac{K_{MY}\,(CV - C^0_M V^0)\,(V^0 + V)\,([M] + k_{M,N}[N]^{m/n})}{K_{NY}\,C^0_M V^0} \quad (30)$$

where the measured value, ([M] + $k_{M,N}$[N]$^{m/n}$), is substituted for the actual value of [M]. When the free concentration ratio [M]/[N] is (much) lower than the selectivity coefficient after the first equivalence point, the electrode can be considered in principle as being selective for N. Therefore, the treatment of this part of the titration is the same as given below for the case when the measured metal reacts in the second part of the titration. In practice, however, the selectivity coefficient is poorly defined at these low [M]/[N] ratios, and theoretical expectations can be unwarranted.

Corrected Gran function. When K_{NY}, or the ratio between K_{MY} and K_{NY}, or both these quantities are insufficiently large to yield a reasonably linear Gran function in the second part of the titration, a linear plot can be obtained in principle only by calculating the value of F_{II}. The functional expression of F_{II} in terms of [M] is obtained by substituting in equation (21) equation (9) for [Y] and the equation

$$[N] = \frac{CV - \{C^0_M V^0 - (V^0 + V)\,([M] - [Y])\}}{K_{NY}\,(V^0 + V)\,[Y]} =$$

$$\frac{K_{MY} CV[M] - \{C^0_M V^0 - (V^0 + V)[M]\}(1 + K_{MY}[M])}{K_{NY}\{C^0_M V^0 - (V^0 + V)[M]\}} \quad (31)$$

for [N]. An equation is obtained that, by analogy with similar equations for other types of titrations, can be termed a "corrected Gran equation." This equation requires the knowledge of both constants and of C^0_M; therefore, it is particularly suitable for titrations with M as the auxiliary metal (see above). It can be used under the condition that the electrode is calibrated to measure the conditional concentration of M.

Other rigorous linear plots. When C^0_M and K_{MY} are known, the second part of the titration can be used in principle for the determination of both K_{NY} and the amount of N. For this purpose, equation (32), obtained by rearranging of equation (21) after substituting for [N] and [Y], can be used:

$$Y = C^0_N V^0 - \left(\frac{1}{K_{NY}}\right) X \quad .. \quad .. \quad .. \quad (32)$$

where:

$$X = (V^0 + V) \times \frac{K_{MY} CV[M] - \{C^0_M V^0 - (V^0 + V)\,[M]\}(1 + K_{MY}[M])}{C^0_M V^0 - (V^0 + V)[M]} \quad (33)$$

$$Y = CV - \{C^0_M V^0 - (V^0 + V)[M]\}\left(1 + \frac{1}{K_{MY}[M]}\right) \quad . . \quad (34)$$

Using the titration parameters and experimental data for calculating X and Y, a rigorous linear plot of Y *versus* X is obtained. The intercept with the abscissa yields the amount of N, and the slope yields K_{NY}. The principle of the method is the same as that of the Hofstee and Scatchard plots for the determination of binding constants.[18,20]

Different rearrangements of equation (21) allow the determination of other pairs of titration parameters.

$K_{NY} >> K_{MY}$

When the metal sensed by the electrode gives the less stable complex with Y, large variations of [M] and of the electrode potential only occur after the first equivalence point, corresponding to the titration of N. Only the second equivalence point, corresponding to the titration of M + N, is detectable on the titration curve.

The ideal linear function is a constant before the first equivalence point, and is represented by equation (21) after it. If K_{MY} is large enough and sufficiently smaller than K_{NY}, it can be assumed that M begins to react exactly at the first equivalence point, and reacts quantitatively until the second; both [N] and [Y] are negligible in equation (21), which therefore reduces to equation (14). Hence, the Gran function (15) is used. Equation (15) is equivalent to equation (19); however, as [N] is small, the interference can be neglected, and equation (19) also reduces to equation (14). Of course, only points after the first equivalence point can be used for extrapolation.

The absolute deviation of G, equations (14) and (15), from F_{II}, equation (21), is

$$G - F_{II} = (V^0 + V)([Y] - [N]) \quad . . \quad (35)$$

In the proximity of the first equivalence point, where [N] ≫ [Y], the deviation is negative; it becomes positive on approaching the second equivalence point, where [Y] ≫ [N]. The relative deviation is expressed by the ratio of the absolute deviation to: (*i*) $(C^0_M + C^0_N)V^0$, if the purpose of the titration is the determination of the total amount of both metals; (*ii*) $C^0_M V^0$, when the amount of N is determined by another method; and (*iii*) $C^0_N V^0$, if M is added in a known amount as the auxiliary metal for the determination of N.

When K_{NY} is only moderately larger than K_{MY} and/or K_{MY} is relatively small, the linear range of the Gran plot is narrow, or completely absent. In this instance, the corrected Gran function introduced above can be used. When the two conditional constants are very similar, and K_{MY} is known, K_{NY} can be determined by plotting equation (32).

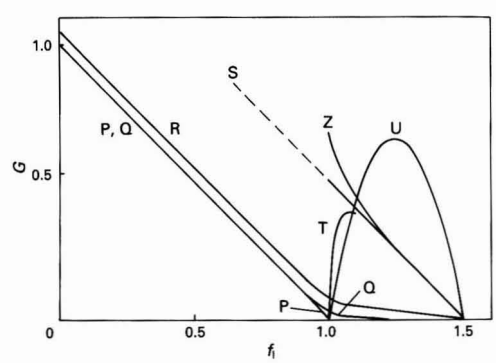

Fig. 3. Plots of "linear" equations for the titration of 1.00×10^{-2} M M ($K_{MY} = 10^{10.00}$) and 0.50×10^{-2} M N ($K_{NY} = 10^{7.00}$) with an electrode for M. Lines P [equation (12)] and S [equation (21)] are the ideal plots for the first and the second equivalence point, respectively. Curves Q and R, equation (19), and curves T and U, equation (30), for $k_{M,N} = 0$ and 0.1, respectively. Curve Z, the same as R with G scale enlarged ×10. Ordinate is normalised

Examples

A few examples are discussed for illustration of the theoretical treatment.

Example 1: $K_{MY} >> K_{NY}$

For the system represented in Fig. 1 ($C^0_M = 1.00 \times 10^{-2}$, $C^0_N = 0.50 \times 10^{-2}$, $\log K_{MY} = 10.00$, $\log K_{NY} = 7.00$), the Gran function for the first equivalence point, calculated with equation (19), is represented in Fig. 3 by line Q for $D = 0$ and $k_{M,N} = 0$, and by line R for $K_{M,N} = 0.1$ (a value larger than in Fig. 1, giving an appreciable interference even in this part of the titration) and $n = m$. The rigorous linear plot, equations (12) and (13), is line P.

The linearity critical condition, equation (18), of the Gran plot (in the absence of electrode interference) is satisfied for δ = 0.01 at pY = 8.7 {where $\log([Y] + [NY]) \approx \log[NY] = \log C^0_M - \delta = -4$; see Fig. 1(*a*), segment *a*}. At this pY value, a titration ratio, $f_I = 0.96$, is calculated with equation (3′). Thus, a titration error of less than 1% on the amount of M is expected if points regularly distributed between $f_I = 0$ and $f_I = 0.96$ are linearised by using equation (15). It must be observed that a small fraction of titrant reacts with N from the beginning of the titration. The largest distance between the curves of log[NY] and log [MY] is −3.3, *i.e.*, the smallest ratio between [NY] and [MY] is 0.005 or 0.5%. Hence, the systematic relative titration error cannot be smaller than this value.

For the second equivalence point, the rigorous linear function, equation (21), is line S in Fig. 3; the corresponding Gran function, calculated with equation (27), is line T.

The point where the modulus of the (negative) relative deviation, $(G_{II} - F_{II})/C^0_N V^0$, decreasing with the progress of the titration after the first equivalence point, becomes smaller than a given value δ, is identified on the logarithmic diagram [Fig. 1(*a*)] by the pY value at which all the following conditions are satisfied:

$$\log([M] - [Y]) - \log C^0_N \approx \log[M] - \log C^0_N \leqslant \log \delta \quad . . \quad (36)$$

$$\log([M] - [Y]) - \log([NY] + [Y] - [M]) \approx \log[M] - \log[NY] \leqslant \log \delta \quad (37)$$

$$\log[M] - \log C^0_M \leqslant \log \delta \quad . . \quad . . \quad (38)$$

[see equation (29) and discussion above]. It can be seen that at pY ≈ 7.25, where condition (37) is met for $|\delta| = 0.01$ [Fig. 1(*a*), segment *b*], both conditions (36) and (38) are largely satisfied. The corresponding titration ratio is $f_I = 1.18$ (after the complete titration of M, 36% of N has also been titrated).

The point at which the (positive) deviation, $(G_{II} - F_{II})/C^0_N V^0$, increasing as the titration approaches to the second equivalence point, reaches a given value δ is identified by the pY value where all the conditions (38), (39) and (40) are satisfied:

$$\log([Y] - [M]) - \log C^0_N \approx \log[Y] - \log C^0_N \leqslant \log \delta \quad . . \quad (39)$$

$$\log([Y] - [M]) - \log([NY] + [Y] - [M]) \approx \log[Y] - \log[NY] \approx \log[Y] - \log C^0_N \leqslant \log \delta \quad (40)$$

It is seen that at pY = 5.3, the smaller pY value where conditions (39) and (40) (almost equivalent) are still satisfied by δ = 0.001 [Fig. 1(*a*), segment *c*], condition (38) is largely satisfied. The corresponding titration ratio is $f_I = 1.49$.

It can be concluded that linear extrapolation of points from $f_I = 1.2$ almost to the second equivalence point yields in principle an accurate end-point for the titration of the sum of metals, particularly if a greater weight is given to points closer

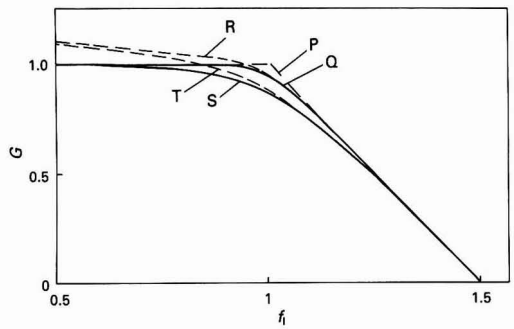

Fig. 4. Plots of "linear" equations for the second equivalence point of the titration of 0.50×10^{-2} M M and 1.00×10^{-2} M N ($K_{NY} = 10^{10.00}$). Linear segments P, ideal plot. Curves Q and R, equation (19) for $k_{M,N} = 0$ and 0.1, respectively, and $K_{MY} = 10^{7.00}$. Curves S and T, equation (19) for $k_{M,N} = 0$ and 0.1, respectively, and $K_{MY} = 10^{8.00}$

to the end of the titration (on the condition that the detection limit of the electrode response is not approached).

Line U in Fig. 3 is the Gran plot for appreciable interference of N in the electrode response, calculated with equation (30) for $k_{M,N} = 0.1$ and $n = m$. It can be seen that linearity is completely lost; however, the equivalence point can still be found (if it is far from the detection limit) by the limiting slope method. Line Z, representing on an enlarged scale line R at $f_I > 1$, shows that, in principle, a large and constant selectivity coefficient allows acceptable extrapolation of the second equivalence point with the Gran function valid for the first.

Example 2: $K_{MY} \ll K_{NY}$

The Gran function for the second equivalence point of the titration represented in Fig. 2 ($C^0_M = 0.50 \times 10^{-2}$, $C^0_N = 1.00 \times 10^{-2}$, $\log K_{MY} = 7.00$, $\log K_{NY} = 10.00$), calculated with equation (19), is represented in Fig. 4 by line Q for $D = 0$ and $k_{M,N} = 0$, and by line R for $k_{M,N} = 0.1$ and $n = m$. The rigorous linear plot is line P. It can be seen that, in principle, the first equivalence point can be determined by extrapolating the linear parts, near the beginning of the titration and approaching the second equivalence point, of line R. Lines S and T are the plots corresponding to lines Q and R, respectively, but for $K_{MY} = 10^{8.00}$.

For this titration, it is convenient to refer deviations of the Gran plot for the second equivalence point to the analyte present in smaller amounts, so obtaining more stringent limits. The point where the modulus of the negative relative deviation $(G - F_{II})/C^0_M V^0$ becomes smaller than a given value, δ, is identified on the logarithmic diagram [Fig. 2(*a*)] by the pY value at which the following condition is satisfied:

$$\log([N] - [Y]) - \log C^0_M \approx \log[N] - \log C^0_M \leqslant \log \delta \quad (41)$$

[see equation (35)]. For $\delta = 0.01$, this condition is reached at pY = 7.7, $f_I = 1.08$ (16% of M has reacted); for $\delta = 0.001$, the same condition is reached at pY = 6.7, $f_I = 1.33$ (two thirds of M has been titrated).

The point approaching the (second) equivalence point, at which the positive deviation reaches a given value δ, is identified by the point where condition (42) is met:

$$\log([Y] - [N]) - \log C^0_M \approx \log[Y] - \log C^0_M \leqslant \log \delta \quad (42)$$

For $\delta = 0.001$, this condition is reached at pY = 5.3, $f_I = 1.49$ (98% of M has been titrated). Therefore, good accuracy must be expected in the determination of the total amount of the metals (or either of them, if the amount of the other is known) if points at f_I higher than about 1.1 are linearised.

Conclusions

Linearisation of potentiometic complexation titrations can solve titration problems for which the traditional end-point methods are unsuccessful. In the above discussion the theoretical foundations have been described for which approximate and rigorous linear plots are obtained. New linear equations have been introduced. Non-ideality and poor reproducibility of the response of the measuring electrode are expected to be the main causes of failure of the theoretical expectations.

It can be expected that some of the procedures introduced here for the evaluation of titration and the treatment of experimental data will be particularly useful for titration with an auxiliary metal. For this type of titration system, after choosing the most suitable auxiliary metal with its own indicating electrode, it should be easy to adjust the experimental parameters to fulfil the optimum conditions for application of the linearisation methods.

References

1. Gran, G., *Analyst*, 1952, **77**, 661.
2. Mascini, M., *Ion-Sel. Electrode Rev.*, 1980, **2**, 17.
3. Carr, P. W., *Anal. Chem.*, 1972, **44**, 452.
4. Johansson, A., *Talanta*, 1973, **20**, 89.
5. Johansson, A., and Wänninen, E., *in* Kolthoff, I. M., and Elving, P. J., *Editors*, "Treatise on Analytical Chemistry, Part I," Volume 11, Interscience, New York, 1975, p. 7117.
6. Anfält, T., and Jagner, D., *Anal. Chem.*, 1973, **45**, 2412.
7. Maccà, C., and Bombi, G. G., *Analyst*, 1989, **114**, 463.
8. Maccà, C., *Analyst*, 1989, **114**, 689.
9. Hannema, U., and den Boef, G., *Anal. Chim. Acta*, 1967, **39**, 167.
10. Hannema, U., and den Boef, G., *Anal. Chim. Acta*, 1967, **39**, 479.
11. Van der Meer, J. M., den Boef, G., and van der Linden, W. E., *Anal. Chim. Acta*, 1975, **76**, 261.
12. IUPAC, "Compendium of Analytical Nomenclature," Pergamon Press, Oxford, 1978, p. 168.
13. Midgley, D., *Analyst*, 1979, **104**, 248.
14. Midgley, D., *Ion-Sel. Electrode Rev.*, 1981, **3**, 43.
15. Neshkova, M., and Sheytanov, H., *Mikrochim. Acta*, 1985, **II**, 161, and references cited therein.
16. Maccà, C., and Bombi, G. G., *Fresenius Z. Anal. Chem.*, 1986, **324**, 52.
17. Maccà, C., *Analyst*, 1983, **108**, 395.
18. Maccà, C., *Fresenius J. Anal. Chem.*, 1990, **336**, 29.
19. Maccà, C., and Cakrt, M., *Anal. Chim. Acta*, 1983, **154**, 51.
20. Connors, K. A., "Binding Constants," Wiley, New York, 1987.

Paper 9/03991K
Received September 18th, 1989
Accepted November 14th, 1989

Comparative Study of Various Polyols as Complexing Agents for the Acidimetric Titration of Tungstate*

Jean-François Verchère, Jean-Paul Sauvage and Guy-Roland Rapaumbya
Laboratoire de Chimie Macromoléculaire, Unité de Recherche Associée 500 du Centre National de la Recherche Scientifique, Faculté des Sciences de Rouen, B.P. 118, 76134 Mont-Saint-Aignan, France

Most polyols (L = alditol or carbohydrate) form dinuclear tungstate complexes according to the over-all equilibrium $2WO_4^{2-} + 2H^+ + L \rightleftharpoons [W_2O_7L]^{2-} + H_2O$. When the reaction is fast and complete, it allows the acidimetric titration of tungstate. The formation constants of the complexes of a series of polyols were determined by potentiometry. Their values were higher at low ionic strengths. Opposite structural factors govern the stabilities and the formation rates of complexes: alditols of *threo* configuration react with tungstate faster than those of *erythro* configuration, but the stability order is *erythro* > *threo*. Of the polyols investigated, only xylitol and D-glucitol (sorbitol) allowed a fast and accurate potentiometric titration. Using 0.02 M HCl as titrand, 0.04 mmol of tungstate was determined in a volume of 100 cm³. The interference of molybdate is discussed in detail.

Keywords: *Tungstate; titrimetry; polyol; carbohydrate; complexation equilibrium*

In addition to its well known metallurgical use, tungsten is now recognised as an important element in biochemistry, as demonstrated by the recent publication of methods[1,2] for the determination of tungstate in biological materials. Several tungsten compounds have been reported[3] to have medicinal activity. This element is usually determined as the tungstate ion (WO_4^{2-}) and the sodium salt $Na_2WO_4.2H_2O$ is a good primary standard. Most usual methods[4] are based on the spectrophotometry of various complexes, the selectivity of which can be improved[5] by using very weakly basic ligands in strongly acidic medium. In contrast, the much easier titrimetric methods seem restricted to re-oxidation of the W^{III} produced by the reduction of W^{VI} using several amalgams,[4] and to acidimetric titration[6–8] after complexation by D-mannitol. However, our own attempts showed the latter method to be unsuitable because formation of the complex was very slow; this confirms another recent report.[9]

Until now, D-mannitol is the only polyol that has been considered for this determination, which is surprising as it is a long time since the relative stabilities of tungstate complexes were investigated qualitatively[10,11] for use in the chromatographic separation of sugars and alditols. Equilibrium constants were determined potentiometrically for the reaction of two hexitols[8,12] and some aldoses.[13] "Pseudo-stability constants" were defined[14] from an electrophoretic study. The structures of hexitol complexes have been determined recently.[15,16]

Considering the simplicity of the acidimetric titration, we tried to improve it by using more appropriate polyols. Common alditols and carbohydrates were investigated as possible complexing agents and the formation constants of their complexes were determined under identical conditions. As most polyols, *e.g.*, D-mannitol, reacted slowly with tungstate, the kinetics of complex formation were taken into account in order to select the best reagents for use.

Experimental

All carbohydrates and alditols were of analytical-reagent grade (Fluka or Aldrich) and were used without further purification. Analytical-reagent grade disodium tungstate dihydrate and disodium molybdate dihydrate (Prolabo) were standardised as described previously.[5,13] In order to avoid possible condensation to unreactive species stock solutions of tungstate were not used. Instead, solutions at the desired concentrations were prepared immediately prior to the titration experiments. The titrand solutions were made by diluting commercial standard HCl solutions (Prolabo, Normadose). Readings of pH were taken using a Metrohm E 632 pH-meter. As tungstate and molybdate solutions are known[17] to attack glass electrodes slowly, the pH-meter was calibrated daily using standard buffers.

The formation constants of the complexes (temperature, 25.0 °C; [KCl], 0.1 M) were determined from measurements on aqueous solutions (100 cm³) ($[WO_4^{2-}]$, 5×10^{-3} M), half-neutralised by 2.50 cm³ of 0.100 M HCl. Weighed amounts of polyol (typically 0.5–1 g) were added and the pH was recorded until stabilisation had occurred. Dilution effects were minimised by introducing the ligands in solid form. The temperature was fixed by performing all experiments in a water-bath. All determinations were, at least, duplicated.

Titrations at different ionic strengths were performed on aqueous solutions (100 cm³) (Na_2WO_4, 10^{-3} M) containing an inert salt (KCl or NaCl of analytical-reagent grade) and the ligand in known concentrations. The titrand was 0.0100 M HCl, hence the end-point was found at 10.00 cm³.

Titrations of dilute solutions were performed on 100 cm³ of 4×10^{-4} M sodium tungstate (KCl, 0.1 M), containing 4.0 g of either xylitol or D-glucitol (sorbitol). The titrand was 0.0200 M HCl, and the end-point was found at 2.00 ± 0.05 cm³. In this instance only, carbon dioxide was excluded by bubbling pure nitrogen into the solution for 15 min before the titration.

We verified that the values of the formation constants were in good agreement by using the data obtained at various tungstate concentrations.

Principle of the Acidimetric Titration of Tungstate

The acidimetric titration of sodium tungstate does not involve simple acid - base equilibria, because of the formation of various isopolyanions. Defining the apparent neutralisation ratio as $x = [H^+]/[WO_4^{2-}]$, the first condensation step is seen to be fast and to yield heptatungstate[18] reversibly for $x = 8/7 = 1.14$ according to the reaction

$$7WO_4^{2-} + 8H^+ \rightleftharpoons [W_7O_{24}]^{6-} + 4H_2O$$

The addition of an excess of acid, *i.e.*, $1.15 < x < 1.50$, initiates the slow and irreversible formation of dodecatung-

* Presented at SAC 89, the 8th SAC International Conference on Analytical Chemistry, Cambridge, UK, 30 July–5 August, 1989.

state,[19] associated with an upward drift in pH, which makes the first end-point difficult to locate accurately. Moreover, the first step is characterised by a buffered zone in the pH range 6–7, which is not favourable for an acidimetric titration.

In the presence of most polyols, the apparent basicity of tungstate is enhanced and a clear end-point is found[10] at exactly $x = 1$. According to previous studies,[12,13] the reaction involves the proton-consuming formation of a dinuclear complex, as for the analogous molybdate - polyol system.[20–22] The general form of the formation equilibria of the complex is

$$2WO_4^{2-} + L + 2H^+ \rightleftharpoons [2,1,2]^{2-} + H_2O \quad .. \quad (1)$$

where L is the polyol.

The simplest formula for the complex, omitting water molecules, would be $[W_2O_7L]^{2-}$ with the formation constant K_{212} being defined as the equilibrium constant of reaction (1).

In all experiments, the polyol was present in a large excess and generally, as the formation constant had a high value, the reaction could be considered quantitative. Defining the initial concentrations of tungstate and polyol as c_W and c_L, respectively, the concentration of acid added was xc_W and the equilibrium concentrations were as follows: $[L] = c_L$, $[WO_4^{2-}] = c_W(1 - x)$ and $[W_2O_7L^{2-}] = c_Wx/2$.

The law of mass action yields the equilibrium constant K_{212} where

$$K_{212} = \frac{[W_2O_7L^{2-}]}{[WO_4^{2-}]^2[L][H^+]^2} = \frac{x}{2c_Lc_W(1-x)^2[H^+]^2} \quad (2)$$

In consequence, when the contributions of other acid - base equilibria could be neglected, the variations of pH with the neutralisation ratio ($0 < x < 1$) were given by equation (3). Therefore, the titration curves resembled those obtained for the titration of a weak base.

$$pH = 1/2(\log K_{212}c_Lc_W) + 1/2\{\log[2(1-x)^2/x]\} \quad .. \quad (3)$$

The formation constants K_{212} were calculated from the pH value at the half-equivalence point, $pH_{\frac{1}{2}}$. For $x = 0.5$, equation (3) reduces to

$$pH_{\frac{1}{2}} = 1/2(\log K_{212}c_Lc_W) \quad .. \quad .. \quad (4)$$

which was used in the following logarithmic form:

$$\text{Log } K_{212} = 2pH_{\frac{1}{2}} - \log c_L - \log c_W \quad .. \quad (5)$$

Results and Discussion

The titration of tungstate in the presence of D-mannitol, following procedures described in the literature,[6,8] was found to be unsatisfactory because the equilibrium was reached very slowly after each addition of acid (typically 10–20 min). This is probably why Selig[9] reported that the method was unsuitable on the microscale. Examination of the literature revealed that this phenomenon had already been mentioned by Weigel and co-workers,[11] who attributed it to an isomerisation of the complex. Similar titrations were performed, substituting various alditols and carbohydrates for D-mannitol and, except for two sugars that did not seem to complex tungstate (D-glucose, D-xylose), all the polyols gave end-points for volumes of acid within 0.5% of the calculated value for one proton per tungstate ion.

For each polyol, the $pH_{\frac{1}{2}}$ values at half-equivalence were recorded at several ligand concentrations, c_L, in order to determine the formation constants. Fig. 1 shows that $pH_{\frac{1}{2}}$ varied linearly with log c_L. To make the comparison easier, all plots were drawn for the same tungstate concentration, *i.e.*, $c_W = 5 \times 10^{-3}$ M. The slope value of 0.50 confirms that 2:1 complexes were the predominating species under our experimental conditions. The alditol plots are generally located above those of the carbohydrates, illustrating the order of stabilities of the complexes.

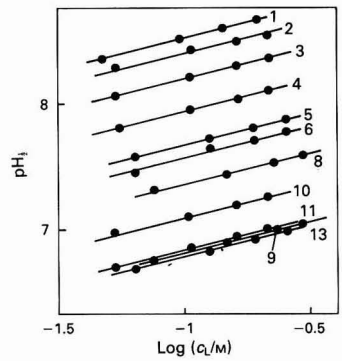

Fig. 1. Variations of $pH_{\frac{1}{2}}$ (pH at half-titration) *versus* log c_L (where c_L is the polyol concentration). c_W, 5×10^{-3} M; temperature, 25 °C; and ionic strength, 0.1 M KCl. Ligands 1–13 are defined in Table 1

Table 1. Potentiometric formation constants and rates of formation of tungstate complexes of polyols. Conditions: temperature, 25 °C; ionic strength, 0.1 M (KCl)

Ligand	Log K_{212}*	Rate	Literature data (reference)
Alditols—			
1 Perseitol† ..	20.35	Slow	
2 Galactitol ..	20.10	Slow	
3 D-Mannitol ..	19.65	Slow	18.78 (12); 20.24 (8)
4 D-Glucitol ..	19.15	Fast	19.26 (12)
5 D-Arabinitol ..	18.65	Slow	
6 Xylitol	18.50	Fast	
7 Ribitol	18.10	Slow	
8 Erythritol ..	18.00	Slow	
9 DL-Threitol ..	16.95	Fast	
Carbohydrates—			
10 D-Mannose ..	17.50‡	Slow	
11 D-Galactose ..	17.00	Slow	
12 D-Fructose ..	16.90	Slow	
13 D-Ribose ..	16.90	Slow	
14 L-Sorbose ..	16.40	Slow	

* The formation constant K_{212} is the equilibrium constant of the reaction $2WO_4^{2-} + L + 2H^+ \rightleftharpoons [W_2O_7L]^{2-} + H_2O$. Accuracy of log K_{212}, ±0.10.

† D-Glycero-D-galacto-heptitol.

‡ From reference 13.

Values of the formation constants, log K_{212}, were calculated by applying equation (5) to the data illustrated in Fig. 1. The results (Table 1) were compared to available literature values and showed good agreement for D-glucitol.[12] Large discrepancies were observed for D-mannitol.[8,12] This was probably due to its slow complexation rate, as the low pH values were obtained when measurements were made before equilibrium was established.

Influence of the Ionic Strength

As increasing the ionic strength had a favourable effect on the stabilities of polytungstates,[23] we examined whether the concentration of two inert salts, NaCl and KCl, could have a similar effect on the formation constants of the dinuclear complexes. The influence on the quality of the determination was checked by titrating 10^{-3} M solutions of tungstate against 10^{-2} M HCl. The results (Table 2) show that the salt effects are comparable when using different alditols, whether they complex tungstate slowly (*e.g.*, mannitol) or rapidly (*e.g.*, glucitol and xylitol). Some general observations can be made. (a) Contrary to the results obtained for the isopolyanions, the formation constants decreased when the salt concentrations

Table 2. Effect of the ionic strength on the formation constants (log K_{212}) of tungstate - alditol complexes. Conditions: temperature, 25 °C

	Log K_{212}*		
	Glucitol	Mannitol	Xylitol
Concentration of NaCl/M—			
0.01	19.30	—	18.65
0.05	19.25	19.45	18.50
0.1	19.10	19.60	18.30
1	18.70	19.05	17.90
Concentration of KCl/M—			
0.01	19.40	—	18.70
0.05	19.30	19.55	18.55
0.1	19.15	19.65	18.50
1	19.10	19.45	18.25

* Accuracy of log K_{212}, ±0.10.

increased. Peculiar behaviour was observed for D-mannitol, the complex of which had a maximum stability at 0.1 M salt concentrations. (b) At high (1 M) salt concentrations, the formation constants were larger in KCl than in NaCl. The magnitude of this effect was too high to be attributed only to variations of the activity coefficients of the aqueous proton.

From the practical point of view, the use of high ionic strengths was unfavourable, because the stabilities of the complexes decreased, resulting in lower values of $pH_{\frac{1}{2}}$ and poorer quality end-points. However, the complete absence of added salt caused unstable pH readings. Therefore, all titrations of dilute tungstate solutions were performed in solutions containing 0.1 M KCl.

Kinetics of the Reaction

The formation constants described above are the major parameters in the design of the titration procedure, as the height of the final pH jump essentially depends on the value of $pH_{\frac{1}{2}}$. This is probably why previous analytical studies have been restricted to D-mannitol, which forms one of the more stable complexes. However, alditols that complex tungstate more rapidly allow much easier titrations. Of the ligands investigated, only DL-threitol, xylitol and D-glucitol were found to give fast reactions with tungstate. It suggested that the presence of *threo* diol groups in the ligand (or the absence of *erythro* diol groups) was associated with a high kinetic reactivity towards tungstate. Accordingly, the comparison of both epimeric tetritols showed that erythritol complexes tungstate much more slowly than threitol.

The opposite is found when the stabilities of the complexes are compared. For example, the erythritol complex is more stable than its threitol homologue. The relationship between the stabilities of the complexes and the alditol structures has been discussed,[24] showing that the formation constants depended mainly on the number of available hydroxyl groups, because the involvement of terminal CH_2OH groups in chelation resulted in a decrease of stability. Within a series of identical chain length, the influence of the configuration was not clear, because pentitols and hexitols could bind tungstate on several different sites. However, xylitol and D-glucitol do not form complexes of outstanding stabilities.

To summarise, it can be concluded that the reactions of tungstate with alditols possessing *erythro* diol groups slowly form complexes of high stabilities, whereas alditols possessing *threo* diol groups rapidly form complexes of lower stabilities.

Acidimetric Titration of Tungstate Solutions

The design of the titration procedure stems from equation (5). The value of $pH_{\frac{1}{2}}$ is equivalent to an "apparent acidity constant" and directly influences the sharpness of the end-point. Hence the best conditions would involve polyols that form complexes with high values of log K_{212}, and high values of c_W and c_L. In fact, the range of c_W is generally low, and the value of c_L is not critical if the ligand is present in excess (*i.e.*, $c_L/c_W > 100$), as $pH_{\frac{1}{2}}$ depends on 1/2(log c_L). For $c_W = 5 \times 10^{-3}$ M, the ligand concentration necessary to obtain a desired $pH_{\frac{1}{2}}$ value can be read graphically from Fig. 1. The range covered in this study was $0.05 \text{ M} > c_L > 0.5 \text{ M}$. Most polyols, including D-mannose, form a complex sufficiently stable (log $K_{212} > 17.50$) to titrate tungstate. Although galactitol and D-mannitol seemed to be the best ligands on the basis of their higher complex stabilities, better results were obtained with D-glucitol and xylitol, which possessed higher reaction rates. Finally, if the cost of analysis must be taken into account, we recommend the use of the cheaper D-glucitol in place of D-mannitol[6–8] for the titration of tungstate.

Special attention must be paid to the initial pH of the solution to be titrated. In order to avoid the formation of isopolyanions of low reactivity,[19] a solution of tungstate should not be kept in acidic medium. If necessary, a few drops of sodium hydroxide must be added to make the solution alkaline. In this instance, the titration curve shows two equivalence points; the first corresponds to the neutralisation of the OH^- ions. The concentration of tungstate is then obtained by difference. Detailed analytical procedures for various tungsten-containing solids are given in reference 7 and these were used without modifications throughout this study. Our pH-metric curves were similar to that shown for a D-mannitol titration in Fig. 1 of that same reference.

The method was used in our laboratory for the standardisation of sodium tungstate solutions, together with a spectrophotometric method based on the formation of the tungstate - catechol complex.[5] The accuracy was checked by determining solutions prepared with weighed amounts of reagent, and the results were within 1% of the calculated values. For routine conditions, 100 cm³ of tungstate solution ($c_W = 10^{-3}$ M) were titrated with standard 10^{-2} M HCl, after the addition of 4 g of polyol (xylitol or D-glucitol). Attempts to determine more dilute tungstate solutions, using 10^{-3} M HCl, showed a severe decrease in the sharpness of the final pH jump, because the $pH_{\frac{1}{2}}$ values decreased, whereas the pH increased after the end-point, owing to the lower concentration of HCl.

Considering that a minimum pH jump should cover at least three pH units, solutions with c_W as low as 4×10^{-4} M could be titrated with 0.02 M HCl using a microburette. The solution volume was 100 cm³ and 4 g of xylitol or D-glucitol were used. Five independent titrations gave a final volume of acid, $V = 2.00 \pm 0.05$ cm³ (theoretical value 2 cm³). A lower concentration of HCl would have given a larger volume, but also unacceptably high pH values after the end-point. Taking $c_W = 4 \times 10^{-4}$ M as the detection limit of tungsten, this corresponds to 73.54 mg l^{-1} or 73.5 p.p.m. A 0.04-mmol amount of tungstate can be determined in 100 cm³.

Interferences

Interferences from most metallic elements can be easily avoided, because the common divalent cations and Fe^{III} are precipitated from the alkaline solution and can be eliminated by filtration. In principle, no interference can arise from other weak acids because the titrand is a strong acid. However, basic species such as ammonia, amines, phosphate or carbonate ions must not be present. Boric acid and borates react easily with polyols[25] and therefore cause serious interference.

Molybdate ions react rapidly with polyols in a similar manner to tungstate. Because their formation constants are not sufficiently different,[12,13] molybdate and tungstate interfere with each other. Hence this interference was studied in detail, using sodium molybdate as the source of molybdenum. Fig. 2 shows a comparison of the titration curves obtained with solutions of tungstate ($c_W = 5 \times 10^{-3}$ M), molybdate ($c_{Mo} = 5 \times 10^{-3}$ M) and a mixture ($c_W = c_{Mo} = 2.5 \times 10^{-3}$ M) under

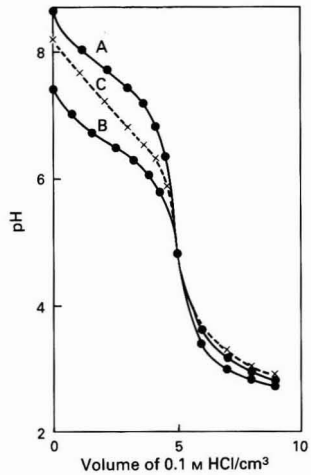

Fig. 2. pH curves for the titration of A, tungstate ($c_W = 5 \times 10^{-3}$ M), B, molybdate ($c_{Mo} = 5 \times 10^{-3}$ M) and C, a mixture ($c_W = c_{Mo} = 2.5 \times 10^{-3}$ M) with 0.1 M HCl. Volume of solution, 100 cm³; ionic strength, 0.1 M KCl. Polyol added, xylitol (4 g)

identical conditions (V = 100 cm³; titrand, 0.1 M HCl; ionic strength, 0.1 M KCl; xylitol added, 4.0 g). Using the relationship defined above for the tungstate species, the $pH_{\frac{1}{2}}$ value for the molybdate curve allowed calculation of the formation constant of the dimolybdate - xylitol complex (log K_{212} = 16.30). As observed for several other polyols,[12,13] it is weaker than its tungstate homologue (log K_{212} = 18.50). Similarly, it was reported[26] that the pH jump in the titration of molybdate, using D-mannitol, was less sharp than that with tungstate and was not suitable analytically.

We checked whether the absence of an inflection point in the titration curve of the mixture could result from the small difference between the $pH_{\frac{1}{2}}$ values corresponding to tungsten and molybdenum ($\Delta pH_{\frac{1}{2}}$ = 1.08) or from the possible formation of a ternary complex $[WMoO_7L]^{2-}$. The curve was found to agree exactly with that expected for the stepwise formation of the ditungstate complex followed by the dimolybdate complex. Accordingly, the pH measured at half-equivalence was equal to $1/2[pH_{\frac{1}{2}}(W) + pH_{\frac{1}{2}}(Mo)]$. Before the end-point, no evidence was found for the existence of a mixed W - Mo species with properties different from those of a simple mixture of both complexes.

A consequence of the similar behaviour of tungstate and molybdate is that the sum of their concentrations, $c_{Mo} + c_W$, can be determined in a mixture by a single acidimetric titration, as shown in Fig. 2.

The authors thank Mrs. E. Leconte for technical assistance.

References

1. Eberhard, A., and Kenyon, G. L., *Analyst*, 1987, **112**, 305.
2. Chakraborty, D., and Das, A. K., *Analyst*, 1989, **114**, 67.
3. Tanaka, S., patents reported in *Chem. Abstr.*, 1985, **102**, 191114y, 191115z, 191117b.
4. Topping, J. J., *Talanta*, 1978, **25**, 61.
5. Poirier, J. M., and Verchère, J. F., *Talanta*, 1979, **26**, 349.
6. Lazarev, A. I., *Zavod. Lab.*, 1960, **26**, 932; *Chem. Abstr.*, 1960, **54**, 24121d.
7. Sinclair, A. G., *Talanta*, 1969, **16**, 459.
8. Lee, W. H., *Kumsok Hakhoe Chi*, 1972, **10**, 207; *Chem. Abstr.*, 1973, **79**, 38259k.
9. Selig, W. S., *Fresenius Z. Anal. Chem.*, 1986, **325**, 297.
10. Angus, H. J. F., and Weigel, H., *J. Chem. Soc.*, 1964, 3994.
11. Angus, H. J. F., Bourne, E. J., and Weigel, H., *J. Chem. Soc.*, 1965, 21.
12. Mikesova, M., and Bartusek, M., *Collect. Czech. Chem. Commun.*, 1978, **43**, 1867.
13. Verchère, J. F., and Chapelle, S., *Polyhedron*, 1989, **8**, 333.
14. Angus, H. J. F., Briggs, J., Sufi, N. A., and Weigel, H., *Carbohydr. Res.*, 1978, **66**, 25.
15. Cervilla, A., Ramirez, J. A., and Beltràn-Porter, A., *Transition Met. Chem.*, 1983, **8**, 21.
16. Llopis, E., Ramirez, J. A., and Cervilla, A., *Polyhedron*, 1986, **5**, 2069.
17. Goldstein, G., Wolff, C. M., and Schwing, J. P., *Bull. Soc. Chim. Fr.*, 1971, 1195.
18. Cruywagen, J. J., and van der Merwe, I. F. J., *J. Chem. Soc., Dalton Trans.*, 1987, 1701.
19. Corsini, A., and Subramanian, K. S., *J. Inorg. Nucl. Chem.*, 1978, **40**, 1777.
20. Bourne, E. J., Hutson, D. H., and Weigel, H., *J. Chem. Soc.*, 1961, 35.
21. Voelter, W., Bayer, E., Records, R., Bunnenberg, E., and Djerassi, C., *Chem. Ber.*, 1969, **102**, 1005.
22. Pettersson, L., *Acta Chem. Scand.*, 1972, **26**, 4067.
23. Goldstein, G., Wolff, C. M., and Schwing, J. P., *Bull. Soc. Chim. Fr.*, 1971, 1201.
24. Verchère, J. F., and Sauvage, J. P., *Bull. Soc. Chim. Fr.*, 1988, 263.
25. Belcher, R., Tully, G. W., and Svehla, G., *Anal. Chim. Acta*, 1970, **50**, 261.
26. Chalmers, R. A., and Sinclair, A. G., *J. Inorg. Nucl. Chem.*, 1967, **29**, 2065.

Paper 9/02967B
Received July 12th, 1989
Accepted October 5th, 1989

Trypsin Inhibitors Analysis: Direct Chromatographic Titration*

Giorgio Raspi, Antonino Lo Moro and Maria Spinetti
Dipartimento di Chimica e Chimica Industriale, Università di Pisa, Via Risorgimento 35, I-56126 Pisa, Italy

A titrimetric method for the standardisation of three human urinary trypsin inhibitors (UTIs) has been developed. The same substances are also present in human plasma, and their amounts in such biological fluids are of bioclinical interest. The method is based on the direct titration of each UTI with a solution of bovine trypsin of known molarity, and monitoring the decreasing residual amounts of the inhibitor by reversed-phase high-performance liquid chromatography. The proposed method provides a suitable alternative to the traditional enzymic - spectrophotometric method. Mean within-day and between-day coefficients of variation and the limit of determination for the standardisation of each UTI are reported.

Keywords: *Trypsin inhibitor; bovine trypsin; high-performance liquid chromatography*

Trypsin inhibitors play an important role in many aspects of normal physiology and disease processes. Three of them[1–3] occur in the plasma and urine of healthy subjects at very low concentrations, rises in which indicate a pathological status.[4–9] It appears essential, therefore, to develop viable methods of identification, separation and standardisation of these compounds, independently from matrices, even considering their eventual use as drugs[10] in the near future.

In recent papers,[11,12] we have developed a chromatographic procedure for the identification, separation and quantitative determination of these inhibitors in urine and plasma. By means of the same procedure we have been able to monitor[13] the fate of the urinary trypsin inhibitors (UTIs), having apparent relative molecular masses of *ca.* 6200 (UTI_6), 18 000 (UTI_{18}) and 72 000 (UTI_{72}), as determined by gel chromatography, in the various steps of the methods proposed[2,14–16] for their purification on a preparative scale. The standardisation of UTIs is usually carried out by an enzymic - spectrophotometric method.[17] This method, based on the inhibition by UTIs of the trypsin-catalysed hydrolysis of an appropriate substrate, under specified conditions, takes advantage of the stable complex that UTIs form[18–20] at *ca.* pH 8.0 with the enzyme. However, the method is non-specific, indirect and limited by the competition between the substrate and inhibitor for the active site of the enzyme. In fact,[17] the inhibition is not directly proportional to inhibitor concentrations up to 100% inhibition; the measurements must be made in the linear part of the inhibition curve. For practical purposes, this is from 20 to 70% inhibition.

In this paper, an assay is proposed for the specific and direct standardisation of such inhibitors, which is a useful alternative to the traditional spectrophotometric detection method. We have investigated the direct titration of each UTI with a standard solution of bovine trypsin, monitoring the decreasing amount of the inhibitor by reversed-phase high-performance liquid chromatography (RP-HPLC), as a result of the chromatographic behaviour of the UTIs previously ascertained and of the stable complexes that they form with trypsin under suitable conditions. The proposed method has been applied to low concentrations of inhibitor.

Experimental

Apparatus

A Model Twincle liquid chromatograph (Jasco, Easton, MD, USA), equipped with a VL-614 injector and a 100- or 1000-µl injection loop and with a Jasco Model GP-A30 Gradient Programmer, was connected to a Jasco Model 100-III variable-wavelength UV detector. The column used was a LiChrosorb RP-18 (250 × 4.6 mm i.d.; 7 µm particle size), supplied by Merck (Darmstadt, FRG), positioned in a CLAR 055 HPLC column block-heater (Violet, Rome, Italy). The output from the detector was displayed on a Chromatopac C-R3A data processor. The HPLC conditions used are presented in Table 1.

Table 1. HPLC conditions

Column	LiChrosorb RP-18 (7 µm)
Temperature	30 ± 0.1 °C
Detector wavelength	200 nm
Injection volume	100–1000 µl
Mobile phase 1	Buffer solution A - acetonitrile (70 + 30)
Mobile phase 2	Buffer solution A - acetonitrile (40 + 60)

Econo-columns (10 × 1.0 cm i.d.) from Bio-Rad (Richmond, CA, USA) were employed for affinity chromatography.

Reagents

Analytical-reagent grade chemicals were used and stored, when necessary, as recommended by the manufacturer. Acetonitrile, sodium perchlorate, orthophosphoric acid and tris(hydroxymethyl)aminomethane hydrochloride (Tris. HCl) were obtained from Merck. All reagents for inhibition and active site measurements, including bovine pancreatic trypsin, Type III, were obtained from Sigma (St. Louis, MO, USA) and used as received. Water purified by a single distillation, followed by passage through a Milli-Q system (Millipore, Bedford, MA, USA), was used to prepare the solutions.

Bovine trypsin was coupled with cyanogen bromide activated Sepharose 4B according to the instructions given by the manufacturer (Pharmacia, Uppsala, Sweden): prolonged washing cycles of alternately high and low pH were necessary in order to obtain an acceptable HPLC background.

Solutions

Buffer solution A (pH 2.2). Prepared from 10.0 mM H_3PO_4 in 0.2 M $NaClO_4$.

Buffer solution B (pH 8.3). Prepared from 0.1 M Tris.HCl in 0.5 M NaCl.

Mobile phases 1 and 2 for HPLC. Prepared by mixing buffer solution A, previously passed through a 0.45-µm membrane filter, with acetonitrile (70 + 30) and (40 + 60), respectively. The solvents were de-aerated by bubbling helium through them.

* Presented at SAC 89, the 8th SAC International Conference on Analytical Chemistry, Cambridge, UK, 30 July–5 August, 1989.

Stock solutions of bovine trypsin. Prepared by dissolving an appropriate amount of enzyme to yield a 2.4 mg ml^{-1} solution in 1×10^{-3} M HCl, containing 0.02 M $CaCl_2$. These solutions were standardised by titration of the active site with 4-nitrophenyl 4′-guanidinobenzoate, according to the method of Chase and Shaw.[21] A set of standard solutions containing 0.5–10.0 nmol ml^{-1} of trypin was prepared by serial dilution of stock solutions with 1×10^{-3} M HCl. Stock and standard trypsin solutions were stored in a freezer at −20 °C; solutions of UTI_6, UTI_{18} and UTI_{72}, from various samples of urine, were processed as described elsewhere.[2,14–16] In a previous paper[13] we have demonstrated that our RP-HPLC method[11] allows an easy and reliable control of the purity of the single inhibitors separated by the cited procedures (see under Check for Purity). When necessary, the single inhibitor was isolated by fractionation with the HPLC technique, which does not destroy the inhibition activity.[11] The resulting solutions were then stored in the dark at −20 °C. The inhibitor concentration of these solutions, expressed in nmol of equivalent trypsin, was determined by the enzymic - spectrophotometric method,[17] using *N*-α-benzoyl-L-arginine-4-nitroanilide as substrate.

Check for Purity

(*a*) The solutions, obtained by various procedures,[2,14–16] adjusted to pH 8.3 with addition of buffer solution B, are passed through a trypsin - Sepharose 4B column (bed volume *ca.* 1.0 ml; loading capacity *ca.* 200 nmol of active trypsin), prepared as described under Reagents and equilibrated with buffer solution B. After washing with *ca.* 20 ml of the same buffer solution, the inhibitors are recovered in a 5-ml calibrated flask from the trypsin - Sepharose 4B column by eluting with 0.8 ml of 1.0 mol l^{-1} H_3PO_4 and buffer solution A up to the mark. In previous papers[11] we reported that, under these conditions of acid elution, the recovery of the inhibitors was ≥98%.

(*b*) A 1000-μl aliquot of the solution resulting from step (*a*) is injected on to the HPLC column and a chromatographic run is performed with isocratic elution for 15 min (mobile phase 1) and then with a linear gradient up to 42% of acetonitrile for 26 min (mobile phase 2), using the described chromatographic conditions.

In Fig. 1 a chromatogram is shown, which was obtained with a sample of urine processed as described above and, therefore, containing all three inhibitors: UTI_6 (peak A), UTI_{72} (peak B) and UTI_{18} (peak C).

For a correct determination using the proposed titration method, the chromatogram must reveal the presence of a single peak.

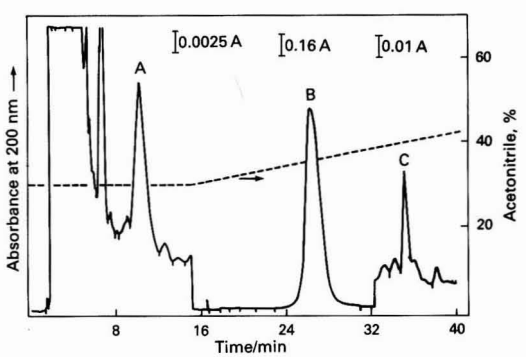

Fig. 1. Typical chromatogram of a 200-ml urine sample. See under Check for Purity for sample treatment. Injection volume, 1000 μl; isocratic elution for 15 min (mobile phase 1) followed by linear-gradient elution (mobile phase 2). A, UTI_6; B, UTI_{72}; and C, UTI_{18}

Procedure for UTI Titration

The procedure involves the following steps: A, formation of the UTI - trypsin complex in the presence of an excess of UTI; B, quantitative separation of the residual UTI from the mixture by affinity chromatography; and C, identification and evaluation of the residual UTI by RP-HPLC.

Step A

At least four identical aliquots were taken, each containing an amount of inhibitor in the range 0.5–20 nmol of equivalent trypsin, and were adjusted to pH 8.3 with buffer solution B. To three of these aliquots were added known and increasing amounts of bovine trypsin standard solution to yield a decrease in the peak area of *ca.* 25, 50 and 75%, respectively, compared with the peak area obtained from the reference (fourth aliquot). The final pH of the solutions was carefully controlled to allow the conservation of the complex, which was very stable over a narrow range centred around pH 8.3. Preliminary tests ensured that the reaction time (*ca.* 5 min) involved in this procedure was sufficient. The rate of attainment of equilibrium was virtually independent of the temperature of incubation.[17] The final volume of each solution was *ca.* 5 ml.

Step B

All four aliquots were passed through a trypsin - Sepharose 4B column, and the residual inhibitor, tightly bound to the immobilised trypsin, was washed and then recovered as described in step A. Immobilised trypsin at pH 8.3 binds only residual UTI: experiments carried out with solutions containing only the UTI - trypsin complex at various levels showed that there was no significant release of UTI. The residual UTI remained tightly bound to the immobilised enzyme; the successive acid elution destroyed the complex and allowed the quantitative recovery of the inhibitor from the affinity column.

Step C

A 100- or 1000-μl aliquot, depending on the amount of UTI in each eluted solution, was injected on to the HPLC column; the temperature and flow-rate were the same as those given in Table 1. The chromatographic conditions for monitoring the titration were simplified (either isocratic or linear-gradient elution) compared with those used under Check for Purity (Fig. 1), owing to the presence of only one of the three inhibitors. Each of them was characterised by a well-shaped peak that appeared at 10.3 min (UTI_6), 20.6 min (UTI_{18}) and 11.2 min (UTI_{72}) (Fig. 2). Isocratic elution with mobile phase 1 was used for UTI_6 [Fig. 2(*a*)], whereas linear-gradient elution was used for UTI_{72} [Fig. 2(*b*)] and UTI_{18} [Fig. 2(*c*)]—acetonitrile: 30–38% for 17 min, and 30–42% for 26 min, respectively.

The peak areas of the inhibitor examined were plotted against the amount (nmol) of bovine trypsin added (Fig. 3). The graphical extrapolation of the straight line obtained gave, on the *x*-axis, the amount of inhibitor, expressed in nmol of equivalent trypsin.

Results

The precision of the proposed method was evaluated by replicate analyses of the samples containing each UTI at three different levels. The results are presented in Table 2, which also shows the results obtained by the enzymic - spectrophotometric method[17] with identical aliquots of the same samples. The within-day precision was assessed from four replicate runs and showed a mean coefficient of variation (CV) of 3.4% for UTI_6, 4.0% for UTI_{18} and 3.1% for UTI_{72}. The between-day precision evaluated over a period of 1 week was determined in the same amount range and showed a mean

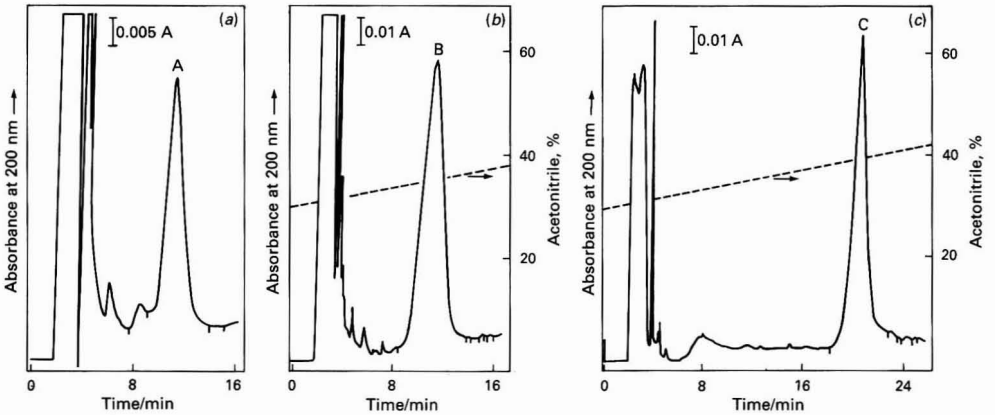

Fig. 2. Chromatograms of purified UTI solutions. (*a*) UTI_6 (A) (1.5 nmol ml^{-1} of equivalent trypsin); injection volume, 1000 μl; isocratic elution with mobile phase 1. (*b*) UTI_{72} (B) (1.0 nmol ml^{-1} of equivalent trypsin); injection volume, 1000 μl; mobile phase 1 and mobile phase 2, linear-gradient elution. (*c*) UTI_{18} (C) (1.24 nmol ml^{-1} of equivalent trypsin); injection volume, 1000 μl; elution as in (*b*)

Table 2. Within- and between-day precision of the titration of UTIs

		Enzymic - spectrophotometric method[17]		Proposed method			
				Within-day		Between-day	
Inhibitor	Sample	Equivalent trypsin*/nmol	CV,† %	Equivalent trypsin*/nmol	CV,† %	Equivalent trypsin*/nmol	CV,† %
UTI_6	1	0.85 ± 0.05	5.9	0.83 ± 0.04	4.8	0.82 ± 0.05	6.1
	2	5.65 ± 0.23	4.1	5.55 ± 0.20	3.6	5.50 ± 0.27	4.9
	3	12.50 ± 0.31	2.5	12.75 ± 0.24	1.9	12.69 ± 0.30	2.4
		Mean	4.2	Mean	3.4	Mean	4.5
UTI_{18}	4	0.72 ± 0.04	5.6	0.70 ± 0.04	5.7	0.70 ± 0.05	7.1
	5	4.38 ± 0.20	4.6	4.45 ± 0.14	3.1	4.48 ± 0.17	3.8
	6	10.05 ± 0.33	3.3	10.20 ± 0.33	3.2	9.90 ± 0.20	2.0
		Mean	4.5	Mean	4.0	Mean	4.3
UTI_{72}	7	0.80 ± 0.04	5.0	0.81 ± 0.04	4.9	0.82 ± 0.04	4.9
	8	6.35 ± 0.26	4.1	6.25 ± 0.15	2.4	6.23 ± 0.37	5.9
	9	20.87 ± 0.25	1.2	21.20 ± 0.42	2.0	21.42 ± 0.47	2.2
		Mean	3.4	Mean	3.1	Mean	4.3

* Mean ($n = 4$) ± standard deviation.
† CV = coefficient of variation.

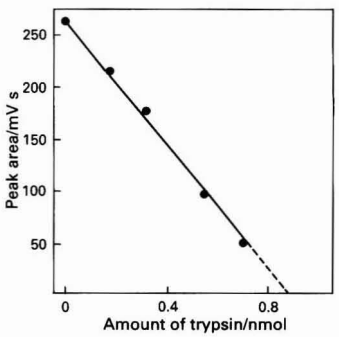

Fig. 3. Typical UTI titration: peak area of the residual UTI_{72} [peak B, Fig. 2(*b*)] plotted against the amount (nmol) of bovine trypsin added

CV (%) of: 4.5 for UTI_6, 4.3 for UTI_{18} and 4.3 for UTI_{72}. The limits of determination were calculated to be, in nmol of equivalent trypsin: 0.7 for UTI_6, 0.5 for UTI_{18} and 0.6 for UTI_{72}, *i.e.*, the levels at which quantitative measurements of the peak areas were consistently possible with an injection volume of 1000 μl.

Discussion

The method depends on the formation of a stable complex between each UTI and bovine trypsin. The direct injection of an aliquot of the resulting solution in step A on to the HPLC column, using a mobile phase of *ca.* pH 8.3, is inadvisable for several reasons; possible formation of precipitates in the mobile phase, presence of inactive trypsin in the sample injected, which complicates the chromatographic trace and contaminates the HPLC column, and scarcely reproducible peak areas either for the complex or for the residual UTI. Instead, the chromatographic peak for each UTI, obtained under the conditions described, was utilised successfully for our purposes.

The most important advantage of the titrimetric method proposed here is the experimental evidence for the inhibitor of interest in the sample. The results presented in Table 2 are in good agreement with those obtained by the enzymic - spectrophotometric method after checks for the purity of the inhibitor and for the linear part of the inhibition curve.

Therefore, the proposed procedure appears to be reliable for the standardisation of the three inhibitors. Further, the method is highly specific, owing to the affinity chromatographic step in combination with the RP-HPLC separation. Other advantages are: the relative speed and ease of use, the exclusion of substrate, the applicability to dilute solutions, and the lack of problems deriving from the biological matrix. The method can be extended to the study of other enzyme - inhibitor systems used for analytical applications.

Conclusions

Titrimetric standardisation of three trypsin inhibitors endogenous in man has been described. These substances are present in human plasma and urine, and their amounts in these biological fluids are of bioclinical interest. The proposed method provides a suitable alternative to the enzymic - spectrophotometric method: the end-point detection by RP-HPLC allows the direct titration of the inhibitor, ensuring unambiguous identification. A simple treatment guarantees reliable analytical results, independently from the matrix, even in dilute samples.

This work was supported by the Consiglio Nazionale delle Ricerche and Ministero della Pubblica Istruzione.

References

1. Reisinger, P., Hochstrasser, K., Albrecht, G. J., Lempart, K., and Salier, J. P., *Biol. Chem. Hoppe-Seyler*, 1985, **366**, 479.
2. Matsuda, K., Ogawa, M., Kitahara, T., Ishida, M., and Mori, T., *Enzyme*, 1985, **34**, 129.
3. Maruyama, M., Yamamoto, T., Sumi, H., Tsushima, H., Mihara, H., and Minamino, N., *Enzyme*, 1986, **35**, 225.
4. Hochstrasser, K., Feuth, H., Fall, J., and Kemkes, B., *Klin. Wochenschr.*, 1974, **52**, 1015.
5. Hochstrasser, K., Feuth, H., Kemkes, B., Fall, J., and Werle, E., *Klin. Wochenschr.*, 1974, **52**, 1018.
6. Feuth, H., Kemkes, B., and Hochstrasser, K., *Langenbecks Arch. Chir. Suppl. Chir. Forum*, 1975, 133.
7. Huhtala, M. L., Kahanpaa, K., Seppala, M., Halila, H., and Stenman, U. H., *Int. J. Cancer*, 1983, **31**, 711.
8. Ogawa, M., Matsuda, K., Shibata, T., Matsuda, Y., Ukai, T., Ohta, M., and Mori, T., *Res. Commun. Chem. Pathol. Pharmacol*, 1985, **50**, 259.
9. Halila, H., Lehtovirta, P., and Stenman, U. H., *Br. J. Cancer*, 1988, **57**, 304.
10. Schnebli, H. P., and Braun, N. J., *in* Barrett, A. J., and Salvesen, G., *Editors*, "Proteinase Inhibitors," Elsevier, Amsterdam, 1986, pp. 613–627.
11. Raspi, G., Lo Moro, A., and Spinetti, M., *Fresenius Z. Anal. Chem.*, 1988, **329**, 786; 1988, **332**, 48.
12. Raspi, G., Lo Moro, A., Spinetti, M., and Molinari, M., *Fresenius Z. Anal. Chem.*, 1989, **335**, 398.
13. Raspi, G., Lo Moro, A., Spinetti, M., and Molinari, M., *Chromatographia*, 1988, **26**, 369.
14. Barthelemy-Clavey, V., Yapo, E. A., Vanhutte, G., and Hayem, A., *Biochim. Biophys. Acta*, 1979, **580**, 154.
15. Tanaka, Y., Maehara, S., Sumi, H., Toki, N., and Moriyama, S., *Biochim, Biophys. Acta*, 1982, **705**, 192.
16. Bromke, B. J., and Kueppers, F., *Biochem. Med.*, 1982, **27**, 56.
17. Fritz, H., Trautschold, L., and Werle, E., *in* Bergmeyer, H. U., *Editor*, "Methods of Enzymatic Analysis," Volume 2, Verlag Chemie, Weinheim; Academic Press, New York, 1974, pp. 1064–1080.
18. Antonini, E., Ascenzi, P., Bolognesi, M., Gatti, G., Guarneri, M., and Menegatti, E., *J. Mol. Biol.*, 1983, **165**, 543.
19. Hochstrasser, K., Bretzel, G., Feuth, H., Hilla, W., and Lempart, K., *Hoppe-Seyler's Z. Physiol. Chem.*, 1976, **357**, 153.
20. Albrecht, G. J., Hochstrasser, K., and Salier, J. P., *Hoppe-Seyler's Z. Physiol. Chem.*, 1983, **364**, 1703.
21. Chase, T., Jr., and Shaw, E., *Biochem. Biophys. Res. Commun.*, 1967, **29**, 508.

Paper 9/03350E
Received August 7th, 1989
Accepted December 19th, 1989

2-Mercaptobenzoic Acid as a Reagent for the Direct Potentiometric Titration of Selenium(IV), Tellurium(IV) and Zinc(II)*

Ismail M. Al-Daher, Fattah A. Fattah and Kassim A. Najm
Department of Chemistry, College of Science, University of Mustansiriyah, Baghdad, Iraq

A simple, direct, rapid and accurate method for the potentiometric determination of selenium(IV), tellurium(IV) and zinc(II) with 2-mercaptobenzoic acid (thiosalicylic acid, TSA) is described. The determinations are also possible in the presence of several metal ions or acids with similar structures to TSA such as benzoic and salicylic acids. The equivalence point is marked by a sharp inflection or sharp peak in all instances and results with an average error of −0.01 to 0.18% were obtained.

Keywords: *2-Mercaptobenzoic acid; selenium(IV); tellurium(IV); zinc(II); potentiometric titration*

The thiol group (–SH) is mainly characterised by its ease of salt formation (mercaptides) and its ready oxidation by mild oxidising agents to the corresponding disulphides.

Misra and Tandon[1] used copper(I) chloride as a titrimetric reagent for the potentiometric determination of 2-mercaptobenzoic acid (thiosalicylic acid, TSA) and several other sulphur compounds. Srivastava[2] determined TSA amperometrically using mercury pool electrodes with an average relative error of 0.23%. Verma[3] determined TSA in acetone by titration with sodium methoxide using Azo Violet as indicator. The relative error was 0.3%. Thiosalicylic acid has been used for the spectrophotometric determination of palladium, rhenium, selenium and nickel[4] and was determined potentiometrically with palladium(II).[5] Al-Daher and Al-Saadi[6] prepared three complexes of TSA with silver, palladium and bismuth. Pastor[7] and Pastor and Antonijevic[8] determined TSA by coulometric titration with electrogenerated manganese(III) and iodine, respectively. Recently, Al-Daher *et al.*[9] have prepared and characterised four complexes of TSA with arsenic(III), selenium(IV), tellurium(IV) and copper(I).

Experimental

Reagents

Thiosalicylic acid (Sigma) was recrystallised from benzene or methanol. Its purity was determined by titration with a standard solution of lead nitrate using Catechol Violet as indicator and boric acid - borax buffer (pH 9.2, 5 ml), the colour change at the end-point being from pink to blue.[10] The purity was found to be 96.53%. Standard solutions of 10^{-2}–2.5×10^{-2} M TSA were prepared daily in 95% ethanol, stored and used under an inert atmosphere of nitrogen to prevent aerial oxidation. Under these conditions the concentration of TSA was found to be unchanged 6 h after preparation.

Selenium(IV) solution was prepared by dissolving the required amount of sodium selenite (Fluka) in doubly distilled water. It was standardised[11] by dissolving 0.22 g of the salt in 25 ml of H_2SO_4 (40% v/v) and diluting to 250 ml. A 12.5-ml volume of H_3PO_4 was added followed by 40 ml of standard 0.02 M potassium permanganate solution. After 30 min the residual permanganate was determined by the addition of a slight excess of 0.1 M ammonium iron(II) sulphate solution and back-titration with standard 0.02 M permanganate solution. The purity was found to be 98.33%.

Tellurium(IV) solution was prepared by dissolving the required amount of tellurium(IV) oxide (Alfa) in 25 ml of concentrated HCl and diluting with doubly distilled water. It was standardised by the same procedure used for the selenium(IV) solution[11] and its purity was found to be 99.99%.

Zinc(II) solution was prepared by dissolving the required amount of AnalaR grade zinc oxide (99.99%, BDH) in 5 ml of concentrated nitric acid and diluting with doubly distilled water.

Other chemicals used for buffer solutions such as sodium carbonate, sodium hydrogen carbonate, sodium acetate, acetic acid, boric acid and borax were high-purity materials and were used as received. Chemicals used as interferences were also of high purity and were used as received.

Titration Procedure

Potentiometric titrations were carried out in an 80-ml glass cell fitted with a Teflon lid containing five openings (two for the electrodes, one for the burette tip and the remaining two as inlet and outlet for the purified nitrogen). The indicating electrode was a bright platinum flag and the reference was a saturated calomel electrode.

A 10- or 20-ml aliquot of the standard solution of TSA was pipetted into the titration vessel then buffer solution and ethanol were added to bring the volume to *ca.* 40 ml. The reference and indicating electrodes were inserted and the solution was stirred with a magnetic stirring bar. Purified nitrogen was bubbled through for about 10 min to de-aerate the solution and then directed over the solution surface to keep the titration under an atmosphere of nitrogen. The nitrogen was used to prevent any possible aerial oxidation of TSA to the disulphide. Titration with solutions of Se^{4+}, Te^{4+} or Zn^{2+} was then started and continued until a potential jump or a peak was obtained.

In the proposed method, TSA can be used either as the titrant, *i.e.*, with the TSA solution in the burette and the metal ion solution in the titration vessel, or as the titrand, *i.e.*, with the reverse situation. In both procedures the same results were obtained. We preferred to use TSA in the titration vessel rather than in the burette, as the burette is connected to the titration bottle in which the elemental solution can be stored for several days without any change in its composition. On the other hand TSA should not be kept overnight as its concentration decreases by about 2% each day as a result of aerial oxidation to the disulphide. A fresh solution of TSA can be used safely as a titrant without further standardisation if the titrations are completed within 4 h.

All titrations were carried out with a Metrohm E536 automatic recording potentiograph with a Metrohm 655 multi-dosimat at a delivery rate of 2 ml min^{-1}. In the titration of TSA with the zinc(II) solution, 10 ml of carbonate - hydrogen carbonate buffer (pH 10) were added before titration and 20 ml of acetate - HCl buffer (pH 2.3) were added

* Presented at SAC 89, the 8th SAC International Conference on Analytical Chemistry, Cambridge, UK, 30 July–5 August, 1989.

when the titration was carried out with selenium(IV).[12] A 2-ml volume of 0.2 M acetic acid was added for the titration with tellurium(IV).

To prepare the sodium acetate buffer solution (pH 2.3), dissolve 136.1 g of sodium acetate trihydrate in water, add 400 ml of 2 M hydrochloric acid and dilute to 1 l with water.

To prepare the carbonate - hydrogen carbonate buffer (pH 10), mix equal volumes of 0.025 M sodium carbonate and 0.025 M sodium hydrogen carbonate solutions.

Two potentiometric titration procedures, *viz.*, normal and first-derivative differential, were used for all the titrations and both the S- and peak-shaped titration curves were recorded. With the differential titration procedure the end-point was located more easily and more accurately.

Results and Discussion

The methods for determining thiols are generally based on the formation of mercaptides with metal ions or on their oxidation to disulphides. This investigation involves potentiometric determination and formation of the mercaptides of TSA with selenium(IV), tellurium(IV) and zinc(II). The method was applied to the determination of these elements at concentration levels of 10^{-2} and 2.5×10^{-2} M, and higher. The average deviation was found to be −0.01 to 0.18% and the relative standard deviation −0.13 to 0.25% as shown in Table 1.

The method is useful for concentrations of TSA and metal ions down to 10^{-2} M and is not confined to between 10^{-2} and 2.5×10^{-2} M but can be used successfully for higher concentrations.

Titrations With Selenium(IV)

The results of the titration of selenium(IV) with TSA are summarised in Table 1. The reaction can be written as follows:

$$4RSH + Se^{4+} \rightarrow (RS)_4Se + 4H^+$$

where RSH represents TSA. The lower concentrations of TSA and selenium(IV) used were in the range 10^{-2}–2.5×10^{-2} M. A mixture of TSA with 95% ethanol and acetate - HCl buffer (pH 2.3) was titrated with an aqueous solution of selenium(IV) (pH 2.0). During the titration a stable complex was formed. This was demonstrated by a high potential jump (200 mV) at the equivalence point, and occurred when the molar ratio of selenium(IV) to TSA was 1 : 4. The results were in good agreement with those obtained by Al-Daher *et al.*[9] These workers prepared and analysed the complex and found the molar ratio to be 1 : 4. Similar, accurate, results were obtained when the titration was carried out using the first-derivative differential method as shown in Fig. 1.

To a mixture of 20 ml of 10^{-2} M TSA and 20 ml of acetate buffer was added 1 ml of a 2.5×10^{-2} M solution of each of the following substances: thallium(I), arsenic(III), lanthanum(III), nickel(II), manganese(II), salicylic acid and benzoic acid and the final mixture was titrated with selenium(IV). Table 1 shows that these substances, added together, do not interfere with the determination of TSA with selenium(IV) or the determination of selenium(IV) with TSA. Bismuth(III) interfered when TSA was titrated with selenium(IV) or tellurium(IV).

Titrations With Tellurium(IV)

The results of the titration of TSA with tellurium(IV) are summarised in Table 1. Thiosalicylic acid has not been used previously as a reagent for determining tellurium(IV) potentiometrically. The reaction is rapid and quantitative and can be described by the following equation:

$$4RSH + Te^{4+} \rightarrow (RS)_4Te + 4H^+$$

A solution of TSA in 95% ethanol at concentrations of 10^{-2}–2.5×10^{-2} M was titrated with similar concentrations of an acidic aqueous solution of tellurium(IV) (pH 0.65). The titrations were carried out using the normal potentiometric

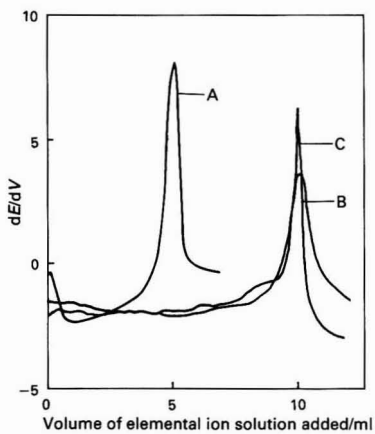

Fig. 1. First-derivative potentiometric titration of A, 20 ml of 0.025 M TSA titrated with a 0.025 M solution of Se^{4+}; B, 20 ml of 0.025 M TSA titrated with a 0.025 M solution of Zn^{2+}; and C, 20 ml of a 0.025 M solution of TSA titrated with a 0.0125 M solution of Te^{4+}. E = potential (mV); V = volume (ml)

Table 1. Results of the potentiometric titration of TSA with selenium(IV), tellurium(IV) and zinc(II)

Titrant	Amount of element/mg		Average deviation, %	Relative standard deviation, %	Molar ratio at inflection point, TSA : element	Approximate potential change at inflection point/mV
	Taken	Recovered*				
Se^{4+}†	9.88	9.90	0.17	0.11	3.99_3	200 (good)
Se^{4+}‡	5.93	5.92	−0.10	0.17	4.00_4	Sharp peak
Se^{4+}§	3.94	3.94	−0.10	0.16	4.00_2	Sharp peak
Te^{4+}†	11.97	11.96	0.16	−0.13	4.00_5	125 (good)
Te^{4+}‡	11.19	11.19	0.02	0.25	3.99_8	Sharp peak
Te^{4+}§	3.95	3.94	−0.01	0.10	4.00_1	Sharp peak
Zn^{2+}†	5.72	5.73	0.10	0.21	1.99_8	75 (good)
Zn^{2+}‡	11.37	11.38	0.18	0.13	1.99_6	Sharp peak
Zn^{2+}§	4.90	4.91	0.04	0.16	1.99_8	Well defined peak

* Average of six determinations.
† Normal potentiometric titration.
‡ Differential potentiometric titration.
§ In the presence of foreign substances added together in the same solution.

method (S-shaped curve) and the first-derivative differential method (peak-shaped curve) as shown in Fig. 1. The results obtained with the two methods were similar and were precise and accurate at a molar ratio of tellurium(IV) to TSA of 1 : 4. The end-point was determined in the same way as for the selenium(IV) titrations. Several substances such as benzoic acid, salicylic acid, arsenic(III), lanthanum(III), nickel(II), zinc(II) and thallium(I) were investigated to study their effects on the titration by adding 2 ml of a 2.5×10^{-2} M solution of each to 20 ml of standard TSA solution and 2 ml of 0.2 M acetic acid, and the mixture was titrated with tellurium(IV). None of the substances tested affected the results or the shape of the potentiometric curve. The determination of tellurium and selenium is very important as both of these elements are poisonous and they can form organometallic compounds termed "ultra-accelerators."[13] The selenium accelerators are used mainly in heat-resistant compounds and the tellurium accelerators in the vulcanisation of butyl rubber. The proposed procedure has several advantages over the conventional methods used for the determination of tellurium(IV) and selenium(IV).[14] It is simple, direct, rapid and accurate and there is no need for indicators or back-titrations. The method can be used for the determination of selenium(IV) and tellurium(IV) by using a standard solution of TSA. On the other hand TSA can be determined quantitatively by titration with standard solutions of selenium(IV) or tellurium(IV).

Although the atomic absorption spectrometric methods for the determination of selenium, tellurium and zinc are more sensitive than the proposed potentiometric method, not every laboratory has access to such an instrument, while the spectrophotometric methods use a very undesirable reagent (3,3′-diaminobenzidine).

Titrations With Zinc(II)

The results of the titration of TSA with zinc(II) are summarised in Table 1. The reaction is rapid and quantitative and occurs as follows:

$$2RSH + Zn^{2+} \xrightarrow{pH\ 10} (RS)_2Zn + 2H^+$$

The concentrations of reagents and the procedure used for detection of the end-point were similar to those used for selenium(IV) and tellurium(IV). The equivalence point occurred when the molar ratio of zinc(II) to TSA was 1 : 2. The proposed method is useful for the determination of zinc(II) using a standard solution of TSA and *vice versa*. Benzoic acid, salicylic acid and arsenic(III) did not interfere with the determination of zinc(II) or TSA, but nickel(II) thallium(I), bismuth(III), lanthanum(III) and manganese(II) interfered when added separately. The procedure proposed here for zinc(II) has the same advantages as those for selenium(IV) and tellurium(IV).

We thank Professor B. Kratochvil of the University of Alberta, Canada, for his encouragement and discussion and for a gift of TSA.

References

1. Misra, G. J., and Tandon, J. P., *Z. Naturforsch.*, 1970, **25**, 30.
2. Srivastava, H. P., *J. Indian Chem. Soc.*, 1976, **53**, 400.
3. Verma, K. K., *Talanta*, 1975, **22**, 920.
4. Naragana, B. C., and Raju, N. A., *J. Indian Chem. Soc.*, 1974, **51**, 870.
5. Koricanac, Z., and Milvanovic, L., *Acta Pharm. Jugosl.*, 1977, **27**, 171.
6. Al-Daher, I. M., and Al-Saadi, B. M., *J. Iraqi Chem. Soc.*, 1985, **10**, 84.
7. Pastor, T. J., *Mikrochim. Acta*, 1984, **I**, 435.
8. Pastor, T. J., and Antonijevic, V. V., *Anal. Chim. Acta*, 1987, **196**, 229.
9. Al-Daher, I. M., Noori, M. A., and Kratochvil, B., *Al-Mustansiriyah Journal of Sciences*, Volume 2, No. 1, in the press.
10. Bahador, K., *Talanta*, 1974, **21**, 968.
11. Vogel, I., "A Textbook of Quantitative Inorganic Analysis," Third Edition, Longman, London, 1961, p. 302.
12. Cresser, M. S., and West, T. S., *Analyst*, 1968, **93**, 595.
13. Supp, G. R., and Jibbs, I., *At. Absorpt. Newsl.*, 1974, **13**, 71.
14. Schrenk, W. T., and Browning, B. L., *J. Am. Chem. Soc.*, 1926, **48**, 2550.

Paper 9/01636H
Received April 18th, 1989
Accepted October 10th, 1989

Determination of Low-energy β-Emitter Radionuclides Deposited on Surfaces by Attapulgite Treatment*

A. Belfiore and G. Panciatici
CRESAM, I-56010 S. Piero a Grado, Pisa, Italy

A. Lo Moro and G. Raspi
Dipartimento di Chimica e Chimica Industriale, Università di Pisa, Via Risorgimento 35, I-56126 Pisa, Italy

A method for the determination of surface contamination of various materials by ^{3}H and ^{99}Tc is reported. Both ^{3}H and $^{99}Tc^{m}$ are widely used in chemical and clinical applications. The isotopes ^{99}Tc, the decay product of $^{99}Tc^{m}$, and ^{3}H are soft β-emitter radionuclides and the use of unsealed sources can frequently produce contamination and excessive internal dosing for workers. The removal of radionuclides from surfaces was effected with attapulgite, a clay with a high absorption capacity for many organic and inorganic substances. The determination was carried out by extracting the absorbed radionuclide from the clay and then measuring it in a β-scintillation counter. The determination limits of the method, 20 Bq cm^{-2} for ^{3}H and 100 Bq cm^{-2} for ^{99}Tc, are below the "derived working limits" for these radionuclides.

Keywords: *Radioanalysis; radioprotection; radionuclide surface contamination; attapulgite; soft β-emitter surface removal*

In chemical research, and particularly in the production and control of new drugs, molecules labelled with ^{3}H and ^{14}C are widely used. In several clinical applications and also in routine procedures, more or less complex molecules labelled with $^{99}Tc^{m}$, which decays to the isomer ^{99}Tc, are handled.

The isotopes ^{3}H, ^{14}C and ^{99}Tc are low-energy β-emitter radionuclides. The use of unsealed sources can frequently produce contamination of laboratory benches, floors and instruments. Excessive doses can lead to internal contamination of workers, therefore, surface contamination "derived working limits" have been recommended.[1] The determination of low-energy β-emitter radionuclides deposited on surfaces is difficult and problems often arise with surveillance and protection in environmental and occupational situations. Direct instrumental measurement techniques cannot reveal the activity present under the surface.

For a better risk evaluation, the fraction of surface contamination that can be transferred under normal working conditions is defined as "removable surface contamination." Indirect measurements, based on the determination of activity removed from surfaces by wiping with a dry or wet material (smear test), provide a rarely satisfactory evaluation, which is difficult to reproduce, of surface contamination that can be removed from the sampling areas. It follows that this problem is far from being solved for low-energy β-emitter radionuclides, which constitute the great majority of contaminants used outside nuclear plants.

During extensive experimental studies[2–4] in recent years, we have obtained very satisfactory results for the removal of α- and γ-emitter radionuclides from non-porous surfaces using a clay (attapulgite) that has a high absorption capacity for many organic and inorganic substances. In this work, the use of attapulgite has been extended to include the removal and determination of the low-energy β-emitters ^{3}H and ^{99}Tc deposited on the surfaces of widely used materials. The procedure consists essentially in the following steps: surface treatment with attapulgite for the determination of radionuclide "removal efficiency"; suspension of the dried clay in water for extraction and centrifugation of the radionuclides; radiometric measurement of the resulting solutions with a liquid scintillation β-counter; and determination of surface contamination using calibration graphs.

* Presented at SAC 89, the 8th SAC International Conference on Analytical Chemistry, Cambridge, UK, 30 July–5 August, 1989.

Experimental

Materials and Specimens

Commercial plastic slabs of poly(vinyl chloride) were obtained from Solvay/CIE (Ferrara, Italy) and of poly(methyl methacrylate) from ICI (Billingham, Cleveland, UK). Stainless steel AISI 304 and aluminium alloy UNI P Al Mg 3.5 were used.

For laboratory tests circular concave samples of o.d. 45 mm with a slightly crushed bottom and for application tests square samples of 100 mm side were prepared from the above materials.

Chemicals

Attapulgite. Attapulgus clay (minimum pore size 100 mesh/regular volatile matter) was obtained from Engelhard Minerals (Menlo Park, NJ, USA). A suspension of the clay in water was prepared with 40% m/m of clay and 60% m/m of distilled water.

Radionuclides. Obtained from Amersham International (Amersham, Buckinghamshire, UK).

For (methyl-^{3}H)thymidine (37 MBq ml^{-1}, specific activity 630 MBq g^{-1}), standard solutions in the range 20–15 000 Bq ml^{-1} were prepared by dilution. For ammonium pertechnetate in 0.1 M ammonia solution (37 MBq ml^{-1}, specific activity 630 MBq g^{-1}), standard solutions in the range 100–20 000 Bq ml^{-1} were prepared by dilution.

Apparatus

Radioactivity measurements were performed using Packard liquid scintillation β-counters with 5- or 20-ml vials and INSTA-GEL II as scintillation liquid. When necessary, the counts were corrected for quenching.

Calibration Graphs

In three series of centrifugal test-tubes, one set of test-tubes for each radionuclide, mix 1.2 g of attapulgite and standard solutions of ^{3}H and ^{99}Tc in the range 20–15 000 and 100–20 000 Bq, respectively. Add distilled water to obtain 1.8 ml of aqueous solution. Mix vigorously and dry in a thermostated

oven at 40 °C. After drying (12 h), treat samples with 10 ml of water, stir for 10 min and centrifuge for 6 min at 3000 rev min^{-1} (*ca.* 1500 *g*). Collect the supernatant liquids and measure them in a β-counter. Plot graphs of measured *versus* theoretical activity.

Procedures

Determination of "removal efficiency"

Cure, according to BS 4247 specification,[5] at least nine specimens for laboratory tests (see Materials and Specimens). Contaminate them with known activities of radionuclide. Add attapulgus clay suspension with a spatula to a thickness of 5 mm, corresponding to 0.5 g cm^{-2}. After 48 h, remove the dried clay and transfer it into the centrifugal test-tubes. Add 10 ml of water, stir for 10 min and centrifuge for 6 min at 3000 rev min^{-1} (*ca.* 1500 *g*). Prepare, for use as references, centrifugal test-tubes with identical activity deposited on the specimen and absorbed with the same amount of clay. Measure the collected liquids, for both samples and references, in a β-counter for the determination of "removal efficiency."

Determination of surface contamination

In experiments performed to check the method we used the specimens for application tests (see Materials and Specimens). Three specimens for each material (three for ^{3}H and three for ^{99}Tc) were accurately cleaned following BS 4247.[5] All the samples were stored at room temperature for at least 15 d after this treatment. Known amounts of the standard solutions of radionuclides were deposited on surfaces at random and dried at room temperature. The attapulgus clay suspension was applied with a spatula to a thickness of 5 mm, corresponding to 0.5 g cm^{-2}. After 48 h the dried clay was quantitatively collected, weighed and uniformly mixed. Aliquots (1.2 g) of the dried clay were treated with 10 ml of water, stirred vigorously for 10 min and centrifuged for 6 min at 3000 rev min^{-1} (*ca.* 1500 *g*). The supernatant liquids were collected and measured in a β-counter. The average activity of the measured aliquots was compared with the calibration graph for ^{3}H or ^{99}Tc. The surface contamination was obtained allowing for the total mass of collected attapulgite, for the percentage removal of radionuclides from different materials, obtained in laboratory tests, and for the surface size treated.

Results and Discussion

The results obtained for the "removal efficiency" are reported in Table 1. For control of the procedure, owing to the low-energy β-emission, we devised an original method consisting in two separate steps: measurement of the activity present in the clay and measurement of the residual activity in the specimens.

For the first step, we followed the procedure described under Determination of "removal efficiency." For the second step, three reference samples were prepared: specimens for laboratory tests were contaminated with either ^{3}H or ^{99}Tc and not treated further with a clay suspension. The specimens, samples and references were treated with 1 ml of 5 M nitric acid. The collected liquids, fully recovered, were measured in a β-counter and the residual activity was evaluated *versus* references. In Tables 2 and 3 the activity balances for ^{3}H and for ^{99}Tc, respectively, are reported.

From Tables 1–3 it appears that the removal of radionuclides, as also confirmed by the activity balance control, is very high except for aluminium alloy contaminated with ^{99}Tc. Further, it is important to note that the results are sufficiently reproducible. Tests carried out on specimens with surface contamination in the range 20–10 000 Bq cm^{-2} gave results that were not appreciably different to those reported in Table 1.

The surface contamination is calculated by using calibration graphs. Two calibration graphs were constructed by measuring 12 different activities of ^{3}H and ^{99}Tc. For each activity of the radionuclides, six replicate measurements were performed. Logarithmic calibration graphs were constructed by plotting the average activity of the radionuclide found *versus* the theoretical activity and were then analysed by a linear least squares treatment. A good linear relationship was obtained in the activity ranges 20–15 000 Bq cm^{-2} for ^{3}H and 100–20 000 Bq cm^{-2} for ^{99}Tc. The recoveries of the activity from the clay for these ranges were *ca.* 25% for ^{3}H and *ca.* 95% for ^{99}Tc, not considering the counting efficiency.

For optimisation of the method we also investigated the conditions for the recovery of the radionuclides from the dried clay using solutions other than water *i.e.*, 1 and 5 M nitric acid, 1 M potassium chloride solution and 5 M hydrochloric acid. We found that water provides the best solution to the problem, considering the reproducibility of the recovery efficiency and quenching of measurements.

Using the procedure described under Determination of surface contamination, we examined many samples of specimens for application tests. The results are reported in Table 4. The percentage error is generally small except for aluminium contaminated with ^{99}Tc, probably owing to the porosity of the material. However, in comparison with the results obtainable by the smear test, this error is largely acceptable.

The proposed procedure is relatively simple and can be extended to any non-porous material and to any molecule labelled with ^{3}H or ^{99}Tc. It is sufficient in each instance to examine the radionuclide removal efficiency for a sample and to prepare calibration graphs for the molecules under con-

Table 1. "Removal efficiency" of ^{3}H and ^{99}Tc activities by attapulgite. Mean of nine determinations ± standard deviation; ^{3}H and ^{99}Tc deposited activity: 2×10^{4} Bq

Material	Radionuclide removal efficiency, %	
	^{3}H	^{99}Tc
Poly(vinyl chloride)	95.8 ± 3.8	94.4 ± 2.4
Poly(methyl methacrylate)	92.8 ± 3.6	90.5 ± 2.8
Stainless steel	97.4 ± 2.2	94.4 ± 2.5
Aluminium alloy	94.5 ± 3.2	63.2 ± 5.8

Table 2. Activity balance for ^{3}H. Mean of nine determinations ± standard deviation; ^{3}H deposited activity: 2×10^{4} Bq

Material	Activity removed by clay, %	Residual activity in specimen, %
Poly(vinyl chloride)	95.8 ± 3.8	3.4 ± 1.9
Poly(methyl methacrylate)	92.8 ± 3.6	1.1 ± 0.1
Stainless steel	97.4 ± 2.2	1.8 ± 0.3
Aluminium alloy	94.5 ± 3.2	2.1 ± 0.4

Table 3. Activity balance for ^{99}Tc. Mean of nine determinations ± standard deviation; ^{99}Tc deposited activity: 2×10^{4} Bq

Material	Activity removed by clay, %	Residual activity in specimen, %
Poly(vinyl chloride)	94.4 ± 2.4	0.7 ± 0.2
Poly(methyl methacrylate)	90.5 ± 2.8	1.5 ± 0.5
Stainless steel	94.4 ± 2.5	0.5 ± 0.3
Aluminium alloy	63.2 ± 5.8	41.0 ± 11.0

Table 4. Determination of surface contamination of ^{3}H and ^{99}Tc in specimens for application tests

	Surface contamination/Bq cm^{-2}			
	^{3}H		^{99}Tc	
Material	Deposited	Found*	Deposited	Found*
Poly(vinyl chloride)	20	18	100	97
	100	103	1000	990
	1000	1050	5000	5250
Poly(methyl methacrylate)	30	31	200	190
	1000	1060	800	870
	10000	9600	5000	4930
Stainless steel	20	19	100	102
	100	112	1000	1060
	1000	983	5000	4600
Aluminium alloy	30	26	200	170
	1000	910	800	730
	10000	10200	5000	4650

* Rounded means of three tests.

sideration. Activity removed by the clay suspension can be considered with a wide safety margin, to be "removable surface contamination." Further, removal by clay can be carried out on limited and circumscribed parts of the surface, including those with complex geometry, and only in the zones of interest, in order to obtain more precise maps of localised contamination.

This method permits the accurate determination of total surface contamination for soft β-emitter radionuclides, which cannot otherwise be determined. The determination limits, 20 Bq cm^{-2} for ^{3}H and 100 Bq cm^{-2} for ^{99}Tc, are lower than the "derived working limits" for these radionuclides and, in our opinion, the proposed method is advantageous for radioprotection.

This work was supported by the Ministero Pubblica Istruzione and Consiglio Nazionale delle Ricerche.

References

1. International Commission on Radiological Protection, "Limits for Intakes of Radionuclides by Workers," Publication 30, Volume 4, Pergamon Press, Oxford, 1980.
2. Belfiore, A., Lo Moro, A., and Panciatici, G., *J. Less-Common Met.*, 1986, **122**, 517.
3. Belfiore, A., and Panciatici, G., *Inorg. Chim. Acta*, 1987, **140**, 351.
4. Belfiore, A., Lo Moro, A., and Panciatici, G., *Sci. Total Environ.*, 1988, **70**, 179.
5. "Recommendations for the Assessment of Surface Materials for Use in Radioactive Areas. Part 1. Method of Test for Ease of Decontamination," BS 4247, Part 1, British Standards Institution, London, 1967.

Paper 9/04596A
Received October 2nd, 1989
Accepted November 22nd, 1989

Spectrophotometric Determination of Taurine in Food Samples With Phenol and Sodium Hypochlorite as Reagents and an Ion-exchange Clean-up*

Oi-Wah Lau, Shiu-Fai Luk† and Teresa P. Y. Chiu
Department of Chemistry, Chinese University of Hong Kong, Shatin, N.T., Hong Kong

A simple and accurate spectrophotometric method is proposed for the determination of taurine in food samples using phenol and sodium hypochlorite as reagents, which form a blue colour with taurine at room temperature and pH 10.35. Ion exchange was used to improve the selectivity of the method. Absorbance measurements were made at 630 nm and the calibration graph was linear from 0 to 180 μg ml^{-1} of taurine with a slope of 0.00242 A (p.p.m.)$^{-1}$. The precision for the determination of taurine (156 μg ml^{-1}) was 0.8% (n = 10). The method was applied successfully to the determination of taurine in milk products and energy drinks.

Keywords: *Taurine determination; spectrophotometry; food analysis; phenol and hypochlorite reagents; ion-exchange clean-up*

Taurine (2-aminoethanesulphonic acid) is present in bile combined with cholic acid, and occurs also in the lungs and flesh extracts of oxen, in shark blood, in mussels and in oysters.[1] Taurine has also been found in milk products and some energy drinks. Several important roles in brain and body functions have been proposed for this compound, including neurotransmitter function, regulation of absorption and digestion of lipids, effects on eating and drinking behaviour and a role in depressive illness.[2]

Many methods have been reported for the determination of taurine, including spectrophotometry using ninhydrin, *o*-phthalaldehyde and urea,[3] and 1-fluoro-2,4-dinitrobenzene[4] as reagents, automatic amino acid analysis,[5] spectrofluorimetry,[6] gas - liquid chromatography[7,8] and high-performance liquid chromatography with pre-column derivatisation.[9–11] Taurine in foods and feeds,[5] human milk, cows' milk and some milk products[12] has been determined using an amino acid analyser.

This paper describes a simple spectrophotometric method for the determination of taurine using phenol and sodium hypochlorite as reagents. The optimum conditions for colour development and the effect of some common food additives on the proposed method were assessed. Several milk products and energy drinks were analysed for their taurine content.

Experimental

Apparatus

The spectra were recorded with a Varian Superscan 3 spectrophotometer using 1-cm glass cells. The pH values of solutions were measured with a Chemtrix Type 60A pH meter.

Reagents

All reagents were of analytical-reagent grade.

Taurine stock solution, 2000 μg ml^{-1}. Prepared by dissolving 0.2000 g of taurine (Fluka) in distilled water and diluting to 100 ml in a calibrated flask, which was then wrapped in aluminium foil to prevent photodegradation. Other standard taurine solutions were prepared by appropriate dilution of the stock solution with distilled water in calibrated flasks, which were also wrapped in aluminium foil.

Phenol solution, 0.68 M. Prepared by dissolving 64 g of phenol in 250 ml of distilled water, heating the mixture to 70 °C if necessary. The solution was then diluted to 1 l with distilled water. As phenol is very corrosive, care should be taken in handling this potentially hazardous chemical.

Sodium hypochlorite solution, 0.45 M. Freshly prepared by appropriate dilution with distilled water of sodium hypochlorite stock solution (Wako, 0.6–0.8 M), the concentration of which was previously determined by iodimetric titration.

Perchloric acid, 0.3 M. Prepared by appropriate dilution of perchloric acid (BDH) with distilled water.

Phosphate buffer. Prepared by dissolving 53.9 g of Na_2HPO_4 and 52.8 g of $Na_3PO_4.12H_2O$ in 1 l of distilled water.

Sample Preparation

Canned milk and milk powder

About 14 g of milk powder were weighed accurately and mixed with 70 ml of distilled water and heated at 60 °C for about 5 min. The mixture was diluted to 100 ml in a calibrated flask and then shaken in an ultrasonic cleaner (Branson) for 30 min. An aliquot (25 ml) of this mixture or of a canned milk sample was mixed with 5 ml of perchloric acid solution (0.3 M) in a centrifuge tube and centrifuged with a Simplex laboratory centrifuge (Christ) for 100 min at 4000 rev min^{-1}. The mixture was then filtered through a Millipore filter of pore size 0.45 μm.

An aliquot (2 ml) of the filtrate was pipetted into a boiling tube and 2–3 g of cation-exchange resin (IR-120, H^+ form, 20–50 mesh) were added. The mixture was shaken for 15 min and then filtered. The resin was washed and the washings were added to the filtrate, which was then diluted to 10 ml with distilled water in a calibrated flask.

Energy drinks

An aliquot (2 ml) of the energy drink was pipetted into a boiling tube, followed by the addition of 4 g of cation-exchange resin. The mixture was shaken for 15 min and then filtered. The filtrate was diluted to 10 ml with distilled water in a calibrated flask.

Determination

Aliquots (2 ml) of standard taurine solutions with concentrations in the range 0–180 μg ml^{-1} were pipetted into 10-ml

* Presented at SAC 89, the 8th SAC International Conference on Analytical Chemistry, Cambridge, UK, 30 July–5 August, 1989.

† Present address: China Cement Company (Hong Kong) Limited, G.P.O. Box 525, Hong Kong.

calibrated flasks. To each flask were added 2 ml of Na_3PO_4 - Na_2HPO_4 buffer, followed by 2 ml of 0.68 M phenol solution. Then, 2 ml of 0.45 M sodium hypochlorite solution were added to each flask and the mixture was diluted to 10 ml with distilled water. After the mixtures had stood at room temperature (25 °C) for 30 min, the absorbance at 630 nm was measured for each solution against a solution containing no taurine as the blank. A calibration graph was obtained by plotting absorbance against taurine concentration.

An aliquot (2 ml) of the sample solution obtained after the sample preparation procedure was treated as described above for the standards. The concentration of taurine in the sample solution was determined using multiple standard addition calibrations, and the taurine content in the original sample was then calculated.

Results and Discussion

The proposed method is based on the blue species formed when taurine is allowed to react with phenol and sodium hypochlorite.[1] The blue species exhibited a single absorption maximum at 630 nm, where the reagent blank had almost zero absorbance. Therefore, 630 nm was used for all subsequent absorbance measurements.

Optimisation of Conditions

Reaction temperature and reaction time

It was found that the reaction was >96% complete after heating at 100 °C for 15 min. However, in the analysis of real samples, the reaction mixtures failed to give the desired blue colour at 100 °C; hence this temperature could not be used. As the reaction proceeded smoothly at room temperature (25 °C) for both standards and real samples, room temperature was used for the proposed method. A reaction time of 30 min was chosen, the reaction being nearly 100% complete.

Effect of pH

Preliminary experiments showed that the reaction gave a dirty orange suspension in CH_3COOH - CH_3COONa buffer. Hence only buffers that operate in the alkaline region were assessed.

An NH_3 - NH_4Cl buffer is not suitable for the proposed method because ammonia will also give a similar blue colour and will interfere with the determination. Further, Na_2CO_3 - $NaHCO_3$ and Na_2HPO_4 - NaH_2PO_4 were found not to be suitable because the absorbance of taurine in these buffers was lower than that in the unbuffered solution. An Na_2HPO_4 - Na_3PO_4 buffer was used to adjust the pH of the reaction mixture from 9.96 to 10.73, and maximum absorbance was observed at pH 10.35, which was used for all subsequent experiments.

Effect of sodium hypochlorite

As sodium hypochlorite solution undergoes self-decomposition at room temperature, the hypochlorite stock solution was placed in a refrigerator and standardised daily before use. The dilute solution used for the determination should be freshly prepared.

Table 1. Results of recovery tests for taurine. Each determination was carried out in triplicate

Sample	Taurine added	Taurine found	Recovery, %
Milk powder	—	34.20 mg per 100 g	
	36.25 mg per 100 g	69.37 mg per 100 g	97.0
Energy drink	—	1.154 mg ml^{-1}	
	1.920 mg ml^{-1}	3.020 mg ml^{-1}	97.2

The absorbances of 10-ml aliquots of solutions containing 2 ml each of taurine solution (79.2 μg ml^{-1}) and phenol solution (0.68 M) and 2 ml of sodium hypochlorite solution with concentrations in the range 0–0.7 M were measured after allowing the solution to stand at room temperature for 30 min. It was found that the absorbance increased with increasing concentration of sodium hypochlorite until the latter reached 0.45 M and then decreased with a further increase in concentration. Hence, the optimum concentration of sodium hypochlorite was 0.45 M.

Effect of phenol

The experiment was repeated using 2 ml of 0.45 M sodium hypochlorite solution and 0–5 ml of 0.68 M phenol solution. The absorbance of the resulting solutions increased with increasing amount of phenol added and then decreased. The optimum volume of phenol solution added per 10 ml of resulting solution was found to be 2 ml.

Recovery Tests

Recovery tests were performed on two real samples. The mean recoveries of three analyses for added taurine were both *ca.* 97% (Table 1), which can be considered to be good.

Interference Studies

In addition to taurine, milk products or energy drinks may contain other amino acids such as phenylalanine, leucine and glutamate, which also form coloured products with phenol and hypochlorite. Ion exchange was used to improve the selectivity of the proposed method as it was found that an ion-exchange column removed all amino acids, cysteic acid, etc., while allowing the quantitative recovery of taurine.[9]

The effects of a number of amino acids and other substances commonly found in milk products and energy drinks were assessed, and the results obtained are given in Table 2. Also included in the study was ammonium ion, as ammonia reacts with phenol and hypochlorite to produce a similar blue colour. The criterion for interference was an absorbance varying by 5% or more from the expected value. None of the compounds studied interfered with the proposed method at the levels indicated, which cover the normal concentration ranges of these compounds.

Table 2. Effect of some common ingredients in milk products and energy drinks on the determination of taurine (100 μg ml^{-1})

Ingredient	Concentration/ μg ml^{-1}	Mass ratio (ingredient : taurine)	Error, %
Ammonium chloride	0.10*	10	−3.0
Ascorbic acid	150	1.5	−3.0
Alanine	318	3.2	+5.0
Aspartic acid	179	1.8	+4.2
Choline	300	3.0	−3.7
Citric acid	0.29*	29	−2.8
L-Cystine	230	2.3	+4.1
Glutamic acid	100	1.0	−4.0
Honey	5*	500	−2.0
Leucine	175	1.8	+4.6
Phenylalanine	186	1.9	−4.9
Serine	181	1.8	+5.0
Sodium citrate	0.10*	10	+1.2
Sucrose	1.5*	150	−2.5
Tyrosine	192	1.9	+4.8
Valine	213	2.1	+5.0

* Concentrations in %.

Table 3. Determination of taurine in milk products and energy drinks

Type of sample	Sample	Proposed method	Label value
Milk products . .	Milk powder (infant formula):		
	Brand 1	0.0299%	0.03%
		0.0278%	
		0.0272%	
		Mean: 0.0283%	
	Brand 2	0.0346%	0.0344%
		0.0340%	
		Mean: 0.0343%	
	Canned milk:		
	Brand 1 (low-iron infant formula)	0.0405 mg ml^{-1}	38 mg per quart* (0.040 mg ml^{-1})
		0.0390 mg ml^{-1}	
		0.0368 mg ml^{-1}	
		Mean: 0.0388 mg ml^{-1}	
	Brand 2 (iron-fortified infant formula)	0.0407 mg ml^{-1}	38 mg per quart* (0.040 mg ml^{-1})
		0.0380 mg ml^{-1}	
		Mean: 0.0393 mg ml^{-1}	
Energy drinks . .	Brand 1	480 μg ml^{-1}	500 μg ml^{-1}
		489 μg ml^{-1}	
		Mean: 484 μg ml^{-1}	
	Brand 2	1134 μg ml^{-1}	1200 μg ml^{-1}
		1194 μg ml^{-1}	
		Mean: 1164 μg ml^{-1}	

* 1 quart = 946.34 ml.

Calibration Graph and Precision

The calibration graph passed through the origin and was linear up to 180 μg ml^{-1} of taurine, having a slope of 0.00242 A (p.p.m.)$^{-1}$ and a correlation coefficient of 0.9999.

The precision of the procedure was checked by calculating the relative standard deviation of ten replicate determinations of a taurine standard solution (156 μg ml^{-1}), and was found to be 0.8%.

Determination of Taurine in Milk Products and Energy Drinks

The food samples analysed included milk powder (infant formula), canned milk (infant formula) and energy drinks. For all of these samples, cation exchange was used to minimise possible interferences from amino acids present in the matrices. For the milk products, perchloric acid was used for deproteinisation. For the milk powder, it was necessary to add hot water to the sample and shake for 30 min, as described previously.

The results of the determinations (Table 3) show a close agreement between the proposed method and the label values.

Conclusion

A simple, rapid and accurate spectrophotometric method has been developed for the determination of taurine in milk products and energy drinks. The selectivity of the method is improved by removing interfering substances using cation exchange. The method is suitable for routine analysis. The proposed method is better than other reported methods in terms of simplicity and convenience as no sophisticated instrumentation is needed. In comparison with other spectrophotometric methods, it is also much simpler as the reagents used are common and cheap and no complicated procedure such as those employed in reported spectrophotometric methods[3,4] is needed.

The authors express their gratitude to Mr. Kon-Leung Wong and Miss Nina L. N. Cheng for experimental assistance.

References

1. Harris, G., *Editor*, "Dictionary of Organic Compounds," Fourth Edition, Volume 5, Eyre & Spottiswoode, London, 1965, p. 2946.
2. Tachiki, K. H., Hendrie, H. C., Kellams, J., and Aprison, M. H., *Clin. Chim. Acta*, 1977, **75**, 455.
3. Gaitonde, M. K., and Short, R. A., *Analyst*, 1971, **96**, 274.
4. Ling, N. R., *J. Clin. Pathol.*, 1957, **10**, 100.
5. Erbersdobler, H. F., Greulich, H., and Trautwein, E., *J. Chromatogr.*, 1983, **254**, 332.
6. McCaman, R., and Stetzler, J., *J. Neurochem.*, 1977, **29**, 739.
7. Stokke, O., and Helland, P., *J. Chromatogr.*, 1978, **146**, 132.
8. Kataoka, H., Ohnishi, N., and Makita, M., *J. Chromatogr., Biomed. Appl.*, 1985, **40**, 370.
9. Larsen, B. R., Grosso, D. S., and Chang, S. Y., *J. Chromatogr. Sci.*, 1980, **18**, 233.
10. Wheler, G. H. T., and Russell, J. T., *J. Liq. Chromatogr.*, 1981, **4**, 1281.
11. Biondi, P. A., Negri, A., and Ioppolo, A., *J. Chromatogr.*, 1986, **369**, 431.
12. Erbersdobler, H. F., and Trautwein, E., *Milchwissenschaft*, 1984, **39**, 722.

Paper 9/03749G
Received September 4th, 1989
Accepted November 16th, 1989

Spectrophotometric Determination of Total Monoterpenols at Low Concentrations*

Juan Cacho
Department of Analytical Chemistry, Faculty of Sciences, University of Zaragoza, Zaragoza, Spain

Vicente Ferreira
Centre of Viticulture and Enology, Movera, Zaragoza, Spain

A method for the determination of low concentrations of monoterpenols in biological samples has been developed. Using phase separation to extract steam distillates and subsequent spectrophotometric determination with sulphuric acid - vanillin reagent, it is possible to determine as little as 3–4 p.p.b. of total monoterpenols.

Keywords: *Terpenol determination; phase separation; extraction spectrophotometry; grape*

Terpenes are a family of compounds that originate in the secondary carotenoid metabolism of plants.[1] Some of them are characterised by an intense smell. Being biosynthetic products controlled by specific genes,[2] they are characteristic of each plant variety and, together with other volatile compounds, they form the plant aroma. Within the alimentary system and together with esters they are responsible for the biosynthetic part of flavour,[3] conferring the organoleptic qualities that make them attractive or otherwise for consumption. If, during maturation time, the amount of these compounds is known, useful information can be established regarding the optimum picking time, because the fruit or plant quality bears a direct relationship to the amount of terpenes present.

Many methods have been described for analysing flavour. All of them involve extraction and further concentration steps. For the extraction stage many solvents have been used, such as dichloromethane,[4] pentane,[5] carbon tetrachloride,[6] several chlorofluorides especially Freon 11,[7] diethyl ether,[8] carbon disulphide,[9] isopentane,[10] supercritical carbon dioxide,[11] ethyl chloride[12] and some of their azeotropes. Different extracting techniques have been used, including simple, continuous, extraction - distillation,[13] phase separation,[14] the use of Amberlite resins[15] and headspace extraction techniques with solvents[16] or different traps, *e.g.*, cold,[17] Tenax,[18] Porapak[19] and Chromosorb 105.[15]

Although chromatographic methods are to be preferred for determining individual components, they are not useful for establishing the blending quality of fruit flavour or of an essence, or for establishing maturation control owing to the lengthy analysis time and the instruments required; further, total results cannot be obtained. For these reasons other methods for aroma and flavour quantification have been developed. Apart from sniffing methods, the most important are chemical and spectrophotometric procedures. The former are based on the oxidising ability of these compounds (chemical oxygen demand, COD),[20] but the results they yield are too general. The latter are based on the formation of a coloured derivative. The most popular method for terpene determination is the vanillin method.[21]

The vanillin method, first used by Attaway *et al.*[22] for the determination of terpenes in citrus juices, was later applied to aromatic raspberries and grapes (mainly muscat).[23,24] At present it is the most commonly used method for the determination of terpenes in these matrices. However, it is not suitable for fruits with less than about 0.12 mg of terpene per litre of juice and hence cannot be applied to the so-called non-aromatic grapes. This is an important restriction because these grapes are used for making wine and it is necessary to know their total terpene content in order to plan the vintage under optimum conditions.[25,26]

In this paper, the possibilities of lowering the detection limit using the vanillin method and organic solvents are considered. The quantification limit of the existing method has been improved more than 11-fold.

Experimental

Apparatus

A Perkin-Elmer Lambda-3 UV - visible spectrophotometer and a Schmidt steam distillation apparatus[27] were used.

Reagents

Propan-1-ol was obtained from Merck. The following solutions were prepared: vanillin solutions, 1.6, 2 and 4% in concentrated sulphuric acid; linalol stock solution, 1 mg ml^{-1}; linalol standard solution, 0.1 mg ml^{-1}, prepared by dilution of the stock solution; and geraniol, nerol, citronelol and terpineol standard solutions, 0.1 mg l^{-1}.

Recommended Procedure

A 100-ml volume of homogenised fruit is placed in a steam distillation apparatus similar to that described by Schmidt[27] and heated to 100 °C. The contents are distilled and the first 25 ml of distillate are recovered in a 100-ml separating funnel. A 2-ml volume of propan-1-ol is added and mixed, then 3.6 g of NaH_2PO_4 and 13.6 g of $(NH_4)_2SO_4$ are added with shaking to effect complete dissolution. The mixture is left until the two phases have separated, then the organic phase is removed.

In a 10-ml Pyrex test-tube fitted with screw-capped silicone-rubber seals, 1.4 ml of the propanolic extract and 0.6 ml of distilled water are shaken, then the tube is cooled to 0 °C in an ice - water bath. One millilitre of the 1.6% vanillin - sulphuric acid reagent is slowly added dropwise by pipette, moving the tip of the pipette over the surface of the tube to avoid local overheating.

The tube is capped and heated for 20 min in a water-bath at 60 ± 1 °C, then cooled in another water-bath to room temperature during 5 min. The absorbance is read at 608 nm against a blank.

To prepare a calibration graph, 25-ml volumes of aqueous solutions containing 0, 2.5, 5, 10, 20, 30, 40, 50 and 60 μg of linalol are prepared, phase separation and reaction are performed following the recommended procedure and the absorbances are read at 608 nm against the blank.

* Presented at SAC 89, the 8th SAC International Conference on Analytical Chemistry, Cambridge, UK, 30 July–5 August, 1989.

Solvent Selection

Various volumes of the organic solvents are placed in 20-ml Pyrex test-tubes and water is added to bring the total volume to 10 ml. The tubes are cooled as before and 5 ml of 2% vanillin in sulphuric acid are added while shaking and further cooling. The tubes are heated for 20 min in a water-bath at 60 °C, then cooled in a water-bath to room temperature and their absorbances are read against distilled water at 608 nm.

Phase Separation Study

Mixtures of ethanol or propan-1-ol and water in different proportions with a total volume of 50 ml are placed in 100-ml Erlenmeyer flasks, then increasing amounts of ammonium sulphate are added up to the beginning of phase separation. Salt addition is continued until saturation.

Reaction Optimisation

A fixed amount of terpene (10 μg) is mixed with various volumes of separated propan-1-ol organic phase in 10-ml test-tubes and distilled water is added to give a final volume of 2 ml. The mixture is cooled in an ice-bath and vanillin - sulphuric acid reagent and occasionally sulphuric acid are added. The tubes are then heated until the blue - green colour from the terpenol - vanillin reaction product develops, cooled to room temperature and the absorbances are read at 608 nm against a blank.

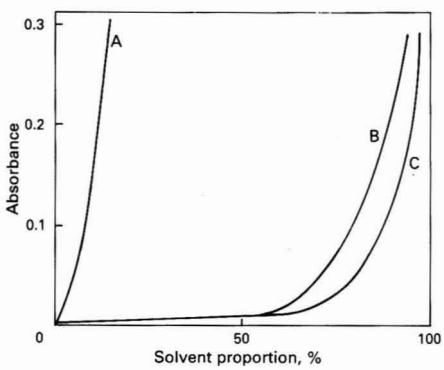

Fig. 1. Solvent interference in the reaction. A, Propan-2-ol, butan-1-ol and acetone; B, propan-1-ol; and C, ethanol

Results and Discussion

Solvent Selection

In order to improve the detection limit of the terpenols it is necessary to concentrate the terpene solution to a much smaller liquid volume than that obtained by steam distillation. This concentration can be carried out by three procedures. Vacuum distillation,[28] can be used, but special conditions and materials are necessary and also these low-volatility compounds tend to remain in the solution or to condense in the manifolds.[28] The second method is solvent extraction with water-immiscible solvents. Although this procedure is simple, it is necessary to find an organic solvent that is both miscible with the vanillin reagent and also non-reactive, which is a serious restriction. The third procedure consists in using water-miscible organic solvents, followed by phase separation by addition of an inorganic salt.

As it was impossible to find an extraction solvent with the required characteristics, we decided to use the third procedure because of its simplicity.

We studied the behaviour of methanol, ethanol, propan-1-ol, propan-2-ol, butan-1-ol and acetone following the described procedure. The last three solvents, although they show good phase separation, react with vanillin giving a strong brown colour that interferes with detection, so they were discarded. Methanol does not undergo phase separation to any useful extent, whereas ethanol and propan-1-ol not only readily give phase separation but also do not give any appreciable reaction when they contain at least 20% of water, as can be appreciated from Fig. 1. For this reason, we studied the optimum phase separation conditions according to the described procedure using only these two solvents.

Phase Separation Conditions

Ammonium sulphate was selected as the phase separation agent, as recommended,[14] and also a constant amount of NaH_2PO_4 was added to improve the phase separation.[29]

Fig. 2 shows the alcohol - water - salt ternary diagrams and the corresponding nodal curves for the binary mixtures. As can be seen in Fig. 2(*a*), the ethanol - water mixtures begin to separate when the proportion of ethanol is at least 10.5% and the upper limit for phase separation is 60% ethanol. Hence under the optimum conditions the organic phase is ethanol - water (60 + 40) and the composition of the separated aqueous phase ethanol - water (10.5 + 89.5). However, the propan-1-ol - water mixture undergoes phase separation from almost 0% to nearly 90% propan-1-ol, the composition of the separated

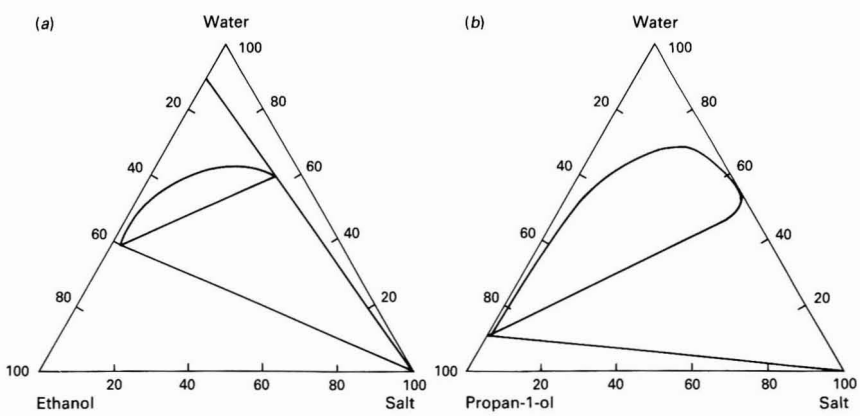

Fig. 2. Ternary diagrams of the solvent - water - salt systems: (*a*) ethanol and (*b*) propan-1-ol. Only the regions of two immiscible liquid phases and two immiscible liquids plus a solid phase are shown

organic phase being propan-1-ol - water (89 + 11) and the separated aqueous phase containing more than 99% water.

It is concluded that propan-1-ol allows better phase separation than ethanol. In addition, the organic phase obtained has a more appropriate composition for dissolving substances such as terpenols owing to its low dielectric constant, whereas the aqueous phase contains hardly any propan-1-ol and all the salt, and hence has a very low affinity for terpenols, so that only a trace amount of terpenols will remain in the aqueous phase after phase separation. For these reasons, in the following only propan-1-ol is considered.

In order to achieve an efficient colorimetric reaction of vanillin, a volume of 1.5 ml of propanolic terpene solution is needed. This volume of phase-separated propan-1-ol is easily obtained by adding 13.6 g of $(NH_4)_2SO_4$ and 3.5 g of NaH_2PO_4 to 25 ml of the distillate to which 2 ml of propan-1-ol have previously been added.

Reaction Optimisation

Minimum proportion of water necessary

It has been observed that propan-1-ol should contain a certain amount of water to prevent its reaction with vanillin. To find the necessary minimum proportion of water to be added to the separated organic phase and to obtain good reproducibility both for the blanks and samples, solutions of 2 ml containing phase-separated propan-1-ol and proportions of water in the range 0–40% were prepared. Another set of solutions was also prepared containing 10 μg of linalol.

Following the described procedure, 1 ml of 2% vanillin - sulphuric acid reagent was added, the mixture was heated at 60 °C for 20 min and cooled in 5 min to room temperature, then the absorbances were read at 608 nm.

Six replicate measurements were made and the mean values of the absorbances for both the sample (against its corresponding blank) and blank (against water) are shown in Fig. 3. It can be seen that up to 70% propan-1-ol the absorbance of the sample increases only slightly as the concentration of phase-separated propan-1-ol increases, and the same applies to the absorbance of the blank. Above 70% of phase-separated propan-1-ol, the absorbance of the blank increases exponentially, causing irreproducibility in the measurements.

In subsequent studies, 0.6 ml of distilled water was added to 1.4 ml of the propanolic extract (*i.e.*, 30% of added water).

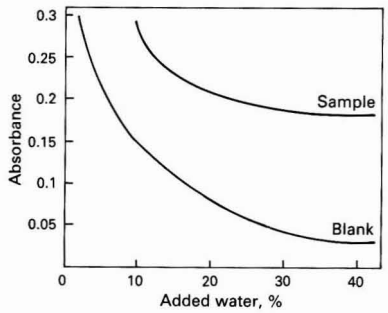

Fig. 3. Absorbances of sample and blank *versus* proportion of water added to the separated phases

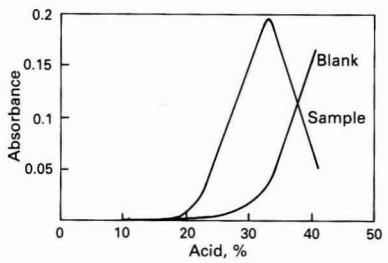

Fig. 4. Absorbances of sample and blank *versus* percentage of sulphuric acid

Influence of acidity

The influence of acidity was studied by adding to the terpenic propan-1-ol - water mixture 0.5 ml of 4% vanillin - sulphuric acid reagent and various volumes of sulphuric acid from 0 to 1.5 ml. The mixture was heated for 20 min at 60 °C following the described procedure. Measurements were made in triplicate and mean absorbance values for both a sample and blank are presented in Fig. 4. The maximum absorbance is obtained when the total volume of sulphuric acid is 1 ml. Under these conditions the absorbances of the blanks were low and the reproducibility of the measurements was fairly good. It is important to take into account that the vanillin - sulphuric acid reagent should be added slowly, shaking the tube to avoid possible local overheating.

Optimum vanillin concentration

The influence of the vanillin concentration was studied by adding to 2-ml blanks and samples 1 ml of vanillin - sulphuric acid reagent with vanillin concentrations between 0.8 and 2.4% m/m. The tubes were incubated to 60 °C for 20 min following the described procedure and three replicate measurements were made. A graph of absorbance *versus* vanillin concentration showed a broad maximum at 1.6%. In subsequent studies (with over 2 ml of sample), 1 ml of 1.6% vanillin - sulphuric acid reagent was added.

Optimum temperature and time of reaction

The described procedure was followed with the optimum values found for the various parameters as described above, heating the solutions at 50, 60 and 70 °C for various times. The results are given in Table 1. At 60 °C the colour was fully developed in 15 min and remained stable for at least 60 min. Nevertheless, in order to ensure total development of colour with all the terpenols, the solutions were heated at 60 °C for 20 min.

Table 1. Optimum reaction times and temperatures (three determinations)

	% of total signal							
	Time/min							
Temperature/°C	0	5	10	15	20	25	30	Blanks SD
50	0	50	65	80	85	90	90	0.0012
60	0	77	95	100	100	100	100	0.0014
70	0	97	100	97	93	92	91	0.0085

Table 2. Standard additions of pure and mixed monoterpenols to a steam distillate from grapes

Terpene	Added/ µg	Found*/ µg	RSD, %	Recovery, %
Linalol	0	14.03	1.93	
	5	18.57	1.99	92.8
	10	23.11	2.03	90.8
	30	41.12	1.62	90.3
	60	69.80	2.24	93.0
Geraniol	0	17.11	1.93	
	5	21.67	2.05	91.2
	10	26.12	2.12	90.1
	30	44.68	1.99	91.9
	60	72.21	2.03	91.8
α-Terpineol	0	9.65	1.93	
	5	14.21	1.77	91.2
	60	63.64	1.78	89.9
Nerol	0	14.09	1.93	
	5	18.67	1.59	91.6
	60	70.20	1.86	93.5
Citronelol	0	15.62	1.93	
	5	20.21	1.79	91.8
	60	71.00	1.87	92.3
Total terpenols	0	14.06	1.93	
	5	18.66	1.65	92.0
	10	23.23	1.69	91.7
	30	41.68	2.05	92.1
	60	69.89	1.82	93.0

* Means of three replicate measurements.

Table 3. Comparison between the proposed method and the Dimitriadis - Williams method[24] in the analysis of two grape samples

	Amount of terpenol/mg l^{-1}			
	Dimitriadis - Williams method		Proposed method	
Fraction	Sample A	Sample B	Sample A	Sample B
1	0.63	0.09	0.62	0.087
2	0.65	0.08	0.61	0.085
3	0.67	0.12	0.62	0.090
4	0.61	0.07	0.63	0.088
5	0.68	0.06	0.60	0.087
6	0.64	0.10	0.64	0.090
Mean	0.65	0.09	0.62	0.088
SD	0.026	0.022	0.014	0.002
RSD, %	4.00	24.8	2.26	2.21

Linear Range, Reproducibility and Characteristic Concentration

Using the above optimum conditions with 25 ml of aqueous solutions of linalol of different concentrations and following the recommended procedure, the range of applicability of Beer's law was studied. Linalol was used as a reference, because it showed the same absorbances as an equimolecular mixture of terpenes, in agreement with the literature,[24] and a calibration graph was constructed.

A linear relationship between absorbance and concentration was obtained up to a linalol concentration in the steam distillate of 5 p.p.m. (that is, when a Schmidt steam distillation apparatus is used, and when the amount of terpenols in the matrix is no higher than about 1.25 p.p.m.). The straight line obtained is represented by the equation $A = -0.0061 + 0.0159\,c$ ($r = 0.9991$), where c is the amount of total terpenols present in 25 ml of steam distillate, expressed as micrograms of linalol, and A is the absorbance obtained against a blank.

In the analysis of ten replicates containing 20 µg of linalol in 25 ml of aqueous solution, the mean absorbance was 0.304 with a standard deviation (SD) of 0.0055 and a relative standard deviation (RSD) of 1.6%.

Table 4. Analysis of non-aromatic grapes (cultivars). Volume of juice taken, 100 ml

Variety	Maturity	Amount of terpenol,* p.p.b.	RSD, %
Carignena	Veraison	16.4	2.8
Carignena	Recolte	38.7	2.6
Tempranillo	Veraison	12.5	2.7
Tempranillo	Recolte	27.2	2.1
Grenache	Veraison	17.3	2.4
Grenache	Recolte	44.5	1.8

* Average of three determinations.

For ten blanks the mean absorbance was 0.037 with SD = 0.0018 and RSD = 4.8%. This implies that the detection limit is 0.34 µg in 25 ml of steam distillate (about 3.4 p.p.b. in the homogenate) and the limit of quantification is 1.125 µg in 25 ml of steam distillate (*i.e.*, about 11.25 p.p.b. in the homogenate).

The characteristic mass (mass of analyte giving an absorbance peak of 0.044) is 3.125 µg of terpenol, *i.e.*, about 31.25 p.p.b. in the homogenate.

Phase Separation as an Extraction Method for Terpenols

The over-all recovery of the terpenols was studied by adding to 25 ml of steam distillate various amounts of individual terpenes and of an equimolar mixture containing linalol, geraniol, α-terpineol, nerol and citronelol. The recovery, both individual and total, was determined by constructing a calibration graph with the individual compounds or with the mixture.

The results are given in Table 2. The recoveries are similar for all the compounds. It is interesting that the slope of the calibration graph constructed with the mixture is the same as that for linalol alone. Hence it is possible to use this compound as a reference in the over-all determination of terpenols.

Application to Grapes

The method was compared with the Dimitriadis - Williams method,[24] analysing six homogenates of table grapes and six of non-aromatic grapes. A 1-kg amount of each variety was crushed under nitrogen and with 20 ml of methanol and divided into six fractions of 100 ml. Each fraction was distilled in a Schmidt distillation apparatus, recovering the first 25 ml of distillate. This was diluted to 35 ml with distilled water and separated in two fractions. One fraction of 10 ml was analysed following the Dimitriadis - Williams method and the other 25-ml fraction was analysed following the proposed method. The results are given in Table 3.

Following the described procedure, various non-aromatic grapes (cultivars) at two different stages of maturity were analysed. The results are given in Table 4.

References

1. Birch, A. J., Boulter, D., Fryer, R. I., Thomson, P. J., and Willis, J. L., *Tetrahedron Lett.*, 1959, **3**, 1.
2. Fujita, Y., and Fujita, S., *Nippon Kagaku Zasshi*, 1967, **88**, 767.
3. Sanderson, G. W., and Graham, H. N., *J. Agric. Food Chem.*, 1973, **21**, 576.
4. Fagan, G. L., Kepner, R. E., and Webb, A. D., *Am. J. Enol. Vitic.*, 1982, **33**, 47.
5. Schreier, P., Drawert, F., and Winkler, F., *J. Agric. Food Chem.*, 1979, **27**, 365.
6. Di Stefano, R., and Castino, M., *Riv. Vitic. Enol.*, 1983, **36**, 245.

7. Williams, P. J., Strauss, C. R., Wilson, B., and Massy-Westrop, R. A., *J. Agric. Food Chem.*, 1982, **30**, 1219.
8. Etievant, P. X., and Bayonove, C. L., *J. Agric. Food Chem.*, 1983, **34**, 393.
9. Snyman, J. P., *Vitis*, 1977, **16**, 295.
10. Cobb, Ch. S., and Bursey, M. M., *J. Agric. Food Chem.*, 1976, **26**, 197.
11. Berger, M., Sagi, F., and Cerles, B., *Fr. Pat.*, 8109894, 1981.
12. Drawert, F., and Rapp, A., *Vitis*, 1983, **5**, 263.
13. Likens, S. F., and Nickerson, G. B., *Proc. Am. Soc. Brew. Chem.*, 1964, 5.
14. Bertrand, A., *Chim. Anal.* (*Paris*), 1971, **53**, 577.
15. Guichard, E., *Sci. Aliments*, 1982, **2**, 173.
16. Rapp, A., and Knipser, W., *Chromatographia*, 1980, **13**, 698.
17. Bayonove, C., and Cordonnier, R., *Ann. Technol. Agric.*, 1970, **19**, 79.
18. Loyaux, D., Roger, S., and Add, A. J., *J. Sci. Food Agric.*, 1981, **32**, 1254.
19. Brander, C. F., Kepner, R. E., and Webb, A. D., *Am. J. Enol. Vitic.*, 1980, **31**, 69.
20. Dougherty, M. H., *Food Technol.* (*Chicago*), 1968, **22**, 1455.
21. Feigl, F., "Qualitative Analysis by Spot Tests," Third Edition, Elsevier, New York, 1946, pp. 340–345.
22. Attaway, J. A., Wolford, R. W., Dougherty, M. H., and Edwards, G. J., *J. Agric. Food Chem.*, 1967, **15**, 688.
23. Latrasse, A., Lantin, B., Mussillon, P., and Sarris, J., *Lebensm.-Wiss. Technol.*, 1982, **15**, 19 and 49.
24. Dimitriadis, E., and Williams, P. J., *Am. J. Enol. Vitic.*, 1984, **35**, 66.
25. Hidalgo, J., *Viña Vino*, 1988, **46**, 67.
26. Foulonneau, C., and Durand, R., *Progr. Agric. Vitic.*, 1986, **103**, 240.
27. Schmidt, H., *Fresenius Z. Anal. Chem.*, 1960, **178**, 173.
28. Forss, P. A., Jacobson, V. M., and Ramshaw, E. H., *J. Agric. Food Chem.*, 1967, **15**, 1104.
29. Mesias, J. L., Maynar, J. I., and Mareca, I., *Rev. Agroquim. Tecnol. Aliment.*, 1981, **21**, 114.

Paper 9/02463H
Received June 12th, 1989
Accepted November 2nd, 1989

CUMULATIVE AUTHOR INDEX

JANUARY–MAY 1990

ANALAO 115(5) 473–664 (1990) May 1990

The Analyst

The Analytical Journal of The Royal Society of Chemistry

CONTENTS

continued inside back cover

Typeset and printed by Black Bear Press Limited, Cambridge, England